ADDIS ABABA UNIVERSITY
COLLEGE OF NATURAL AND COMPUTATIONAL SCIENCES
DEPARTMENT OF CHEMISTRY

PhD DISSERTATION

PHYTOCHEMICAL STUDIES OF *MYRICA SALICIFOLIA*, *CLEMATIS SIMENSIS* AND *OLINIA USAMBARENSIS*

BY: ABRAHAM DILNESA

JUNE, 2024

ADDIS ABABA, ETHIOPIA

Phytochemical Studies of *Myrica salicifolia*, *Clematis simensis* and *Olinia usambarensis*

By Abraham Dilnesa Gashaw

Advisors: Dr. Mekonnen Abebayehu Desta &
Dr. Estifanos Ele Yaya

A Dissertation Submitted to Department of Chemistry, College of Natural Sciences, Addis Ababa University in a Partial Fulfillment for the Degree of Doctor of Philosophy in Chemistry

June, 2024

Addis Ababa, Ethiopia

Addis Ababa University

College of Natural and Computational Sciences

School of Graduate Studies

Department of Chemistry

It is certified that the research work presented in this dissertation, entitled "Phytochemical Studies of *Myrica salicifolia*, *Clematis simensis,* and *Olinia usambarensis*", has been carried out by Abraham Dilnesa under my supervision for the fulfillment of the requirements of a Ph.D. degree in Chemistry (Organic stream) complies with the regulation of the University and meets the accepted standards with respect to originality and quality during the session 2019-2024. Approved by the examining committee:

Name	Signature	Date
External examiner		
_____	_____	_____
Internal examiner		
_____	_____	_____
Internal examiner		
_____	_____	_____
Advisor		
_____	_____	_____
Chairman of the Department		
_____	_____	_____

DECLARATION OF THE CANDIDATE

I, Abraham Dilnesa, hereby declare that this dissertation entitled "Phytochemical Studies of *Myrica salicifolia*, *Clematis simensis,* and *Olinia usambarensis*" is my original work submitted at Addis Ababa University, College of Natural and Computational Sciences, Addis Ababa, Ethiopia, and has not been submitted previously for any degree or examination elsewhere. All sources of information have been duly acknowledged and properly cited in the text.

This work was done from September 2019 to June 2024 at Department of Chemistry, College of Natural and Computational Sciences, Addis Ababa University under the supervision of Dr. Mekonnen Abebayehu Desta and Dr. Estifanos Ele Yaya.

Phytochemical Studies of *Myrica salicifolia*, *Clematis simensis* and *Olinia usambarensis*

Abraham Dilnesa Gashaw

Department of Chemistry, Addis Ababa University

Abstract

Myrica salicifolia A Rich (Myricaceae) is a tree growing in Central and East Africa. Traditionally the plant is applicable in the treatment of malaria, respiratory disorders, inflammations, and infections. The leaves and stem barks of *Clematis simensis* are traditionally used to treat tinea capitis, dermatitis, tropical ulcers, wounds and cancer. One of the African medicinal plants, *Olinia usambarensis,* is well known for its traditional use in various forms of medicine to treat fever, respiratory issues, digestive issues, headaches, and scabies. In this study, the plant materials were collected from Debresina, and Northern Shewa, Ethiopia. The essential oil extractions of the samples were carried out *via* hydro-distillation. The composition of the essential oil from roots and leaves of *Myrica salicifolia*, aerial part of *Clematis simensis,* and barks of *Olinia usambarensis* was analyzed by GC-MS. A total of 79 compounds were identified by GC-MS. The major compounds in the essential oils from roots and leaves of *Myrica salicifolia* were *trans*-3-hexen-1-ol (52.62%) and n-hexadecanoic acid (46.69%). On the other hand, the essential oil obtained from the aerial part of *Clematis simensis* and barks of *Olinia usambarensis* were predominantly (*E*)-2-nonen-1-ol (38.33%), 4-cyclopentene-1,3-dione (28.69%), and n-hexadecanoic acid (28.83%). Three terpenes, namely squalene (**77**), β-carotene (**78**), and β-sitosterol (**80**), and one chlorin, namely pheophytin a (**79**), were isolated from the leaves of *M. salicifolia*. The chloroform-methanol (2:1) crude extract of the stem barks of *M. salicifolia* was fractionated using column chromatography to afford three diarylheptanoids (myricanone (**28**), myricanol (**29**), myricanol-11-*O*-β-D-xylopyranoside (**32**)), four triterpenoids (taraxerone (**81**), taraxerol (**82**), myricadiol (**83**), 3β-*O*-*trans*-caffeoylisomyricadiol (**84**)), one pyranoside (methyl-β-D-glucopyranoside (**85**)). This is the first report of compounds **81**, **82**, **83**, **84**, and **85** from the stem barks of *M. salicifolia*. Five compounds, namely taraxerol (**82**), β-sitosterol (**80**), sitoindoside I (**87**), myricanone (**28**), and myricanol 5-*O*-β-D-glucopyranoside (**30**), were also isolated from the roots of *M. salicifolia.* Furthermore,

three compounds, namely 2-deoxy-D-ribono-1,4-lactone (**88**), 5-hydroxylevulinic acid (**89**), and β-sitosterol-3-*O*-β-D-glucoside (**90**), were isolated from the aerial part of *Clematis simensis.* Three compounds, namely lupeol (**91**), n-pentacosyl *trans*-ferulate (**92**), and 4-*O*-β-D-glucopyranosylcaffeic acid (**72**), were isolated and characterized from the barks of *Olinia usambarensis.* The structures of these compounds were determined using a comprehensive analysis of 1D/2D NMR, HR-MS, FT-IR and comparison with literature data. In this work, the isolated compounds and crude extracts of *Myrica salicifolia*, and aerial part of *Clematis simensis* were screened for antibacterial activity using disk diffusion agar method, and the activities revealed that both myricanol-11-*O*-β-D-xylopyranoside (**32**) and 3β-*O*-*trans*-caffeoylisomyricadiol (**84**) showed modest antibacterial activity with inhibition zones of 10.0 mm against *S. pyogenes* and 9.0 mm against *S. aureus* at 250 µg/mL. The antioxidant activities of the crude extracts and isolated compounds were also evaluated using the diphenylpicrylhydrazyl (DPPH) assay method. The crude extracts and isolated compounds from the stem barks of *Myrica salicifolia*, roots of *Myrica salicifolia,* aerial part of *Clematis simensis,* and barks of *Olinia usambarensis* showed very weak (IC_{50} = 458.8 µg/ml) to very strong (IC_{50} = 2.97 µg/ml) DPPH scavenging activities. The observed IC_{50} value showed that roots of *Myrica salicifolia* exhibited highest antioxidant activity (IC_{50} = 2.97 µg/ml).

Contents

List of Figures

List of Tables

.

List of Appendices

List of Abbreviations and Acronyms

AA	Ascorbic Acid
ATCC	American type culture collection
BTH	Butylated hydroxytoluene
CE	Crude Extract
CLSI	Clinical and Laboratory Standards Institute
COSY	^{1}H-^{1}H Correlation Spectroscopy
Cy	Cyclohexane
DCM	Dichloromethane
DEPT-135	Distortionless Enhancement by Polarization Transfer 135
DHB	2,5-Dihydroxybenzoic acid
DMSO	Dimethyl sulfoxide
1D-NMR	One-dimensional Nuclear Magnetic Resonance Spectroscopy
2D-NMR	Two-dimensional Nuclear Magnetic Resonance Spectroscopy
DPPH	2, 2-Diphenyl-1-picrylhydrazyl
EtOAc	Ethyl acetate
G	Gram
GC-MS	Gas Chromatography-Mass Spectroscopy
H	Hour
HMBC	Heteronuclear Multiple Bond Correlation
HRESIMS	High Resolution Electrospray Ionization Mass Spectroscopy
HSQC	Heteronuclear Single Quantum Coherence
IC_{50}	Half Maximal Inhibitory Concentration
IR	Infrared Spectroscopy
MeOH	Methanol
Mg	Milligram
mL	Milliliter
MSD	Mass Selective Detection
NIST	National Institute of Standards and Technology
NOSY	Nuclear Overhauser Enhancement Spectroscopy
NP	Natural Product

PC	Paper chromatography
PET	Petrolum ether
RF	Retention factor
RSA	Radical scavenging activity
TLC	Thin Layer Chromatography
TMS	Tetramethylsilane
TOF-MS	Time-of-Flight Mass Spectrometry
UV-Vis	Ultraviolet-Visible

Acknowledgments

I would like to express my deepest gratitude and appreciation to my research supervisors, Dr. Mekonnen Abebayehu Desta and Dr. Estifanos Ele Yaya, for their guidance, encouragement, and continuous support throughout the completion of this Ph.D. dissertation

I am also grateful to Dr. Kibrom Gebreheiwot Bedane and Prof. Wendimagegn Mammo, for their insightful feedback and constructive criticism of my work and NMR measurements of samples. I extend my thanks to Dr. Estifanos Ele for running GC-MS and his scientific support during GC-MS data analysis.

I would like to express my sincere gratitude to Dr. Kibrom Gebreheiwot Bedane, Taye B. Demissie, and Japheth O. Ombito for generously allowing me to utilize the laboratory facilities of the Department of Chemistry, University of Botswana for some parts of the research conducted in this dissertation. The opportunity to access equipment and resources has been invaluable in the successful completion of this project.

I would like to thank Prof. Wendimagegn Mammo and Dr. Estifanos Ele for their support by providing reading materials, articles and relevant courses in my study. Dr. Yonas Chebude should be acknowledged for running IR.

Ato Melaku Wondafrash of the National Herbarium is thanked for the authentication of the *Myrica salicifolia*, *Clematis simensis* and *Olinia usambarensis* species. I extend my thanks to the Department of Chemistry, Addis Ababa University, for providing the necessary resources and facilities for conducting my research. Special thanks to the lab technicians for their assistance during experiments. I would like to to be grateful to the Department of Chemistry at Addis Ababa University and the Ethiopian Forest Development Institute, which enabled me to pursue my Ph.D. studies. Your support has been instrumental in the successful completion of this dissertation.

1 Introduction

There are about 374,000 plant species in the world, of which approximately 308,312 are vascular plants, with 295,383 are flowering plants.[1]Approximately 25% of the world's plant genetic resources, or up to 45,000 plant species, are found in Africa. More than 5,000 plant species from this vast African resource are utilized in traditional medicines.[2] Ethiopia is endowed with 6500–7000 plant species, with 12–19% of them are being endemic.[3] For centuries, Ethiopian people have heavily relied on traditional medicine for their health care needs. It is estimated that about 80% of the population and 90% of livestock rely on these traditional medicinal practices.[4-5] Since ancient times, medicinal plants have been used around the world to treat a wide range of ailments, diseases, and wounds.[6] Medicinal plants are a rich source of phytochemicals such as alkaloids, terpenes, glucosinolates, phenolics, and flavonoids.[7] Plant-derived products and their corresponding metabolites have garnered considerable interest at the clinical, pharmacological, cosmetic and even industrial levels.[8] Indeed, natural products are extremely rich sources of biomolecules useful for a multitude of applications. Despite major scientific and technological progress in combinatorial chemistry, drugs derived from natural products still make an enormous contribution to drug discovery today.[9] In addition to the discovery of new chemical entities for therapeutic application, the natural products provide an important foundation as potential lead compounds for the development of new and more effective drugs through structural modification. Although natural products possess diverse and complex chemical structures, the plant secondary metabolites are seemed to exhibit greater biological friendliness and drug-likeness than those derived from purely synthetic sources. Consequently, the molecules from natural origin are supposed to be better candidates for further drug development.[10-11] Natural products and their derivatives represent over 60% of all drugs clinically used worldwide where natural products from medicinal plants alone contribute to 25% of total drugs.[12] Natural products and related drugs are reportedly used for example as antibacterial, anticancer, anticoagulant, antiparasitic and immunosuppressant agents to treat 87% of all categorized human diseases.[13] Of the 1,135 new drugs approved from 1981 to 2010, 50% were of natural product origin (natural, derivatives and analogues).[14] Well known examples include the widely used breast cancer drug, paclitaxel (**1**), isolated from

the bark of the *Taxus brevifolia*[15], trabectedin (**2**) was isolated from the *Ecteinascidia turbinate*[16], and mevastatin (**3**) was isolated from *Penicillium citrinum*.[17]

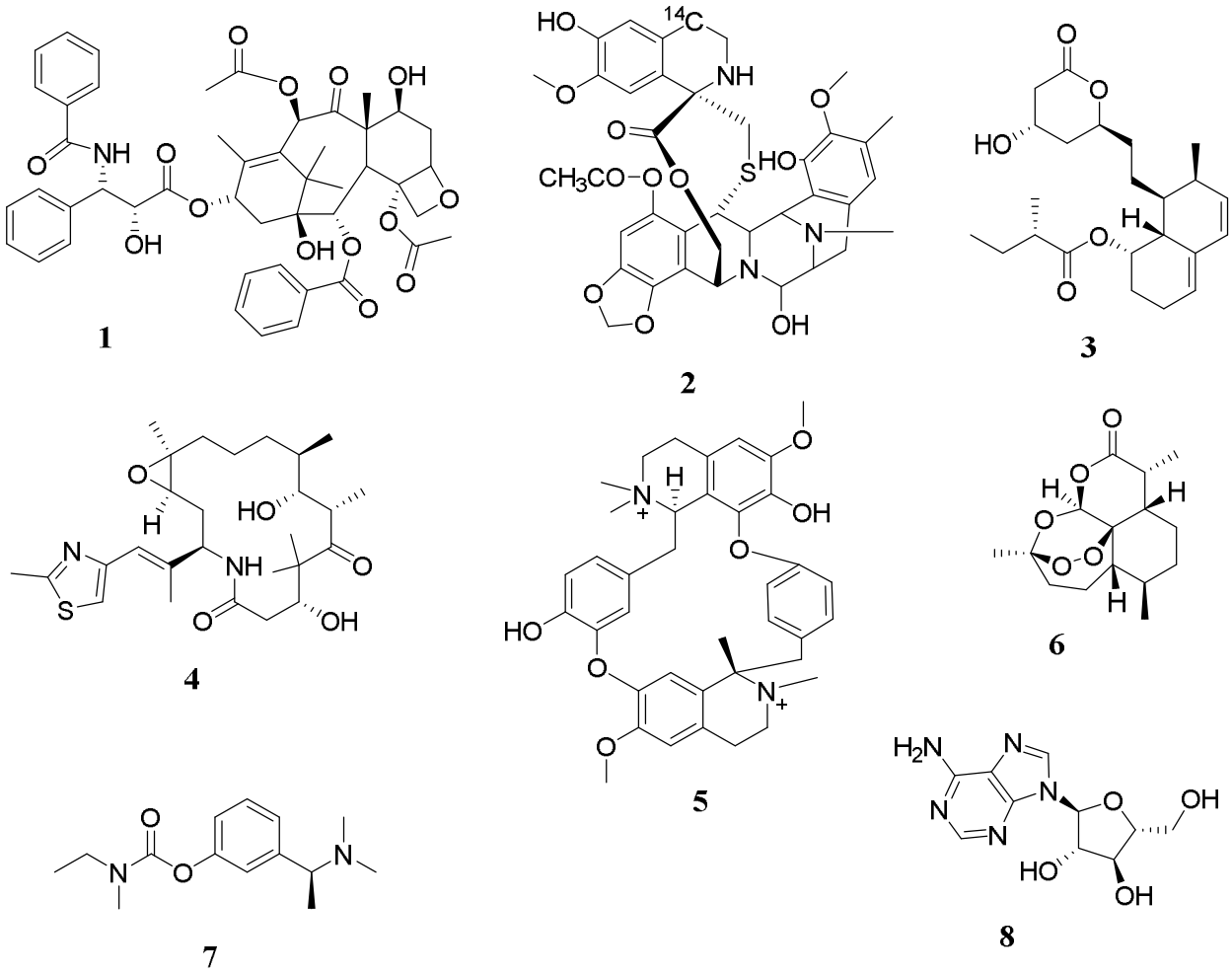

Figure 1: Chemical structures of FAD approved drugs frome natural products.

Several other natural products or natural products-derived drugs including tubocurarine (**4**)[18], ixabepilone (**5**)[19], artemisinin (**6**)[20], rivastigmine (**7**)[21,] and vidarabine (**8**)[22], are examples approved by food and drug administration (FDA) (Figure 1). As a result of increasing interest in the plant kingdom as a potential source of new therapeutic agents, several techniques have been developed for the extraction and isolation of natural products.[23] Several sample preparation and pre-purification steps are used prior to the isolation and/or analysis of natural products. Extraction methods are used as a pre-purification step to selectively remove interfering components and/or to isolate the active compounds. The extraction method includes microwave, maceration, sublimation,

supercritical fluid, soxhlet, steam distillation or hydro-distillation and ultrasonic. Initial extraction with low-polarity solvents yields the more lipophilic components, while ethanolic solvents obtain a larger spectrum of non-polar and polar material.[24] Other pre-purification methods includes filtration, precipitation, sephadex LH-20, centrifugal partition chromatography, and solid-phase extraction.[25] Chromatographic techniques are used in the isolation of various types of natural products may be classified broadly into two categories, older chromatographic techniques, and modern chromatographic techniques. The classical chromatographic techniques include vacuum liquid chromatography (VLC), flash chromatography (FC), column chromatography (CC), size exclusion chromatography (SEC), thin layer chromatography (TLC), and preparative thin layer chromatography (PTLC) whereas chromatotron, droplet counter-current chromatography (DCC), high performance thin layer chromatography (HPTLC), High-performance liquid chromatography (HPLC), sephadex (SPE), vacuum liquid chromatography (VLC), and a number of hyphenated techniques may be considered to be modern chromatographic techniques. In identifying a plant constituent, once it has been isolated and purified, its homogeneity must be checked carefully beforehand, as a single spot in several TLC and/or PC systems. The class of compound is usually clear from its response to color tests, its solubility and RF properties and its UV spectral characteristics.[26] Complete identification within the class depends on measuring other properties and then comparing these data with those in the literature. These properties include melting point (for solids), boiling point (for liquids), optical rotation (for optically active compounds) and RF (under standard conditions). However, equally informative data on a plant substance are its spectral characteristics: these include ultraviolet (UV), infrared (IR), nuclear magnetic resonance (NMR) and mass spectral (MS) measurements.[26]

1.1 Statement of the Problem

According to WHO (2011), as commercialization of the herbal medicines is going on, assurance of safety, quality and efficacy become an important issue.[27] Even though quite a number of plants used in folk medicine have been identified in Ethiopia, the use of complicated, individualized treatments and the absence of standards for herbal remedies are issues that complicate clinical studies of complementary and alternative medicine. In

Ethiopia, there is a lack of scientific data on the phytochemical composition of many medicinal plants that contribute to the standardization and formulation of drugs.[28-29]

One of the top threats to global development and public health is antibiotic drug resistance. Many bacterial strains have become resistant to widely used antibiotics, which can result in treatment failures and the spread of infections bacterial strains that are challenging to treat like *Staphylococcus aureus*, *Escherichia coli*, *Streptococcus pyogenes*, and *Pseudomonas aeruginosa*, which are the four major antibiotic-resistant bacteria of the ten most dangerous reported antibiotic-resistant bacteria.[30]

Due to the increasing level of drug resistance of these pathogens against the current chemotherapeutics, the need for new drugs discovery became important. To address some of the challenges outlined above, the present study was designed to investigate the unexplored ethnomedicinal knowledge of some Ethiopian plants towards the treatment of infectious diseases. Based on ethnobotanical studies, three plants namely *Myrica salicifolia*, *Clematis simensis,* and *Olinia usambarensis,* were selected for the study. Prior to this study, little was known about the antimicrobial activity of different extracts of *Myrica salicifolia*[31], *Clematis simensis*[32], and *Olinia usambarensis*.[33]

Hence, this study was initiated to search for new phytochemicals that can serve as an alternative therapeutic agent from the leaves, roots, and barks of *Myrica salicifolia,* the leaves of *Clematis simensis,* and the barks of *Olinia usambarensis.*

1.2 Rationale

Ethiopia is one of the most biodiverse countries in the world, with a wide variety of plant species that have not been fully explored for their medicinal properties[34-35]and therefore, phytochemical investigation of *Myrica salicifolia, Clematis simensis*, and *Olinia usambarensis* plants can uncover new compounds with therapeutic potential, contributing to the discovery of novel drugs and treatments. Traditional herbal medicine plays a significant role in the healthcare system of Ethiopia, especially in rural areas where access to modern healthcare facilities is limited[36] and, as a result, investigating the phytochemical properties of medicinal plants can help validate their traditional uses and provide scientific evidences for their efficacy and safety. Ethiopia's rich biodiversity and traditional

knowledge of medicinal plants present an opportunity for the development of the pharmaceutical and herbal medicine industries[36-37] and consequently, phytochemical investigation of *Myrica salicifolia, Clematis simensis,* and *Olinia usambarensis* plants can lead to the identification of valuable compounds that can be commercialized, benefiting both the economy and local communities.

1.3 Objectives of the Study

1.3.1 General Objective

The main objective of this research work has been to investigate the chemical composition and evaluate the biological activities of crude extracts and isolated compounds of *Myrica salicifolia, Clematis simensis,* and *Olinia usambarensis* plant species.

1.3.2 Specific Objectives

1) Extraction and characterization of essential oils of the *Myrica salicifolia, Clematis simensis* and *Olinia usambarensis.*
2) Isolation and characterization of secondary metabolites from the leaves, roots and barks of *Myrica salicifolia,* the aerial part of *Clematis simensis,* and the barks of *Olinia usambarensis.*
3) Evaluation of the antioxidant activities of the extracts and isolated compounds of the roots and barks of *Myrica salicifolia,* the aerial part of *Clematis simensis,* and the barks of *Olinia usambarensis.*
4) Evaluation of antibacterial activities of the extracts and isolated compounds of the barks of *Myrica salicifolia,* and the aerial part of *Clematis simensis.*

2 Literature Review

2.1 Phytochemistry and Biological activities of *Myrica salicifolia*

The Myricaceae is a small family comprising three genera (*Myrica, Comptonia* and *Canacomyrica*) and widely distributed in both temperate and sub-tropical regions.[1] Macdonald[38] stated reasons for cut off *Myrica* genus in two, *Myrica* and *Morella*, and his arguments were accepted in 2002 and the genus was split.[39] To clarify the distinction a taxonomic key was published in 2005.[40] As a result, a large number of species that were previously classified in the *Myrica* genus have been reclassified into the *Morella* genus. In the field of natural product research, this taxonomic reclassification has several consequences. The isolation of secondary metabolites from the *Myrica* species has been reported in a number of studies published prior to 2005, which are now *Morella* species, and this may result in false reports about secondary metabolites that are discovered in the genus for the first time. But it can also result in more recent works that still refer to the earlier scientific name and consequently not be appropriately identified in a literature review.[41]

Morella is by far the largest genus, which has roughly 50 species that have been identified and are distributed widely throughout Africa, Europe, North America, and Asia.[40] The members of the *Myrica* and *Morella* genera are woody shrubs or tree pioneers in nitrogen-poor soils to fix nitrogen through nitrogen-fixing root nodules.[42] These species are valued for their raw fruits, which are also used to make jams, syrups, and juices. Their economic value extends beyond their use as a source of barks for paper and rope, as well as for biomass production and land reclamation[43], and their applications in traditional medicine are also remarkable.[44] For instance, in Chinese or Japanese folk medicine, they are used to treat diarrhea, digestive problems, headaches, burns, and skin diseases. treat bleeding, and stomach pain[45], dyspepsia[46], burns, and skin diseases[47], enteritis[48], asthma, coughing, and shortness of breath[49], treat painful menstruation, colds, coughs, and headaches, and enhance male sexual performance[50], management of sugar related disorder and as laxatives to treat constipation[51], treat fever and inflammation[39], intestinal worms, cardiac disorders, and aching muscles.[52] This potential sparked necessary and obligatory research to try to

validate the beneficial effects recommended by traditional medicine as well as to look for the active ingredients responsible for the activities demonstrated.

A review literature showed more than 100 compounds were isolated from *Myrica* and *Morella* species, most of them are cyclic diarylheptanoids, flavonoids and pentacyclic triterpenoids.[53-54] Some cyclic diarylheptanoids, specially, myricanone (**20**) and myricanol (**21**), and some pentacyclic triterpenoids should be used as *Myrica*/*Morella* genus chemotaxonomic markers[53-54], while unusual *C*-methylated dihydrochalcones and flavonoids may support the segregation of some *Myrica* species to a new genus.[54] Several new diarylheptanoids, which have a unique 1,7-diphenylheptane structure and are distributed in a few botanic genera[55], have been isolated over the years from the *Myrica* genus (e.g., *Myrica rubra*).[56] Diarylheptanoids are known for their remarkable antioxidant, anti-inflammatory, antitumor, leishmanicidal, hepatoprotective, melanogenesis, and neuroprotective activities.[55, 57]

Myrica salicifolia (Figure 2, synonyms: *Morella salicifolia*, *Myrica humilis* sensu, *Myrica kilimandscharica*, *Myrica usambarensis*) Local name: '*shinet*' or '*Kalava*' in Amharic, '*Abay*', '*Kataba*' or '*Radji*' (*Tona*) in Affan Oromo, '*Nihibi*' in Tigrigna, '*Abeyi*' in Guaragegna, '*Gawada*' in Kabategna, and '*Kowada*' in Hadyagna[58-59] belongs to the genus *Myrica Lin.* It is a deciduous shrub with a trunk diameter of up to 1 m and can grow up to 20 meters in height. It is found in Central and East Africa, including Ethiopia, Zambia, Kenya, Burundi, Malawi, Uganda, Madagascar, Zaire, Rwanda, Tanzania and also in Saudi Arabia.[60-61]It is typically grown in humid lower highlands. The plant has a long history of use as a traditional medicine in Tanzania, where it is used to treat a variety of illnesses, including pneumonia, chronic constipation, cryptococcal meningitis, herpes zoster, stomach pain, and headaches as well as for managing of HIV.[62-63]*M. salicifolia* has also been used to treat erectile dysfunction and male sexual impotence in Uganda.[64] In Ethiopia, it is used to treat lung diseases, inflammation, and skin diseases.[65-66]

The compounds isolated from *M. salicifolia* have shown a range of biological activities. Marealle *et al*. reported the antimycobacterial activity of compounds isolated from *M. salicifolia* against three nonpathogenic mycobacterial species. Maslinic acid showed the

highest MICs value of 17, 28, and 56 µg/ml against *Mycobacterium madagascariense*, standard *Mycobacterium tuberculosis* strain $H_{37}RV$, and rifampicin resistant *M. tuberculosis* clinical isolates, respectively.[67]

Figure 2: *Myrica salicifolia* leaves (a) and barks (b) (By Dr. Mekonnen Abebayehu, July 2020, Debresina, Northern Shewa, Amhara region, Ethiopia).

It has been linked to antimalarial[59], antiplasmodial[68], strong analgesic effect[69], and lowering blood glucose effects.[70] Recently, Rehman and coworkers reported that the root extract of *M. salicifolia* inhibited the activation of tumor necrosis factor-alpha (TNF-alpha) and interleukin-6 (IL-6) in the colonic tissues of the ulcerative colitis model in rats.[71] Earlier studies focused on the evaluation of the antimicrobial and antimalarial activities of this plant. This led to the identification and isolation of the diarylheptanoids derivatives as the potential active constituents against *anti-Helicobacter pylori* activity[31] and ellagic acid derivatives active against all *Plasmodium falciparum* strains.[72] A preliminary phytochemical analysis of the methanolic extracts of the stem barks[58], roots[59], and leaves[73] revealed the presence of polyphenols, unsaturated, saponins, glycosides, sterols/triterpenes, alkaloids, tannins, flavonoids, protein, and carbohydrates. These constituents possess a wide range of biological activities including anti-inflammatory, antibacterial, antioxidant, and cytotoxic activities.[74] Different compound classes, such as seventeen cyclic diarylheptanoids, eight proanthocyanidins, three methylated ellagic acid glycosides, one ellagitannin, and two more were isolated from *M. salicifolia* (Figure 3 and Table 1).[67, 75-76]

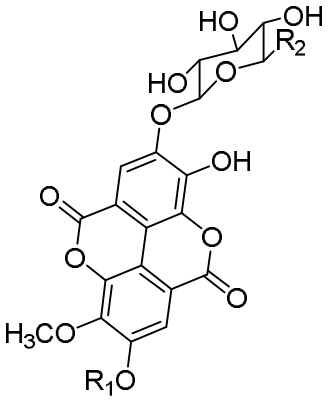

	R_1	R_2
9: myriside	CH_3	H
10: lagertannin	CH_3	CH_2OH
11: ducheside A	H	H

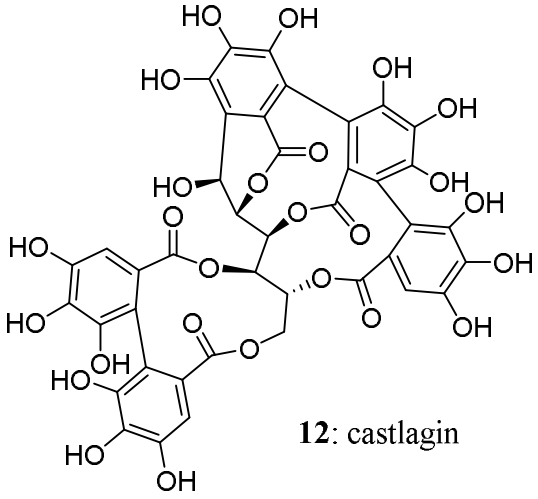

12: castlagin

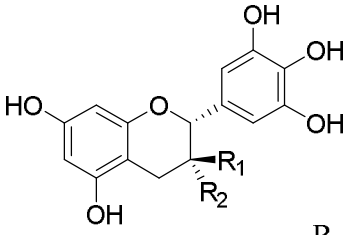

	R_1	R_2
13: gallocatechin	H	OH
14: epigallocatechin-3-*O*-gallate	galloyl	H

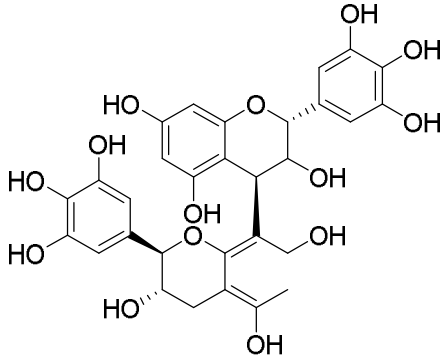

15: prodelphinidin B1

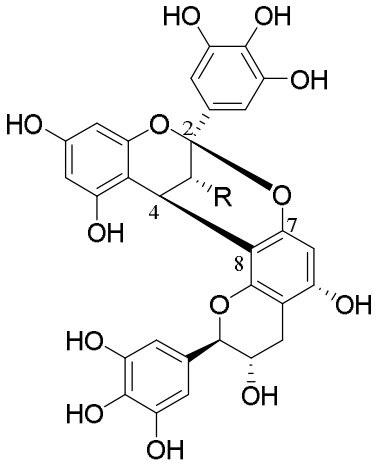

16: epigallocatechin-3-*O*-gallate-(2$\beta\rightarrow$*O*$\rightarrow$7,4$\beta\rightarrow$8)-gallocatechin, R=galloyl

17: ephedrannin D5, R=OH

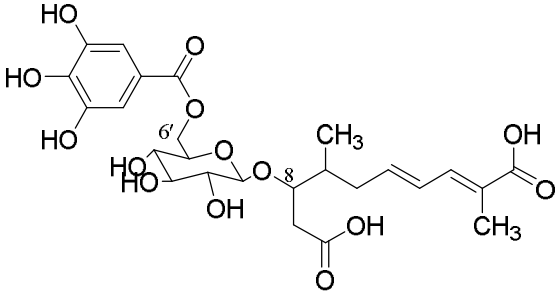

18: 2,7-dimethyl-8-*O*-(6′-*O*-galloyl)-β-D-glucopyranoside-deca-2*E*,4*E*- dienedioic acid

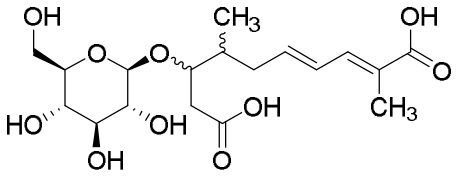

19: 2,7-dimethyl-8-*O*-*β*-D glucopyranoside-deca-2*E*,4*E*-dienedioic acid

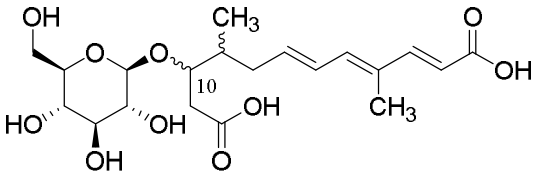

20: 4,9-dimethyl-10-*O*-*β*-D glucopyranoside-do deca-2*E*,4*E*,6*E*-trienedioic acid

Figure 3: Structures of some selected compounds isolated from *Myrica salicifolia.*

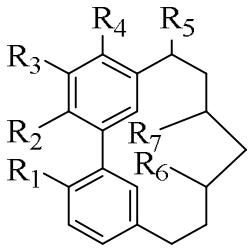

Table 1: Some of cyclic diarylheptanoids isolated from *Myrica salicifolia*.

Cds No	Name of compounds	R_1	R_2	R_3	R_4	R_5	R_6	R_7
21	salicimeckol	OH	OCH_3	OCH_3	*β*-D-glucopyranoside	OH	OH	H
22	juglanin B	OH	*β*-D-glucopyranoside	OCH_3	H	H	OH	H
23	salicireneol B	OH	*β*-D-glucopyranoside	OH	OCH_3	H	OH	H
24	saliciclaireone A	OH	OCH_3	OCH_3	*β*-D-glucopyranosyl-(1→6)-*β*-D-glucopyranoside	H	=O	H
25	saliciclaireone B	OH	OCH_3	OCH_3	*β*-D-glucopyranosyl-(1→6)-*β*-D-glucopyranoside	H	H	=O

26	myricanone 17- α-l-arabinofuranosyl-(1→6)-*β*-D-glucopyranoside	α-L-arabino-furanosyl-(1→6)-*β*-D-glucopyranoside	OH	OCH_3	OCH_3	H	=O	H
27	juglanin B 11-sulfate	OH	OH	OCH_3	H	H	OSO_3H	H
28	myricanone	OH	OCH_3	OCH_3	OH	H	=O	H
29	myricanol	OH	OCH_3	OCH_3	OH	H	OH	H
30	myricanol 5-*O*-*β*-D-glucopyranoside	OH	OCH_3	OCH_3	*β*-D-glucopyranoside	H	OH	H
31	myricanone 5-*O*-*β*-D-glucopyranoside	OH	OCH_3	OCH_3	*β*-D-glucopyranoside	H	=O	H
32	myricanol 11-*O*-*β*-D-xylopyranoside	OH	OCH_3	OCH_3	OH	H	*β*-D-xylopyranoside	H
33	myricanol 5-*O*-*β*-D-(6′-*O*-galloyl)-glucopyranoside	OH	OCH_3	OCH_3	*β*-D-(6′-*O*-galloyl)-glucopyranoside	H	OH	H
34	myricanone 5-*O*-*β*-D-(6′-*O*-galloyl)-glucopyranoside	OH	OCH_3	OCH_3	*β*-D-(6′-*O*-galloyl)-glucopyranoside	H	=O	H
35	myricanol 5-*O*-α-l-arabinofuranosyl-(1→6)-*β*-D-glucopyranoside	OH	OCH_3	OCH_3	α-L-arabino-furanosyl-	H	OH	H

36	myricanol 5-*O*-*β*-D-glucopranosyl-(1→6)-*β*-D-glucopyranoside	OH	OCH_3	OCH_3	(1→6)-*β*-D-glucopyranoside *β*-D-glucopyranosyl-(1→6)-*β*-D-glucopyranoside	H	OH	H

2.2 Phytochemistry and Biological activites of *Clematis simensis*

The *Ranunculaceae* is a large family comprising 60 genera and 2,200 species widely distributed worldwide, mainly in the temperate regions of the northern hemisphere. It consists of herbs such as small shrubs and woody vines.[77] The genus *Clematis* is a large genus within dicotyledons. Globally, about 300 species are known. Many *Clematis* species are found throughout the northern hemisphere and are widely utilized as traditional medicines worldwide.[78] The aerial parts of different species of *Clematis* are used as diuretics, antidotes for snake bites, antimalarials, antidysentery, and to treat rheumatic pain, fever, gout, eye infections, bone diseases, gonorrheal symptoms, chronic skin disorders, and varicosity in Europe, Eastern Asia, Africa, and India.[79-83] *Clematis* species have a broad range of constituents such as polyphenols, alkaloids, flavonoids, coumarins, triterpenes, volatile oils, lignans, steroids, macrocyclic compounds, organic acids, etc. A review of the literature, different classes and more than 250 compounds were isolated from *Clematis* species[79] and some are shown in Figure **4**. These constituents possess a wide range of biological activities that includ anti-inflammatory, anticancer, antioxidant, antipyretic activity, and analgesic, antiangiogenic, antigonorrhoeal, arthritis, apoptosis, antimicrobial, cartilage protective, diuretic, hypotensive, hepatoprotective, and HIV-1 protease inhibitors activitie.[79, 84-87]

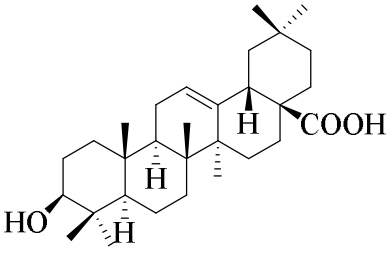

37: hederagenic acid

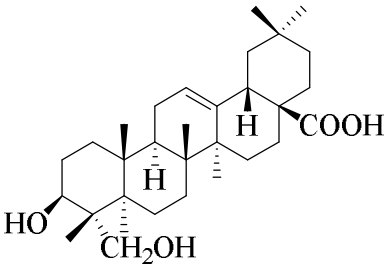

38: oleanolic acid

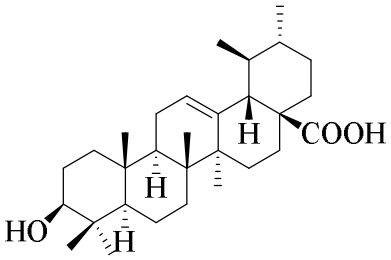

39: clematibetoside B

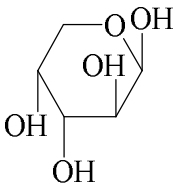

40: α-L-arabinopyranosyl

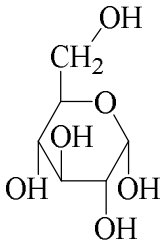

41: β-D-glucopyranosyl

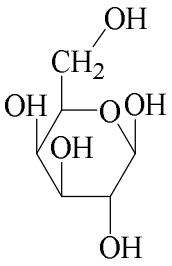

42: β-D-galactopyranosyl

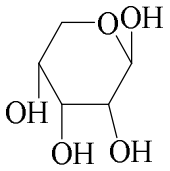

43: β-D-ribopyranosyl

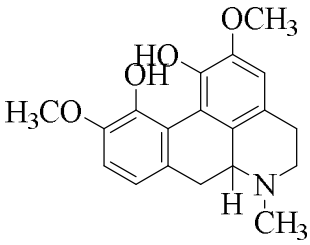

44: corytuberine

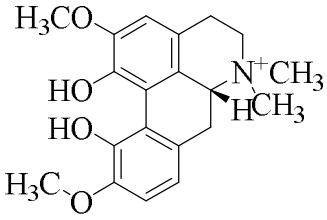

45*:* β-magnoflorine

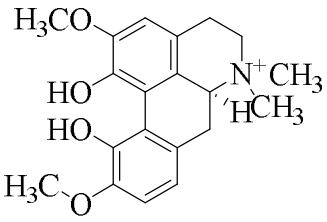

46: *α*-magnoflorine

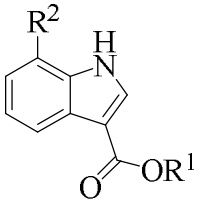

47: me-7-methoxy-3-indolecarbonate

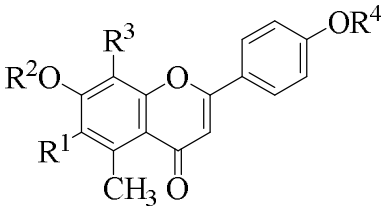

	R^1	R^2	R^3	R^4
48: linarin	H	Rha(1 → 6)-Glc	H	Me
49: apigenin	H	H	H	H

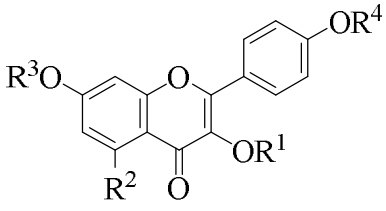

	R^1	R^2	R^3	R^4
50: 4',7-dimethoxykaempferol	H	OH	Me	Me
51: isokaempferide	Me	OH	H	H
52: kaempferol	H	OH	H	H

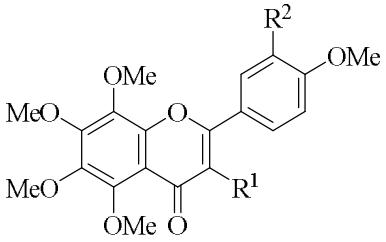

	R^1	R^2
53: 3,4,6,7,8,3′,4′-heptamethoxyflavone	OMe	OMe
54: nobiletin	H	OMe
55: tangeritin	H	H

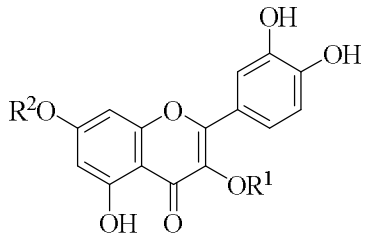

	R^1	R^2
56: quercetin	H	H
57: isoquercetin	Glc	H
58: rutin	Rha(1→6)-Glc	H

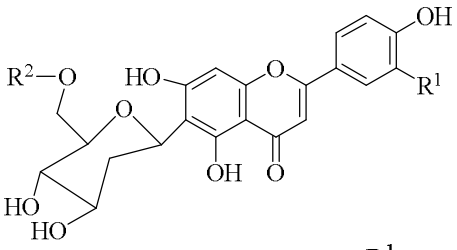

	R^1	R^2
59: isovitexin-6-*O*-*E*-*p*-coumarate	H	*E*-*p*-coumaroyl
60: isoorientin	OH	H

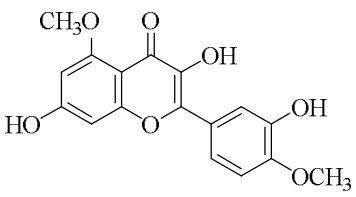

61: 3,3',7-trihydroxy-4',5-dimethoxy flavones

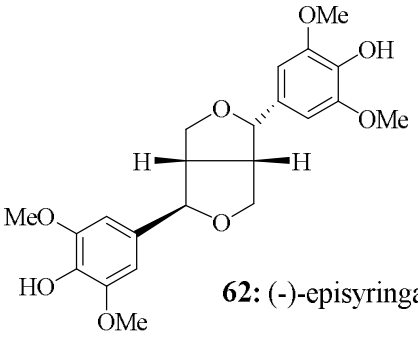

62: (-)-episyringaresinol

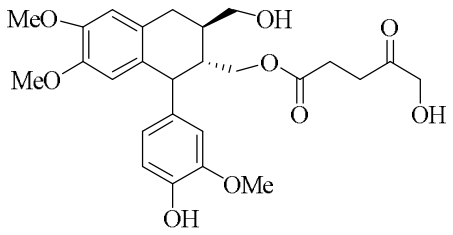

66: (+)-clemomanshurinane A

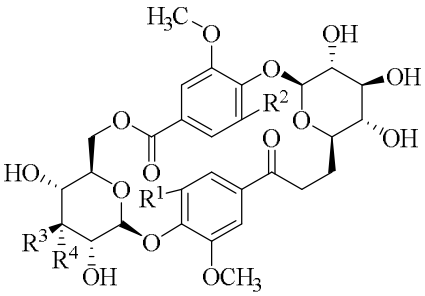

	R^1	R^2	R^3	R^4
63: clemahexapetoside A	OCH_3	H	H	OH
64: clemahexapetoside B	H	H	H	OH
65: clemochinenoside A	OCH_3	OCH_3	OH	H

Figure 4: Structures of compounds isolated from genus *Clematis*.

Clematis simensis (Figure 5, synonyms: *Clematis orientalis, Clematis altissima Hutch, Clematis kissenyensis, Clematis orientalis*) is a tall, climbing shrubby plant that can grow up to 20 m, often behaving as a strong liane; younger stems are more or less hairy; leaves are unequally pinnate with five leaflets; flower buds ellipsoid.[88] The genus *Clematis* L. is widely spread in the northern hemisphere.[89] It is native and distributed in Eritrea, Ethiopia, Sudan, Malawi, Zimbabwe, Mozambique, Cameroon, Republic of the Congo, and Angola.[88]

Locally it is known as 'Fiide′ in Sidama[90], 'azo-hareg′[91] and 'Enderifa′[92] in Amaharic, and Feetii/Hidda[93] in Afaan oromo. The leaves of this plant are traditionally used in Ethiopia to treat tinea capitis, dermatitis, tropical ulcers, and wounds. The seeds of this plant are also used to alleviate rheumatic pain, and the sap is used to treat animal bloat and as a febrifuge.[94] The stem barks of *C. simensis* is used for the treatment of toothache and cancer.[95] According to a recent study, the leaves of *C. simensis* have been used in combination with another plant belonging to the same family.[96-97]

Solvent extracts of the plant showed different biological activities. The aqueous and methanol extracts of *C. simensis* leaves showed inhibition against bacteria including *Staphylococcus aureus*, *Pseudomonas aeruginosa*, and *fungus Candida albicans.*[32, 98] Methanol and acetone extracts of *C. simenses* exhibited anti-inflammatory and antinociceptive activity at doses of 400 mg/kg and 800 mg/kg, respectively.[99] Recently, Birhan and coworkers reported that an 80% methanol extract displayed that *Staphylococcus aureus* was the most susceptible bacteria, followed by *Pseudomonas aeruginosae.*[95] The chloroform fraction of *C. simensis* was cytotoxic against breast cancer cell lines (JIMT-1, MCF-7, and HCC1937).[100]

A preliminary phytochemical screening of the extracts of the stem barks[101], roots[102], and leaves[103] revealed the presence of polyphenols, alkaloids, steroids, terpenoids, tannins, and flavonoids. However, there is no previously report on phytochemical investigation secondary metabolites of this plant.

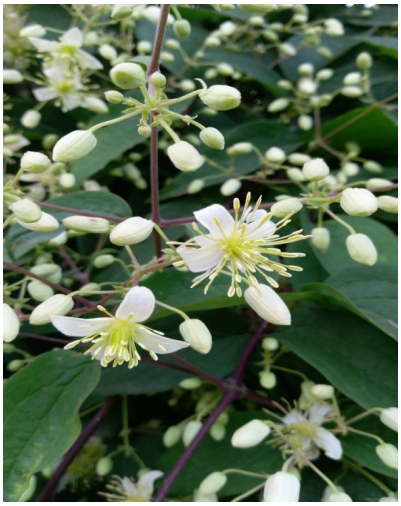

Figure 5: *Clematis simensis* (By Dr. Mekonnen Abebayehu, June 2019, Debresina, Northern Shewa, Amhara region, Ethiopia).

2.3 Phytochemistry and Biological activites of *Olinia usambarensis*

The Oliniaceae is a small family comprises one genus (*Olinia*) and 8-10 species. They are trees and shrubs widely distributed in the montane and coastal forests of eastern and Southern Africa, and also on the island of St. Helena.[104] *Olinia usambarensis* is also called *Olinia rochetiana* and belongs to the family Oliniaceae. Decoctions of the roots are drunk to cure fever. A bark decoction is ingested for rheumatism, bronchitis, dyspepsia, and to induce tapeworm emission.[105]

Olinia usambarensis is a shrub, small tree or less often a large tree, evergreen and frost resistant, usually 1.2-16 meters tall, but occasionally reach 27 meters and endemic to some Eastern and southern African countries.[33, 106] It is distinguished by branchlets and quadrangular branches, flowers organized in triads, and an inflorescence placement is axillary and/or terminal.[88]

In Ethiopia, the barks and leaves of *O.usambarensis* (Figure 6, locally known as “Tife” in Amharic and Guna in Hadiyyisa) are used traditionally to treat toothache, scabies, acne, and eczema.[107-109] In Tanzania and Kenya, Ogiek community uses the barks as well as leaves remedy for colds, protects against pneumonia, other chest-related ailments and chewing as mouth freshener.[110]

Figure 6: *Olinia usambarensis* (By Dr. Mekonnen Abebayehu, February 2022, Debresina, Amhara region, Ethiopia).

The plant has wormicidal and antimicrobial activities. These include antibacterial and antifungal effects of *O. rochetiana* used in the management of urinary tract infections and oral candidiasis.[111] It is also used to cure menstrual pain and intestinal worms.[105] Barks or roots are pounded, water added and the resulting paste applied on swellings such as those on the throat and other tumors. Additionally, it has been reported that this plant's inner bark is combined with those of *Brucea spp*. and *Myrica salicifolia*, and consumed in a meat soup as a remedy for treatment of measles, cough, and abscess. The juice of its roots is also claimed to be used for malaria treatment.[112]

The ethanol (leaves and stem-barks) extracts of *O. rochetiana* showed very good inhibit against the growth of bacterial strains (*Escherichia coli, Pseudomonas aeruginosa, Salmonella Typhi* and *Staphylococcus aureus)* at a concentration of 250 mg/mL.[33] Caffeoyloxy-5,6-dihydro-4-methyl-(2H)-pyran-2-one (**67**) is considered to be the most active compound from *O. usambarensis* leaves, reported as a good candidate as an anti-inflammatory agent.[113] A preliminary phytochemical screening of the ethanol extracts of the leaves revealed the presence of phenols, tannin, glycosides, steroids, terpenoids, and saponin whereas, chloroform crude extract showed presence of tannin, terpenoid and

glycoside. On the other hand, ethanol extract of stem-barks showed presence of tannin, phenol, terpenoid and steroid.[33] These constituents possess a wide range of biological activities including antifeedant activity[114], anticancer[113], antifungal and antibacterial.[111] Some compounds were isolated from the root barks and leaves of *O. rochetiana* (Figure 7).[114-115]

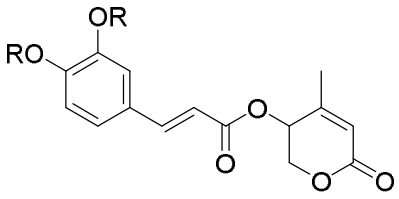

	R
67: caffeoyloxy-5,6-dihydro-4-methyl-(2H)-pyran-2-one	H
68: 4-methyl-6-oxo-3,6-dihydro-2H-pyran-3-yl (*E*)-3-(3,4-bis(carboxyoxy)phenyl)acrylate	Ac

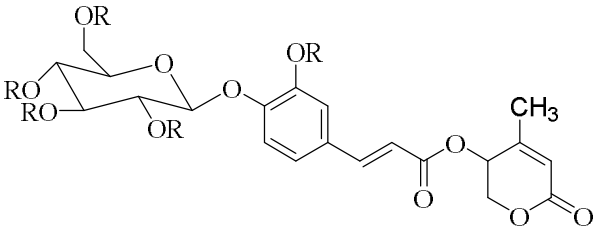

	R
69: olinioside	H
70: pentaacetyl olinioside	Ac

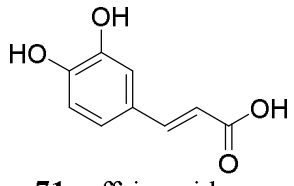

71:caffeic acid

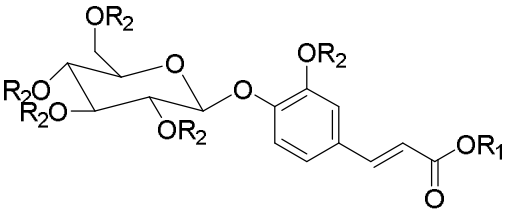

	R_1	R_2
72: 4-*O*-β-D-glucopyranosylcaffeic acid	H	H
73: pentaacetyl-4-*O*-β-D-glucopyranosylcaffeic acid	H	Ac
74: methyl pentaacetyl-4-*O*-β-D glucopyranosylcaffeate	Me	Ac

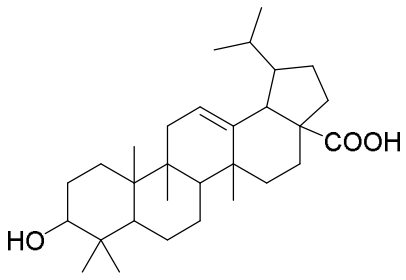

75: 3-hydroxylup-12-en-28-oic acid

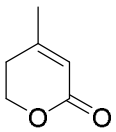

76: mevalonolactone

Figure 7: Structures of compounds isolated from *Olinia usambarensis.*

3 Results and Discussion

The leaves, roots, and barks of *Myrica salicifolia,* aerial parts of *Clematis simensis,* and barks of *Olinia usambarensis*, belonging to the Myricaceae, Ranunculaceae, and Oliniaceae family, respectively, were studied for their chemical compositions. The methanol-chloroform extracts from these three species were subjected to extensive chromatography separation such as column chromatography and preparative thin layer chromatography to yield twenty-four pure compounds.

Eighteen compounds were isolated from the leaves, roots, and barks extract of *Myrica salicifolia*, namely diarylheptanoids, triterpenoids, and alphatic derivatives. The four isolated diarylheptanoids were myricanone (**28**), myricanol (**29**), myricanol-11-*O*-β-D-xylopyranoside (**32**), and myricanol 5-*O*-β-D-glucopyranoside (**30**). One cerebroside (contortamide (**29**)) and one pyranoside (methyl-β-D-glucopyranoside (**85**)) were isolated**.** Seven terpenoid derivatives, namely squalene (**77**), β-carotene (**78),** taraxerone (**81**), taraxerol (**82**), myricadiol (**83**), β-sitosterol (**80**), and sitoindoside I (**87**), were also isolated from this plant. Of the compounds elucidated, 3β-O-*trans*-caffeoylisomyricadiol (**84**) was found to be a new compound that isolated for the first time in this work. Additonaliy, a chlorin compound, namely a pheophytin A (**79**), was isolated. The chemical study of *Clematis simensis* yielded three compounds, namely 2-deoxy-D-ribono-1,4-lactone (**88**), 5-hydroxylevulinic acid (**89**), and β-sitosterol-3-*O*-β-D-glucoside (**90**). Three compounds, namely lupeol (**91**), n-pentacosyl *trans*-ferulate (**92**), and 4-*O*-β-D-glucopyranosylcaffeic acid (**72)**, were successfully isolated and characterized from the chloroform-methanol extract of *Olinia usambarensis* barks. The structural elucidations of those isolated compounds were conducted using spectroscopic methods. Complete ^{1}H, ^{13}C, DEPT-NMR, HSQC and HMBC spectral data are given for compounds and also comparison was made with the literature data for known compounds.

3.1 Phytochemical Investigation of the Leaves of *Myrica salicifolia*

The leaves, barks and roots of *M. salicifolia* were collected from Debresina, Northern Shewa, Amhara region, 192 km from Addis Ababa, Ethiopia, in July 2020 by Dr.

Mekonnen Abebayehu. The plant specimens were identified by Mr. Melaku Wendafrash, Addis Ababa University, Ethiopia. A voucher specimen of the plant material has been deposited in the National Herbarium, Addis Ababa University, with a voucher/specimen number of MA/2007/12. Phytochemical analysis of the leaves extract of *M. salicifolia* resulted in the isolation of four compounds, namely, squalene (**77**), β-carotene (**78**), pheophytin a (**79**), and β-sitosterol (**80**). The phytochemical studies of the leaves of this plant have never been reported before. The phytochemical investigation on the leaves of *M. salicifolia* is discussed in the following sections.

3.1.1 Characterization of Essential Oil of the Leaves of *Myrica salicifolia*

The essential oil from the *M. salicifolia* leaves samples were extracted by hydrodistillation following the method described by Katekar.[116] Plant material (520 g) was hydrodistilled to afford clear colorless oil (0.4 mL). The essential oil was then analyzed by gas chromatography-mass spectroscopy (GC-MS). The GC-MS analysis of the essential oil of the fresh leaves of *M. salicifolia* revealed the presence of 21 major compounds (Figure 8 and Table 2) after comparing the data with NIST-14 mass spectral database, with qualities greater than 80%. The analyzed essential oil was composed of different compounds of different classes: fatty acid, aromatic phenols, aliphatic alcohols, hydrocarbons, and terpenes. The major volatile compounds were *trans*-3-hexen-1-ol (52.62%), terpineol (7.93%), benzaldehyde (6.28%), *p*-cymen-8-ol (3.99%) and terpinen-4-ol (3.60%). Scientific reports revealed that some of the identified compounds have a considerable potential for therapeutic use. For example, *trans*-3-hexen-1-ol is the major volatile organic compound that has antifungal activity[117], flavor and fragrance application[119], It is also used as an organic chemical synthesis intermediate[120] and stimulates the antennae of male *Hyphantria cunea* moths.[120] The second major compound**,** α-terpineol has a wide range of biological applications as an antioxidant, anticancer, anticonvulsant, antiulcer, antihypertensive, anti-nociceptive.[121] Benzaldehyde, the third major component of the essential oil has insecticidal, antimicrobial, and antioxidant activities.[122]

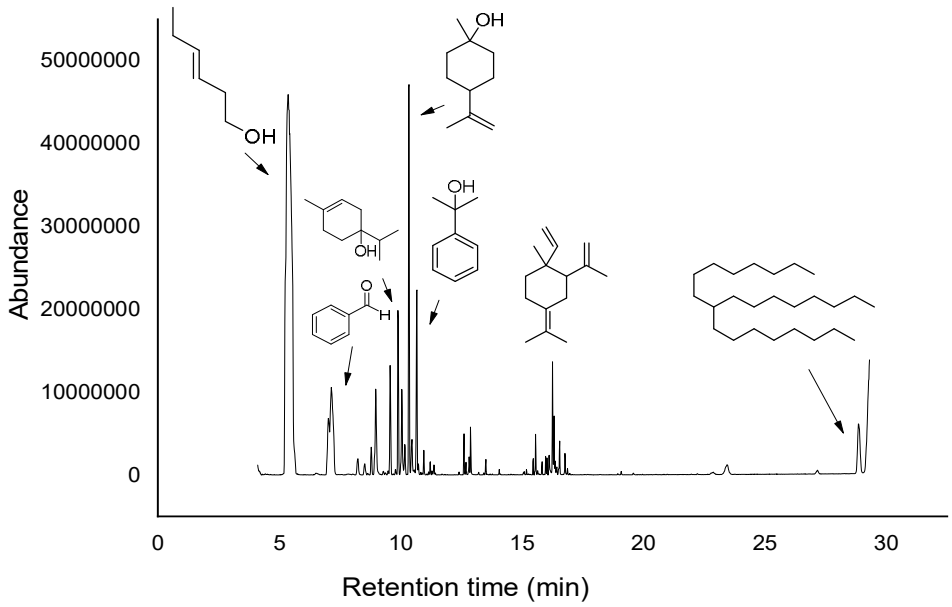

Figure 8: GC-MS chromatogram of the essential oil of leaves of *Myrica salicifolia*.

Table 2: Compounds identified from the essential oil of the leaves of *Myrica salicifolia* by GC-MS

PK	RT	Area Pct	Compound names		Q	CF
1	5.37	52.62	*trans*-3-hexen-1-ol	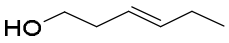	91	$C_6H_{12}O$
2	7.03	2.55	Eucalyptol	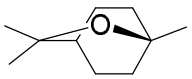	86	$C_{10}H_{18}O$
3	7.14	6.28	Benzaldehyde	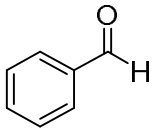	95	C_7H_6O
4	8.24	0.59	*m*-Methylisopropylbenzene	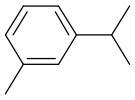	89	$C_{10}H_{14}$
5	8.79	0.63	Linalool	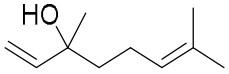	80	$C_{10}H_{18}O$
6	8.97	2.87	Benzyl alcohol	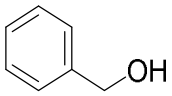	95	C_7H_8O
7	9.57	2.63	(+)-Sabinol	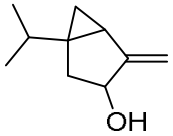	81	$C_{10}H_{16}O$
8	9.89	3.60	Terpinen-4-ol	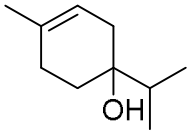	94	$C_{10}H_{18}O$
9	10.05	2.36	Carveol	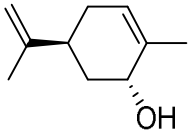	76	$C_{10}H_{16}O$
10	10.17	1.02	(+)-Borneol	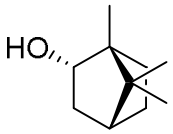	91	$C_{10}H_{18}O$
11	10.34	7.93	Terpineol	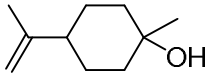	91	$C1_8H_{18}O$

12	10.46	1.50	Methyl salicylate	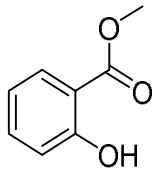	96	$C_8H_8O_3$
13	10.66	3.99	*p*-Cymen-8-ol	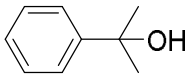	81	$C_{10}H_{14}O$
14	10.73	0.53	Methyl phenethyl ether	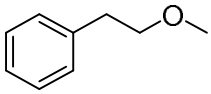	62	$C_{10}H_{12}O$
15	11.21	0.22	*cis*-*p*-Mentha-1(7),8-dien-2-ol	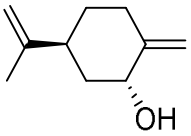	93	$C_{10}H_{16}O$
16	12.61	0.50	Thymol	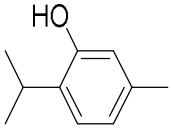	94	$C_{10}H_{14}O$
17	12.88	0.69	3-Methyl-4-isopropylphenol	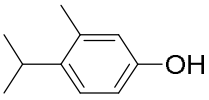	94	$C_{10}H_{14}O$
18	15.45	0.21	(+)-Spathulenol	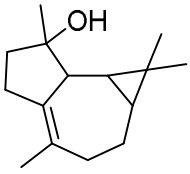	58	$C_{15}H_{24}O$
19	15.55	0.57	2-Hexadecen-5-olide	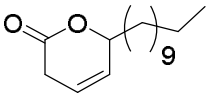	59	$C_{16}H_{28}O_2$
20	16.02	0.21	Tau-Muurolol	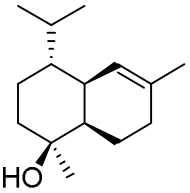	70	$C_{15}H_{26}O$
21	16.11	0.45	(-)-Cedreanol	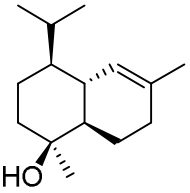	81	$C_{15}H_{26}O$
22	16.25	1.59	Elixene	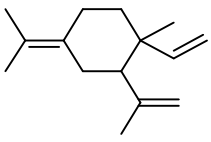	87	$C_{15}H_{24}$

23	16.31	1.14	α-Caryophylladienol	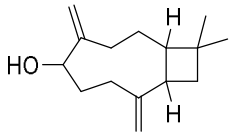	91	$C_{15}H_{24}O$
24	16.55	0.60	(1*R*,7*S*,*E*)-7-Isopropyl-4,10-dimethylenecyclodec-5-enol	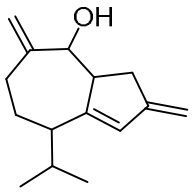	77	$C_{13}H_{20}O_2$
25	28.85	2.95	9-Octylheptadecane	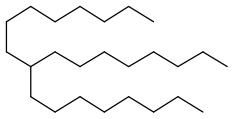	86	$C_{25}H_{52}$

Pk = peak number, Rt = retention time (min), Area Pct. = area percentage, Q = quality

3.1.2 Characterization of Compounds Isolated from the Leaves Extract of *Myrica salicifolia*

3.1.2.1 Characterization of Compound 77

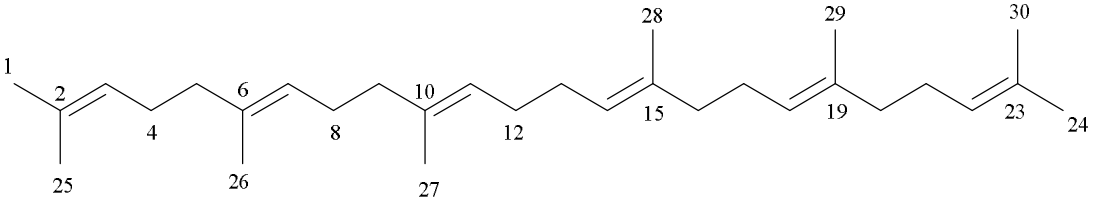

77

Compound **77** was isolated as colourless oil. The compound gave a dark blue spots on TLC with cerium ammonium molybdate spraying with the R_f value of 0.80 in Cy (100%). Its molecular formula was deduced to be $C_{30}H_{50}$ from TOF-ESI-MS (Appendix 7) showed a fragment ion peak $[M+H+CO-41]^+$ at *m/z* 398.2412 corresponds to a fragment, C_3H_5, of the proposed compound **77**. The ^{13}C-NMR spectrum showed 15 carbon resonances signals indicating 30 carbons suggesting that the molecule was symmetrical. ^{1}H-NMR (Table 3 and Appendix 1) showed signals at δ_H 1.60 (*s*, 18H) and δ_H 1.68 (*s*, 6H) for eight methyl groups attached to olefinic bond, two overlapping multiplets at δ_H 2.02 (H-12/13) and δ_H 2.07 (4/21, 8/17) for ten methylene protons each and a broad multiplet signal at δ_H 5.10-5.11 for six olefinic protons. The ^{13}C-NMR (Appendix 2 and Table 3) and DEPT-NMR

spectrum (Appendix 3 and Table 3) of compound **77** revealed 15 carbon signals at δ_C 135.1, 134.9 and 131.2, belonging to quaternary carbons, at δ_C 124.4, 124.3, and 124.3 for methine carbons, at δ_C 39.8, 39.8, 28.3, 26.8, and 26.7 for methylene carbons and at δ_C 25.7, 17.7, 16.1, and 16.0 for methyl groups. ^{13}C-NMR spectrum showed carbon signals at δ_C 25.7, 26.7, 26.8, 39.8, 124.3, 124.4, 131.2, and 134.9 resemble the reported values of farnesene.[123] A long COSY spectrum revealed (Appendix 4) the methylene proton signals at δ_H 1.98 (*m*, H-5, 9, 16, 20) correlated with the methylene proton signals at δ_H 2.07 (H-4, 8, 17, 20), indicating a head to tail attachments of the isoprene units. It also showed olefinic methine proton signals at δ_H 5.10-5.1 were correlated with methylene proton at δ_H 2.07. In HMBC spectrum (Appendix 6), a singlet methyl signal at δ_H 1.60 (H-25/30, 26/29, 27/28) correlated with a quaternary carbon signals at δ_C 135.1 (C-2/23), 134.9 (C-6/19), and methine carbon signals at δ_C 124.3 (C-3/22, 7/18, 11/14) indicated that a methyl was attached to the quaternary carbon (C-2/23). The correlation of a methyl signal at δ_H 1.68 (H-1/24) with a quaternary carbon signals at δ_C 131.25 (C-2/23), and a methine carbon signal at δ_C 124.3 (C-3/22) revealed that a methyl group was attached to a quaternary carbon (C-2/23). The fusion of one isoprene unit to the second unit in a squalene is head-to-tail and tail-to-tail.[124] The tail-to-tail linkage is supported by the chemical shift of C-12/13 at δ_C 28.3 which shows it is located adjacent to an olefinic methin at C-11/14, and not to a methyl group at this position in head-to-tail linkage, it is observed that the chemical shift of the head of an isoprene which is adjacent to the methyl at δ_C 39.8 (C-5/20) and δ_C 39.8 (C- 9/16) were attached to upfield shift carbon of the tail of an isoprene at δ_C 25.7 (1/24), δ_C 26.8 (4/21), δ_C 26.7 (8/17) and δ_C 28.3 (12/13).[125] On the basis of above assignments and the literature[126-127] reported the structure of this sesquiterpene hydrocarbon was established as (*E*)-2,6,10,15,19,23-hexamethyl-2,6,10,14,18,22-tetracosahexaene and was designated as squalene.

Table 3: ^{1}H-and ^{13}C-NMR data for compound **77**

Position	**77** ^{1}H-NMR (400 MHz, $CDCl_3$) ^{13}C-NMR (101 MHz, $CDCl_3$)		**Lit.**[126-127] ^{1}H-NMR (300 MHz, $CDCl_3$) ^{13}C-NMR (75 MHz, $CDCl_3$)	
	δc	δH	δc	δH
1/24	25.7	1.68 (*s*, 6H)	25.7	1.68 (*s*)
2/23	131.2	-	131.2	-
3/22	124.3	5.14 (*d*, *J* = 6.2 Hz, 1H)	124.2	5.11(*t*)
4/21	26.8	2.07 (*m*, 2H)	26.8	2.07 (*m*)
5/20	39.8	1.98 (*m*, 2H)	39.8	1.98 (*m*)
6/19	134.9	-	134.8	-
7/18	124.4	5.10 (*m*, 1H)	124.4	5.11(*m*)
8/17	26.7	2.07 (*m*, 2H)	26.6	2.07 (*m*)
9/16	39.8	1.98 (*m*, 2H)	39.7	1.98 (*m*)
10/15	135.1	-	135.0	-
11/14	124.3	5.10 (*m*, 1H)	124.3	5.11(*m*)
12/13	28.3	2.02 (*d*, *J* = 6.8 Hz, 2H)	28.3	2.01 (*dd, J,* 6.8*,* 3.3)
25/30	17.7	1.60 (*s*, 6H)	17.6	1.60 (*s*)
26/29	16.0	1.60 (*s*, 6H)	16.0	1.60 (*s*)
27/28	16.1	1.60 (*s*, 6H)	16.0	1.60 (*s*)

3.1.2.2 Characterization of Compound 78

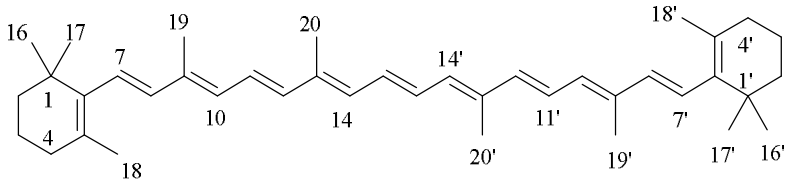

78

Compound **78** was isolated as a red powder with a melting point of 177-178 °C. The compound gave a dark blue spots on TLC with cerium ammonium molybdate spraying with the R_f value of 0.39 in Cy (100%). Colour of the compound indicates a highly conjugated system characteristic of a carotenoid.[128] The IR spectrum revealed the presence of double bond CH stretching at 2923.56 cm^{-1}, and aliphatic C-H stretching at 2854.13 cm^{-1}, and aliphatic C = C stretching at 1640.8 cm^{-1}. The positive ion TOF-ESI-MS of **78** (Appendix 15) showed a fragment ion peak $[M-332.769+H]^+$ at *m/z* 203.1051 corresponds to a known fragment, $C_{15}H_{22}$, of the proposed compound **78**.[129]

Table 4: ^{1}H- and ^{13}C-NMR data for compound **78**

Position	**78** ^{1}H-NMR (400 MHz, $CDCl_3$) ^{13}C-NMR (101 MHz, $CDCl_3$)		**Lit.**[133] ^{1}H-NMR (400 MHz, $CDCl_3$) ^{13}C-NMR (100 MHz, $CDCl_3$)	
	δc	δ_H	δc	δ_H
1, 1′	34.2	-	34.3	-
2, 2′	39.6	1.45 (*dd*, *J* = 16.0, 5.7 Hz, 4H)	39.7	1.46 (*dd*, *J* = 3.6, 6.0 Hz, 4H)
3, 3′	19.3	1.62 *(m*, 4H)	19.3	1.6 (4H)
4, 4′	33.1	2.03 (*d*, *J* = 6.4 Hz, 4H)	33.1	2.02 (*t*, *J* = 6.4 Hz, 4H)
5, 5′	129.4	-	129.4	-
6, 6′	137.9	-	137.9	-
7, 7′	126.7	6.16 (*m*, 2H)	126.7	6.18 (2H)
8, 8′	137.8	6.11 (*m*, 2H)	137.8	6.14 (2H)
9, 9′	136.0	-	136.0	-
10, 10′	132.4	6.25 (*m*, 1H);6.27 (*m*, 1H)	132.4	6.22;6.26 (2H)
11, 11′	129.9	6.17 (*d*, *J* = 7.0 Hz, 2H)	130.0	6.61 (2H)
12,12′	137.2	6.37 (*d*, *J* = 14.9 Hz, 2H)	137.2	6.35 (*d*, *J* = 14.8 Hz, 2H)
13, 13′	136.5	-	136.5	-
14, 14′	130.8	6.27 (*d*, *J* = 8.3 Hz, 2H)	130.9	6.12 (2H)
15, 15′	125.0	6.65 (*d*, *J* = 10.3 Hz, 2H)	125.0	6.65 (2H)
16, 16′	29.0	1.04 (*s*, 6H)	29.0	1.03 (s, 6H)
17, 17′	28.9	1.04 (*s*, 6H)	28.9	1.03 (s, 6H)
18, 18′	21.8;21.9	1.74 (*s*, 6H)	21.7;21.8	1.72;1.713 (s, 6H)
19, 19′	12.8	1.99 (*s,* 6H)	12.83	1.97 (s, 6H)
20, 20′	12.8	1.99 (*s*, 6H)	12.78	1.97 (s, 6H)

The ^{1}H-NMR spectrum (Table 4 and Appendix 8) of **78** showed the presence of fourteen olefinic methine proton signals in a conjugated system at δ_H 6.12 (*m*, 2H-8/ 8′), 6.16 (*m*, 2H-7/7′), 6.17 (*d*, *J* = 7.0 Hz, 3H-11/11′), 6.25 (*m*, 6H-10′), 6.27 (*m*, 1H-14/14′), 6.27 (*m*, 6H-10), 6.37 (*d*, *J* = 14.9 Hz, 1H-12/12′), and 6.65 (*d*, *J* = 10.3 Hz, 2H-15/15′) and ten methyl singlets protons at δ_H 1.04 (6H-16/16′), 1.04 (6H-17/17′), 1.74 (3H-18/18′), and 1.99 (6H-19/19′, 20/20′). ^{13}C-NMR (Appendix 9) and DEPT-135 spectral data (Table 4 and Appendix 10) showed resonances for twenty-one carbons which were attributed to seven olefinic methine carbons signals at δ_C 137.8 (C-8/8′), 137.2 (C-12/12′), 132.4 (C-10/10′), 130.8 (C-14/14′), 129.9 (C-11/11′), 126.7 (C-7/7′), and 125.0 (C-15/15′), a ten quaternary carbon signals δ_C 136.5 (C-13/13′), 136.0 (C-9/9′), 129.4 (C-5/5′), 34.2 (C-1/1′), and 29.0 (C-16/16′), three methylene carbons signals at δ_C 39.6 (C-2/2′), 33.11 (C-4/4′), and 19.3 (C-3/3′), and five methyl carbons signals δ_C 29.0 (C-16/16′), 28.9 (C-17/17′), 21.81/21.9 (C-18/18″), 12.8 (C-19/19′), and 12.8 (C-20/20′). Since many carotenoids are

symmetrical both in the aliphatic and olefinic regions, most of the carbon resonances are also overlapping.[130-131] The ^{1}H-^{1}H COSY spectrum (Appendix 11) of **78** showed correlations for four spin systems: H-2/H-3/H-4 and H-2'/H-3'/H-4', H-7/H-8 and H-7'/H-8', H-10/H-l1/H-12 and H-10'/H-11'/H-12', and H-14/H-15 and H-14'/H-15'. In the COSY spectrum, the methyl protons signals (H-19 and H-20) correlated with proton signals *trans* to the methyl group (H-10, and H-14), but not to protons in a single bonds *trans* position (H-8 and H-12) are the characteristics of carotenoids[132]. In HSQC spectra (Table 4 and Appendix 12), a methylene proton signal at δ_H 1.45 (*dd*, *J* = 16.0, 5.7 Hz, 4H) correlated with a carbon signal at δ_C 39.6 (C-2, 2′). The signal at δ_H 1.62 (*m*, 4H) correlated with carbon signal at δ_C 19.3 (C-3, 3′). A methylene proton signal at δ_H 2.03 (*d*, *J* = 6.4 Hz, 4H) correlated with a carbon signal at δ_C 33.1 (C-4, 4′), a proton signal at δ_H 6.16 (*m*, 2H) correlated with carbon signal at δ_C 126.7 (C-7, 7′), and a proton signal at δ_H 6.25 (*m*, 1H) and 6.27 (*m*, 1H) correlated with a carbon signal at δ_C 132.4 (C-10, 10′). A methine proton signal at δ_H 6.17 (*d*, *J* = 7.0 Hz, 2H) correlated with a carbon signal at δ_C 129.9 (C-11, 11′), a proton signal at δ_H 6.37 (*d*, *J* = 14.9 Hz, 2H) correlated with carbon signal at δ_C 137.2 (C-12,12′), a proton signal at δ_H 6.27 (*d*, *J* = 8.3 Hz, 2H) correlated with a carbon signal at δ_C 130.8 (C-14, 14′). The methine proton signal at δ_H 6.65 (*d*, *J* = 10.3 Hz, 2H) correlated with carbon signal at δ_C 125.0 (C-15, 15′). The HMBC spectrum of **78** showed correlations of H-16/17 with C-1, C-2 and C-6, indicated the two methyl groups of C-16/17 were attached to C-1. The methyl proton (H-19/19′) signal at δ_H 1.99 showed HMBC correlation with the quaternary carbon at δ_C 136.0 (C-9/9′) and the two methin protons at δ_C 137.8 (C-8/8′) and δ_C 132.4 (C-10/10). Similarly, HMBC spectrum (Appendix 13) showed correlations of the methyl proton signal of H-20/20′ at δ_H 1.99 with the quaternary carbon signal at δ_C 136.5 (C-13/13′) and the two methin carbon sinals at δ_C 137.2 (C-12/12′) and δ_C 130.8 (C-14/14′) which revealed that a methyl was attached to C-13. The relative stereochemistry of **78** was obtained from the NOESY spectrum (Appendix 14). Since there are no chiral centers in the structure of **78**, the NOESY spectrum was used to confirm the *trans* configuration of the olefinic protons located in the acyclic part of the molecule and also verified the assignments of the methyl groups in the cyclic system of the molecule. The following are the NOESY correlations that were observed: H-17/H-7/H-19/H-1l/H-20/H-15 were found on the same side of the molecule and H-18/H-8 were on the opposite side of the molecule. In summary, NMR

spectral data (Table 4) of compound **78** revealed a very close agreement with the reported literature data.[133] Therefore, compound **78** was identified as β-carotene.

3.1.2.3 Characterization of Compound 79

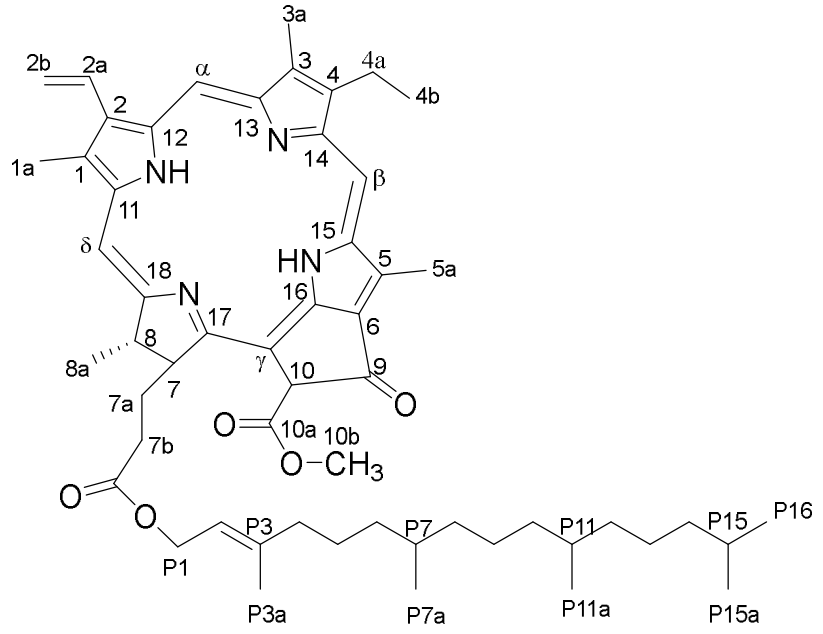

79

Compound **79** was isolated as a dark bluish waxy with a melting point of 115-117 °C. The compound gave a dark blue spots on TLC with cerium ammonium molybdate spraying with the R_f value of 0.53 in $CHCl_3$ (100%). The IR spectrum showed a broad band signal for N-H bond stretching at 3461.6 cm^{-1}, aliphatic C-H stretching at 2918.6 cm^{-1} and 2847 cm^{-1}, C=O stretching of ester at 1738 cm^{-1}, and a medium C=N stretching at 1644.6 cm^{-1}. ^{1}H-NMR spectrum (Table 5 and Appendix 16) of compound **79** showed the presence of eleven methyls, fourteen methylenes, and eleven methines. The three singlet signals at δ_H 9.54 (H-β), 9.39 (H-α) and 8.67 (H-δ) were indicative of the presence of the porphyrin unit of olefinic methine protons bridging the pyrrole ring. The methine assignments for methyl pheophorbide a are based on the considerations that the proton lies between a pyrrole and a pyrroline ring and should, therefore, be the most shielded methine proton and that the β methine proton, because of its proximity to the keto carbonyl group is more strongly

deshielded than the α proton.[134] Also, the three methyl signals at δ_H 3.72 (*s*, 3H-5a), 3.25 (*s*, 3H-3a) and 3.41 (*s*, 3H-1a) corresponds to substituents attached to the pyrrole ring of the porphyrin unit, these proton siganls are highly dishielded due the ring current effect.[134] The proton signals at δ_H 4.50 (*m*, 2H-P1) and δ_H 5.17 (*m*, 1H-P2) could be attributed to the oxymethylene protons of ester and olefinic methin of the phytyl group, respectively. The signals at δ_H 1.59 (*s*, 3H), 0.82 (*m,* 3H), 0.82 (*m,* 3H) and 0.83 (*m*, 3H) were assigned to the four methyl substituents at P3a, P7a, P11a, and P15a, respectively, for phytol group. The multiplet signals at δ_H 1.24 to 1.36 was assigned to the methylene protons of phytol group. The remaining signal at δ_H 1.92 could be attributed to methylene protons labeled to P4. The ^{13}C-NMR Spectrum (Table 5 and Appendix 17) showed 55 carbon signals which were attributed two carbonyl signals at δ_C 173.0 (C-7c) and 169.6 (C-10a), a cyclic ketone carbon signal at δ_c 189.7 (C-9), one oxymethylene carbon signal at δ_C 61.5 (C-P1), eleven methine carbons signal at δ_C 129.1 (C-2a), 97.5 (C-α), 104.5 (C-β), 64.7 (C-10), 51.7 (C-7), 50.2 (C-8), 93.4 (C-δ), 117.7 (C-P2), 32.6 (C-P7), 32.8 (C-P11), and 32.8 (C-P11) of which seven methine carbons were found in the pheophorbide moiety and four in the phytyl side chain of **79**. The four methylene carbon signals at δ_C 19.5 (C-4a), 31.2 (C-7a), 29.8 (C-7b) and 122.9 (C-2b) were in the pheophorbide moiety and ten methylene carbon signals at δ_C 61.5 (C-P1), 39.8 (C-P4), 25.0 (C-P5), 36.6(C-P6), 37.3(C-P8), 24.4(C-P9), 37.4 (C-P10), 37.3 (C-P12), 24.8 (C-P13), and 39.4 (C-P14) were in the phytyl side chain. The olefinic methine (=CH) carbon signals at δ_C 104.5 (C-β), 97.5 (C-α) and 93.4 (C-δ), and methine carbon signals at δ_C 51.9 (C-7) and 50.4 (C-8) are the characterstic of the presence of porphyrin moiety.[135] The oxymethylene carbon signals at δ_C 61.5 (C-P1) and olefinic carbon signal at δ_C 117.7 (C-P2) were in the phytyl group moiety. HSQC spectrum (Table 5 and Appendix 19) showed singlet methine proton signal at δ_H 9.54, 9.39, and 8.67 correlated with the carbon signals at δ_C 104.5 (C-β), 97.5 (C-α), and 93.4 (C-δ) in porphyrin unit, respectively, the three singlet methyl proton signals at δ_H 3.7, 3.4, and 3.2 correlated with the carbon signals at δ_C 12.1 (C-5a), 12.2 (C-1a), and 11.3 (C-3a) in pyrrole ring, respectively, a methylene proton at δ_H 6.2 and 6.3 correlated with C-2b at δc 122.9, a methine proton at δ_C 8.0 correlated with C-2a at δ_C 129.1, a methoxy proton at δ_H 3.50 correlated with C-10b at δ_C 52.9 indicated a methoxy group was attached to carbonyl carbon. Based on HMBC Spectrum (Table 5 and Appendix 20), the triplet signal at δ_H 8.05

(H-2a) showed a strong correlation with the olefinic methylene carbon signal at δ_C 122.9 (C-2b) and 136.3 (C-2). In comparison, the doublet signal at δ_H 6.29 ($1H_2$-2b) and 6.18 (H-2b) showed a correlation to the olefinic methine carbon signal at δc 129.1 (C-2a), indicating the vinyl group (-CH=CH_2) was attached to C-2. The methyl proton signal at δ_H 1.70 (H-4b) showed a correlation with the methylene carbon signal at δ_C 19.5 (C-4a) and 145.2 (C-4) indicating the ethyl group was attached to C-4. The methine proton signals at δ_H 4.25 (H-7) and 4.50 (H-8) also correlated with C-17 through ^2J and ^3J coupling, respectively.

The methyl proton signal at δ_H 1.80 (H-8a) connected to carbon signal at δ_C 51.9 (C-7) and δ_C 50.4 (C-8) through ^3J and ^2J coupling, respectively. Oxymethylene proton signal at δ_H 4.50 (H-P1) correlated with the olefinic carbon signals at δ_C 117.7 (C-P2) and 173.0 (C-7c), indicated the phytyl group was attached to ester group at C-7c. The methine proton signal at δ_H 6.3 (H-10) showed correlation with the carbon signal at δ_C 169.6 (C-10a) indicated an ester group was attached to C-10. All of the above data were similar to the literature data of pheophytin A[137] which is well-known *chlorophyll*.

Table 5: ^{1}H- and ^{13}C-NMR data for compound **79**

Position	**79** ^{1}H-NMR (400 MHz, $CDCl_3$) ^{13}C-NMR (101 MHz, $CDCl_3$)		**Lite.**[136] ^{1}H-NMR (500 MHz, $CDCl_3$) ^{13}C-NMR (125 MHz, $CDCl_3$)	
	δc	δ_H	δc	δ_H
1	132.0	-	132.1	-
2	136.3	-	136.4	-
3	136.1	-	136.0	-
4	145.2	-	145	-
5	129.2	-	128.9	-
6	129.3	-	130.1	-
7	51.7	4.25 (*m*, 1H)	52.1	4.41
8	50.2	4.50 (*m*, 1H)	50.8	4.46
9	189.7	-	189.2	-
10	64.7	6.31 (*s*, 1H)	66.4	6.26
11	142.9	-	142.2	-
12	136.6	-	136.5	-
13	155.2	-	155.6	-
14	151.1	-	151.4	
15	138.0	-	138.5	-
16	149.8	-	149.9	-
17	161.5	-	162.1	-
18	172.4	-	172.8	-
α	97.5	9.39 (*s*, 1H)	97.5	9.38
β	104.5	9.54 (*s*, 1H)	104.4	9.52
γ	105.4	-	106.8	-

δ	93.4	8.67 (*s*, 1H)	93.9	8.55
1a	12.2	3.41 (*s*, 3H)	11.9	3.40
2a	129.1	8.05 (*dd*, *J* = 17.8, 11.5 Hz, 1H)	129.7	8.00
2b	122.9	6.29 (*dt*, *J* = 11.2, 1.7 Hz, 1H); 6.18 (*m*, 2H)	122.1	6.28/6.18
3a	11.3	3.25 (*d*, *J* = 5.2 Hz, 3H)	10.8	3.23
4a	19.5	3.71 (*d*, *J* = 11.3 Hz, 2H)	19.5	3.68
4b	17.4	1.70 (*td*, *J* = 7.6, 4.9 Hz, 3H)	17.4	1.69
5a	12.1	3.72 (*s*, 3H)	11.7	3.68
7a	31.2	2.19 (*m*, 2H)	31.7	2.63
7b	29.8	2.35 (*m*, 1H); 1.27 (*m*, 1H)	30.2	2.26
7c	173.0	-	172.9	
8a	23.1	1.8 (*d*, *J* = 7.3 Hz, 3H)	23.3	1.80
10a	169.6	-	169.9	
10b	52.9	3.50 (*s*, 3H)	52.5	3.88
P1	61.5	4.5 (*m*, 2H)	61.4	4.50
P2	117.7	5.17 (*m*, 1H)	119.5	5.13
P3	142.1	-	142.2	
P3a	16.3	1.59 (*m*, 3H)	16.2	1.56
P4	39.8	1.92 (*dt*, *J* = 10.8, 5.4 Hz, 2H)	40.5	1.90
P5	25.0	1.24-1.36 (*m*, 2H)	25.8	1.0-1.3
P6	36.6	1.24-1.36 (*m*, 2H)	37.4	1.0-1.3
P7	32.6	1.24-1.36 (*m*, 1H)	33.5	1.0-1.3
P7a	19.7	0.82 (*m*, 3H)	19.9	0.85
P8	37.3	1.24-1.36 (*m*, 2H)	38.1	1.0-1.3
P9	24.4	1.24-1.36 (*m*, 2H)	25.2	1.0-1.3
P10	37.4	1.24-1.36 (*m*, 2H)	38.1	1.0-1.3
P11	32.8	1.24-1.36 (*m*, 1H)	33.6	1.0-1.3
P11a	19.7	0.82 (*m*, 3H)	19.9	0.85
P12	37.3	1.24-1.36 (*m*, 2H)	38.1	1.0-1.3
P13	24.8	1.24-1.36 (*m*, 2H)	25.6	1.0-1.3
P14	39.4	1.24-1.36 (*m*, 2H)	40.2	1.0-1.3
P15	28.0	1.24-1.36 (*m*, 1H)	28.8	1.0-1.3
P15a	22.6	0.83 (*m*, 3H)	22.9	0.80
P16	22.7	0.87 (*m*, 3H)	23.0	1.0-1.3

3.1.2.4 Characterization of Compound 80

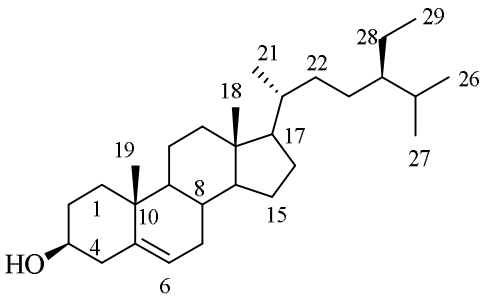

80

Compound **80** was isolated as a white powder with a melting point of 133-134 °C. The compound gave a dark blue spots on TLC with cerium ammonium molybdate spraying with the R_f value of 0.46 in $CHCl_3$:MeOH (1:0.1). The IR spectrum revealed the presence of O-H stretching at 3436.34 cm^{-1}, aliphatic C-H stretching at 2918.2 cm^{-1} and 2851.4 cm^{-1}, and C=C cyclic alkene stretching at 1639.32 cm^{-1}. The molecular formula was established as $C_{29}H_{50}O$ by the sodiated-molecular-ion peak in the TOF-ESI-MS (Appendix 30) at *m/z* 472.6723 $[M+CH_3OH+Na+3H]^{4+}$ (calcd for $C_{30}H_{57}O_2Na$, 472.7067). ^{1}H-NMR spectrum (Table 6 and Appendix 23) revealed the presence of six methyl signals, two of which appeared as angular methyl singlets at δ_H 0.68 (H-18) and 1.00 (H-19), three methyl doublet proton signals at δ_H 0.93 (*d*, *J* = 6.5 Hz, 3H-21), 0.82 (*d*, *J* = 7.6 Hz, 3H-27), and 0.80 (*d*, *J* = 6.3 Hz, 3H-26), and a methyl triplet proton signal at position δ_H 0.84 (*d*, *J* = 6.5 Hz, 3H-29). One olefinic proton signal was also detected in ^{1}H-NMR spectra at δ_H 5.34 (*dd*, *J* = 5.1, 2.6 Hz, H-6). In ^{1}H-NMR spectrum, a triplet of triplet at δ_H 3.53 was assigned to an oxymethine proton (H-3). ^{13}C-NMR (Table 6 and Appendix 24) and DEPT-135 spectra (Table 6 and Appendix 25) showed the presence of 29 carbon signals which were attributed to six methyls, eleven methylenes, nine methines, and three quaternary carbons. The signals at δ_C 140.8 (C-5) and 121.7 (C-6) were indicative of the presence of a double bond. The carbon signals at δ_C 19.2 and 12.1 were assigned to angular methyl carbons. The carbon signal at δ_C 71.8 could be attributed to oxymethine carbon of C-3. The COSY spectrum (Appendix 26) showed a triplet of triplet signal at δ_H 3.53 (*tt*, *J* = 10.7, 4.7 Hz, 1H-3) correlated with a proton signal at δ_H 2.22 (H-4). Olefinic methine proton signal at δ_H 5.35 (*dd*, *J* = 5.1, 2.6 Hz, H-6) was coupled with the proton signal at δ_H 1.98 (H-7). A proton signal of methyl at δ_H 0.93 (*d*, *J* = 6.5 Hz, 3H-21) correlated with a methine proton signal at δ_H 1.36 (*m*, 1H-20). In COSY spectrum, proton signals at δ_H 0.82 (*d*, *J* = 7.6 Hz, 3H-27) and δ_H 0.80 (*d*, *J* = 2.3 Hz, 3H-26) correlated with a methine proton signal at δ_H 1.65 (H-25). A signal at δ_H 0.84 (H-29) correlated with a methylene proton at δ_H 1.26 (*m*, 2H-28). HSQC spectrum (Appendix 27) showed an oxymethin proton signal at δ_H 3.53 (1H-3) correlated with a carbon signal at δ_C 71.58 (C-3). The signal at δ_H 5.34 (*dd*, *J* = 5.1,

2.6 Hz, 1H) correlated with carbon signal at δ_C 121.7 (C-6). A methyl proton signal at δ_H 0.93 (*d*, *J* = 6.5 Hz, 3H) correlated with a carbon signals at δ_C 18.9 (C-21), a proton signal at δ_H 0.80 (*d*, *J* = 6.3 Hz, 3H) correlated with carbon signal at δ_C 19.4 (C-26), and a proton signal at δ_H 0.82 (*d*, *J* = 6.5 Hz, 3H) correlated with a carbon signal at δ_C 19.9 (C-27). The two singlet signals at δ_H 1.00 (*s*, 3H-19) and 0.68 (*s*, 3H-18) correlated with angular methyl carbon signals at δ_C 19.2 (C-19) and 11.8 (C-18), respectively. A proton signal at δ_H 0.84 (*d*, *J* = 6.5 Hz, 3H) correlated with carbon signal at δ_C 11.8 (C-29). The HMBC Spectrum (Appendix 28) of compound **80** showed that the oxymethin proton at δ_H 3.53 (1H-3) correlated with methylene carbons at δ_C 42.4 (C-4) and δ_C 31.7 (C-2), indicated the hydroxyl group was linked to C-3. The doublet proton signal at δ_H 5.35 (H-6) correlated with the methylene carbon signal at δ_C 42.4 (C-4), methylene carbon signal at δ_C 31.8 (C-7) and methine carbon signal at δ_C 36.5 (C-10), similarly, a carbon signal at δ_C 140.8 (C-5) correlated with H-4 at δ_H 2.27 (*m*, 1H), and δ_H 0.93 (*m*, H-9) indicated the double bond was attached to C-7, C-4, and C-10. The protons singlet signal at δ_H 1.00 (3H-19) showed correlation with the carbon signals at δ_C 37.3 (C-1), 36.5 (C-10), 50.2 (C-9), and 140.8 (C-5) indicated the angular methyl proton was attached to C-20. The protons singlet signal at δ_H 0.68 (H-18) showed correlation to the carbon signals at δ_C 39.5 (C-12), 42.4 (C-13), 56.8 (C-14), and 56.0 (C-17) confirmed the connection of the angular methyl group to C-13. A doublet methyl proton signal at δ_H 0.80 (H-26) correlated with C-25 at δ_C 29.2 and C-24 at δ_C 45.7 and C-27 at δ_C 19.9. Similarly, a doublet methyl proton signal at δ_H 0.82 (H-27) correlated with C-25 at δ_C 29.2 and C-24 at δ_C 45.7 and C-26 at δ_C 19.4. Thus, the two methyl protons shared the same carbon atom (C-25), indicated the two methyl groups were attached to C-25. The location of the isopropyl group was deduced using the correlations between C-24 with H-28 and H-29. Comparison of the above spectral data of **80** with those reported in the literature[137] for β-sitosterol revealed a very close resemblance.

Table 6: ^{1}H- and ^{13}C-NMR data for compound **80**

Position	**80** ^{1}H-NMR (600 MHz, DMSO-d_6) ^{13}C-NMR (151 MHz, DMSO-d_6)		**Lite.**[137] ^{1}H-NMR (300 MHz, $CDCl_3$) ^{13}C-NMR (100 MHz, $CDCl_3$)	
	δ_c	δ_H	δ_c	δ_H
1	37.3	1.07 (*m*, 1H); 1.83 (*m*, 1H)	37.2	1.08 (*m*, 1H); 1.83 (*m*, 1H)
2	31.7	1.48 (*m*, 1H);1.80 (*m*, 1H)	31.6	1.49 (*m*, 1H); 1.82 (*m*, 1H)
3	71.8	3.53 (*tt*, *J* = 10.7, 4.7 Hz, 1H)	71.8	3.53 (*m*, 1H)
4	42.4	2.22 (*m*, 1H);2.27 (*m*, 1H)	42.27	2.24 (*m*, 1H);2.28 (*m*, 1H)
5	140.8	-	140.7	
6	121.7	5.35 (*dd*, *J* = 5.1, 2.6 Hz, 1H)	121.7	5.35 (*J* = 4.7 Hz)
7	31.8	1.57 (*m*, 1H);1.98 (*m*, 1H)	31.9	1.59 (*m*, 1H);1.98 (*m*, 1H)
8	31.8	1.48 (*m*, 1H)	31.9	1.49 (*m*, 1H)
9	50.2	0.93 (*m*, 1H)	50.1	0.94 (*m*, 1H)

10	36.5	-	36.5	-
11	21.2	1.48 (*m*, 1H); 1.50 (*m*, 1H)	21.06	1.45 (*m*, $1H_2$); 1.48 (*m*, $1H_2$)
12	39.5	2.00 (*m*, 1H); 1.15 (*m*, 1H)	39.8	1.15 (*m*, 1H); 1.97 (*m*, 1H)
13	42.4	-	42.19	-
14	56.8	1.07 (*m*, 1H)	56.7	1.03 (*m*, 1H)
15	24.4	1.55 (*d*, *J* = 6.5 Hz, 1H); 1.01 (*m*, 1H)	24.3	1.05 (*m*, 1H); 1.55 (*m*, 1H)
16	27.9	1.86 (*m*, 1H);1.27 (*m*,1H)	28.2	1.24 (*m*, 1H)
17	56.0	1.11 (*m*, 1H)	56.0	1.13 (*m*, 1H)
18	12.0	0.68 (*s*, 3H)	11.97	0.68 (*s*, 3H)
19	19.2	1.00 (*s*, 3H)	19.4	1.01(*s*, 3H)
20	36.2	1.36 (*m*, 1H)	36.1	1.36 (*m*, 1H)
21	18.9	0.93 (*d*, *J* = 6.5 Hz, 3H)	18.8	0.94 (*d*, 3H)
22	33.9	1.37 (*m*, 1H);1.05 (*m*, 1H)	33.9	1.32 (*m*, 2H)
23	26.0	1.14 (*m*, 2H)	26.0	1.15 (*m*, 2H)
24	45.7	0.92 (*m*, 1H)	45.8	0.93 (*m*, 1H)
25	29.2	1.65 (*m*, 1H)	29.1	1.65 (*m*, 1H)
26	19.4	0.80 (*d*, *J* = 6.3 Hz, 3H)	19.02	0.82 (*J* = 6.3 Hz, 3H)
27	19.9	0.82 (*d*, *J* = 6.5 Hz, 3H)	19.8	0.83 (*J* = 6.1 Hz, 3H)
28	22.8	1.26 (*m*, 2H)	23.0	1.22 (*m*, 3H)
29	11.8	0.84 (*d*, *J* = 6.5 Hz, 3H)	11.8	0.85 (*m*, 3H)

3.2 Phytochemical Invesigation of the Stem Barks of *Myrica salicifolia*

The stem barks of *M. salicifolia* was collected from Debresina, Northern Shewa, Amhara region, 192 km from Addis Ababa, Ethiopia, in July 2020 by Dr. Mekonnen Abebayehu. The plant specimens were identified by Mr. Melaku Wendafrash, Addis Ababa University, Ethiopia. A voucher specimen of the plant material has been deposited in the National Herbarium, Addis Ababa University, with a voucher specimen number of MA/2007/12. Phytochemical analysis of the plant extract resulted in the isolation of nine compounds, namely, myricanone (**28**), myricanol (**29**), myricanol-11-*O*-β-D-xylopyranoside (**32**), taraxerone (**81**), taraxerol (**82**), myricadiol (**83**), 3β-*O*-*trans*-caffeoylisomyricadiol (**84**), methyl-β-D-glucopyranoside (**85**) and contortamide (**86**). Antibacterial activities and DPPH radical scavenging activities of the isolated compounds were also determined in this study. The compounds showed a wide range of DPPH scavenging activities from very weak (IC_{50} value = 282.61 μM) to very strong (IC_{50} = 13.48 μM). Antibacterial activities of the compounds were evaluated using the disk diffusion agar method, where some of the compounds showed modest antibacterial activities against *S. pyogenes* and *S. aureus* at

250 µg/mL. The phytochemical investigation on the stem barks of *M. salicifolia* is discussed in the following sections.

3.2.1 Characterization of Compounds Isolated from the Stem Barks of *Myrica salicifolia*

3.2.1.1 Characterization of Compound 28

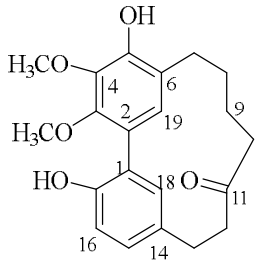

28

Compound **28** was isolated as a white powder with the melting point of 193-195 °C. The compound gave a dark blue spots on TLC with cerium ammonium molybdate spraying with the R_f value of 0.81 in $CHCl_3$:EtOAc (1:0.5). The IR spectrum revealed the presence of O-H stretching at 3369.8 cm^{-1}, C-H stretching at 2924.2 cm^{-1} and 2855.6 cm^{-1}, aliphatic ketone, C=O stretching at 1704.2 cm^{-1}, and C=C stretching at 1614.8 cm^{-1}. The molecular formula was established as $C_{21}H_{24}O_5$ by the sodiated-molecular-ion peak in the HPLC-ESI-MS (Appendix 37) at *m/z* 379.1516 for $[M+Na]^+$ (calcd for $C_{21}H_{24}O_5Na$, 379.1516). The ^{1}H-NMR spectrum (Table 7 and Appendix 32) of the aromatic region confirmed the presence of four aromatic protons, with a singlet signal at δ_H 6.31 (H-19) and three mutually coupled proton signals at δ_H 6.95 (H-15), 6.72 (H-16), and 6.51 (H-18), indicating the presence of one proton in one of the aromatic ring and three in 1,2,4-relative positions in the other aromatic ring. Additionally, four deshielded carbon signals at δ_C 140.4 (C-4), 148.5 (C-3), 149.1 (C-5), and 152.7 (C-17) were indicative of the the presence of oxygenated aromatic carbons. Three aromatic proton signals were observed as an ABX system at 6.95 (*dd*, *J* = 8.2, 2.4 Hz, H-15), 6.72 (*d*, *J* = 8.2 Hz, H-16), and 6.51 (*d*, *J* = 2.5 Hz, H-18) in the ^{1}H-NMR spectra. The presence of two methoxy groups was deduced from the ^{1}H-NMR spectra at δ_H 3.76 (3H-21) and 3.74 (3H-20), and the ^{13}C-NMR spectrum at δ_C 60.9 (C-21) and 60.5 (C-20). The ^{13}C-NMR (Table 7 and Appendix 32) spectrum revealed 21 carbon signals due to two methyls, six methylenes, four methines, and eight quaternary carbon signals, as well as the typical peaks of a carbonyl carbon and twelve aromatic carbons (Table 7). The HMBC (Appendix 36) showed a correlation between the deshielded methoxyl proton signals at δ_H 3.74 (H-20) and δ_H 3.76 (H-21) and the aromatic

carbon signals at δ_C 148.5 (C-3) and 140.3 (C-4), respectively, indicative of a di-*ortho*-substitution. The HMBC spectrum (Appendix 36) reveled OH-protons signals at δ_H 8.87 and δ_H 8.62 correlated with carbon signal at δ_C 149.1 (C-5) and at δ_C 152.7 (C-17), respectively, indicated the two OH groups were attaced to the phenol ring. The two hydroxy groups were resonating highly down field than expected since it forms an intramolecular hydrogen bond with the methoxy groups in the compound structure.[138]

Table 7: ^{1}H-and ^{13}C-NMR data for compound **28**

Position	**28** ^{1}H-NMR (600 MHz, DMSO) ^{13}C-NMR (151 MHz, DMSO)		**Lit.**[139] ^{1}H-NMR (400 MHz, $CDCl_3$) ^{13}C-NMR (100 MHz, $CDCl_3$)	
	δ_c	δ_H	δ_c	δ_H
1	126.9	-	125.5	-
2	122.8	-	123.3	-
3	148.5	-	146.1	-
4	140.4	-	138.8	-
5	149.1	-	147.9	-
6	122.3	-	123.1	-
7	27.2	2.56 (*m*, 2H)	26.9	2.72, *m*
8	24.5	1.78 (*m*, 2H)	24.6	1.95, *m*
9	21.8	1.58 (*m*, 2H)	21.9	1.85, *m*
10	45.9	2.66 (*t*, *J* = 7.2, 2H)	46.2	2.75, *m*
11	213.8	-	213.5	
12	42.4	2.73 (*m*, 2H)	42.6	2.78, *m*
13	28.8	2.82 (*m*, 2H)	29.0	3.02, *m*
14	131.4	-	132.4	-
15	128.3	6.95 (*dd*, *J* = 8.2, 2.4 Hz, 1H)	129.0	7.06 (*dd*, *J* = 8.0, 2.0 Hz, 1H)
16	115.9	6.72 (*d*, *J* = 8.2 Hz, 1H)	117.0	6.88 (*d*, *J* = 8.0 Hz, 1H)
17	152.7	-	151.8	-
18	133.5	6.51 (*d*, *J* = 2.5 Hz, 1H)	132.5	6.75 (*d*, *J* = 2.0 Hz, 1H)
19	129.1	6.31 (*s*, 1H)	129.0	6.61,s
20	60.5	3.74 (*s*, 3H)	61.5	5.83,s
21	60. 9	3.76 (*s*, 3H)	61.5	7.63,s

The COSY spectra (Appendix 34) showed correlations of protons H-7/H-8/H-9/H-10 and H-12/H-13 which confirmed the presence of alphatic moiety. The HMBC (Appendix 36) spectrum of **28** showed correlations of the methylene proton signals of H-9, H-10, H-12, and H-13 with carbon signal of C-11 revealed that C-10 and C-12 were connected through a C=O group at C-11. The HMBC spectrum showed correlation between a methylene proton signal δ_H 2.56 (H-7) and aromatic carbon signals δ_C 149.1 (C-5), 122.3 (C-6), and 129.1 (C-19), and correlation between a methylene proton signal δ_H 2.82 (H-13) and aromatic carbon signals δ_C 128.3 (C-15), and 131.4 (C-14) indicated the aliphatic chain

were link to the diphenyl moiety. Consequently, compound **28** was determined as myricanone by comparison of these data (Table 7) and the literature data.[139]

3.2.1.2 Characterization of Compound 29

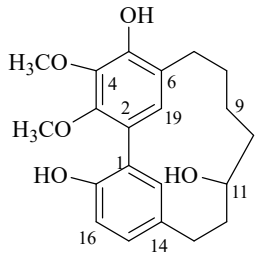

29

Compound **29** was isolated as an amorphous white powder with a melting point of 102-110 °C. The compound gave a dark blue spots on TLC with cerium ammonium molybdate spraying with the R_f value of 0.50 in $CHCl_3$:EtOAc (1:0.5). The IR spectrum of compound **29** revealed the presence of a broad O-H stretch at 3369.8 cm^{-1}, C-H stretching of the aliphatic chain at 2924.2 cm^{-1} and 2855.6 cm^{-1}, and C=C stretching of aromatic at 1610.8 cm^{-1}-1444.0 cm^{-1}. The molecular formula, $C_{21}H_{26}O_5$, was determined from HPLC-ESI-MS (Appendix 44) at *m/z* 381.1670 for $[M+Na]^+$ (calcd for $C_{21}H_{26}O_5Na$, 381.1672). The ^{1}H-NMR spectrum (Table 8 and Appendix 38) of compound **29** was very similar to that of **28**, except the aliphatic side chain contained OH at C-11. This observation was supported by a methine proton signal at δ_H 3.98 could be attributed to C-11 (δ_C 67.1). The ^{13}C-NMR (Appendix 39) and DEPT spectra (Appendix 41) revealed 21 carbon signals due to two methyl, six methylene, five methine, and eight quaternary carbon signals, as well as the typical peaks of an oxymethine group and twelve aromatic carbons.

Table 8**:** ^{1}H-and ^{13}C-NMR data for compound **29**

Position	**29** ^{1}H-NMR (600 MHz, Acetone) ^{13}C-NMR (151 MHz, Acetone)		**Lit.**[140] ^{1}H-NMR (400 MHz, $CDCl_3$) ^{13}C-NMR (100 MHz, $CDCl_3$)	
	δ_C	δ_H	δ_C	δ_H
1	124.8	-	124.7	-
2	122.7	-	123.4	-
3	146.6	-	145.9	-
4	139.4	-	138.7	-
5	148.8		147.7	-
6	122.9	-	122.6	-
7	25.5	2.54 (*m*, 1H); 2.78 (*m*, 1H)	25.4	2.56;2.81
		-		
8	25.8	1.91 (*m*, 1H);1.98 (*m*, 1H)	25.8	1.89-1.99
9	22.9	1.50 (*m*, 1H);1.68 (*m*, 1H)	22.9	1.50-1.62;1.63-1.77
10	39.5	1.54 (*dd*, *J* = 13.6, 11.5 Hz, 1H); 1.83 (*m*, 1H)	39.4	1.50-1.62;1.89-1.99
11	67.1	3.98 (*m*, 1H)	68.6	4.10
12	36.7	1.67 (*m*, 1H);2.30 (*m*, 1H)	34.7	1.63-1.77;2.35
13	26.7	2.81 (*d*, *J* = 4.7 Hz, 1H); 2.91 (*m*, 1H)	26.9	2.93
14	130.8	-	130.7	-
15	129.5	7.05 (*dd*, *J* = 8.2, 2.4 Hz, 1H)	129.9	7.10
16	116.2	6.8 (*d, J* = 8.2)	116.8	6.92
17	151.5	-	151.4	-
18	133.3	7.22 (*m*, 1H)	133.1	7.19
19	129.0	6.91 (*s*, 1H)	129.4	6.92
20	60.8	3.89, (*s*, 3H)	61.4	3.89
21	60.6	3.91 (*s*, 3H)	61.4	4.01

The ^{1}H-^{1}H correlation spectroscopy (COSY) spectrum (Appendix 41) showed correlation between H-7 and H-8, H-8/H-9/H-10, H-11/H-12 and H-13 for alphatic chain, and a proton signal of H-15 correlated with proton signals of H-16 and H-18 indicated the presence of 1,3,4-trisubstituted benzene ring. The ^{13}C-NMR data (Table 8 and Appendix 39) were similar to those of compound **28**, except for position 11. In contrast, the carbonyl group at C-11 (δ_C 213.8) in **28** was replaced by a hydroxyl group (δ_C 67.1). As a result of the long-range coupling between the proton signal of H-15 and H-18, a weak cross-peak was also notice. In the HMBC spectrum (Appendix 43) of **29**, correlation between proton signal of H-7 and carbon signal of C-19, C-8, and C-9, and correlation between proton signal of H-13 and carbon signals of C-18, C-14, and C-15, indicated alkyl chain was attached benzene rings. A connection between carbon signal of C-4 and proton signal of H-20, and carbon signal of C-5 and proton signal of H-21 in the HMBC showed where the methoxyl groups

were located. Furthermore, HMBC showed correlation of oxymethine proton signal at δ_H 3.98 with carbon signal of C-10 and C-12 indicated the hydroxyl group was attached to C-11. As a result, compound **29** was identified as myricanol by comparison of these data (Table 8) and those found in the literature.[140]

3.2.1.3 Characterization of Compound 32

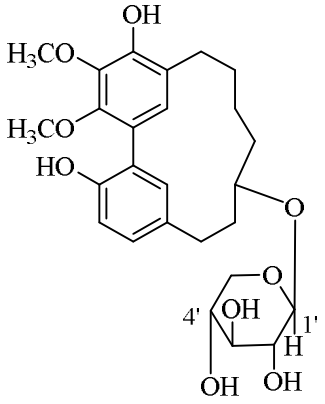

32

Compound **32** was isolated as an amorphous white powder with a melting point of 231-232 °C. The compound gave a dark blue spots on TLC with cerium ammonium molybdate spraying with the R_f value of 0.54 in $CHCl_3$:MeOH (1:0.15). The IR spectrum of compound **32** revealed a broad absorption band of O-H stretching at 3390.8 cm^{-1}, C-H stretching at 2927.8 cm^{-1} and 2849.6 cm^{-1}, C-C stretching of aromatics at 1501.8 cm^{-1}-1406.2 cm^{-1}, and C-O-C stretching of aromatic methoxy at 1352.6 cm^{-1} and 1235.8 cm^{-1}. The molecular formula was established to be $C_{26}H_{34}O_9$ from HPLC-ESI-MS (Appendix 52) at *m/z* 513.2095 for $[M+Na]^+$ (calcd for $C_{26}H_{34}O_9Na$, 513.2095). The ^1H and ^{13}C-NMR spectra (Appendix 45 and Appendix 46) of compound **32** were similar to those of compound **29**, except for an additional sugar moiety at C-11. Twenty six carbon atoms were identified by the ^{13}C-NMR (Appendix 46) and DEPT spectra (Table 9 and Appendix 47). These signals included two methyls, seven methylenes, nine methines, and eight quaternary carbon signals, in addition to the characteristic peaks of an oxymethine group, twelve aromatic carbons and characteristic peaks of xylose. The anomeric proton and carbon signals of the sugar moiety were at δ_H 3.98 (*d*, *J* = 7.4 Hz, H-1′) and δ_C 101.4 (C-1′) in the ^1H and ^{13}C-

NMR spectra, respectively. The remaining sugar carbons characteristic of xylose [141] were appeared at δ_C 66.1 (5′), 70.1 (C-4′), 73.6 (C-2′), and 77.0 (C-3′). The relative configuration of the xylose sugar moiety was also assigned by ^{1}H-^{1}H coupling constants and NOESY correlations (Appendix 51). The anomeric proton signal of H-1′ (δ_H 3.98) and oxymethine proton signal of H-2′ (δ_H 2.89) are located at axial positions which was confirmed by the large coupling constant value of ^{3}JH1′-H2′ (7.4 Hz). The coupling constant of 8.9 Hz between H-2′ (δ_H 2.89) and H-3′ (δ_H 3.05) also indicated their axial–axial relationship. The large coupling value (8.9 Hz) between H-3′ and H-4′ revealed that H-3′ (δ_H 3.05) and H-4′ (δ_H 3.21) are located on the axial positions of the sugar. Furthermore, the NOESY correlations of H-1′ (δ_H 3.98) and H-3′ (δ_H 3.05) assigned that these two protons were found in the same plane, while H-2′ (δ_H 2.89) and H-4′ (δ_H 3.21) protons were found on the other side. So that, the OH at H-3′ is *trans* to H-2′ and H-4′. If two adjacent hydrogen atoms in a six-membered ring are *trans* (i.e., diaxial) a value of 7-10 Hz should be observed, while only 2-4 Hz should be observed if the hydrogen atoms are gauche (i.e., axial-equatorial) [34]. The attachment of the sugar moiety at C-11 was supported by the HMBC correlation (Appendix 50) between the anomeric proton at δ_H 3.98 (H-1′) and C-11 (δ_C 75.4). Hence, based on the above data (Table 9) and comparison with the literature data, compound **32** was proposed to be 11-*O*-β-D-xylopyranosylmyricanol.[39]

Table 9: ^{1}H-and ^{13}C-NMR data for compound **32**

Position	**32** ^{1}H-NMR (600 MHz, DMSO-d_6) ^{13}C-NMR (151 MHz, DMSO-d_6)		Lite.[39] H-NMR (500 MHz, $CDCl_3$) ^{13}C-NMR (125.8 MHz, $CDCl_3$)	
	δ_C	δ_H	δ_C	δ_H
1	126.5	-	124.6	-
2	122.9	-	123.0	-
3	148.4	-	146.0	-
4	140.3	-	138.9	-
5	149.1	-	148.0	-
6	121.8	-	122.7	-
7	25.9	2.46 (*m*, 1H); 2.63 (*m*, 1H)	25.5	2.51;2.74
8	25.4	1.77 (*m*, 2H)	25.5	1.77;1.82
9	22.7	1.37 (*m*, 1H); 1.47 (*m*, 1H)	22.5	1.49;1.61
10	35.6	1.62 (*dd*, *J* = 7.9, 4.7 Hz, 2H)	35.1	1.61;1.82
11	75.4	3.73 (*d*, *J* = 3.3 Hz, 1H)	75.2	3.98
12	33.3	1.70 (*m*, 1H); 2.12 (*m*, 1H)	32.9	1.82;2.18
13	27.0	2.69 (*m,* 1H); 2.78 (*m*, 1H)	26.7	2.79;2.85
14	130.3	-	131.0	-
15	129.5	6.94 (*d*, *J* = 3.6 Hz, 1H)	129.7	7.00
16	116.2	6.72 (*d*, *J* = 8.8 Hz, 1H)	116.5	6.81
17	152.1	-	150.9	-
18	134.1	6.93 (*d*, *J* = 2.7Hz, 1H)	132.6	7.07
19	129.8	6.53 (*s*, 1H)	129.3	6.79
20	60.5	3.80 (*s*, 3H)	61.3	3.82
21	61.0	3.78 (*s*, 3H)	61.1	3.90
1′	101.4	3.98 (*d*, *J* = 7.4 Hz, 1H)	100.1	4.2
2′	73.6	2.89 (*ddd*, *J* = 8.9, 7.4, 5.2 Hz, 1H)	72.1	3.24
3′	77.0	3.05 (*td*, *J* = 8.7, 4.7 Hz, 1H)	74.7	3.37
4′	70.1	3.23 (*ddt*, *J* = 10.2, 8.6, 5.2 Hz, 1H)	69.4	3.49
5′	66.1	2.84 (*dd*, *J* = 11.5, 9.9 Hz, 1H); 3.49 (*dd*, *J* = 11.4, 5.3 Hz, 1H)	64.2	2.98;3.67

3.2.1.4 Characterization of Compound 81

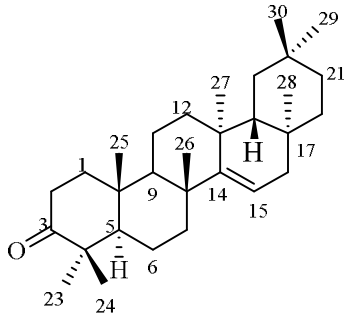

81

Compound **81** was isolated as a white powder with a melting point of 272–274 °C. The compound gave a dark blue spots on TLC with cerium ammonium molybdate spraying with the R_f value of 0.33 in $CHCl_3$ (100%). The IR spectrum of compound **81** revealed the presence of =C-H stretching at 3051.4 cm^{-1}, C-H stretching of alkanes at 2929.0 cm^{-1} and 2860.4 cm^{-1}, and C=O stretching at 1709 cm^{-1}. The molecular formula was deduced to be $C_{30}H_{48}O$ by the MALDI-MS (Appendix 60) from the molecular ion peak at *m/z* 449.9 for $[M+Na+H]^{2+}$ (calc. for $[C_{30}H_{48}ONaH]^{2+}$, 449.7). ^{1}H-NMR (Table 10 and Appendix **53**) and ^{13}C-NMR spectra (Table 10 and Appendix 55) showed eight singlet methyl signals at chemical shifts of δ_H 1.15 (H-27), 1.12 (H-25), 1.11 (H-23), 1.01 (H-24), 0.98 (H-29), 0.94 (H-30), 0.93 (H-26), and 0.85 (H-28), which were associated with the carbon resonances at δ_C 33.4 (C-29), 29.9 (C-26), 29.8 (C-28), 26.1 (C-23), 25.6 (C-27), 21.5 (C-24), 21.4 (C-30), and 14.8 (C-25), suggesting the presence of a pentacyclic triterpenoid structure.[142] There were four methine proton signals, the doublate at δ_H 5.58 (H-15) was assigned to the olefinic proton of C-15. A multiplet at δ_H 1.34, 1.53, and a doublet of doublet at δ_H 1.01 (*J* = 14.8, 8.1) was assigned to the methine proton signals of C-5, C-9, and C-18, respectively. ^{13}C-NMR and DEPT spectra showed 30 carbon signals: eight methyls, ten methylenes, four methines, and four quaternary carbons, of which one of the quaternary carbon at δ_C 217.5 (C-3) was a carbonyl carbon.

Table 10: ^{1}H-and ^{13}C-NMR data for compound **81**

Position	**81** ^{1}H-NMR (600 MHz, DMSO-d_6) ^{13}C-NMR (151 MHz, DMSO-d_6)		**Lit.** [142] ^{1}H-NMR (500 MHz, $CDCl_3$) ^{13}C-NMR (126 MHz, $CDCl_3$)	
	δ_C	δ_H	δ_C	δ_H
1	38.4	1.40 (*m*, 1H); 1.90 (*m*, 1H)	38.57	
2	34.1	2.35 (*m*, 1H); 2.60 (*m*, 1H)	34.34	
3	217.5	-	217.74	-
4	47.6	-	47.76	-
5	55.8	1.34 (*m*, 1H)	55.96	
6	20.0	1.57 (*m*, 1H); 1.62 (*m*, 1H)	20.15	
7	35.1	1.04 (*m*, 1H); 1.40 (*m*, 1H)	35.26	
8	38.9	-	39.06	-
9	48.8	1.53 (*m*, 1H)	49.98	
10	35.8	-	35.95	-
11	17.5	1.57 (*m*, 1H);	17.63	

		1.69 (*m*, 1H)		
12	37.7	1.90 (*m*, 1H);	37.88	
		1.95 (*m*, 1H)		
13	37.5	-	37.93	-
14	157.6	-	157.78	-
15	117.2	5.58 (*dd*, *J* = 8.2, 3.2 Hz, 1H)	117.37	5,56 (*dd*, *J* = 8,4, 3,0 Hz)
16	36.7	1.69 (*m*, 1H);	36.83	
		1.95 (*m*, 1H)		
17	37.7	-	37.72	-
18	48.7	1.01 (*m*, 1H)	48.98	
19	40.6	2.10 (*m*, 1H); 1.39 (*m*, 1H)	40.82	
20	28.8	-	28.98	-
21	33.6	1.57 (*m*, 1H); 1.62 (*m*, 1H)	33.73	
22	33.1	1.34 (*m*, 1H);	33.24	
		1.39 (*m*, 1H)		
23	26.1	1.11 (*s*, 3H)	26.25	1.07
24	21.5	1.01 (*s*, 3H)	21.68	1.06
25	14.8	1.11 (*s*, 3H)	14.99	1.08
26	29.9	0.93 (*s*, 3H)	30.03	0.90
27	25.6	1.15 (*s*, 3H)	25.77	1.13
28	29.9	0.85 (*s*, 3H)	30.11	0.82
29	33.4	0.98 (*s*, 3H)	33.55	0.95
30	21.4	0.94 (*s*, 3H)	21.53	0.91

^{1}H-NMR spectrum showed ten methylene signals at δ_H 1.40 (*m*, H_1-1), 1.90 (*m*, H_2-1), 2.35 (*m*, H_1-2), 2.60 (*m*, H_2-2), 1.57 (*m*, H_1-6), 1.62 (*m*, H_2-6), 1.04 (*m*, H_1-7), 1.40 (*m*, H_2-7), 1.57 (*m*, H_1-11), 1.69 (*m*, H_2-11), 1.00 (*d*, *J* = 3.7 Hz, H_1-12), 1.34 (*m*, H_2-12), 1.69 (*m*, H_1-16), 1.95 (*m*, H_2-16), 2.10 (*m,* H_1-19), 1.39 (*m*, H_2-19), 1.57 (*m*, H_1-21), 1.62 (*m*, H_2-21), 1.34 (*m*, H_1-22), and 1.39 (*m*, H_2-22). The COSY spectrum (Appendix 56) of compound **81** showed correlations between the proton signals of H-1 and H-2, H-6 and H-7, H-15 and H-16, H-21 and H_2-22, H-9 and H-11, H-5 and H_2-6, and H-18 and H-19. The olefin was attributed to C-14 based on long-range HMBC correlations (Appendix 58) of the methyl singlets H-26 and H-27 with C-14 and H-16 with C-14. NOESY correlations (Appendix 59) showed that H-24/H-25, H-26/H-18, and H-30/H-26/H-28 were found on the same side of the molecule, whereas H-23/H-5, H-5/H-9, and H9/H-27 were found on the opposite side of the molecule. Therefore, the structure of compound **81** was determined to be taraxerone.[142]

3.2.1.5 Characterization of Compound 82

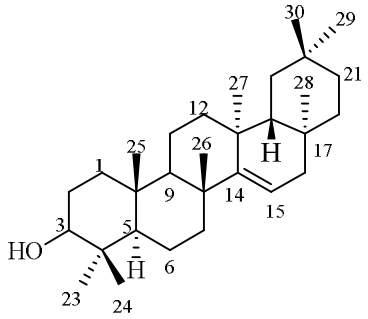

82

Compound **82** was isolated as a white powder with a melting point of 257–260 °C. The compound gave a dark blue spots on TLC with cerium ammonium molybdate spraying with the R_f value of 0.76 in $CHCl_3$:EtOAc (1:0.5). The IR spectrum showed the presence of O-H stretching at 3430.8 cm^{-1}, =C-H stretching at 3051.4 cm^{-1}, and C=C stretching at 1620 cm^{-1}. The molecular formula was deduced to be $C_{30}H_{50}O$ using the MALDI-MS (Appendix 68) at *m/z* 449.9 for $[M+Na]^+$ (calc. for $C_{30}H_{50}ONa$, 449.7). The ^{1}H-NMR spectrum (Table 11 and Appendix 61) of **82** showed the presence of a double doublet at δ_H 5.53 (*dd*, *J* = 8, 3.2 Hz, H-15) that could be attributed to an olefinic proton. The proton signal at δ_H 3.22 (H-3) was assigned to an oxymethine proton. Six methyl singlet protons were identified at δ_H 1.11, 1.00, 0.97, 0.95, 0.85, and 0.83. Two identical methyl moieties' protons were shown at δ_H 0.93. The ^{13}C-NMR spectrum (Table 11 and Appendix 62) revealed carbon signals at δ_C 33.4, 29.9, 29.8, 28.0, 25.9, 21.3, 15.5, and 15.4 that could be attributed to eight methyl carbons. The presence of a double bond involving a quaternary carbon atom is consistent with the carbon signals located at δ_C 158.1 (C-14). The sp^3 hybridized carbon linked to an OH group causes a chemical shift at δ_C 79.10 that could be attributed to the C-3. Its NMR spectroscopic data was identical to that of **81**, except for the absence of carbonyl carbon signals in **81,** which was replaced by an OH group at C-3. This was confirmed by the shielded chemical shift of C-3 at δ_C 79.1, the proton signal at δ_H 3.22 (H-3) correlated with proton signal of H-2 (δ_H 1.63 (*m*, 1H) in COSY spectrum (Appendix 64), and the methyl proton signals δ_H 1.00 (*s*, H-23) and 0.95 (*s*, H-24) correlated with a carbon signal at δ_C 79.1 (C-3) in the HMBC spectrum (Appendix 66). The relative configuration of OH was determined to be 3β from the NOESY correlations (Appendix 68) of H-3 and H-5. Therefore, the structure of compound **82** was elucidated as taraxerol.[143]

Table 11: ^{1}H and ^{13}C-NMR data for Compound **82**.

Position	**82** ^{1}H-NMR (600 MHz, DMSO-d_6) ^{13}C-NMR (151 MHz, DMSO-d_6)		Lit. [143] ^{1}H-NMR (400 MHz, $CDCl_3$) ^{13}C-NMR (100 MHz, $CDCl_3$)	
	δ_c	δ_H	δ_c	δ_H
1	37.7	1.63 (*m*, 2H)	38.1	0.99;1.63
2	27.2	1.59 (*m*, 1H); 1.63 (*m*, 1H)	27.3	1.62
3	79.1	3.22 (*dt*, *J* = 10.6, 5.1 Hz, 1H)	79.2	3.19 (*dd*, *J* = 11.2, 4.8 Hz, 1H)
4	38.9	-	38.9	-
5	55.5	0.80 (*m*, 1H)	55.7	0.88
6	18.8	1.50 (*m*, 1H); 1.63 (*m*, 1H)	18.9	1.62;1.45
7	41.3	1.37 (*m*, 1H); 2.06 (*dt*, 12.8, 3.3 Hz, 1H)	41.5	1.36;2.03
8	38.8	-	39.1	-
9	48.8	0.98 (*m*, 1H)	48.9	1.43
10	38.0	-	37.9	-
11	17.5	1.44 (*m*, 1H); 1.63 (*m*, 1H)	17.7	1.63;1.49
12	33.1	1.26 (*m*, 1H); 1.37 (*m*, 1H)	33.2	1.53;1.64
13	37.6	-	37.9	-
14	158.1	-	158.2	-
15	116.9	5.56 (*d*, *J* = 8.2, 3.2 Hz, 1H)	117.0	5.53 (*dd*, J= 8, 3.2 Hz, 1H)
16	37.7	1.63 (*m*, 1H); 1.94 (*dd*, *J* = 14.8, 3.2 Hz, 1H)	36.8	1.59; 1.92 (*dd*, *J* = 14.8, 3.2 Hz, 1H)
17	35.8	-	35.3	-
18	49.3	1.44 (*m*, 1H)	49.4	0.99
19	36.7	1.00 (*m*, 1H); 1.33 (*m*, 1H)	37.7	1.02;1.33
20	28.8	-	28.9	-
21	33.7	1.25 (*m*, 1H); 1.59 (*m*, 1H)	33.8	1.25;1.38
22	35.1	1.04 (*m*, 1H); 1.38 (*m*, 1H)	35.9	1.00;1.38
23	28.0	1.00 (*s*, 3H)	28.2	0.97
24	15.5	0.95 (*s*, 3H)	15.6	0.80
25	15.4	0.83 (*s*, 3H)	15.6	0.92
26	25.9	1.11 (*s*, 3H)	26.1	1.10
27	21.3	0.93 (*s*, 3H)	21.5	0.91
28	29.8	0.85 (*s*, 3H)	29.9	0.82
29	33.4	0.97 (*s*, 3H)	33.5	0.95
30	29.9	0.93 (*s*, 3H)	30.1	0.91

3.2.1.6 Characterization of Compound 83

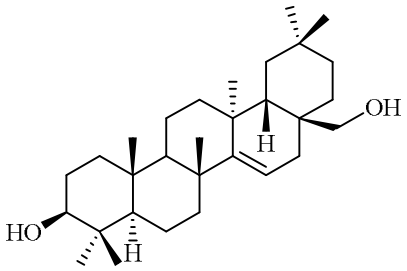

83

Compound **83** was isolated as a white amorphous powder with a melting point of 266-268 °C. The compound gave a dark blue spots on TLC with cerium ammonium molybdate spraying with the R_f value of 0.71 in $CHCl_3$:EtOAc (1:0.5). The IR spectrum showed the presence of O-H stretching at 3392, C-H stretching at 2936 and 2855, and C=C stretching at 1644.4. The molecular formula was deduced to be $C_{30}H_{50}O_2$ from the MALDI-MS (Appendix 76) at *m/z* 442.1 for $[M]^+$ (calc. for $C_{30}H_{50}O_2$, 442.7). The ^{1}H-NMR spectrum (Table 12 and Appendix 69) showed the presence of seven tertiary methyl signals at δ_H 0.82 (H-24), 0.92 (H-30), 0.94 (H-25), 0.98 (H-27), 0.99 (H-29), 1.07 (H-26) and 1.00 (H-23) (s, each 3H), and resonances at δ_H 3.16 and 3.31 were ascribed to proton signals connected to an oxygenated methylene carbon (C-28). The appearance of a second oxymethine proton signal at δ_H 3.22 (*dt*, *J* = 10.7, 5.0 Hz) indicates that hydroxyl group was linked to C-3. One olefinic proton of a trisubstituted double bond was identified in the ^{1}H-NMR spectrum at δ_H 5.53 (*dd*, *J* = 8.2, 3.3 Hz, 1H-15) which was linked with protons of a methylene at δ_H 2.14 (*dd*, *J* = 15.2, 8.2 Hz, $1H_2$-16), and 1.77 (*dd*, *J* = 15.4, 3.3 Hz, $1H_1$-16) in the COSY spectrum. Its spectroscopic data were identical to those of compound **83**, except for the presence of a hydroxylated carbon signal at δ_C 65.5 (C-28) in the ^{13}C-NMR spectrum of compound **83** (Appendix 70). From DEPT (Appendix 71) and HSQC spectra (Table 12 and Appendix 73), 30 carbon signals were identified as four methines, seven methyls, ten methylenes, six quaternary carbons, one oxygen-bearing secondary carbon, and a trisubstituted double bond. Five of the six degrees of unsaturation were indicative of a pentacyclic skeleton and one of them was caused by a trisubstituted double bond at δ_C 117.2 and 159.2. The HMBC correlations (Appendix 74) from 1.07 (*s*, 3H-26), 0.98 (*s*, 3H-27), and 2.14 (*dd*, *J* = 15.2, 8.2 Hz, 1H-16) to δ_C 159.2 (C-140) were used to identify a double bond. The presence of this additional hydroxyl group was confirmed by the ^{1}H-NMR signals for diastereotopic protons at δ_H 3.16 and 3.31 (H-28), as shown by the HMBC correlations with C-17 (δ_C 40.4), C-22 (δ_C 27.9), and C-16 (δ_C 30.8). NOESY correlations (Appendix 75) showed that H-24/H-25/H-26 and H-18/H-28/H-30 were all classified as β-oriented due to their appearances on the same side of the molecule. Whereas, the H-3/H-23/H-5, H-5/H-9, and H9/H-27 NOESY correlations showed that they were α-

configured. Based on the spectroscopic data (Table 12) and comparison with the literature data, compound **83** was determined to be myricadiol.[144]

Table 12: ^{1}H-and ^{13}C-NMR data for compound **83**.

Position	**83** ^{1}H-NMR (600 MHz, DMSO-d_6) ^{13}C-NMR (151 MHz, DMSO-d_6)		**Lit.** [144] ^{1}H-NMR (400 MHz, $CDCl_3$) ^{13}C-NMR (100 MHz, $CDCl_3$)	
	δ_c	δ_H	δ_c	δ_H
1	37.7	1.63 (*m*, 2H)	37.5	1.61 (*m*, 1H), 1.58 (*m*, 1H)
2	27.1	1.57 (*m*, 1H); 1.62 (*m*, 1H)	26.9	1.60 (*m*, 1H), 1.59 (*m*, 1H)
3	79	3.22 (*dt*, *J* = 10.7, 5.0 Hz, 1H)	78.5	3.16 (*dd*, *J* = 10.8, 4.8 Hz, 1H)
4	38.8	-	38.5	-
5	55.8	0.80 (*dd*, *J* = 12.2, 2.5)	55.3	0.77(*dd*, *J* = 2.4 Hz, 1H)
6	18.8	1.50 (*m*, 1H); 1.65 (*m*, 1H)	18.5	
7	41.3	1.36 (*dd*, *J* = 12.9, 4.0 Hz, 1H); 2.01 (*dt*, *J* = 12.8, 3.3 Hz, 1H)	41.1	2.01 (*dt*, *J* = 12.6, 3.0 Hz, 1H); 1.33 (*dt*, *J* = 12, 3.0 Hz, 1H)
8	39.1	-	38.8	-
9	49.1	1.42 (*m*, 1H)	48.9	1.42 (*m*, 1H)
10	37.9	-	37.7	-
11	17.4	1.50 (*m*, 1H);1.64 (*m*, 1H)	17.1	
12	33.4	1.53 (*d*, *J* = 3.2); 1.66 (*m*, 1H)	33.2	1.66 (*m*, 1H), 1.62 (*m*, 1H)
13	37.5	-	37.2	-
14	159.2	-	158.6	-
15	117.2	5.53 (*dd*, *J* = 8.2, 3.3 Hz, 1H)	115.6	5.51 (*dd*, *J* = 8.4, 3.0 Hz, 1H)
16	30.8	1.77 (*dd*, *J* = 15.4, 3.3 Hz, 1H); 2.14 (*dd*, *J* = 15.2,8.2 Hz, 1H)	30.4	2.14 (*dd*, *J* = 15.0, 8.4.0 Hz, 1H); 1.70 (*dd*, *J* = 3.0, 15.0 Hz, 1H)
17	40.4	-	40.2	-
18	44.8	0.63 (*dd*, *J* = 13.7, 3.8 Hz, 1H)	44.6	0.57 (*dd*, *J* = 13.8, 3.6 Hz, 1H)
19	35.8	1.05 (*m*, 1H); 1.43 (*m*, 1H)	35.6	1.00 (*dd*, *J* = 3.6, 13 Hz, 1H)
20	28.6	-	28.3	-
21	32.7	1.29 (*m*, 2H)	32.4	1.26 (*m*, 1H), 1.24 (*m*, 1H)
22	27.9	1.17 (*m*, 1H); 1.46 (*m*, 1H)	27.6	1.50 (*m*, 1H), 1.47 (*m*, 1H)
23	28.0	1.00 (*s*, 3H)	27.8	0.97 (s, 3H)
24	15.4	0.82 (*s*, 3H)	15.3	0.79 (s, 3H)
25	15.4	0.94 (*s*, 3H)	15.2	0.91 (s, 3H)
26	26.0	1.07 (*s*, 3H)	25.8	1.06 (s, 3H))
27	21.6	0.98 (*s*, 3H)	21.3	0.96 (s, 3H)
28	65.5	3.16 (*dd*, *J* = 10.9, 4.8 Hz, 1H); 3.31 (*dd*, *J* = 10.9, 5.3 Hz, 1H)	64.8	3.10 (*d*, *J* = 10.8 Hz, 1H)
29	33.5	0.99 (*s*, 3H)	33.3	0.969 (s, 3H))
30	29.9	0.92 (*s*, 3H)	29.6	0.89 (s, 3H)

3.2.1.7 Characterization of Compound 84

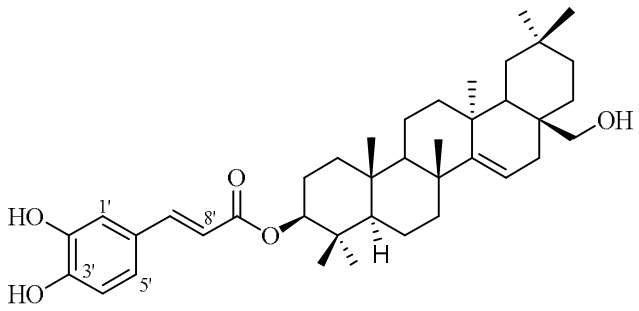

84

Compound **84** was isolated as a white powder with a melting point of 292–294 °C. The compound gave a dark blue spots on TLC with cerium ammonium molybdate spraying with the R_f value of 0.39 in $CHCl_3$:EtOAc (1:0.5). The IR spectrum (Appendix 85) showed the presence of O-H stretching at 3434.2 cm^{-1}, C-H stretching at 2937.8 cm^{-1} and 2868.4 cm^{-1}, C=O stretching at 1695.6 cm^{-1}, and C=C stretching at 1616.6 cm^{-1}. The molecular formula was found to be $C_{39}H_{56}O_5$, *via* the MALDI-MS (Appendix 84) at *m/z* 897.8 for $[M+(DHB-H_2O)_2+Na-2H]^+$ (calc. for $C_{39}H_{56}O_5$, 897.0) with a mass fragment ion peak at m/z 449.9 [M + Na – CH_3 –$PhCH_2CO$] and 425 [M –$PhCH_2CO_2$]. The ^{1}H-NMR (Appendix 77) and ^{13}C-NMR (Appendix 78) spectra of compounds **84** and **83** were nearly superimposable for the pentacyclic moiety. Differences were observed due to the signals of a *trans*-caffeoyl moiety in **84**. This group was identified in the ^{1}H-NMR from olefinic *trans* coupled proton signals at δ_H 7.45 (*d*, *J* = 15.8 Hz, H-7′) and 6.24 (*d*, *J* = 15.9 Hz, H-8′), and three aromatic proton signals at δ_H 6.76 (*d*, *J* = 8.1 Hz, H-4′), 7.00 (*dd*, *J* = 8.2, 2.1 Hz, H-5′), and 7.04 (*d*, *J* = 2.1 Hz, H-1′); the coupling relationship established a 1,3,4-substituted benzene ring.[145] In COSY spectrum, the second set of signals displayed seven singlet methyl proton signals at δ_H 1.04, 0.95, 0.94, 0.93, 0.92, 0.86, and 0.84 correlated with carbon resonances signals at δ_C 26.3, 33.9, 15.6, 21.8, 17.1, 30.2, and 28.2 respectively, which suggested the presence of a pentacyclic triterpenoid partial structure. In HSQC spectrum, a trisubstituted double bond proton signal at δ_H 5.58 (*dd*, *J* = 8.2, 3.2 Hz, 1H) correlated with carbon sinals at δ_C 116.4, 158.0, and a hydroxymethylene proton signals at δ_H 3.00 (*m*, 1H), 2.88 (*m*, 1H) correlated with a carbon signal at δ_C 63.5 C-28).

Table 13: ^{1}H (600 MHz), ^{13}C (151 MHz, DMSO-d6), HMBC (600 MHz) and COSY (600 MHz) NMR spectroscopic data of compounds **7.**

position	δc	δ_H	COSY	HMBC	position	δc	δ_H	COSY	HMBC
1	37.3	1.00 (H_1)	H_2-2	C-2, 3, 10	21	32.9	1.17(H_1)	H_1-22	C-20
		1.56 (H_2)	H_2-2	C-5, 10, 25			1.24(H_2)	H_2-22	C-17, 22, 20, 21, 30, 29
2	23.7	1.58(H_1)	H_1-1	C-1,3,4,10	22	27.8	1.00(H_1)	H_2-21	C-21
		1.63(H_2)	H_1-1	C-1,3,4,10			1.49(H_2)	H_2-21	C-20
3	80.2	4.49 (dd, *J* = 11.7, 4.5 Hz)	H_2--2	C-2, 4, 5, 23, 24, 9′	23	28.2	0.84		C-3, 4, 5, 24
4	37.9				24	17.1	0.92		C-3, 4
5	55.5	0.92	H_2-6	C-3, 6, 7, 9, 24, 25	25	15.6	0.94		C-1, 5, 9
6	18.7	1.49 (H_1)		C-4, 5, 7	26	26.3	1.04		C-7, 9, 14
		1.58(H_2)	H-5	C-4, 5, 7					
7	41.3	1.31(H_1)	H_2-6	C-9, 26	27	21.8	0.933		C-13, 14
		1.99(H_2)	H_1-7	C-5, 8, 9, 26					
8	38.9	-			28	63.5	2.89(H_1)	H_2-28	C-16, 17
							3.00(H_2)	H_1-28	C-16, 17, 22
9	48.9	1.44	H_2-11	C-5, 11, 25, 26	29	33.9	0.95		C-20, 21
10	37.8				30	30.2	0.87		C-19, 20, 21, 29
11	17.4	1.46 (H_1)	H_1-12	C-9, 12, 13	1′	115.2	7.04 (d, *J* = 2.1 Hz, 1H)		C-2′, 3′, 5′, 7′
		1.61(H_2)		C-8, 9, 13,					
12	33.6	1.47(H_1)	H_1-11	C-9, 11, 13, 14, 27	2′	146.2	-		
		1.61(H_2)		C-9, 11, 13, 14, 27					

13	37.4	-			3′	148.8	-		
14	158.0				4′	116.2	6.76 (d, *J* = 8.1 Hz, 1H-4′)	H-5′	C-2′, 3′, 5′, 6′
15	116.4	δ 5.58 (dd, *J* = 8.2, 3.2 Hz)	H_2-16	C-8, 13, 16, 17	5′	121.7	7.00 (dd, *J* = 8.2, 2.1 Hz, 1H),	H-4′	C-1′, 3′, 7′
16	30.6	1.56(H_1)		C-14, 15, 28	6′	125.9	-		
		2.12(dd, *J* = 14.8, 8.1 Hz) (H_2)	H-15	C-14, 15, 17, 18, 28					
17	40.5	-			7′	145.2	7.45 (d, *J* = 15.8 Hz)	H-8′	C-1′, 6′, 8′
18	45.0	0.47 (dd, *J* = 13.6, 3.6 Hz)	H_1-19	C-13, 17, 19	8′	114.9	6.24 (d, *J* = 15.9 Hz)	H-7′	C-6′, 9′
			H_2-19						
19	36.0	1.00(H_1)		C-18, 20, 30	9′	166.8	-		
		1.37(H_2)		C-18, 20, 30					
20	28.8								

In addition, there are ten methylene, ten methine and five quaternary carbon signals which suggested the presence of a taraxerane-type caffeoyl.[146] The HMBC (Appendix 82) spectrum showed correlation of H-3 at δ_H 4.49 with carbonyl carbon C-9′ at δ_C 166.8, indicating the caffeoyl group was attached to C-3 *via* an ester linkage. The relative configuration of the stereogenic center of **84** was deduced from the ^{1}H-^{1}H coupling constant and the NOESY experiment (Appendix 83). The typical coupling constant for H-3 (J = 11.7, 4.5 Hz) in the ^{1}H-NMR spectrum revealed that H-3 was in the α-orientation. The difference in the multiplicity with a larger coupling constant of H-3 in **84** was in agreement with the respective coupling patterns (axial-equatorial and axial-axial) of H-3 and H-2, indicating that H-3 is situated in an axial position.[147-148] Additionally, *α*-orientation of H-3, H-5, H-9, H-23, and H-27 was suggested by the NOESY interactions of H-3 to H-23/H-5 and H-9 to H-5/H-23/H-27. Thus, the structure of compound **84** was determined to be 3β-(3′, 4′-dihydroxy-*trans*-cinnamoyloxy)-D-friedoolean-14-en-3α, 28-diol and named with a trivial name 3β-*O*-trans-caffeoylisomyricadiol.

3.2.1.8 Characterization of Compound 85

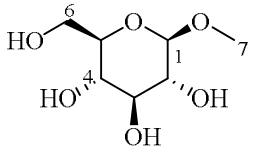

85

Compound **85** was isolated as a colorless crystal with a melting point of 104–106 °C. The compound gave a dark blue spots on TLC with cerium ammonium molybdate spraying with the R_f value of 0.25 in $CHCl_3$:MeOH (1:0.25). The IR spectrum showed the presence of O-H group at 3420 cm^{-1}, C-H stretching of CH_3, CH_2, and CH at 2928.2 cm^{-1} and 2858.6 cm^{-1}. The molecular formula was established as $C_7H_{14}O_6$ by an HPLC-ESI-MS (Appendix 92) at *m/z* 217.06848 for $[M+Na]^+$ (calcd for $C_7H_{14}O_6$, 217.06826). The ^{13}C-NMR (Table 14 and Appendix 87) and DEPT spectra (Table 14 and Appendix 88) showed seven carbon signals at δ_C 55.9 to δ_C 104.0, indicating the presence of a sugar moiety. These signals included a methyl, an oxymethylene, a methylene and five methine signals. The ^{1}H-NMR spectrum (Table 14 and Appendix 86) showed the proton signals at δ_H 3.18 and 4.19, which corresponds to the resonance location of protons on carbons linked to oxygen.

Table 14: ^{1}H-and ^{13}C-NMR data for compound **85**.

Position	**85** ^{1}H-NMR (600 MHz, MeOD) ^{13}C-NMR (151 MHz, MeOD)		**Lit.** [149] ^{1}H-NMR (500.16 MHz, D_2O) ^{13}C-NMR (125.78 MHz, D_2O)	
	δ_C	δ_H	δ_C	δ_H
1	104.0	4.19 (*d*, *J* = 7.8 Hz, 1H)	103.82	4.364
2	73.7	3.18 (*d*, *J* = 9.6 Hz, 1H)	73.75	3.247
3	76.7	3.36 (*t*, *J* = 8.8 Hz, 1H)	76.42	3.474
4	70.2	3.29 (*m*, 1H)	70.31	3.366
5	76.6	3.31 (*d*, *J* = 9.6 Hz, 1H)	76.57	3.447
6	61.4	3.89 (*m*, 1H); 3.69 (*dd*, *J* = 11.7, 6.6 Hz, 1H)	61.41	3.710;3.912
7	55.9	3.55 (*s*, 3H)	57.82	3.56

In the HSQC spectrum (Appendix 90), connectivities between H-1 (δ_H 4.19) and C-1 (δ_C 104.0), H-2 (δ_H 3.18) and C-2 (δ_C 73.7), H-3 (δ_H 3.36) and C-3 (δ_C 76.7), H-4 (δ_H 3.29) and C-4 (δ_C 70. 2), H-5 (δ_H 3.31) and C-5 (δ_C 76.6), and, H-6 (δ_H 3.89) and C-6 (δ_C 61.4) were indicative of a pyranoside. At δ_H 4.19, the anomeric proton (H-1) with the highest downfield doublet signal had a significant coupling constant ($^{3}J_{1,2}$ 7.8), which is typical of a β-linked glucopyranose ring. A singlet sigal at δ_H 3.55 was integrated for three protons, which was assigned to a methoxyl (OMe) protons. The HMBC spectrum (Appendix 91) showed correlation of the methoxy proton signal at δ_H 3.55 (*s*, 3H) with the anomeric carbon signal at δ_H 104.0, indicating a methoxy group was attached to C-1. Additionally, in HMBC spectrum, the anomeric proton signal at 4.19 (H-1) gave a strong cross-peak with a carbon signal at δ_C 73.7 (C-2), and this carbon signal gave cross-peaks with two proton signals at δ_H 3.36 (H-3) and 3.28 (H-4). A detailed analysis of ^{1}H-NMR and ^{13}C-NMR spectra (Table 14) and comparison with the literature[149] indicated the results were in line with those for methyl-β-D-glucopyranoside.

3.2.1.9 Characterization of Compound 86

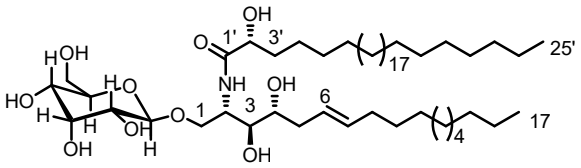

86

Compound 86 was isolated as an amorphous white powder with a melting point of 198-200 °C. The compound gave a dark blue spots on TLC with cerium ammonium molybdate spraying with the R_f value of 0.50 in $CHCl_3$:MeOH (1:0.25). The IR Spectrum showed broad absorption peak at 3436.1 cm^{-1} and 3418.2 cm^{-1} indicating the presence of –OH and NH group, aliphatic C-H stretching at 2920.4 and 2851.2 cm^{-1}, amide C=O stretching at 1746.8 cm^{-1} and, N-H bending at 1535.2 cm^{-1}, and C=C stretching at 1635.6 cm^{-1}. ^{1}H-NMR

spectrum (Table 15 and Appendix 93) revealed the proton resonance signals of two terminal methyl groups at δ_H 0.92, a broad signal range of methylene proton signals at δ_H 1.26-1.38, a sugar an anomeric proton signal at δ_H 4.30 (*d*, *J* = 7.7 Hz, 1H), carbinol proton signals appearing as multiplets between δ_H 4.04 and 3.20. Two olefinic proton signals at δ_H 5.44 (*m*, 2H-7) and 5.33 (*m*, H-6), attributable to the presence of one disubstituted double bond. A signal appearing at δ_H 4.30 (*dd*, *J* = 9.9, 7.4 Hz, 1H-2) was assigned to a methine proton vicinal to the nitrogen atom, clearly suggesting a cerebroside containing hydroxy fatty acid.[150]

Table 15: ^{1}H-and ^{13}C-NMR data for compound **86**

Position	**86** ^{1}H-NMR (600 MHz, MeOD) ^{13}C-NMR (151 MHz, MeOD)		Lit. [151] ^{1}H-NMR (400 MHz, CD_3OD) ^{13}C-NMR (100 MHz, CD_3OD)	
Sphingoid base moieties	δ_C	δ_H	δ_C	δ_H
1	68.6	4.07 (*dd*, *J* = 10.5, 6.3 Hz, 1H); 3.83 (*dt*, *J* = 10.5, 3.2 Hz, 1H)	68.5	4.02 (*m*, 1H); 3.79 (*dd*, *J* = 7.2; 14.8 Hz, 1H)
2	50.2	4.30 (*dd*, *J* = 9.9, 7.4 Hz, 1H)	50.3	(*m*, 1H)
3	74.1	3.62 (*t*, *J* = 6.1 Hz, 1H)	74.4	(*t*, *J* = 6.1Hz, 1H)
4	71.5	3.54 (*m,* 1H)	71.4	(*m*, 1H)
5	32.3	2.09 (*m,* 2H)	32.4	(*m*, 1H); 1.98 (*m*, 1H)
6	129.3	5.33 (*m*, 1H)	129.4	5.40 (*dt*, *J* =14.4 Hz, 1H)
7	129.5	5.44 (*m*, 1H)	130.4	5.46 (*dt*, *J* = 14.4 Hz, H)
8	32.4	1.98 (*m*, 2H)	32.0	1.64 (*m*, 1H)
9-16	22.3-31.4	1.26-1.38H (*brs*, 58H)	22.2-31.7	1.28-1.40 (*brs*, 58H)
17	13.1	0.92 (*t*, *J* = 6.9 Hz, 3H)	13.1	0.89 (*t*, *J* = 6.7 Hz, 3H)
N-acyl unit				
1′	175.7	-	176.2	-
2′	71.6	4.04 (*m*, 1H)	71.5	4.00 (*m*, 1H)
3′	34.3	1.76 (*m*, 1H); 1.62 (*m*, 1H)	34.4	1.73 (*m*, 1H); 1.63 (*m*, 1H
4′-24′	22.3-31.5	1.26-1.38 (*brs*, 58H)	22.2-31.7	1.28-1.40 (*brs*, 58H)
25′	13.1	0.92 (*t*, *J* = 6.9 Hz, 3H)	13.1	0.89 (*t*, *J* = 6.7 Hz, 3H)
β-glucopyranose moiety				
1″	103.3	4.30 (*d*, *J* = 7.7 Hz, 1H)	103.3	4.26 (*d*, *J* = 7.8 Hz, 1H)
2″	73.6	3.20 (*dd*, *J* = 9.3, 7.8 Hz, 2H)	73.6	3.20 (*m*, 2H)
3″	76.5	3.37 (*m*, 2H)	76.6	3.33 (*m*, 2H)
4″	70.1	3.29 (*m*, 2H)	70.2	3.26 (*dd*, *J* = 12.3; 4 Hz, 2H)
5″	76.6	3.29 (*m*, 2H)	76.0	3.27 (*m*, 2H)
6″	61.2	3.68 (*m*, 1H); 3.89 (*m*, 1H)	61.3	3.85 (*dd*, *J* = 11.2 Hz, 1H); 3.64 (*dd*, *J* = 4.4; 11.2 Hz, 1H)

The ^{13}C-NMR spectrum (Table 15 and Appendix 94) revealed carbonyl carbon signal at δ_C 175, amide carbon signal at δ_C 50.2 (C-2), methylene carbon signals at δ_C 22.3–31.5, two terminal methyl carbon signals δ_C 13.1 (C-17 and C-25′). One olefinic carbon signal at δ_C 129.3 (C-6) and 129.5 (C-7) were indicative of the presence of one double bond. In the ^{13}C-NMR spectrum, the six oxygenated carbon resonances signals were appeared at δ_C 61.2 (C-6″), 70.1 (C-4″), 73.6 (C-2″), 76.6 (C-5″), 76.5 (C-3″), and 103.3 (C-1″), revealing the presence of a glucopyranoside. [152] Besides the methine signals for a glucose unit, the ^{1}H-NMR spectrum (Table 15 and Appendix 93) of **86** also showed three other methine signals at δ_H 4.04 (*m*, H-2′), 3.62 (*m*, H-3) and 3.54 (*m*, H-4). Similarliy, ^{13}C-NMR spectrum (Table 15 and Appendix 94) showed methine carbon signals at δ_C 71.6 (C-2′), 74.1 (C-3) and 71.5 (C-4). Olefinic bond was confirmed to have a (*E*)-configuration as stated by Ai-Qun.[153] Typically, the signals of a carbon next to a *trans* double bond[153-154] appear between δ_C 32 and 33 while those of a *cis* double bond[155] appear between δ_C 27.0 and 28.0. ^{1}H-^{1}H COSY (Appendix 96) showed correlation of the proton signal of H-2 (δ_H 4.30) with proton signals of H_1-1 (δ_H 3.83) and H-3 (δ_H 3.62), a methylene proton at δ_H 2.09 (H-5) correlated with a olefinic proton H-6 (δ_H 5.33) and an oxymethine proton H-4 (δ_H 3.54). It also showed an oxymethine proton at δ_H 4.04 (H-2′) correlated to H-3′ at δ_H 1.76 and δ_H 1.62. COSY spectrum showed an oxymethine proton at δ_H 4.04 (H-2′) correlated with H-3′ at δ_H 1.76 and δ_H 1.62. The anomeric proton (H-1″) of the β-glucose unit exhibited a long-range HMBC correlation (Appendix 98) with C-1 at δ_C 68.6; indicating the glucose moiety was attached to C-1. In HMBC spectrum, the proton signals at 4.30 (*dd*, *J* = 9.9, 7.4 Hz, 1H-2) and 4.04 (*m*, 1H-2′) correlated with carbonyl signal at 175.7 (C-1′), indicated the acyl moiety is attached to NH of the sphingosine. In HMBC, proton signal of H-2 correlated with carbon signal of C-1 at δ_C 68.6, C-3 at δ_C 74.1 and C-4 at δ_C 71.5. HMBC spectrum showed the proton signal at δ_H 2.09 (H-5) and 1.98 (H-8) correlated with carbon signal at δ_C 129.3 (C-6) and 129.5 (C-7), respectively, indicating the double bond was attached at C-5 and C-8. Based on the spectroscopic data (Table 15) and comparison with the literature data, compound **86** was determined to be contortamide.[151]

3.2.2 Biological Activities of the Crude Extract and Isolated Compounds from the Stem Barks of *Myrica salicifolia*

3.2.2.1 DPPH Radical Scavenging Assays of the Crude Extract and Isolated Compounds from Stem Barks of *Myrica salicifolia*

The antioxidant capacities of the isolated compounds, expressed as the DPPH free radical inhibition and the IC_{50} values, are presented in Table 16. According to antioxidant activity parameters, the IC_{50} value category is very strong if the IC_{50} value is <10μg/mL, strong if the IC_{50} value is between 10 and 50 μg/mL, mild if the IC_{50} value is between 50 and 100

μg/mL, weak if the IC_{50} value is between 100 and 250 μg/mL, and not active if IC_{50} is above 250 μg/m.[156] The relative IC_{50} values for the isolated compounds were in the range of 4.83 μg/mL – 138 μg/mL (Table 16). Compound **28** (IC_{50} = 4.83 μg/mL) showed the highest antioxidant activity compared to other isolated compounds, while compound **85** (IC_{50} = 138 μg/mL) showed the lowest antioxidant activity. The IC_{50} values recorded for diarylheptanoid compounds **29**, **32**, and **28** were 6.96 μg/mL, 4.85 μg/mL, and 4.83 μg/mL, respectively, whereas 120.84 μg/mL, 120.78 μg/mL, 26.26 μg/mL, and 14.48 μg/mL were reported for compounds **81**, **82**, **83**, and **84**, respectively. In diarylheptanoid compounds, the most susceptible OH group is the phenolic hydroxyl group, which confirms the importance of the enolic-OH moiety for the highest antioxidant activity of compound **28**. The presence of the ketone functional group in compound **29** and the sugar moiety in compound **32** might be responsible for their reduced-antioxidant activity in comparison to compound **28**.[157-158] Of the triterpenoid compounds, compound **84** has a phenylpropanoid moiety, which increases its antioxidant activity compared to other terpenes. This suggests that the phenylpropanoid moiety is an essential functional group for the observed antioxidant activity.

Table 16: Percent radical scavenging activity and IC_{50} values of the isolated compounds.

Cpds	% DPPH inhibition at					r^2	IC_{50} (μg/mL)
	50 μg/mL	25 μg/mL	12.5 μg/mL	6.25 μg/mL	3.12 μg/mL		
28	79.59	68.98	58.91	46.59	35.59	0.99	6.96
29	88.86	86.68	79.06	67.45	52.74	0.93	4.83
32	82.10	76.92	67.30	57.33	45.30	0.98	4.84
81	35.71	26.73	24.13	22.26	20.85	0.84	120.84
82	31.78	27.33	24.91	23.14	21.65	0.95	120.78
83	52.22	41.74	31.26	25.57	22.54	0.95	26.26
84	96.23	87.32	46.23	24.15	13.88	0.95	14.48
85	33.69	27.36	24.21	22.28	20.59	0.92	138
Ascorbic acid	97.32	97.27	97.25	97.19	96.96	0.81	0.31

Note: r^2 - coefficient of determination; IC_{50} - half maximal inhibitory concentration.

3.2.2.2 Antibacterial Activities of the crude Extract and Compounds of the Stem Barks of *Myrica salicifolia*

The *in-vitro* antibacterial activities of compounds **28-29, 32, 81**–**84** against gram-positive (*S. aureus* and *S. pyogenes*) and gram-negative (*E. coli* and *P. aeruginosa*) bacterial strains were examined at doses of 250 µg/mL and 500 µg/mL compared with 10 µg/mL of positive controls. The measured inhibition zones of the compounds are presented in Table 17.

Table 17: Antibacterial activities of isolated compounds

Bactria strains:	Gram-positive bacteria				Gram-negative bacteria			
	S. pyogenes		*S. aureus*		*P. aeruginosa*		*E. coil*	
Conc. (µg/ml):	250	500	250	500	250	500	250	500
28	8.0	9.0	7.5	8.5	7.0	8.0	7.0	8.0
29	9.0	10.5	8.5	10.0	8.0	9.0	8.0	9.0
32	10.0	11.5	9.0	10.5	8.5	10	9.0	11.0
81	7.5	8.0	7.0	7.5	6.5	7.0	6.5	7.5
82	8.0	9.0	8.0	8.5	7.0	8.0	7.0	8.0
83	9.0	10.0	8.5	9.0	7.5	8.5	8.0	9.0
84	10.0	11.0	9.0	10.0	8.0	9.0	8.5	10.0
Amp	14.0	-	13.0	-	12.5	-	13.0	-

Note: **28**-**84**: compounds, Amp: Ampicillin (+ve control), Conc: concentration.

The inhibition zone for the seven isolated compounds against *E. coli* ranges from 6.5 to 9.5 mm at a concentration 250 µg/mL. The compound having better activity against *E. coli* was compound **32** (inhibition zone of 9.0 mm) compared to other isolated compounds. Compounds **32** (10.0 mm) and **84** (10.0 mm) displayed the highest activity against *S. pyogenes*, while compound **81** showed the lowest inhibition zone (7.0 mm) against *S. aureus*, followed by compounds **83** (8.5 mm) and **84** (9.0 mm). Against the gram-negative bacteria *P. aeruginosa*, the highest activity was recorded for compound **32** (8.5 mm), followed by compound **84** (8.0 mm) at a concentration of 250 µg/mL. The results of the present study generally indicate that compounds **32** and **84** displayed better activities to inhibit the growth of both gram-positive and gram-negative bacterial strains compared to other compounds, and the lowest activity was exhibited by compound **81**. All the isolated compounds showed relatively weaker activities compared to the standard drugs ampicillin and ciprofloxacin. However, compared to the growth of gram-negative bacteria, it was more effective against the growth of gram-positive bacteria. Several studies suggest that

the antibacterial activity of polyphenols is generally more effective against Gram-positive than Gram-negative bacteria due to cell walls linked to a molecularly complex outer membrane that slows down the passage of chemicals.[159] The results from this study suggest that the higher antibacterial and antioxidant activity of compounds **32** and **84** could be attributed to the complex phenolic compounds. In the case of compound **32** with the skeletal structure of two aromatic rings linked together with seven carbon chains and possesses strong nucleophilic properties, which may allow it to donate an electron pair to electrophilic functional groups of plasma membrane proteins and/or lipids, probably leading to membrane dysfunction.[160] For the activity displayed by compound **84**, the presence of caffeoyl group might be responsible. In this finding, compounds **32** and **84** showed better antibacterial activites than the other isolated compounds.

3.3 Phytochemical Investigation of the Roots of *Myrica salicifolia*

Phytochemical analysis of the roots extract of *M. salicifolia* resulted in the isolation of five compounds, namely taraxerol (**82**), β-sitosterol (**80**), sitoindoside I (**87**), myricanone (**28**), and myricanol 5-*O*-β-D-glucopyranoside (**30**). DPPH radical scavenging activities of the isolated compounds and crude extrac were also determined in this study. The compounds showed a wide range of DPPH scavenging activities from very weak (IC_{50} = 368.75 µg/ml) to very strong (IC_{50} = 2.97 µg/ml).

3.3.1 Characterization of Essential Oil of the Roots of *Myrica salicifolia*

The essential oils from the roots of *Myrica Salicifolia* samples were extracted by hydrodistillation following the method described by Katekar.[116] Plant material (536 g) was hydrodistilled to afford clear colorless oil (0.2 mL). The essential oil was then analyzed by gas chromatography-mass spectroscopy (GC-MS). An Agilent Technologies 7820A GC system with Agilent Technologies 5977E MSD was used for the analysis. The physical properties of the essential oil and its main compound are given in Table 18, and the chemical constitution of the essential oil in Table 18. The GC-MS analysis of the essential oil of the roots of *Myrica Salicifolia* revealed the presence of 5 major compounds with qualities greater than 80% after comparing the data with NIST mass spectral database (Figure 9 and Table 6). The analyzed essential oil was composed of different compounds

of different metabolite classes: sesquiterpenoids, fatty group and aromatic phenols, aliphatic alcohols, hydrocarbons, and terpenes. The major volatile compounds were *n*-hexadecanoic acid (46.69%), 1-ethyl-2,4-dimethylbenzene (7.30%), *E*-7-dodecen-1-ol acetate (7.29%) and dicumene (6.86%), and *trans*-α-Bergamotene (5.34%). Scientific reports revealed that some of the identified compounds have a considerable potential for therapeutic use. For example, n-hexadecanoic acid is the major volatile organic compound that has hypocholesterolemic, antioxidant, anti-inflammatory, nematicide, and pesticide.[161] Whereas, *E*-7-dodecen-1-ol acetate, the third major component of in the essential oil has adverse effects on target pests like *Eucosma gloriola* (Eastern pine shoot borer). The other eight bioactive components of the essential oil, with their various pharmacological activities have been reported in many studies as antioxidant, anticancer, antiulcer, anticonvulsant, antihypertensive, antibacterial, anti-nociceptive and anti-inflammation activities.[162-163] The *trans*-α-bergamotene compound has been identified as an active compound that can attract ectoparasites such as *Melittobia digitata* (wasps), serving as a trapping strategy, where pests are attracted away from the main crop.[164] (-)-Tau-muurolol has a role as a plant metabolite, a fungicide, a volatile oil component, a marine metabolite and a bacterial metabolite.[165]

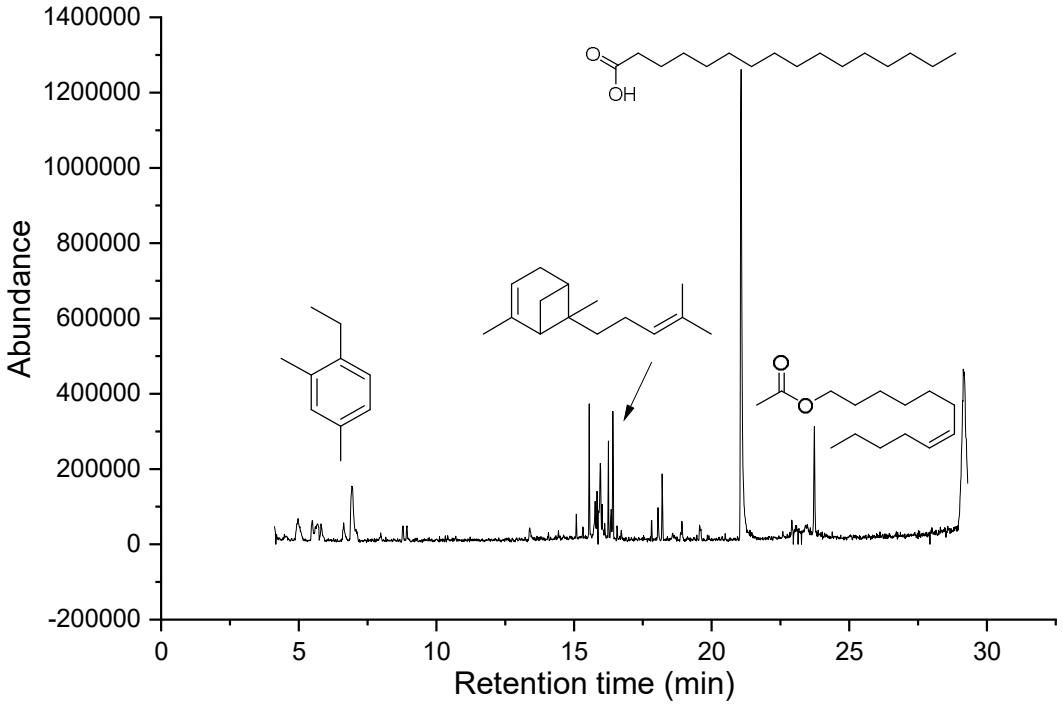

Figure 9: GC-MS chromatogram of the essential oil of roots of *Myrica Salicifolia*.

Table 18: Compounds identified from the essential oil of the roots of *Myrica salicifolia* by GC-MS.

PK	RT	Peak Pct	Compound names	Structure of compounds	Q	CF
1	6.93	7.30	1-Ethyl-2,4-dimethylbenzene	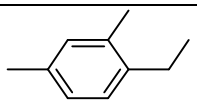	82	$C_{10}H_{14}$
2	15.83	2.19	Cadina-1,3,5-triene	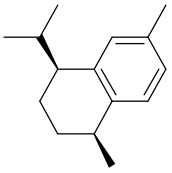	55	$C_{15}H_2$
3	15.96	6.86	Dicumene	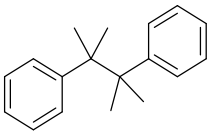	95	$C_{15}H_{24}O$
4	16.25	3.56	(-)-*Tau-muurolol*	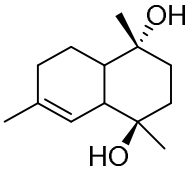	90	$C_{15}H_{26}O$
5	16.42	5.34	*trans*-α-Bergamotene	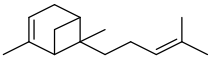	99	$C_{14}H_{28}O_2$
6	18.21	3.03	Hexahydrofarnesyl acetone	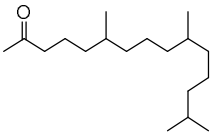	78	$C_{18}H_{36}O$
7	21.07	46.69	n-Hexadecanoic acid	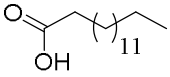	78	
8	23.73	7.29	*E*-7-Dodecen-1-ol acetate	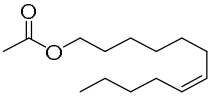	91	$C_{16}H_{32}O_2$

Pk = peak number, Rt = retention time (min), Area Pct. = area percentage, Q = quality

3.3.2 Characterization of Compounds Isolated from the Roots of *Myrica salicifolia*

3.3.2.1 Characterization of Compound 82

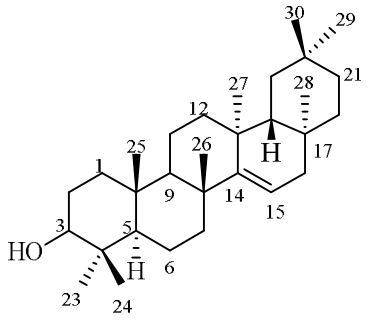

82

Compound **82** was isolated as a white solid with a melting point of 281–282 °C. The IR spectrum showed the presence of O-H stretching at 3492.4 cm^{-1}, C-H stretching at 2930.8 cm^{-1} and 2851.2 cm^{-1}, and C=C stretching at 1634.2 cm^{-1}. The molecular formula was deduced to be $C_{30}H_{50}O$ using the TOF-ESI-MS (Appendix 105) at *m/z* 472.6723 for $[M+2Na]^+$ (calc. for $C_{30}H_{50}ONa$, 472.6980). The ^{1}H-NMR (Table 19 and Appendix 99), ^{13}C-NMR (Table 19 and Appendix 100), COSY (Appendix 102), and HMBC spectra (Appendix 104) of this compound were similar with previously isolated compound **82** from leave of the *Myrica salicifolia* in this study. Therefore, it was established that compound **82** has the structure that is shown by comparing with reported literature data.[166]

Table 19: ^{1}H-and ^{13}C-NMR data for compound **82**.

Position	**82** ^{1}H-NMR (400 MHz, $CDCl_3$) ^{13}C-NMR (1oo MHz, $CDCl_3$)		Lit.[166] ^{1}H-NMR (400 MHz, $CDCl_3$) ^{13}C-NMR (100 MHz, $CDCl_3$)	
	δ_C	δ_H	δ_C	δ_H
1	37.7	0.98 (*m*, 1H),1.63 (*m*, 1H)	38.1	0.99;1.63
2	27.2	1.59 (*m*, 1H); 1.63 (*m*, 1H)	27.3	1.62
3	79.1	3.22 (*dt*, *J* = 10.6, 5.1 Hz, 1H)	79.2	3.19 (*dd*, *J* = 11.2, 4.8 Hz, 1H)
4	38.9	-	38.9	
5	55.5	0.80 (*m*, 1H)	55.7	0.88
6	18.8	1.50 (*m*, 1H); 1.63 (*m*, 1H)	18.9	1.62;1.45
7	41.3	1.37 (*m*, 1H); 2.06 (*dt*, 12.8, 3.3 Hz, 1H)	41.5	1.36;2.03
8	38.8	-	39.1	
9	48.8	0.98 (*m*, 1H)	48.9	1.43
10	38.0	-	37.9	
11	17.5	1.44 (*m*, 1H); 1.63 (*m*, 1H)	17.7	1.63;1.49
12	33.1	1.26 (*m*, 1H); 1.37 (*m*, 1H)	33.2	1.53;1.64
13	37.6	-	37.9	
14	158.1	-	158.2	
15	116.9	5.56 (*d*, *J* = 8.2, 3.2 Hz, 1H)	117.0	5.53 (*dd*, *J* = 8, 3.2 Hz, 1H)
16	37.7	1.63 (*m*, 1H); 1.94 (*dd*, *J* = 14.8, 3.2 Hz, 1H)	36.8	1.59; 1.92(*dd*, *J* = 14.8, 3.2 Hz, 1H)
17	35.8	-	35.3	
18	49.3	1.44 (*m*, 1H)	49.4	0.99
19	36.7	1.00 (*m*, 1H); 1.33 (*m*, 1H)	37.7	1.02;1.33
20	28.8	-	28.9	
21	33.7	1.25 (*m*, 1H); 1.59 (*m*, 1H)	33.8	1.25;1.38
22	35.1	1.04 (*m*, 1H); 1.38 (*m*, 1H)	35.9	1.00;1.38
23	28.0	1.00 (*s*, 3H)	28.2	0.97
24	15.5	0.95 (*s*, 3H)	15.6	0.80
25	15.4	0.83 (*s*, 3H)	15.6	0.92
26	25.9	1.11 (*s*, 3H)	26.1	1.10
27	21.3	0.93 (*s*, 3H)	21.5	0.91
28	29.8	0.85 (*s*, 3H)	29.9	0.82
29	33.4	0.97 (*s*, 3H)	33.5	0.95
30	29.9	0.93 (*s*, 3H)	30.1	0.91

3.3.2.2 Characterization of Compound 80

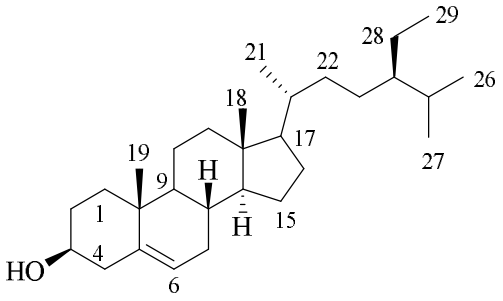

80

Compound 80 was isolated as an amorphous white powder with a melting point of 133-135°. The IR Spectrum showed the presence of O-H stretching at 3424.6 cm^{-1}, aliphatic C-H stretching at 2928 and 2849.2 cm^{-1} and C=C stretching at 1618.4 and 1645 cm^{-1}. Moreover, this result was further supported by the TOF-MS (Appendix 112) analysis that gave a *m/z* at 416.2167 for $[M+2H]^{2+}$, corresponds to the molecular formula of $C_{29}H_{50}O$ (calc 414.7077). ^{1}H-NMR (Table 20 and Appendix 106), ^{13}C-NMR (Appendix 107), DEPT (Appendix 108), and COSY (Appendix 109) spectra of compound (**80)** were similar with previously isolated compound from leave of the *Myrica salicifolia* in this study. Comparison of the spectroscopic data of **80** with those reported in the literature for β-sitosterol showed that the two compounds are identical.[137]

Table 20: ^{1}H- and ^{13}C-NMR data for compound **80**.

Position	**80** ^{1}H-NMR (600 MHz, DMSO-d_6) ^{13}C-NMR (151 MHz, DMSO-d_6)		**Lit.**[137] ^{1}H-NMR (300 MHz, $CDCl_3$) **^{13}**C-NMR (100 MHz, $CDCl_3$)	
	δ_C	δ_H	δ_C	δ_H
1	37.3	1.07 (*m*, $1H_2$); 1.83 (*m*, $1H_1$)	37.2	1.08;1.83
2	31.7	1.48 (*m*, 1H);1.80 (*m*, 1H)	31.6	1.49;1.82
3	71.8	3.53 (*tt*, *J* = 10.7, 4.7 Hz, 1H)	71.8	3.53
4	42.4	2.22 (*m*, 1H-);2.27 (*m*, 1H)	42.27	2.24;2.28
5	140.8	-	140.7	-
6	121.7	5.35 (*dd*, *J* = 5.1, 2.6 Hz, 1H)	121.7	5.35 (*J* = 4.7 Hz)
7	31.8	1.57 (*m*, 1H);1.98 (*m*, 1H)	31.9	1.59;1.98
8	31.8	1.48 (*m*, 1H)	31.9	1.49
9	50.2	0.93 (*m*, 1H)	50.1	0.94
10	36.5	-	36.5	-
11	21.0	1.48 (*m*, $1H_2$); 1.50 (*m*, $1H_1$)	21.06	1.45;1.48
12	39.5	2.00 (*tt*, *J* = 14.6, 3.1 Hz, $1H_1$); 1.15 (*m*, $1H_2$)	39.8	1.15; 1.97
13	42.4	-	42.19	-
14	56.8	1.07 (*m*, 1H)	56.7	1.03
15	24.4	1.55 (*d*, *J* = 6.5 Hz, $1H_1$); 1.01 (*m*, 1H)	24.3	1.05;1.55
16	27.9	1.86 (*m*, $1H_1$);1.27 (*m*,$1H_2$)	28.2	1.24
17	56.0	1.11 (*m*, 1H)	56.0	1.13
18	11.8	0.68 (*s*, 3H)	11.97	0.68(*s*, 3H)
19	19.2	1.00 (*s*, 3H)	19.4	1.01(*s*, 3H)
20	36.2	1.36 (*m*, 1H)	36.1	1.36
21	18.9	0.93 (*d*, *J* = 6.5 Hz, 3H)	18.8	0.94(*d*, 3H)
22	33.9	1.37 (*m*, 1H);1.05 (*m*, 1H)	33.9	1.32
23	26.0	1.14 (*m*, 2H)	26.0	1.15
24	45.7	0.92 (*m*, 1H)	45.8	0.93
25	29.2	1.65 (*m*, 1H)	29.1	1.65
26	19.4	0.80 (*d*, *J* = 2.3 Hz, 3H)	19.02	0.82 (6.3 Hz, 3H)
27	19.9	0.82 (*d*, *J* = 7.6 Hz, 3H)	19.8	0.83 (6.1 Hz, 3H)
28	22.8	1.26 (*m*, 2H)	23.0	1.22
29	11.8	0.84 (*d*, *J* = 6.5 Hz, 3H)	11.8	0.85

3.3.2.3 Characterization of Compound 87

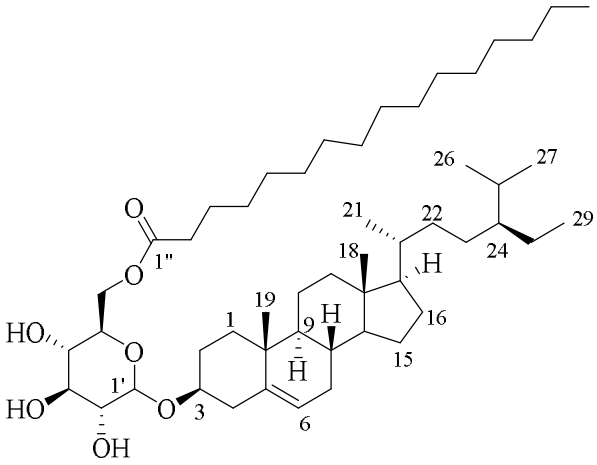

87

Compound 87 was isolated as an amorphous white powder with a melting point of 198-200 °C. The compound gave a dark blue spots on TLC with cerium ammonium molybdate spraying with the R_f value of 0.83 in $CHCl_3$:MeOH (1:0.25). The IR spectrum showed a broad absorption band of O-H group at 3432.8 cm^{-1}, aliphatic C-H stretching at 2918.2 and 2851.6 cm^{-1}, C=O stretching of ester at 1747.6 cm^{-1}, and C=C stretching at 1625.6 cm^{-1}. The molecular formula was established to be $C_{51}H_{90}O_7$ from TOF-ESI-MS (Appendix 119) at *m/z* 815.6644 for $[M]^+$ (calcd for $C_{51}H_{90}O_7$ 815.2580). ^{1}H-NMR spectrum (Table 21 and Appendix 113) of steroidal skeleton revealed the presence of two angular methyl singlet signals at δ 0.68 (H-18) and 1.00 (H-19), three methyl doublet signals at δ_H 0.93 (*d*, *J* = 6.3 Hz, 3H-21), 0.83 (*d*, *J* = 7.0 Hz, 3H-27), and 0.81 (*d*, *J* = 7.0 Hz, 3H-26), one olefinic proton signal at δ_H 5.39 (*dd*, *J* = 5.1, 2.6 Hz, H-6), oxymethine proton signal as multiples at δ_H 3.58 (H-3), oxymethine and oxymethylene proton peaks of a hexose unit signals between H-1' (δ_H 4.39) to H-4' (δ_H 3.4), and H-2" (δ_H 2.35) to H-16" (δ_H 0.89) for a long aliphatic chain. The signal at δ_H 4.39 (*d*, *J* = 7.8 Hz) was assigned to the anomeric proton (H-1') of the glucose moiety. ^{13}C-NMR (Table 21 and Appendix 114) and DEPT spectra (Table 21 and Appendix 115) showed seven methyls, fourteen methines, and four quaternary carbons. It revealed a carboyl carbon signal at δ_C 174.0, sugar moiety carbon signals at δ_C 63.4-101.2 and aliphatic chain carbon signals at δ_C 14.2-34.3. The carbon signals at δ_C 140.3 (C-5) and 122.2 (C-6) indicated the presence of a double bond. The

carbon signal at δ_C 19.4 and 11.9 was assigned to angular methyl carbon. The methine carbon signal at δ_C 79.7 indicated the hydroxyl group was attached to C-3. The COSY spectrum (Appendix 116) showed a multiples at δ_H 3.58 (*d*, *J* = 8.8 Hz, 3H-3) correlated with δ_H 2.36 (H-4). Olefinic methine proton at δ_H 5.39 (*d*, *J* = 5.6 Hz, 1H-6) was linked to H_1-7 at δ_H 1.99 for a methylene proton. A doublet signal of methyl at δ_H 0.93 (*d*, *J* = 6.3 Hz, 3H-21) correlated with a methine proton signal at δ_H 1.35 (*m*, 1H-20). A methyl signals at δ_H 0.83 (*d*, *J* = 7.0 Hz, 3H-27) and δ_H 0.81 (*d*, *J* = 7.0 Hz, 3H-26) correlated with a methine proton H-25 at δ_H 1.66. In the HSQC spectrum (Appendix 117), a proton signal at δ_H 3.58 (1H-3) correlated with carbon signal at δ_C 79.70 (C-3). The signal at δ_H 5.39 (*d*, *J* = 5.6, Hz, 1H-6) correlated with olefinic methine carbon signal at δ_C 122.2 (C-6) indicated the presence of double bond. Three doublet signals of methyl at δ_H 0.93 (*d*, *J* = 6.3 Hz, 3H), 0.81 (*d*, *J* = 7.0 Hz, 3H) and 0.83 (*d*, *J* = 7.0 Hz, 3H) correlated with a methine carbon at δ_C 18.8 (C-21), 19.0 (C-26), and 19.8 (C-27), respectively. The two singlet signals at δ_H 1.00 (*s*, 3H) and 0.68 (*s*, 3H) corresponds to angular methyl carbon signals at δ_C 19.38 (C-19) and 11.87 (C-18), respectively. A proton signal at δ_H 0.85 (*m*, 3H) correlated with C-29 at δ_C 11.99. The HMBC Spectrum (Appendix 118) of compound **87** showed that a carbon signal at δ_C 140.3 (C-5) correlated to H-4 at δ_H 2.36 (*m*, 1H), and δ_H 0.91 (*m*, H-9) indicating the double bond was attached to C-7, C-4, and C-10. The proton singlet signals at δ_H 1.00 (3H-19) correlated to the carbon signal at δ_C 37.3 (C-1), 36.7 (C-10), 50.2 (C-9), and 140.3 (C-5) indicating the angular methyl protons was attached to C-20. The protons singlet signal at δ_H 0.68 (3H-18) correlated with the carbon signals at δ_C 39.8 (C-12), 42.3 (C-13), 56.8 (C-14), and 56.1 (C-17) confirmed the angular methyl group was to C-13. A doublet methyl proton signals at δ_H 0.81 (3H-26) connected to C-25 at δ_C 29.1, C-24 at δ_C 45.8, and C-27 at δ_C 19.8. similarly, a doublet methyl proton signal at δ_H 0.83 (3H-27) correlated with C-25 at δ_C 29.1, C-24 at δ_C 45.8 and C-26 at δ_C 19.0, indicated the two methyl groups were attached to C-25. In HMBC spectrum, the anomeric proton signal at δ_H 3.58 (*d*, *J* = 8.8 Hz, 1H-3) correlated with C-1' (101.2) of the sugar moiety, indicating the steroid moiety was attached to C-1' of the sugar moiety. This was also confirmed by the de-shielded position of the C-3 at δ_C 79.7 compared to **80** (δ_C 71.8). The presence of the extra fatty acid moiety of **87** in comparison to **80** was evidenced by the presence of peaks corresponds to the long CH_2 chain in the upfield region of the ^1H and ^{13}C-NMR

spectra. The aliphatic chain was attached to C-6′ position of the glucose unit through an ester linkage. This fact was confirmed by the long range HMBC correlations observed between the carbonyl carbon at δ_C 174.0 of the ester moiety and the diasterotopic protons H_1-6 and H_2-6 of the sugar unit. All of the observed long-range correlations spectral data and the literature were in line with the compound **87** structure. The spectroscopic data of compound **87** (sitoindoside I or sitosteryl (6'-*O*-palmitoyl)-3-beta-D-glucopyranoside) is in agreement with those reported in the literature.[167] This is the first report of the isolation of **87** from this plant and from the genus Mayrica.

Table 21: ^{1}H- and ^{13}C-NMR data for compound **87**.

Position	**87** ^{1}H-NMR (400 MHz, $CDCl_3$) ^{13}C-NMR (101 MHz, $CDCl_3$)		Lit. [167] ^{1}H-NMR (600 MHz, $CDCl_3$) ^{13}C-NMR (150 MHz, $CDCl_3$)	
β-Sitosterol	δ_C	δ_H	δ_C	δ_H
1	37.3	1.86 (*m*, 1H); 1.06 (*m*, 1H)	37.27	1.06 (*m*); 1.85 (*m*)
2	29.7	1.95 (*m*, 1H); 1.61 (*m*, 1H)	29.70	1.61 (*m*); 1.95 (*m*)
3	79.7	3.58 (*d*, *J* = 8.8 Hz, 1H)	79.64	3.54 (*m,* 1H)
4	38.9	2.36 (*m*, 1H), 2.26 (*m,* 1H)	38.91	2.27 (*m,* 1H); 2.36 (*m,* 1H)
5	140.3	-	140.30	-
6	122.2	5.39 (*d*, *J* = 5.6 Hz, 1H).	122.14	(*m*, 1H)
7	31.9	1.26 (*m*, 1H); 1.99 (*m*, 1H)	31.94	1.98 (*m,* 2H)
8	31.9	1.50 (*m*, 1H)	31.88	1.52 (*m,* 1H)
9	50.2	0.91 (*m*, 1H)	50.14	0.93 (*m,* 1H)
10	36.7	-	36.70	-
11	21.1	1.49 (*m*, 2H)	21.04	1.02 (*m*);1.56 (*m*)
12	39.8	2.03 (*m*, 1H); 1.15 (*m*, 1H)	39.76	1.18 (*m*), 2.02 (*m*)
13	42.3	-	42.33	-
14	56.8	0.99 (*m*, 1H)	56.76	(*m*)
15	24.3	1.60 (*m,*1H);1.00 (*m,*1H)	24.30	1.08 (*m*);1.12 (*m*)
16	28.3	1.85 (*m*, 2H)	28.26	1.83 (*m*);1.86 (*m*)
17	56.1	1.11 (*m*, 1H)	56.11	1.12 (*m*)
18	11.9	0.68 (*s*, 3H)	11.85	0.68 (*s*)
19	19.4	1.00 (*s*, 3H)	19.37	(*s,* 3H)
20	36.2	1.35 (*m*, 1H)	36.19	1.36 (*m*)
21	18.8	0.93 (*d*, *J* = 6.3 Hz, 3H)	4.18.76	0.92 (*d*, *J* = 6.4, 3H)
22	33.9	1.32 (*m*, 1H);1.00 (*s*, 1H)	33.92	1.34 (*m*), 1.00 (*s*)
23	26.1	1.15 (*m*, 2H)	26.10	1.18 (*m,* 2H)

24	45.8	0.93 (*m*, 1H)	45.81	0.95 (*m*)
25	29.1	1.66 (*m*, 1H)	29.10	1.66 (*m*)
26	19.0	0.81 (*d*, *J* = 7.0 Hz, 3H)	19.02	(*d*, *J* = 6.8, 3H)
27	19.8	0.83 (*d,* *J* = 7.0 Hz, 3H)	19.82	(*d*, *J* = 6.8, 3H)
28	23.1	1.26 (*brs*)	23.06	1.26 (*bs*)
29	12.0	0.85 (*m*, 3H)	11.97	0.84 (*t,* *J* = 7.6, 3H)
Glucopyranoside				
1′	101.2	4.39 (*d,* *J* = 7.8 Hz, 1H)	101.24	4.38 (*d*, *J* = 7.7, 1H)
2′	73.8	3.5 (*td*, *J* = 9.0, 4.4 Hz, 1H)	73.45	3.35 (*dd*, *J* = 7.7, 8.7, 1H)
3′	76.1	3.58 (*d*, *J* = 8.8 Hz, 1H	76.07	3.57 (*dd*, *J* = 8.7, 9.9, 1H)
4′	70.2	3.40 (*td*, *J* = 9.0, 4.4 Hz, 1H)	70.23	3.38 (*dd*, *J* = 9.9, 8.6, 1H)
5′	73.5	3.37 (*m*, 1H)	73.82	3.45 (*m,* 1H)
6′	63.4	4.31 (*d*, *J* = 12.1 Hz, 1H); 4.39 (*d*, *J* = 12.1 Hz, 1H)	63.41	4.42 (*dd*, *J* = 12.1, 5.3, 1H) 4.29 (*dd*, *J* = 12.1, 1.7, 1H)
Palmitic acid				
1″	174.0	-	174.56	-
2″	34.3	2.35 (*t*, *J* = 8.1 Hz, 2H)	34.26	2.34 (*t*, *J* = 7.6, 2H)
3″	25.0	1.61 (*m*, 2H)	24.97	1.61 (*m*)
4″	29.3	1.26 (brs)	29.26	1.28 (bs)
5″	29.4	1.26 (brs)	29.45	1.26 (bs)
6″	29.8	1.26 (brs)	29.68	1.26 (bs)
7″-12″	29.6	1.26 (brs)	29.78	1.26 (bs)
13″	29.3	1.26 (brs)	29.40	1.26 (bs)
14″	32.0	1.26 (brs)	31.90	1.26 (bs)
15″	22.7	1.28 (brs)	22.70	1.30 (bs)
16″	14.2	0.89 (*t*, 7.1 Hz, 3H)	14.13	0.88 (*t*, *J* = 7.1 Hz, 3H)

3.3.2.4 Characterization of Compound 28

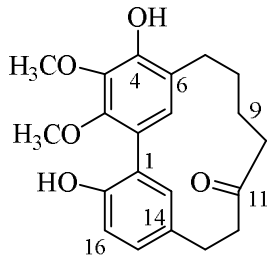

28

Compound 28 was isolated as a white powder with a melting point of 187-192 °C. The IR spectrum revealed the presence of O-H stretching at 3424.4 cm^{-1}, C-H stretching 2919.2 cm^{-1} and 2854.9 cm^{-1}, C=O stretching at 1705.2 cm^{-1}, C=C stretching at 1642.2 cm^{-1} and 1613.2 cm^{-1}. The molecular formula was established as $C_{21}H_{24}O_5$ by the sodiated-molecular-ion peak in the TOF-ESI-MS (Appendix 125) at *m/z* 379.1512 for $[M+Na]^+$ (calcd for $C_{21}H_{24}O_5Na$, 379.1516). Comparsion of its ^1H and ^{13}C-NMR data (Table 22)

with the previous reported literature[139], compound **28** was identified to be myricanone. Myricanone (**28**) was previously isolated from the $CHCl_3$-MeOH extract of the leaves of *Myrica salicifolia* in this study.

Table 22: ^{1}H-and ^{13}C-NMR data for compound **28**.

Position	DEPT-135	**28** ^{1}H-NMR (400 MHz, $CDCl_3$) ^{13}C-NMR (101 MHz, $CDCl_3$)		**Lit.** [139] ^{1}H-NMR (400 MHz, $CDCl_3$) ^{13}C-NMR (100 MHz, $CDCl_3$)	
		δ_C	δ_H	δ_C	δ_H
1	C	125.5	-	125.5	-
2	C	123.2	-	123.3	-
3	C	146.0	-	146.1	-
4	C	138.6	-	138.8	-
5	C	147.8	-	147.9	-
6	C	123.1	-	123.1	-
7	CH_2	26.9	2.74 (*m*, 2H)	26.9	2.72 (*m*, 2H)
8	CH_2	24.5	2.74 (*m*, 1H); 1.97 (*dd*, *J* = 8.5, 5.0 Hz, 1H)	24.6	1.95 (*m*, 2H)
9	CH_2	21.9	1.89 (*dd*, *J* = 7.4, 7.0 Hz, 1H); 2.79 (*m*, 1H)	21.9	1.85 (*m*, 2H)
10	CH_2	46.2	3.01 (*m*, 1H); 2.79 (*m*, 1H)	46.2	2.75 (*m*, 2H)
11	C	213.6	-	213.5	-
12	CH_2	42.6	2.82 (*dt*, *J* = 13.6, 6.2 Hz, 2H)	42.6	2.78 (*m*, 2H)
13	CH_2	28.9	2.89 (*m*, 1H); 3.04 (*m*, 1H)	29.0	3.02 (*m*, 2H)
14	C	132.3	-	132.4	-
15	CH	128.9	7.08 (*dd*, *J* = 8.2, 2.4 Hz, 1H)	129.0	7.06 (*dd, J* = 2.0, 8.0 Hz)
16	CH	115.9	6.90 (*d*, *J* = 8.2 Hz, 1H)	117.0	6.88 (*d*, *J* = 8.0 Hz)
17	C	151.7	-	151.8	-
18	CH	132.4	6.76 (*d*, *J* = 2.4 Hz, 1H)	132.5	6.75 (*d, J* = 2.0 Hz)
19	CH	128.9	6.63 (*s*, 1H)	129.0	6.61 (*s*, 1H)
20	CH_3	61.5	4.00 (*s*, 3H)	61.5	5.83 (*s*, 3H)
21	CH_3	61.4	3.87 (*s*, 3H)	61.5	7.63 (*s*, 3H)

3.3.2.5 Characterization of Compound 30

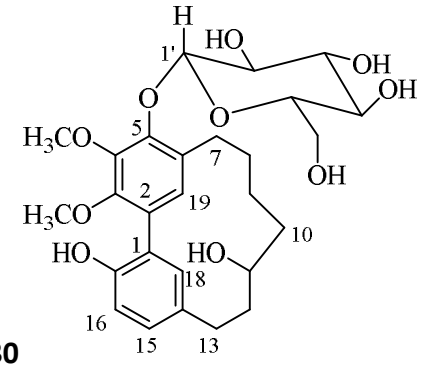

30

Compound **30** was isolated as an amorphous white powder with a melting point of 220-223 °C. The compound gave a dark blue spots on TLC with cerium ammonium molybdate spraying with the R_f value of 0.37 in $CHCl_3$:MeOH (1:0.1). The IR spectrum of compound **30** revealed the presence of O-H stretching at 3455.8 cm^{-1} and 3408 cm^{-1}, C-H stretching at 2919.2 cm^{-1} and 2849.2 cm^{-1}, and C=C stretching of aromatics at 1640.4-1453.6 cm^{-1}. The molecular formula was established to be $C_{27}H_{36}O_{10}$ from TOF-ESI-MS (Appendix 132) at *m/z* 543.2219 for $[M+Na]^+$, 359.1845 $[(M + H)\text{-Glu}]^+$ (calcd for $C_{27}H_{36}O_{10}Na$, 543.5595). Twenty-seven carbon signals were identified by the ^{13}C-NMR (Table 23 and Appendix 127) and DEPT spectra (Table 23 and Appendix 128). These signals include two methyls, seven methylenes, ten methines, and eight quaternary carbon signals. Some of them identified characteristic peaks of aromatic moiety and glucopyranoside. 1D/2D-NMR analyses of compound **30** revealed that it was a cyclic diarylheptanoid closely linked to myricanone (**30**) but different due to lack of glucopyranoside at C-5 of compound **28**, and the carbonyl group at C-11 (δ_C 213.6) of **28** was replaced by a hydroxyl group (δ_C 67.8) in compound **30**. ^{1}H-NMR revealed the presence of six upfield methylene group signal (δ_H 1.47-2.97) and a hydroxyl signal at δ_H 3.93 (H-11), characteristic of heptanoid moiety[168] of compound **30**. The anomeric proton of the glucose moiety was shown at δ_H 5.03 (*d*, *J* = 7.3 Hz, H-1′), indicating β-configuration.

Table 23: ^{1}H-and ^{13}C-NMR data for compound **30**.

Position	**30** ^{1}H-NMR (400 MHz, MeOD) ^{13}C-NMR (101 MHz, MeOD)		**Lit.**[169] ^{1}H-NMR (500 MHz, $CDCl_3$) ^{13}C-NMR (125 MHz, $CDCl_3$)	
	δ_c	δ_H	δ_c	δ_H
1	128.2	-	128.4	
2	129.8	-	128.0	
3	148.0	-	148.3	
4	145.1	-	145.1	
5	148.5	-	148.8	
6	125.2	-	126.0	
7	25.7	2.97 (*dd*, *J* = 16.0, 3.1 Hz, 1H-7); 1.90 (*m*, 1H)	25.8	2.54
8	26.1	2.73 (*m*, 1H)	26.0	2.71
9	22.6	1.58 (*d*, *J* = 8.7 Hz, 1H); 1.47 (*dd*, *J* = 13.3, 12.3, 6.0 Hz, 1H)	22.5	1.28;1.21
10	39.1	1.87 (*m*, 1H); 1.56 (*d*, *J* = 11.6 Hz, 1H)	39.3	1.63;1.35
11	67.8	3.93 (*m*, 1H)	66.7	3.95
12	34.3	2.29 (*ddd*, *J* = 16.0, 11.5, 5.0 Hz, 1H); 1.66 (*m*, 1H)	34.4	2.09;1.49
13	26.7	2.87 (*m*, 2H)	26.8	2.83;2.78
14	130.5	-	129.4	-
15	129.7	7.06 (*dd*, *J* = 8.2, 2.3 Hz, 1H)	129.1	6.96 (*dd*, *J* = 6.6, 1.5 Hz)
16	115.9	6.80 (*d*, *J* = 8.2 Hz, 1H)	115.6	6.74 (*d*, *J* = 6.6 Hz)
17	151.6	-	152.0	-
18	133.7	7.12 (*d*, *J* = 2.4 Hz, 1H)	134.6	6.92
19	129.1	6.86 (*s*, 1H)	129.5	6.60
20	60.3	3.91 (*s*, 3H)	60.1	3.81
21	60.6	3.99 (*s*, 3H)	60.8	3.83
1′	104.0	5.03 (*d*, *J* = 7.3 Hz, 1H)	103.9	4.84 (*d*, *J* = 7.6 Hz)
2′	74.4	3.46 (*m*, 1H)	74.0	3.04
3′	76.9	3.27 (*ddd*, *J* = 9.2, 5.3, 2.3 Hz, 1H)	77.1	3.06
4′	70.1	3.41 (*m*, 1H)	69.9	3.17
5′	76.7	3.47 (*m*, 1H)	76.5	3.23
6′	61.2	3.83 (*dd*, *J* = 12.0, 2.4 Hz, 1H); 3.69 (*dd*, *J* = 12.0, 5.3 Hz, 1H)	60.9	3.58;3.42

The COSY spectrum (Appendix 129) showed correlations for two spin systems: H-7/H-8/H-9/H-10 and H-12/H-13 which confirmed the presence of a alphatic moiety. The ^{13}C-NMR spectrum (Table 23 and Appendix 127) showed the signal of the sugar's anomeric carbon at δ_C 101.4 (C-1′) and the other sugar carbon signals are characteristic of D-glucopyranoside[169] which were appeared at δ_C 76.9 (C-3′), 76.7 (C-5′), 74.4 (C-2′), and 70.1 (C-4′), and a methylene carbon signal at δ_C 61.2 (C-6′). Sugar protons typical of a

glucose resonating between δ_H 3.27 and 5.03 were assigned to H-1′ to H-6′ based on the COSY experiment (Appendix 129). The COSY spectrum showed five methine proton signals at δ_H 5.03 (*d*, *J* = 7.3 Hz, 1H-1′), 3.47 (*m*, 1H-5′), 3.46 (*m*, 1H- 2′), 3.41 (*m*, 1H) and 3.27 (*ddd*, *J* = 9.2, 5.3, 2.3 Hz, 1H-3′) in the spin system, which coupled to their neighbors in this sequence. It also showed coupling occurs between the last methine proton (H-5′) signal and the methylene proton signals at δ_H 3.83 (*dd*, *J* = 12.0, 2.4 Hz, 1H-6′) and 3.69 (*dd*, *J* = 12.0, 5.3 Hz, 1H-6′). An oxymethine proton signal resonated at δ_H 3.93 (*m*) was assigned to H-11 following a proton coupling from the COSY and HMBC long-range correlations (Appendix 131). The HMBC spectrum showed correlation between the anomeric proton signal at δ_H 5.03 (H-1') and carbon signal at δ_H 148.5 (C-5), indicating glycosylation was occurred at C-5. Hence, based on the above data (Table 23) and comparison with the literature[169], compound **30** was proposed to be myricanol 5-*O*-β-D-glucopyranoside.

3.3.3 Biological Activities of Crude Extract and Isolated Compounds from the Roots of *Myrica salicifolia*

3.3.3.1 DPPH Radical Scavenging Assay of Crude Extract and Isolated Compounds from the Roots of *Myrica salicifolia*

The effect of the addition of an antiradical agent can be determined spectrophotometrically by monitoring the change in the DPPH free radical concentration. The amount of the stable DPPH free radicals remaining was expressed as the % RSA which was used to calculate the IC_{50} values. The IC_{50} values (Table 24) indicate 50% of the maximal inhibitory concentration. Thus, the IC_{50} is inversely proportional to the antioxidant activity; a compound with a low IC_{50} value has a high antioxidant capacity, the vice versa holds. The crude extract showed the lowest IC_{50} values and thus the best antioxidant capacities. The IC_{50} values of 2.97–368.75 µg/ml were recorded. The compound **80** had very high IC_{50} values corresponding to low antioxidant activities. The order of the antioxidant activity among the compounds was **CE > 28 > 82 > 30 > 87 > 80**. Hydroxyl groups in a conjugated environment are known to provide antioxidant activity; for example, polyphenols rely on them for their activity. It is one of the most important and common pharmacophores.

Table 24: Percent radical scavenging activity and IC_{50} values of the isolated compounds.

	DPPH Inhibition at					
Compounds/ Extracts	50 µg/mL	25 µg/mL	12.5 µg/mL	6.25 µg/mL	3.12 µg/mL	**IC_{50}** (µg/mL)
EC	96.54	92.31	69.79	50.40	39.35	2.97
28	79.59	68.98	58.91	46.59	35.59	6.96
30	28.82	24.53	22.45	22.17	21.18	183.9
87	24.84	22.45	22.34	21.15	20.23	337.37
82	31.78	27.33	24.91	23.14	21.65	120.78
80	24.60	22.94	21.38	21.24	20.92	368.75
Ascorbic acid	97.32	97.27	97.25	97.19	96.96	0.31

Note: r^2 - coefficient of determination; **EC**: crude Extract; IC_{50} - half maximal inhibitory concentration.

Increasing or decreasing the number of hydroxyls in a molecule affects the overall radical scavenging activity accordingly.[171] Functionalization (e.g., methylation) of the hydroxyl groups also results in a steep drop in the antioxidant activity, demonstrating that the mobile H is essential for it.[172] Increasing the glycosylation of the molecules led to lower activity.[173] Their antioxidant effect was related to the number of free hydroxyl groups in their structures.

3.4 Phytochemical Investigation of the Aerial Parts of *Clematis simensis*

The aerial parts of *C. simensis* were collected from Debresina, Northern Shewa, Amhara region, 192 km from Addis Ababa, in June 2020 by Dr. Mekonnen Abebayehu. The plant specimens were identified by the Department of Plant Science, Addis Ababa University, Ethiopia. Voucher specimens were deposited at the Herbarium, Addis Ababa University (No. AD001 *C. simenses).* The chloroform-methanol extract of the air-dried aerial parts of *C. simensis* afforded three compounds namely 2-deoxy-D-ribono-1,4-lactone (**88**), 5-hydroxylevulinic acid (**89**), and β-sitosterol-3-O-β-D-glucoside (**90**). Their structures were elucidated by 1D- and 2D-NMR spectroscopy, FAB-MS, HR-EI-MS and HR-ESI-MS. The chemical compositions of the essential oils obtained by hydrodistillation from the aerial part of *Clematis simensis* were determined by GC/MS, which led to the detection of ten

major compounds: (*E*)-2-nonen-1-ol (38.33%), 4-cyclopentene-1,3-dione (28.69%), cyclofenchene (5.65%), benzene acetaldehyde (4.74%), methyl salicylate (2.77%), salicylaldehyde (2.68%), benzaldehyde (2.60%), α-terpineol (2.10%), eucalyptol (1.21%), and 2,6-dimethylcyclohexanol (1.15%). Compound **89** showed high antioxidant activity (IC_{50} = 14.89 μg/ml) but have no antibacterial activity against both Gram-positive and Gram-negative bacterial strains. According to the antimicrobial parameters, crude extract showed very weak activity at 500 mg/ml, 250 mg/ml, and 125 mg/ml. To our knowledge, this is the first report on the isolation of secondery metabolites from *Clematis simensis*.

3.4.1 Characterization of Essential Oil of the Aerial Parts of *Clematis simensis*

The essential oils from the *Clematis simensis* aerial parts were extracted by hydrodistillation following the method described by Katekar.[116] Plant material (440 g) was hydrodistilled to afford clear colorless oil (2.0 mL). The essential oil was then analyzed by gas chromatography-mass spectroscopy (GC-MS). The chemical constitutes and physical properties of the essential oil are given in Table 25. The GC-MS analysis of the essential oil of the fresh aerial part of *Clematis simensis* revealed the presence of 20 major compounds with qualities greater than 80% after comparing the data with NIST mass spectral database (Figure 10 and Table 25). The analyzed essential oil was composed of different compounds of different metabolite classes: phenols, aliphatic alcohols, hydrocarbons, and terpenes. The major volatile compounds were (*E*)-2-nonen-1-ol (38.33%), 4-cyclopentene-1,3-dione (28.69%), cyclofenchene (5.65%), benzene acetaldehyde (4.74%), methyl salicylate (2.77%), salicylaldehyde (2.68%), benzaldehyde (2.60%), α-terpineol (2.10%), eucalyptol (1.21%), and 2,6-dimethylcyclohexanol (1.15%). Scientific reports revealed that some of the identified compounds have a considerable potential for therapeutic use. For example, (*E*)-2-nonen-1-ol (38.33%) is the major volatile organic compound that has antifungal activity[174], antimicrobial activity[175], sex pheromone[176], flavoring agent[177], antibacterial quorum sensing (anti-QS)[178], and deorphanize odorant receptors[179]. Whereas, 4-cyclopentene-1, 3-dione (28.69%), the second major component of in the *essential oil* has antifungal[180] and anticancer activity[181]. The other eight bioactive components of the essential oil, with their various pharmacological activities have been reported in many studies as antioxidant, anticancer,

antiulcer, anticonvulsant, antihypertensive, anti-nociceptive, analgesic, antiinflammatory, and rubefacient/counterirritant properties.[121, 182]

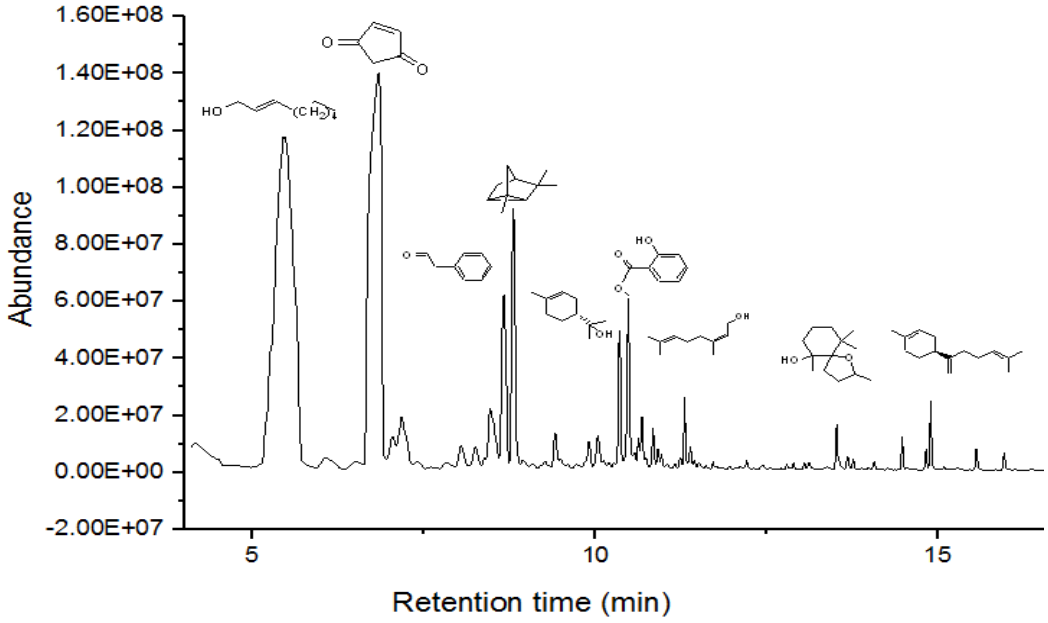

Figure 10: GC-MS chromatogram of the essential oil of aerial parts of *Clematis simensis*.

Table 25: Compounds identified from the essential oil of the aerial parts of *Clematis simensis by* GC-MS.

PK	RT	Area Pct	Compound names	Structure	Q	CF
1	5.45	38.32	(*E*)-2-Nonen-1-ol	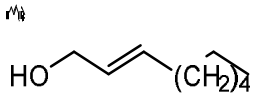	78	$C_9H_{18}O$
2	6.06	0.81	5-Methyl-2(3H)-Furanone	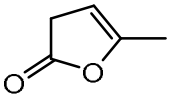	83	$C_5H_6O_2$
3	6.84	28.69	4-Cyclopentene-1,3-dione	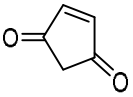	75.1	$C_5H_4O_2$
4	7.04	1.21	Eucalyptol	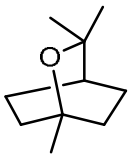	89	$C_{10}H_{18}O$
5	7.17	2.60	Benzaldehyde	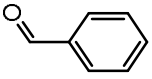	97	C_6H_5CHO
6	8.04	0.84	(*E*,*E*)-2,4-Heptadienal	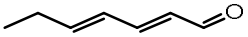	76	$C_7H_{10}O$
7	8.25	0.78	*cis*-Linalool oxide	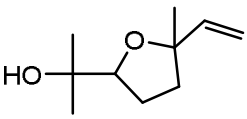	70.3	$C_{10}H_{18}O_2$
8	8.47	2.68	Salicylaldehyde	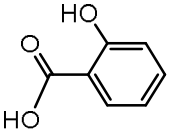	97	$C_7H_6O_2$
9	8.66	4.74	Benzeneacetaldehyde	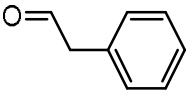	94	

PK	RT	Area Pct	Compound names	Structure	Q	CF
						C_8H_8O
10	8.80	5.65	Cyclofenchene		83	$C_{10}H_{16}$
11	9.41	1.15	2,6-Dimethyl Cyclohexanol	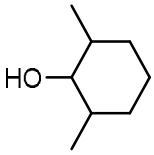	76	$C_8H_{16}O$
12	9.91	0.65	Terpinen-4-ol	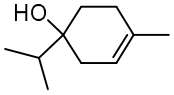	83	$C_{10}H_{18}O$
13	10.04	0.79	Isopinocarveol	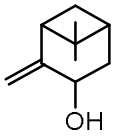	74.4	$C_{10}H_{16}O$
14	10.35	2.10	α-Terpineol	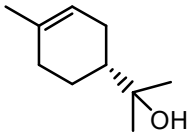	95	$C_{10}H_{18}O$
15	10.48	2.77	Methyl salicylate	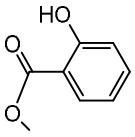	94	$C_8H_8O_3$
16	10.57	0.26	α-Terpinen-7-al	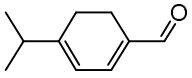	78	$C_{10}H_{14}O$
17	10.63	0.36	*p*-Cymen-8-ol	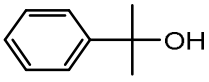	86	$C_{10}H_{14}O$

PK	RT	Area Pct	Compound names	Structure	Q	CF
18	10.68	0.78	*m*-Cymenene	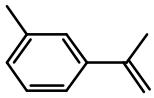	95	$C_{10}H_{14}$
19	10.84	0.58	β-Cyclocitral	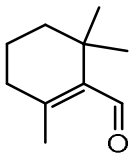	95	$C_{10}H_{16}O$
20	10.92	0.28	3-Carene	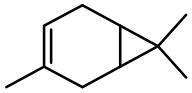	87	$C_{10}H_{16}$
21	10.96	0.19	(-)-*cis*-Carveol	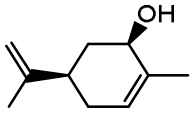	95	$C_{10}H_{16}O$
22	11.24	0.17	β-Homocyclocitral	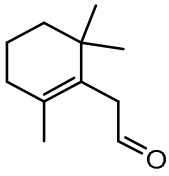	74.8	$C_{11}H_{18}O$
23	11.30	0.76	*cis*-Geraniol	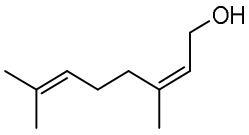	91	$C_{10}H_{18}O$
24	11.38	0.34	D-Carvone	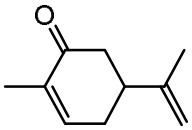	94	$C_{10}H_{14}O$
25	13.52	0.59	6-Hydroxydihydrotheaspirane	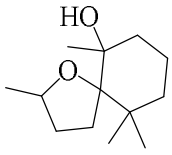	67.8	$C_{13}H_{24}O_2$

PK	RT	Area Pct	Compound names	Structure	Q	CF
26	13.68	0.13	*cis*-Jasmone	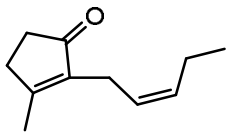	98	$C_{11}H_{16}O$
27	14.48	0.29	β-Ionene	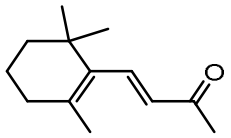	98	$C_{13}H_{20}O$
28	14.82	0.22	β-Ionone epoxide	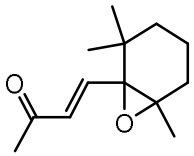	79.8	$C_{13}H_{20}O_2$
29	14.89	0.67	β-Bisabolene	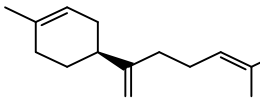	76	$C_{15}H_{24}$
30	15.56	0.25	5-pentyl-1,3-Benzenediol	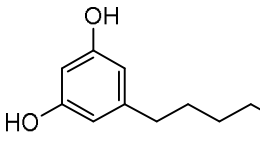	78	$C_{11}H_{16}O_2$
31	15.96	0.20	2-Methyl-5-octyn-4-ol	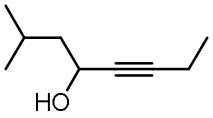	83	$C_9H_{16}O$

Pk = peak number, Rt = retention time (min), Area Pct. = area percentage, Q = quality

3.4.2 Characterization of Compounds Isolated from the Aerial parts of *Clematis simensis*

3.4.2.1 Characterization of Compound 88

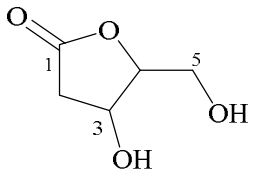

88

Compound **88** was isolated as white powder with a melting point of 134-135 °C. The IR spectrum showed the presence of O-H stretching at 3408 cm^{-1}, C-H stretching at 2915cm^{-1} and 2847cm^{-1}, and C=O stretching at 1634 cm^{-1}. The HR-EI-MS spectrum (Appendix 139) of compound **88** revealed fragment ion at *m/z* = 104.0515 due to the loss of $[CO]^+$ and *m/z* 101.0279 due to loss of $[CH_2OH]^+$ from a compound which are characteristic of dihydroxylated γ-lactone[183] with the molecular weight of 132.0427. The ^{1}H-NMR spectrum (Table 26 and Appendix 133) showed diastereotopic protons signals at δ_H 3.52 and 3.57 could be attributed to H-5. The diastereotopic proton signals at δ_H 2.82 and 2.24 were assigned to methylene protons (H-2) which were alpha to the carbonyl carbon. Hydroxyl proton signals at δ_H 5.5 (*brs*, 1H) and 5.07 (*s*, 1H) could be attributed to C-5 and C-3, respectively. ^{13}C-NMR (Table 26 and Appendix 134) and DEPT (Table 26 and Appendix 135) spectra showed two methine carbon signals at δ_C 67.8 (C-3) and 88.3 (C-4), one carbonyl group signal at δ_C 176.3 (C-1), and two methylene group signals at δ_C 60.8 (C-5) and at δ_C 38.1 (C-2). The HMBC spectrum showed correlations between H-2 (δ_H 2.24) with C-1 (δ_C 176.3) and C-3 (δ_C 67.8), and H-5 (δ_H 3.52) with C-3 (δ_C 67.8) and C-4 (δ_C 88.3). Based on these results and by comparing the spectral data (Table 26) with values published in the literature, compound **88** was determined to be 2-deoxy-D-ribono-1, 4-lactone.[184]

Table 26: ^{1}H and ^{13}C-NMR data for compound **88**.

Position	**88** ^{1}H-NMR (600 MHz, DMSO) ^{13}C-NMR (151 MHz, DMSO)		**Lite.**[184] ^{1}H-NMR (500 MHz, Pyridine-d_5) ^{13}C-NMR (125 MHz, Pyridine-d_5)	
	δ_C	δ_H	δ_C	δ_H
1	176.3	-	177.11	-
2	38.0	2.82 (*dd*, *J* = 17.7, 6.5 Hz, 1H); 2.24 (*dd*, *J* = 17.7, 2.3 Hz, 1H)	39.46	2.86 (*dd*, *J* = 2.5, 17.5,1H); 3.33 (*dd*, *J* = 6.5, 17.5, 1H)
3	67.8	4.34 – 4.18 (*m*, 1H)	69.23	5.00 (*ddd*, *J* = 2.0, 2.5, 6.5,1H)
4	88.3	4.34 – 4.18 (*m*, 1H)	89.76	4.91(*ddd*, *J* = 2.0, 3.5, 3.5, 1H)
5	60.8	3.52 (*m*, H); 3.57 (*m*, H)	62.07	4.34 (*dd*, *J* = 3.5, 12.0, 1H), 4.13 (*dd*, *J* = 3.5, 12.0, 1H)

3.4.2.2 Characterization of Compound 89

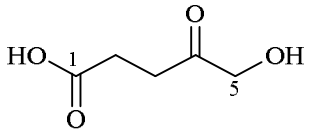

89

Compound **89** was isolated as a white powder with a melting point of 97-100 ^{0}C. The IR spectrum of compound **89** showed the presence of O-H stretching at 3443 cm^{-1}, C-H stretching at 2926 cm^{-1} and 2855 cm^{-1}, C=O stretching at 1736 cm^{-1} and 1634 cm^{-1}. The HR-EI-MS spectrum (Appendix 145) of Compound **89** showed fragment ion peaks at *m/z* = 101 consistent with the loss of $[CH_2OH]^+$ from a 5-hydroxy-4-oxopentanoic acid with a molecular weight of 132.0427. The ^{1}H-NMR spectrum (Table 27 and Appendix 140) of compound **89** showed triplet signals at δ_H 2.59 (*t*, *J* = 6.7 Hz, H-2) and δ_H 2. 70 (*t*, *J* = 6.7 Hz, H-3) due to the two linked methylene protons, a singlet signal at δ_H 4.24 (H-5), indicated the protons of methylene unit were flanked between a hydroxyl group and a carbonyl carbon. The ^{13}C-NMR (Table 27 and Appendix 141) spectrum revealed five carbon signals due to a carboxylic acid carbon at δ_C 176.4 (C-1), one carbonyl carbon at δ_C 211.1 (C-4), a methylene carbon adjacent to the hydroxyl at δ_C 68.9 (C-5) and two

methylene carbon next to the carboxylic acid at δ_C 33.9 (C-3) and δ_C 28.5 (C-2). The ^{1}H-^{1}H correlation spectroscopy (COSY) spectrum (Appendix 142) showed a proton signal at δ_H 2.59 (*t*, *J* = 6.7 Hz, H-2) correlated with a proton signal at δ_H 2.70 (*t*, *J* = 6.7 Hz, 2H-3), indicated two protons were in an adjacent environment. HMBC spectrum (Appendix 144) showed a proton signal of H-2 at 2.59 (*t*, *J* = 6.7 Hz) correlated with a carbon signal of aliphatic acid at δ_C 176.8 (C-1). The most intense proton signals at δ_H 4.24 (H-5) and 2.69 (H-3) correlated with a carbonyl carbon signal at δ_C 211.1 (C-4), indicated the carbonyl carbon was attached to hydoxymethylene and methylene groups. Based on these results and by comparing the spectral data with values published in the literature, the chemical structure of compound **89** was determined to be 5-hydroxylevulinic acid which was previously isolated from *Clematis delavayi var. spinescens.*[185]

Table 27: ^{1}H and ^{13}C-NMR data for compound **89**.

position	**89** ^{1}H-NMR (601 MHz, DMSO) ^{13}C-NMR (151 MHz, DMSO)		**Lite.**[186-187] ^{1}H-NMR (90 MHz, $CDCl_3$) ^{13}C-NMR (90 MHz, $CDCl_3$)	
	δ_C	δ_H	δ_C	δ_H
1	176.4	-	176.5	-
2	28.5	2.59 (*t*, *J* = 6.7 Hz, 2H).	28.5	2.62 (*t*, *J* = 5.9 Hz)
3	33.9	2.70 (*t*, *J* = 6.7 Hz, 2H)	33.9	2.72 (*t*, *J* = 5.9 Hz,)
4	211.1	-	211.2	-
5	68.9	4.24 (*s*, 2H)	68.8	4.21 (*s*, 2H)

3.4.2.3 Characterization of Compound 90

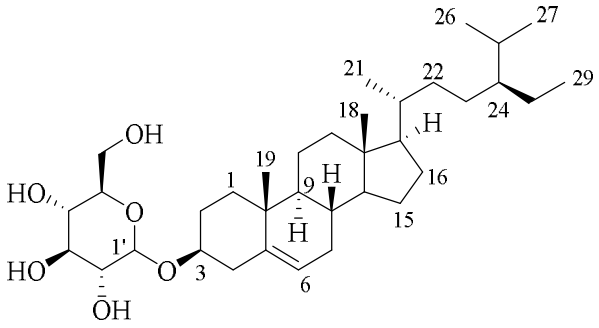

90

Compound **90** was isolated as a white powder with a melting point of 285-287 °C. The IR showed the presence of O-H stretching at 3436 cm^{-1}, C-H stretching at 2918 cm^{-1}, and C=C

stretching at 1620 cm^{-1}. The molecular formula was established as $C_{35}H_{60}O_6$ by FAB-MS (Appendix 152) at m/z 599.4236 for $[M+Na]^+$ (calc. for $C_{35}H_{60}O_6$, 599.8384). The ^{1}H-NMR spectrum of compound **90** (Table 28 and Appendix 146) showed the presence of two methyl singlet signals at δ_H 0.65 (H-18) and δ_H 0.96 (H-19), three doublet signals at δ_H 18.99 (H-27), δ_H 19.04 (H-21) and δ_H 19.78 (H-26). The triplet signal at δ_H 0.82 (H-29) indicated the methyl group was attached to a methylene group (H-28). A multiplet signal at δ_H 5.30 (H-6) was assigned to olefinic methine proton. The ^{1}H-NMR spectra of compound **90** (Table 28) showed a triplet of doublet signal at δ_H 3.42 (H-3), oxymethine proton signals of glucose at δ_H 3.01-4.22 as a multiplet. Anomeric proton and other proton signals of the glucose moiety were shown at δ_H 4.22 (H-1′), δ_H 3.65 (H_1-6′), δ_H 3.41 (H_2-6′), δ_H 3.12 (H-3′), δ_H 3.07 (H-5′), δ_H 3.01 (H-4′), and δ_H 2.88 (H-2′) and the coupling constant for H-3 was 11.7, indicating that the hydroxyl function was β-oriented. The ^{1}H-NMR and ^{13}C-NMR spectral data of **90** were similar to β-sitosterol, except for the sugar moiety, which was linked to C-3 as C-3 shifted toward downfield from δ_C 71.0 to δ_C 77.0, compared with β-sitosterol.[188] The ^{13}C-NMR and DEPT-NMR spectra showed 35 carbon signals which are attributed to six methyl carbons, eleven methylene carbons, nine methine carbons, and three quarternary carbons. The anomeric carbon signal was shown at δ_C 100.8 (C-1′). The remaining sugar carbon signals resonated in the range of C-3′ (δ_C 76.8) to C-6′ (61.1). The ^{13}C-NMR spectrum contained signals for a methylene carbon (C-6′) was shown at δ_C 61.1 and other four carbon signals was shown at δ_C 76.8 (C-3′), 76.8 (C-5′), 73.5 (C-2′), and 70.17 (C-4′). In the COSY spectrum (Appendix 149), the olefinic methine proton signal at δ_H 5.30 (H-6) was coupled with H-7 at δ_H 1.52, oxymethine proton signal at δ_H 3.42 (H-3) coupled with H-4 at δ_H 2.36 and H-2 at δ_H 1.81, and methine proton signal at δ_H 1.38 (H-8) coupled with H-7 at δ_H 1.52 and H-14 δ_H 0.99. In HSQC (Appendix 150) spectrum, the proton signal at δ_H 3.42 (H-3) correlated with the carbon signal at δ_C 76.9 (C-3) which confirmed the presence of oxymethine group at C-3. A doublet olefinic proton signal at δ_H 5.30 (H-6) correlated with the carbon signal at δ_C 121.3 (C-6). The HMBC spectrum (Appendix 151) showed correlation of H-1′ at δ_H 4.22 with C-3 at δ_C 76.9 indicated that glucose moiety was linked to the sitosterol at C-3. The methine proton signal at δ_H 5.30 (H-6) showed HMBC correlation with the carbon signal at δ_C 36.3 (C-10), 31.5 (C-7), and 31.4 (C-8) which located the olefinic bond at C-6 and C-5. The signals at δ_H

2.36 (H_1-4) and δ_H 2.17 (H_2-4) showed long-range HMBC correlations with the carbons at δ_C 140.5 (C-5), 121.3 (C-6), 76.9 (C-3), and 36.3 (C-10). Comparison of ^{1}H and ^{13}C-NMR data of compound **90** (Table 28) with literature value confirmed that compound **90** is β-sitosterol-3-*O*-β-D-glucoside.[189]

Table 28: ^{1}H-and ^{13}C-NMR data for compound **90**

Position	**90** ^{1}H-NMR (601 MHz, DMSO) ^{13}C-NMR (151 MHz, DMSO)		Lite.[189] ^{1}H-NMR (400 MHz, $CDCl_3$) ^{13}C-NMR (100 MHz, $CDCl_3$)	
	δc	δ_H	δc	δ_H
1	36.9	1.79 (*m*, 1H); 1.00 (*d*, *J* = 6.6 Hz, 1H)	36.79	1.40 *m*;1.0 *m*
2	29.3	1.81 (*m*, 1H);1.42 (*m*, 1H)	29.23	1.58 *m*;1.26 *m*
3	76.9	3.42 (*td*, *J* = 11.2, 5.6 Hz)	76.85	2.98 *m*
4	38.4	2.36 (*m*, 1H);2.17 (*m*, 1H)	39.28	2.26 *m*;1.98 *m*
5	140.5	-		-
6	121.3	5.30 (*m*, 1H)	121.20	5.35 *(t*, *J* = 3.6)
7	31.5	1.92 (*m*, 1H);1.52 (*m*, 1H)	31.38	1.95 *m*;1.73 *m*
8	31.4	1.38 (*m*, 1H)	31.26	1.36 *m*
9	49.7	0.83 (*m*, 1H)	49.55	0.85 *m*
10	36.3	-		-
11	20.5	1.21 (*d*, *J* = 5.7 Hz, 1H); 1.01 (*d*, *J* = 9.7 Hz, 1H)	20.56	1.42 *m*
12	39.3	1.94 (*m*, 1H); 1.11 (*dd*, *J* = 11.9, 3.7 Hz, 1H)	38.26	1.52 (*dd*, *J* = 12.37,4.3); 1.20 *m*
13	41.9	-	41.82	-
14	56.2	0.99 (*m*, 1H)	56.13	0.95 *m*
15	23.9	1.57 (*m*, 1H);1.08 (*m*, 1H)	23.83	1.57 *m*;1.05 *m*
16	27.9	1.84 (*m*, 1H);1.24 (*m*, 1H)	27.76	1.85 *m*;1.25 *m*
17	55.5	1.12 (*m*, 1H)	55.38	1.20 *m*
18	12.3	0.65 (*s*, 3H)	11.64	0.70 *s*
19	19.2	0.96 (*s*, 3H)	19.07	0.94 *s*
20	35.6	1.35 (*m*, 1H)	35.45	1.40 *m*
21	19.0	0.78 (*d*, *J* = 7.7 Hz, 3H)	18.58	0.95(*d*, *J* = 6.5)
22	33.4	1.34 (*m*, 1H);1.04 (*m*, 1H)	33.29	1.20 *m*
23	25.4	1.15 (*m*, 2H)	25.36	1.25 *m*
24	45.2	0.91 (*m*, 1H)	45.09	0.94 *m*
25	28.7	1.63 (*m*, 1H)	28.64	1.68 *m*
26	19.8	0.80 (*d*, *J* = 5.4 Hz, 3H)	19.69	0.87 (*d*, *J* = 7.0)
27	19.0	0.87 (*d*, *J* = 4.4 Hz, 3H)	18.89	0.88 (*d*, *J* = 7.0)
28	23.0	1.22 (*m*, 2H)	22.06	1.30 *m*
29	11.7	0.82 (*t*, *J* = 7.2 Hz, 3H)	11.75	0.97 *(t*, *J* = 7.5)
1′	100.8	4.22 (*d*, *J* = 7.8 Hz, 1H)	100.73	4.20 (*d*, *J* = 7.9)

2′	73.5	2.88 (*m*, 1H)	73.42	2.89 (*dt*, *J* = 4.5, 8.0)
3′	76.8	3.12 (*td*, *J* = 8.8, 4.7 Hz, 1H)	76.86	3.27 (*dt*, 8.0, *J* = 4.5, 8.0)
4′	70.2	3.01 (*td*, *J* = 9.1, 5.1 Hz, 1H)	70.04	3.00 (*dt*, *J* = 4.5, 8.0)
5′	76.8	3.07 (*ddd*, *J* = 9.7, 5.9, 2.1 Hz, 1H)	76.72	3.06 (*dt*, , *J* = 4.5, 8.0)
6′	61.1	3.65 (*ddd*, *J* = 11.7, 5.8, 2.0 Hz, 1H); 3.41 (*dt*, *J* = 11.7, 5.9 Hz, 1H	62.82	4.55 (*dd*, *J* = 2.5,11.77); 4.40 (*dd*, *J* = 5.211.77)

3.4.3 Biological Activities of the Crude Extract and Isolated Compounds from the Aerial Part of *Clematis simensis*

3.4.3.1 DPPH Radical Scavenging Assay of the Crude Extract and Isolated Compounds from the Aerial Parts of *Clematis simensis*

The antioxidant capacities of the crude extract and isolated compounds, expressed as the DPPH free radical inhibition and the IC_{50} values, are presented in Table 29.

Table 29: Percent radical scavenging activity and IC_{50} values of the crude extract and the isolated compounds

	% DPPH inhibition at					
Compounds/ Crude extract	50 µg/mL	25 µg/mL	12.5 µg/mL	6.25 µg/mL	3.12 µg/mL	IC_{50} µg/mL
CE	47.8	36.7	30.1	25.8	22.7	52.9
88	47.8	46.2	44.9	44.4	44.2	26.96
89	43.8	42.9	39.0	38.5	36.8	14.89
90	38.5	31.9	25.0	24.7	23.5	26.99
AA	97.32	97.27	97.25	97.19	96.96	0.36

Note: IC_{50} - half maximal inhibitory concentration; CE-crude extract

In the current study, the antioxidant activities of the crude extract of the aerial part of *C. simensis* and the isolated compounds were evaluated using a DPPH assay. The DPPH method is the most common, cost-effective, and quick method to evaluate the antioxidant activities of natural products.[190] According to the parameters used, the IC_{50} value category is very strong if the IC_{50} value is < 10 µg/mL, strong if the IC_{50} value is between 10 and 50 µg/mL, mild if the IC_{50} value is between 50 and 100 µg/mL, weak if the IC_{50} value is between 100 and 250 µg/mL and not active if the IC_{50} is above 250 µg/mL.[156] The crude extract (52 µg/mL) showed mild antioxidant activity (Table 29). The isolated compounds **88**, **89**, and **90** showed strong antioxidant activity with the IC_{50} values in the range of 14.89-26.99 µg/mL but were very low compared to the standard ascorbic acid (0.36 µg/mL).

3.4.3.2 Antibacterial Activities of the Crude Extract and Compounds from the Aerial Part of *Clematis simensis*

The antibacterial activity of the crude extract and isolated compounds were determined by the disk diffusion method as recommended by the National Committee for Clinical Laboratory Standards against Gram-positive microorganisms *Staphyloccocus aureus* (MTCC 1430), and Gram-negative microorganisms *Escherichia coli* (MTCC 42), *Pseudomonas aeruginosa* (MTCC 1034), and *Salmonella typhi* (ATCC 6539) at 125-500 mg/mL concentrations, using 10% dimethyl sulfoxide (DMSO) as a solvent.

Table 30: Antibacterial activities of isolated compounds.

Organism	Conc.	Zones of inhibition in mm			
		Crude extract (mg/ml)	88 (μg/ml)	89 (μg/ml)	*Ciprofloxacin*
S. aureus	125	ND	ND	ND	18±0.3 (at 5 μg/ml)
	250	3.0±0.3	ND	ND	
	500	5.0±0.1	ND	ND	
P. aeruginosa	125	ND	ND	ND	15±0.8 (at 5 μg/ml)
	250	2.0±0.8	ND	ND	
	500	5.0±0.2	ND	ND	
E. coil	125	ND	ND	ND	32±1.0 (at 5 μg/ml)
	250	2.0±0.2	ND	ND	
	500	4.0±0.5	ND	ND	
S. typhi	125		ND	ND	27±0.6 (at 5 μg/ml)
	250	2.0±0.1	ND	ND	
	500	4.0±0.6	ND	ND	

Note: Conc: Concentration, ND: not detected

The tested extract of *C. simensis* had antibacterial activity against both gram-positive and gram-negative bacteria at different concentrations (Table 30). A higher inhibition zone (3.0±0.3 mm) was detected against *S. aureus,* followed by *P. aeruginosa* with a mean zone of inhibition of 2.0±0.8 mm at 250 mg/mL, which is one of the most common causes of a wide range of infections, such as skin infections, food poisoning, pneumonia, sepsis, and osteomyelitis.[191] The results showed that the $CHCl_3$:MeOH (2:1) extracts of *C. simensis* leaves possessed relatively better antibacterial activity against the tested bacteria. Compounds **88** and **89** did not show any inhibition against the tested microorganisms. Ciprofloxacin, which was used as a positive control, produced a zone of inhibition of 15–32 mm. The antibacterial effects of the crude extract of *C. simensis* were far below the

commercial antibiotic, ciprofloxacin (5 µg/mL**)**. This could attribute to the fact that the antibacterial activities found in the plant are less potent.

3.5 Phytochemical Investigation of the Barks of *Olinia usambarensis*

The barks of *Olinia usambarensis* was collected from Debresina, Northern Shewa, Amhara region, 192 km from Addis Ababa, Ethiopia, in February 2022 by Dr. Mekonnen Abebayehu. The plant specimens were identified by Mr. Melaku Wendafrash, Addis Ababa University, Ethiopia. A voucher specimen of the plant material has been deposited in the National Herbarium, Addis Ababa University, with a voucher/specimen number of OR001 *O. rochetiana*. The chloroform-methanol extract of the barks of *Olinia usambarensis* afforded four compounds namely lupeol (**91**), n-pentacosyl *trans*-ferulate (**92**), and 4-*O*-β-D-glucopyranosylcaffeic acid (**72**). Their structures were elucidated by FT-IR, 1D-and 2D-NMR spectroscopy, and HR-MS. DPPH radical scavenging activities of the isolated compounds and crude extract were also determined in this study. The compounds showed a wide range of DPPH scavenging activities from very weak (IC_{50} = 458.8 µg/ml) to very strong (IC_{50} = 22.1 µg/ml). The phytochemical investigation on the barks of *Olinia usambarensis* is discussed in the following sections.

3.5.1 Characterization of Essential Oil of the Barks of *Olinia usambarensis*

The essential oils from the *Olinia usambarensis* barks were extracted by hydrodistillation following the method described by Katekar.[116] Plant material (570 g) was hydrodistilled to afford clear colorless oil (0.7 mL). The essential oil was then analyzed by gas chromatography-mass spectroscopy (GC-MS). The chemical constitutes and physical properties of the essential oil are given in Table 31. The GC-MS analysis of the essential oil of the fresh Barks of *Olinia usambarensis* revealed the presence of 12 major compounds with qualities greater than 80% after comparing the data with NIST mass spectral database (Figure 11 and Table 31). The analyzed essential oil was composed of different compounds of different metabolite classes: phenols, saponins, and aliphatic acides. The major volatile compounds were n-hexadecanoic acid (28.83%), seudenone (25.80%), 9, 12-octadecadienoic acid (*Z*,*Z*)- (15.84%), and benzaldehyde (9.49%). Scientific reports revealed that some of the identified compounds have a considerable potential for

therapeutic use. For example, hexadecanoic acid (28.83%) is the major volatile organic compound that has antioxidants, hypocholesterolemic, nematicide, and pesticide activity[192], Whereas, seudenone (25.80%), the second major component of in the essential oil has is an insect pheromone, used in nut flavor and can be used as a starting material: In the total synthesis of (−)-*ar*-teunifolene, a naturally occurring aromatic sesquiterpene.[193-194] The third major component, benzaldehyde (9.49%), is used as flavor and fragrance agent, synthesis of pharmaceuticals, including antihistamines, antipsychotic drugs, and antibiotics, production of various polymers and resins.[195-196]

The other bioactive components of the essential oil, with their various pharmacological activities have been reported in many studies as added to foods as antioxidant, a preservative, antimicrobial activity, anticancer effects, treat genital herpes and acquired immunodeficiency syndrome (AIDS), used in the formulation of cosmetic and personal care products, flavoring agent, lubricants, surfactants, and detergents.[197-199]

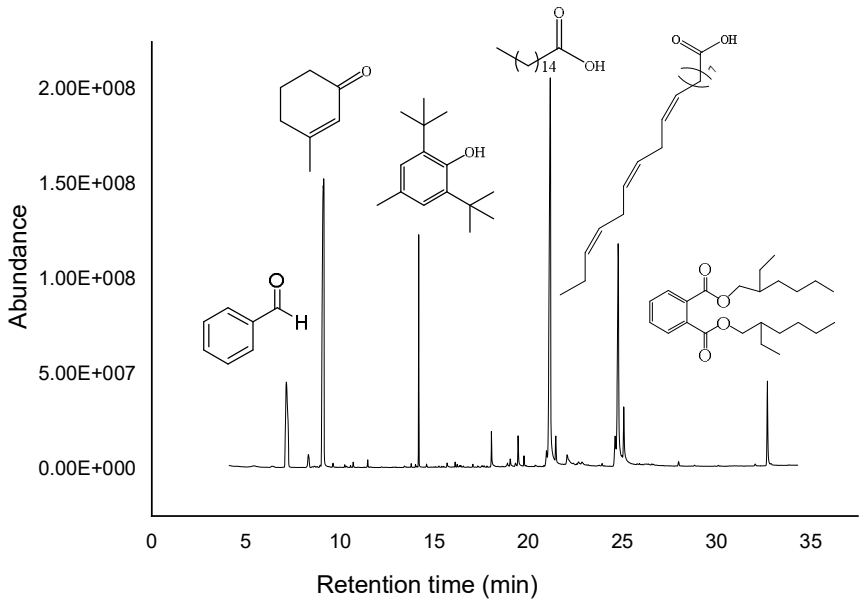

Figure 11: GC-MS chromatogram of the essential oil of Barks of *O. usambarensis*.

Table 31: Compounds identified from the essential oil of the bark of *O. usambarensis* by GC-MS

PK	RT	Area Pct	Compound names	Structure of compounds	Q	CF
1	7.15	9.49	Benzaldehyde	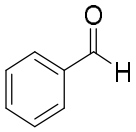	97	C_7H_6O
2	8.32	0.90	Succinic anhydride	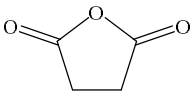	85	$C_{10}H_{18}O$
3	9.13	25.80	Seudenone	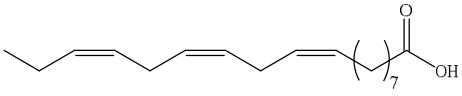	77	$C_7H_{10}O$
4	14.18	5.07	BHT	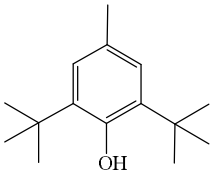	95	$C_{15}H_{24}O$
5	18.04	1.20	Tetradecanoic acid	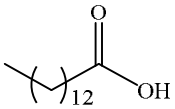	99	$C_{14}H_{28}O_2$
6	19.46	1.18	Pentadecanoic acid	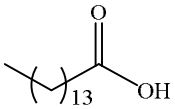	99	$C_{15}H_{30}O_2$
7	20.97	0.87	Palmitoleic acid	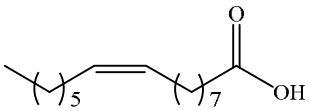	99	$C_{15}H_{30}O_2$
8	21.16	28.83	n-Hexadecanoic acid	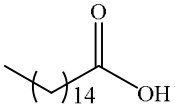	93	$C_{16}H_{32}O_2$
9	21.46	1.32	butyl isobutyl phthalate	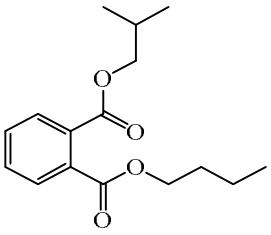	95	$C_{16}H_{22}O$

10	24.61	1.94	Oleic Acid	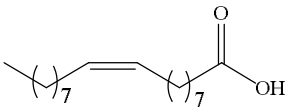	99	$C_{18}H_{34}O_2$
11	24.77	15.84	*cis*,*cis*-Linoleic acid	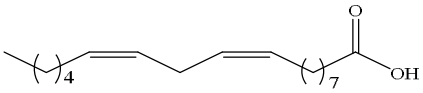	99	$C_{18}H_{32}O$
12	25.07	3.83	Linolenic acid	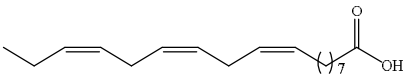	98	$C_{18}H_{30}O$
13	32.70	3.68	Bis(2-ethylhexyl) phthalate	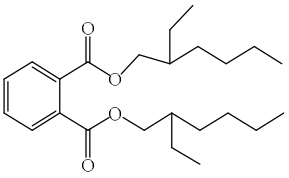	91	$C_{24}H_{38}O_4$

Pk = peak number, Rt = retention time (min), Area Pct. = area percentage, Q = quality

3.5.2 Characterization of Compounds Isolated from the Barks of *Olinia usambarensis*

3.5.2.1 Characterization of Compound 91

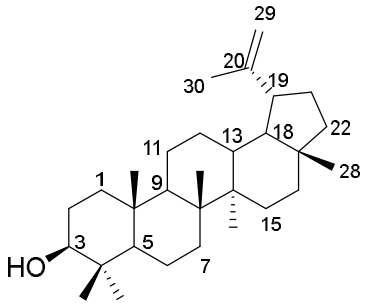

91

Compound **91** was isolated as a white powder with a melting point of 213-215 °C. This compound gave a magenta spot on TLC with 1% vanillin-sulfuric acid spraying reagent with an R_f value of 0.68 in Hex:EtOAc (9:1). The IR spectrum revealed the presence of O-H stretching at 3437.2 cm^{-1}, C-H stretching at 2919.2 cm^{-1} and 2853.6 cm^{-1}, and the C=C stretching at 1642.2 cm^{-1}. The molecular formula was established as $C_{30}H_{50}O$ by the sodiated-molecular-ion peak in the TOF-ESI-MS (Appendix 159) at *m/z* 449.3441 for $[M+Na]^+$ (calcd for $C_{30}H_{50}ONa$, 449.7082). The ^{1}H-NMR spectrum (Table 32 and Appendix 153) showed the seven methyl proton signals at δ_H 1.66 (*s*, 3H), 1.01 (s, 3H), 0.95 (*s*, 3H), 0.93 (s, 3H), 0.81 (s, 3H), 0.77 (s, 3H), and 0.74 (s, 3H). In the ^{1}H-NMR spectrum showed an oxygenated methine proton signal appeared as a doublet of doublet at

δ_H 3.17 with a *J* coupling of 11.2 indicated the α-oriented hydrogen of 3β-hydroxy triterpene. It also showed two olefinic protons at 4.67 (*d*, *J* = 2.5 Hz, 1H-29) and 4.55 (*s*, 1H-29) was assigned to a terminal double bond. These two signals with a methyl proton signal at δ_H 1.66 (H-30) indicated the presence of an isopropenyl group in the structure of **91**. The ^{13}C-NMR spectrum (Table 32 and Appendix 154) of the compound (**91**) revealed 30 carbon signals which could be attributed to seven methyls, eleven methylenes, six methines and six quaternary carbons for the terpenoid of lupane skeleton. A carbon attached to the hydroxyl group was shown at δ_H 79.2 (C-3). The olefinic carbon signals of the exocyclic double bond were shown at δ_C 151.2 (C-20) and 109.6 (C-29). The COSY spectrum (Appendix 156) of **91** revealed correlations of H-19 at δ_H 2.29 with H-21 at δ_H 1.90 and H-18 at δ_H 1.27, and the oxymethine proton signal at δ_H 3.17 (H-3) was coupled with H-2 at δ_H 1.57. It also showed a methine proton at δ_H 0.68 (H-5) correlated with methylene proton at δ_H 1.37 (H-6). From HMBC spectrum (Appendix 158), the methine proton signal at δ_H 3.17 (H-3) showed correlation with a methyl carbon signal at δ_C 15.6 (C-24), and a methyl carbon signal of δ_C 28.2 (C-23) and a quaternary carbon of δ_C 40 (C-4). The two methyl proton signal at δ_H 0.95 (H-23) and δ_H 0.74 (H-24) correlated with the carbon signal at δ_C 79.2 (C-3), 55.6 (C-5) and 40.0 (C-4) indicated the two methyl were attached to the quaternary carbon (C-4). The methyl signal at δ_H 1.66 (H-30) showed correlation with a terminal carbon signal of C-29 at δc 109.6, quaternary carbon signal at δ_C 151.2 (C-20), and methine carbon signal at δ_C 48.2 (C-19) indicated the a methyl group was attached to C-20. The two vicinal protons at δ_H 4.67 (H-29) and 4.55 (H-29) showed correlation with a quaternary carbon signal at δ_C 151.2 (C-20), a methyl carbon at δ_C 19.5 (C-30) and methine carbon signal at δ_C 48.2 (C-19) revealed that an isopropenyl group was attached to C-19. Thus, compound **91** was identified as lupeol based on the above spectroscopic data (Table 32) and reported literature values.[200]

Table 32: ^{1}H- and ^{13}C-NMR data for compound **91**

Position	**91** ^{1}H NMR (400 MHz, $CDCl_3$) ^{13}C NMR (101 MHz, $CDCl_3$)		Lite.[200] ^{1}H NMR (500 MHz, $CDCl_3$) ^{13}C NMR (125 MHz, $CDCl_3$)	
	δ_C	δ_H	δ_C	δ_H
1	38.9	1.59 (*m*, 1H); 0.89 (*m*, 1H)	38.9	1.65 (*m*, 1H); 0.90 (*m*, 1H)
2	27.6	1.57 (*dd*, *J* = 12.0, 3.3 Hz, 1H); 1.61 (*m*, 1H)	27.5	1.59 (*m*, 1H)
3	79.2	3.17 (*dd*, *J* = 11.2, 5.0 Hz-1H)	79.1	3.18 (*dd*, *J* = 11.4, 4.8 Hz, 1H)
4	40.0	-	39.0	-
5	55.6	0.68 (*t*, *J* = 7.9 Hz, 1H)	55.5	0.67 (*m*, 1H)
6	18.5	1.37 (*m*, 1H); 1.50 (*m*, 1H)	18.5	1.51 (*m*, 1H); 1.38 (*m*, 1H)
7	34.5	3.71 (*m*, 2H)	34.5	1.39 (*m*, 1H)
8	41.1	-	41.0	-
9	50.6	1.24 (*s*, 1H)	50.6	1.26 (*m*, 1H)

10	37.4	-	37.3	-
11	21.1	1.39 (*m*, 1H); 1.25 (*m*, 1H)	21.1	1.41(*m*, 1H)
12	26.0	1.65 (*m*, 1H)	25.3	1.64 (*m*, 1H)
13	38.2	1.63 (*m*, 1H)	38.2	1.65 (*m*, 1H)
14	43.0	-	43.0	-
15	27.6	1.67 (*m*, 1H); 1.5 (*m*, 1H)	27.6	1.66 (*m*, 1H)
16	35.8	1.44 (m, 2H)	35.8	1.48 (*m*, 1H)
17	43.2	-	43.2	-
18	48.5	1.27 (*m*, 1H)	48.5	1.36 (*m*, 1H)
19	48.2	2.29 (*m*, 1H)	48.1	2.37 (*m*, 1H)
20	151.2	-	151.1	-
21	30.0	1.90 (*m*, 1H); 1.22 (*m*, 1H)	30	1.29 (*m*, 1H); 1.91 (*m*, 1H)
22	40.2	1.13 (*m*, 1H); 1.30 (m, 1H)	40.2	1.20 (*m*, 1H); 1.37 (*m*, 1H)
23	28.2	0.95 (*s*, 3H)	28.2	0.97 (*s*, 3H)
24	15.6	0.74 (s, 3H)	15.5	0.76 (*s*, 3H)
25	16.3	0.81 (s, 3H)	16.3	0.83 (*s*, 3H)
26	16.2	1.01 (s, 3H),	16.2	1.03 (*s*, 3H)
27	14.8	0.93 (s, 3H),	14.7	0.94 (*s*, 3H)
28	18.2	0.77 (s, 3H),	18.2	0.79 (*s*, 3H)
29	109.6	4.67 (*d*, *J* = 2.5 Hz, 1H); 4.55 (*s*, 1H)	109.5	4.56 (*s*, 1H); 4.69 (*s*, 1H)
30	19.5	1.66 (*s*, 3H)	19.5	1.68 (*s*, 3H)

3.5.2.2 Characterization of Compound 92

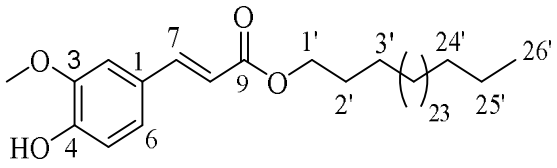

92

Compound **92** was isolated as white amorphous powder with a melting point of 195-200 ºC. This compound gave a magenta spot on TLC with 1% vanillin-sulfuric acid spraying reagent with an R_f value of 0.67 in Hex:EtOAc (2:0.2). The IR spectrum showed the presence of O-H stretching at 3450.2 cm^{-1}, C−H stretchings at 2936 and 2866 cm^{-1}, C=O stretching at 1751.4 cm^{-1}, and aromatic C=C stretching 1635 cm^{-1}. The TOF-ESI-MS spectrum (Appendix 166) showed the molecular ion peak $[M]^+$ at m/z 544.3618 (calcd. for $C_{35}H_{60}O_4$, 544.8498) in accordance with the molecular formula of $C_{35}H_{60}O_4$. The ^{1}H-NMR spectrum (Table 33 and Appendix 160) showed three aromatic signals at δ_H 7.01 (*dd*, *J* = 8.2, 1.9 Hz, 1H-6), 6.97 (*d*, *J* = 1.8 Hz, 1H-2), and 6.85 (*d*, *J* = 8.1 Hz, 1H-5) which

confirmed the presence of a 1,3,4-trisubstituted benzene moiety. The signals at δ_H 7.54 (*d*, *J* = 15.9 Hz, 1H-7) and δ_H 6.23 (*d*, *J* = 15.9 Hz, 1H-8) were assigned to a *trans* double bond in the molecule. Two triplet signals at δ_H 4.12 (*t*, *J* = 6.8 Hz, H-1′) and 0.81 (*t*, *J* = 6.7 Hz, H-26′) were assigned to oxymethylene protons and terminal methyl protons, respectively. A singlet signal at δ_H 3.89 (*s*, 3H) was allocated to methoxy group. The multiplet broad signals at δ_H 1.18 (*brs*, 47H) indicated the presence of methylene groups. The ^{13}C-NMR (Appendix 161) and DEPT-NMR spectrum (Table 33 and Appendix 162) showed four quartenary carbons, five methines, one methyl, one methoxy and twenty-five methylenes. In the COSY spectrum (Appendix 163), the oxymethylene proton signal at δ_H 4.12 (H-1′) was coupled with the signal at δ_H 1.63 (H-2′) which was coupled with the signal at δ_H 1.31 (H-3′). It also showed a homonuclear coupling between H-8/H-9 and H-5/H-6. In HSQC spectrum (Appendix 164) showed a methine proton signal at δ_H 6.97 (*d*, *J* = 1.8 Hz, 1H) correlated with a carbon signal at δ_C 109.2 (C-2). The signal at δ_H 56.85 (*d*, *J* = 8.1 Hz, 1H) correlated with carbon signal at δ_C 114.7 (C-5). A methine proton signal at δ_H 7.01 (*dd*, *J* = 8.2, 1.9 Hz, 1H) correlated with a carbon signal at δ_C 123.1 (C-6), a proton signal at δ_H 7.54 (*d*, *J* = 15.9 Hz, 1H) correlated with carbon signal at δ_C 144.7 (C-7), and a proton signal at δ_H 6.23 (*d*, *J* = 15.9 Hz, 1H) correlated with a carbon signal at δ_C 115.7 (C-8). The singlet signal at δ_H 3.89 (*s*, 3H) correlated with carbon signal at δ_C 55.9 (3-OMe). A proton signal at δ_H 4.12 (*t*, *J* = 6.8 Hz, 2H) correlated with carbon signal at δ_C 64.6 (C-1′). From the HMBC spectrum (Appendix 165) the correlations from H-5 to C-4, from H-26′ to C-24′, from H-25′ to C-24′, and OCH_3 to C-3 were observed for the feruloyl and aliphatic moiety. Especially, the HMBC correlations from H-1′ to C-8 confirmed the aliphatic chain was linked with feruloyl moiety at C-1′. Compound **92** was identified as n-pentacosyl-*trans*-ferulate after a comparison of the aforementioned NMR spectroscopic data (Table 33) and published data.[201]

Table 33: ^{1}H and ^{13}C-NMR data for compound **92**.

Position	**92** ^{1}H-NMR (600 MHz, Acetone) ^{13}C-NMR (151 MHz, Acetone)		**Lite.**[201] ^{1}H-NMR (500 MHz, $CDCl_3$) ^{13}C-NMR (125 MHz, $CDCl_3$)	
	δ_C	δ_H	δ_C	δ_H
1	127.0	-	127.1	-
2	109.2	6.97 (*d*, *J* = 1.8 Hz, 1H)	109.3	7.03 (*d*, *J* = 2.6 Hz, 1H)
3	147.9	-	147.9	-
4	146.7	-	146.8	-
5	114.7	6.85 (*d*, *J* = 8.1 Hz, 1H)	114.7	6.89 (*d*, *J* = 8.0 Hz, 1H)
6	123.1	7.01 (*dd*, *J* = 8.2, 1.9 Hz, 1H)	123.0	7.05 (*dd*, *J* = 8.0, 2.6 Hz, 1H)
7	144.7	7.54 (*d*, *J* = 15.9 Hz, 1H)	144.6	7.59 (*d*, *J* = 15.9 Hz, 1H)
8	115.7	6.23 (*d*, *J* = 15.9 Hz, 1H)	115.7	6.27 (*d*, *J* = 15.9)
9	167.4	-	167.4	-
3-OMe	55.9	3.89 (*s*, 3H)	55.9	3.91 (*brs*, 3H)
1′	64.6	4.12 (*t*, *J* = 6.8 Hz, 2H)	64.6	4.17 (*t*, *J* = 6.7 Hz, 2H)
2′	28.8	1.18, 1.63	28.8	1.67 (*t*, *J* = 6.6 Hz, 2H)
3′	26.0	1.31 (*d*, *J* = 8.2 Hz, 2H)	26.0	1.23 (*brs*)

4′-23′	29.7-29.3	1.18-1.63 (*brs*, 50H)	29.7-29.4	1.23 (*brs*)
24′	31.9	1.18 (*s*, 50H)	31.95	1.23 (*brs*)
25′	22.7	1.18 (*s*, 50H)	22.7	1.23 (*brs*)
26′	14.2	0.81 (*t*, *J* = 6.7 Hz, 5H)	14.1	6.7 (*d*, *J* = 6.7)

3.5.2.3 Characterization of Compound 72

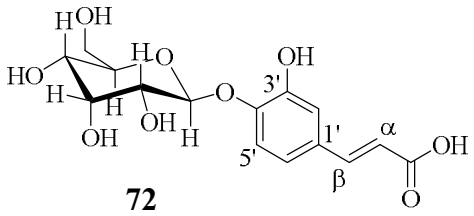

72

Compound **72** was isolated as white amorphous powder. This compound gave a magenta spot on TLC with 1% vanillin-sulfuric acid spraying reagent with an R_f value of 0.35 in EtOAc:MeOH (2:1). The IR spectrum revealed the presence of O-H stretching at 3429.4 cm^{-1}, C−H stretching 2866 and 2936 cm^{-1}, C=O stretching at 1747.8 cm^{-1}, and C=C stretching at 1651.5 cm^{-1}, aromatic ring at 1610, 1506.2, and 1464 cm^{-1}, and C-O-C stretching at 1072.4 cm^{-1}. The TOF-ESI-MS spectrum (Appendix 173) showed the molecular ion peak $[M+H]^+$ at m/z 343.1019 (calcd. for $C_{15}H_{19}O_9$, 343.3065), corresponds to a molecular formula of $C_{15}H_{18}O_9$. The ^{1}H-NMR spectrum (Table 34 and Appendix 167) showed three aromatic signals at δ_H 7.22 (*d*, *J* = 8.4 Hz, 1H-5′), 7.12 (*d*, *J* = 2.1 Hz, 1H-2′), and 7.06 (*dd*, *J* = 8.4, 2.1 Hz, 1H-6′) which indicated the presence of a 1,3,4-trisubstituted benzene moiety. The signals at δ_H 7.57 (*d*, *J* = 15.9 Hz, 1H-β) and 6.34 (*d*, *J* = 15.9 Hz, 1H-α) was assigned to a *trans* double bond in the molecule. Furthermore, *β*-glucose units were identified by a characteristic anomeric signal at δ_H 4.88 with a coupling constant of ∼7.0 Hz and carbinol proton signals appearing as multiplet between δ_H = 3.93 and 3.45. The ^{13}C-NMR spectrum (Table 34 and Appendix 168) showed 15 carbon signals which are attributed to two oxygenated olefine quaternary carbons at δ_C 148.7 (C-3'), 148.4 (C-4'), one olefine quaternary carbon δc 131.1 (C-1'), and three olefine methine carbons at δ_C 122.1 (C-6′), 118.0 (C-2′), 115.8 (C-5′), 117.8 (C-α), 146.0 (C-β) and one carbonyl quaternary carbon at δ_C 170.7, indicating the presence of a caffeic acid moiety. The other six oxygenated carbon signals appeared at δ_C 103.4 (C-1), 78.3 (C-5), 77.4 (C-3), 74.7 (C-2), 71.2 (C-4), and 62.3 (C-6), revealing the presence of a β–glucopyranoside. Assignments

of the above protons were further established by the COSY spectrum (Appendix 170). The signal of olefinic proton at δ_H 7.57 (H-β) showed correlation with the signal at δ_H 6.34 (H-α) in the COSY spectrum. In the aromatic region, the signal at δ_H 7.06 (H-6′) showed ortho and meta correlation with the signal at δ_H 7.22 (H-5′) and 7.12 (H-2′) in the COSY spectrum.

Table 34: ^{1}H-and ^{13}C-NMR data for compound **72**.

Position	**72** ^{1}H-NMR (400 MHz, MeOD) ^{13}C-NMR (101 MHz, MeOD)		Lite. [202] ^{1}H-NMR (600 MHz, $CDCl_3$) ^{13}C-NMR (125 MHz, $CDCl_3$)	
Caffeic acid	δ_C	δ_H	δ_C	δ_H
CO	170.6	-	170.6	-
α	117.8	6.34 (*d*, *J* = 15.9 Hz, 1H)	117.9	6.30 (*d*, *J* = 15.6)
β	146.0	7.57 (*d*, *J* = 15.9 Hz, 1H)	146.0	7.42 (*d, J* = 15.6)
1′	131.1	-	131.2	-
2′	118.0	7.12 (*d*, *J* = 2.1 Hz, 1H)	118.2	7.10 (*d*, *J* = 2.6)
3′	148.7	-	148.7	-
4′	148.4	-	148.5	-
5′	115.8	7.22 (*d*, *J* = 8.4 Hz, 1H)	115.7	7.14 (*d, J* = 7.8)
6′	122.1	7.06 (*dd*, *J* = 8.4, 2.1 Hz, 1H)	122.1	7.03 (*dd*, J = 7.8; 2.6)
Glucose				
1	103.4	4.88 (*d*, *J* = 7.0 Hz, 1H)	103.5	overlapped
2	74.7	3.52 (*m,* 1H)	74.8	3.42 (*dd*, *J* = 9.1; 7.8)
3	77.5	3.52 (*d*, *J* = 7.0 Hz, 1H)	77.5	3.51 (*t*, *J* = 9.1)
4	71.2	3.45 (*m,* 1H)	71.3	3.48 (*t*, *J* = 9.1)
5	78.3	3.45 (*m,* 1H)	78.4	3.44 (*ddd, J*=9.1; 5.2; 1.7*)*
6	62.3	3.93 (*dd*, *J* = 12.1, 2.0 Hz, 1H); 3.74 (*dd*, *J* = 12.1, 5.1 Hz, 1H)	62.4	3.90 (*dd*, *J* = 12; 1.7); 3.71 (*dd*, *J* = 12; 5.2)

HSQC spectrum (Appendix 171) showed a methine proton signal at δ_H 6.34 (*d*, *J* = 15.9 Hz, 1H) correlated with a carbon signal at δ_C 117.8 (C-α). The signal at δ_H 7.57 (*d*, *J* = 15.9 Hz, 1H) correlated with carbon signal at δ_C 146.0 (C-β). A methine proton signal at δ_H 7.12 (*d*, *J* = 2.1 Hz, 1H) correlated with a carbon signal at δ_C 118.0 (C-2′), a proton signal at δ_H 7.22 (*d*, *J* = 8.4 Hz, 1H) correlated with carbon signal at δ_C 115.8 (C-5′), and a proton signal at δ_H 7.06 (*dd*, *J* = 8.4, 2.1 Hz, 1H) correlated with a carbon signal at δ_C 122.1 (C-6′). The anomeric proton signal at δ_H 4.88 (*d*, *J* = 7.0 Hz, 1H) correlated with carbon signal at δ_C 103.4 (C-1). In the caffeic acid moiety, HMBC showed correlations from H-α and H-β to carbonyl carbon and H-6′ to C-5′, H-5′ to C-4′and C-1′, and H-2′ to C-3′and C-1′. From the HMBC spectrum (Appendix 172) the correlations from H-β to C-6′ and C-1′ indicated the olefinic

carbon at C-β (δ_C 145.98) was attached to C-1. The anomeric proton (H-1) of the β-glucose unit showed a long′-range ^{1}H-^{13}C correlation with C-4′ at δ_H 148.39 which located the glucose moiety at C-4′. Based on the analysis of the spectroscopic data, compound **72** was identified to be 4-*O*-β-D-glucopyranosylcaffeicacid. Comparison of the spectroscopic data (Table 34) of **72** with those reported in the literature[202] for 4-*O*-β-D-glucopyranosylcaffeic acid showed that the two compounds are identical.

3.5.3 Biological Activities of the Crude Extract and Isolated Compounds from *Olinia usambarensis* Barks

3.5.3.1 DPPH Radical Scavenging Assay of the Crude Extract and Isolated Compounds from *Olinia usambarensis Bark*

Table 35: Percent radical scavenging activity and IC_{50} values of the isolated compounds.

Compounds/ Extracts	% DPPH Inhibition at							
	100 µg/mL	**50** µg/mL	**25** µg/mL	**12.5** µg/mL	**6.25** µg/mL	**3.12** µg/mL	r^2	IC_{50} (µg/ml)
CE	92.9	80.2	62.5	43.8	34.4	28.1	0.93	22.1
91	27.1	22.6	22.2	21.8	20.9	20.1	0.94	458.8
92	35.8	28.4	27.1	24.4	23.9	23.	0.99	217.4
72	35.8	27.8	25.2	23.1	22.1	21.5	0.92	198.8
Ascorbic acid		97.32	97.27	97.25	97.19	96.96	0.81	0.31

Note: r^2 - coefficient of determination; IC_{50} - half maximal inhibitory concentration.

The antioxidant capacities of the extract and isolated compounds, expressed as the DPPH free radical inhibition and the IC_{50} values, are presented in Table 35. According to antioxidant activity parameters, a lower IC_{50} value corresponding with a higher antioxidant power.[156] The relative IC_{50} values for the isolated compounds and extract were in the range of 22.1–458.8 µg/ml (Table 35). According to antioxidant activity parameters, crude extract (IC_{50} = 22.1 µg/ml) showed strong in antioxidant activity compared to isolated compounds, while compound **91** (IC_{50} = 458.8 µg/ml) showed the lowest antioxidant activity. The order of the antioxidant activity among the compounds was **CE > 72 > 92 > 91**. As observed from Table 35, the isolated compounds and extract showed higer IC_{50} values compared to ascorbic acid (0.31µg/mL).

4 Experimental Section

4.1 General Experimental Procedures

All chemicals used in this study were analytical/HPLC grade and purchased from Sigma-Aldrich, Germany and Fisher Scientific, UK. Analytical-grade methanol (HPLC, > 99.9%), DCM (ACS, > 99.9%), ethyl acetate (ACS, > 99.9%), chloroform (ACS Reagent, > 99.9%), petroleum ether (ACS, > 99.9%) and hexane (Lab grade) were used throughout the laboratory work. Whatman filter paper No. 3 was used for filtration, and samples were concentrated by a rotary evaporator (Heidolph Hei-VAP, Germany). NMR experiments (1D and 2D) were recorded on a 600.0 MHz Bruker Avance III spectrometer using DMSO-d_6, MeOD, $CDCl_3$ solvents, and TMS as an internal reference. Mass spectra were recorded on a high-resolution mass spectrometer (Thermo Scientific, USA) equipped with an electrospray ionization (ESI) ion source. The Matrix-assisted laser desorption/ionization high resolution mass spectrometry (MALDI-HR-MS) was conducted using an Applied Biosystems 4800 Proteomics Analyzer equipped with an Nd/YAG laser (λ=335 nm), operated at a repetition rate of 200 Hz on a Bruker New ultrafleXtremeTM instrument. FT-IR (PerkinElmer) in the range 4000-400 cm^{-1} (resolution: 4 cm^{-1}, number of scans: 4) was used using KBr discs. Melting point was recorded using a METTLER TOLEDO FP82HT hot stage coupled with a METTLER TOLEDO FP90 central processor. Gas chromatography-mass spectrometry (GC-MS) experiments were conducted on Agilent Technologies 7820A GC system coupled with Agilent Technologies 5977E MSD, USA. Chromatographic peaks were identified by using NIST 2014 mass spectrometry data center library. For column chromatography, silica gel 60 (70–230 mesh ASTM) and Sephadex LH−20 (18−111 μm, GE Healthcare Bio-Sciences AB, Sweden) were used. The isolation process was monitored by TLC (pre-coated sheets, ALUGRAM, Xtra SIL G/UV_{254}, 20x20 cm, coated with silica gel 60 fluorescent indicator, Germany), which was visualized under UV light and also sprayed with vanillin (1 g vanillin with 5% H_2SO_4 in MeOH) and cerium molybdate stain (ammonium molybdate (12 g), ceric ammonium molybdate (0.5 g), and conc. H_2SO_4 (15 mL) in distilled water (235 mL) followed by heating for a few seconds.

4.2 Plant Materials

Myrica salicifolia

The leaves, roots and stem barks of *M. salicifolia* were collected from Debresina, Northern Shewa, Amhara region, 192 km from Addis Ababa, Ethiopia, in July 2020 by Dr. Mekonnen Abebayehu. The plant specimens were identified by Mr. Melaku Wendafrash, Department of Plant Sciences, Addis Ababa University, Ethiopia. A voucher specimen of the plant material was deposited at the National Herbarium, Addis Ababa University (No. MA/2007/12).

Clematis simensis

The aerial parts of *C. simensis* were collected from Debresina, Northern Shewa, Amhara region, 192 km from Addis Ababa, in June 2019 by Dr. Mekonnen Abebayehu. The plant specimen was identified by the Department of Plant Science, Addis Ababa University, Ethiopia. A voucher specimen was deposited at the National Herbarium, Addis Ababa University (No. AD001 *C. simenses).*

Olinia usambarensis

The barks of *Olinia usambarensis* were collected from Debresina, Northern Shewa, Amhara region, 192 km from Addis Ababa, in February 2022 by Dr. Mekonnen Abebayehu. The plant specimen was identified by the Department of Plant Science, Addis Ababa University, Ethiopia. A voucher specimen was deposited at the National Herbarium, Addis Ababa University (No. OR001 *O. rochetiana).*

4.3 Extraction and Characterization

4.3.1 Extraction and Characterization of Compounds from the Leaves of *Myrica salicifolia*

4.3.1.1 Extraction of Essential Oil by Hydrodistillation

The fresh leaves of *Myrica salicifolia* were crushed and prepared for hydrodistillation following previously published report.[203] Plant material (520 g) was placed into distillation flask (4 L) filled with 2 L distilled water and then the flask was attached to Clevenger

apparatus which was connected to a condenser. On a heating mantle, the flask's contents were brought to boiling, and then hydrodistillation was carried out for eight hours. The essential oil was collected (~0.4 mL), dried over anhydrous Na_2SO_4, and stored in a sealed vial in the dark at 4 ^{0}C, until analysis by GC-MS.

4.3.1.2 Characterization of the Essential Oil from the Leaves of *Myrica salicifolia*

The essential oil obtained from leaves of *Myrica salicifolia* were analyzed by using an Agilent Technology 7820A GC system coupled with an Agilent Technology 5977E MSD system equipped with an autosampler. The chromatographic separation was done on a column 30 m in length and 0.25 μm in thickness coated with HP-5MS, (5%-phenyl)-methylpolysiloxane, at a pressure of 8 psi and a flow rate of 0.97989 mL/min. Ultra-high pure helium (99.999%) was used as carrier gas at constant flow mode. An Agilent G4567A autosampler was used to inject 1 μL of the sample with a splitless injection mode into the inlet heated to 275 ºC with a total run time of 29.33 min. Oven temperature was programmed with the initial column temperature of 60 ºC and hold-time 2 min. The column temperature was increased at a rate of 10 ºC/min until the temperature reached 200 ºC and then heated again at the rate of 3 ºC/min until the temperature reached 240 ºC. No mass spectra were collected during the first 4 min of the solvent delay. The transfer line and the ion source temperatures were 280 ºC and 230 ºC, respectively. The detector voltage was 1600 V and the electron energy was 70 eV. Mass spectral data were collected from 40–650 *m*/*z*. The names and structures of peaks were determined through National Institute of Standards and Technology (NIST) 2014 library search.

4.3.1.3 Solvent Extraction of the Leaves of *Myrica salicifolia*

The collected fresh leaves of *M. salicifolia* were air-dried at room temperature. The dried plant materials were ground using an electric grinder to obtain a fine powder. The powder (1.22 kg) was soaked and homogenized exhaustively using MeOH:$CHCl_3$ mixture at a ratio of 1:1 (3 x 1L, 24 h each day). The mixture was filtered using a Buchner funnel with Whatman filter paper. The filtrates were concentrated using a rotary evaporator under reduced pressure at a temperature of 40 °C. The concentrated crude extracts were allowed to dry to a constant weight at room temperature and furnished dark green gummy extract

(41 g). The fractionation was done using slightly modified version of Kupchan method (Figure 12) of solvent-solvent partitioning[117] and yielded four partitionates; n-Pet ether (PE), chloroform ($CHCl_3$), ethylacetate (EtOAc), and methanol (MeOH) aqueous fraction which were stored in 4°C.

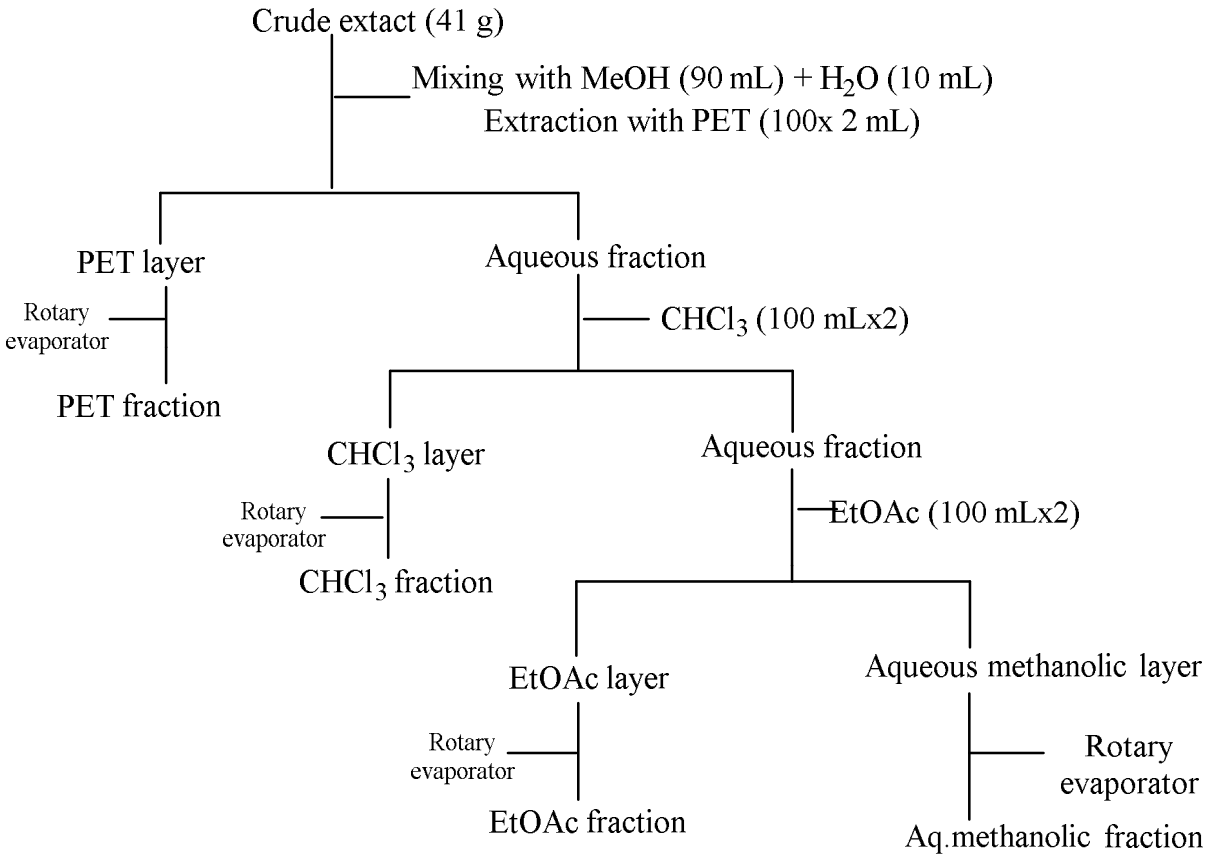

Figure 12: Schematic representation of the modified Kupachan partitioning of leaves crude extracts of *M. salicifolia.*

4.3.1.4 Fractionation of the Crude Extract of the Leaves of *Myrica salicifolia*

Each fraction was concentrated to dryness under reduced pressure to give PET fraction (15.40 g), $CHCl_3$ fraction (8.80 g), EtOAc fraction (5.40 g), and MeOH fraction (7.56 g). PET fraction (15.40 g) was dissolved in PET and EtOAc mixture, and adsorbed on 15 g of silica gel, mixed well and dried by a rotary evaporator. The dried sample (Figure 13) was loaded to a glass column packed with silica gel (390 g, 70–230 mesh ASTM) and fractionated using gradient solvent system PET:$CHCl_3$ (100:0 to 75:25, v/v) to give ten fractions (MSLP-1 to MSLP-10) each 200 mL. Fraction MSLP-2 (1.32 g) was subjected to

column chromatography over silica gel (80 g) using a gradient solvent system of Cy:EtOAc (100:0.00, v/v) to give 11 subfractions (MSLP-2-1 to MSLP-2-11) each 200 mL. Aliquot of MSLP-2-8 fraction was purified with acetone to give compound **77** (8.2 mg). Fraction MSLP-6 (3.17 g) was subjected to column chromatography over silica gel (200 g) using a gradient solvent system of PET:EtOAc (100:0.00 to 90:10,, v/v) to give 14 subfractions (MSLP-6-1 to MSLP-6-14) each 200 mL. Aliquot of MSLP-6-2 and MSLP-6-8 fraction was recrystallized from acetone to give compound **78 (**3.5 mg**)**. Fraction MSLP-10 was chromatographed over a column of silica gel using Cy:EtOAc (90:10 to 85:15, v/v) as eluent to afford 8 subfractions (MSLP-10-1 to MSLP-10-8). Subfraction MSLP-10-5 was rechromatographed over a column of silica gel using solvent system, $CHCl_3$ (100%) to give compounds **79** (12.47 mg). Chloroform fraction (8.80 g) was dissolved in chloroform and adsorbed on 10.00 g of silica gel, mixed well and dried by a rotary evaporator. The dried sample was loaded to a glass column packed with silica gel (350.00 g, 70–230 mesh ASTM) and fractionated using gradient solvent system $CHCl_3$:MeOH (100:0 to 68:32, v/v) to give 8 fractions (MSLC-1 to MSLC-8) each 200 mL (Figure 14). Fraction MSLC-5 (1.00 g) was subjected to column chromatography over silica gel (100 g, 70–230 mesh ASTM) using solvent sysyem of $CHCl_3$:MeOH (95:5, v/v) to give 8 subfractions (MSLC-5-1 to MSLC-5-8). Aliquot of MSLC-5-4 fraction was recrystallized from acetone to get compound **80** (9.32 mg).

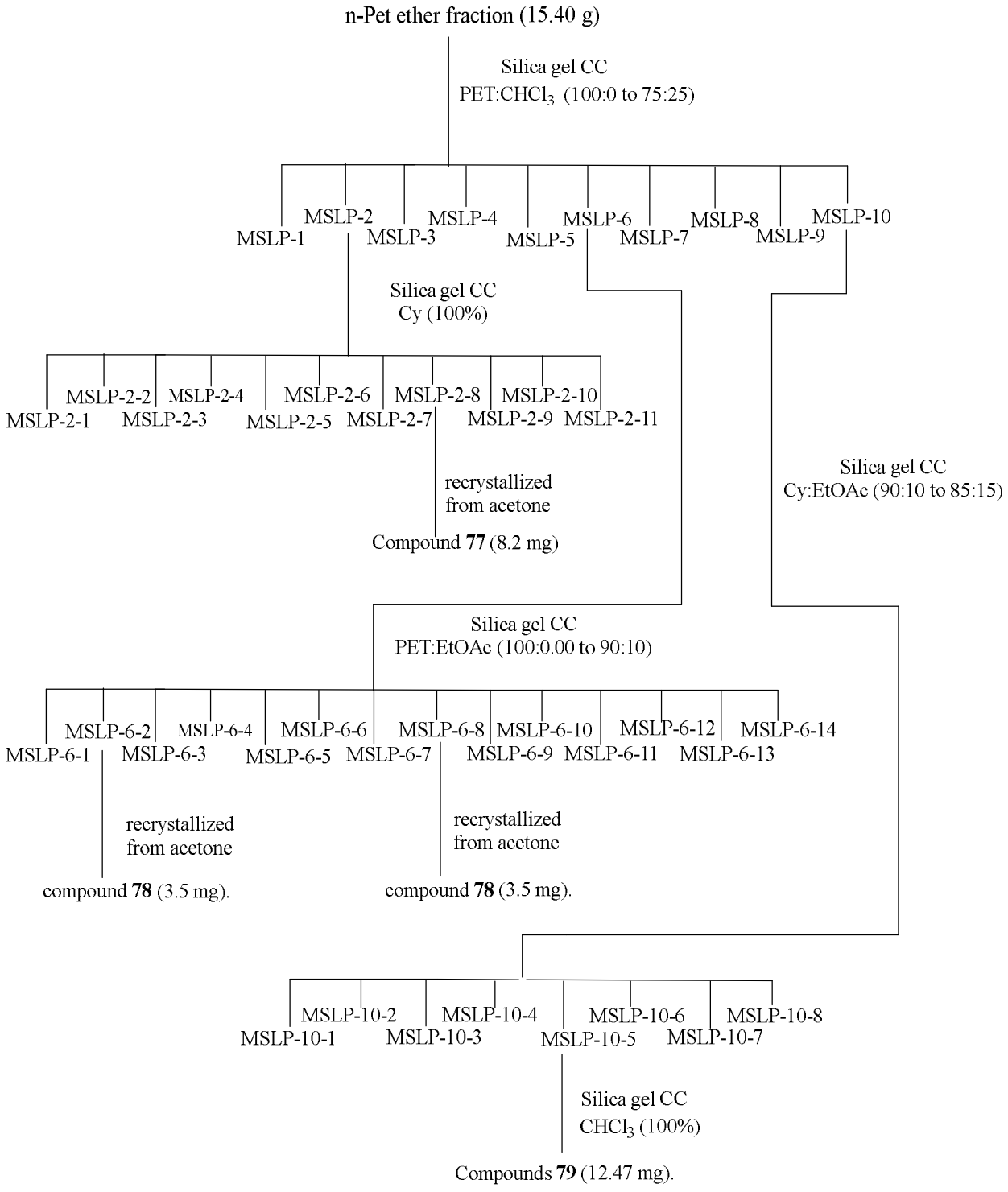

Figure 13: Fractionations and isolation compounds from n-Pet ether fraction of Leaves of *Myrica salicifolia.*

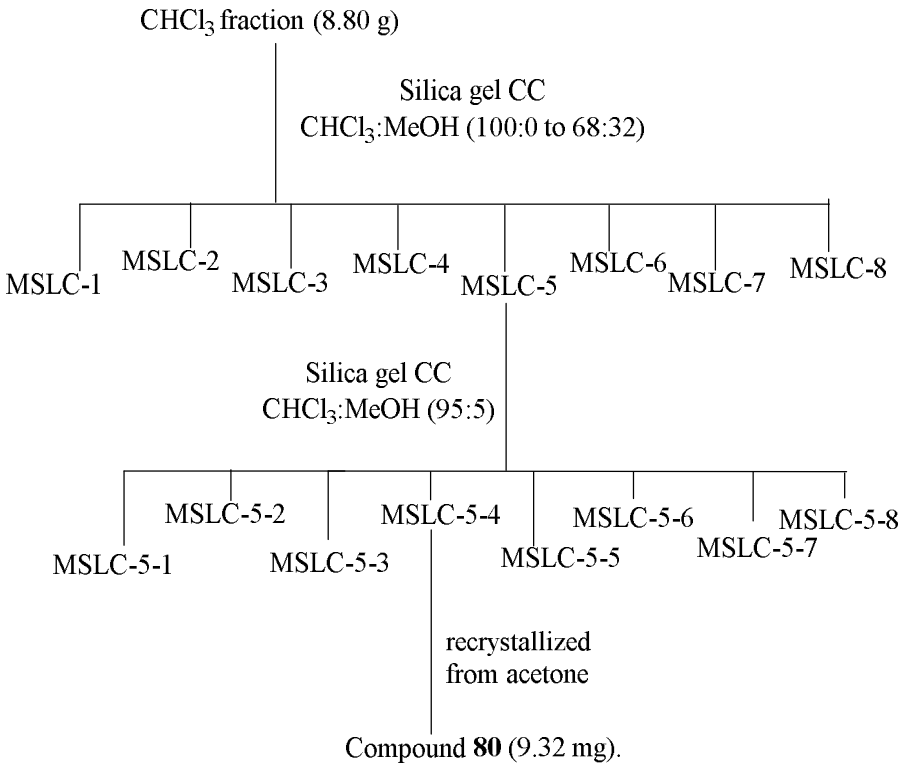

Figure 14: Fractionations and isolation compounds from chloroform fraction of leaves of *Myrica salicifolia*.

4.3.1.5 Physical and Spectroscopic Data of Compounds Isolated from the Leaves of *Myrica salicifolia*

Squalene (**77**): colourless oil; TOF-ESI-MS *m/z* 505.7191 $[M+4Na+3H]^{7+}$ (calc. for $C_{30}H_{53}Na4$, 505.7020); ^{1}H-NMR (400 MHz, $CDCl_3$) δ 5.14 (*d*, *J* = 6.2 Hz, 1H-3/22), 5.10 (*m*, 1H-7/18), 5.10 (*m*, 1H-11/14), 2.07 (*m*, 2H-8/17), 2.07 (*m*, 2H-4/21), 2.02 (*d*, *J* = 6.8 Hz, 2H-12/13), 1.98 (*m*, 2H-9/16), 1.98 (*m*, 2H-5/20), 1.68 (*s*, 6H-1/24), 1.60 (*s*, 6H-27/28), 1.60 (*s*, 6H-25/30), 1.60 (*s*, 6H-26/29). ^{13}C-NMR (101 MHz, $CDCl_3$) δ 135.1 (C-10/15), 134.9 (C-6/19), 131.2 (C-2/23), 124.4 (C-7/18), 124.3 (C-11/14), 124.3 (C-3/22), 39.8 (C-5/20), 39.8 (C-9/16), 28.3 (C-12/13), 26.8 (C-4/21), 26.7 (C-8/17), 25.7 (C-1/24), 17.7 (C-25/30), 16.1 (C-27/28), 16.0 (C-26/29).

Beta-carotene (**78**): red powder; m.p. 177 °C to 178 °C; IR_v (KBr, cm^{-1}): 2923.56, 2854.13, 1640.8; TOF-ESI-MS at *m/z* 203.1051 [M-332.769+H] (calc. for $C_{15}H_{23}$, 203.3436); ^{1}H-NMR (400 MHz, $CDCl_3$) δ 6.65 (*d*, *J* = 10.3 Hz, 2H -15, 15′), 6.37 (*d*, *J* =

14.9 Hz, H-12,12′), 6.27 (*d*, *J* = 8.3 Hz, 1H-14, 14′), 6.25/6.27 (*m*, 2H-10, 10′), 6.17 (*d*, *J* = 7.0 Hz, 3H -11, 11′), 6.16 (*m*, 2H-7, 7′), 6.12 (*m*, 2H-8, 8′), 1.04 (*s*, 6H-16, 16′), 2.03 (*d*, *J* = 6.4 Hz, 2H -4, 4′), 1.99 (*s,* 6H-19, 19′), 1.99 (*s*, 6H-20, 20′), 1.74 (*s*, 6H-18, 18′), 1.62 (*m*, H-3, 3′), 1.45 (*dd*, *J* = 16.0, 5.7 Hz, 4H-2, 2′), 1.04 (*s*, 6H-17, 17′). ^{13}C-NMR (150 MHz, $CDCl_3$) δ 137.9 (C-6, 6′), 137.8 (C-8, 8′), 137.2 (C-12,12′), 136.5 (C-13, 13′), 136.0 (C-9, 9′), 132.4 (C-10, 10′), 130.8 (C-1, 1′), 129.9 (C-11, 11′), 129.4 (C-5, 5′), 126.7 (C-7, 7′), 125.0 (C-14, 14′), 39.6 (C-2, 2′), 34.2 (C-1, 1′), 33.11(C-4, 4′), 29.0 (C-16, 16′), 28.9 (C-17, 17′), 21.81/21.9 (C-18, 18″), 19.3 (C-3, 3′), 12.8 (C-19, 19′), 12.8 (C-20, 20′).

Pheophytin A (**79**): dark bluish waxy; m.p. 115-117 °C; IR_v (KBr, cm^{-1}): 3461.6, 2918.6, 2847, 1738, 1644.6; ^{1}H-NMR (400 MHz, $CDCl_3$) δ 9.54 (*s*, 1H- β), 9.39 (*s*, 1H- α), 8.67 (*s*, 1H- δ), 8.05 (*dd*, *J* = 17.8, 11.5 Hz, 1H-2a), 6.31 (*s*, 1H-10), 6.18 (*m*, $2H_2$-2b), 6.29 (*dt*, *J* = 11.2, 1.7 Hz, $1H_2$-2b), 5.17 (*m*, 1H-P2), 4.50 (*m*, 1H-8), 4.50 (*m*, 2H-P1), 4.25 (*m*, 1H-7), 3.72 (*s*, 3H-5a), 3.71 (*d*, *J* = 11.3 Hz, 5H-4a), 3.5 (*s*, 3H-10b), 3.41 (*s*, 3H-1a), 3.25 (*s*, 3H-3a), 2.35 (*m*, 1H7b), 2.19 (*m*, 2H-7a), 1.92 (*dt*, *J* = 10.8, 5.4 Hz, 2H- P4), 1.80 (*d*, *J* = 7.3 Hz, 2H-8a), 1.70 (*td*, *J* = 7.6, 4.9 Hz, 3H-4b), 1.59 (*s*, 3H- P3a), 0.87 (*m*, H4- P15a), 0.87 (*m*, 4H- P16), 0.82 (*m*, 6H-P7a, P11a). ^{13}C-NMR (101 MHz, $CDCl_3$) δ 189.7 (C-9), 173.0 (C-7c), 172.4 (C-18), 169.6 (C-10a), 161.5 (C-17), 155.2 (C-13), 151.1 (C-14), 149.8 (C-16), 145.2 (C-4), 142.9 (C-11), 142.1(C-P3), 138.0 (C-15), 136.6 (C-12), 136.3 (C-2), 136.1 (C-3), 132.0 (C-1), 129.3 (C-6), 129.2 (C-5), 129.1 (C-2a), 122.9 (C-2b), 117.7 (C-P2), 105.4 (C- γ), 104.5 (C- β), 97.5 (C- α), 93.4 (C- δ), 64.7 (C-10), 61.5 (C-P1), 52.9 (C-10b), 51.7 (C-7), 50.2 (C-8), 39.8 (C- P4), 39.4 (C- P14), 37.4 (C-P10), 37.3 (C-P12), 37.3 (C- P8), 36.6 (C-P6), 32.8 (C-P11), 32.6 (C-P7), 31.2 (C-7a), 29.8 (C-7b), 28.0 (C- P15), 25.0 (C-P5), 24.8 (C- P13), 24.4 (C- P9), 23.1 (C-8a), 22.7 (C- P16), 22.6 (C-P15a), 19.7 (C- P7a), 19.6 (C- P11a), 19.5 (C-4a), 17.4 (C-4b), 16.3 (C- P3a), 12.2 (C-1a), 12.1 (C-5a), 11.3 (C-3a).

***β*-sitosterol** (**80**): white powder; m.p. 133-134 °C; IR_v (KBr, cm^{-1}): 3436.34, 2918.2 8, 2851.4 6, 1639.32; TOF-ESI-MS *m/z* 472.6723 $[M+CH_3OH+Na+3H]^{4+}$ (calcd for $C_{30}H_{57}O_2Na$, 472.7067); ^{1}H-NMR (400 MHz, $CDCl_3$) δ 5.35 (*dd*, *J* = 5.1, 2.6 Hz, 1H-6), 3.53 (*tt*, *J* = 10.7, 4.7 Hz, 1H-3), 2.27 (*m*, $1H_1$ -4), 2.22 (*m*, $1H_2$-4), 1.98 (*m*, 1H-7), 2.00 (*tt*, *J* = 14.6, 3.1 Hz, $1H_1$-12), 1.86 (*m*, $1H_1$-16), 1.83 (*m*, $1H_1$-1), 1.80 (*m*, 1H-2), 1.65 (*m*,

1H-25), 1.57 (*m*, 1H-7), 1.55 (*d*, *J* = 6.5 Hz, 1H1-15), 1.50 (*m*, $1H_1$ -11), 1.48 (*m*, $1H_2$-11), 1.48 (*m*, 1H-3, 8, 11), 1.37 (*m*, 1H-22), 1.36 (*m*, 1H-20), 1.27 (*m*, $1H_2$-16), 1.26 (*m*, 2H-28), 1.15 (*m*, $1H_2$ -12), 1.14 (*m,* H-23), 1.11 (*m*, 1H-17), 1.07 (*m*, 1H2-1, 14), 1.05 (*m*, 1H-22), 1.01 (*m*, 1H-15), 1.00 (*s*, 3H-19), 0.93 (*d*, *J* = 6.5 Hz, 4H-9, 21), 0.92 (*m*, 1H-24), 0.84 (*d*, *J* = 6.5 Hz, 3H -29), 0.82 (*d*, *J* = 6.5 Hz, 3H-27), 0.68 (*s*, 3H-18), 0.80 (*d*, *J* = 6.3 Hz, 3H-26). ^{13}C-NMR (101 MHz, $CDCl_3$) δ 140.8 (C-5), 121.7 (C-6), 71.8 (C-3), 56.8 (C-14), 56.0 (C-17), 50.2 (C-9), 45.7 (C-24), 42.4 (C-13), 42.4 (C-4), 39.5 (C-12), 37.3 (C-1), 36.5 (C-10), 36.2 (C-20), 34.4 (C-22), 31.8 (C-8), 31.8 (C-7), 31.7 (C-2), 29.2 (C-25), 27.9 (C-16), 26.0 (C-23), 24.4 (C-15), 22.8 (C-28), 21.2 (C-11), 19.9 (C-27), 19.6 (C-26), 19.2 (C-19), 18.9 (C-21), 11.8 (C-29), 12.0 (C-18).

4.3.2 Extraction and Characterization of Compounds from the Stem Barks of *Myrica salicifolia*

4.3.2.1 Solvent Extraction of the Stem Barks of *Myrica salicifolia*

The collected fresh stem bark of *M. salicifolia* was air-dried at room temperature. The dried plant materials were ground using an electric grinder to obtain a fine powder. The powder (1.41 kg) was soaked and homogenized exhaustively using MeOH and $CHCl_3$ mixture at a ratio of 2:1. The mixture was filtered using a Buchner funnel with Whatman filter paper. The filtrates were concentrated using a rotary evaporator under reduced pressure at a temperature of 40 °C. The concentrated crude extracts were allowed to dry to a constant weight at room temperature and furnished a mass of 98 g.

4.3.2.2 Fractionation of the Stem Barks Extract of *Myrica salicifolia*

The crude extract (26.4 g) was redissolved in chloroform and adsorbed on 25 g of silica gel, mixed well and dried by a rotary evaporator. The dried sample was loaded to a glass column packed with silica gel (330 g, 70–230 mesh ASTM) and fractionated using gradient solvent system pet ether:$CHCl_3$ (25:75 to 10:90, v/v), $CHCl_3$:EtOAc (90:10 to 0:100, v/v), and EtOAc:MeOH (95:5 to 20:80, v/v) to give 25 fractions each 200 mL. Fractions with similar TLC profiles were combined to give twenty fractions (MS-1 to MS-20) (Figure 15). Fraction MS-7 (5.3 g) was subjected to column chromatography over silica gel (120 g)

using gradient solvent system of pet ether:$CHCl_3$ (0:100 to 5:95, v/v) and $CHCl_3$:EtOAc (0:100 to 5:95, v/v) to give 14 subfraction, which were recombined into four groups (MS-7-1 to MS-7-4) based on their TLC profile. Subfraction MS-7-1 (205.5 mg) was applied to a Sephadex LH-20 column chromatography and eluted using $CHCl_3$:MeOH (1:1) to give compound **28** (12.4 mg). Fraction MS-9 (1.2 g) was subjected to column chromatography over silica gel (40 g) using gradient of pet ether:$CHCl_3$ (23:77 to 0:100, v/v) and $CHCl_3$:EtOAct (98:2 to 65:35, v/v) to give 10 subfractions, which were combined into three groups (MS-9-1 to MS-9-3) based on their TLC profile. Subfraction MS-9-2 (170.7 mg) was subjected to column chromatography over Sephadex LH-20 (90 g) using $CHCl_3$:MeOH (2:1) as eluent to give compound **29** (8.8 mg). Fraction MS-16 (2.1 g) was rechromatographed over silica gel (100 g) eluted using $CHCl_3$:EtOAc (10:90 to 5:95), followed by EtOAc:MeOH (97:3 to 70:30, v/v). Seven fractions (MS-16-1 to MS-16-7) were collected. Subfraction MS-16-4 (87 mg) was allowed to pass over Sephadex LH-20 column (90 g) eluted with $CHCl_3$:MeOH (2:1), and the fractionated eluents were concentrated to give compound **32** (13 mg). The subfractions MS-1 (325.5 mg) and MS-6 (102.5 mg) from pet ether:$CHCl_3$ (30:70, v/v), and pet ether:$CHCl_3$ (10:90, v/v) were recrystallized with MeOH to give compound **81** (10.2 mg) and compound **82** (7.6 mg), respectively. Subfraction MS-7-3 (102.5 mg) was was recrystallized to give compound **83** (42.12 mg) as a white solid. The major fraction MS-11 was concentrated and dissolved in acetone to give a precipitate named compound **84** (11.2 mg). Fraction MS-20 (1.42g) was rechromatographed over silica gel (100 g) eluted with EtOAc:MeOH mixtures (96:4 to 40:60, v/v). Five fractions (MS-20-1 to MS-20-5) were collected. Subfraction MS-20-4 (23 mg) was applied to the Sephadex LH-20 column (90 g) and eluted with $CHCl_3$:MeOH (2:1), and the collected fractions were concentrated to give compound **85** (5.2 mg) and compound **86 (**7.1 mg**)**.

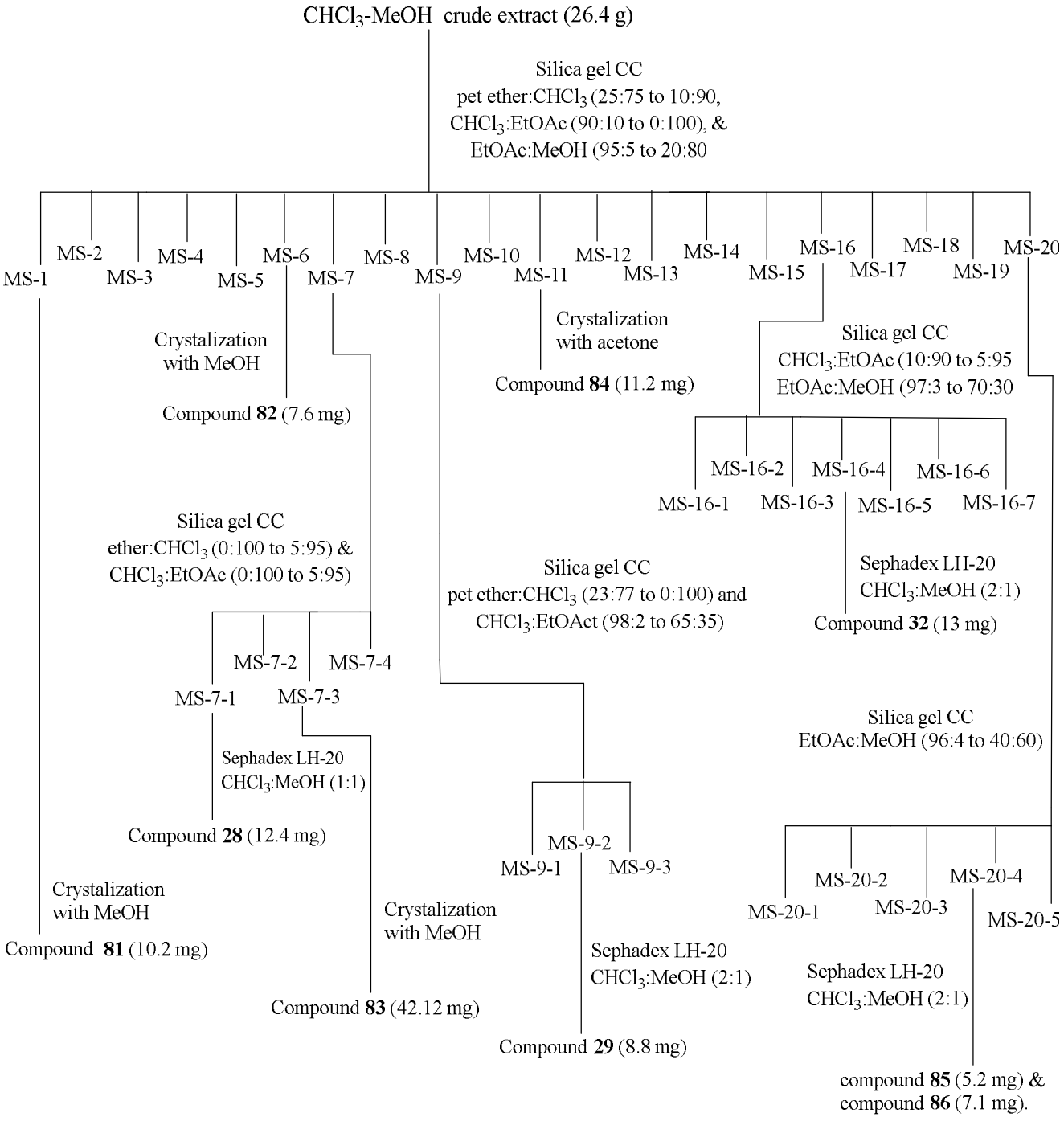

Figure 15: Fractionations and isolation of compounds from stem bark extract of *Myrica salicifolia*.

4.3.2.3 Physical and Spectroscopic Data of Compounds Isolated from the Stem Barks of *Myrica salicifolia*

Myricanone (**28**): white powder; m.p. 193-195 °C; IR_v (KB, cm^{-1}): 3409.2, 2934, 2857.2 1704.2, 1604.2; HPLC-ESI-MS (positive-ion mode) *m/z* 379.1516 $[M+Na]^+$ (calc. for $C_{21}H_{24}O_5$, 379.1515); ^{1}H-NMR (600 MHz, DMSO) δ 8.85 (*s*, OH-5), 8.70 (*s*, OH-17), 6.95 (*dd*, *J* = 8.2, 2.4 Hz, 1H-15), 6.72 (*d*, *J* = 8.2 Hz, 1H-16), 6.50 (*d*, *J* = 2.5 Hz, 1H-18), 6.32 (*s*, 1H-19), 3.76 (*s*, 3H-21), 3.74 (*s*, 3H-20), 2.85–2.78 (*m*, 2H-13), 2.76–2.71 (*m*, 2H-12), 2.66 (*t*, *J* = 7.2 Hz, 2H-10), 2.59–2.54 (*m*, 2H-7), 1.78 (*p*, *J* = 6.3 Hz, 2H-8), 1.58 (*p*, *J* = 7.1 Hz, 2H-9). ^{13}C-NMR (151 MHz, DMSO) δ 213.8 (C-11), 152.7 (C-17), 149.1 (C-5), 148.5 (C-3), 140.4 (C-4), 133.5 (C-18), 131.4 (C-14), 129.2 (C-19), 128.4 (C-15), 126.9 (C-1), 122.8 (C-2), 122.3 (C-6), 115.9 (C-16), 60.9 (C-21), 60.5 (C-20), 45.9 (C-10), 42.4 (C-12), 28.8 (C-13), 27.2 (C-7), 24.5 (C-8), 21.8 (C-9).

Myricanol (**29**): white powder; m.p. 102-110 °C; IR_v (KBr, cm^{-1}): 3369.8, 2924.2, 2855.6, 1610.8-1444; HPLC-ESI-MS (positive-ion mode) *m/z* 381.16707 $[M+Na]^+$ (calc. for $C_{21}H_{26}O_5$, 381.16724); ^{1}H-NMR (600 MHz, Acetone) δ 7.22 (*m*, 1H-18), 7.04 (*dd*, *J* = 8.2, 2.4 Hz, 1H-15), 6.91 (*s*, 1H-19), 6.80 (*d*, *J* = 8.2 Hz, 1H-16), 3.98 (*t*, *J* = 9.1 Hz, 1H-11), 3.91 (*s*, 3H-21), 3.89 (*s*, 3H-20), 2.93 (*ddd*, *J* = 16.3, 13.2, 2.7 Hz, 1H-13), 2.81 (*d*, *J* = 4.7 Hz, 1H-13), 2.78 (*m*, 1H-7), 2.54 (*ddd*, *J* = 17.9, 11.4, 3.9 Hz, 1H-7), 2.29 (*ddd*, *J* = 15.5, 13.0, 2.8 Hz, 1H-12), 1.91 (*ddd*, *J* = 13.7, 6.8, 3.8 Hz, 2H-8), 1.83 (*ddd*, *J* = 13.3, 10.4, 7.3 Hz, 1H-10), 16.7 (*m*, 1H-12), 1.57 (*dd*, *J* = 13.6, 11.5 Hz, 1H-10), 1.50 (*ddt*, *J* = 14.4, 10.9, 7.6 Hz, 1H-9). ^{13}C-NMR (151 MHz, Acetone) δ 151.5 (C-17), 148.7 (C-3), 146.8 (C-4), 139.4 (C-5), 133.3 (C-18), 130.8 (C-14), 129.5 (C-15), 129.0 (C-19), 124.8 (C-6), 123.0 (C-2), 122.7 (C-1), 116.2 (C-16), 67.1 (C-11), 60.8 (C-20), 60.6 (C-21), 39.5 (C-10), 34.6 (C-12), 26.7 (C-13), 25.8 (C-8), 25.5 (C-7), 22.9 (C-9).

11-*O*-*β*-D-xylopyranosylmyricanol (**32**): white powder; m.p. 231-232 °C; IR_v (KBr, cm^{-1}): 3390.8, 2927.8, 2849.6, 1501.8-1406.2; HPLC-ESI-MS (positive-ion mode) *m/z* 513.20956 $[M+H]^+$ (calc. for $C_{26}H_{34}O_9$, 513.20950); ^{1}H-NMR (600 MHz, DMSO) δ 6.94 (*d*, *J* = 3.6 Hz, 1H-15), 6.93 (*dt*, *J* = 2.7 Hz, 1H-18), 6.74 (*d*, *J* = 8.8 Hz, 1H-16), 6.53 (*s*, 1H-19), 3.98 (*d*, *J* = 7.4 Hz, 1H-1′), 3.80 (*s*, 3H-20), 3.78 (*s*, 3H-21), 3.73 (*d*, *J* = 3.3 Hz,

1H-11), 3.49 (*dd*, *J* = 11.4, 5.3 Hz, 1H-5′), 3.21 (*ddt*, 10.2, 8.6, 5.2 H, 1H-4′), 3.05 (*td*, *J* = 8.7, 4.7 Hz, 1H-3′), 2.89 (*ddd*, *J* = 8.9, 7.4, 5.2 Hz, 1H-2′), 2.78 (*m*, 1H-13), 2.69 (*dt*, *J* = 16.6, 3.8 Hz, 1H-13), 2.63 (*dt*, *J* = 17.7, 3.8 Hz, 1H-7), 2.50–2.43 (*m*, 1H-7), 2.12 (*m*, 1H-12), 1.70 (*m*, 1H-12), 1.77 (*m*, 2H-8), 1.63 (*dd*, *J* = 7.9, 4.7 Hz, 2H-10), 1.47 (*m*, 1H-9), 1.37 (*dt*, *J* = 9.7, 4.4 Hz, 1H-9). ^{13}C-NMR (151 MHz, DMSO) δ 129.5 (C-15), 134.1 (C-18), 116.2 (C-16), 129.8 (C-19), 102.0 (C-1′), 60.5 (C-20), 61.0 (C-21), 75.4 (C-11), 66.1 (C-5′), 70.1 (C-4′), 77.0 (C-3′), 73.6 (C-2′), 27.0 (C-13), 25.9 (C-7), 33.3 (C-12), 25.4 (C-8), 35.6 (C-10), 22.7 (C-9).

Taraxerone (**81**): white powder; m.p. 272-274 °C; IR_v (KBr, cm^{-1}): 2928.4, 2847.8, 1709; MALDI-MS (positive-ion mode) *m/z* 449.9 $[M+Na+H]^{2+}$ (calc. for $[C_{30}H_{48}ONaH]^{2+}$, 449.7); ^{1}H-NMR (600 MHz, $CDCl_3$) δ 5.58 (*dd*, *J* = 8.2, 3.2 Hz, 1H-15), 2.60 (*m*, 1H-2), 2.35 (*m*, 1H-2), 2.10 (*m*, 1H-19), 1.95 (*dd*, *J* = 14.7, 3.2 Hz, 1H-12), 1.90 (*ddd*, *J* = 13.2, 7.1, 3.3 Hz, 1H-12), 1.15 (*s*, 3H-27), 1.103 (*s*, 1H-23), 1.11 (*d*, *J* = 3.7 Hz, 3H-25), 1.09 (*s*, 3H-24), 1.103 (*s*, 1H-23), 1.01 (*m*, 1H-18), 0.98 (*s*, 3H-29), 0.94 (*s*, 3H-30), 0.93 (*s*, 3H-26), 0.85 (*s*, 3H-28). ^{13}C-NMR (125 MHz, $CDCl_3$) δ: 38.4 (C-1), 34.1 (C-2), 217.5 (C-3), 47.6 (C-4), 55.8 (C-5), 20 (C-6), 35.1 (C-7), 38.9 (C-8), 48.8 (C-9), 35.8 (C-10), 17.5 (C-11), 37.7 (C-12), 37.5 (C-13), 157.6 (C-14), 117.2 (C-15), 36.7 (C-16), 37.7 (C-17), 48.7 (C-18), 40.6 (C-19), 28.8 (C-20), 33.6 (C-21), 33.1 (C-22), 26.1 (C-23), 21.5 (C-24),14.8 (C-25), 29.9 (C-26), 25.6 (C-27), 29.9 (C-28), 33.3 (C-29), 21.3 (C-30).

Taraxerol (**82**): white powder; m.p. 257-260 °C; IR_v (KBr, cm^{-1}): 3430.8, 3051.4, 2929, 2860.4, 1751.2, 1620; MALDI-MS (positive-ion mode) *m/z* 449.9 $[M+Na]^+$ (calc. for $[C_{30}H_{50}ONa]^+$, 449.73); ^{1}H-NMR (600 MHz, $CDCl_3$) δ 5.56 (*dd*, *J* = 8.2, 3.2 Hz, 1H-15), 3.22 (*dt*, *J* = 10.6, 5.1 Hz, 1H-3), 2.06 (*dt*, *J* = 12.8, 3.3 Hz, 1H-7), 1.94 (*dd*, *J* = 14.8, 3.2 Hz, 1H-16), 1.63 (*m*, 1H-16), 1.63 (*m*, 1H-1), 1.63 (*m*, 1H-2), 1.59 (*m*, 1H-21), 1.59 (*m*, 1H-2), 1.50 (*m*, 2H-6), 1.44 (*m*, 2H-18), 1.44 (*m*, 2H-11), 1.37 (*m*, 2H-7), 1.38 (*m*, 2H-22), 1.33 (*m*, 1H-19), 1.25 (*m*, 2H-21), 1.11 (*s*, 3H-26), 1.00 (*s*, 1H-22), 1.00 (*m*, 3H-23), 0.97 (*s*, 3H-29), 0.95 (*s*, 3H-24), 0.93 (*s*, 3H-30), 0.93 (*s*, 3H-27), 0.83 (*s*, 3H-25), 0.80 (*m*, 1H-5). ^{13}C-NMR (100 MHz, $CDCl_3$): 15.5 (C-24), 15.4 (C-25), 17.5 (C-11), 18.8 (C-6), 21.3 (C-27), 25.9 (C-26), 27.2 (C-2), 28.0 (C-23), 28.8 (C-20), 29.8 (C-28), 29.9 (C-30), 33.1 (C-12), 33.4 (C-29), 33.7 (C-21), 35.8 (C-17), 35.1 (C-22), 36.7 (C-16), 37.74 (C-19),

37.6 (C-13), 38 (C-10), 37.7 (C-1), 38.9 (C-4), 38.8 (C-8), 41.3 (C-7), 48.8 (C-9), 49.3 (C-18), 55.0 (C-5), 79.1 (C-3), 116.9 (C-15), 158.1 (C-14).

Myricadiol (**83**): white powder; m.p. 266-268 °C; IR_v (KBr, cm^{-1}): 3392, 2936, 2855, 1644.4; MALDI-MS (positive-ion mode) *m/z* 442.10 $[M]^+$ (calc. for $C_{30}H_{50}O_2$, 442.717); ^{1}H-NMR (600 MHz, $CDCl_3$) δ 5.53 (*dd*, *J* = 8.2, 3.3 Hz, 1H-15), 3.31 (*dd*, *J* = 10.9, 5.3 Hz, 1H-28), 3.22 (*dt*, *J* = 10.7, 5.0 Hz, 1H-3), 3.16 (*dd*, *J* = 10.9, 4.8 Hz, 1H-28), 2.14 (*dd*, *J* = 15.2, 8.2 Hz, 1H-16), 1.77 (*dd*, *J* = 15.4, 3.3 Hz, 1H-16), 1.62 (*m*, 1H-2), 1.66 (*m*, 1H-12), 1.54 (*d*, *J* = 3.2 Hz, 1H-12), 1.50 (*m*, 4H-11), 1.42 (*m*, 1H-9), 142 (*m*, 1H-9), 1.29 (*m*, 2H-21), 1.17 (*m*, 4H-26),1.00 (*s*, 3H-23), 0.99 (*s*, 3H-29), 0.98 (*s*, 3H-27), 0.92 (*s*, 3H-30), 0.94 (*s*, 3H-25), 0.82 (*s*, 3H-24), 0.80 (*dd*, *J* = 12.2, 2.5 Hz, 1H-5), 0.63 (*dd*, *J* = 13.7, 3.8 Hz, 1H-18). ^{13}C-NMR (125 MHz, $CDCl_3$) δ: 37.7 (C-1), 27.1 (C-2), 79.0 (C-3), 38.8 (C-4), 55.8 (C-5), 18.8 (C-6), 41.1 (C-7), 39.1 (C-8), 49.1 (C-9), 37.9 (C-10), 17.4 (C-11), 33.4 (C-12), 37.5 (C-13), 159.2 (C-14), 117.2 (C-15), 30.8 (C-16), 40.4 (C-17), 44.8 (C-18), 35.8 (C-19), 28.6 (C-20), 32.7 (C-21), 27.9 (C-22), 28.0 (C-23), 15.4 (C-24), 15.4 (C-25), 26.0 (C-26), 21.6 (C-27), 65.5 (C-28), 33.5 (C-29), 29.9 (C-30).

3β-*O-trans*-caffeoylisomyricadiol (84): white powder; m.p. 292-294 °C; IR_v (KBr, cm^{-1}): 3434.2, 2937.8, 2868.4, 1695.6, 1616.6; MALDI-MS *m/z* 897.8 as $[M+(DHB-H_2O)_2+Na]^+$ (calc. for $C_{39}H_{56}O_5$, 897.0); ^{1}H NMR (600 MHz, DMSO) δ 7.45 (*d*, *J* = 15.8 Hz, 1H-7′), 7.04 (*d*, *J* = 2.1 Hz, 1H-1′), 7.00 (*dd*, *J* = 8.2, 2.1 Hz, 1H-5′), 6.76 (*d*, *J* = 8.1 Hz, 1H-4′), 6.24 (*d*, *J* = 15.9 Hz, 1H-8′), 5.43 (*dd*, *J* = 8.4, 3.1 Hz, 1H-15), 4.49 (*dd*, *J* = 11.7, 4.5 Hz, 1H-3), 4.30 (*s*, OH-28), 3.00 (*d*, *J* = 10.3 Hz, 1H-28), 2.89 (*d*, *J* = 10.2 Hz, 1H-28), 2.12 (*dd*, *J* = 14.8, 8.1 Hz, 1H-16), 1.99 (*dt*, *J* = 13.3, 3.4 Hz, 1H-7), 1.37 (*s*, 1H-19), 1.27–1.11 (*m*, 2H-21), 1.04 (*s*, 3H-26), 1.00 (*m*, 2H-19, 22), 0.95 (*s*, 3H-29), 0.94 (*s*, 3H-25), 0.933 (*s*, 3H-27), 0.92 (*s*, 3H-24), 0.918 (*m*, 1H-5) 0.87 (*s*, 3H-30), 0.84 (*s*, 3H-23), 0.47 (*dd*, *J* = 13.6, 3.6 Hz, 1H-18). ^{13}C-NMR (151 MHz, DMSO) δ 166.7 (C-9′), 158.0 (C-14), 148.8 (C-3′), 146.0 (C-2′), 145.3 (C-7′), 126.0 (C-6′), 121.7 (C-5′), 116.4 (C-15), 116.2 (C-4′), 115.3 (C-1′), 114.9 (C-8′), 80.2 (C-3), 63.7 (C-28), 55.3 (C-5), 48.9 (C-9), 45.0 (C-18), 40.5 (C-17), 41.3 (C-7), 39.0 (C-8), 37.9 (C-4), 37.9 (C-10), 37.4 (C-13), 37.3 (C-1), 36.0 (C-19), 34.0 (C-29), 33.6 (C-12), 32.9 (C-21), 30.6 (C-16), 30.2 (C-30), 28.7 (C-20), 28.2

(C-23), 27.8 (C-22), 26.3 (C-26), 23.7 (C-2), 21.8 (C-27), 18.7 (C-6), 17.4 (C-11), 17.1 (C-24), 15.6 (C-25).

Methyl-β-D-glucopyranoses (**85**): white powder; m.p. 104-106 °C; IR_v (KBr, cm^{-1}): 3420, 2928.2, 2858.6; HPLC-ESI-MS (positive-ion mode) *m/z* 217.0684 $[M+H]^+$ (calc. for $C_7H_{14}O_6$, 217.0682; ^{1}H-NMR (600 MHz, MeOD) δ 4.19 (*d*, *J* = 7.8 Hz, 1H-1), 3.69 (*dd*, *J* = 11.7, 6.6 Hz, 1H-6), 3.55 (*s*, H-7), 3.37 (*t*, *J* = 8.8 Hz, 1H-3), 3.31 (*d*, *J* = 9.6 Hz, 1H-5), 3.29 (*m*, 1H-4), 3.18 (*dd*, *J* = 9.2, 7.8 Hz, 1H-2). ^{13}C-NMR (151 MHz, MeOD) δ 104.0 (C-1), 61.3 (C-6), 55.9 (C-7), 76.7 (C-3), 70.2 (C-4), 76.5 (C-5), 73.7 (C-2).

Contortamide (86): white powder; m.p. 198-200 °C; IR_v (KBr, cm^{-1}): 3436.1, 3418.2, 2920.4, 2851.2, 1746.8-1635.6, 1535.2-1465.3; ^{1}H NMR (600 MHz, MeOD) δ 5.44 (*m*, 1H-7), 5.33 (*m*, 1H-6), 4.30 (*dd*, *J* = 9.9, 7.4 Hz, 2H-2), 4.30 (*d, J* = 7.7 Hz, 1H-1″), 4.07 (*dd*, *J* = 10.5, 6.3 Hz, 1H1-1), 4.04 (*m*, 1H-2′), 3.89 (*m*, 2H1-6″), 3.83 (*dt*, *J* = 10.5, 3.2 Hz, 1H2-1), 3.68 (*m*, 2H2-6″), 3.62 (*t*, *J* = 6.1 Hz-3), 3.54 (*m*, 1H-4), 3.37 (*m*, 2H-3″), 3.29 (*m*, 2H-5″), 3.29 (*m*, 2H-4″), 3.20 (*dd*, *J* = 9.3, 7.8 Hz, 2H-2″), 2.09 (*m*, 1H-5), 1.98 (*m*, 2H-8), 1.76 (*m*, 1H1-3′), 1.62 (*m*, 1H2-3′), 1.26-1.38H (*brs*, 58H-9-16), 1.26-1.38 (*brs*, 58H-4′-24′), 0.92 (*t*, *J* = 6.9 Hz, 3H-25′), 0.92 (*t*, *J* = 6.9 Hz, 3H-17). ^{13}C NMR (151 MHz, MeOD) δ 175.70 (C-1′), 129.53 (C-7), 129.34 (C-6), 103.28 (C-1″), 76.60 (C-5″), 76.48 (C-3″), 74.15 (C-3), 73.60 (C-2″), 71.56 (C-2′), 71.46 (C-4), 70.16 (C-4″), 68.51 (C-1), 61.24 (C-6″), 50.24 (C-2), 34.32 (C-3′), 22.2-31.7 (C-9–16/C-4′–24′), 22.34 (C-1), 13.04 (C-17, 25′).

4.3.2.4 Biological Activities of the Crude Extract and Isolated Compounds from the Stem Barks of *Myrica salicifolia*

4.3.2.4.1 DPPH Radical Scavenging Assay of the Extract and Isolated Compounds from the Stem Barks of *Myrica salicifolia*

The antioxidant activities of the isolated compounds were assessed using DPPH radical scavenging activity with ascorbic acid as the positive control as per the previously described method.[204] The standard solution of 0.1mM DPPH was prepared by dissolving 4mg of DPPH in 100 mL of methanol. All extracted and isolated compounds were

separately dissolved in DMSO (1 mg/mL). Briefly, 4 ml of methanol solution of DPPH (0.1mM) was mixed with 1 ml of extract and each of isolated compound solution at different concentrations (3.12, 6.25, 12.5, 25, and 50 µg/mL). The mixture was incubated in the dark for 30 minutes, and the absorbance was read off at 517 nm wavelength using a UV-Vis spectrophotometer. An ascorbic acid solution of the same concentration (3.12 µg/mL to 50 µg/mL) was prepared in similar fashion and measured. The DPPH radical scavenging activity of each of the tested compounds was reported as percentage inhibition using the formula given by Eq. 1:

$$\%\ \text{DPPH Inhibition} = \left[\frac{\text{A control} - \text{B sample}}{\text{A control}}\right] \times 100 \quad \ldots\ldots\ldots\ldots\ldots\text{Eq. 1}$$

Where A control is the absorbance of DPPH solution, and B sample is the absorbance of the test sample (DPPH solution plus compound). The DPPH solution was used as a negative control. The relative half-maximal inhibitory concentration (IC_{50}) values were calculated *via* linear regression analysis (y = bx + a), where y = 50 and x denote IC_{50}. The final antioxidant activity of each compound was expressed as the IC_{50} value.

4.3.2.4.2 Antibacterial Activities of the Crude Extract and Isolated Compounds from the Stem Barks of *Myrica salicifolia*

The four common standard ATCC strains, *Staphylococcus aureus*, *Escherichia coli*, *Streptococcus pyogenes*, and *Pseudomonas aeruginosa* were obtained from Adama Science and Technology University (ASTU). Experiments were conducted in close consultation with the Microbiology Laboratory of the Applied Biology Department of ASTU. The *in-vitro* antibacterial susceptibility test was determined by disk diffusion method.[203] The medium was prepared by dissolving 38 g of Mueller Hinton agar in 1000 mL of distilled water in 2.5 L flask. The flask was placed on a hot plate with a magnetic stirrer, and the mixture was heated slowly until the powder was completely dissolved, then autoclaved at 121 °C for 15 min. The autoclaved medium was poured into sterile petri dishes (20 mL/plate), and the plates were allowed to solidify under sterile conditions at room temperature. Then, the plates were seeded with an overnight grown culture approximately 1.5 x 10^8 CFU/mL by swabbing evenly on the surface of the medium with a sterile cotton swab. The isolated compounds at concentrations of 250 µg/mL and 500

μg/mL were prepared by dissolving in 10% DMSO in water.[205-206] Six mm in diameter discs made of Whatman filter paper No. 1 were infused with the solutions of the isolated compounds and placed on the surface of the medium by gently pressed down to ensure contact with the MHA. Plates were inverted and incubated at 37 ℃ for 24 hours. Ampicillin was used as a standard antibiotic positive control[207], while 10% DMSO in water was used as a negative control. After incubation, the inhibition zones were evaluated by measuring the diameter (mm) of the clear zone around the discs. All the experiments were performed in triplicate and interpreted using the CLSI zone diameter interpretative standards[203], and compared with 10 μg/mL controls.

4.3.3 Extraction and Characterization of Compounds from the Roots of *Myrica salicifolia*

4.3.3.1 Extraction of Essential Oil by Hydrodistillation

The roots of *Myrica salicifolia* were crushed and prepared for hydrodistillation following previously published report.[116] Plant material (536 g) was placed into distillation flask (4 L) filled with 2 L distilled water, which was then attached to Clevenger apparatus. On a heating mantle, the flask's contents were brought to boiling, and then hydrodistillation was carried out for eight hours. The essential oil was collected (~0.2 mL), dried over anhydrous Na_2SO_4, and stored in a sealed vial in the dark at 4 ^{0}C, until analysis by GC-MS.

4.3.3.2 Characterization of the Essential Oil from the Roots of *Myrica salicifolia*

The essential oil obtained from roots of *Myrica salicifolia* were analyzed by using an Agilent Technology 7820A GC system coupled with an Agilent Technology 5977E MSD system equipped with an autosampler. The chromatographic separation was done on a column 30 m in length and 0.25 μm in thickness coated with HP-5MS, (5%-phenyl)-methylpolysiloxane, at a pressure of 8 psi and a flow rate of 0.97989 mL/min. Ultra-high pure helium (99.999%) was used as carrier gas at constant flow mode. An Agilent G4567A autosampler was used to inject 1 μL of the sample with a splitless injection mode into the inlet heated to 275 ºC with a total run time of 29.33 min. Oven temperature was programmed with the initial column temperature of 60 ºC and hold-time 2 min. The column temperature was increased at a rate of 10 ºC/min until the temperature reached 200 ºC and then heated again at the rate of 3 ºC/min until the temperature reached 240 ºC. No mass

spectra were collected during the first 4 min of the solvent delay. The transfer line and the ion source temperatures were 280 ºC and 230 ºC, respectively. The detector voltage was 1600 V and the electron energy was 70 eV. Mass spectral data were collected from 40–650 *m*/*z*. The names and structures were determined through National Institute of Standards and Technology (NIST) 2014 library search.

4.3.3.3 Solvent Extraction of the Roots of *Myrica salicifolia*

The collected fresh roots of *M. salicifolia* were air-dried at room temperature. The dried plant materials were ground using an electric grinder to obtain a fine powder. The powder (1.31 kg) was soaked and homogenized exhaustively using MeOH and $CHCl_3$ mixture at a ratio of 1:2. The mixture was filtered using a Buchner funnel with Whatman filter paper. The filtrates were concentrated using a rotary evaporator under reduced pressure at a temperature of 40 °C. The concentrated crude extracts were allowed to dry to a constant weight at room temperature and furnished a mass of 44.3 g. Crude extract was fractionated using modified 'Kupchan method of solvent-solvent partitioning.[117] Solvents based with varying in density and polarities were used for fractionation. n-Hexane (Hex), chloroform ($CHCl_3$), ethyacetate (EtOAc) and methanol (MeOH) were successively added in separating funnel gave four fractions (Figure 16).

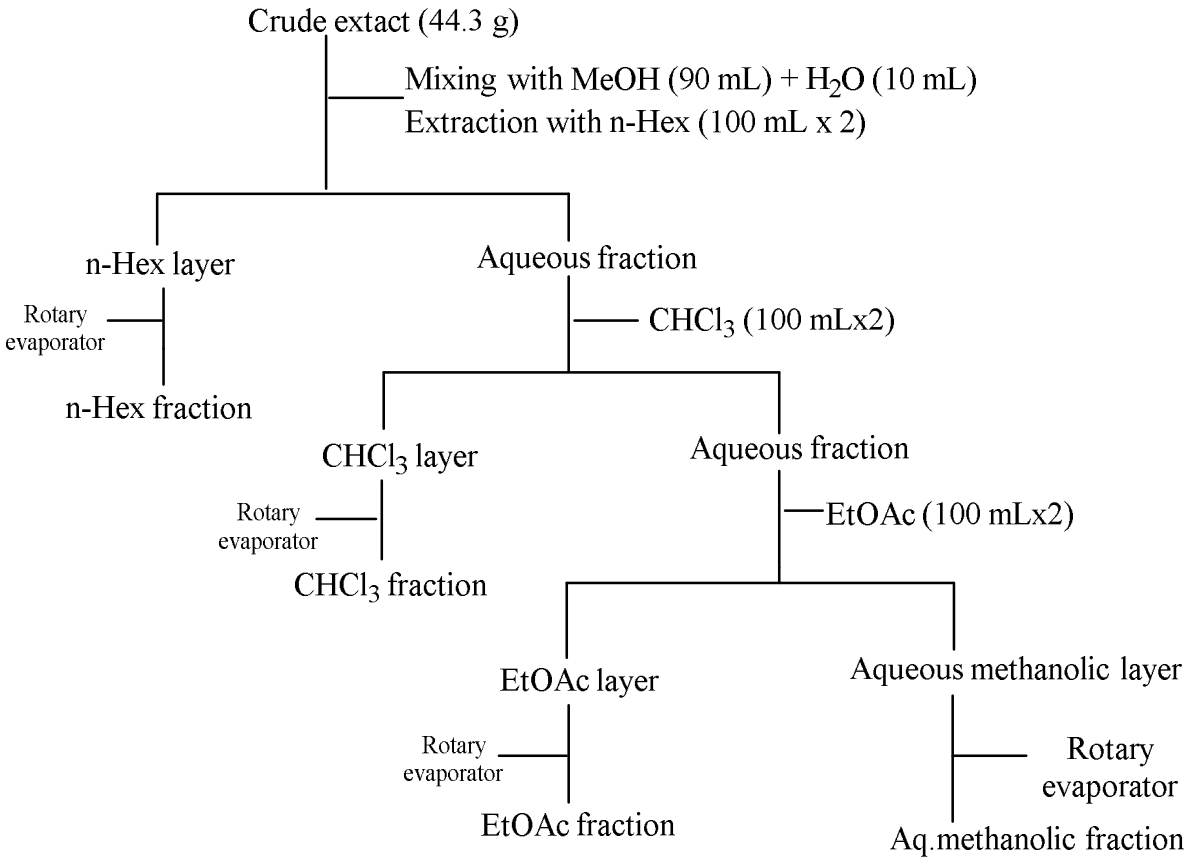

Figure 16: Schematic representation of the modified Kupachan partitioning of roots crude extracts of *M. salicifolia.*

4.3.3.4 Fractionation of the Roots Extract of *Myrica salicifolia*

Each fraction was concentrated to dryness under reduced pressure to yield n-Hex (6.24 g) fraction, $CHCl_3$ fraction (5.60 g), EtOAc fraction (9.11 g), and MeOH fraction (10.96 g). Chloroform fraction (5.60 g) was redissolved in chloroform and adsorbed on 6 g of silica gel, mixed well and dried by a rotary evaporator. The dried sample was loaded to a glass column packed with silica gel (200 g, 70–230 mesh ASTM) and fractionated using gradient solvent system PET:$CHCl_3$ (95:5 to 20:80, v/v), $CHCl_3$:EtOAc (90:10 to 0:100, v/v), and EtOAc:MeOH (95:5 to 60:40, v/v) gave 12 fractions (MSRC-1 to MSRC-12) each 150 mL (Figure 17). The fraction MSRC-4 (655 mg) was rechromatographed on silica gel column chromatography (40 g) and eluted using pet ether:$CHCl_3$ (20:80, v/v) gave 15 subfractions. Subfractions from MSRC-4-3 to MSRC-4-7 were mixed and recrystallized using MeOH gave compound **82** (12 mg). Fraction MSRC-5 (1.68 g) was subjected to column

chromatography over silica gel (50 g) using a gradient solvent system of pet ether:$CHCl_3$ (80:20 to 10:90, v/v) gave 10 subfractions (MSRC-5-1 to MSRC-5-10) each 150 mL. Fraction MSRC-5-6 and MSRC-5-7 were recombined into one fraction based on their TLC profile and allowed to pass over Sephadex LH-20 column eluted using $CHCl_3$:MeOH (2:1) as eluent gave compound **80** (8.9 mg). EtOAc fraction (9.11 g) was redissolved using EtOAc and adsorbed on 10 g of silica gel, mixed well and dried by a rotary evaporator. The dried sample was loaded to a glass column packed with silica gel (370 g, 70–230 mesh ASTM) and fractionated using gradient solvent system $CHCl_3$:EtOAc (50:50 to 0:100, v/v), and EtOAc:MeOH (98:2 to 0:100, v/v) gave 34 fractions each 200 mL (Figure 18), which were combined into 9 groups (MSRE-1 to MSRE-9) based on their TLC profile. Fraction MSRE-2 (324.4 mg) was subjected to column chromatography over silica gel (20 g, 70–230 mesh ASTM) using gradient solvent system of $CHCl_3$:MeOH (100:0 to 75:25, v/v) gave 6 subfractions (MSRE-2-1 to MSRE-2-6). Aliquot of MSRE-2-1 fraction was recrystallized using acetone gave compound **87** (5.73 mg). Fraction MSRE-3 (2.36 g) was subjected to column chromatography over silica gel (120 g, 70–230 mesh ASTM) using $CHCl_3$:MeOH (100:0 to 75:25, v/v) (0:100 to 5:95, v/v) gave 18 subfraction which were recombined into 8 groups (MSRE-3-1 to MSRE-3-8) based on their TLC profiles. Subfraction MSRE-3-5 to MSRE-3-8 (215.7 mg) were mixed and further fractionated by Sephadex LH-20 using $CHCl_3$:MeOH (1:1) as eluent gave compound **28** (5.94 mg). Fraction MSRE-8 (3.77 g) was subjected to column chromatography over silica gel (150 g, 70–230 mesh ASTM) using a gradient solvent system of EtOAc:MeOH (100:0 to 75:25, v/v) to give 12 subfraction (MSRE-8-1 to MSRE-7-12) based on their TLC profiles. Subfraction MSRE-8-4 (316 mg) was further fractionated by column chromatography over silica gel (120 g) using $CHCl_3$:MeOH (1:0.5) as eluent to give compound **30** (10.1 mg).

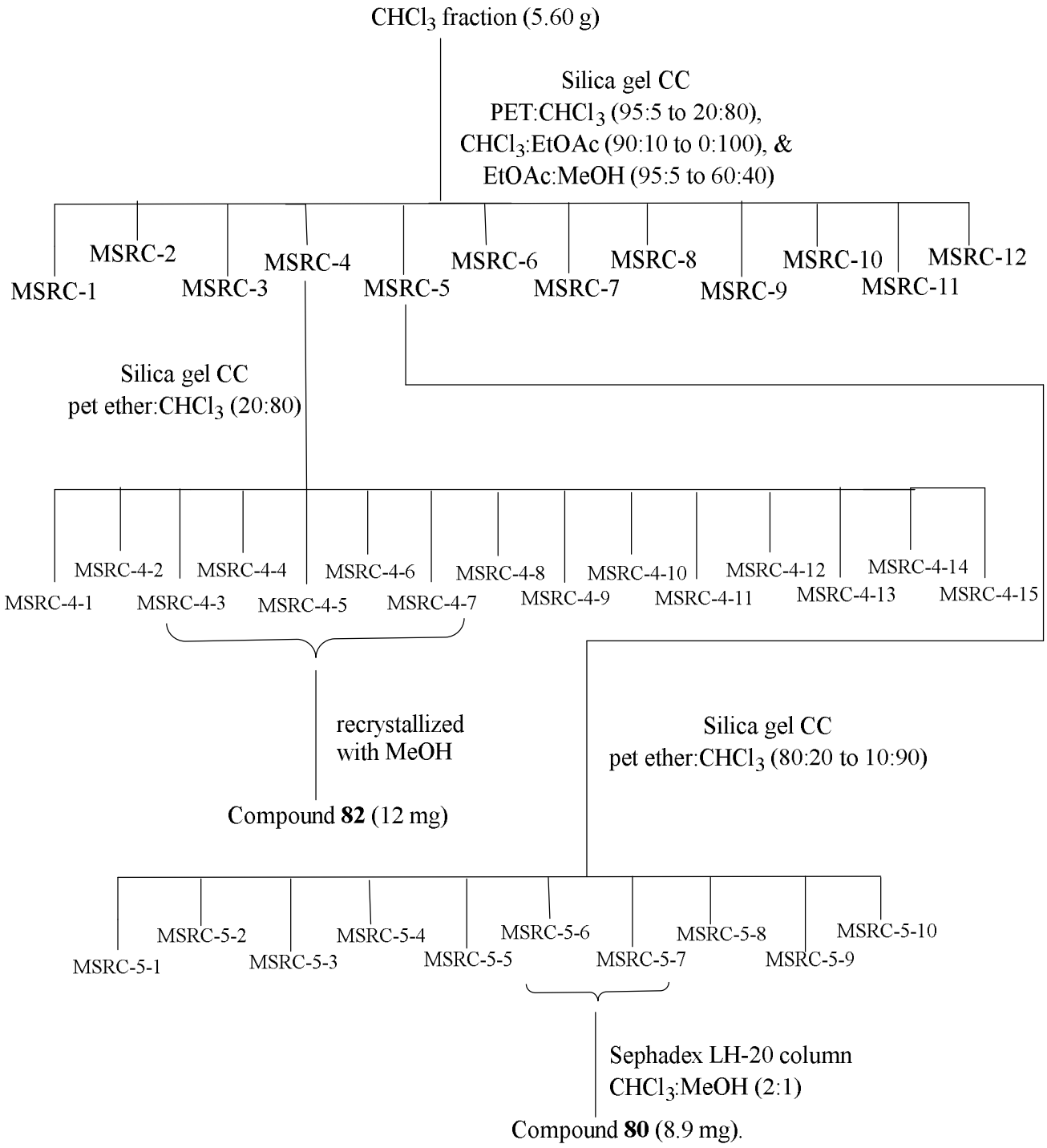

Figure 17: Fractionations and isolation of compounds from chloroform fraction of roots extract of *Myrica salicifolia.*

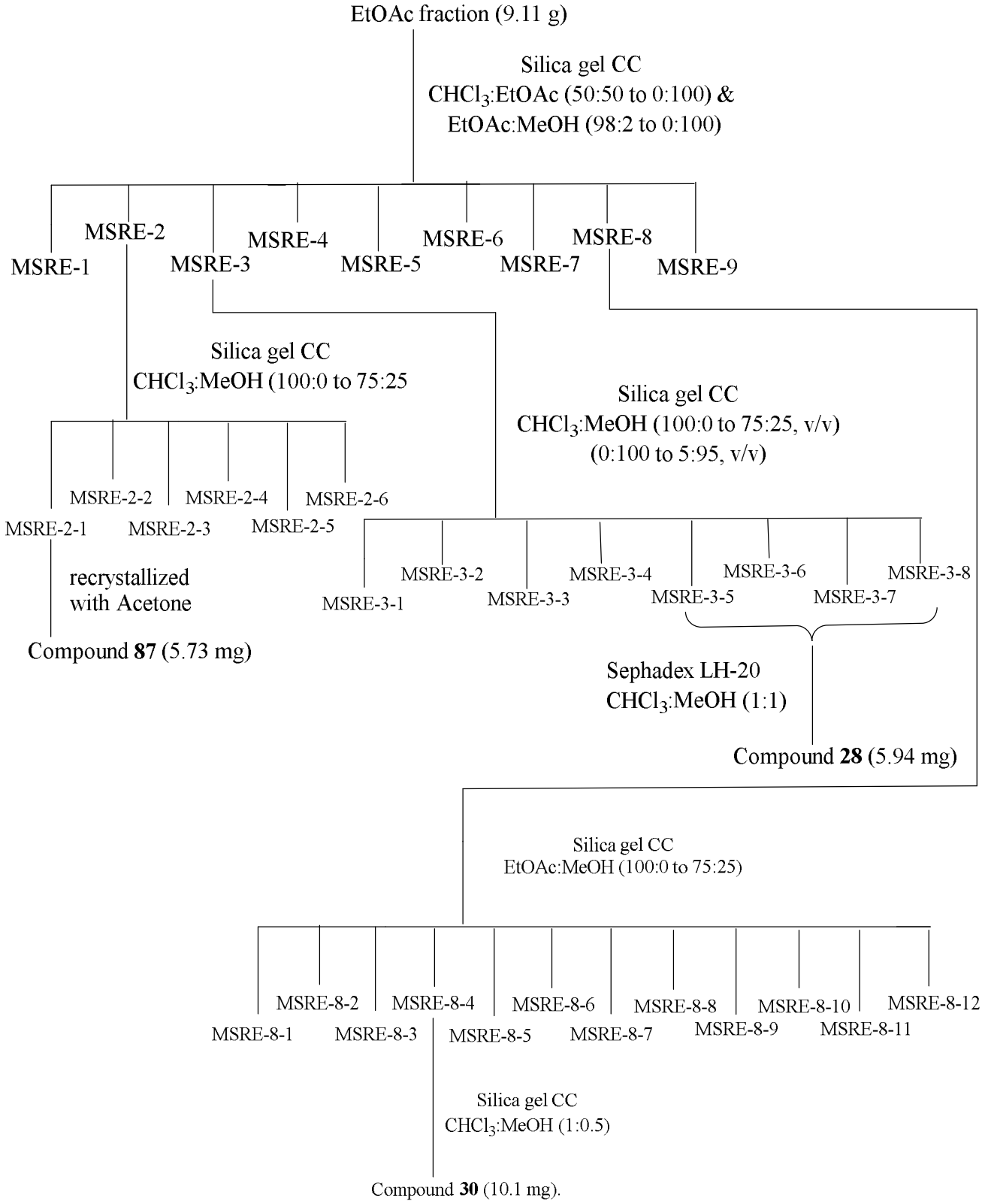

Figure 18: Fractionations and isolation of compounds from ethyl acetate fraction of roots extract of *Myrica salicifolia.*

4.3.3.5 Physical and Spectroscopic Data of Compounds Isolated from the Roots of *Myrica salicifolia*

Taraxerol (82): white powder; m.p. 257–260 °C; IR_v (KBr, cm^{-1}): 3492.4, 2930.8, 2851.2, 1634.2-1618; TOF-ESI-MS at *m/z* 472.6723 $[M+2Na]^+$ (calc. for $C_{30}H_{50}ONa$, 472.6980); ^{1}H-NMR (600 MHz, $CDCl_3$) δ 5.56 (*dd*, *J* = 8.2, 3.2 Hz, 1H-15), 3.22 (*dt*, *J* = 10.6, 5.1 Hz, 1H-3), 2.06 (*dt*, *J* = 12.8, 3.3 Hz, 1H-7), 1.94 (*dd*, *J* = 14.8, 3.2 Hz, 1H-19), 1.63 (*m*, 2H-21), 1.63 (*m*, 2H-1), 1.63 (*m*, 2H-2), 1.59 (*m*, 1H-21), 1.59 (*m*, 1H-2), 1.50 (*m*, 2H-11), 1.50 (*m*, 2H-6), 1.43 (*m*, 2H-18), 1.43 (*m*, 2H-11), 1.38 (*m*, 2H-7), 1.38 (*m*, 2H-22), 1.33 (*m*, 1H-19), 1.26 (*m*, 2H-21), 1.11 (*d*, *J* = 0.9 Hz, 3H-26), 1.00 (*s*, 3H-22), 0.97 (*s*, 3H-23), 0.95 (*s*, 3H-29), 0.93 (*d*, *J* = 1.4 Hz, 3H-30), 0.93 (*d*, *J* = 1.4 Hz, 3H-27), 0.83 (*s*, 3H-28), 0.81 (*m*, 1H-5). ^{13}C-NMR (100 MHz, $CDCl_3$) δ 15.5 (C-24), 15.4 (C-25), 17.5 (C-11), 18.8 (C-6), 21.3 (C-27), 25.9 (C-26), 27.2 (C-2), 28.0 (C-23), 28.8 (C-20), 29.8 (C-28), 29.9 (C-30), 33.1 (C-12), 33.4 (C-29), 33.7 (C-21), 35.8 (C-17), 35.1 (C-22), 36.7 (C-16), 37.74 (C-19), 37.6 (C-13), 38 (C-10), 37.7 (C-1), 38.9 (C-4), 38.8 (C-8), 41.3 (C-7), 48.8 (C-9), 49.3 (C-18), 55.0 (C-5), 79.1 (C-3), 116.9 (C-15), 158.1 (C-14).

***β*-Sitosterol (80)**: white powder; m.p. 133-135 °C; IR_v (KBr, cm^{-1}): 3424.6, 2928, 2849.2, 1618.4-1645; TOF-ESI-MS at m/z 416.2167 $[M+2H]^{2+}$ (calc. for $C_{29}H_{52}O$, 416.7236); ^{1}H-NMR (400 MHz, $CDCl_3$) δ 5.35 (*d*, *J* = 5.1 Hz, 1H-6), 3.53 (*tt*, *J* = 10.6, 4.7 Hz, 1H-3), 2.27 (*m*, $1H_1$-4), 2.22 (*m*, $1H_2$-4), 1.98 (*m*, 1H-7), 2.00 (*tt*, *J* = 14.6, 3.1 Hz, $1H_1$-12), 1.83 (*m*, $3H_1$-1), 1.65 (*m*, 1H-25), 1.57 (*m*, 1H-7), 1.48 (*m*, 1H-8), 1.37 (*m*, 1H-22), 1.14 (*td*, *J* = 14.2, 11.4, 5.8 Hz, 2H-23), 1.00 (*s*, 3H-19), 0.93 (*d*, *J* = 6.4 Hz, 4H-21), 0.84 (*d*, *J* = 6.5 Hz, 3H-29), 0.82 (*d*, *J* = 7.6 Hz, 3H-27), 0.80 (*d*, *J* = 2.3 Hz, 3H-26), 0.68 (*s*, 3H-18). ^{13}C-NMR (101 MHz, $CDCl_3$) δ 140.8 (C-5), 121.7 (C-6), 71.8 (C-3), 56.8 (C-14), 56.0 (C-17), 50.2 (C-9), 45.7 (C-24), 42.4 (C-4), 39.5 (C-12), 33.9 (C-22), 31.8 (C-7), 31.8 (C-8), 31.7 (C-2), 29.2 (C-25), 27.9 (C-16), 26.0 (C-23), 24.4 (C-15), 22.8 (C-28), 21.2 (C-11), 19.9 (C-27), 19.4 (C-19), 19.4 (C-26), 18.9 (C-21), 11.8 (C-18), 11.9 (C-29).

Sitoindoside I (87): white powder; m.p. 198-200 °C; IR_v (KBr, cm^{-1}): 3432.8, 2918.2, 2851.6, 1747.6, 1625.6; TOF-ESI-MS at *m/z* 815.6644 $[M]^+$ (calcd. for $C_{51}H_{90}O_7$ 815.2580); ^{1}H-NMR (400 MHz, $CDCl_3$) δ 0.68 (*s*, 4H-18), 0.81 (*s*, 3H-26), 0.83 (*d*, *J* = 2.1

Hz, 5H-27), 0.85 (*m*, 3H-29), 0.88 (*d*, *J* = 7.0 Hz, 2H-16″), 0.93 (*d*, *J* = 6.3 Hz, 1H-21), 1.00 (*s*, 3H-19), 1.32 (*s*, 6H-22), 1.35 (*d*, *J* = 7.3 Hz, 2H-20), 1.66 (*m*, 1H-25), 2.00–2 .06 (*m*, 2H-12), 2.35 (*t*, *J* = 8.1 Hz, 2H-2″), 3.37 (*td*, *J* = 9.0, 4.4 Hz, 1H-4′), 3.55 (*d*, *J* = 8.8 Hz, 1H-3′), 4.31 (*d*, *J* = 12.1 Hz, 1H-6′), 4.39 (*d*, *J* = 7.8 Hz, 1H-6′), 5.36 (*d*, *J* = 5.6 Hz, 1H-6). ^{13}C-NMR (101 MHz, $CDCl_3$) δ 174.6 (C-1″), 140.3 (C-5), 122.2 (C-6), 101.2 (C-1′), 79.7 (C-3), 76.1 (C-3′), 73.8 (C-2′), 73.5 (C-5′), 70.2 (C-4′), 63.4 (C-6′), 56.8 (C-14), 56.1 (C-17), 50.2 (C-9), 45.8 (C-24), 42.3 (C-13), 39.8 (C-12), 38.9 (C-4), 37.3 (C-1), 36.7 (C-10), 36.2 (C-20), 34.3 (C-2″), 33.9 (C-22), 32.0 (C-14″), 31.9 (C-8), 29.8 (C-6″), 29.7-29.6 (C-7″-14″), 29.4 (C-5″), 29.3 (C-4″), 29.1 (C-25), 28.3 (C-16), 26.1 (C-23), 25.0 (C-3″), 24.3 (C-15), 23.1 (C-28), 22.7 (C-15″), 21.1 (C-11), 19.8 (C-27), 19.4 (C-19), 19.0 (C-26), 18.8 (C-21), 14.2 (C-16″), 12.0 (C-29), 11.9 (C-18).

Myricanon (28): white powder; m.p. 187-192 °C; IR_v (KBr, cm^{-1}): 3424.4, 2919.2, 2854.9, 1705.2, 1642.2-1613.2; TOF-ESI-MS at *m/z* 379.1512 $[M+Na]^+$ (calcd for $C_{21}H_{24}O_5Na$, 379.1516); ^{1}H-NMR (400 MHz, $CDCl_3$) δ 1.89 (*d*, *J* = 7.4, 7.0 Hz, 1H-9), 1.97 (*dd*, *J* = 8.5, 5.0 Hz, 1H-8), 2.74 (*m*, 2H-7, 8), 2.79 (*m*, 1H-10), 2.82 (*dt*, *J* = 13.6, 6.2 Hz, 2H-12), 2.89 (*m*, 2H), 3.01 (*m*, 2H-10), 3.04 (*m*, 1H), 3.87 (*s*, 3H-21), 4.00 (*s*, 3H-20), 5.91 (*s*, OH-5), 6.63 (*s*, 1H-19), 6.76 (*d*, *J* = 2.4 Hz, 1H-18), 6.90 (*d*, *J* = 8.2 Hz, 1H-16), 7.08 (*dd*, *J* = 8.2, 2.4 Hz, 1H-15), 7.69 (*s*, OH-17). ^{13}C-NMR (101 MHz, $CDCl_3$) δ 21.9 (C-9), 24.5 (C-8), 26.9 (C-7), 28.9 (C-13), 42.6 (C-12), 46.2 (C-10), 61.4 (C-21), 61.5 (C-20) , 115.9 (C-16), 123.1 (C-6), 123.2 (C-2), 125.5 (C-1), 128.9 (C-19), 128.9 (C-15), 132.3 (C-14), 132.4 (C-18), 138.6 (C-4), 146.0 (C-3), 147.8 (C-5), 151.7 (C-17), 213.6 (C-11).

Myricanol 5-*O*-β-D-Glucopyranoside (30): white powder; m.p. 220-223 °C; IR_v (KBr, cm^{-1}): 3455.8, 2919.2, 2849.2, 1640.4 -1453.6; TOF-ESI-MS at *m/z* 543.2219 $[M+Na]^+$ (calcd for $C_{27}H_{36}O_{10}Na$, 543.5595). ^{1}H-NMR (400 MHz, MeOD) δ 7.12 (*d*, *J* = 2.4 Hz, 1H-18), 7.06 (*dd*, *J* = 8.2, 2.3 Hz, 1H-15), 6.86 (*s*, 1H-19), 6.80 (*d*, *J* = 8.2 Hz, 1H-16), 5.03 (*d*, *J* = 7.3 Hz, 1H-1′), 3.99 (*s*, 3H-21), 3.93 (*m*, 1H-11), 3.91 (*s*, 3H-20), 3.83 (*dd*, *J* = 12.0, 2.4 Hz, 1H-6′), 3.69 (*dd*, *J* = 12.0, 5.3 Hz, 1H-6′), 3.47 (*m*, 1H-5′), 3.46 (*m*, 1H- 2′), 3.41 *(m*, 1H-4′), 3.27 (*ddd*, *J* = 9.2, 5.3, 2.3 Hz, 1H-3′), 2.97 (*dd*, *J* = 16.0, 3.1 Hz, 1H-7), 2.87 (*m*, 2H-13), 2.73 (*m*, 1H-8), 2.29 (*ddd*, *J* = 16.0, 11.5, 5.0 Hz, 1H-12), 1.66 (*m*, 1H-12), 1.90 (*m*, 1H-7), 1.87 (*m*, 1H-10), 1.58 (*d*, *J* = 8.7 Hz, 1H-9), 1.56 (*d*, *J* = 11.6 Hz, 1H-

9), 1.47 (*dd*, *J* = 13.3, 12.3, 6.0 Hz, 1H-9). ^{13}C-NMR (101 MHz, MeOD) δ 151.6 (C-17), 148.5 (C-5), 148.0 (C-3), 145.0 (C-4), 133.7 (C-18), 130.5 (C-14), 129.8 (C-2), 129.7 (C-15), 129.1 (C-19), 128.2 (C-1), 125.2 (C-6), 115.9 (C-16), 103.9 (C-1′), 76.9 (C-3′), 76.7 (C-5′), 74.4 (C-2′), 70.1 (C-4′), 67.8 (C-11), 61.2 (C-6′), 60.6 (C-21), 60.3 (C-20), 39.1 (C-10), 34.3 (C-12), 26.7 (C-13), 26.1 (C-8), 25.7 (C-7), 22.6 (C-9).

4.3.3.6 Biological Activities of the Crude Extract and Isolated Compounds from the Roots of *Myrica salicifolia*

4.3.3.6.1 DPPH Radical Scavenging Assay of the Crude Extract and Isolated Compounds from the Roots of *Myrica salicifolia*

The antioxidant activities of the isolated compounds were assessed using DPPH radical scavenging activity with ascorbic acid as the positive control as per the previously described method.[204] The standard solution of 0.1mM DPPH was prepared by dissolving 4mg of DPPH in 100 mL of methanol. All extracted and isolated compounds were separately dissolved in DMSO (1 mg/mL). Briefly, 4 ml of methanol solution of DPPH (0.1mM) was mixed with 1 ml of extract and each of isolated compound solution at different concentrations (3.12, 6.25, 12.5, 25, and 50 µg/mL). The mixture was incubated in the dark for 30 minutes, and the absorbance was read off at 517 nm wavelength using a UV-Vis spectrophotometer. An ascorbic acid solution of the same concentration (3.12 µg/mL to 50 µg/mL) was prepared in similar fashion and measured. The DPPH radical scavenging activity of each of the tested compounds was reported as percentage inhibition using the formula given by Eq. 1.

$$\%\ \text{DPPH Inhibition} = \left[\frac{\text{A control} - \text{B sample}}{\text{A control}}\right] \times 100 \quad \text{.....Eq. 1}$$

Where A control is the absorbance of DPPH solution, and B sample is the absorbance of the test sample (DPPH solution plus compound). The DPPH solution was used as a negative control. The relative half-maximal inhibitory concentration (IC_{50}) values were calculated *via* linear regression analysis (y = bx + a), where y = 50 and x denote IC_{50}. The final antioxidant activity of each compound was expressed as the IC_{50} value.

4.3.4 Extraction and Characterization of Compounds from the Aerial Part of *Clematis simensis*

4.3.4.1 Extraction of Essential Oil by Hydrodistillation

The fresh aerial parts of *C. simensis* were crushed and prepared for hydrodistillation following previously published report.[208] Plant material (440 g) was placed into distillation flask (4 L) filled with 2 L distilled water and the flask was attached to Clevenger apparatus which was connected to a condenser. On a heating mantle, the flask's contents were brought to boiling, and then hydrodistillation was carried out for eight hours. The essential oil was collected (~2.0 mL), dried over anhydrous Na_2SO_4, and stored in a sealed vial in the dark at 4 ^{0}C, until analysis by GC-MS.

4.3.4.2 Characterization of the Essential Oil from the Aerial Parts of *Clematis simensis*

The essential oil obtained from aerial parts of *clematis simensis* were analyzed by using an Agilent Technology 7820A GC system coupled with an Agilent Technology 5977E MSD system equipped with an autosampler. The chromatographic separation was done on a column 30 m in length and 0.25 μm in thickness coated with HP-5MS, (5%-phenyl)-methylpolysiloxane, at a pressure of 8 psi and a flow rate of 0.97989 mL/min. Ultra-high pure helium (99.999%) was used as carrier gas at constant flow mode. An Agilent G4567A autosampler was used to inject 1 μL of the sample with a splitless injection mode into the inlet heated to 275 ºC with a total run time of 29.33 min. Oven temperature was programmed with the initial column temperature of 60 ºC and hold-time 2 min. The column temperature was increased at a rate of 10 ºC/min until the temperature reached 200 ºC and then heated again at the rate of 3 ºC/min until the temperature reached 240 ºC. No mass spectra were collected during the first 4 min of the solvent delay. The transfer line and the ion source temperatures were 280 ºC and 230 ºC, respectively. The detector voltage was 1600 V and the electron energy was 70 eV. Mass spectral data were collected from 40–650 *m*/*z*. The names and structures were determined through National Institute of Standards and Technology (NIST) 2014 library search.

4.3.4.3 Solvent Extraction of the Aerial Part of *Clematis simensis*

The collected fresh aerial parts of *C. simenses* were air dried at room temperature for two weeks under a shed until it became well dried. The dry plant materials were ground using an electric grinder to obtain a fine powder. The powder (0.5 kg) was soaked in 1:1 ratio of MeOH to $CHCl_3$ (2 L x 3, 24 h each) at room temperature. The mixture was filtered using a Buchner funnel with Whatman filter paper. The combined filtrates were concentrated by a rotary evaporator under reduced pressure at a 45 °C. The concentrated crude extracts were allowed to dry to a constant weight at room temperature, and gave a total mass of 52.6 g.

4.3.4.4 Fractionation of the Crude Extract of the Aerial Parts of *Clematis simensis*

The MeOH-$CHCl_3$ crude extract (22.0 g) was redissolved in small amount of chloroform-methanol and adsorbed on 20 g silica gel, then stirred well and dried by rotary evaporator until a fine dry powder remains. The dried powder was applied to a glass column packed with silica gel and fractionated using a gradient solvent system containing pet ether:$CHCl_3$ (from 50:50 to 0:100, v/v), $CHCl_3$:EtOAc (95:5 to 0:100, v/v), and $CHCl_3$:MeOH (90:10 to 62.5:37.5, v/v) gave a total of 31 fractions (Figure 19). The fractions were combined based on their TLC profiles into twenty fractions (CSA-1C to CSA-20C). Fraction CSA-17C (2.70 g) was subjected to column chromatography over silica gel (150 g) using pet ether:$CHCl_3$ (50:50 to 0:100, v/v) and $CHCl_3$:EtOAc (94:6 to 0:100, v/v) to give 64 subfraction, which were combined into seven groups (CSA-17C-1 to CSA-17C-7) based on their TLC profiles. Subfractions CSA-17C-3 and CSA-17C-5 were redissolved in diethyl ether and left overnight, the insoluble part was separated gave compounds **88** (9.6 mg) and **89** (7.3 mg) as white solids. Fraction 20C (2.2 g) was further chromatographed on a glass column packed with silica gel (130 g) which was eluting with 40% ethyl acetate in hexane gave compound **90** (11.8 mg).

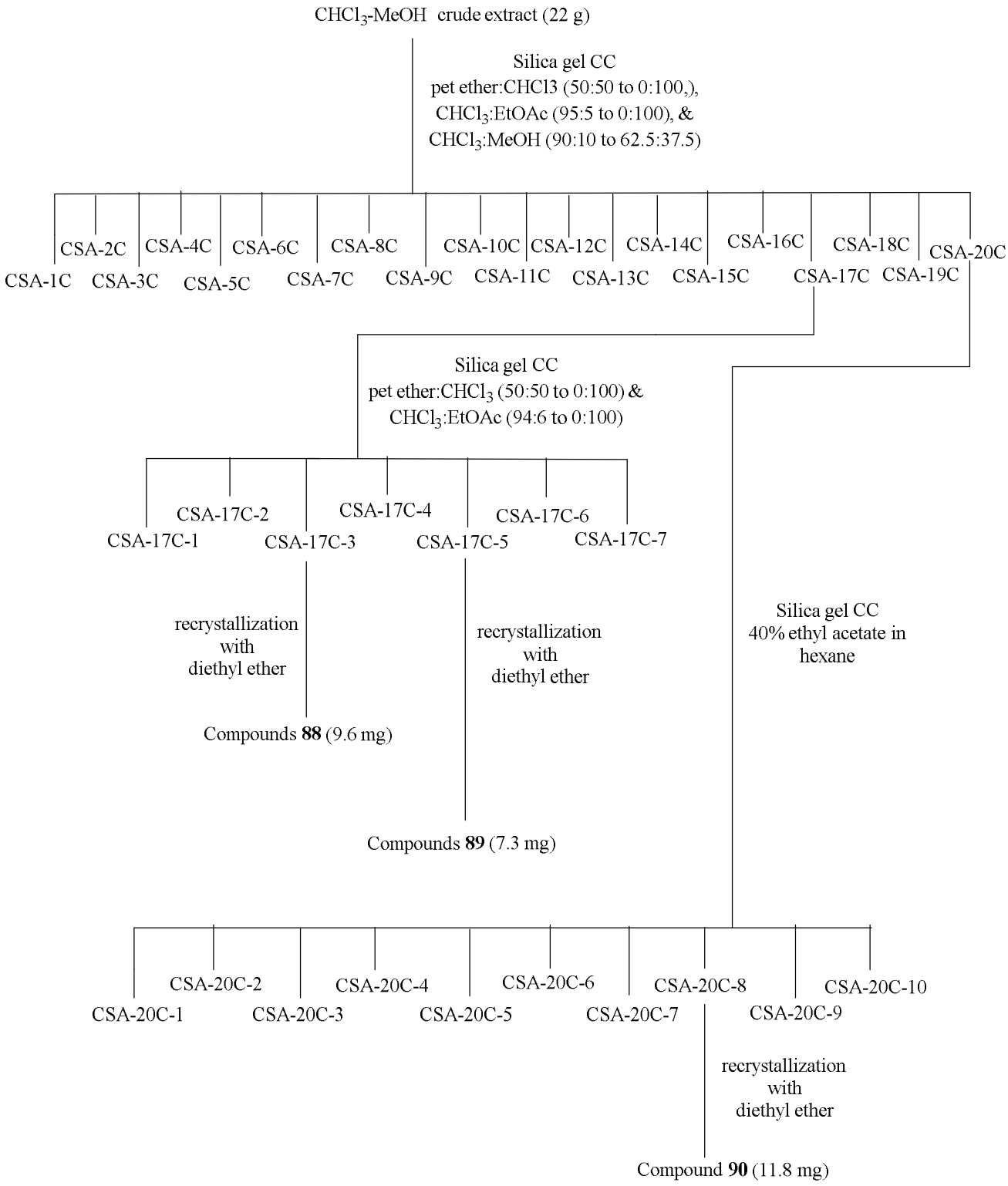

Figure 19: Fractionations and isolation of compounds from chloroform-methanol crude extract of aerial parts of *C. simenses.*

4.3.4.5 Physical and Spectroscopic Data of Compounds from the Aerial Part of *Clematis simensis*

2-Deoxy-D-Ribono-1, 4-Lactone (88): white powder; m.p. 134-135 ^{0}C; IR$_{v}$ (KBr, csm^{-1}): 3408, 2915, 2847, 1634; ^{1}H-NMR (600 MHz, DMSO) δ 5.50 (*s*, OH-3), 5.07 (*s*, OH-5), 4.34–4.18 (*m*, 1H-3, 4), 3.55 (*qd*, *J* = 12.3, 3.4 Hz, 2H-5), 2.82 (*dd*, *J* = 17.7, 6.5 Hz, 1H$_1$-2), 2.24 (*dd*, *J* = 17.7, 2.3 Hz, 1H$_2$-2); ^{13}C-NMR (151 MHz, DMSO) δ 176.3 (C-1), 88.3 (C-4), 67.8 (C-3), 60.8 (C-5), 38.1 (C-2).

5-Hydroxylevulinic acid (89): white powder; m.p. 97-100 ^{0}C; IR$_{v}$ (KBr, cm^{-1}): 3443, 2926, 2855, 1739, 1634; ^{1}H-NMR (600 MHz, CH_3OH) δ 4.24 (*s*, 1H-5), 2.70 (*t*, *J* = 6.7 Hz, 1H-3), 2.59 (*t*, *J* = 6.7 Hz, 1H-2); ^{13}C-NMR (151 MHz, CH_3OH) δ 211.1 (C-4), 176.4 (C-1), 68.9 (C-5), 33.9 (C-3), 28.5 (C-2).

β-sitosterol-3-*O*-β-D-glucoside (90): white powder; m.p. 285 - 287 °C; IR$_{v}$ (KBr, cm^{-1}): 3436, 2918, 2848, 1620; FAB-MS (positive ion mode) m/z 599.4236 [M + Na] $^{+}$ (calcd. for $C_{35}H_{60}O_{6,}$ 599.8384). ^{1}H-NMR (601 MHz, DMSO) δ 5.30 (*m*, 1H-6), 4.22 (*d*, *J* = 7.8 Hz, 1H-1′), 3.65 (*ddd*, *J* = 11.7, 5.8, 2.0 Hz, 1H-6′), 3.42 (*m*, 1H-3), 3.41 (*dt*, *J* = 11.7, 5.9 Hz, 1H-6′), 3.12 (*td*, *J* = 8.8, 4.7 Hz, 1H-3′), 3.07 (*ddd*, *J* = 9.7, 5.9, 2.1 Hz, 1H-5′), 3.01 (*td*, *J* = 9.1, 5.1 Hz, 1H-4′), 2.88 (*m*, 1H-2′), 2.36 (*m*, 1H-4), 2.17 (*m*, 1H-4), 1.94 (*m*, 1H-12), 1.92 (*m*, 1H-7), 1.84 (*m*, 1H-16), 1.81 (*m*, 1H-2), 1.79 (*m*, 1H-1), 1.63 (*m*, 1H-25), 1.57 (*m*, 1H-15), 1.52 (*m*, 1H-7), 1.42 (*m*, 1H-2), 1.38 (*m*, 1H-8), 1.35 (*m*, 1H-20), 1.34 (*m*, 1H-22), 1.24 (*m*, 1H-16), 1.22 (*m*, 1H-28), 1.21 (*d*, *J* = 5.7 Hz, 1H-11), 1.15 (*m*, 1H-23), 1.12 (*m*, 1H-17), 1.11 (*dd*, *J* = 11.9, 3.7 Hz, 1H-12), 1.08 (*m*, 1H-15), 1.04 (*m*, 1H), 1.01 (*d*, *J* = 9.7 Hz, 1H-11), 1.00 (*d*, *J* = 6.6 Hz, 1H-1), 0.99 (*m*, 1H-14), 0.96 (*s*, 3H-19), 0.91 (*m*, 1H-24), 0.83 (*m*, 1H-9), 0.87 (*d*, *J* = 4.4 Hz, 1H), 0.82 (*t*, *J* = 7.2 Hz, 3H-29), 0.80 (*d*, *J* = 5.4 Hz, 3H-26), 0.78 (*d*, *J* = 7.7 Hz, 3H-21), 0.65 (*s*, 3H-18). ^{13}C-NMR (151 MHz, DMSO) δ 121.2 (C-6), 100.8 (C-1′), 76.9 (C-3) , 76.8 (C-3′), 73.5 (C-2′), 70.1 (C-4′), 61.1 (C-6′), 56.2 (C-14), 55.4 (C-17), 49.6 (C-9), 45.1 (C-24), 41.9 (C-13), 39.3 (H-12), 38.3 (C-4), 36.8 (C-1), 36.2 (C-10), 35.5 (C-20), 33.3 (C-22), 31.4 (C-7), 31.4 (C-8), 29.3 (C-2), 28.7 (C-25), 27.8 (C-16), 25.4 (C-23), 23.9 (C-15), 20.6 (C-11), 19.7 (C-26), 19.1 (C-19), 18.9 (C-26), 18.6 (C-27), 11.8 (C-18), 11.7 (C-29).

4.3.4.6 Biological Activities of the Crude Extract and Isolated Compounds from Aerial Part of *Clematis simensis*

4.3.4.6.1 DPPH Radical Scavenging Assay of the Crude Extract and Isolated Compounds from the Aerial Parts of *Clematis simensis*

The antioxidant activities of the isolated compounds were assessed using DPPH radical scavenging activity with ascorbic acid as the positive control as per the previously described method.[204] The standard solution of 0.1mM DPPH was prepared by dissolving 4mg of DPPH in 100 mL of methanol. All extracted and isolated compounds were separately dissolved in DMSO (1 mg/mL). Briefly, 4 ml of methanol solution of DPPH (0.1mM) was mixed with 1 ml of extract and each of isolated compound solution at different concentrations (3.12, 6.25, 12.5, 25, and 50 µg/mL). The mixture was incubated in the dark for 30 minutes, and the absorbance was read off at 517 nm wavelength using a UV-Vis spectrophotometer. An ascorbic acid solution of the same concentration (3.12 µg/mL to 50 µg/mL) was prepared in similar fashion and measured. The DPPH radical scavenging activity of each of the tested compounds was reported as percentage inhibition using the formula given by Eq. 1.

$$\%\ \text{DPPH Inhibition} = \left[\frac{\text{A control} - \text{B sample}}{\text{A control}}\right] \times 100 \quad \ldots\ldots\ldots\ldots\ldots\text{Eq. 1}$$

Where A control is the absorbance of DPPH solution, and B sample is the absorbance of the test sample (DPPH solution plus compound). The DPPH solution was used as a negative control. The relative half-maximal inhibitory concentration (IC_{50}) values were calculated *via* linear regression analysis (y = bx + a), where y = 50 and x denote IC_{50}. The final antioxidant activity of each compound was expressed as the IC_{50} value.

Antibacterial activities of the Crude Extract and Isolated Compounds from the Aerial Parts of *Clematis simensis*

The four common human bacterial strains: *Staphylococcus aureus*, *Escherichia coli*, *Salmonella typhi*, and *Pseudomonas aeruginosa*, were collected from the Addis Ababa University. Experiments were done in collaboration with the Microbiology Laboratory of Biology Department of Addis Ababa University. *In vitro* antibacterial susceptibility tests

were determined by the disk diffusion method.[203] The medium was prepared by dissolving 38 g of Mueller Hinton agar (MHA) in 1000 mL distilled water, and autoclaved at 121 °C for 15 min. The autoclaved medium was poured into sterile petri dishes (20 mL/plate), and the plates were allowed to solidify under sterile conditions at room temperature. After solidification, the plates were seeded with an overnight grown culture approximately 1.5 X 10^8 CFU/mL by swabbing evenly on the surface of the medium with a sterile cotton swab. The crude extract and isolated compounds at concentrations of 125 mg/mL-500 mg/mL and 125-1000 µg/mL, respectively, were prepared by dissolving in 10% DMSO. Whatman filter paper No. 1 was used to prepare discs of 6 mm in diameter. The sterile discs were infused with the isolated compounds, placed on the surface of the medium with sterile forceps, and gently pressed down to ensure contact with the (MHA). Ciprofloxacin was used as a positive control, and then the plates were inverted and incubated at 37 ℃ for 24 hours. After incubation, the inhibition zone produced by the isolated compounds was evaluated by measuring the diameter (mm) of the clear zone around the disc and comparing it with 5 µg/ml positive controls.

4.3.5 Extraction and Characterization of Compounds from the Steam Barks of *Olinia usambarensis*

4.3.5.1 Extraction of Essential Oil by Hydrodistillation

The Barks of *Olinia usambarensis* were crushed and prepared for hydrodistillation following previously published report.[208] Plant material (570 g) was placed into distillation flask (4 L) filled with 2 L distilled water and the flask was attached to Clevenger apparatus which was connected to a condenser. On a heating mantle, the flask's contents were brought to boiling, and then hydrodistillation was carried out for eight hours. The essential oil was collected (~0.7 mL), dried over anhydrous Na_2SO_4, and stored in a sealed vial in the dark at 4 ^{0}C, until analysis by GC-MS.

4.3.5.2 Characterization of the Essential Oil from the Barks of *Olinia usambarensis*

The essential oil obtained from barks of *Olinia usambarensis* were analyzed by using an Agilent Technology 7820A GC system coupled with an Agilent Technology 5977E MSD

system equipped with an autosampler. The chromatographic separation was done on a column 30 m in length and 0.25 μm in thickness coated with HP-5MS, (5%-phenyl)-methylpolysiloxane, at a pressure of 8 psi and a flow rate of 0.97989 mL/min. Ultra-high pure helium (99.999%) was used as carrier gas at constant flow mode. An Agilent G4567A autosampler was used to inject 1 μL of the sample with a splitless injection mode into the inlet heated to 275 ºC with a total run time of 33.00 min. Oven temperature was programmed with the initial column temperature of 60 ºC and hold-time 2 min. The column temperature was increased at a rate of 10 ºC/min until the temperature reached 200 ºC and then heated again at the rate of 3 ºC/min until the temperature reached 240 ºC. No mass spectra were collected during the first 4 min of the solvent delay. The transfer line and the ion source temperatures were 280 ºC and 230 ºC, respectively. The detector voltage was 1600 V and the electron energy was 70 eV. Mass spectral data were collected from 40–650 *m*/*z*. The names and structures were determined through National Institute of Standards and Technology (NIST) 2014 library search.

4.3.5.3 Solvent Extraction of the Barks of *Olinia usambarensis*

The collected fresh barks of *Olinia usambarensis* were dried at room temperature. The dried plant materials were ground using an electric grinder to obtain a fine powder. The powder (0.894 kg) was soaked and homogenized exhaustively using MeOH and $CHCl_3$ mixture (2 L x 3, 24 h each) at a ratio of 1:1at room temperature. The mixture was filtered using a Buchner funnel with Whatman filter paper. The filtrates were concentrated using a rotary evaporator under reduced pressure at a temperature of 40 °C. The concentrated crude extracts were allowed to dry to a constant weight at room temperature and furnished brown gummy crude (93 g).

4.3.5.4 Fractionation of the Crude Extract of Barks of *Olinia usambarensis*

The crude extract (40.42 g) was redissolved in chloroform-methanol and adsorbed on 40 g of silica gel, mixed well and dried by a rotary evaporator. The dried sample was loaded to a glass column packed with silica gel (700 g, 70–230 mesh ASTM) and fractionated using gradient solvent system Hex:EtOAc (100:0 to 50:50, v/v), and EtOAc:MeOH (90:10 to 0:100, v/v) to give 47 fractions each 250 mL. Fractions with similar TLC profiles were

combined to give eleven fractions (OR-1 to OR-11) (Figure 20). Fraction OR-2 (3.3 g) was subjected to column chromatography over silica gel (180 g) using Hex:EtOAc (100:0 to 71:29, v/v) to give 14 (OR-2-1 to OR-2-14) subfraction. Sub-fraction OR-2-3 was crystallized from MeOH afforded compound **91 (**7.4 mg). Fraction OR-2-12 (276.7 mg) was further fractionated by PTLC using pet ether:EtOAc (80:20, v/v) as eluent to give compound **92** (3.4 mg). Fraction OR-9 (604.2 mg) was subjected to column chromatography over silica gel (80 g) using MeOH in $CHCl_3$ (10:80 to 23:77, v/v) as eluent. A total of 11 subfractions (OR-9-1 to OR-9-11) were collected. Subfraction OR-9-8 (125 mg) was rechromatographed over silica gel (20 g) using solvent system of $CHCl_3$:MeOH (80:20, v/v) as eluent to give compound **72** (9.4 mg).

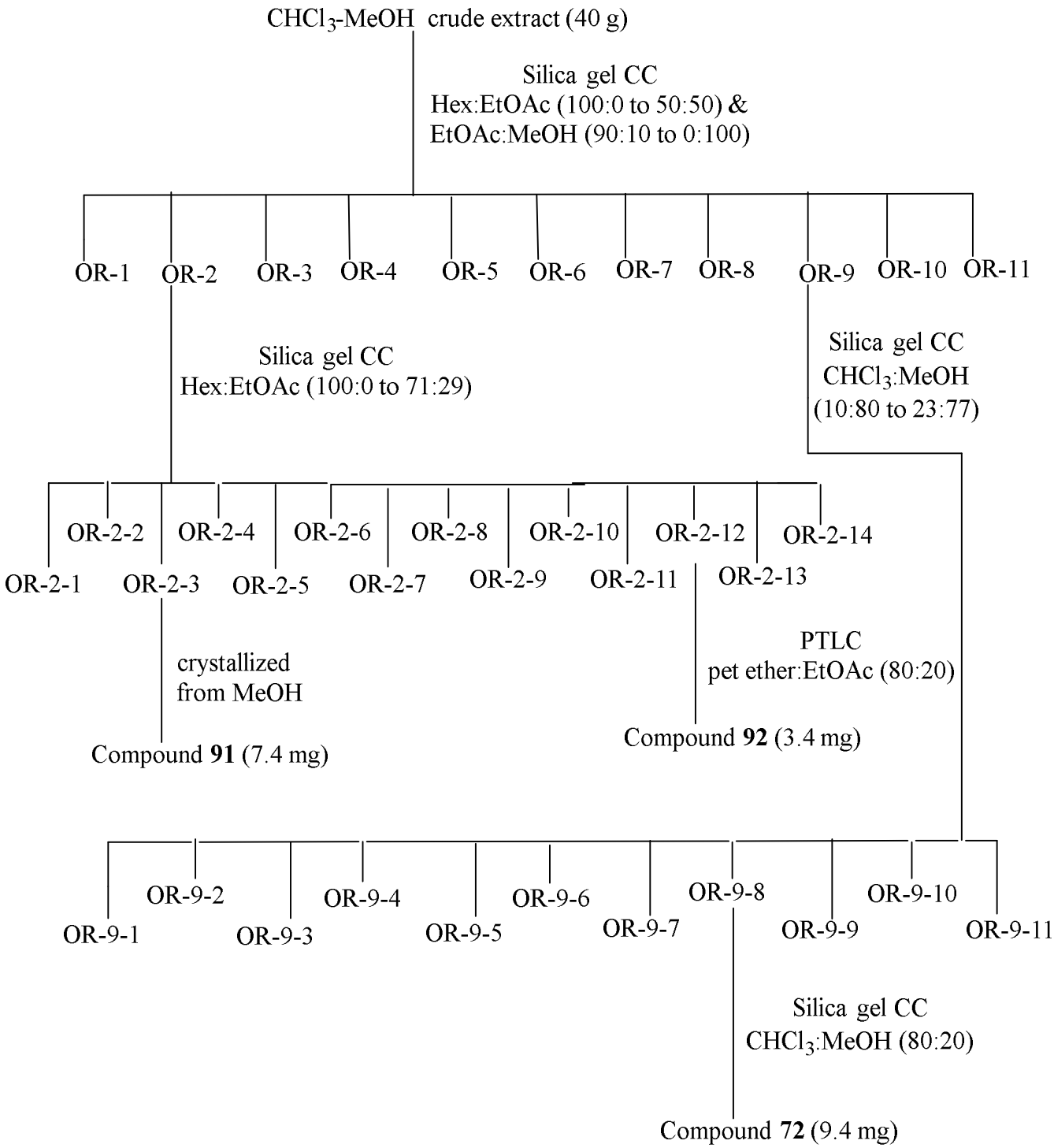

Figure 20: Fractionations and isolation of compounds from the barks extract of *Olinia usambarensis*.

4.3.5.5 Physical and Spectroscopic Data of Compounds Isolated from the Barks of *Olinia usambarensis*

Lupeol (91): white powder; m.p. 213-215 °C; IR_v (KBr, cm^{-1}): 3437.2, 2919.2, 2853.6, 1642.2; TOF-ESI-MS at *m/z* 449.3441 $[M+Na]^+$ (calcd for $C_{30}H_{50}ONa$, 449.7082); ^{1}H-NMR (400 MHz, $CDCl_3$) δ 4.67 (*d*, *J* = 2.5 Hz, 1H-29), 4.55 (*s*, 1H-29), 3.71 (*m*,1H -7), 3.17 (*dd*, *J* = 11.2, 5.0 Hz, H-3), 2.29 (*m*,1H -19), 1.90 (*m*,1H $_1$-21) 1.67 (*m*,1H -15), 1.66 (s, 3H-30), 1.65 (*m*,1H -12), 1.63 (*m*,1H -13), 1.59 (*m*,1H $_1$-1), 1.57 (*dd*, *J* = 12.0, 3.3 Hz, 1H-2), 1.61 (*m*,1H-2), 1.50 (*m*,1H$_1$-6), 1.44 (*m*,1H-16), 1.5 (*m*, 1H-15), 1.39 (*m*, 1H$_1$-11), 1.37 (*m*, 1H$_2$-6), 1.30 (*m*, 1H$_1$-22), 1.27 (*m*, 1H-18), 1.25 (*m*,1H *m*, 1H$_2$-11), 1.24 (s, 1H-9), 1.22 (*m*, 1H$_2$-21), 1.13 (*m*, 1H$_2$-22), 1.01 (*s*, 3H-26), 0.95 (*s*, 3H-23), 0.93 (*s,* 3H-27), 0.89 (*m*, 1H $_2$-1), 0.81 (*s*, 3H-25), 0.77 (*s*, 3H-28), 0.74 (*s*, 3H-24), 0.68 (*t*, *J* = 7.9 Hz, 1H-5). ^{13}C-NMR (101 MHz, $CDCl_3$) δ 109.6 (C-29), 79.2 (C-3), 55.6 (C-5), 50.6 (C-9), 48.5 (C-18), 48.2 (C-19), 43.2 (C-17), 43.0 (C-14), 41.1 (C-8), 40.2 (C-22), 40.0 (C-4), 38.9 (C-1), 38.2 (C-13), 37.4 (C-10), 35.8 (C-16), 34.5 (C-7), 30.0 (C-21), 28.2 (C-23), 27.6 (C-2), 27.6 (C-15), 26.0 (C-12), 21.1 (C-11), 19.5 (C-30), 18.5 (C-6), 18.2 (C-28), 16.3 (C-25), 16.2 (C-26), 151.2 (C-20), 15.6 (C-24, 14.8 (C-27).

n-Pentacosyl *trans*-Ferulate (92): white powder; m..p. 197-200 ^{0}C; IR_v (KBr, cm^{-1}): 3450.2, 2866, 2936, 1751.4, 1635; TOF-ESI-MS at m/z 343.1019 $[M+H]^+$ (calcd. for $C_{15}H_{19}O_9$, 343.30655); ^{1}H-NMR (400 MHz, $CDCl_3$) δ 4. 7.54 (*d*, *J* = 15.9 Hz, 1H-7), 7.01 (*dd*, *J* = 8.2, 1.9 Hz, 1H-6), 6.97 (*d*, *J* = 1.8 Hz, 1H-2), 6.85 (*d*, *J* = 8.1 Hz, 1H-5), 6.23 (*d*, *J* = 15.9 Hz, 1H-8), 4.12 (*t*, *J* = 6.8 Hz, 2H-1′), 3.86 (*s*, -OCH_3), 1.62 (*q*, *J* = 7.1 Hz, 2H-2′), 1.31 (*d*, *J* = 8.2 Hz, 2H-3′), 1.18 (*brs*, 64H 4′-25′), 0.81 (*t*, *J* = 6.7 Hz, 3H-26′). ^{13}C-NMR (101 MHz, $CDCl_3$) δ 167.4 (C-9), 147.9 (C-3), 146.7 (C-4), 144.6 (C-7), 127.1 (C-1), 123.1 (C-6), 115.7 (C-8), 114.7 (C-5), 109.2 (C-2), 64.6 (C-1′), 55.9 (-OCH_3), 31.9 (C-24′), 29.7- 29.3 (4′-23′), 28.0 (C-2′), 26.0 (C-3′), 22.7 (C-25′), 14.2 (C-26′).

4-*O*-β-D-Glucopyranosylcaffeicacid (72): white powder; m.p. 209-2015 ^{0}C; IR_v (KBr, cm^{-1}): 3429.4, 2866, 2936, 1747.8, 1651.5, 1610, 1506.2, 1464, 1072.4; TOF-ESI-MS at m/z 343.1019 $[M+H]^+$ (calcd. for $C_{15}H_{19}O_9$, 343.3065); ^{1}H-NMR (400 MHz, MeOD) δ 7.57 (*d*, *J* = 15.9 Hz, 1H-β), 7.22 (*d*, *J* = 8.4 Hz, 1H-5′), 7.12 (*d*, *J* = 2.1 Hz, 1H-2′), 7.06 (*dd*, *J* = 8.4, 2.1 Hz, 1H-6′), 6.34 (*d*, *J* = 15.9 Hz, 1H-α), 4.88 (*d*, *J* = 7.0 Hz, 1H-1), 3.93

(*dd*, *J* = 12.1, 2.0 Hz, 1H-6), 3.74 (*dd*, *J* = 12.1, 5.1 Hz, 1H-6), 3.52 (*m*, H-2), 3.52 (*d*, *J* = 7.0 Hz, 1H-3), 3.45 (*m*, H- 4, 5). ^{13}C-NMR (101 MHz, MeOD) δ 170.6 (C=O), 148.7 (C-3′), 148.4 (C-4′), 146.0 (C-β), 131.1 (C-1′), 122.1 (C-6′), 118.0 (C-α), 117.8 (C-2′), 115.8 (C-5′), 103.4 (C-1), 78.3 (C-5), 77.4 (C-3), 74.7 (C-2), 71.2 (C-4), 62.3 (C-6).

4.3.5.6 Biological Activities of the Crude Extract and Isolated Compounds from the Barks of *Olinia usambarensis*

4.3.5.6.1 DPPH Radical Scavenging Assay of the Crude Extract and Isolated Compounds from the Barks of *Olinia usambarensis*

The antioxidant activities of the isolated compounds were assessed using DPPH radical scavenging activity with ascorbic acid as the positive control as per the previously described method. The standard solution of 0.1mM DPPH was prepared by dissolving 4mg of DPPH in 100 mL of methanol. All extracted and isolated compounds were separately dissolved in DMSO (1 mg/mL). Briefly, 4 ml of methanol solution of DPPH (0.1mM) was mixed with 1 ml of extract and each of isolated compound solution at different concentrations (3.12, 6.25, 12.5, 25, and 50 µg/mL). The mixture was incubated in the dark for 30 minutes, and the absorbance was read off at 517 nm wavelength using a UV-Vis spectrophotometer. An ascorbic acid solution of the same concentration (3.12 µg/mL to 50 µg/mL) was prepared in similar fashion and measured. The DPPH radical scavenging activity of each of the tested compounds was reported as percentage inhibition using the formula given by Eq. 1.

$$\%\ \text{DPPH Inhibition} = \left[\frac{\text{A control} - \text{B sample}}{\text{A control}}\right] \times 100 \quad \ldots\ldots\ldots\ldots\ldots\text{Eq. 1}$$

Where A control is the absorbance of DPPH solution, and B sample is the absorbance of the test sample (DPPH solution plus compound). The DPPH solution was used as a negative control. The relative half-maximal inhibitory concentration (IC_{50}) values were calculated *via* linear regression analysis (y = bx + a), where y = 50 and x denote IC_{50}. The final antioxidant activity of each compound was expressed as the IC_{50} value.

5 Conclusion

The main objective of this research work has been to investigate the chemical constituents, antioxidant and antibacterial activities of extracts and isolated compounds of *Myrica salicifolia, Clematis simensis,* and *Olinia usambarensis,* and analysis of the composition of its essential oil. The phytochemical investigation of leaves, roots, and barks of *Myrica salicifolia* led to the isolation of eighteen compounds, of which twelve compounds are reported in this work for the first time from this plant. To the best of our knowledge, of the compounds isolated one was new compound, 3β-*O-trans*-caffeoylisomyricadiol (**84**). The phytochemical study of *Clematis simensis* and *Olinia usambarensis* yielded six compounds, of which five compounds are reported in this work for the first time. It is noteworthy that squalene (**77**), β-carotene (**78**), pheophytin A (79), 3β-*O-trans*-caffeoylisomyricadiol (**84**), methyl-β-D-glucopyranoside (**85**), contortamide **(86)**, sitoindoside I **(87)**, lupeol **(91)**, n-pentacosyl *trans*-ferulate **(92)** are new compounds to the genus. The GC-MS analysis of the major components of the essential oils were found to be 3-hexen-1-ol (52.62 %), n-hexadecanoic acid (46.69 %), n-(*E*)-2-nonen-1-ol (38.33 %) and n-hexadecanoic acid (28.83%), in leaves, roots of *Myrica salicifolia*, leaves of *Clematis simensis* and barks of *Olinia usambarensis* respectively. The antioxidant activites of crude extracts and isolated compounds were determined using DPPH assye as aresult the roots crude extract of *Myrica salicifolia* showed very strong antioxidant activity. The antibacterial activites of crude extracts and compounds were investigated using disk diffusion method against four bacterial strains, compounds **32** and **84** showed modest antibacterial activity against gram positive bacteria. Thus, this study has brought new information and additional constituents for the chemical diversity of *M. salicifolia*, *C. simensis* and *O. usambarensis*, as well as which updated the previous study and may provide vital information to this traditional plant for the further researchers and development of drug. As a result, we deduced that the current study bring new scientific report of the new isolated compound and other compounds. It also contributes to standardization of these plants and conservation efforts by highlighting the importance of preserving these species for their potential medicinal value. Further research is warranted

to explore the bioactivity and therapeutic potential of these compounds, thereby harnessing the full potential of these plants in traditional medicine and drug discovery endeavors.

Summary of isolated compounds

No	Compound Structures	source
77	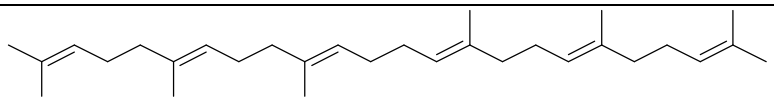	leaves of Myrica salicifolia
78	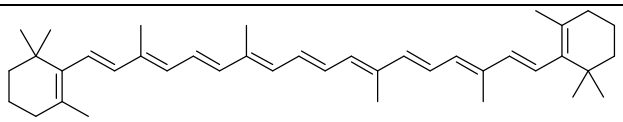	
79	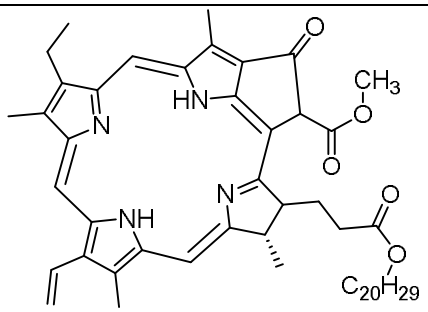	
80	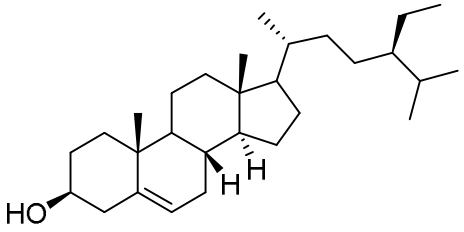	
28	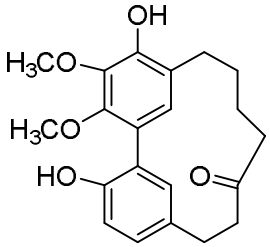	Steam barks of *Myrica salicifolia*
29	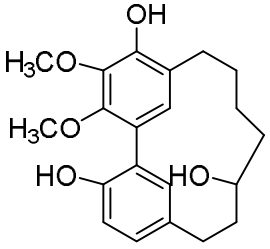	

32	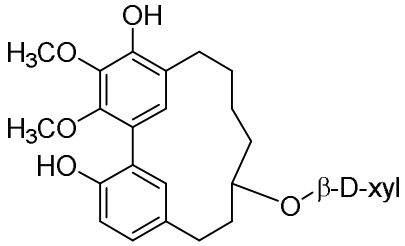	Steam barks of *Myrica salicifolia*
81	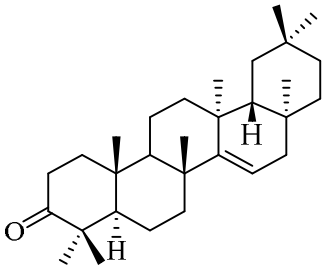	
82	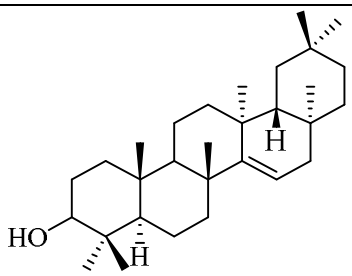	
86	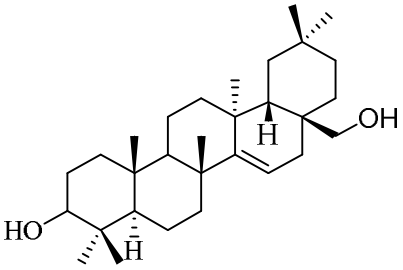	
84	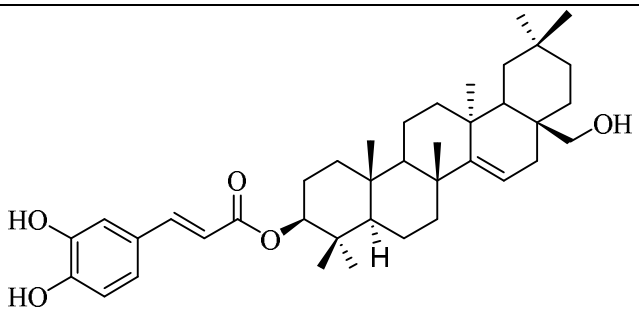	
85	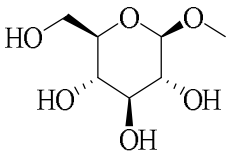	

86	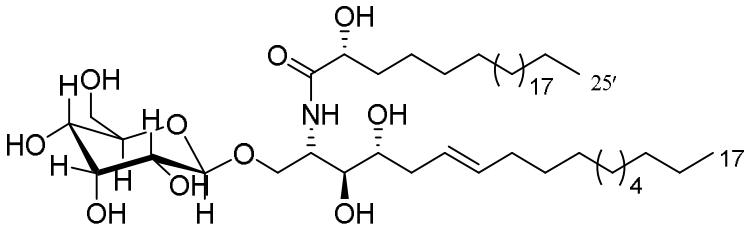	Steam barks of *Myrica salicifolia*
82	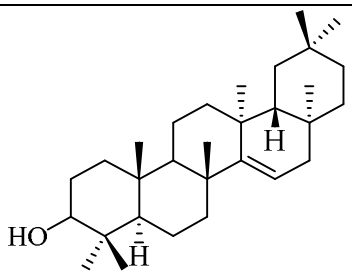	Roots of *Myrica salicifolia*
80	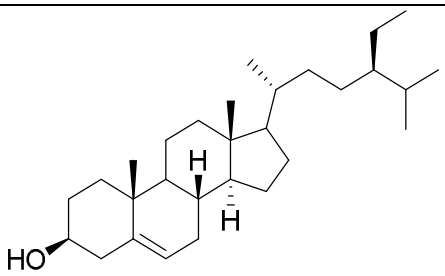	
87	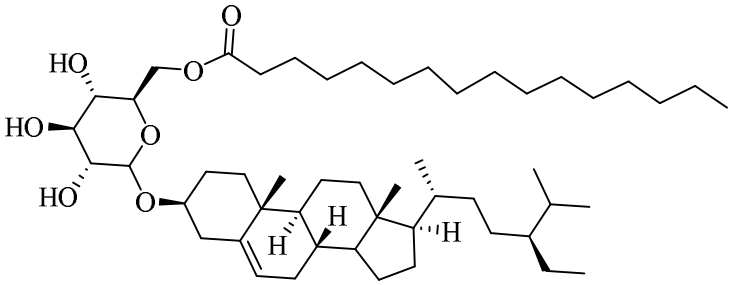	
28	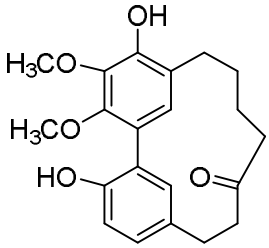	
30	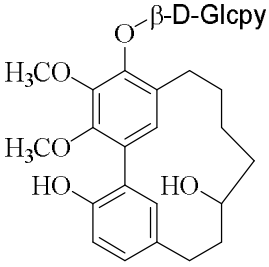	

88	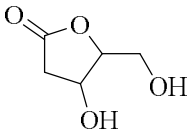	Aerial parts of *Clematis simensis*
89	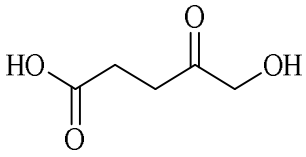	
90	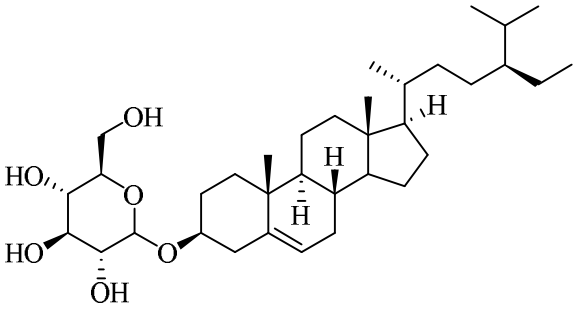	
91	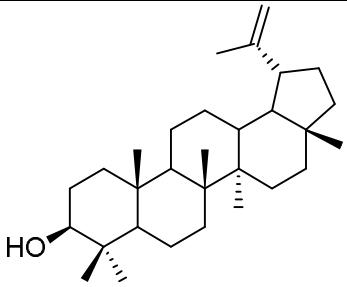	Barks of *Olinia usambarensis*
92	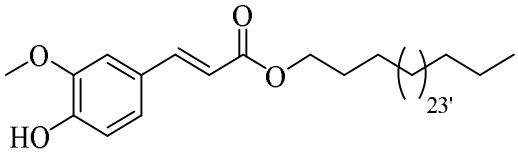	
72	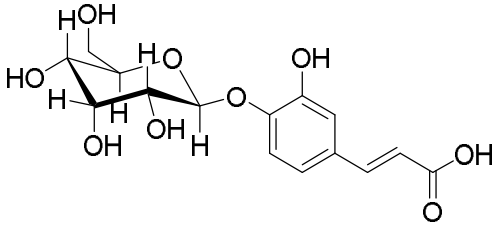	

6 References

(1) Christenhusz, M. J.; Byng, J. W.; Christenhusz, M. J.; Byng, J. W. The Number of Known Plants Species in the World and Its Annual Increase. *Phytotaxa* **2016**, *261* (3), 201–217.

(2) Bhat, R. A.; Hakeem, K. R.; Dervash, M. A. *Phytomedicine : A Treasure of Pharmacologically Active Products from Plants*; Academic Press: London, 2021

(3) Ayalew, H.; Tewelde, E.; Abebe, B.; Alebachew, Y.; Tadesse, S. Endemic Medicinal Plants of Ethiopia: Ethnomedicinal Uses, Biological Activities and Chemical Constituents. *J. Ethnopharmacol.* **2022**, *293* (115307), 115307. https://doi.org/10.1016/j.jep.2022.115307.

(4) Kidane, B.; van Andel, T.; van der Maesen, L. J. G.; Asfaw, Z. Use and Management of Traditional Medicinal Plants by Maale and Ari Ethnic Communities in Southern Ethiopia. *J. Ethnobiol. Ethnomed.* **2014**, *10* (1), 46. https://doi.org/10.1186/1746-4269-10-46.

(5) Oyda, S. Review on Traditional Ethno-Veterinary Medicine and Medicinal Plants Used by Indigenous People in Ethiopia: Practice and Application System. *Int. J. Res. Granthaalayah* **2017**, *5* (8), 109–119. https://doi.org/10.29121/granthaalayah.v5.i8.2017.2193.

(6) Kumar, B.; Vijayakumar, M.; Govindarajan, R.; Pushpangadan, P. Ethnopharmacological Approaches to Wound Healing-Exploring Medicinal Plants of India. *Journal of ethnopharmacol*. **2007**, *114* (2), 103–113.

(7) Velavan, S. Phytochemical Techniques-a Review. *World j. sci. res*. ***2015*** (2), 80–91.

(8) Femenia, A. *High-Value Co-Products from Plant Foods: Cosmetics and Pharmaceuticals. In Handbook of Waste Management and Co-Product Recovery in Food Processing*; Elsevier, 2007.

(9) Cragg, G. M.; Newman, D. J. Natural Products: A Continuing Source of Novel Drug Leads. *Biochim. Biophys. Acta.* **2013**, *1830* (6), 3670–3695. https://doi.org/10.1016/j.bbagen.2013.02.008.

(10) Balunas, M. J.; Kinghorn, A. D. Drug Discovery from Medicinal Plants. *Life Sci.* **2005**, *78* (5), 431–441. https://doi.org/10.1016/j.lfs.2005.09.012.

(11) Drahl, C.; Cravatt, B. F.; Sorensen, E. J. Protein-Reactive Natural Products. *Angew. Chem. Int. Ed Engl.* **2005**, *44* (36), 5788–5809. https://doi.org/10.1002/anie.200500900.

(12) Gurib-Fakim, A. Traditional Roles and Future Prospects for Medicinal Plants in Health Care. *Asian Biotechn Dev R.* **2011**, *13*, 77–83.

(13) Bhattarai, S.; Feitosa, C. M.; Rai, M. An Introduction to the Ethnopharmacology of Wild Plants. In *Ethnopharmacology of Wild Plants*; CRC Press: First edition. | Boca Raton : CRC Press, 2021.

(14) Yeung, A. W. K.; Mocan, A.; Tzvetkov, N. T.; Šmejkal, K.; Heiss, E. H.; Atanasov, A. G. Natural Products, the Continuous Source of Therapeutic Molecules for Various Diseases: Literature Landscape Analysis. *Curr. Mol. Pharmacol.* **2021**, *14* (6), 993–1002. https://doi.org/10.2174/1874467213666201214124327.

(15) Yang, F.; Guo, X.; Ni, K. *Research Progress on Forage Production, Processing and Utilization in China*; Springer Nature, 2022.

(16) Barreca, M.; Spanò, V.; Montalbano, A.; Cueto, M.; Díaz Marrero, A. R.; Deniz, I.; Erdoğan, A.; Lukić Bilela, L.; Moulin, C.; Taffin-de-Givenchy, E.; Spriano, F.; Perale, G.; Mehiri, M.; Rotter, A.; P Thomas, O.; Barraja, P.; Gaudêncio, S. P.; Bertoni, F. Marine Anticancer Agents: An Overview with a Particular Focus on Their Chemical Classes. *Mar. Drugs* **2020**, *18* (12), 619. https://doi.org/10.3390/md18120619.

(17) Ahmad, A.; Panda, B. P.; Mujeeb, M. Screening of Nutrient Parameters for Mevastatin Production by Penicillium Citrinum MTCC 1256 under Submerged Fermentation Using the Plackett-Burman Design. *J. Pharm. Bioallied Sci.* **2010**, *2* (1), 44–46. https://doi.org/10.4103/0975-7406.62709.

(18) Guan-Hua Du. *Natural Small Molecule Drugs from Plants*; Springer. C: Singapore, 2018.

(19) Hunt, J. T. Discovery of Ixabepilone. *Mol. Cancer Ther.* **2009**, *8* (2), 275–281. https://doi.org/10.1158/1535-7163.mct-08-0999.

(20) Bero, J.; Frédérich, M.; Quetin-Leclercq, J. Antimalarial Compounds Isolated from Plants Used in Traditional Medicine. *J. Pharm. Pharmacol.* **2009**, *61* (11), 1401–1433. https://doi.org/10.1211/jpp/61.11.0001.

(21) Emre, M.; Aarsland, D.; Albanese, A.; Byrne, E. J.; Deuschl, G.; De Deyn, P. P.; Durif, F.; Kulisevsky, J.; van Laar, T.; Lees, A.; Poewe, W.; Robillard, A.; Rosa, M. M.; Wolters, E.; Quarg, P.; Tekin, S.; Lane, R. Rivastigmine for Dementia Associated with Parkinson's Disease. *N. Engl. J. Med***. 2004**, *351* (24), 2509–2518. https://doi.org/10.1056/nejmoa041470

(22) Elfawal, M. A.; Towler, M. J.; Reich, N. G.; Golenbock, D.; Weathers, P. J.; Rich, S. M. Dried Whole Plant Artemisia Annua as an Antimalarial Therapy. *PLoS One* **2012**, *7* (12), e52746. https://doi.org/10.1371/journal.pone.0052746.

(23) Sarker, S. D.; Nahar, L. An Introduction to Natural Products Isolation. *Methods Mol. Biol.* **2012**, *864*, 1–25. https://doi.org/10.1007/978-1-61779-624-1_1.

(24) K. Hostettmann; Marston, A.; Maryse Hostettmann. *Preparative Chromatography Techniques*; Springer Science & Business Media, 2013

(25) Sticher, O. Natural Product Isolation. *Nat. Prod. Rep.* **2008**, *25* (3), 517–554. https://doi.org/10.1039/b700306b.

(26) Richardson, P. M.; Harborne, J. B. Phytochemical Methods: A Guide to Modern Techniques of Plant Analysis. Second Edition. *Brittonia* **1990**, *42* (2), 115. https://doi.org/10.2307/2807624.

(27) Qi, Z.; Kelley, E. The WHO Traditional Medicine Strategy 2014-2023: A Perspective. *Science* **2014**, *346* (6216), S5–S6.

(28) Moges, A.; Moges, Y. Ethiopian Common Medicinal Plants: Their Parts and Uses in Traditional Medicine-Ecology and Quality Control. Plant Science-Structure, Anatomy and Physiology in Plants Cultured in Vivo. 2019, *21*, 78–101.

(29) Dubale, S.; Edris, R.; Abebe, E.; Kebebe, D.; Abdissa, N.; Debela, A.; Zeynudin, A.; Suleman, S. Traditional Medicine Regulatory Framework and Legal Basis in Ethiopia: A Critical Evaluation of Challenges and Opportunities for Policy Implementation. *Res Sq.* **2023**. https://doi.org/10.21203/rs.3.rs-3298134/v1.

(30) Mancuso, G.; Midiri, A.; Gerace, E.; Biondo, C. Bacterial Antibiotic Resistance: The Most Critical Pathogens. *Pathog.* **2021**, *10* (10), 1310. https://doi.org/10.3390/pathogens10101310.

(31) Lee, H.-B. Anti-Helicobacter Pylori Diarylheptanoid Identified in the Rhizome of Alpinia Officinarum. *J. Korean Soc. Appl. Biol. Chem.* **2009**, *52* (4), 367–370. https://doi.org/10.3839/jksabc.2009.065.

(32) Desta, B. Ethiopian Traditional Herbal Drugs. Part II: Antimicrobial Activity of 63 Medicinal Plants. *J. Ethnopharmacol.* **1993**, *39* (2), 129–139. https://doi.org/10.1016/0378-8741(93)90028-4.

(33) Nigussie, G.; Erdedo, A.; Ashenafi, S. In Vitro Anti-Bacterial Activities of Aqueous, Ethanol and Chloroform Crude Extracts of Olinia Rochetiana and Vernonia Myriantha. *J. Trop. Pharm. Chem.* **2020**, *5* (2), 98–110. https://doi.org/10.25026/jtpc.v5i2.243.

(34) Husen, A., Mishra, V.K., Semwal, K. and Kumar, D. Biodiversity Status in Ethiopia and Challenges (In: 'Environmental Pollution and Biodiversity‟ Vol. -1, Bharati K. P., Chauhan A. and Kumar P., Eds., Discovery Publishing House Pvt Ltd. New Delhi, India, 2012, *1*, 31–79.

(35) Bekalo, T. H.; Woodmatas, S. D.; Woldemariam, Z. A. An Ethnobotanical Study of Medicinal Plants Used by Local People in the Lowlands of Konta Special Woreda, Southern Nations, Nationalities and Peoples Regional State, Ethiopia. *J. Ethnobiol. Ethnomed.* **2009**, *5* (1), 26. https://doi.org/10.1186/1746-4269-5-26.

(36) Yeshiwas, Y.; Tadele, E.; Tiruneh, W. The Dynamics of Medicinal Plants Utilization Practice Nexus Its Health and Economic Role in Ethiopia: A Review Paper. *Int. J. Biodivers. 2019* (1), 31–47.

(37) Hill, R. A. Making Scientific Sense of Traditional Medicine: Efficacy, Bioprospecting, and the Enduring Hope of Drug Discovery in Ethiopia. *hopp* **2022**, *63* (2), 270–301. https://doi.org/10.3368/hopp.63.2.270.

(38) Herbert, J. Systematics and Biogeography of Myricaceae. Ph.D. Dissertation, University of St Andrews, *Scotland,* 2005. https://hdl.handle.net/10023/2687 (accessed 2023-03-12)

(39) Tene, M.; Wabo, H. K.; Kamnaing, P.; Tsopmo, A.; Tane, P.; Ayafor, J. F.; Sterner, O. Diarylheptanoids from Myrica Arborea. *Phytochem.* **2000**, *54* (8), 975–978. https://doi.org/10.1016/s0031-9422(00)00164-3.

(40) Herbert, J. New Combinations and a New Species in Morella (Myricaceae). *Novon* **2005**, 293–295.

(41) Silva, B. J. C.; Seca, A. M. L.; Barreto, M. do C.; Pinto, D. C. G. A. Recent Breakthroughs in the Antioxidant and Anti-Inflammatory Effects of Morella and Myrica Species. *Int. J. Mol. Sci.* **2015**, *16* (8), 17160–17180. https://doi.org/10.3390/ijms160817160.

(42) Scaria, S. S.; Ravi, L. Symbiotic Associations of Frankia in Actinorhizal Plants. In *Microbial Symbionts*; Elsevier, 2023; pp 397–416.

(43) Yanthan, M.; Misra, A. K. Molecular Approach to the Classification of Medicinally Important Actinorhizal Genus. Myrica. *Indian J Biotechnol*. **2013**, 12(1):133-136

(44) World Health Organization. WHO Traditional Medicine Strategy: 2014-2023. *Who.int.* **2014**. https://doi.org/9789241506090.

.(45) Taiwanese Native Medicinal Plants. Phytopharmacology and Therapeutic Values by Thomas S. c. Li (Pacific Agri-Food Research Center, Summerland, British Columbia). CRC Press/Taylor & Francis, Boca Raton. 2006. Xiv + 379 Pp. 16 × 24 Cm. $189.95. ISBN 0-8493-9249-7. *J. Nat. Prod.* **2006**, *69* (9), 1377–1377. https://doi.org/10.1021/np068235x.

(46) Yu, Y.-F.; Lu, Q.; Guo, L.; Mei, R.-Q.; Liang, H.-X.; Luo, D.-Q.; Cheng, Y.-X. Myricananone and Myricananadiol: Two New Cyclic ‘Diarylheptanoids’ from the

Roots ofMyrica Nana. *Helv. Chim. Acta* **2007**, *90* (9), 1691–1696. https://doi.org/10.1002/hlca.200790175.

(47) Wang, J.-F.; Zhang, C.-L.; Lu, Q.; Yu, Y.-F.; Zhong, H.-M.; Long, C.-L.; Cheng, Y.-X. ChemInform Abstract: Three New Diarylheptanoids from Myrica Nana. *Chem. Inform*. **2010**, *41* (1), no-no. https://doi.org/10.1002/chin.201001222.

(48) Lee, S.; Xiao, C.; Pei, S. Ethnobotanical Survey of Medicinal Plants at Periodic Markets of Honghe Prefecture in Yunnan Province, SW China. *J. Ethnopharmacol.* **2008**, *117* (2), 362–377. https://doi.org/10.1016/j.jep.2008.02.001.

(49) Schmidt, E.; Lotter, M.; Mccleland, W. *Trees and Shrubs of Mpumalanga and Kruger National Park*; Jacana Media, 2002.

(50) *Sesotho Plant & Animal Names & Plants Used by the Basotho*; Rodney Moffett. SUN Press: Bloemfontain, South Africa, 2010.

(51) Ashafa, A. O. T. Medicinal Potential of Morella Serata (Lam.) Killick (Myricaceae) Root Extracts: Biological and Pharmacological Activities. *BMC Complement. Altern. Med.* **2013**, *13* (1), 163. https://doi.org/10.1186/1472-6882-13-163.

(52) Small, E. *North American Cornucopia: Top 100 Indigenous Food Plants*; CRC Press, 2013.

(53) Ene, M.; Tane, P.; Connolly, J. D. Triterpenoids and Diarylheptanoids from Myrica Arborea. *Biochemical Systematics and Ecology* **2008**, *36* (11), 872–874.

(54) Fang, J.; Paetz, C.; Schneider, B. C-Methylated Flavanones and Dihydrochalcones from Myrica Gale Seeds. *Biochem. Syst. Ecol.* **2011**, *39* (1), 68–70. https://doi.org/10.1016/j.bse.2011.01.009.

(55) Lv, H.; She, G. Naturally Occurring Diarylheptanoids. *Nat. Prod. Commun.* **2010**, *5* (10), 1687–1708. https://doi.org/10.1177/1934578x1000501035.

(56) Un, C.; Huang, H.; Xu, C.; Li, X.; Chen, K. Biological Activities of Extracts from Chinese Bayberry (Myrica Rubra Sieb. et Zucc.): A Review. *Plant Foods Hum. Nutr*. **2013**, *68*, 97–106.

(57) Lv, H.; She, G. Naturally Occurring Diarylheptanoids-A Supplementary Version. *Rec. Nat. Prod.* **2012**, *6*.

(58) Meniso, B. G.; Boru, A. D.; Ganjinaboyina, N. B. Phytochemical Investigation and Evaluation of Antimicrobial Activities of Stem Bark of Morella Salicifolia. *Bull. Chem. Soc. Ethiop.* **2019**, *33* (2), 293–306.

(59) Kifle, Z. D.; Adinew, G. M.; Mengistie, M. G.; Gurmu, A. E.; Enyew, E. F.; Goshu, B. T.; Amare, G. G. Evaluation of Antimalarial Activity of Methanolic Root Extract of Myrica Salicifolia A Rich (Myricaceae) against Plasmodium Berghei-Infected Mice. *J. Evid. Based Integr. Med.* **2020**, *25*, 2515690X20920539. https://doi.org/10.1177/2515690X20920539.

(60) Mbuya, L.; Msanga, H.; Ruffo, C.; Birnie, A.; Tengnäs, B. *Useful Trees and Shrubs for Tanzania: Identification, Propagation and Management for Agricultural and Pastoral Communities. Regional Soil Conservation Unit*; 1994.

(61) Kokwaro, J. O. Medicinal Plants of East Africa; Nairobi, Kenya Univ. Of Nairobi Press, 2009.

(62) Schlage, C.; Mabula, C.; Mahunnah, R. L. A.; Heinrich, M. Medicinal Plants of the Washambaa (Tanzania): Documentation and Ethnopharmacological Evaluation. *Plant Biol. (Stuttg.)* **2000**, *2* (1), 83–92. https://doi.org/10.1055/s-2000-296.

(63) Hedberg, I.; Hedberg, O.; Madat, P. J.; Mshigeni, K. E.; Mshiu, E. N.; Samuelsson, G. Inventory of Plants Used in Traditional Medicine in Tanzania. II. Plants of the Families Dilleniaceae—Opiliaceae. *J. Ethnopharmacol.* **1983**, *9* (1), 105–127. https://doi.org/10.1016/0378-8741(83)90030-2.

(64) Kamatenesi-Mugisha, M.; Oryem-Origa, H. Traditional Herbal Remedies Used in the Management of Sexual Impotence and Erectile Dysfunction in Western Uganda. *Afr. Health Sci.* **2005**, *5* (1), 40–49.

(65) Alelign, T.; Chalchisa, D.; Fekadu, N.; Solomon, D.; Sisay, T.; Debella, A.; Petros, B. Evaluation of Acute and Sub-Acute Toxicity of Selected Traditional Antiurolithiatic Medicinal Plant Extracts in Wistar Albino Rats. *Toxicol. Rep.* **2020**, *7*, 1356–1365. https://doi.org/10.1016/j.toxrep.2020.10.001.

(66) Eklay, A.; Abera, B.; Giday, M. An Ethnobotanical Study of Medicinal Plants Used in Kilte Awulaelo District, Tigray Region of Ethiopia. *J. Ethnobiol. Ethnomed.* ***2013*** (1), 1–23.

(67) Marealle, A. I.; Innocent, E.; Andrae-Marobela, K.; Qwarse, M.; Machumi, F.; Nondo, R. S. O.; Heydenreich, M.; Moshi, M. J. Safety Evaluation and Bioassay-Guided Isolation of Antimycobacterial Compounds from Morella Salicifolia Root Ethanolic Extract. *J. Ethnopharmacol.* **2022**, *296* (115501), 115501. https://doi.org/10.1016/j.jep.2022.115501.

(68) Kirira, P. G.; Rukunga, G. M.; Wanyonyi, A. W.; Muregi, F. M.; Gathirwa, J. W.; Muthaura, C. N.; Omar, S. A.; Tolo, F.; Mungai, G. M.; Ndiege, I. O. Anti-Plasmodial Activity and Toxicity of Extracts of Plants Used in Traditional Malaria Therapy in Meru and Kilifi Districts of Kenya. *J. Ethnopharmacol.* **2006**, *106* (3), 403–407. https://doi.org/10.1016/j.jep.2006.01.017.

(69) Njung'e, K.; Muriuki, G.; Mwangi, J. W.; Kuria, K. A. M. Analgesic and Antipyretic Effects of Myrica Salicifolia (Myricaceae). *Phytother. Res.* **2002**, *16* (S1), 73–74. https://doi.org/10.1002/ptr.761.

(70) Emiru, Y. K.; Periasamy, G.; Karim, A.; Ur Rehman, N.; Ansari, M. N. Evaluation of in Vitro α-Amylase Inhibitory Activity and Antidiabetic Effect of Myrica Salicifolia in Streptozotocin-Induced Diabetic Mice. *Pak. J. Pharm. Sci.* **2020**, *33* (4(Supplementary)), 1917–1926.

(71) Rehman, N. U.; Ansari, M. N.; Palla, A. H.; Karim, A.; Imam, F.; Raish, M.; Hamad, A. M.; Noman, M. Myrica Salicifolia Hochst. Ex A. Rich. Suppress Acetic Acid-Induced Ulcerative Colitis in Rats by Reducing TNF-Alpha and Interleukin-6, Oxidative Stress Parameters and Improving Mucosal Protection. *Hum. Exp. Toxicol.* **2022**, *41*, 9603271221102518. https://doi.org/10.1177/09603271221102518.

(72) Soh, P. N.; Witkowski, B.; Olagnier, D.; Nicolau, M.-L.; Garcia-Alvarez, M.-C.; Berry, A.; Benoit-Vical, F. In Vitro and in Vivo Properties of Ellagic Acid in Malaria Treatment. *Antimicrob. Agents Chemother.* **2009**, *53* (3), 1100–1106. https://doi.org/10.1128/AAC.01175-08.

(73) Geyid, A.; Abebe, D.; Debella, A.; Makonnen, Z.; Aberra, F.; Teka, F.; Kebede, T.; Urga, K.; Yersaw, K.; Biza, T.; Mariam, B. H.; Guta, M. Screening of Some Medicinal Plants of Ethiopia for Their Anti-Microbial Properties and Chemical

Profiles. *J. Ethnopharmacol.* **2005**, *97* (3), 421–427. https://doi.org/10.1016/j.jep.2004.08.021.

(74) Ganapathy, G.; Preethi, R.; Moses, J. A.; Anandharamakrishnan, C. Diarylheptanoids as Nutraceutical: A Review. *Biocatal. Agric. Biotechnol.* **2019**, *19* (101109), 101109. https://doi.org/10.1016/j.bcab.2019.101109.

(75) Makule, E. E.; Kraus, B.; Jürgenliemk, G.; Heilmann, J.; Wiesneth, S. Dioic Acid Glycosides, Tannins and Methylated Ellagic Acid Glycosides from Morella Salicifolia Bark. *Phytochem. Lett.* **2018**, *28*, 76–83. https://doi.org/10.1016/j.phytol.2018.09.013.

(76) Makule, E.; Schmidt, T.; Heilmann, J.; Kraus, B. Diarylheptanoid Glycosides of Morella Salicifolia Bark. *Mol.* **2017**, *22* (12), 2266. https://doi.org/10.3390/molecules22122266.

(77) Da-Cheng, H.; Pei-Gen, X.; Hong-Ying, M.; Yong, P.; Chun-Nian, H. Mining Chemodiversity from Biodiversity: Pharmacophylogeny of Medicinal Plants of Ranunculaceae. *Chin. J. Nat*. **2015**, *13*, 507–520.

(78) Ma, X.; Qian, R.; Zhang, X.; Hu, Q.; Liu, H.; Zheng, J. Contrasting Growth, Physiological and Gene Expression Responses of Clematis Crassifolia and Clematis Cadmia to Different Irradiance Conditions. *Sci. Rep.* **2019**, *9* (1), 17842. https://doi.org/10.1038/s41598-019-54428-z.

(79) Chawla, R.; Kumar, S.; Sharma, A. The Genus Clematis (Ranunculaceae): Chemical and Pharmacological Perspectives. *J. Ethnopharmacol.* **2012**, *143* (1), 116–150. https://doi.org/10.1016/j.jep.2012.06.014.

(80) Motjotji, L.; Moteetee, A.; Seleteng-Kose, L. Medicinal Plants of Lesotho: A Review of Ethnomedicinal, Pharmacological and Conservation Studies: Lesotho Medicinal Plants. *Ethnobot. Res. Appl*. **2023**, *25*, 1–19.

(81) Hawaze, S.; Deti, H.; Suleman, S. In Vitro Antimicrobial Activity and Phytochemical Screening of Clematis Species Indigenous to Ethiopia. *Indian J. Pharm. Sci.* **2012**, *74* (1), 29–35. https://doi.org/10.4103/0250-474X.102540.

(82) Rajeev Rattan. Bioactive species of genus clematis-a report. *Int. J. Creat. Res. Thoughts* **2023**, *11* (5). 718-724.

(83) Wu, W.; Xu, X.; Dai, Y.; Xia, L. Therapeutic Effect of the Saponin Fraction from Clematis Chinensis Osbeck Roots on Osteoarthritis Induced by Monosodium Iodoacetate through Protecting Articular Cartilage: THERAPEUTIC EFFECT OF CLEMATIS CHINENSIS OSBECK ON OSTEOARTHRITIS. *Phytother. Res.* **2010**, *24* (4), 538–546. https://doi.org/10.1002/ptr.2977.

(84) Yesilada, E.; Küpeli, E. Clematis Vitalba L. Aerial Part Exhibits Potent Anti-Inflammatory, Antinociceptive and Antipyretic Effects. *J. Ethnopharmacol.* **2007**, *110* (3), 504–515. https://doi.org/10.1016/j.jep.2006.10.016.

(85) Du, Z.-Z.; Yang, X.-W.; Han, H.; Cai, X.-H.; Luo, X.-D. A New Flavone C-Glycoside from Clematis Rehderiana. *Molecules* **2010**, *15* (2), 672–679. https://doi.org/10.3390/molecules15020672.

(86) Chen, J.-H.; Du, Z.-Z.; Shen, Y.-M.; Yang, Y.-P. Aporphine Alkaloids from Clematis Parviloba and Their Antifungal Activity. *Arch. Pharm. Res.* **2009**, *32* (1), 3–5. https://doi.org/10.1007/s12272-009-1111-7.

(87) Fu, Q.; Zan, K.; Zhao, M.; Zhou, S.; Shi, S.; Jiang, Y.; Tu, P. Triterpene Saponins from Clematis Chinensis and Their Potential Anti-Inflammatory Activity. *J. Nat. Prod.* **2010**, *73* (7), 1234–1239. https://doi.org/10.1021/np100057y.

(88) Sebola, R. J.; Balkwill, K. A Monographic Study of the Oliniaceae. *Kew Bull.* **2013**, *68* (3), 419–456. https://doi.org/10.1007/s12225-013-9465-x.

(89) Hao, D. C.; Gu, X.-J.; Xiao, P. G. Chemical and Biological Research of Clematis Medicinal Resources. In *Medicinal Plants*; Elsevier, 2015; pp 341–371.

(90) Tuasha, N.; Petros, B.; Asfaw, Z. Medicinal Plants Used by Traditional Healers to Treat Malignancies and Other Human Ailments in Dalle District, Sidama Zone, Ethiopia. *J. Ethnobiol. Ethnomed.* **2018**, *14* (1). https://doi.org/10.1186/s13002-018-0213-z.

(91) Tuasha, N.; Petros, B.; Asfaw, Z. Plants Used as Anticancer Agents in the Ethiopian Traditional Medical Practices: A Systematic Review. *Evid. Based. Complement. Alternat. Med.* **2018**, *2018*, 6274021. https://doi.org/10.1155/2018/6274021.

(92) Wubetu, M.; Sintayehu, M.; Aeta, M. A. Ethnobotany of Medicinal Plants Used to Treat Various Mental Illnesses in Ethiopia: A Systematic Review Muluken Wubetu1, Mezinew Sintayehu2, Mohammedbrhan Abdelwuhab Aeta2, Haimanot Reta2 and Dagninet Derebe2. *Asian J. Plant Sci*. **2018**, *8* (1), 9–33.

(93) Amenu, E. Use and Management of Medicinal Plants by Indigenous People of Ejaji Area (Chelya Woreda) West Shoa, Ethiopia: An Ethnobotanical Approach. *M. Sc. Thesis*, Addis Ababa University. Addis Ababa, 2007. http://thesisbank.jhia.ac.ke/id/eprint/6141 (accessed 2022-02-16).

(94) Tedila, H.; Assefa, A. In Vitro Antibacterial Activity of Rumex Nervosus and Clematis Simensis Plants against Some Bacterial Human Pathogens. *Afr. J. Microbiol. Res.* **2019**, *13* (1), 14–22.

(95) Birhan, M.; Kenubih, A.; Mekuriyaw, A.; Yayeh, M.; Nuru, A. Assessment of Antimicrobial Effects, Antioxidant Activity and Phytochemical Analysis of Clematis Simensis Leaves Extract. *Asian J. Med. Pharm. Res.* **2018**, *8* (3), 15–25.

(96) Addis, G.; Abebe, D.; Urga, K. *A Survey of Traditional Medicinal Plants in Shirka District*; Arsi Zone, Ethiopia, *Ethiop. Pharm. J.* **2001**, 19, 30-47.

(97) Gedif, T.; Hahn, H. Traditional Treatment of Skin Disorders in Butajira, South-Central Ethiopia. *Ethiop. Pharm. J.* **2001**, *19*, 48–56.

(98) Costa, E. S.; Hiruma-Lima, C. A.; Lima, E. O.; Sucupira, G. C.; Bertolin, A. O.; Lolis, S. F.; Andrade, F. D. P.; Vilegas, W.; Souza-Brito, A. R. M. Antimicrobial Activity of Some Medicinal Plants of the Cerrado, Brazil. *Phytother. Res.* **2008**, *22* (5), 705–707. https://doi.org/10.1002/ptr.2397.

(99) Tadele, A.; Asres, K.; Melaku, D.; Mekonnen, W. In Vivo Anti-Inflammatory and Antinociceptive Activities of the Leaf Extracts of Clematis Simensis Fresen. *Ethiop. Pharm. J.* **2010**, *27* (1). https://doi.org/10.4314/epj.v27i1.51117.

(100) Tuasha, N.; Seifu, D.; Gadisa, E.; Petros, B.; Oredsson, S. Cytotoxicity of Selected Ethiopian Medicinal Plants Used in Traditional Breast Cancer Treatment against Breast-Derived Cell Lines. *J. Med. Plant Res.* **2019**, *13* (9), 188–198.

(101) Ayana, M. T.; Mehari, Y. G.; Beyene, B. B. A Phytochemical Investigation and Evaluation of the Antioxidant and Antibacterial Activities of the Stem Bark Extract of *Clematis Simensis (Yeazo Hareg)*. *J. Chem. Res.* **2022**, *46* (5), 174751982211273-174751982211273. https://doi.org/10.1177/17475198221127398.

(102) Alemayehu, M. A.; Abdelwuhab, M.; Gelayee, D. A. In-Vivo Anti-Malarial Activity of Crude Extract and Solvent Fractions of the Roots of Clematis Simensis Fresen.(Ranunculaceae) in Plasmodium Berghei Infected Mice. *IOSR J. Pharm.* **2020** (5), 52–62.

(103) Teshome, N.; Degu, A.; Ashenafi, E.; Ayele, E.; Abebe, A. Evaluation of Wound Healing and Anti-Inflammatory Activity of Hydroalcoholic Leaf Extract of Clematis Simensis Fresen (Ranunculaceae). *Clin. Cosmet. Investig. Dermatol.* **2022**, *15*, 1883–1897. https://doi.org/10.2147/CCID.S384419.

(104) Cufodontis, G. Die Identifizierung von Tephea Delile Und Andere Die Oliniaceae Betreffende Feststellungen. *Oesterr. Bot. Z. Alternative* **1960**, *107*, 106–112.

(105) Kokwaro, J. O. Medicinal Plants of East Africa. In *Kenya Literature Bureau 401p. ISBN*; Nairobi, 1993; Vol. 9966.

(106) Kebede, M.; Yirdaw, E.; Luukkanen, O.; Lemenih, M. Plant Community Analysis and Effect of Environmental Factors on the Diversity of Woody Species in the Moist Afromontane Forest of Wondo Genet, South Central Ethiopia. *Biodivers. Res. Conserv.* **2013**, *29* (1), 63–80. https://doi.org/10.2478/biorc-2013-0003.

(107) Negesse, G.; Woldearegay, M. Floristic Diversity, Structure and Regeneration Status of Menfeskidus Monastery Forest in Berehet District, North Shoa, Central Ethiopia. *Trees For. People* **2022**, *7* (100191), 100191. https://doi.org/10.1016/j.tfp.2022.100191.

(108) Abebe, D.; Ayehu, A. *Medicinal Plants and Enigmatic Health Practices of Northern Ethiopia*; B.S.P.E, Addis Ababa, Ethiopia, 1993.

(109) Abate, G.; Demissew, S. Etse Debdabe. *Ethiopian Traditional Medicine.* Addis Ababa University Press; 1989, 99–183.

(110) Lulekal, E.; Asfaw, Z.; Kelbessa, E.; Van Damme, P. Ethnomedicinal Study of Plants Used for Human Ailments in Ankober District, North Shewa Zone, Amhara Region, Ethiopia. *J. Ethnobiol. Ethnomed.* **2013**, *9* (1), 63. https://doi.org/10.1186/1746-4269-9-63.

(111) Tadeg, H.; Mohammed, E.; Asres, K.; Gebre-Mariam, T. Antimicrobial Activities of Some Selected Traditional Ethiopian Medicinal Plants Used in the Treatment of Skin Disorders. *J. Ethnopharmacol.* **2005**, *100* (1–2), 168–175. https://doi.org/10.1016/j.jep.2005.02.031.

(112) Mugweru, F.; Nyamai, D.; Arika, W.; Mworia, J.; Ngugi, M.; Njagi, E.; Ngeranwa, J. In Vivo Safety of Aqueous Extracts of Maytemus Putterlickoides, Senna Spectabilis and Olinia Usambarensis on Mice Models. *J. Clin. Toxicol.* **2016**, *6* (3).

(113) Deyou, T.; Woo, J.-H.; Choi, J.-H.; Jang, Y. P. A New Natural Product from the Leaves of Olinia Usambarensis and Evaluation of Its Constituents for Cytotoxicity against Human Ovarian Cancer Cells. *S. Afr. J. Bot.* **2017**, *113*, 182–185. https://doi.org/10.1016/j.sajb.2017.08.011.

(114) Nyandat, E.; Rwekika, E.; Galeffi, C.; Palazzino, G.; Nicoletti, M. Olinioside, 5-(4′-O-β-d-Glucopyranosyl)-Caffeoyloxy-5, 6-Dihydro-4-Methyl-(2H)-Pyran-2-One from Olinia Usambarensis. *Phytochem.* **1993**, *33* (6), 1493–1496.

(115) Kang, S.-Y.; Shin, J.-S.; Kim, S.-Y.; Noh, Y. S.; Lee, S.-J.; Hwang, H.; Deyou, T.; Jang, Y. P.; Lee, K.-T. Caffeoyloxy-5, 6-Dihydro-4-Methyl-(2H)-Pyran-2-One Isolated from the Leaves of Olinia Usambarensis Attenuates LPS-Induced Inflammatory Mediators by Inactivating AP-1 and NF-κB. *Chem. -Biol. Interact*. **2019**, *309* (2019). 1-202

(116) Katekar, V. P.; Rao, A. B.; Sardeshpande, V. R. Review of the Rose Essential Oil Extraction by Hydrodistillation: An Investigation for the Optimum Operating Condition for Maximum Yield. *Sustain. Chem. Pharm.* **2022**, *29* (100783), 100783. https://doi.org/10.1016/j.scp.2022.100783.

(117) Beckett, M.; Stenlake, O. Modified Kupchan Partition. *J. Med. Chem*. **1986**, *52*, 1525–1529.

(118) Selli, S.; Cabaroglu, T.; Canbas, A. Volatile Flavour Components of Orange Juice Obtained from the Cv. Kozan of Turkey. *J. Food Compost. Anal.* **2004**, *17* (6), 789–796. https://doi.org/10.1016/j.jfca.2003.10.005.

(119) Ou, W.; Liu, H.; Wang, R. A Review on Chemical Synthesis of Leaf Alcohol. *Curr. Org. Chem.* **2022**, *26* (16), 1512–1529. https://doi.org/10.2174/1385272827666221103102328.

(120) Tang, R.; Zhang, J. P.; Zhang, Z. N. Electrophysiological and Behavioral Responses of Male Fall Webworm Moths (Hyphantria Cunea) to Herbivory-Induced Mulberry (Morus Alba) Leaf Volatiles. *PLoS One* **2012**, *7* (11), e49256. https://doi.org/10.1371/journal.pone.0049256.

(121) Khaleel, C.; Tabanca, N.; Buchbauer, G. α-Terpineol, a Natural Monoterpene: A Review of Its Biological Properties. *Open Chem.* **2018**, *16* (1), 349–361. https://doi.org/10.1515/chem-2018-0040.

(122) Ullah, I.; Khan, A. L.; Ali, L.; Khan, A. R.; Waqas, M.; Hussain, J.; Lee, I.-J.; Shin, J.-H. Benzaldehyde as an Insecticidal, Antimicrobial, and Antioxidant Compound Produced by Photorhabdus Temperata M1021. *J. Microbiol.* **2015**, *53* (2), 127–133. https://doi.org/10.1007/s12275-015-4632-4.

(123) Ahmad, V. U.; Ahmad, V. U. Linear. *13C-NMR of Natural Products*; Springer Science & Business Media, 1992, 177–205.

(124) P.B.C. Panawala; D.C. Abeysinghe; R.M. Dharmadasa. Phytochemical Distribution and Bioactivity of Different Parts and Leaf Positions of Pimenta Dioica (L.) Merr (Myrtaceae). *J. Plant Physiol*. **2016**, *4* (5), 143–146. https://doi.org/10.12691/wjar-4-5-3.

(125) Mahmood, U.; Kaul, V. K.; Singh, B. Sesquiterpene and Long Chain Ester from Tanacetum Longifolium. *Chem. Inform.* **2003**, *34* (17). https://doi.org/10.1002/chin.200317162.

(126) Pogliani, L.; Ceruti, M.; Ricchiardi, G.; Viterbo, D. An NMR and Molecular Mechanics Study of Squalene and Squalene Derivatives. *Chem. Phys. Lipids* **1994**, *70* (1), 21–34. https://doi.org/10.1016/0009-3084(94)90044-2.

(127) Ragasa, C.; Tan, M.; Fortin, D.; Shen, C.-C. Chemical Constituents of Ixora Philippinensis Merr. *J. Appl. Pharm. Sci.* **2015**, 062–067. https://doi.org/10.7324/japs.2015.50912.

(128) Khoo, H.-E.; Prasad, K. N.; Kong, K.-W.; Jiang, Y.; Ismail, A. Carotenoids and Their Isomers: Color Pigments in Fruits and Vegetables. *Mol.* **2011**, *16* (2), 1710–1738. https://doi.org/10.3390/molecules16021710.

(129) van Breemen, R. B.; Dong, L.; Pajkovic, N. D. Atmospheric Pressure Chemical Ionization Tandem Mass Spectrometry of Carotenoids. *Int. J. Mass Spectrom.* **2012**, *312*, 163–172. https://doi.org/10.1016/j.ijms.2011.07.030.

(130) Lederer, E. Cis-Trans Isomeric Carotenoids, Vitamins A and Arylpolyenes. *J. Chromatogr. A* **1963**, *10*, 252. https://doi.org/10.1016/s0021-9673(01)92305-2.

(131) Structure Elucidation of Î²-Stigmasterol and Î²-Sitosterol from Sesbania Grandifora [Linn.] Pers. and Î²-Carotene from Heliotropium Indicum Linn. by NMR Spectroscop β-Carotene from Heliotropium Indicum Linn. by NMR Spectroscopy. *Kimika* **2004**, *20* (1), 5–12.

(132) Lutnaes, B. F.; Bruås, L.; Kildahl-Andersen, G.; Krane, J.; Liaaen-Jensen, S. The Charge Delocalised β,β-Carotene Dication—Preparation, Structure Elucidation by NMR and Reactions with Nucleophiles. *Org. Biomol. Chem.* **2003**, *1* (22), 4064–4072. https://doi.org/10.1039/b307531a.

(133) Ragasa, C. Structure Elucidation of Stigmasterol and β-Sitosterol from Sesbania Grandiflora Linn Pers. and B-Carotene from Heliotropium Indicum Linn. by NMR Spectroscopy. *Kimika* **2004**, *20* (1).

(134) Katz, J. J.; Brown, C. E. ChemInform Abstract: Nuclear Magnetic Resonance Spectroscopy Of Chlorophylls and Corrins. *Chem. Inf.* **1985**, *16* (33). https://doi.org/10.1002/chin.198533395.

(135) Peter, O.; Ngozi, A.; Ekene, O.; Chiaguguom, I.; Grace, F. Isolation of Pheophytin a and β-Amyrin from Newbouldia Laevis (P. Beauv) Leaf Extract. *Path Sci.* **2022**, *8* (6), 7001–7012. https://doi.org/10.22178/pos.82-16.

(136) Lötjönen, S.; Hynninen, P. H. Carbon-13 NMR Spectra of Chlorophyll a, Chlorophyll A′, Pyrochlorophyll a and the Corresponding Pheophytins. *Org. Magn. Reson.* **1983**, *21* (12), 757–765. https://doi.org/10.1002/omr.1270211208.

(137) Jan-Michael, C.; Ragasa, C. Structure Elucidation of Stigmasterol and B-Sitosterol from Sesbania Grandiflora Linn Pers. and B-Carotene from Heliotropium Indicum Linn. by NMR Spectroscopy. *Kimika* **2004**, *20* (1), 5–12.

(138) Charisiadis, P.; Kontogianni, V. G.; Tsiafoulis, C. G.; Tzakos, A. G.; Siskos, M.; Gerothanassis, I. P. 1H-NMR as a Structural and Analytical Tool of Intra- and Intermolecular Hydrogen Bonds of Phenol-Containing Natural Products and Model Compounds. *Mol.* **2014**, *19* (9), 13643–13682. https://doi.org/10.3390/molecules190913643.

(139) Joshi, B. S.; Pelletier, S. W.; Newton, M. G.; Lee, D.; Mcgaughey, G. B.; Puar, M. S. Extensive 1D, 2D NMR Spectra of Some [7.0] Metacyclophanes and X-Ray Analysis of (±)-Myricanol. *J. Nat. Prod.* **1996**, *59* (8), 759–764.

(140) Jones, J. R.; Lebar, M. D.; Jinwal, U. K.; Abisambra, J. F.; Koren, I.; Blair, J.; Leary, L.; Davey, J. C.; Trotter, Z.; Johnson, J. The Diarylheptanoid (+)-a R, 11 S-Myricanol and Two Flavones from Bayberry (Myrica Cerifera) Destabilize the Microtubule-Associated Protein Tau. *J. Nat. Prod.* **2011**, *74* (1), 38–44.

(141) Marino, D.; Iorizzi, S.; Zollo, M.; Minale, F.; Amsler, L.; Baker, C. D.; Mcclintock, B. J. Isolation, Structure Elucidation, and Biological Activity of the Steroid Oligoglycosides and Polyhydroxysteroids from the Antarctic Starfish Acodontaster Conspicuus. *J. Nat. Prod.* **1997**, *60* (10), 959–966.

(142) Trimedona, N.; Nurdin, H.; Darwis, D.; Efdi, M. Isolation of Triterpenoid from Stem Bark of Pometia Pinnata. *Int. J. Pharm. Res*. **2015**.

(143) Abouelela, M. E.; Orabi, M. A.; Abdelhamid, R. A.; Abdelkader, M. S.; Darwish, F. M. Chemical and Cytotoxic Investigation of Non-Polar Extract from Ceiba

Pentandra (L.) Gaertn: A Study Supported by Computer Based Screening. *J. Appl. Pharm. Sci*. **2018**, *8* (7), 57–064.

(144) Merfort, I.; Buddrus, J.; Nawwar, M. A. M.; Lambert, J. A Triterpene from the Bark of Tamarix Aphylla. *Phytochem.* **1992**, *31* (11), 4031–4032. https://doi.org/10.1016/s0031-9422(00)97580-0.

(145) Orfali, R. S.; Ebada, S. S.; El-Shafae, A. M.; Al-Taweel, A. M.; Lin, W. H.; Wray, V.; Proksch, P. 3-O-Trans-Caffeoylisomyricadiol: A New Triterpenoid from Tamarix Nilotica Growing in Saudi Arabia. *Z. Naturforsch. C.* **2009**, *64* (9–10), 637–643. https://doi.org/10.1515/znc-2009-9-1006.

(146) Hu, X.; Luo, Y.; Chen, R.; Zhou, L. Study Advances on Taraxerane Triterpenoids and Their Spectroscopic Characteristic. *Nat. Prod. Res. Dev.* **2007**, *19*, 170–178.

(147) Jin, Y.; Xu, Y.; Huang, Z.; Zhou, Z.; Wei, X. Metabolite Pattern in Root Nodules of the Actinorhizal Plant Casuarina Equisetifolia. *Phytochem.* **2021**, *186* (112724), 112724. https://doi.org/10.1016/j.phytochem.2021.112724.

(148) Laphookhieo, S.; Karalai, C.; Ponglimanont, C.; Chantrapromma, K. Pentacyclic Triterpenoid Esters from the Fruits of Bruguiera c Ylindrica. *J. Nat. Prod.* **2004**, *67* (5), 886–888.

(149) Roslund, M. U.; Tähtinen, P.; Niemitz, M.; Sjöholm, R. Complete Assignments of the 1H and 13C Chemical Shifts and JH, H Coupling Constants in NMR Spectra of D-Glucopyranose and All D-Glucopyranosyl-D-Glucopyranosides. *Carbohydr. Res.* **2008**, *343* (1), 101–112.

(150) Thomford, A. K.; Ahmed Abdelhameed, R. F.; Yamada, K. Chemical Studies on the Parasitic Plant Thonningia Sanguinea Vahl. *RSC Adv.* **2018**, *8* (37), 21002–21011. https://doi.org/10.1039/c8ra03913e.

(151) Ebede, G. R.; Ndongo, J. T.; Mbing, J. N.; Kenfack, H. C. M.; Pegnyemb, D. E.; Bochet, C. G. Contortamide, a New Anti-Colon Cancer Cerebroside and Other Constituents from Tabernaemontana Contorta Stapf (Apocynaceae). *Nat. Prod. Res.* **2021**, *35* (11), 1757–1765. https://doi.org/10.1080/14786419.2019.1636243.

(152) Mansoor, T. A.; Shinde, P. B.; Luo, X.; Hong, J.; Lee, C.-O.; Sim, C. J.; Son, B. W.; Jung, J. H. Renierosides, Cerebrosides from a Marine Sponge Haliclona (Reniera) Sp. *J. Nat. Prod.* **2007**, *70* (9), 1481–1486. https://doi.org/10.1021/np070078u.

(153) Jia, A.-Q.; Yang, X.; Wang, W.-X.; Jia, Y.-H. Glycocerebroside Bearing a Novel Long-Chain Base from Sagina Japonica (Caryophyllaceae). *Fitoterapia* **2010**, *81* (6), 540–545. https://doi.org/10.1016/j.fitote.2010.01.015.

(154) Huang, X. Z.; Yin, Y.; Dai, J. H.; Liang, H.; Dai, Y.; Bai, L. Two New Ceramides from the Stems of Piper Betle L. *Chin. Chem. Lett.* **2010**, *21* (4), 433–436. https://doi.org/10.1016/j.cclet.2009.11.047.

(155) Liu, H.; Orjala, J.; Sticher, O.; Rali, T. Acylated Flavonol Glycosides from Leaves of Stenochlaena Palustris. *J. Nat. Prod.* **1999**, *62* (1), 70–75. https://doi.org/10.1021/np980179f.

(156) Reviana, R.; Usman, A. N.; Raya, I.; Aliyah; Dirpan, A.; Arsyad, A.; Fendi, F. Analysis of Antioxidant Activity on Cocktail Honey Products as Female Pre-Conception Supplements. *Gac. Sanit.* **2021**, *35 Suppl 2*, S202–S205. https://doi.org/10.1016/j.gaceta.2021.10.021.

(157) Vellosa, J. C. R.; Regasini, L. O.; Khalil, N. M.; Bolzani, V. da S.; Khalil, O. A. K.; Manente, F. A.; Pasquini Netto, H.; Oliveira, O. M. M. de F. Antioxidant and Cytotoxic Studies for Kaempferol, Quercetin and Isoquercitrin. *Eclét. Quím. J.* **2011**, *36* (2), 07–20. https://doi.org/10.1590/s0100-46702011000200001.

(158) Rusmana, D.; Wahyudianingsih, R.; Elisabeth, M.; Balqis, B.; Maesaroh, M.; Widowati, W. Antioxidant Activity of Phyllanthus Niruri Extract, Rutin and Quercetin. *Indones. Biomed. J.* **2017**, *9* (2), 84. https://doi.org/10.18585/inabj.v9i2.281.

(159) Inouye, S.; Takizawa, T.; Yamaguchi, H. Antibacterial Activity of Essential Oils and Their Major Constituents against Respiratory Tract Pathogens by Gaseous Contact. *J. Antimicrob. Chemother.* **2001**, *47* (5), 565–573. https://doi.org/10.1093/jac/47.5.565.

(160) Miklasińska-Majdanik, M.; Kępa, M.; Wojtyczka, R. D.; Idzik, D.; Wąsik, T. J. Phenolic Compounds Diminish Antibiotic Resistance of Staphylococcus Aureus Clinical Strains. *Int. J. Environ. Res. Public Health* **2018**, *15* (10), 2321. https://doi.org/10.3390/ijerph15102321.

(161) Kalpana Devi, V.; Shanmugasundaram, R.; Mohan, V. GC-MS Analysis of Ethanol Extract of Entada Pursaetha DC Seed. *Biosci. Discov.* **2012** (1), 30–33.

(162) Avoseh, O. N.; Mtunzi, F. M.; Ogunwande, I. A.; Ascrizzi, R.; Guido, F. Albizia Lebbeck and Albizia Zygia Volatile Oils Exhibit Anti-Nociceptive and Anti-Inflammatory Properties in Pain Models. *J. Ethnopharmacol.* **2021**, *268* (113676), 113676. https://doi.org/10.1016/j.jep.2020.113676.

(163) Wei, G.; Kong, L.; Zhang, J.; Ma, C.; Wu, X.; Li, X.; Jiang, H. Essential Oil Composition and Antibacterial Activity of Lindera Nacusua (D. Don) Merr. *Nat. Prod. Res.* **2016**, *30* (23), 1–3. https://doi.org/10.1080/14786419.2015.1135145.

(164) Pinto, K. B.; Santos, P. H. B. dos; Krause, L. C.; Caramão, E. B.; Bjerk, T. R. Preliminary Prospection of Phytotherapic Compounds from the Essential Oils from Barks and Leaves of Umburana (Commiphora Leptophloeos). *Braz. J. Pharm. Sci.* **2022**, *58*. https://doi.org/10.1590/s2175-97902022e21609.

(165) Antil, R.; Singh, L.; Gahlawat, D. K.; Dahiya, P. Investigation of Chemical Composition of Methanolic Extract of Anisomeles Indica (L.) Kuntze by Using FTIR and GC-MS. *J. Pharmacogn. Phytochem.* **2019**, *8* (4), 49–54.

(166) Oladoye, S. O.; Ayodele, E. T.; Abdul-Hammed, M.; Idowu, O. T. Characterisation and Identification of Taraxerol and Taraxer-14-En-3-One from Jatropha Tanjorensis (Ellis and Saroja) Leaves: Terpeniods from Jatropha Tanjorensis. *Pakistan Journal of Scientific & Industrial Research Series A: Phys. Sci*. **2015**, *58* (1), 46–50.

(167) Nguyen, A. T.; Malonne, H.; Duez, P.; Vanhaelen-Fastre, R.; Vanhaelen, M.; Fontaine, J. Cytotoxic Constituents from Plumbago Zeylanica. *Fitoterapia* **2004**, *75* (5), 500–504. https://doi.org/10.1016/j.fitote.2004.03.009.

(168) Akihisa, T.; Taguchi, Y.; Yasukawa, K.; Tokuda, H.; Akazawa, H.; Suzuki, T.; Kimura, Y. Acerogenin M, a Cyclic Diarylheptanoid, and Other Phenolic Compounds from Acer Nikoense and Their Anti-Inflammatory and Anti-Tumor-

Promoting Effects. *Chem. Pharm. Bull. (Tokyo)* **2006**, *54* (5), 735–739. https://doi.org/10.1248/cpb.54.735.

(169) Marino, D.; Iorizzi, S.; Palagiano, M.; Zollo, E.; Roussakis, F. Starfish Saponins. 55. Isolation, Structure Elucidation, and Biological Activity of the Steroid Oligoglycosides from an Antarctic Starfish of the Family Asteriidae. *Nat. Prod.* **1998**, No. 11, 1319–1327.

(170) R M Ibrahim, S.; A Mohamed, G.; I M Khedr, A.; M Aljaeid, B. Anti-Oxidant and Anti-Inflammatory Cyclic Diarylheptanoids from Alnus Japonica Stem Bark. *Iran. J. Pharm. Res.* **2017**, *16* (Suppl), 83–91.

(171) Heijnen, C. G.; Haenen, G. R.; van Acker, F. A.; van der Vijgh, W. J.; Bast, A. Flavonoids as Peroxynitrite Scavengers: The Role of the Hydroxyl Groups. *In Vitro Toxicol.* **2001**, *15* (1), 3–6. https://doi.org/10.1016/s0887-2333(00)00053-9.

(172) Li, X.; Jiang, Q.; Wang, T.; Liu, J.; Chen, D. Comparison of the Antioxidant Effects of Quercitrin and Isoquercitrin: Understanding the Role of the 6 ″-OH Group. *Mol.* **2016**, *21* (9).

(173) Cai, Y.; Sun, M.; Corke, H. Antioxidant Activity of Betalains from Plants of the Amaranthaceae. *J. Agric. Food Chem.* **2003**, *51* (8), 2288–2294. https://doi.org/10.1021/jf030045u.

(174) She, J.; Mohottige, C. U.; King, M.; Jiang, Y.; Mlsna, M.; Clark, S.; Baird, R.; Mlsna, T. Estimation of Total Phenolic Compounds and Non-Targeted Volatile Metabolomics in Leaf Tissues of American Chestnut (Castanea Dentata), Chinese Chestnut (Castanea Mollissima) and the Backcross Breeding Generations. *J. Agric. Chem. Environ.* **2021** (2), 222–256.

(175) Nirubama, K.; Kanchana, G.; Rubalakshmi, G. Bioactive Compounds in Andrographis Echiodes (L.) Nees. Leaves by GC-MS Analysis. *Int. J. Curr. Res. Biosci. Plant Biol*. **2014** (3), 92–97.

(176) Derek; Nakanishi, K.; Meth-Cohn, O. Comprehensive Natural Products Chemistry: Miscellaneous Natural Products Including Marine Natural Products, Pheromones, Plant Hormones, and Aspects of Ecology; Elsevier Publishing Company, 1999.

(177) Smith, R.; Waddell, W.; Cohen, S. M.; Feron, V.; Marnett, L.; Portoghese, P.; Rietjens, I.; Adams, T.; Gavin, C. L.; Mcgowen, M. GRAS Flavoring Substances 24. *Food Technol.* **2009**, *63* (6), 46–105.

(178) Husain, F. M.; Al-Shabib, N. A.; Noor, S.; Khan, R. A.; Khan, M. S.; Ansari, F. A.; Khan, M. S.; Khan, A.; Ahmad, I. Current Strategy to Target Bacterial Quorum Sensing and Virulence by Phytocompounds. In *New Look to Phytomedicine*; Elsevier, 2019; pp 301–329.

(179) Pelletier, J.; Xu, P.; Yoon, K. S.; Clark, J. M.; Leal, W. S. Odorant Receptor-Based Discovery of Natural Repellents of Human Lice. *Insect Biochem. Mol. Biol*. **2015**, *66*, 103–109. https://doi.org/10.1016/j.ibmb.2015.10.009.

(180) Mokhtari, M.; Jackson, M. D.; Brown, A. S.; Ackerley, D. F.; Ritson, N. J.; Keyzers, R. A.; Munkacsi, A. B. Bioactivity-Guided Metabolite Profiling of Feijoa (*Acca Sellowiana*) Cultivars Identifies 4-Cyclopentene-1,3-Dione as a Potent Antifungal Inhibitor of Chitin Synthesis. *J. Agric. Food Chem.* **2018**, *66* (22), 5531–5539. https://doi.org/10.1021/acs.jafc.7b06154

(181) Baccelli, M.; Kobayashi, K.; Sereboff, S. C.; Hiratsuka, M. *Advanced Software and Patents: A Patentability Balance for Fostering Technology, Human-Centric Computing in a Data-Driven Society: 14th IFIP TC 9 International Conference on Human Choice and Computers*; Springer: Tokyo, Japan, 2020.

(182) Dasgupta, A.; Wahed, A. Common Poisonings Including Heavy Metal Poisoning. In *Clinical Chemistry, Immunology and Laboratory Quality Control*; Elsevier, 2021; pp 405–419.

(183) Crotti, A. E. M.; Fonseca, T.; Hong, H.; Staunton, J.; Galembeck, S. E.; Lopes, N. P.; Gates, P. J. The Fragmentation Mechanism of Five-Membered Lactones by Electrospray Ionisation Tandem Mass Spectrometry. *Int. J. Mass Spectrom.* **2004**, *232* (3), 271–276. https://doi.org/10.1016/j.ijms.2004.02.009.

(184) Kitajima, J.; Ishikawa, T.; Tanaka, T.; Ida, Y. Water-Soluble Constituents of Fennel. IX. Glucides and Nucleosides. *Chem. Pharm. Bull. (Tokyo)* **1999**, *47* (7), 988–992. https://doi.org/10.1248/cpb.47.988.

(185) Li, Y.; Wang, S.-F.; Zhao, Y.-L.; Liu, K.-C.; Wang, X.-M.; Yang, Y.-P.; Li, X.-L. Chemical Constituents from Clematis Delavayi Var. Spinescens. *Mol.* **2009**, *14* (11), 4433–4439. https://doi.org/10.3390/molecules14114433.

(186) *5-Hydroxy-4-oxopentanoic acid - SpectraBase*. Spectrabase.com. https://spectrabase.com/compound/8kH3c7mgZjh (accessed 2024-06-11).

(187) Cottier, L.; G. Descotes; Eymard, L.; Rapp, K. Syntheses of γ-Oxo Acids or γ-Oxo Esters by Photooxygenation of Furanic Compounds and Reduction under Ultrasound: Application to the Synthesis of 5-Aminolevulinic Acid Hydrochloride. *Synthesis* **1995**, *1995* (03), 303–306. https://doi.org/10.1055/s-1995-3897.

(188) Sadikun, A.; Aminah, I.; Ismail, N.; Ibrahim, P. Sterols and Sterol Glycosides from the Leaves of Gynura Procumbens. *Nat. Prod. Sci.* **1996**, *2* (1), 19–23.

(189) Peshin, T.; Kar, H. Isolation and Characterization of β-Sitosterol-3-O-β-D-Glucoside from the Extract of the Flowers of Viola Odorata. *Br. J. Pharm. Res.* **2017**, *16* (4), 1–8. https://doi.org/10.9734/bjpr/2017/33160.

(190) Arulmozhi, S.; Mazumder, P. M.; Ashok, P.; Narayanan, L. S. In Vitro Antioxidant and Free Radical Scavenging Activity of Alstonia Scholaris Linn. *Iran J. Pharm. Res*. **2007**, *6* (2), 191–196.

(191) Kakai, R.; Wamola, I. A. Minimising Antibiotic Resistance to Staphylococcus Aureus in Developing Countries. *East Afr. Med. J.* **2002**, *79* (11), 574–579. https://doi.org/10.4314/eamj.v79i11.8801.

(192) Yagi, T.; Agarwal, M. Gas Chromatography-Mass Spectrometry Analysis of Bioactive Constituents in the Ethanolic Extract of Pistia Stratiotes L. *J. Appl. Med. Sci*. **2017**, *7* (1), 14–21.

(193) Silvestre, A. J.; Válega, M.; Cavaleiro, J. A. Chemical Transformation of 1, 8-Cineole: Synthesis of Seudenone, an Insect Pheromone. *Ind. Crops Prod*. **2000**, *12* (1), 53–56.

(194) Shaw, K.; Niyogi, S.; Bisai, V. Catalytic Enantioselective Total Synthesis of (−)-Ar-Tenuifolene. *Tetrahedron Lett.* **2020**, *61* (20), 151850. https://doi.org/10.1016/j.tetlet.2020.151850.

(195) Andersen, A. Final Report on the Safety Assessment of Benzaldehyde. *Int. J. Toxicol.* **2006**, *25 Suppl 1* (1_suppl), 11–27. https://doi.org/10.1080/10915810600716612.

(196) Satrio, J. A. B.; Doraiswamy, L. K. Production of Benzaldehyde: A Case Study in a Possible Industrial Application of Phase-Transfer Catalysis. *Chem. Eng. J.* **2001**, *82* (1–3), 43–56. https://doi.org/10.1016/s1385-8947(00)00351-x.

(197) Shah, N. N.; Soni, N.; Singhal, R. S. Modification of Proteins and Polysaccharides Using Dodecenyl Succinic Anhydride: Synthesis, Properties and Applications—A Review. *Int. J. Biol. Macromol.* **2018**, *107*, 2224–2233. https://doi.org/10.1016/j.ijbiomac.2017.10.099.

(198) Yehye, W. A.; Rahman, N. A.; Ariffin, A.; Abd Hamid, S. B.; Alhadi, A. A.; Kadir, F. A.; Yaeghoobi, M. Understanding the Chemistry behind the Antioxidant Activities of Butylated Hydroxytoluene (BHT): A Review. *Eur. J. Med. Chem.* **2015**, *101*, 295–312. https://doi.org/10.1016/j.ejmech.2015.06.026.

(199) Whelan, L. *Oleic Acid and its potential health effects*; Nova Science Pub Incorporated, 2014.

(200) Ghani, M. S. A.; Zakaria, N.; Mohd Arshad, N.; Kamarulzaman, E. E.; Awang, K.; Litaudon, M.; Taib, M. N. A. M. Pentacyclic Triterpenoids Isolated from Diospyros Foxworthyi Bakh.(Ebenaceae) with Its Cytotoxic Activity against Ht-29 Human Colon Cancer Cell. *Malays. J. Chem.* **2022** (4), 19–25.

(201) Chang, S.-J.; Lin, T.-H.; Chen, C.-C. Constituents from the Stems of Dendrobium Clavatum Var. Aurantiacum. *J. Chin. Med.* **2001**, *12* (3), 211–218.

(202) Yu, Y.; Jiang, Z.; Song, W.; Yang, Y.; Li, Y.; Jiang, J.; Shi, J. Glucosylated Caffeoylquinic Acid Derivatives from the Flower Buds of Lonicera Japonica. *Acta. Pharm. Sin. B.* **2015**, *5* (3), 210–214. https://doi.org/10.1016/j.apsb.2015.01.012.

(203) National Committee for Clinical Laboratory Standards. Performance standards for antimicrobial susceptibility testing. Twelfth informational supplement, M100-S12. Wayne, PA; 2002.

(204) Isika, D. K.; Özkömeç, F. N.; Çeşme, M.; Sadik, O. A. Synthesis, Biological and Computational Studies of Flavonoid Acetamide Derivatives. *RSC. Adv.* **2022**, *12* (16), 10037–10050. https://doi.org/10.1039/d2ra01375d.

(205) Ohemeng, K.; Schwender, C.; Fu, K.; Barrett, J. DNA Gyrase Inhibitory and Antibacterial Activity of Some Flavones (1). *Bioorg. Med. Chem. Lett*. **1993**, *3* (2), 225–230.

(206) Okolo, E. N.; Ugwu, D. I.; Ezema, B. E.; Ndefo, J. C.; Eze, F. U.; Ezema, C. G.; Ezugwu, J. A.; Ujam, O. T. New Chalcone Derivatives as Potential Antimicrobial and Antioxidant Agent. *Sci. Rep.* **2021**, *11* (1), 21781. https://doi.org/10.1038/s41598-021-01292-5.

(207) Konaté, K.; Mavoungou, J. F.; Lepengué, A. N.; Aworet-Samseny, R. R.; Hilou, A.; Souza, A.; Dicko, M. H.; Batchi, B. Antibacterial Activity against β-Lactamase Producing Methicillin and Ampicillin-Resistants Staphylococcus Aureus: Fractional Inhibitory Concentration Index (FICI) Determination. *Ann. Clin. Microbiol. Antimicrob*. **2012**, *11*, 1–12.

(208) Elyemni, M.; Louaste, B.; Nechad, I.; Elkamli, T.; Bouia, A.; Taleb, M.; Chaouch, M.; Eloutassi, N. Extraction of Essential Oils of Rosmarinus Officinalis L. by Two Different Methods: Hydrodistillation and Microwave Assisted Hydrodistillation. *Sci. World J.* **2019**, *2019*, 3659432. https://doi.org/10.1155/2019/3659432.

7 Appendices

Appendix 1: ^{1}H-NMR (400 MHz, $CDCl_3$) Spectrum of Compound **77**

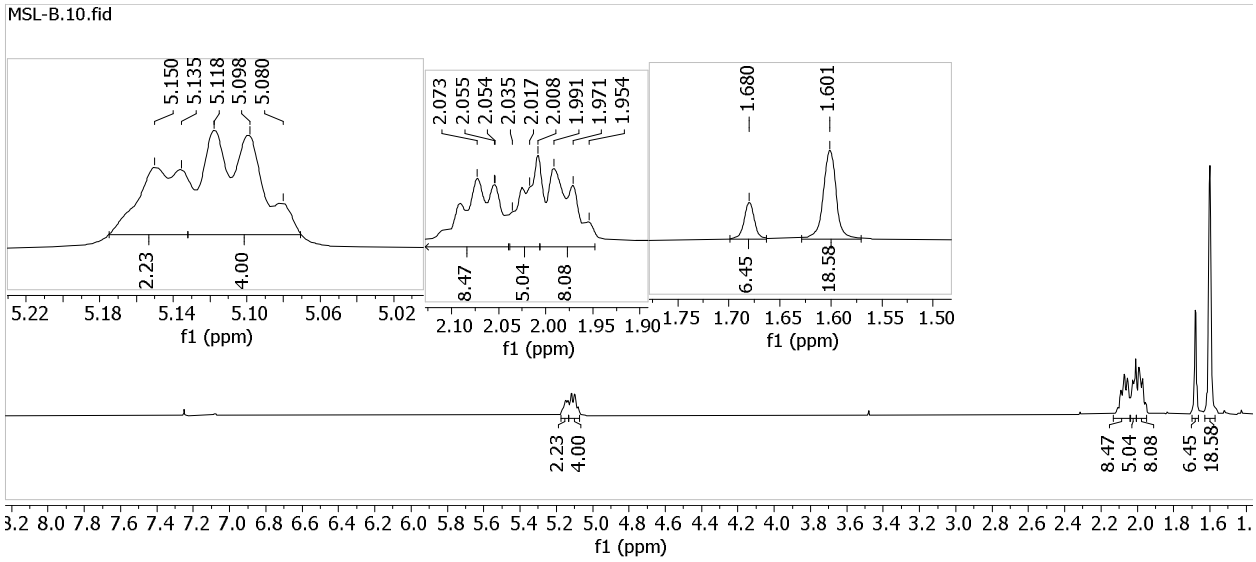

Appendix 2: ^{13}C-NMR (101 MHz, $CDCl_3$) Spectrum of Compound **77**

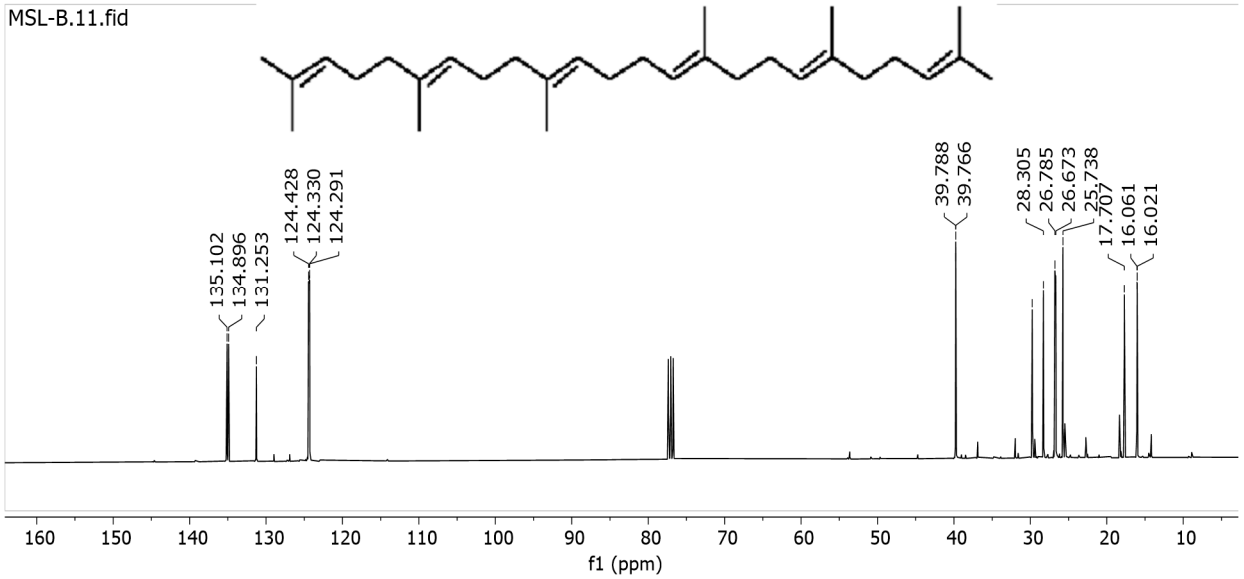

Appendix 3: DEPT-135 Spectrum of Compound 77

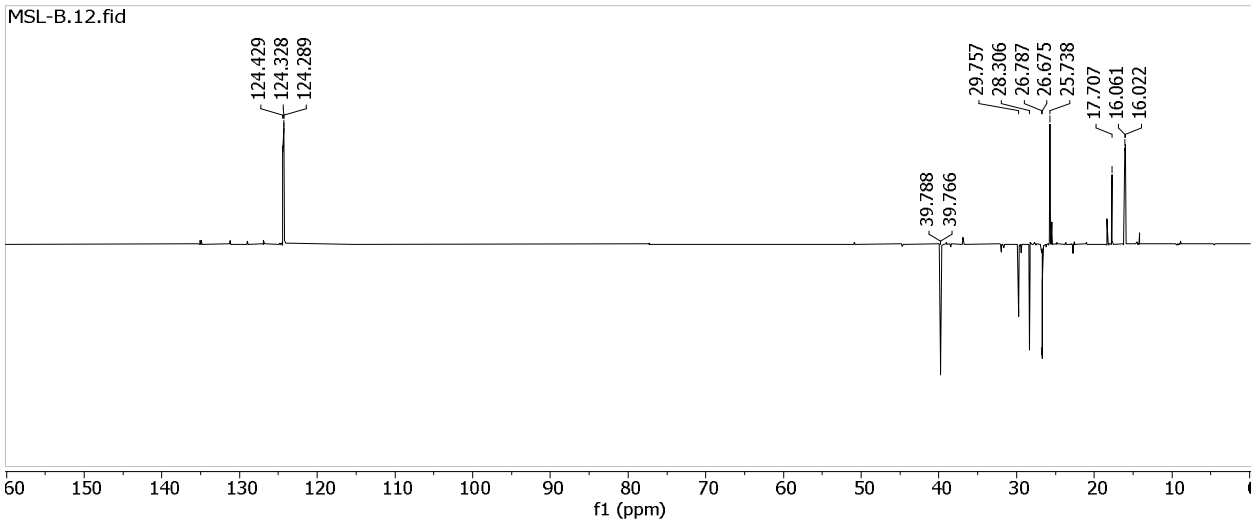

Appendix 4: ^{1}H-^{1}H COSY Spectrum of Compound **77**

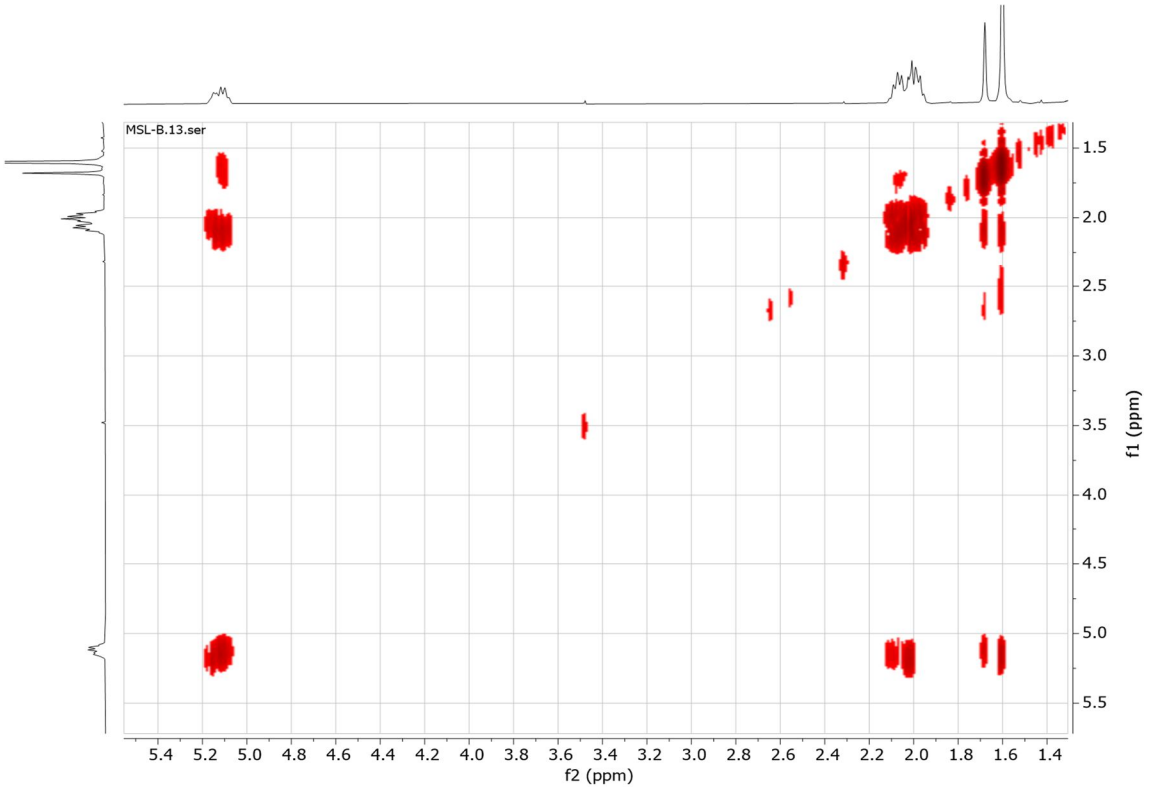

Appendix 5: HSQC Spectrum of Compound **77**

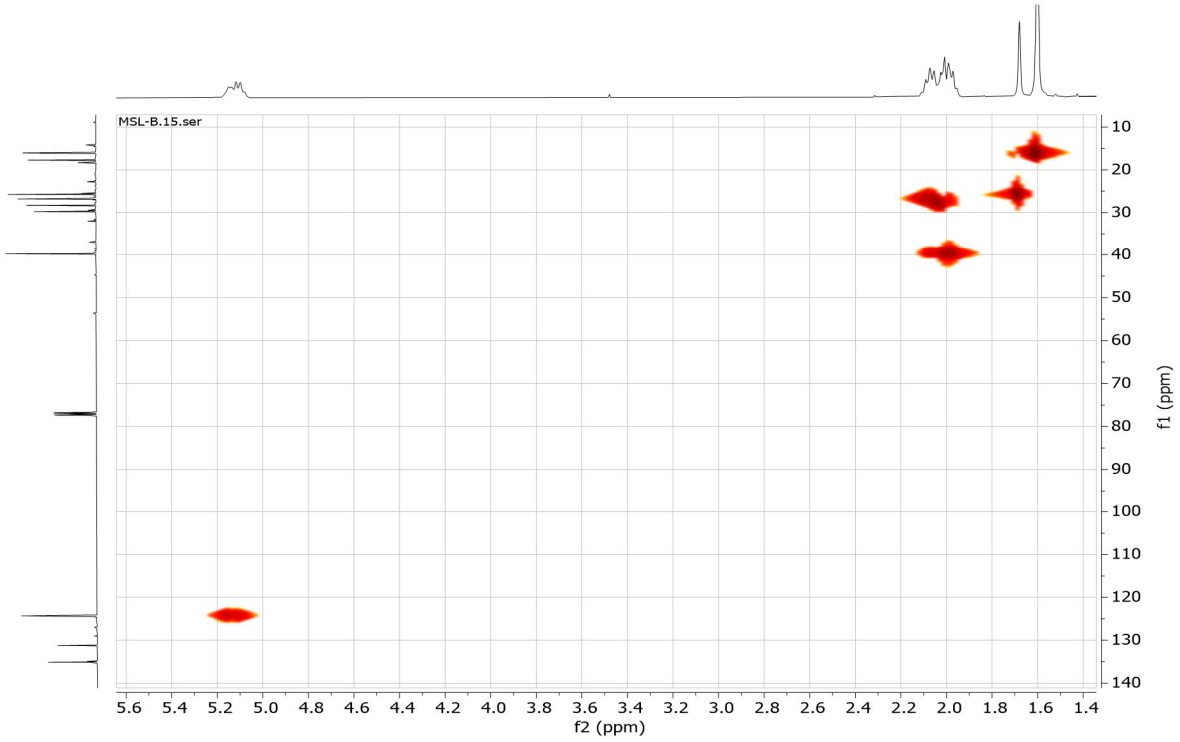

Appendix 6: HMBC Spectrum of Compound **77**

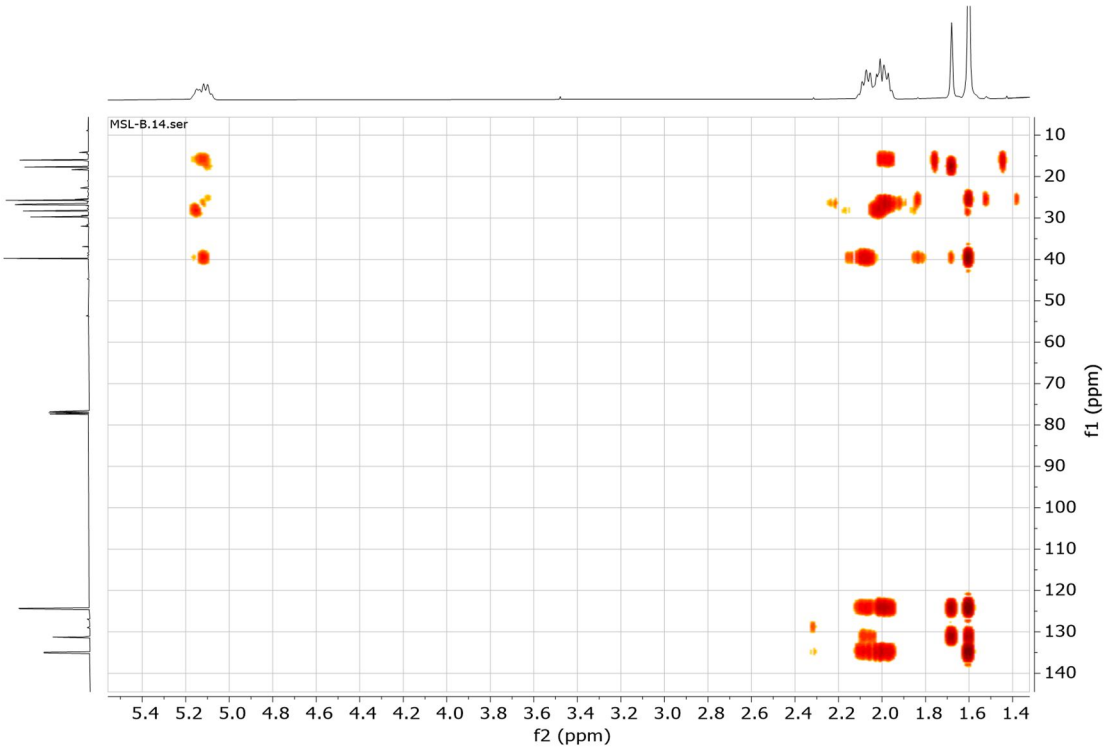

Appendix 7: TOF-MS Spectrum of Compound **77**

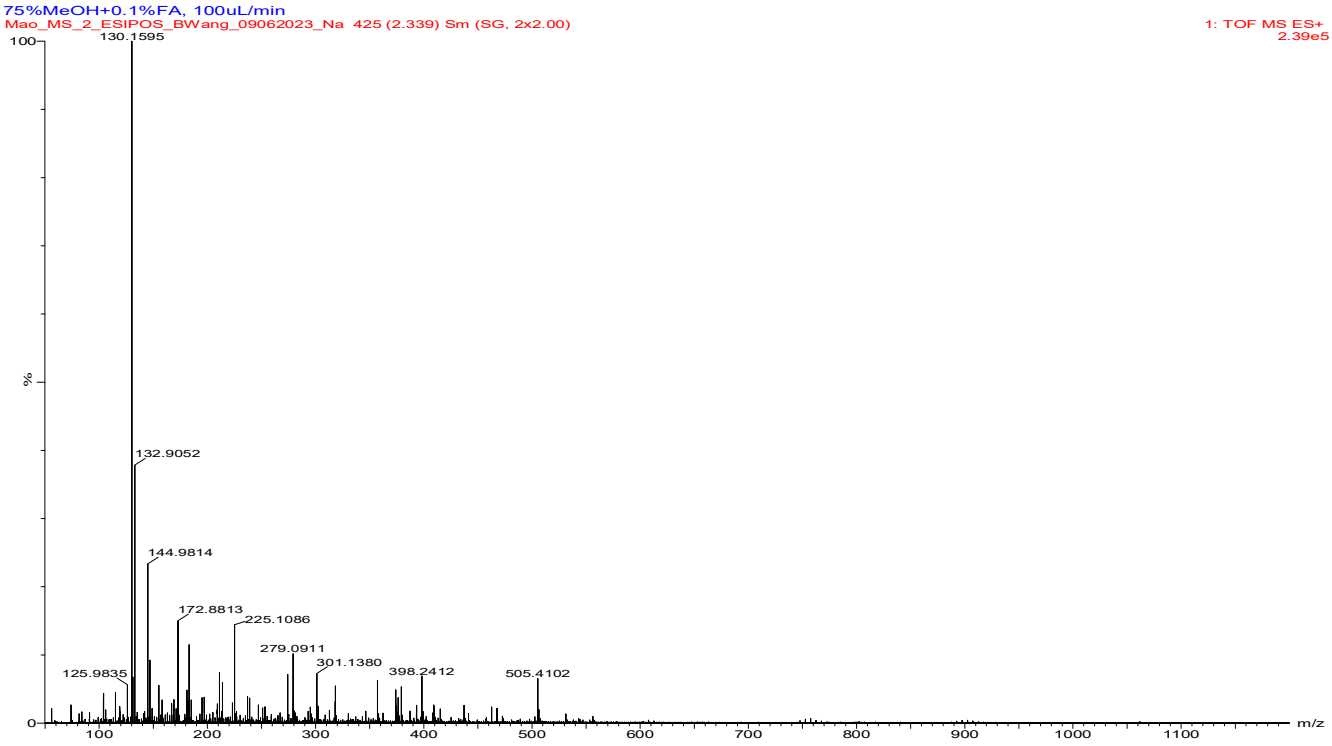

Appendix 8: ^{1}H-NMR (400 MHz, $CDCl_3$) Spectrum of Compound **78**

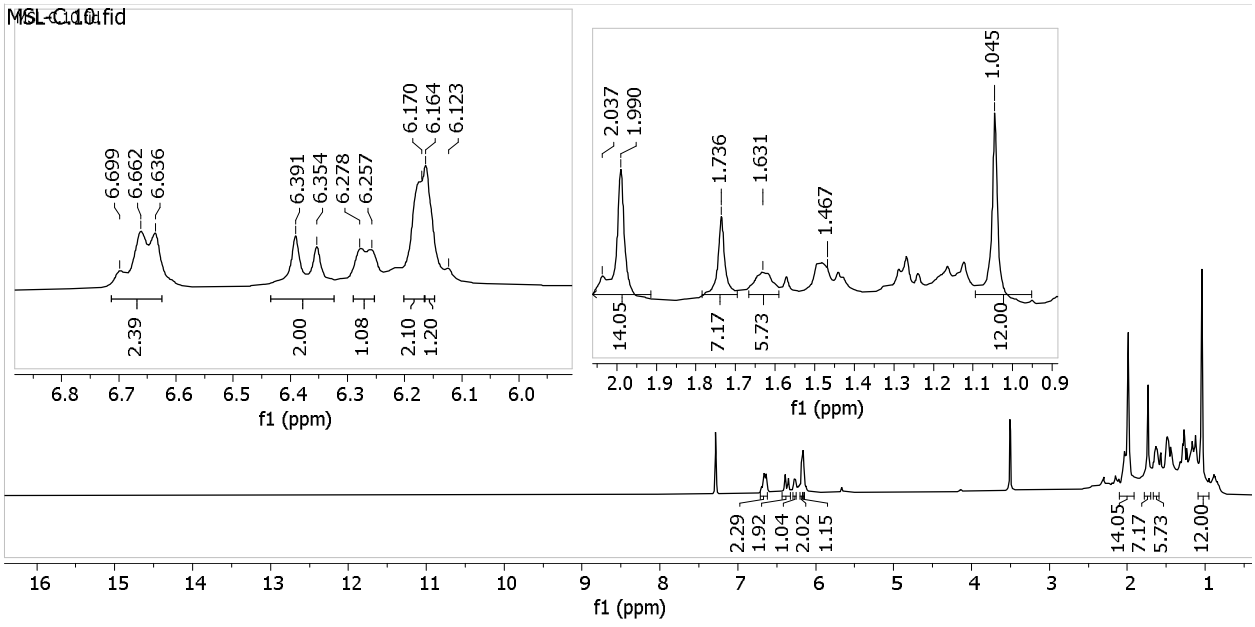

Appendix 9: ^{13}C-NMR (101 MHz, $CDCl_3$) Spectrum of Compound **78**

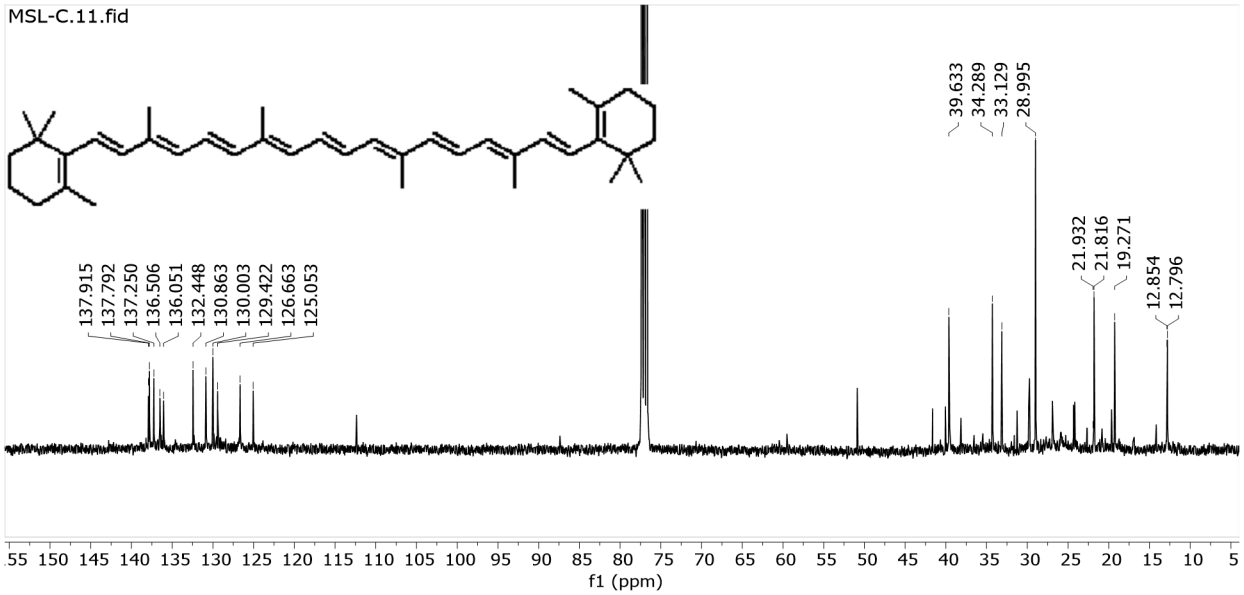

Appendix 10: DEPT-135 Spectrum of Compound **78**

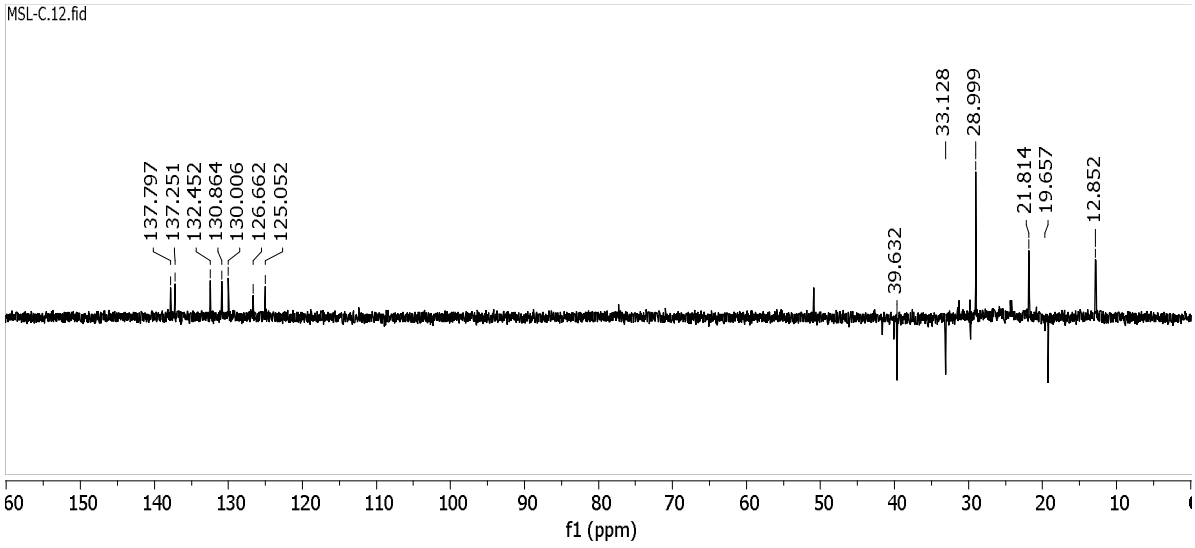

Appendix 11: ^{1}H-^{1}H COSY Spectrum of Compound **78**

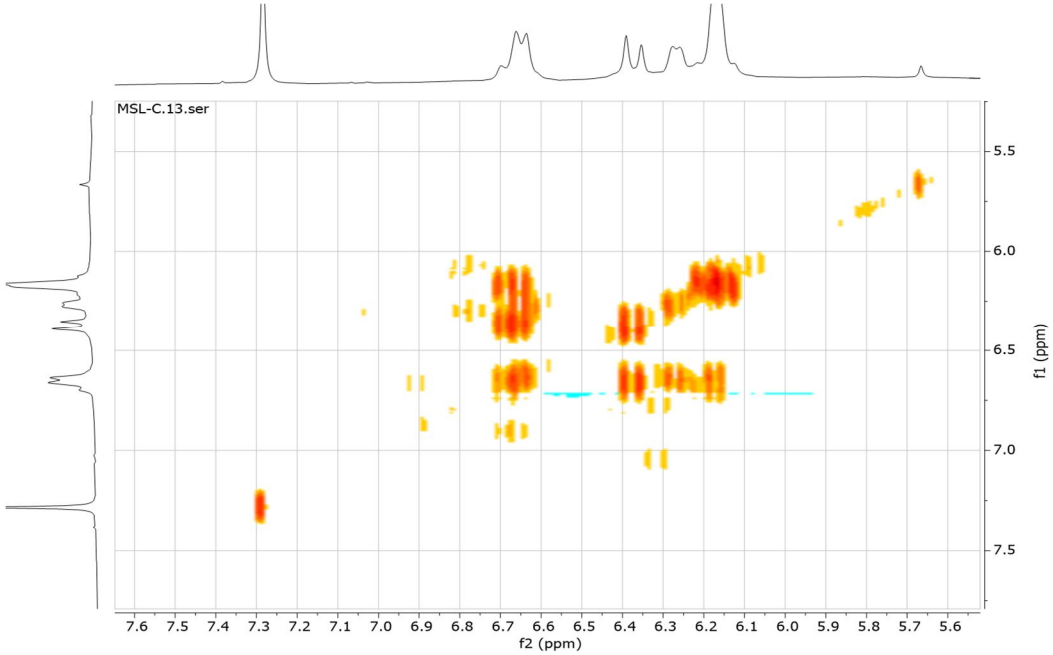

Appendix 12: HSQC Spectrum of Compound **78**

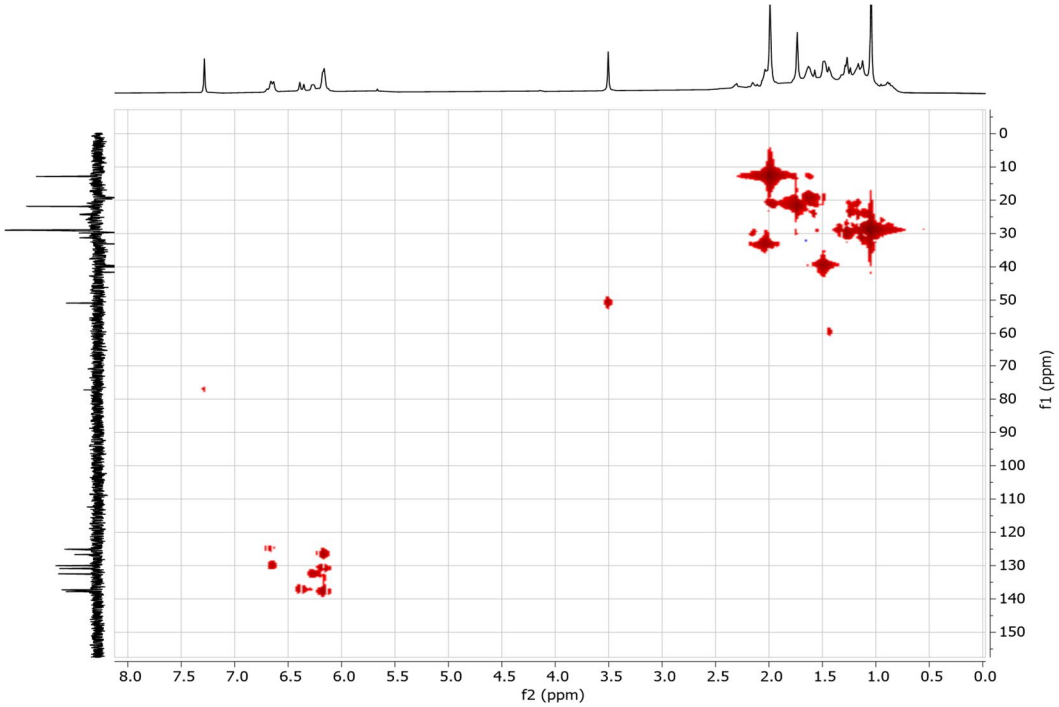

Appendix 13: HMBC Spectrum of Compound **78**

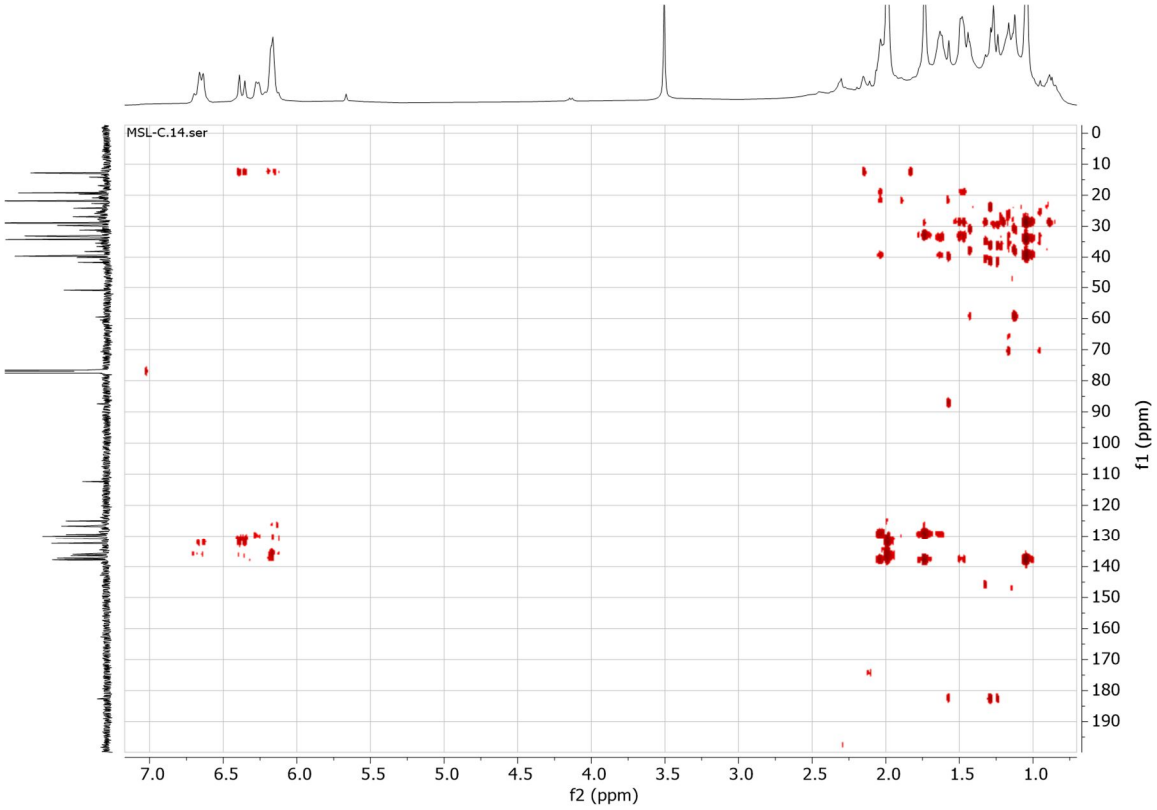

Appendix 14: NOES Spectrum of Compound **78**

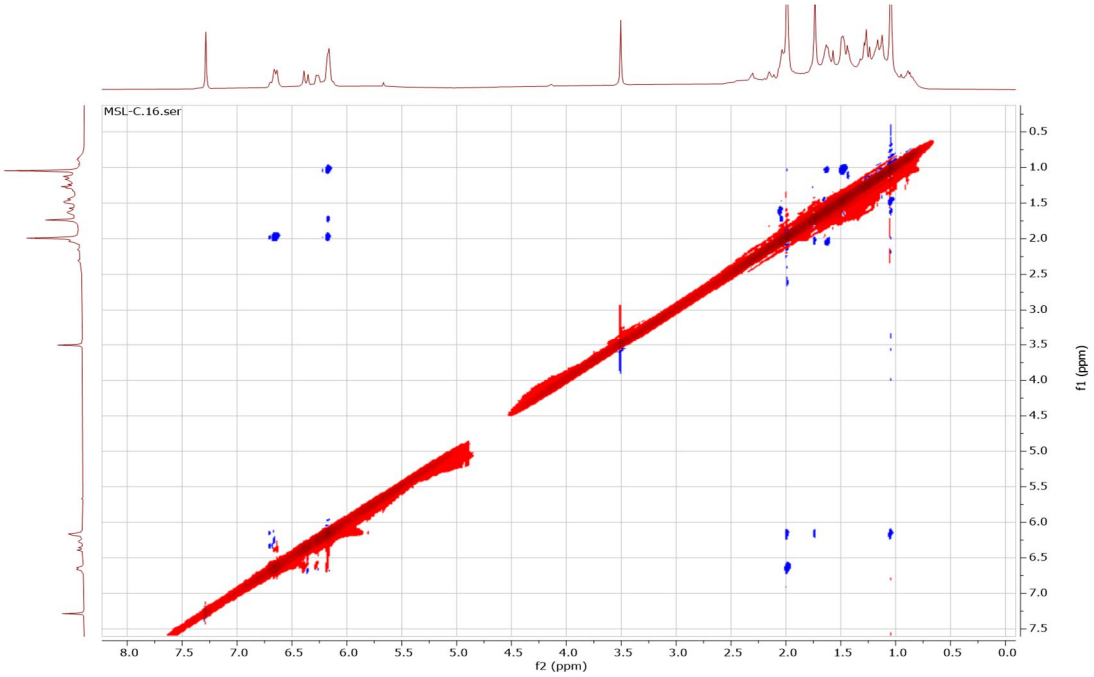

Appendix 15: TOF-MS Spectrum of Compound **78**

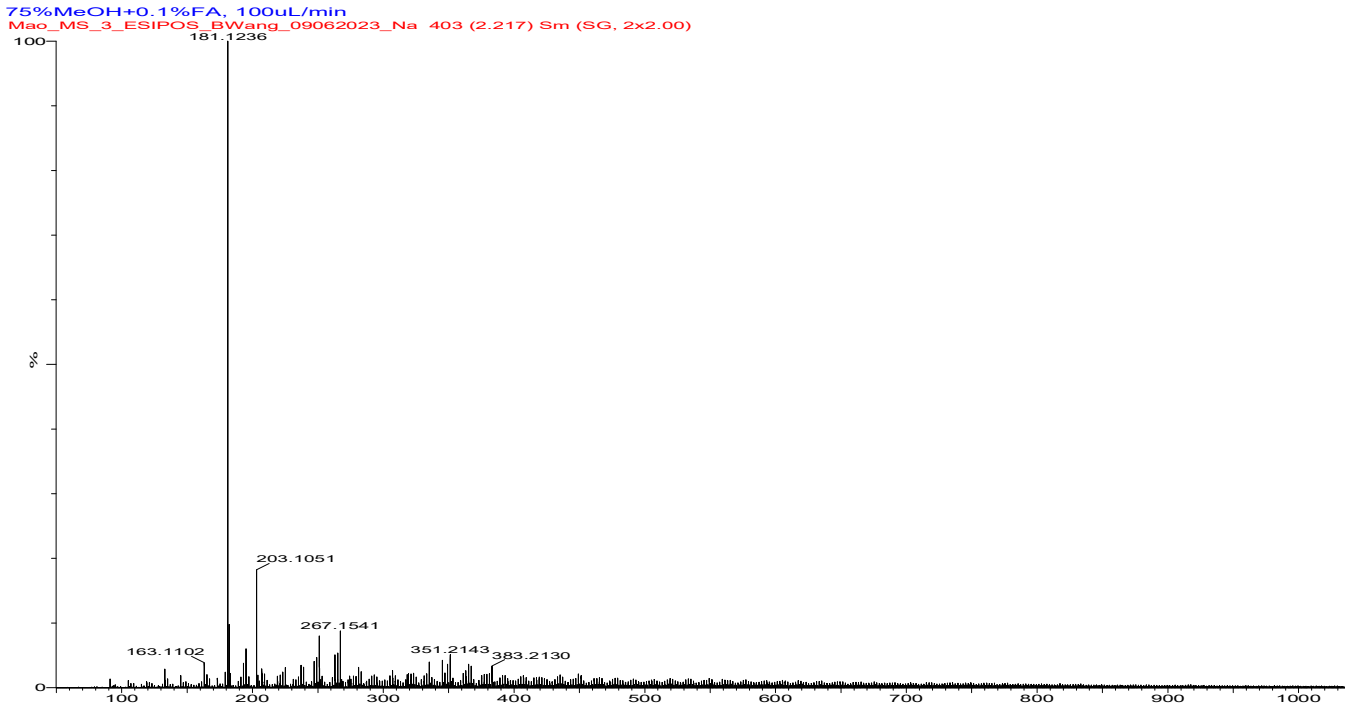

Appendix 16: ^{1}H-NMR (400 MHz, $CDCl_3$) Spectrum of Compound **79**

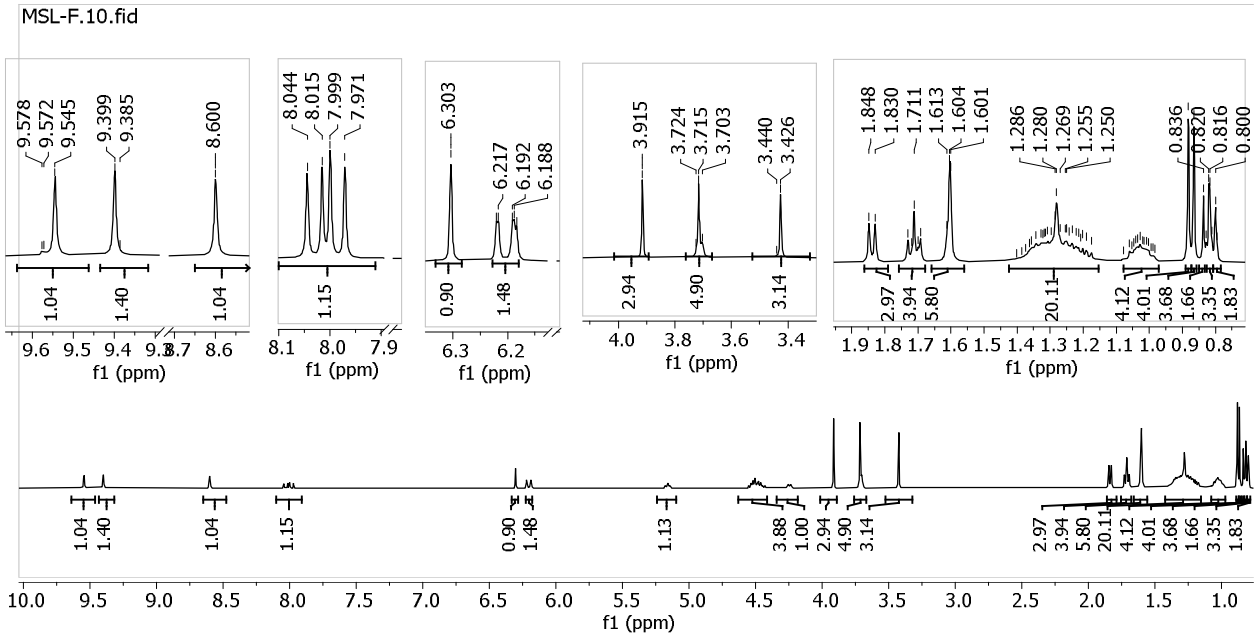

Appendix 17: ^{13}C-NMR (101 MHz, $CDCl_3$) Spectrum of Compound **79**

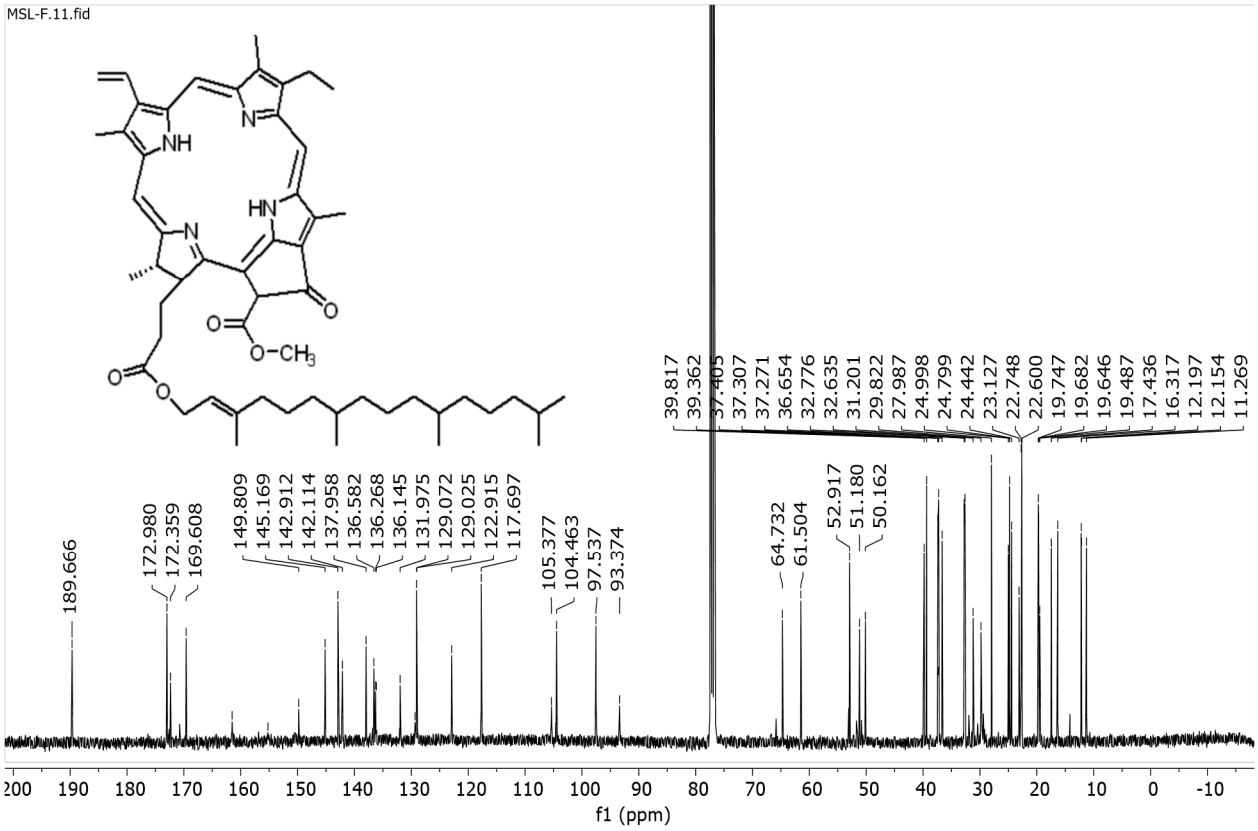

Appendix 18: DEPT-135 Spectrum of Compound **79**

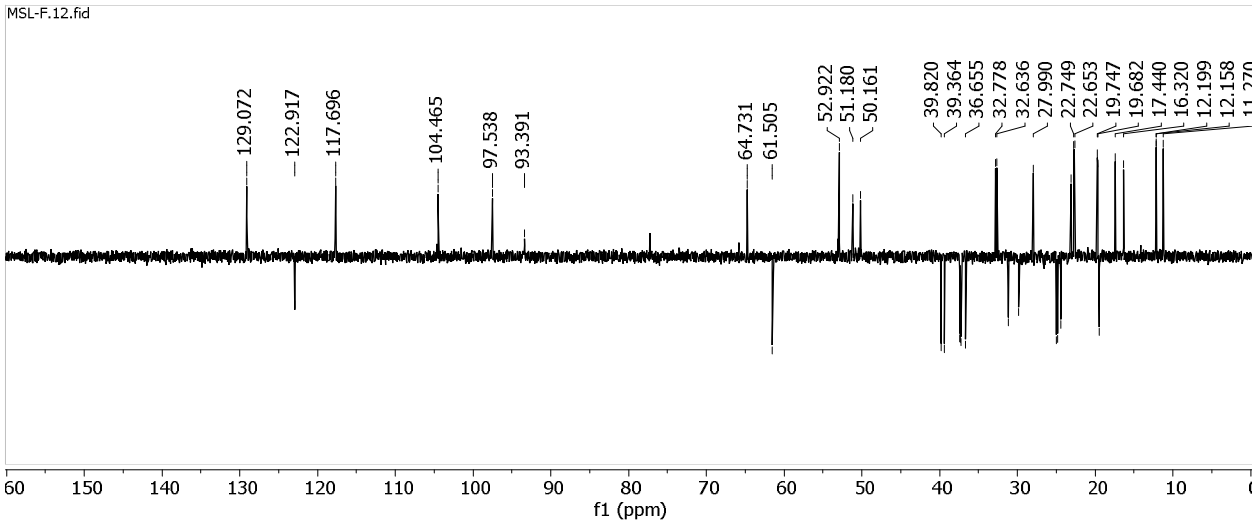

Appendix 19: HSQC Spectrum of Compound **79**

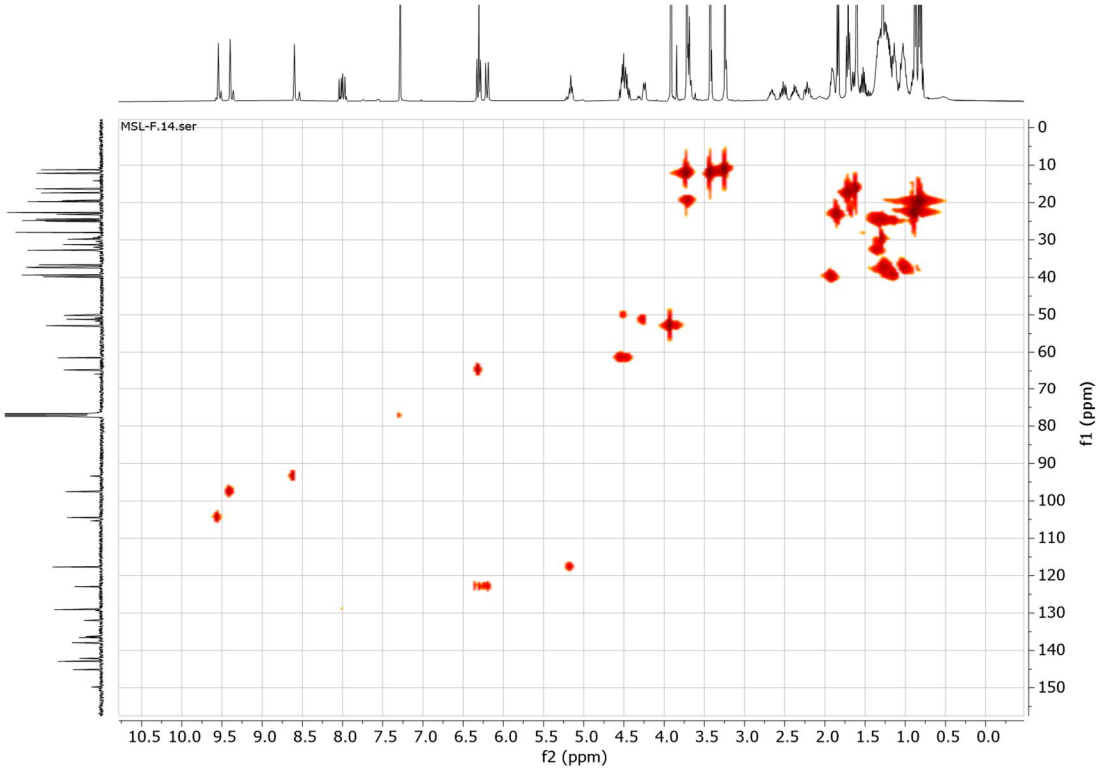

Appendix 20: HMBC Spectrum of Compound **79**

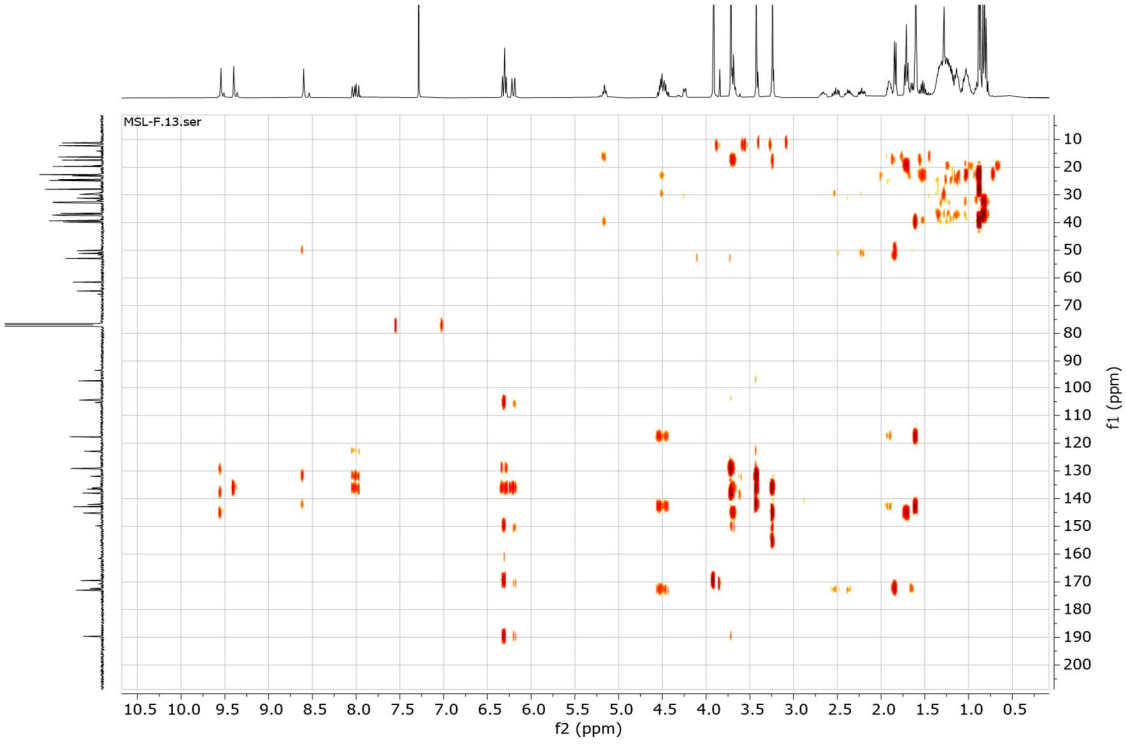

Appendix 21: NOES Spectrum of Compound **79**

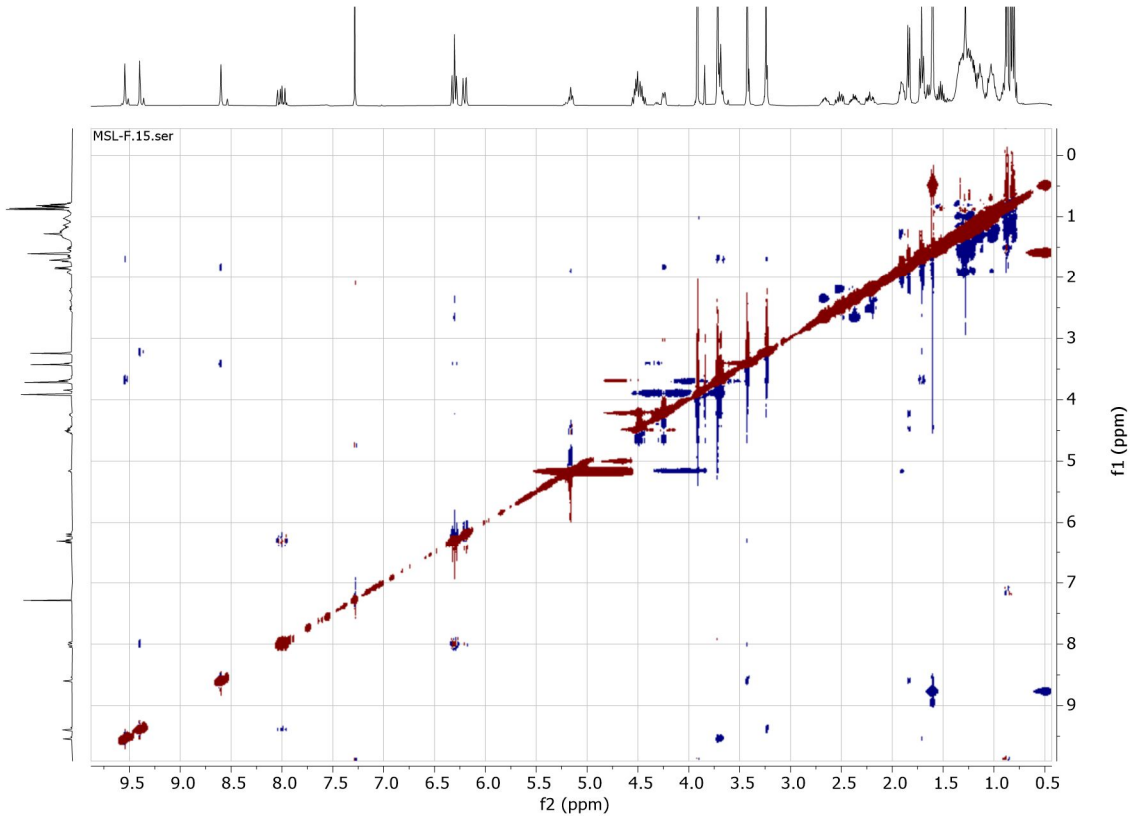

Appendix 22: TOF-MS Spectrum of Compound **79**

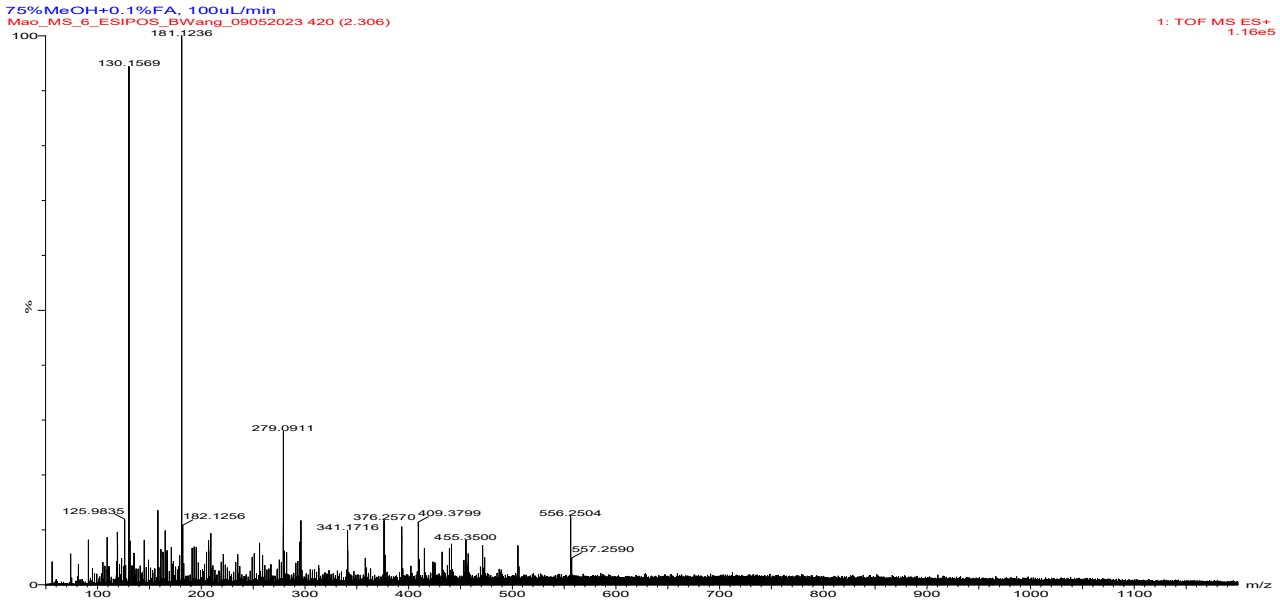

Appendix 23: ^{1}H-NMR (400 MHz, $CDCl_3$) Spectrum of Compound **80**

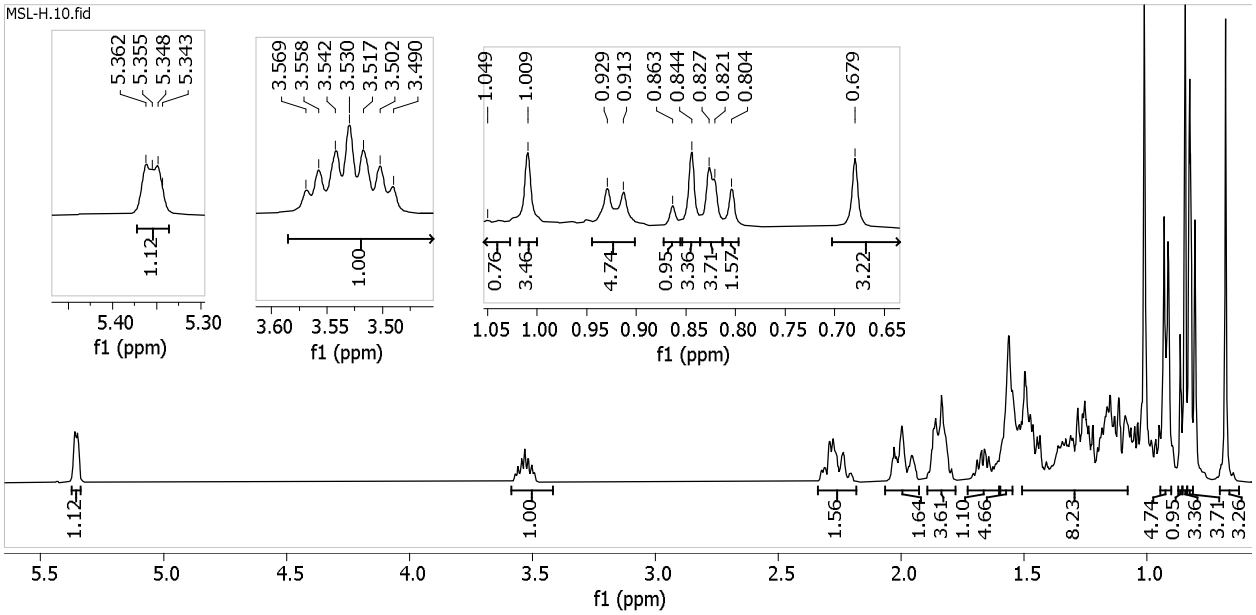

Appendix 24: ^{13}C-NMR (101 MHz, $CDCl_3$) Spectrum of Compound **80**

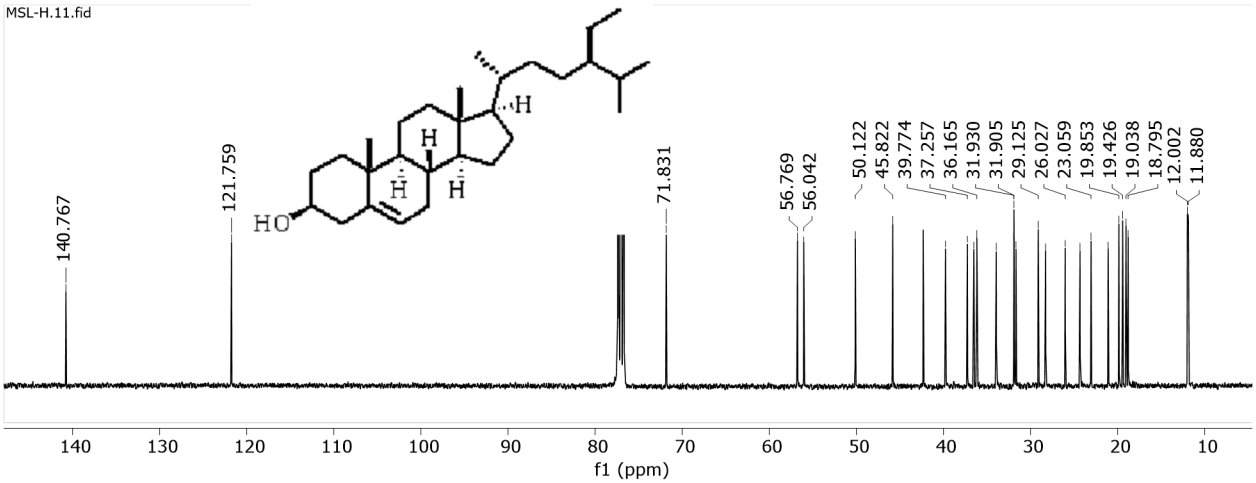

Appendix 25: DEPT-135 Spectrum of Compound **80**

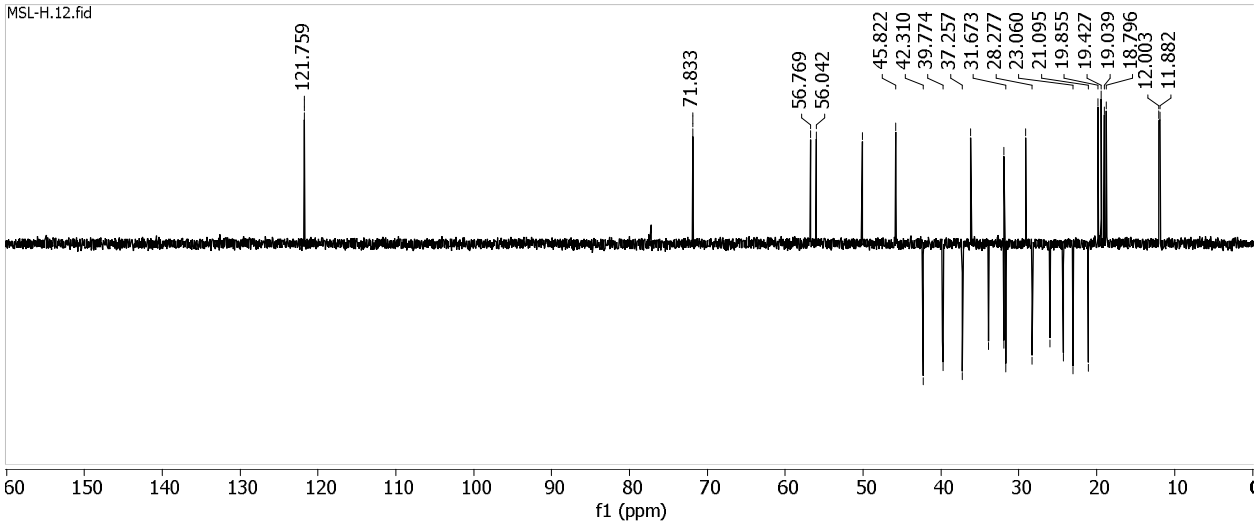

Appendix 26: ^{1}H-^{1}H COSY Spectrum of Compound **80**

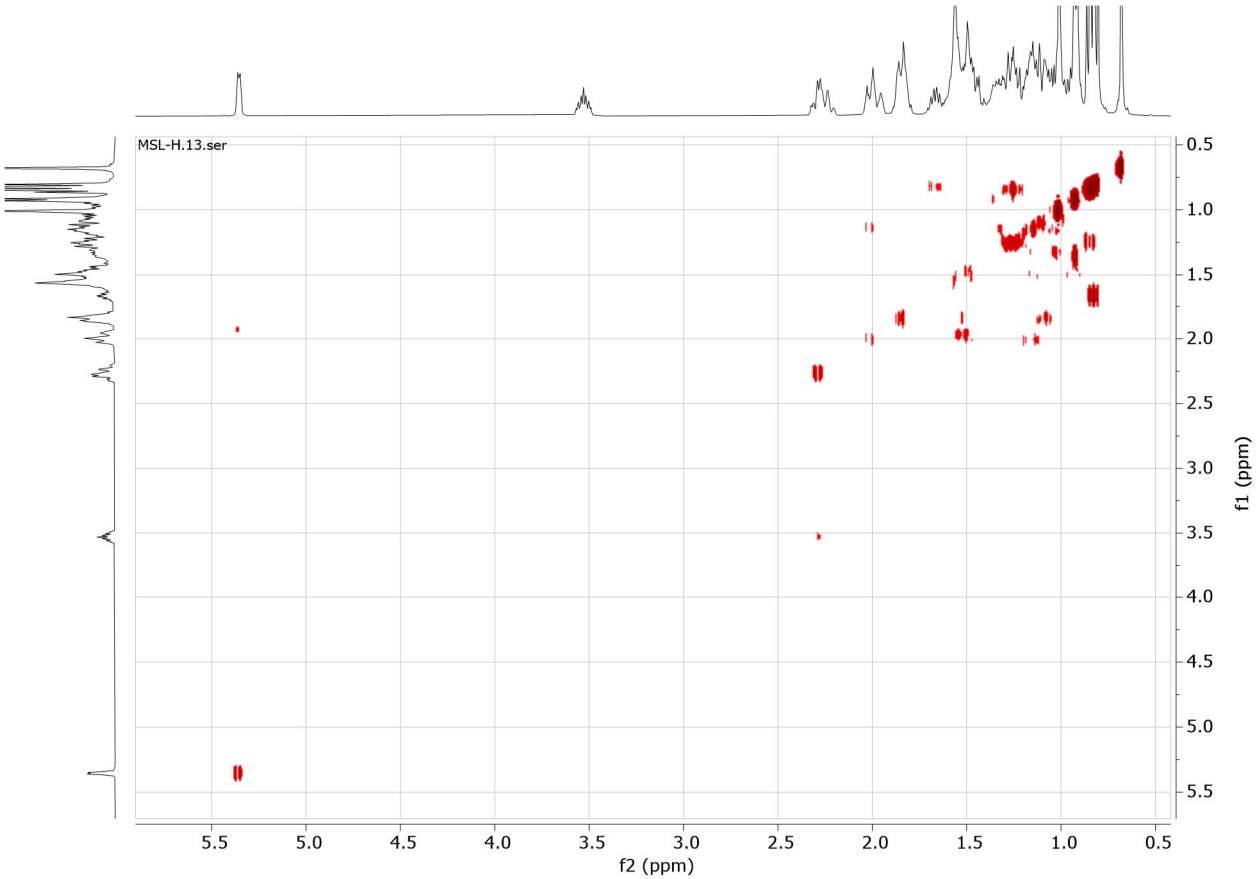

Appendix 27: HSQC Spectrum of Compound **80**

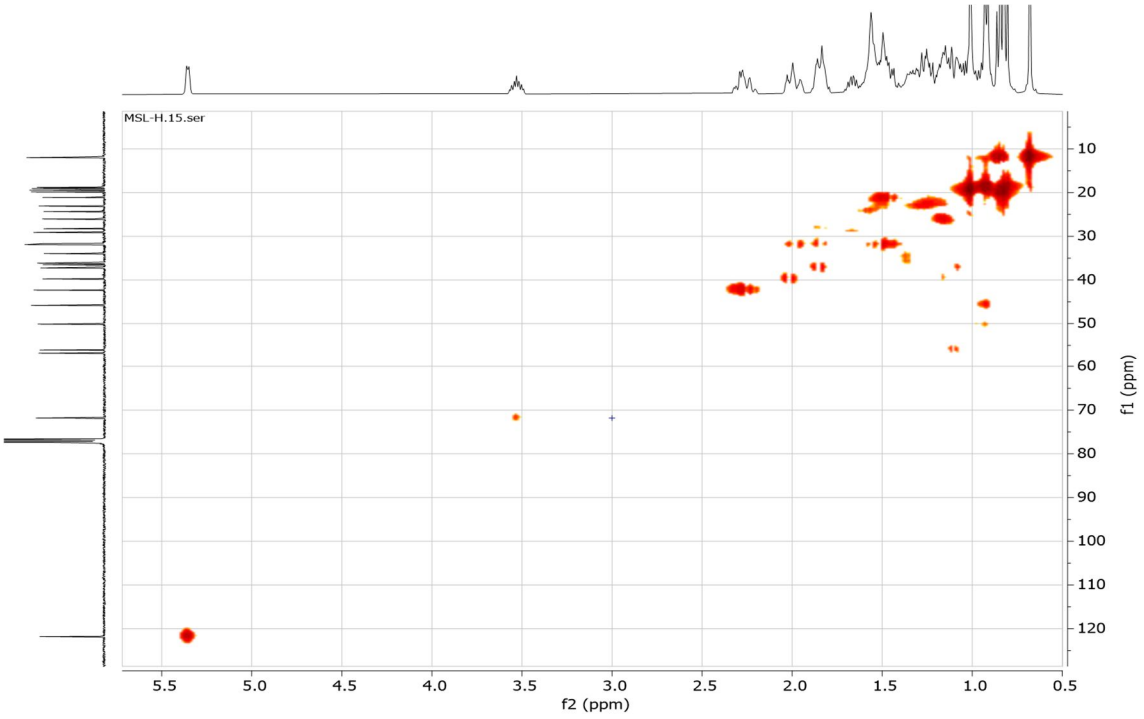

Appendix 28: HMBC Spectrum of Compound **80**

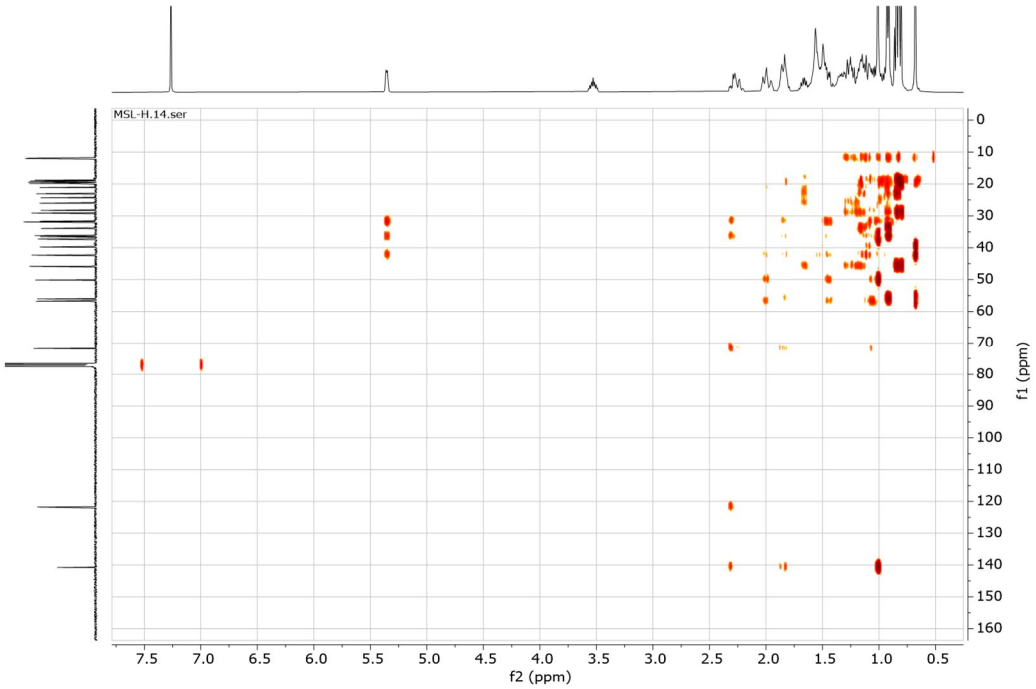

Appendix 29: NOES Spectrum of Compound **80**

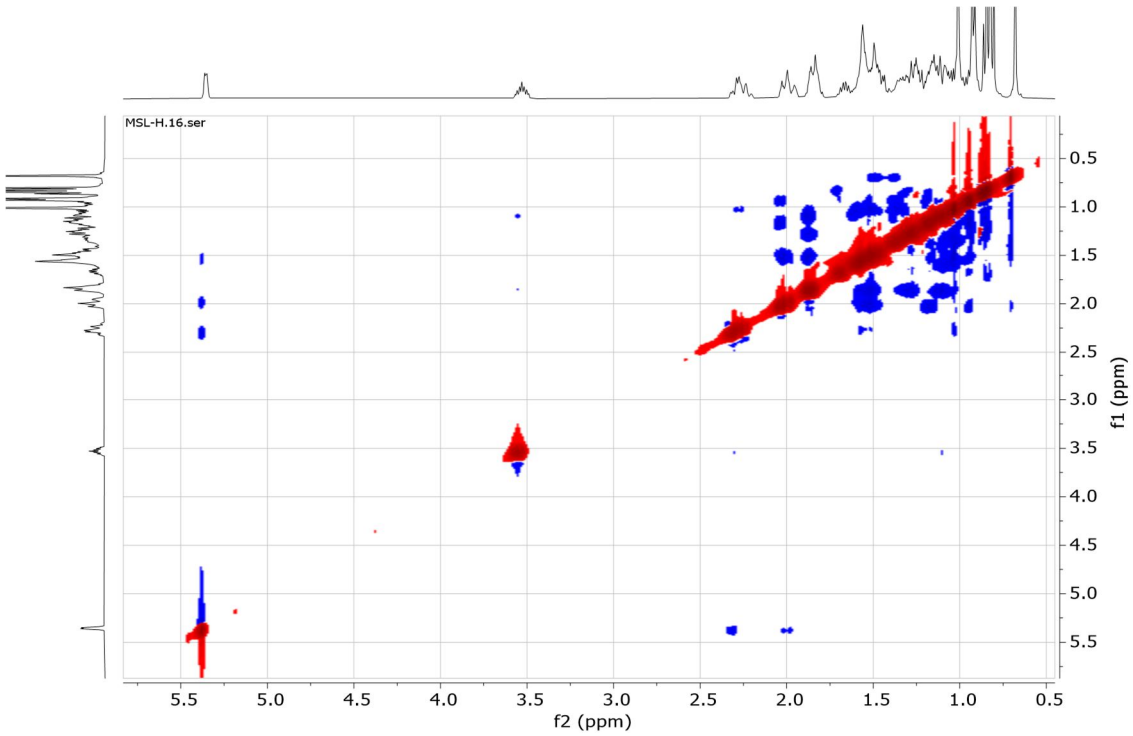

Appendix 30: TOF-MS Spectrum of Compound **80**

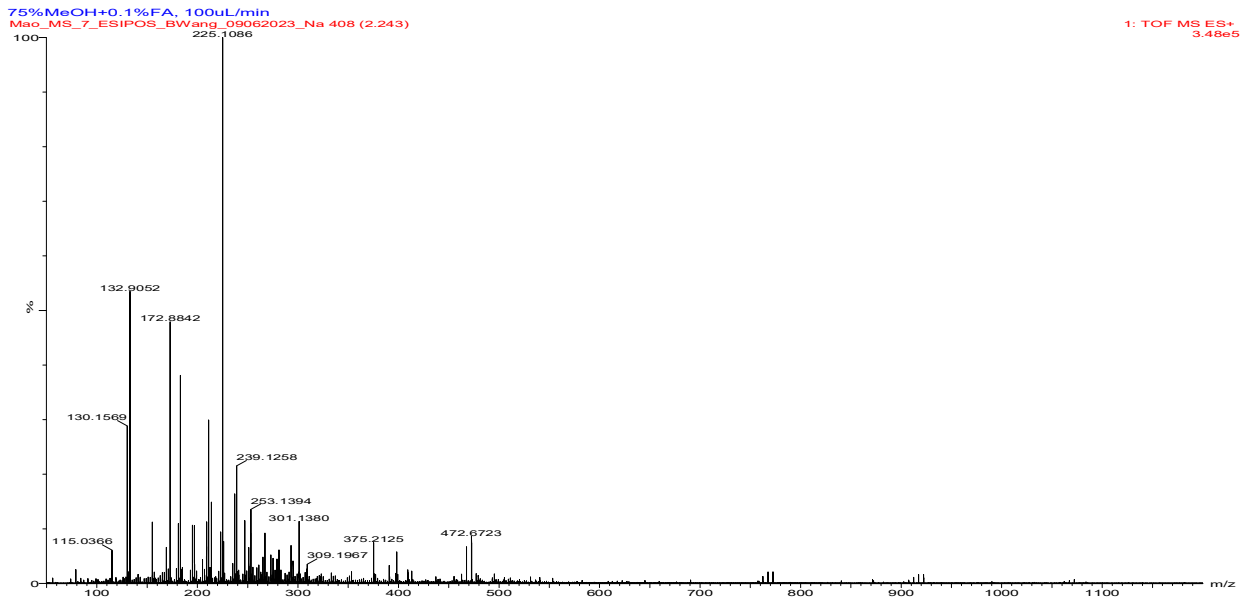

Appendix 31: ^{1}H-NMR (600 MHz, DMSO) Spectrum of Compound **28**

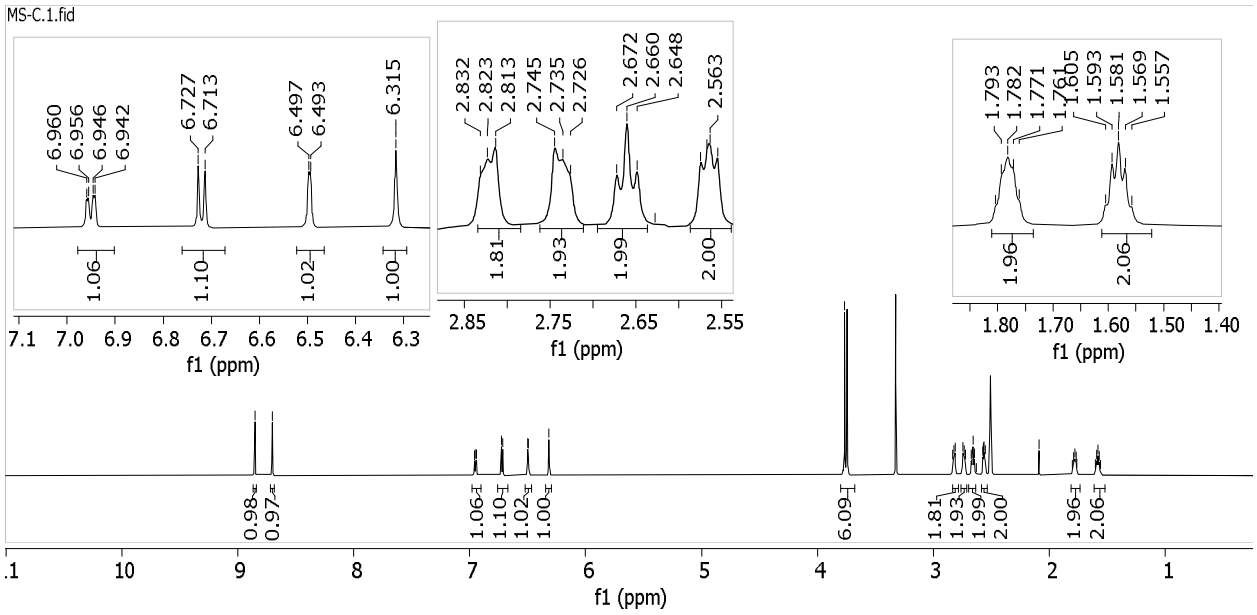

Appendix 32: ^{13}C-NMR (151 MHz, DMSO) Spectrum of Compound **28**

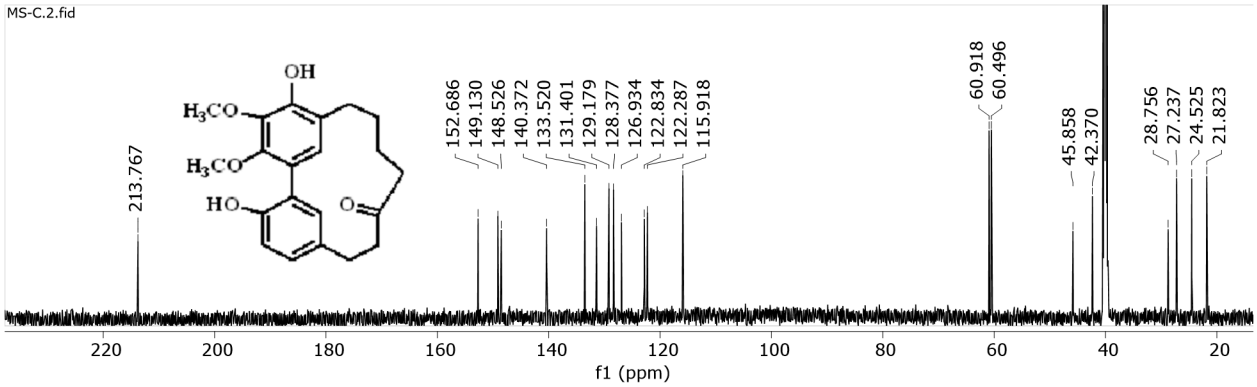

Appendix 33: DEPT-135 Spectrum of Compound **28**

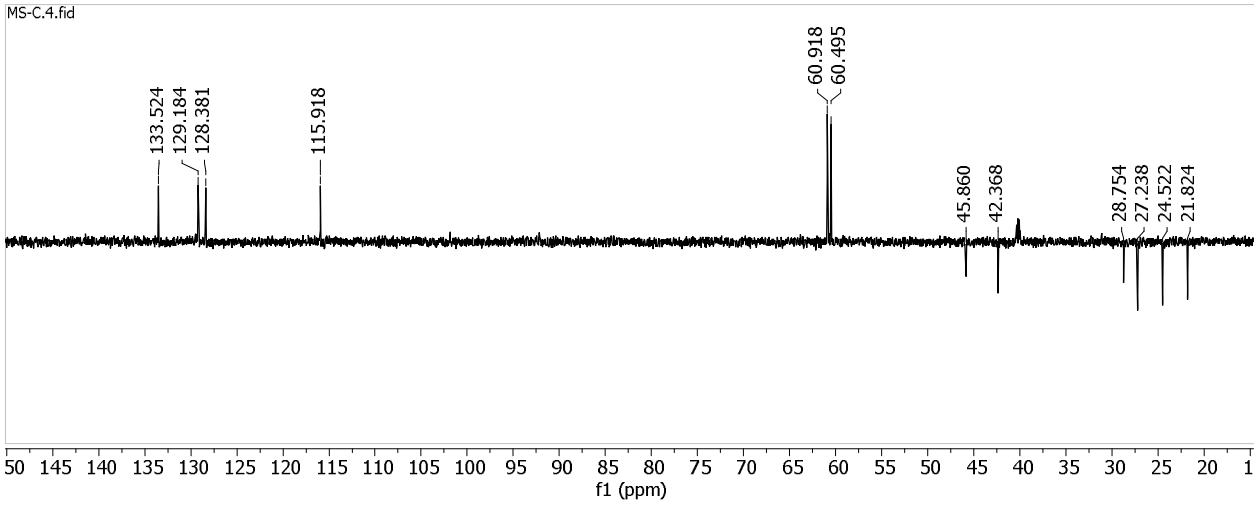

Appendix 34: ^{1}H-^{1}H COSY Spectrum of Compound **28**

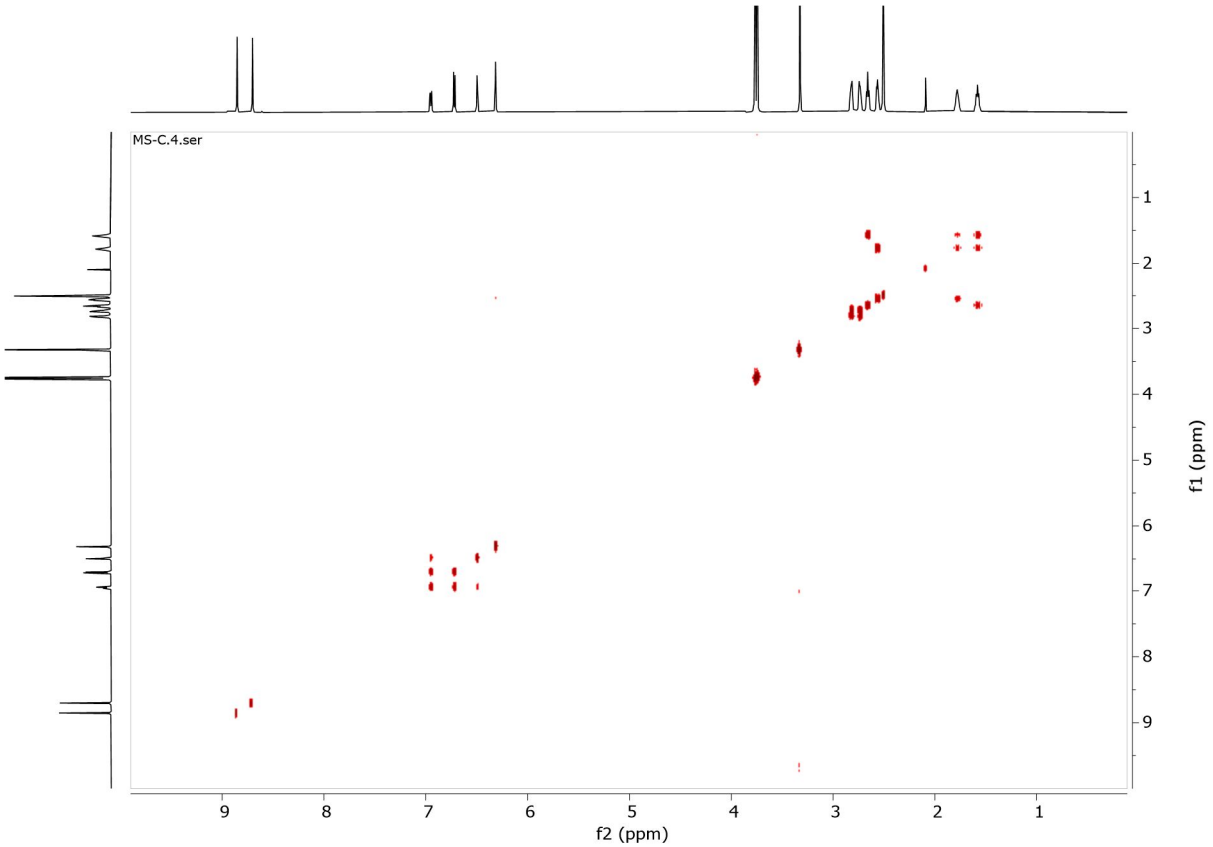

Appendix 35: HSQC Spectrum of Compound **28**

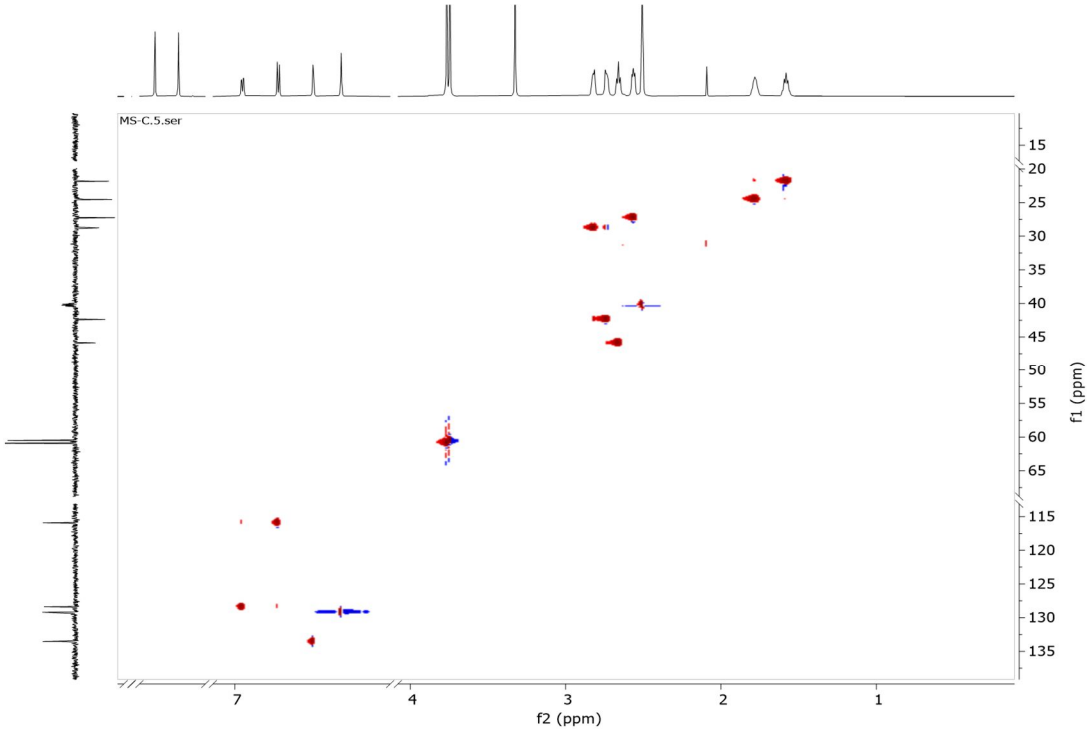

Appendix 36: HMBC Spectrum of Compound **28**

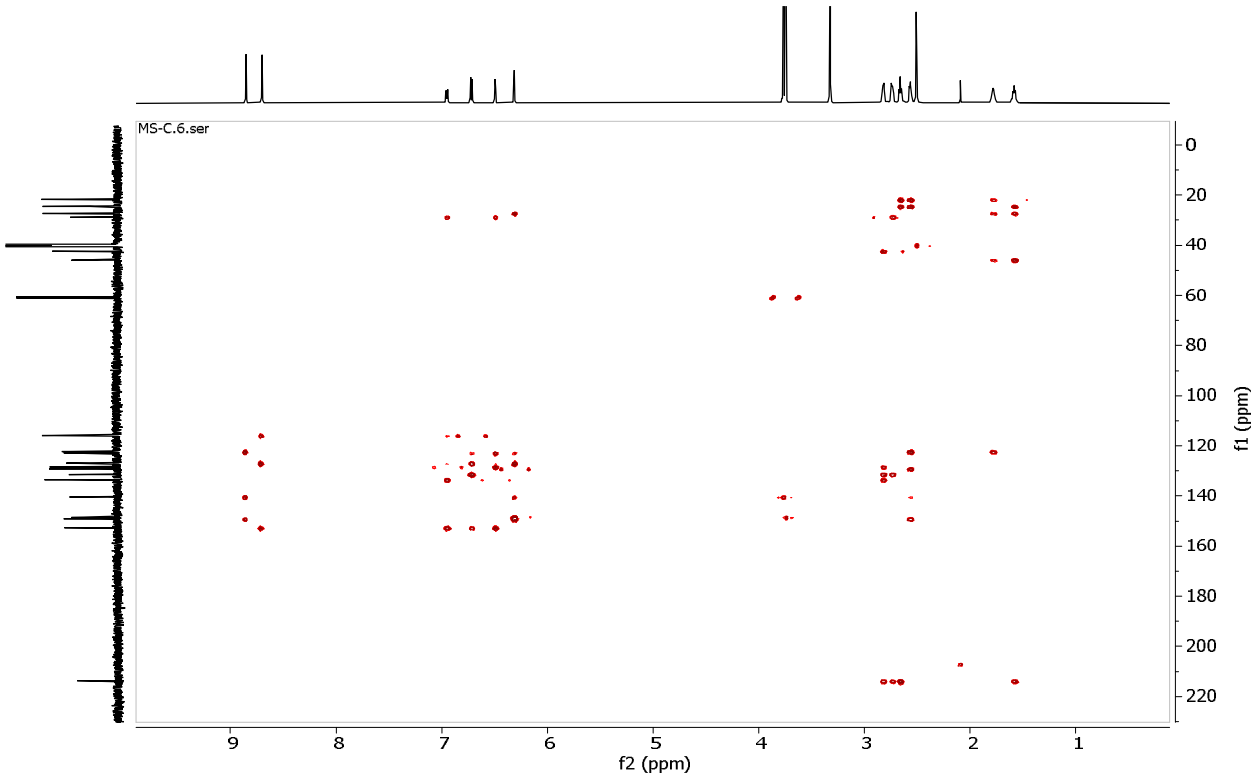

Appendix 37: HPLC-MS Spectrum of Compound **28**

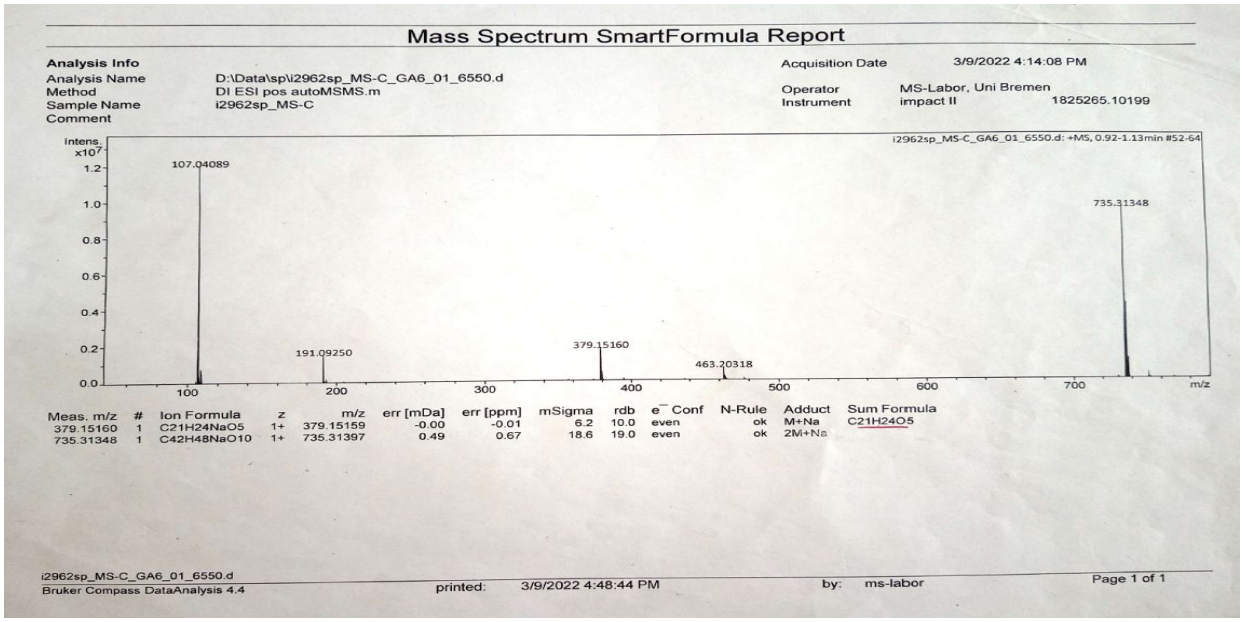

Appendix 38: ^{1}H-NMR (600 MHz, Acetone) Spectrum of Compound **29**

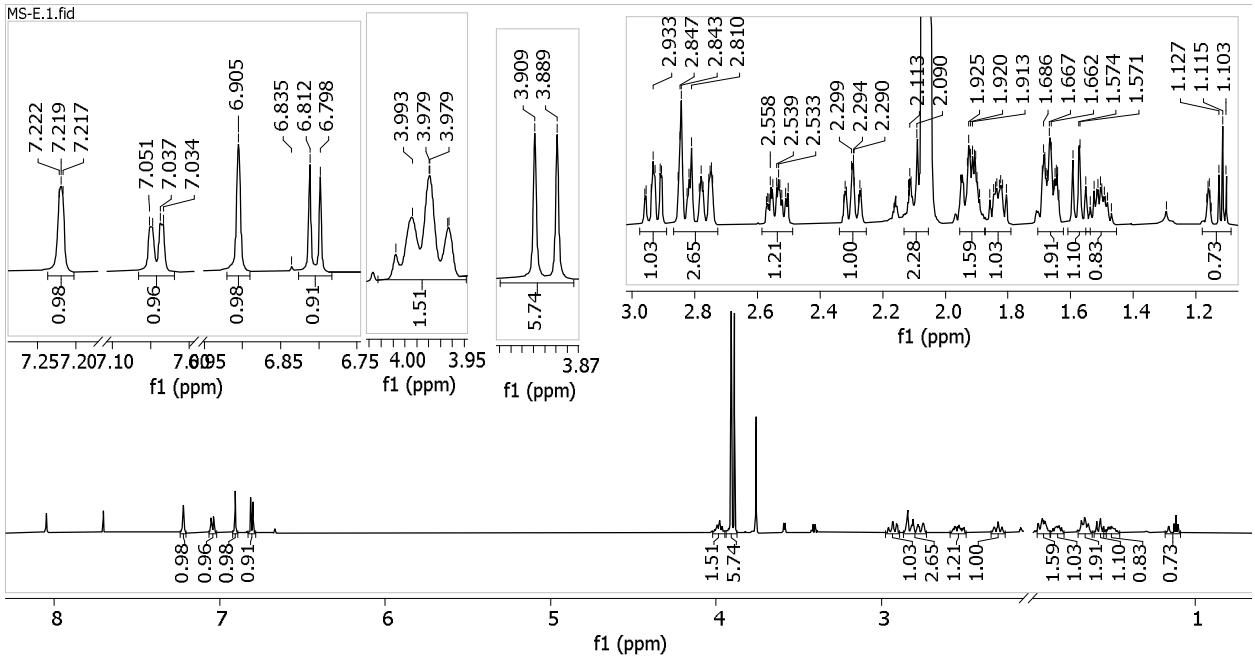

Appendix 39: ^{13}C-NMR (151 MHz, Acetone) Spectrum of Compound **29**

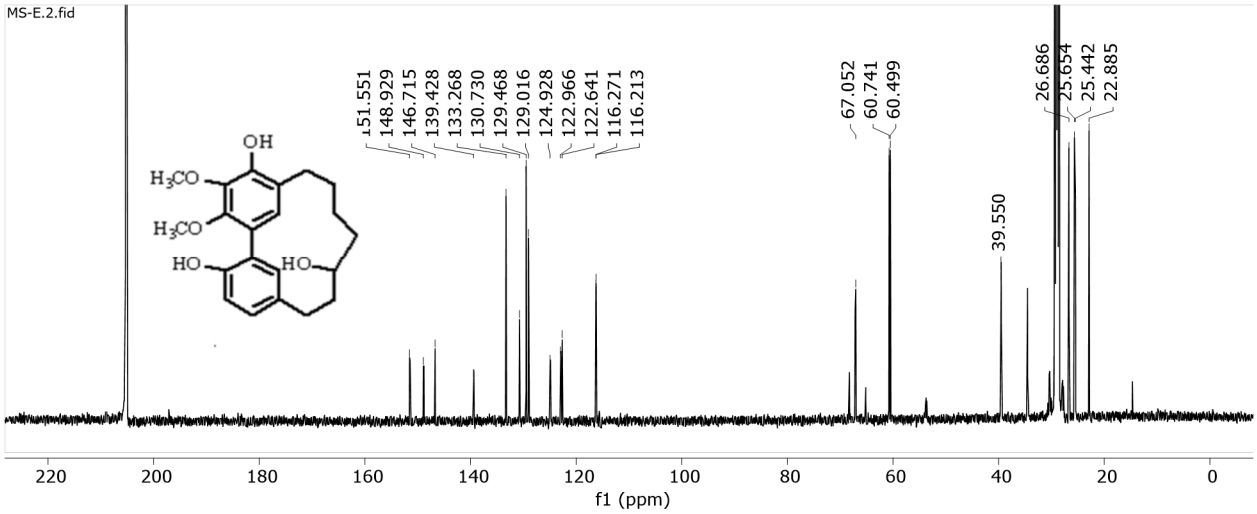

Appendix 40: DEPT-135 Spectrum of Compound **29**

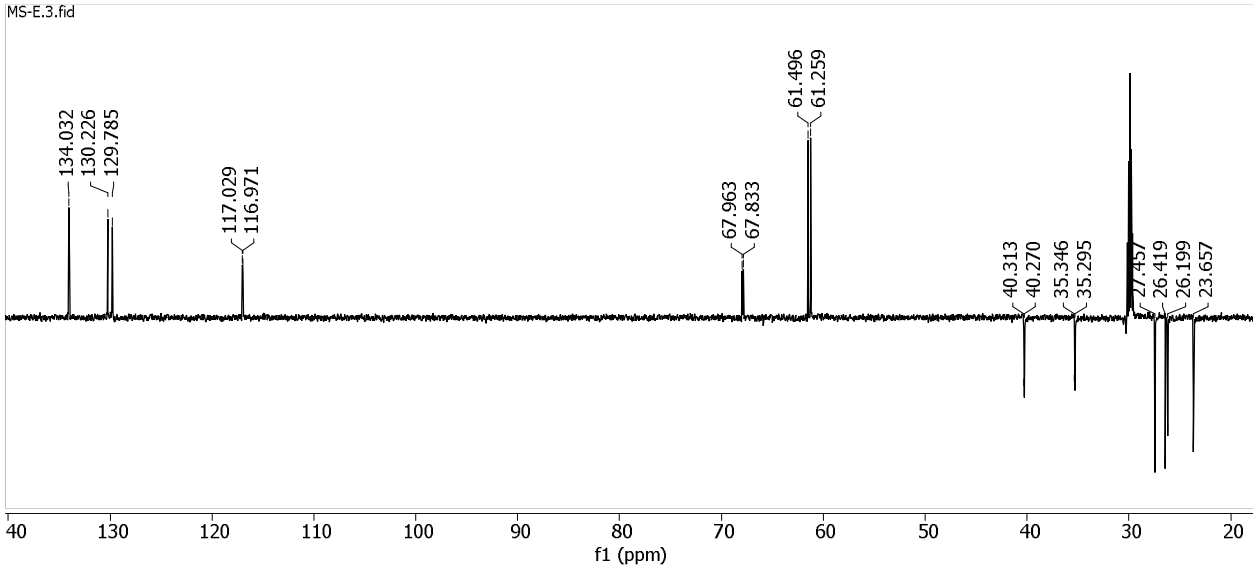

Appendix 41: ^{1}H-^{1}H COSY Spectrum of Compound **29**

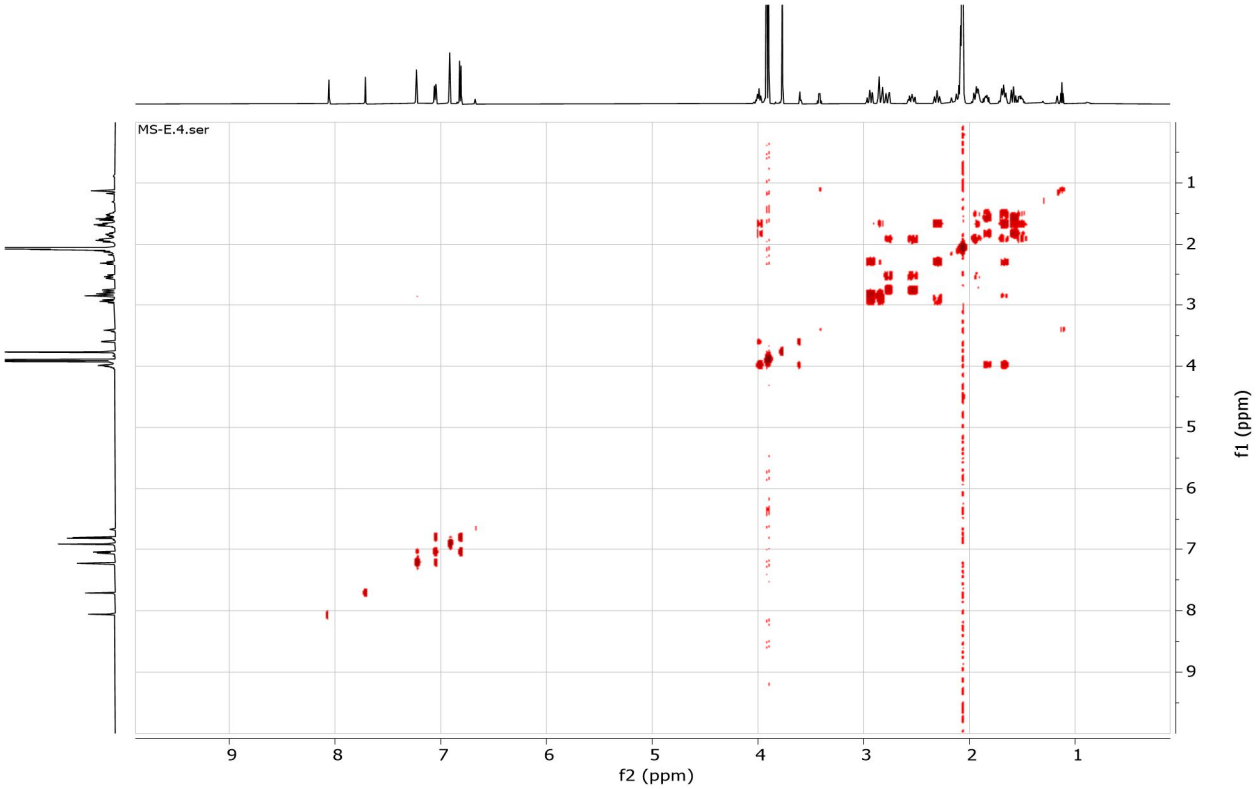

Appendix 42: HSQC Spectrum of Compound **29**

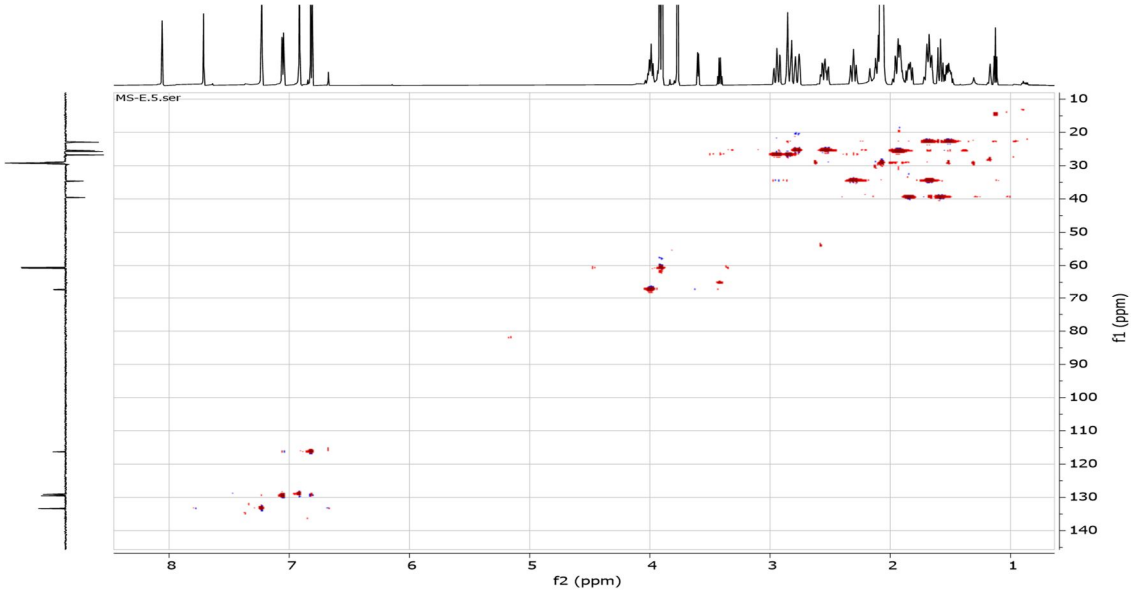

Appendix 43: HMBC Spectrum of Compound **29**

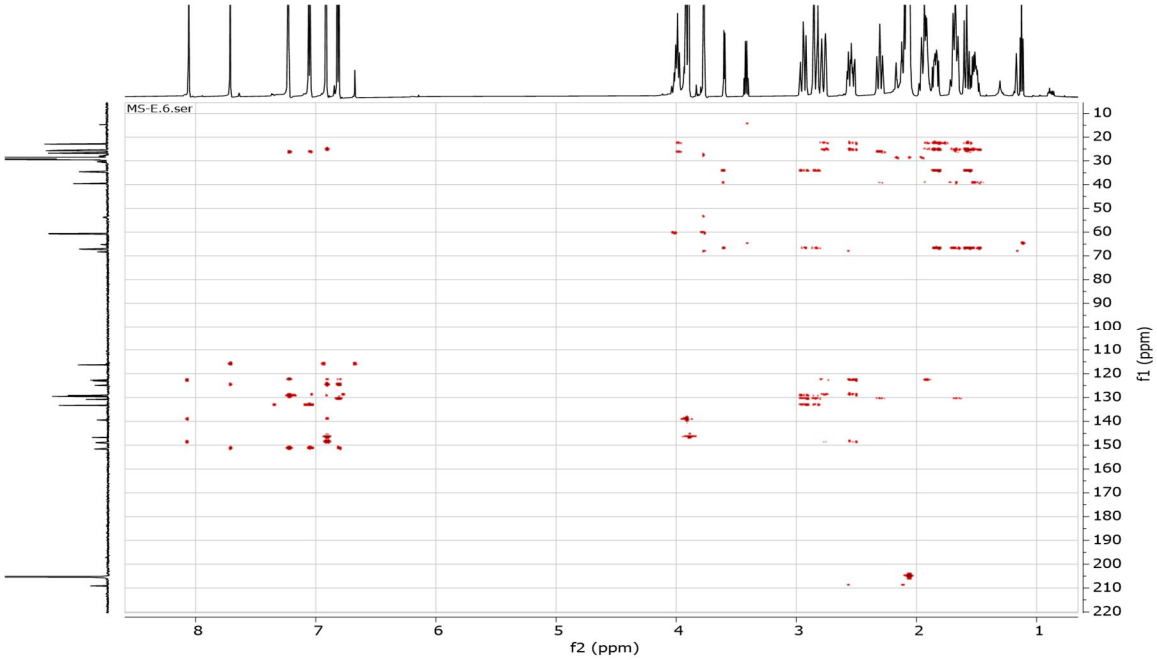

Appendix 44: HPLC-MS Spectrum of Compound **29**

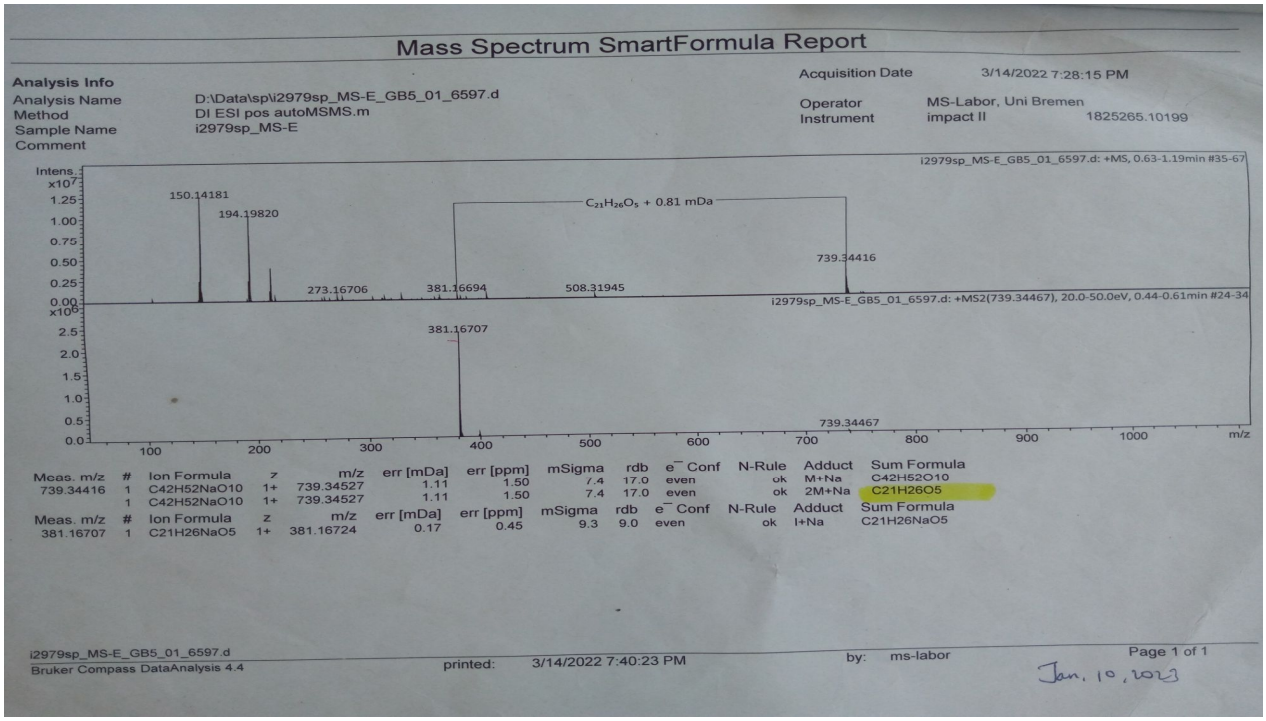

Appendix 45: ^{1}H-NMR (600 MHz, DMSO) Spectrum of Compound **32**

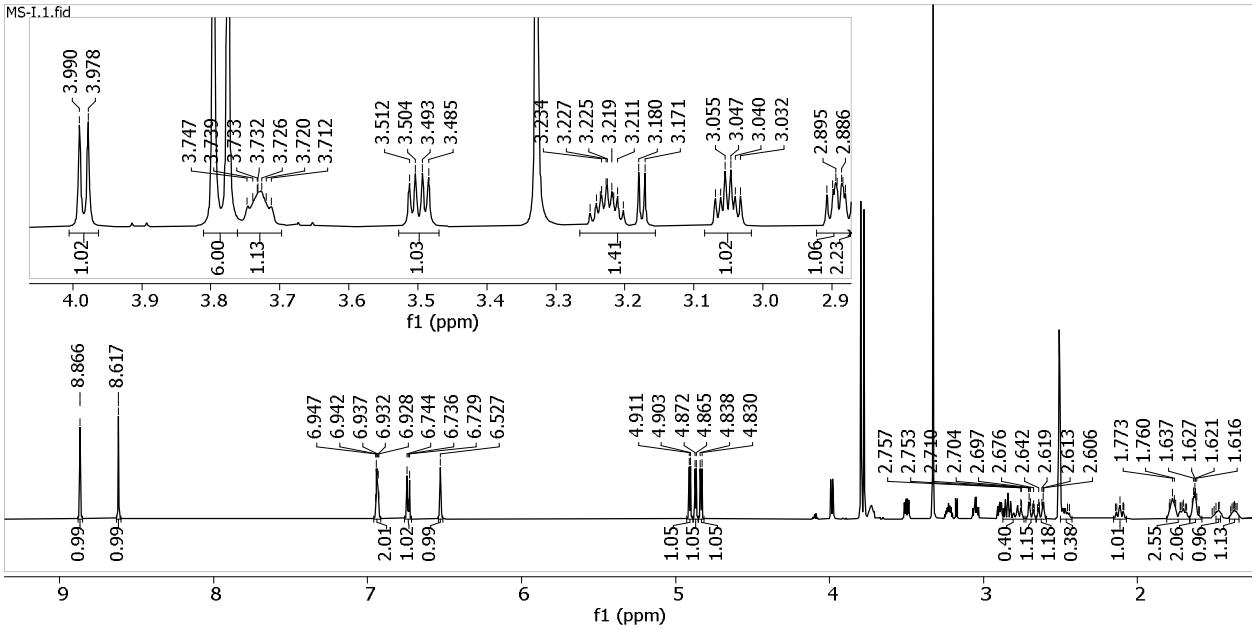

Appendix 46: ^{13}C-NMR (151 MHz, DMSO) Spectrum of Compound **32**

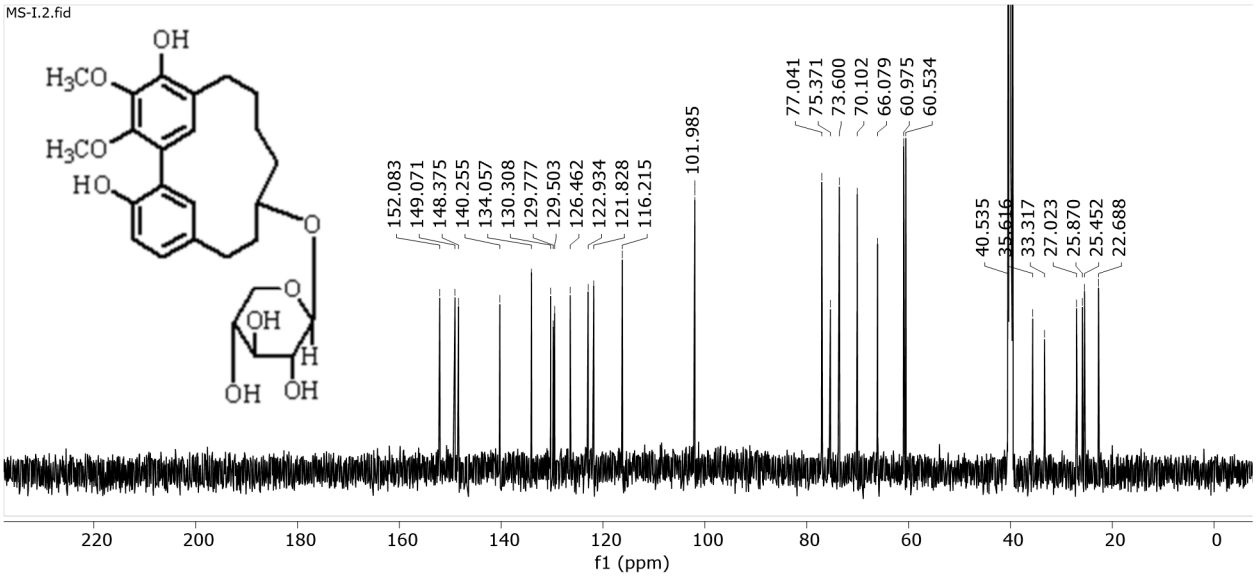

Appendix 47: DEPT-135 Spectrum of Compound **32**

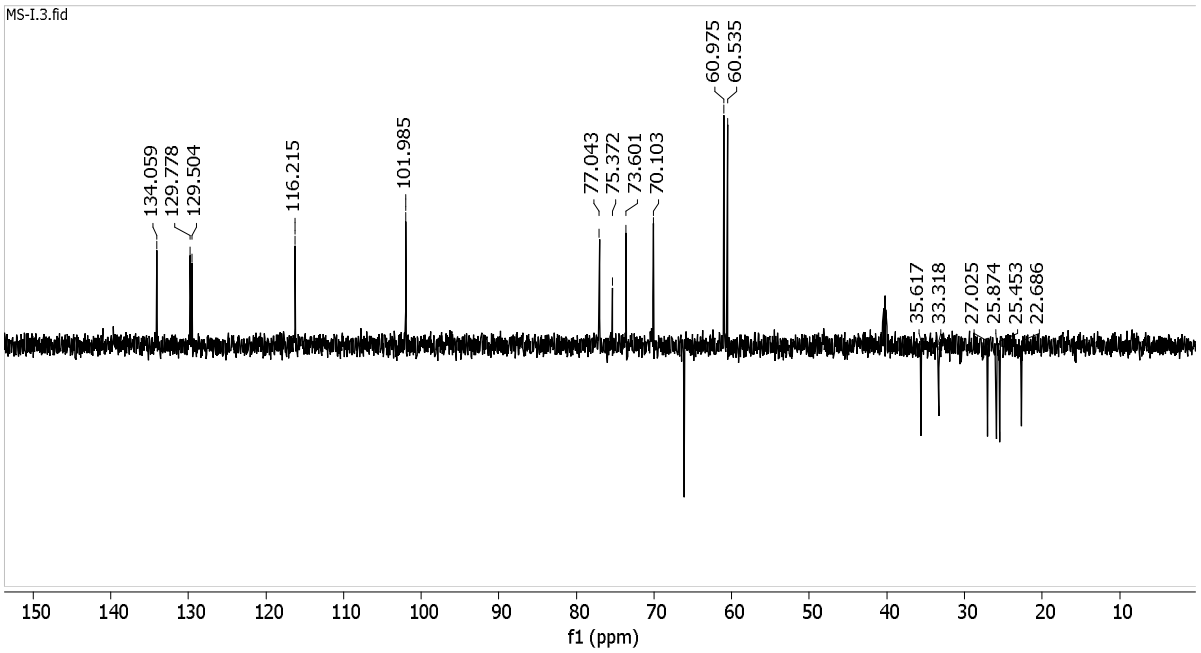

Appendix 48: ^{1}H-^{1}H COSY Spectrum of Compound **32**

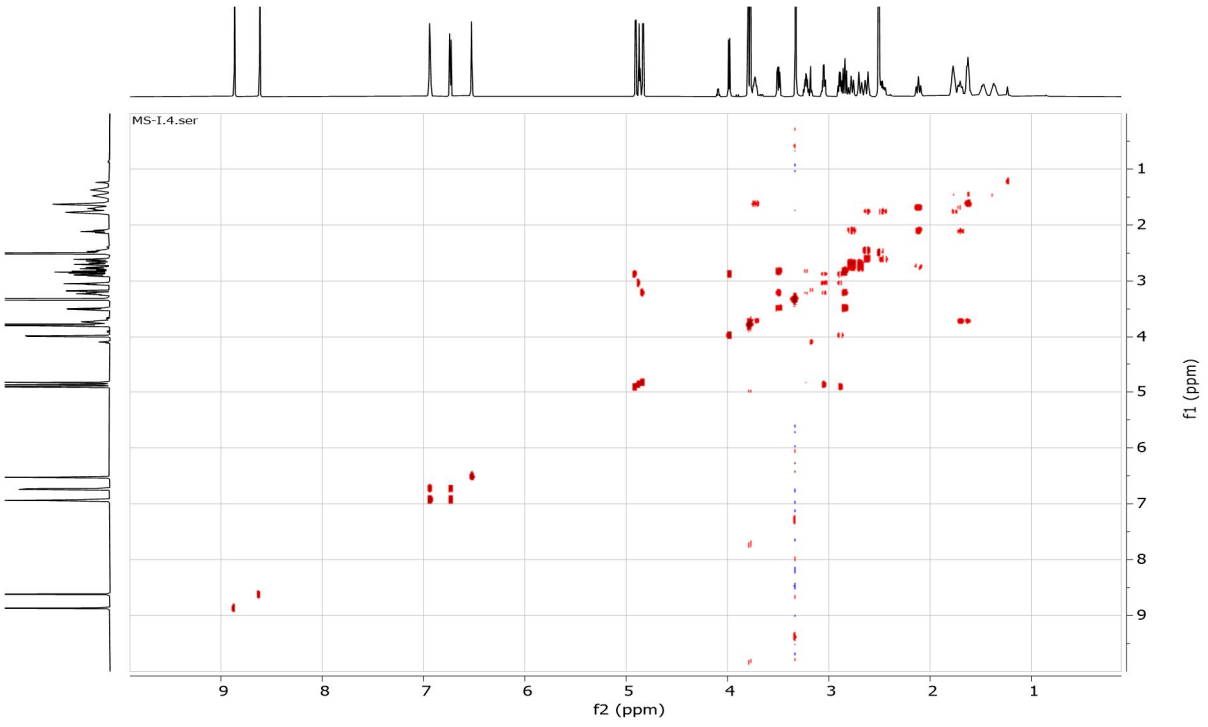

Appendix 49: HSQC Spectrum of Compound **32**

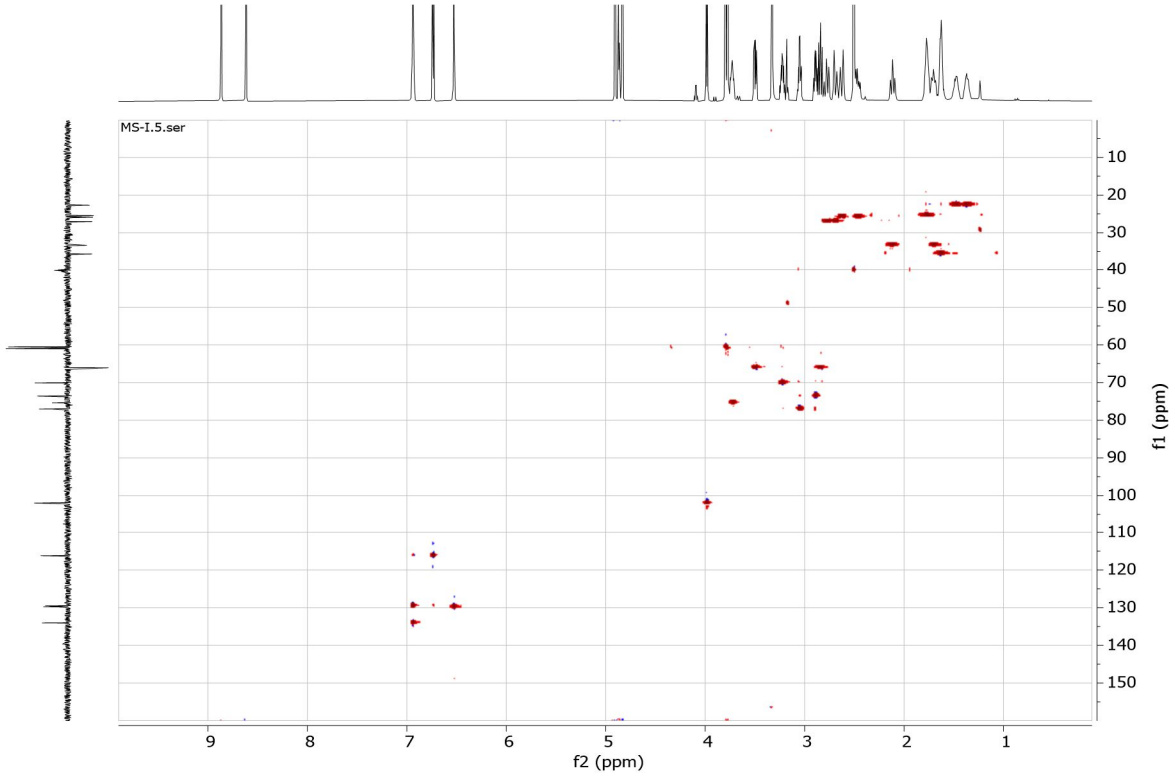

Appendix 50: HMBC Spectrum of Compound **32**

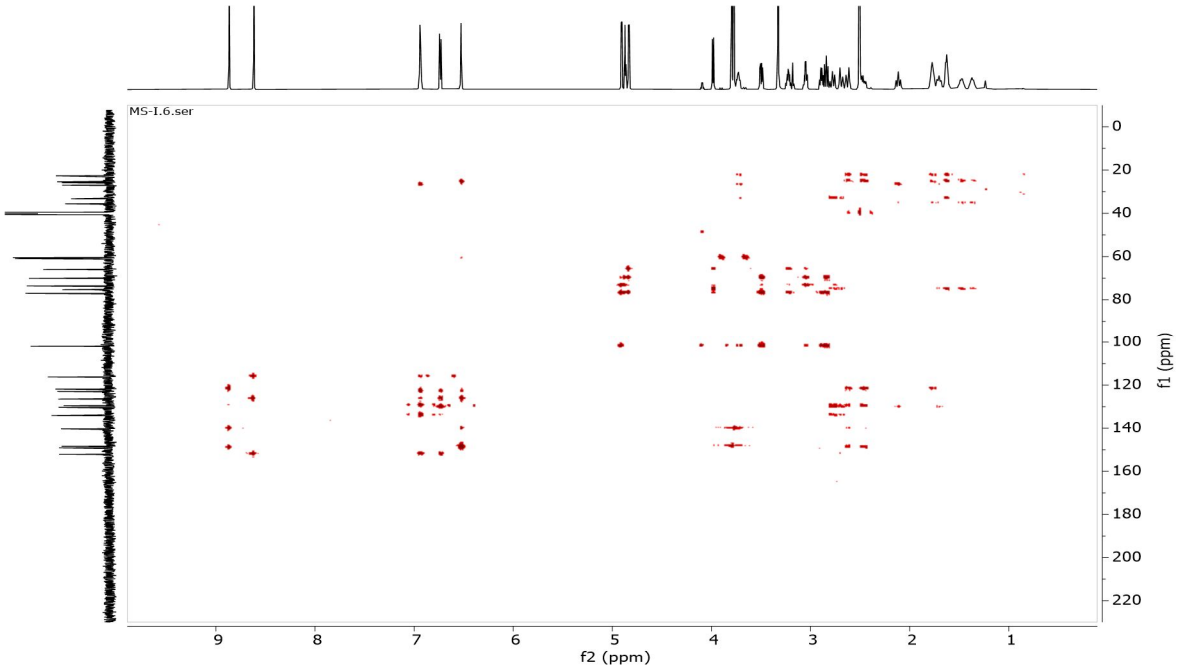

Appendix 51: NOES Spectrum of Compound **32**

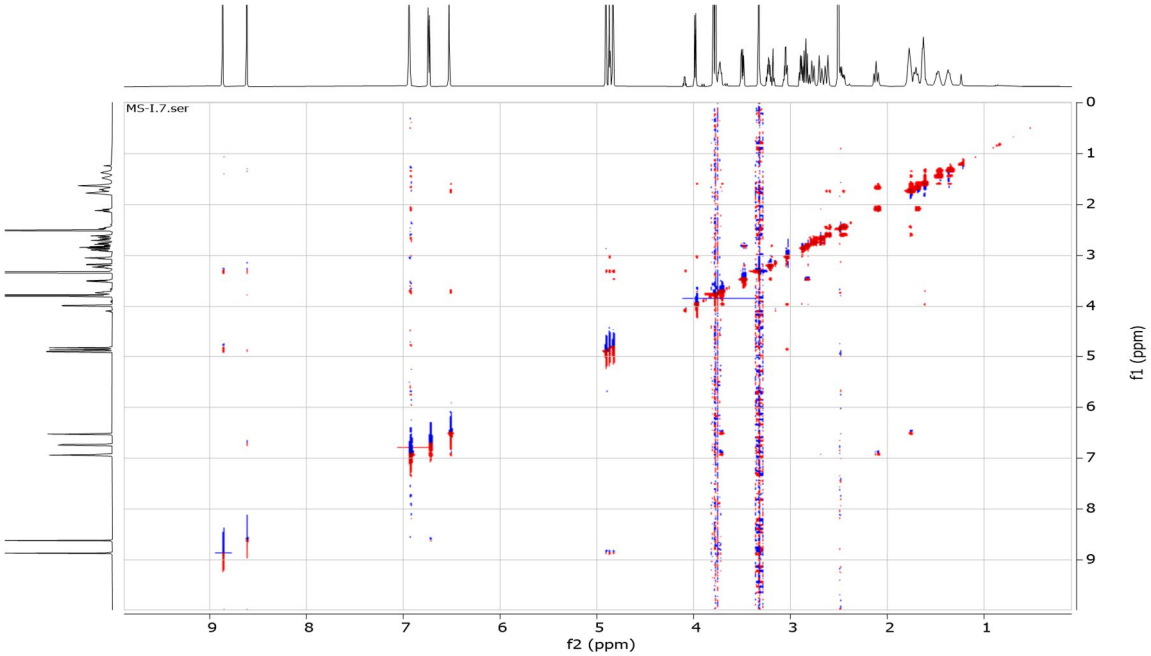

Appendix 52: HPLC-MS Spectrum of Compound **32**

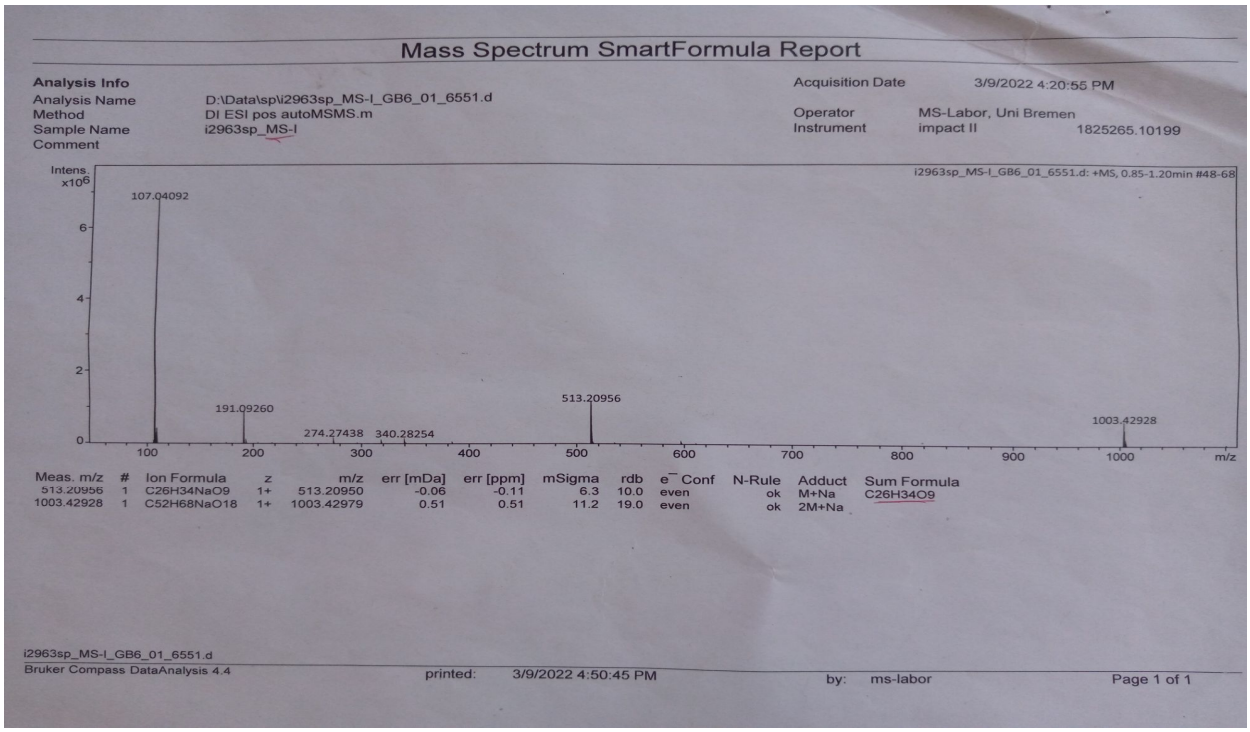

Appendix 53: ^{1}H-NMR (600 MHz, $CDCl_3$) Spectrum of Compound **81**

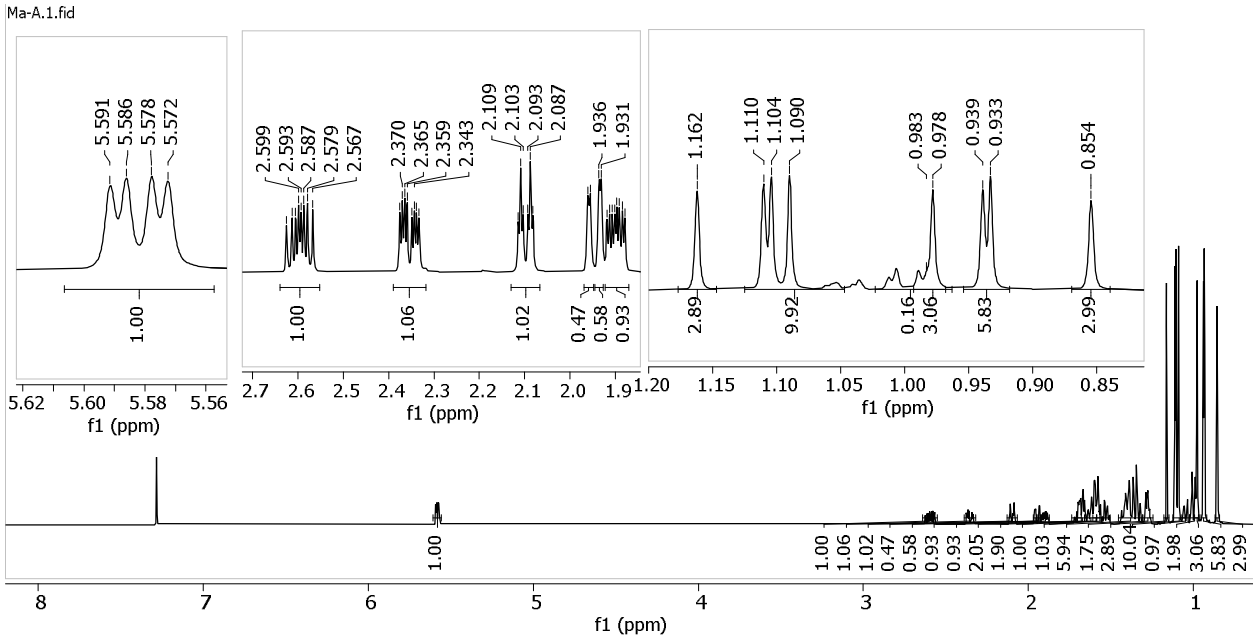

Appendix 54: ^{13}C-NMR (125 MHz, $CDCl_3$) Spectrum of Compound **81**

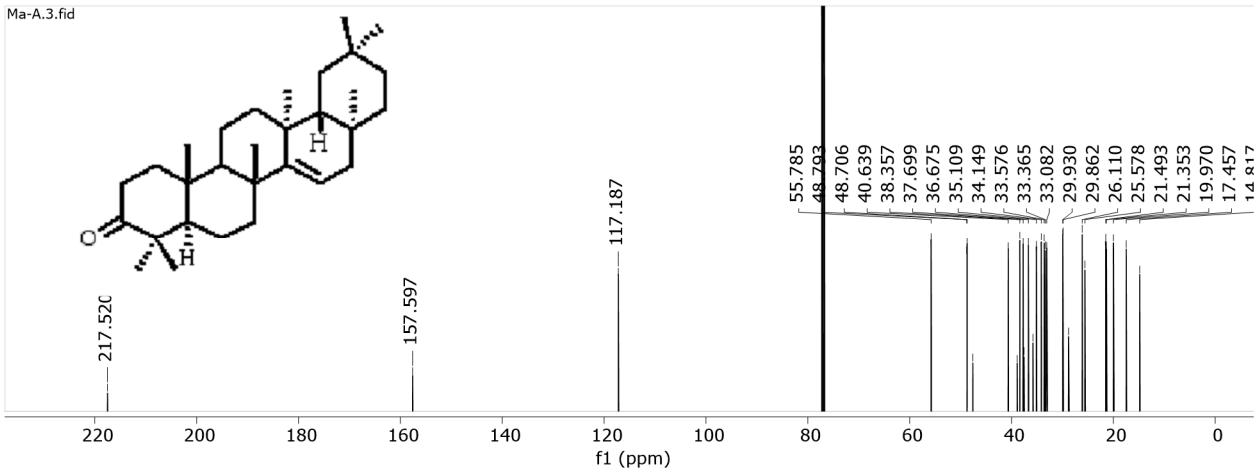

Appendix 55: DEPT-135 Spectrum of Compound **81**

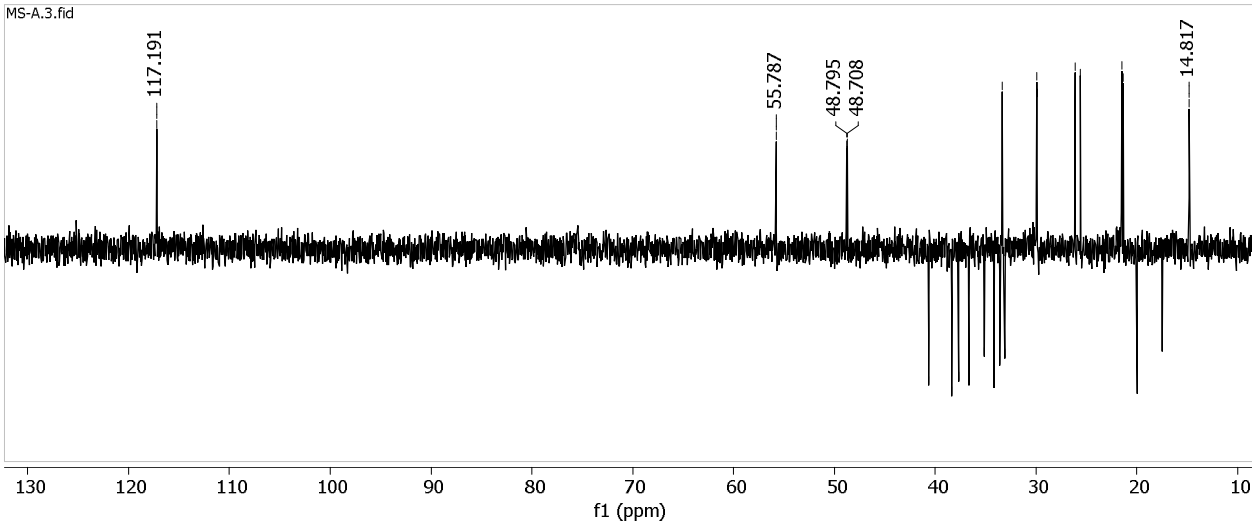

Appendix 56: ^{1}H-^{1}H COSY Spectrum of Compound **81**

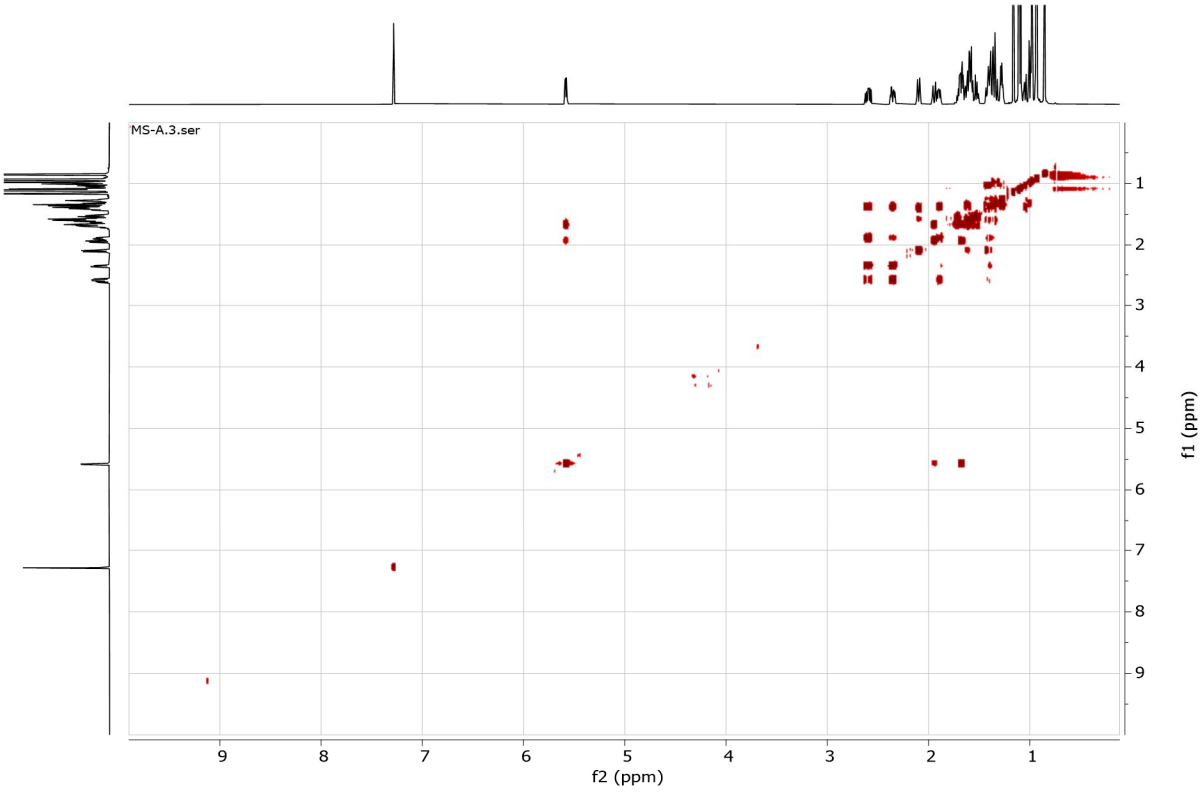

Appendix 57: HSQC Spectrum of Compound **81**

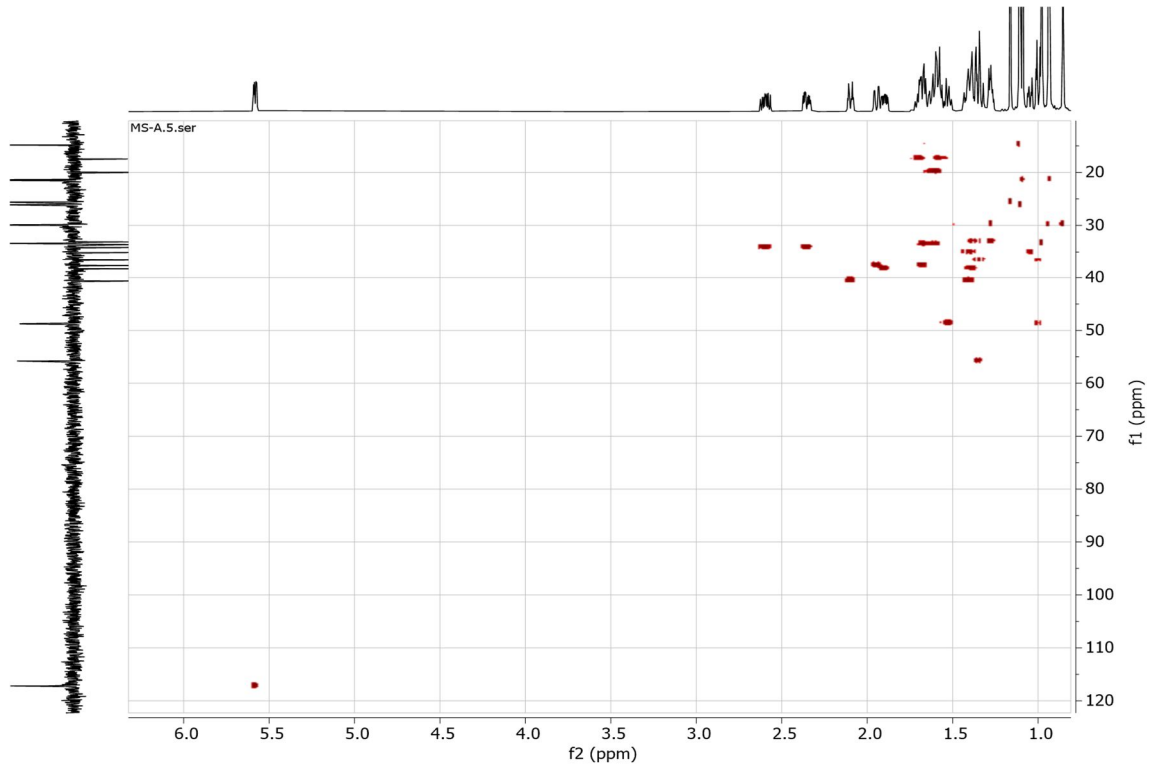

Appendix 58: HMBC Spectrum of Compound **81**

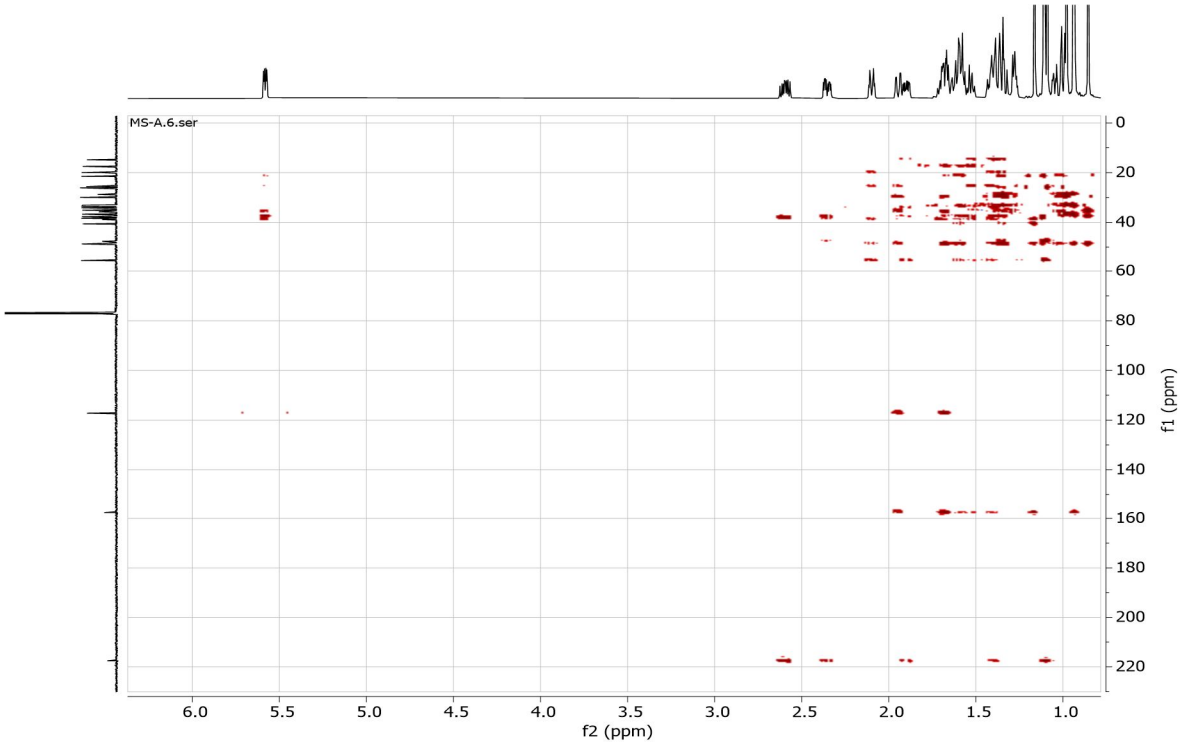

Appendix 59: NOES Spectrum of Compound **81**

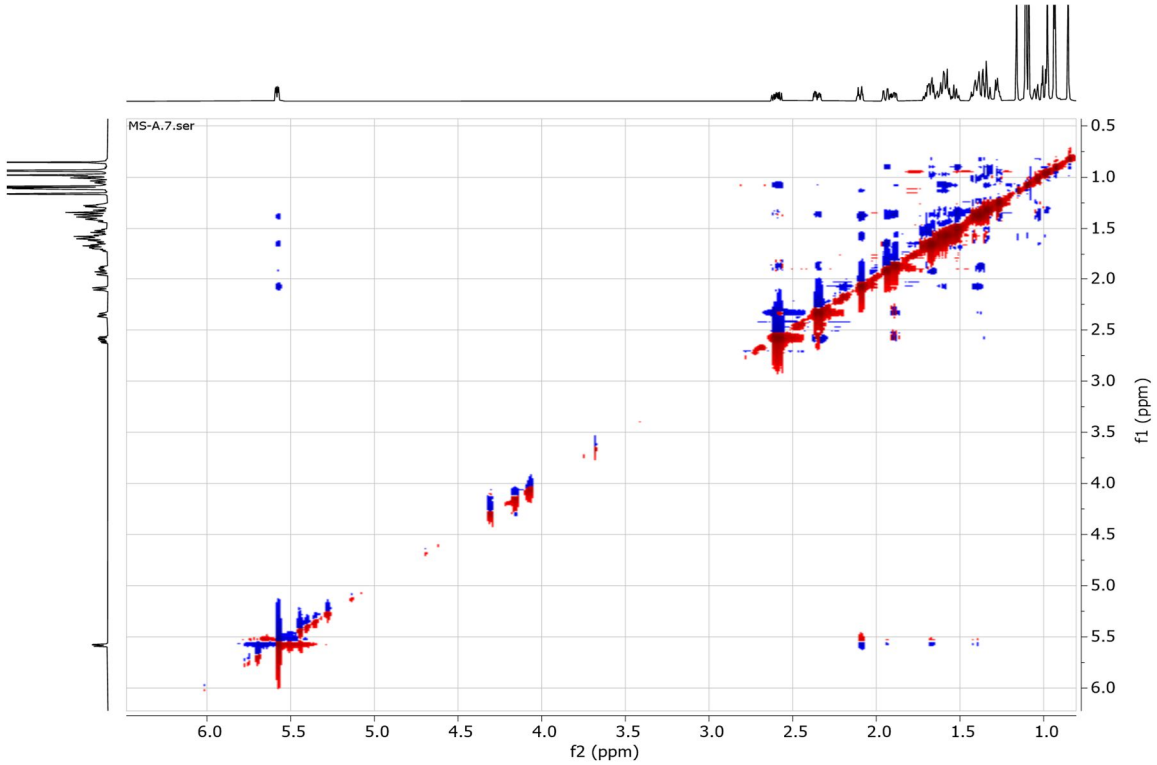

Appendix 60: MALDI-MS Spectrum of Compound **81**

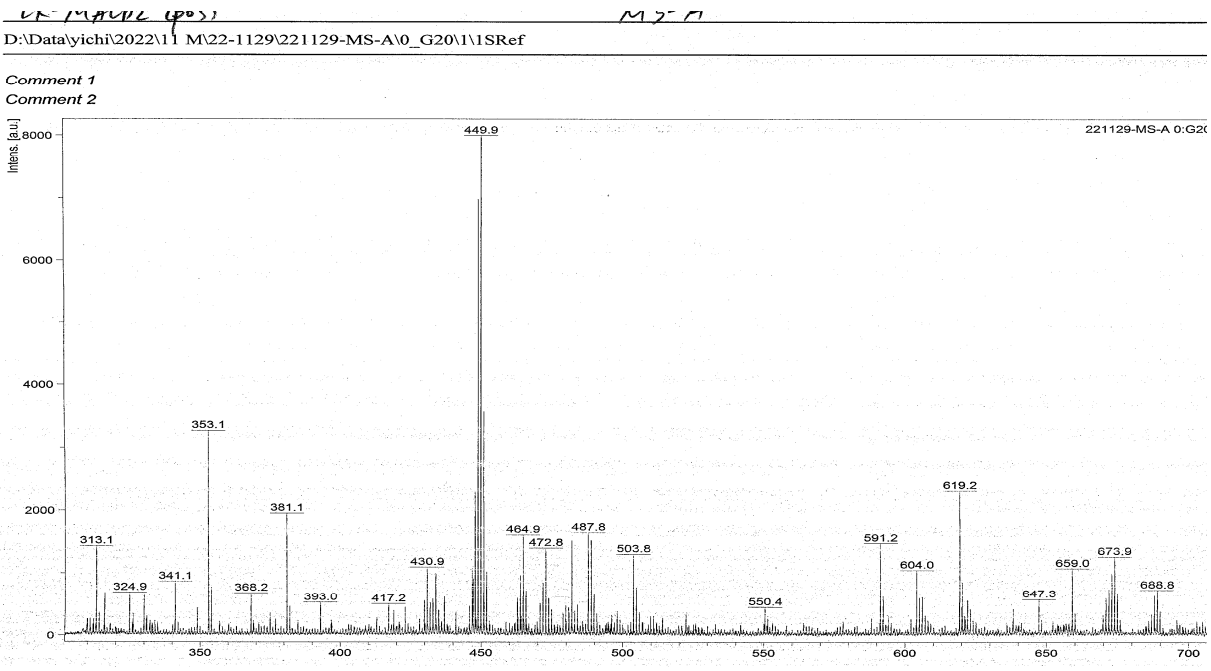

Appendix 61: ^{1}H-NMR (600 MHz, $CDCl_3$) Spectrum of Compound **82**

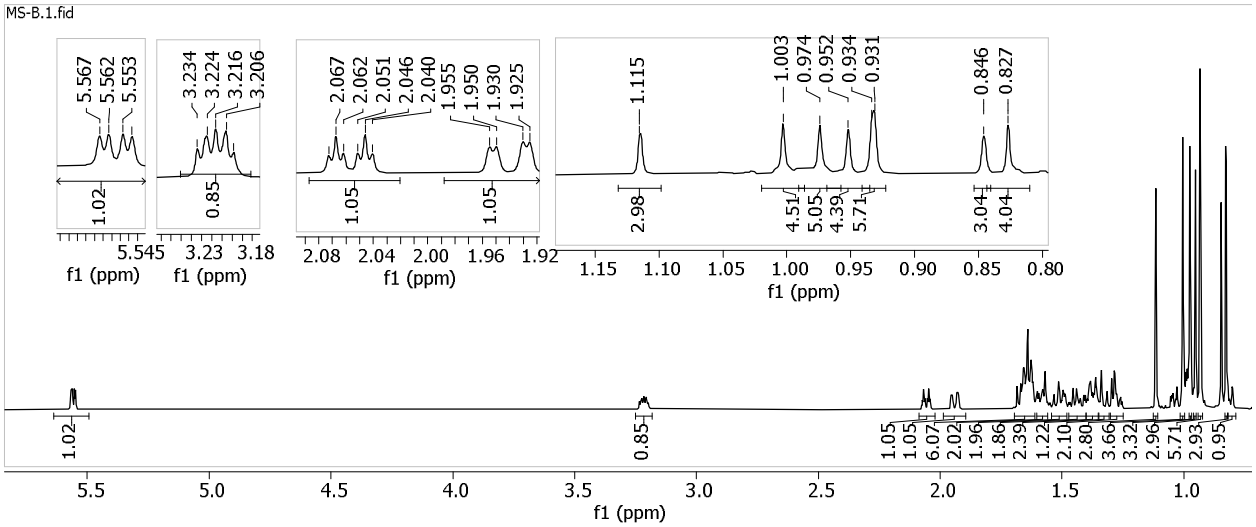

Appendix 62: ^{13}C-NMR (100 MHz, $CDCl_3$) Spectrum of Compound **82**

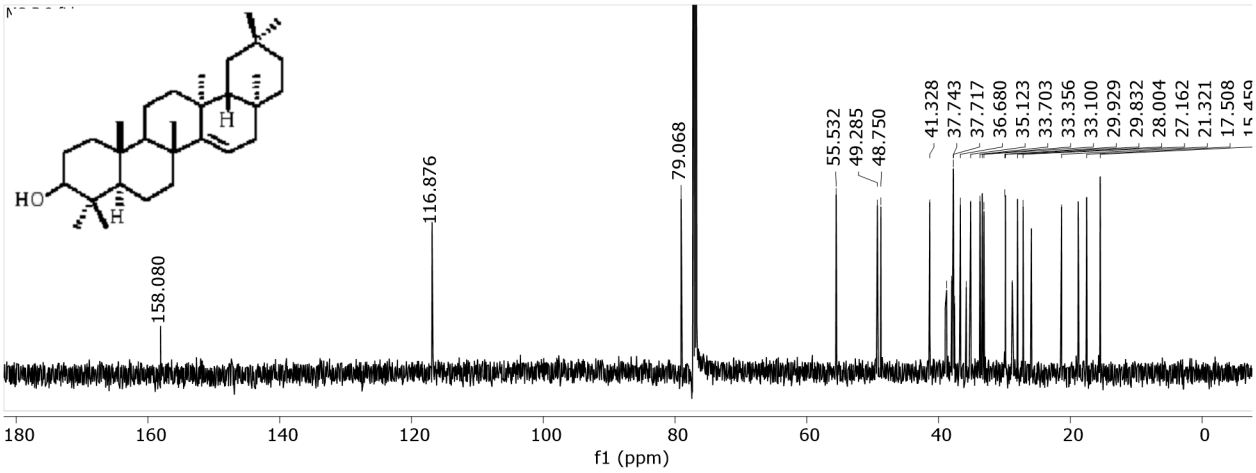

Appendix 63: DEPT-135 Spectrum of Compound **82**

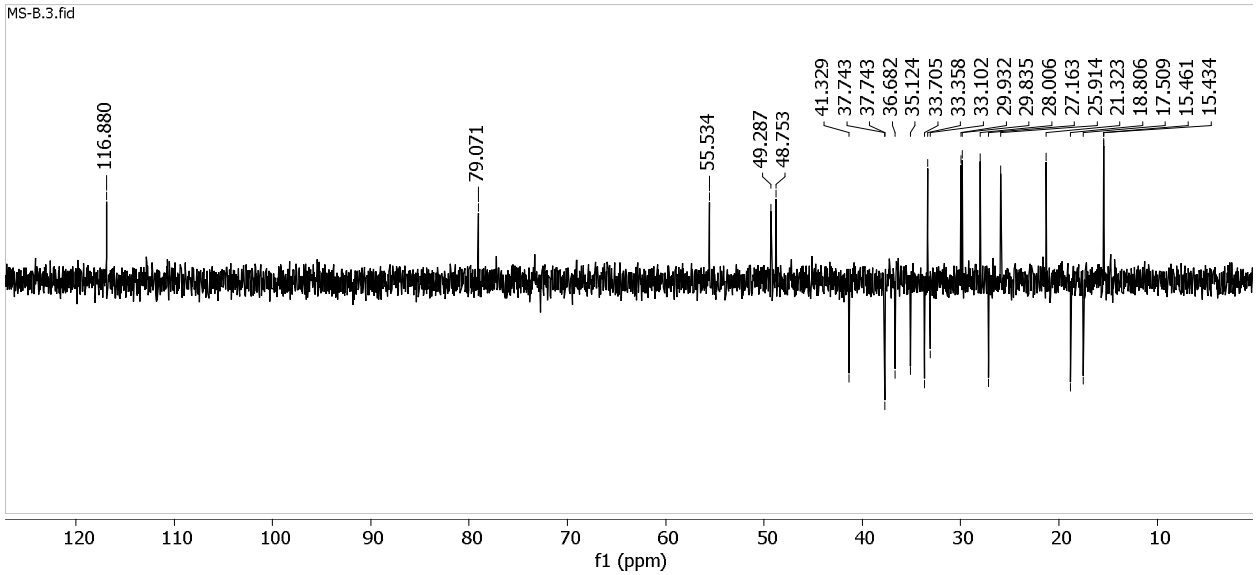

Appendix 64: ^{1}H-^{1}H COSY Spectrum of Compound **82**

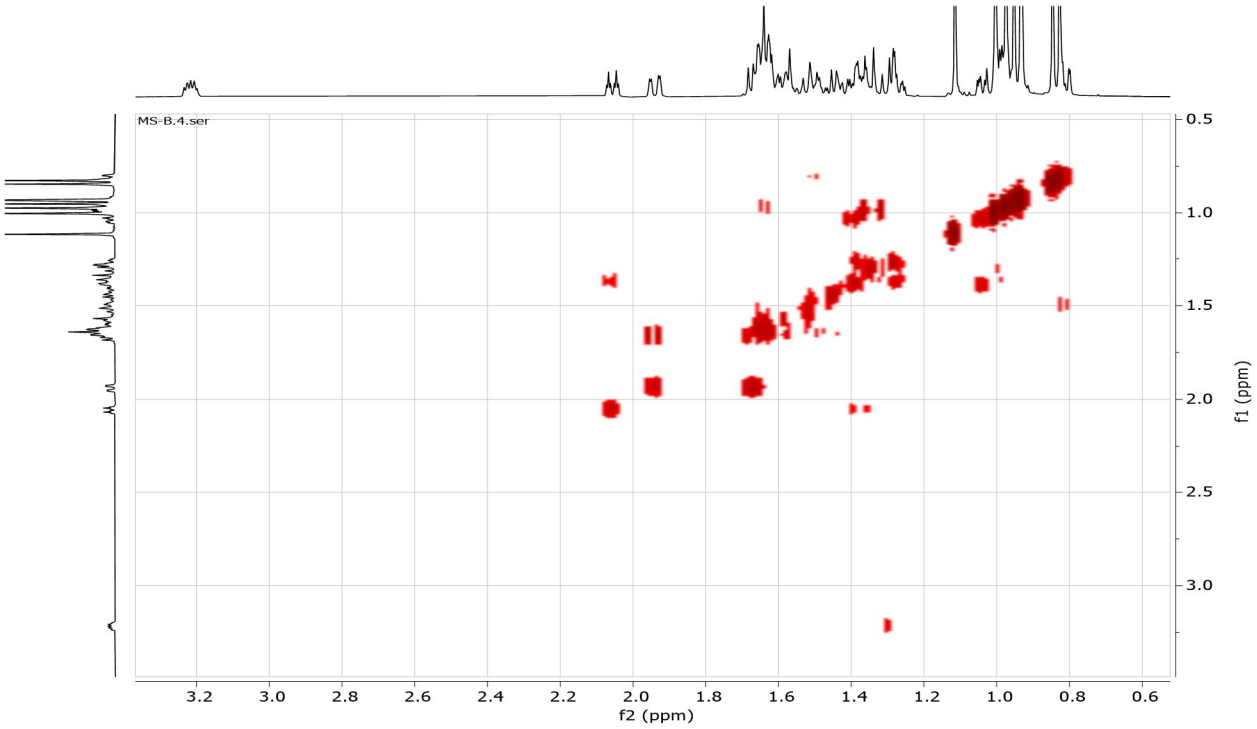

Appendix 65: HSQC Spectrum of Compound **82**

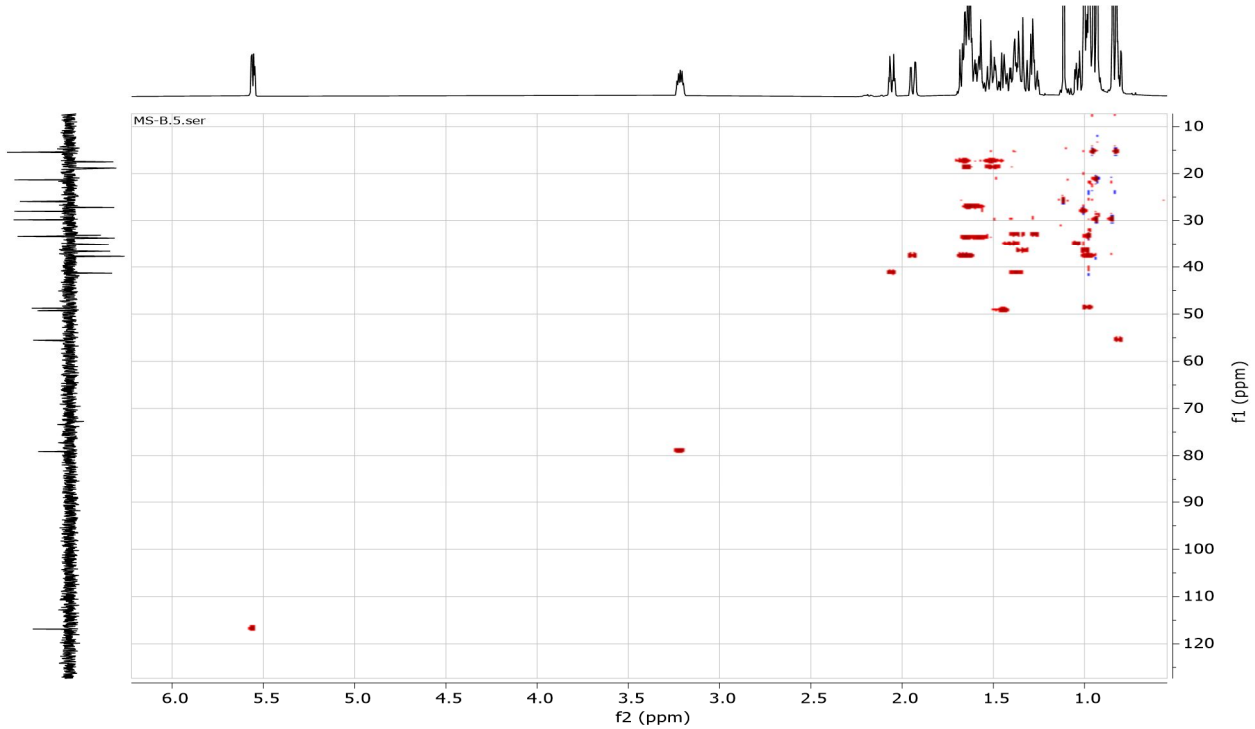

Appendix 66: HMBC Spectrum of Compound **82**

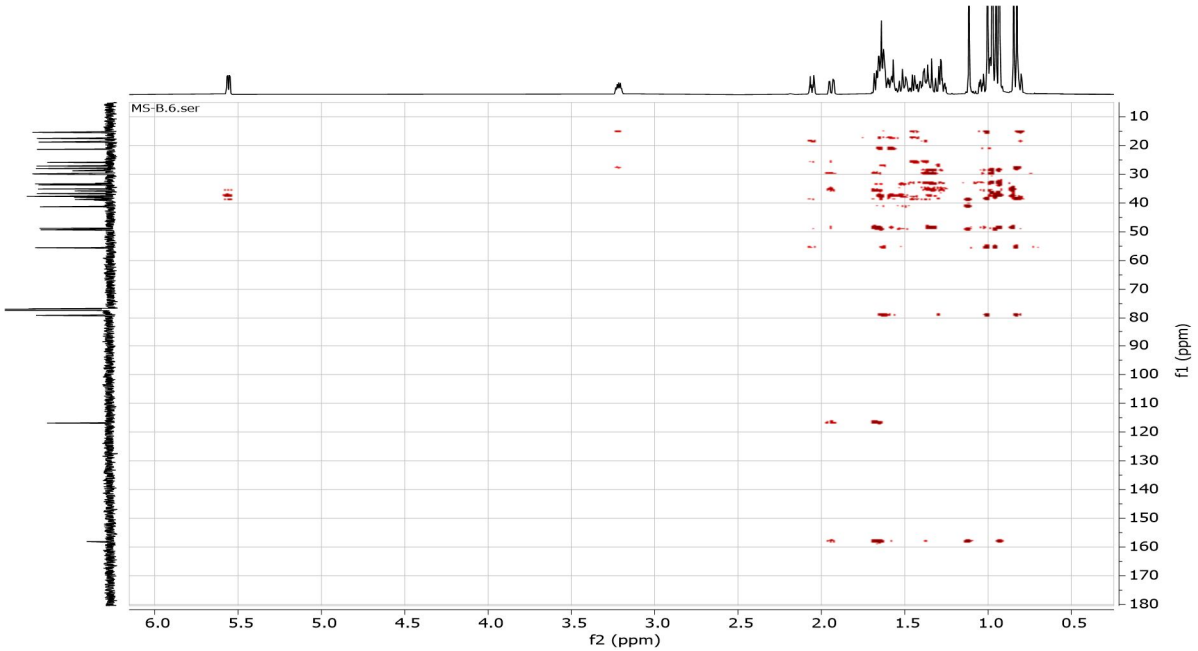

Appendix 67: NOES Spectrum of Compound **82**

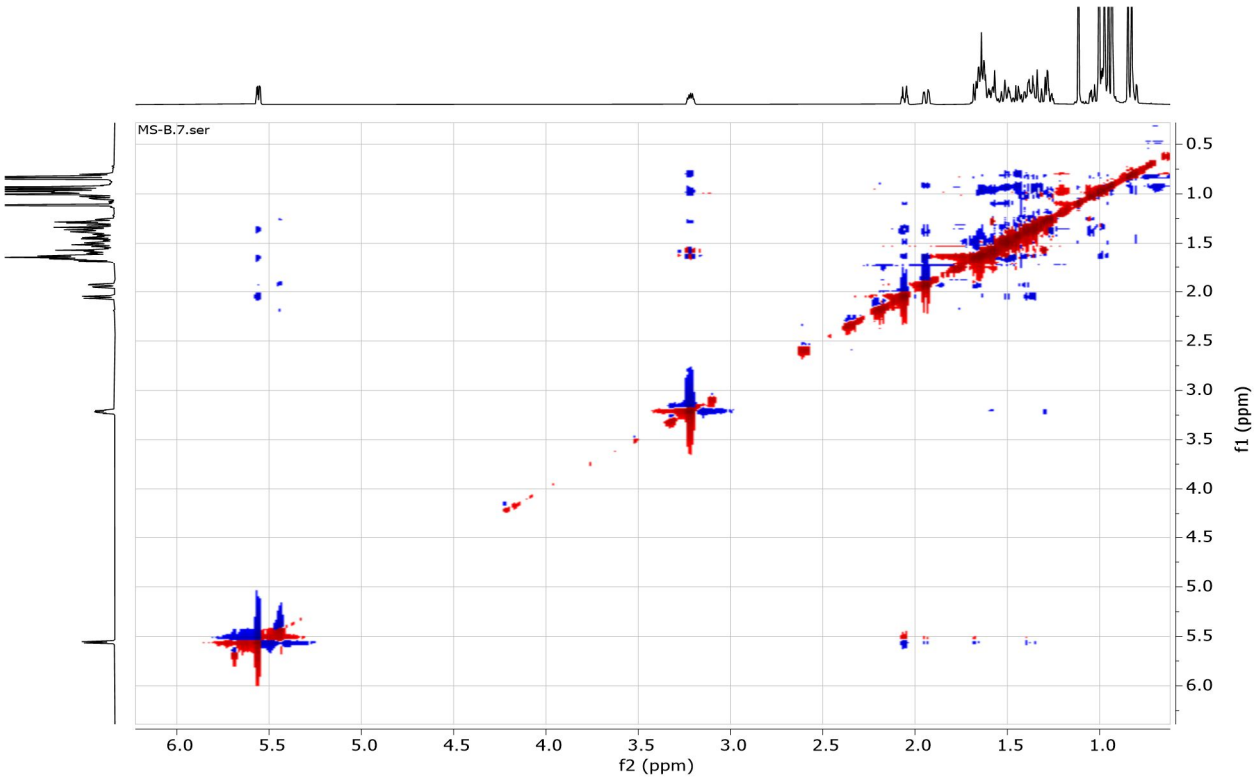

Appendix 68: MALDI-MS Spectrum of Compound **82**

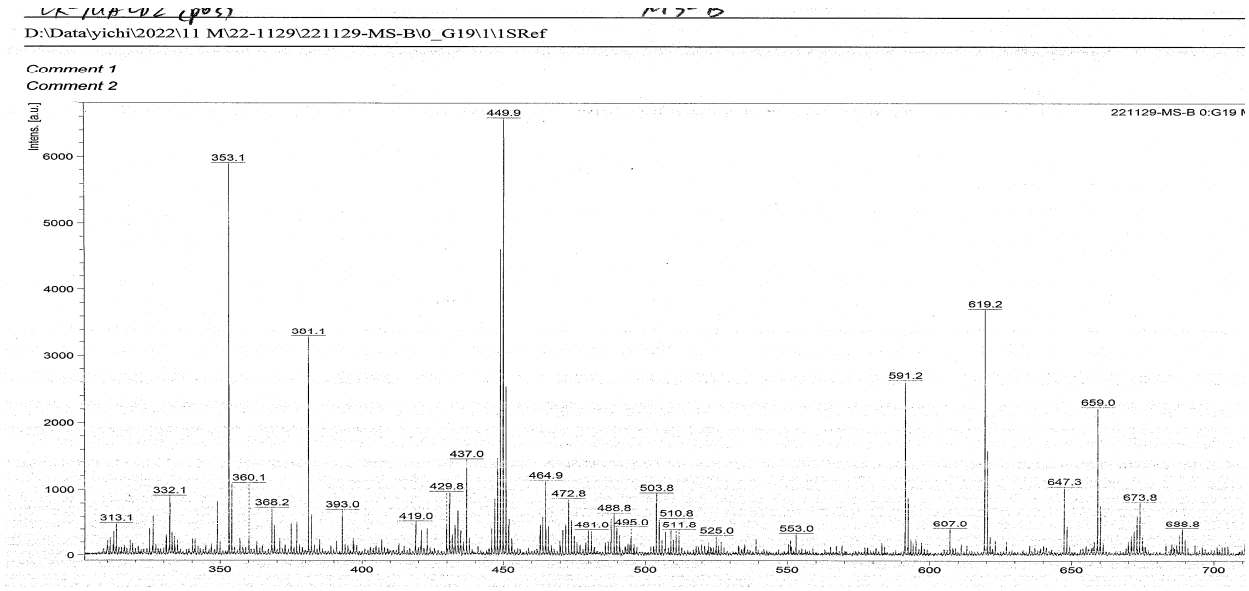

Appendix 69: ^{1}H-NMR (600 MHz, $CDCl_3$) Spectrum of Compound **83**

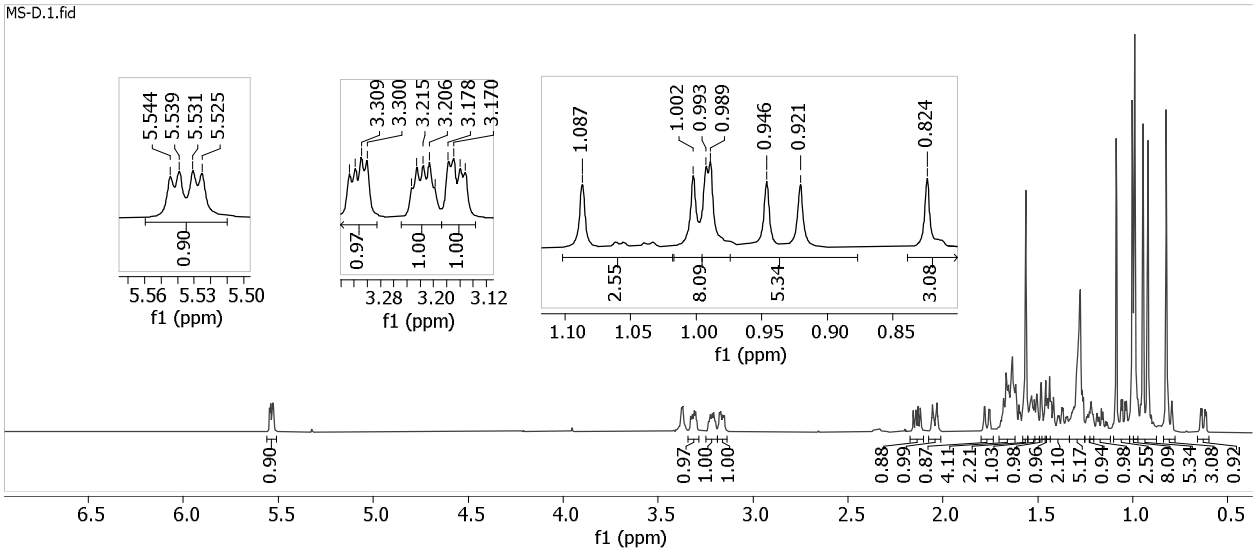

Appendix 70: ^{13}C-NMR (125 MHz, $CDCl_3$) Spectrum of Compound **83**

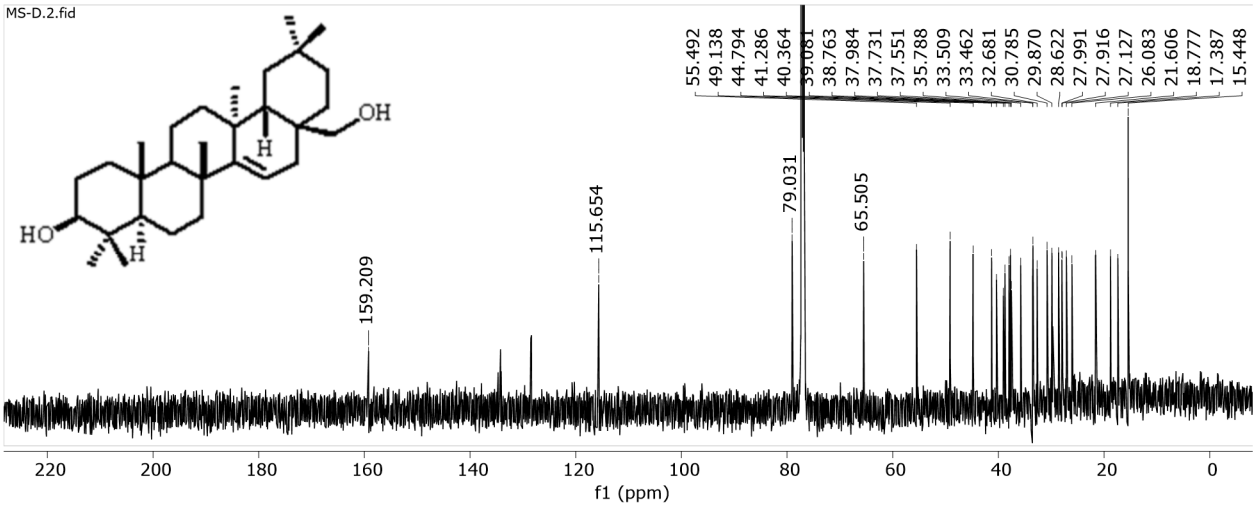

Appendix 71: DEPT-135 Spectrum of Compound **83**

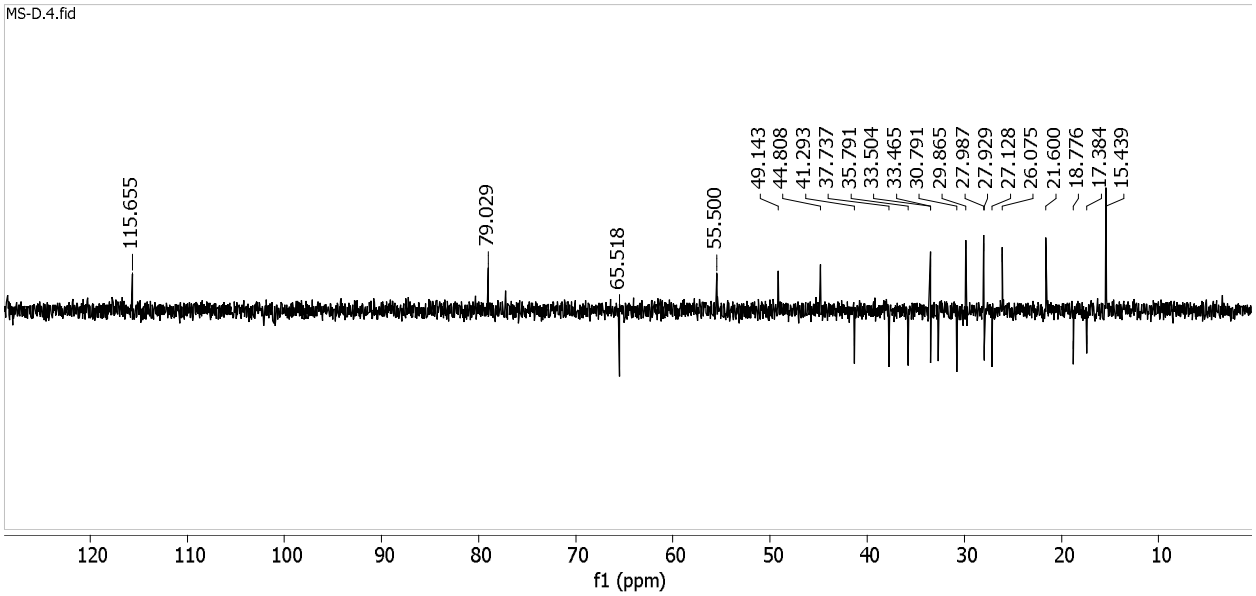

Appendix 72: ^{1}H-^{1}H COSY Spectrum of Compound **83**

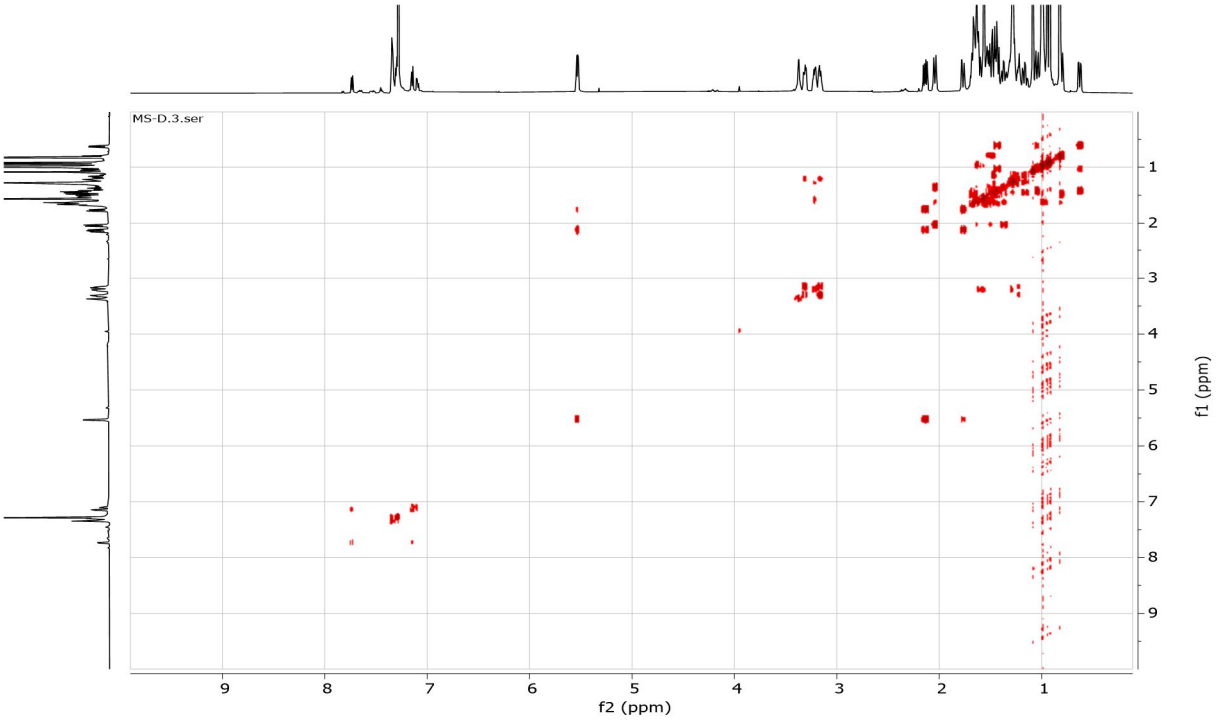

Appendix 73: HSQC Spectrum of Compound **83**

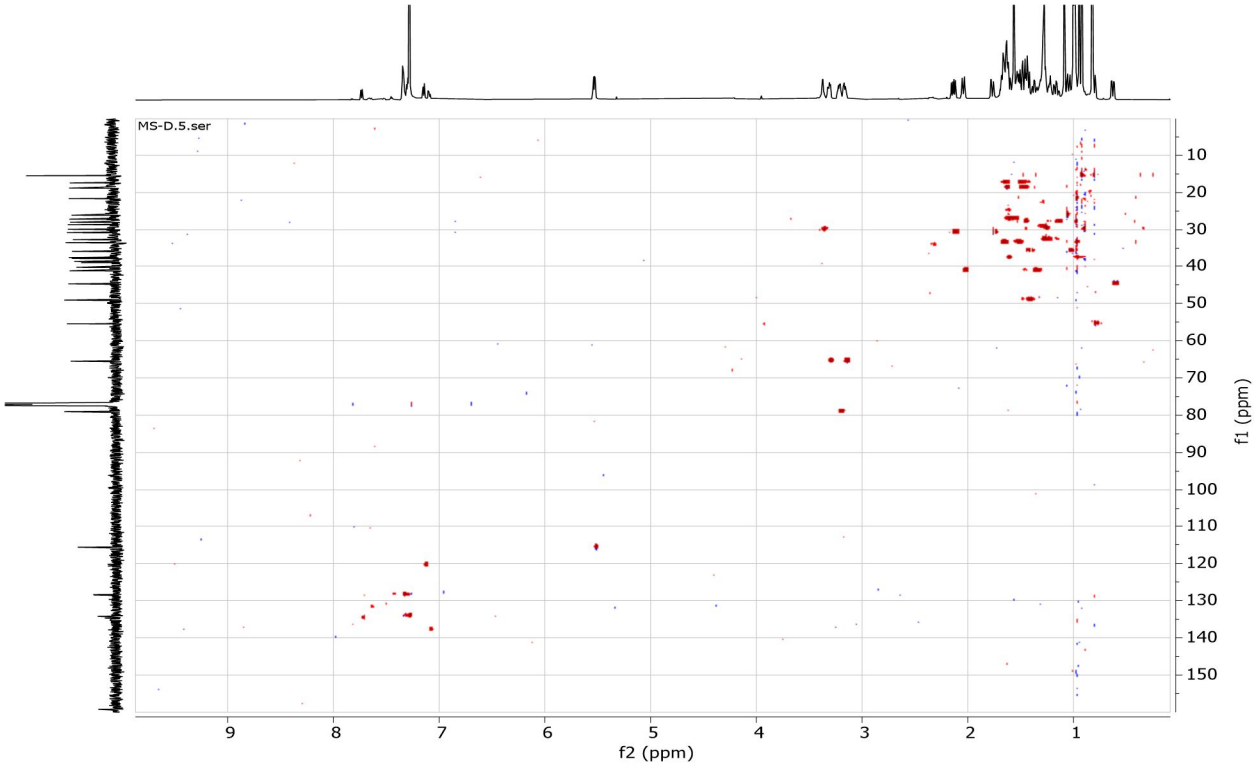

Appendix 74: HMBC Spectrum of Compound **83**

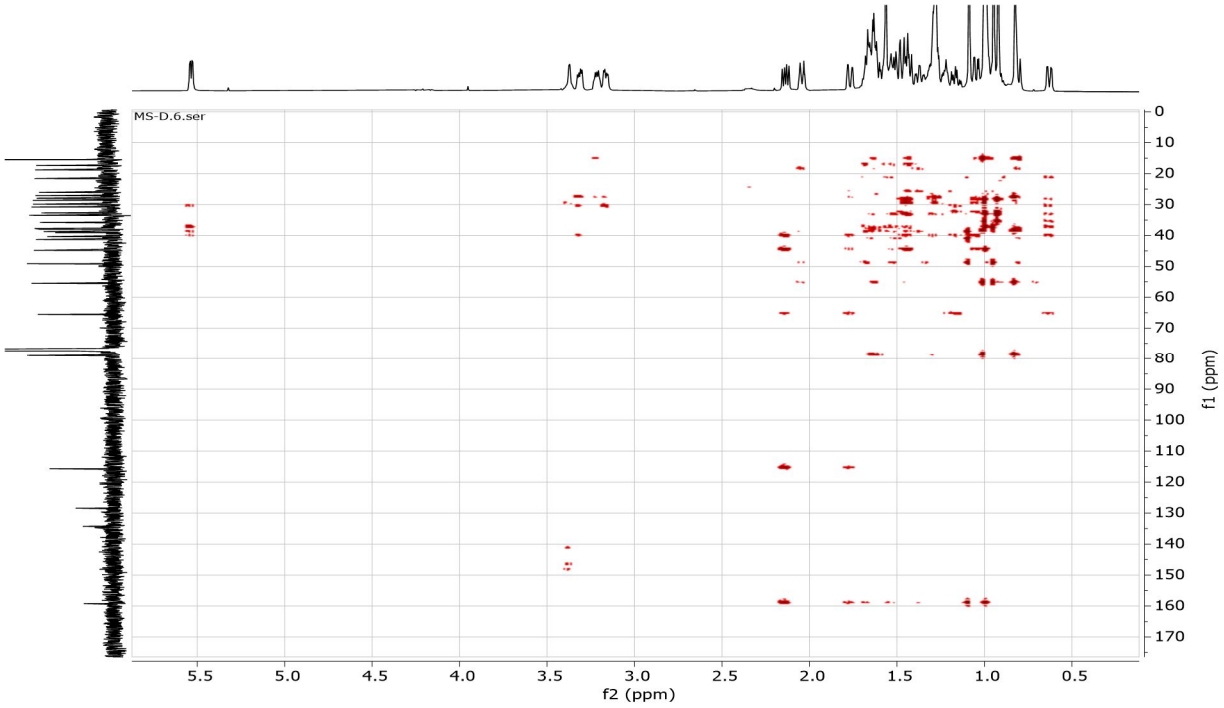

Appendix 75: NOES Spectrum of Compound **83**

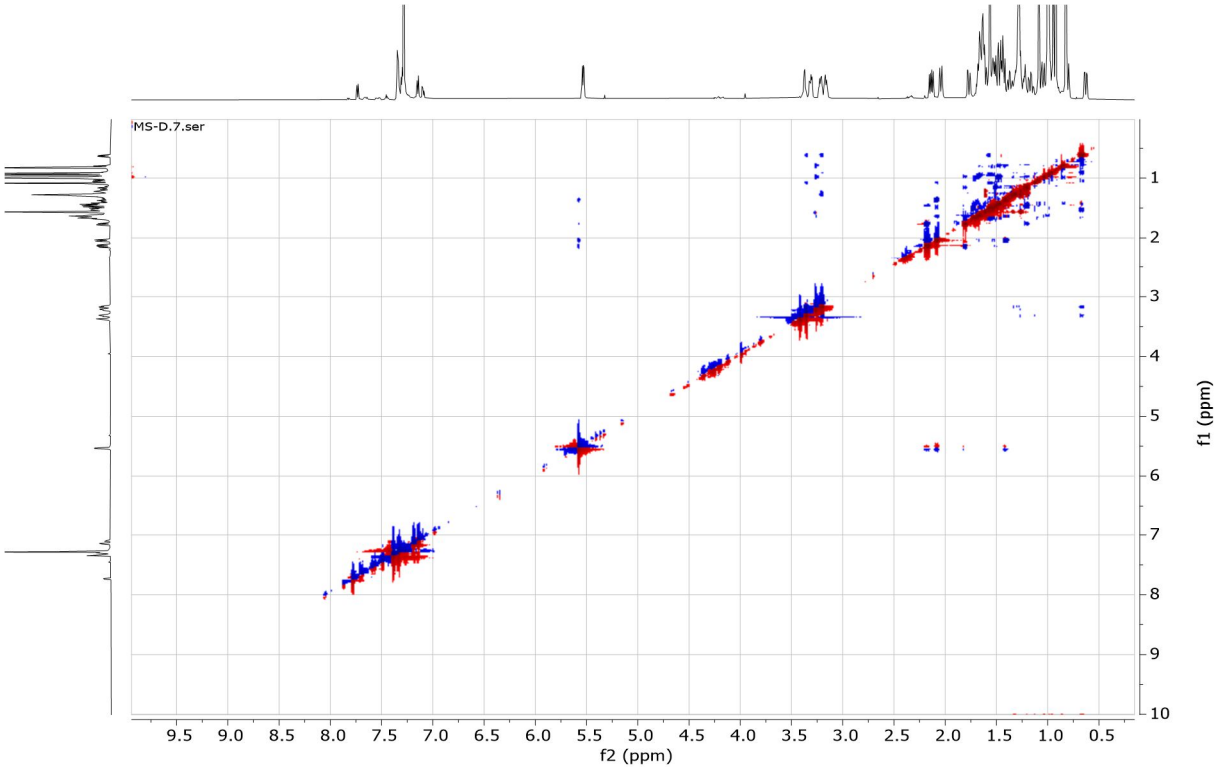

Appendix 76: MALDI-MS Spectrum of Compound **83**

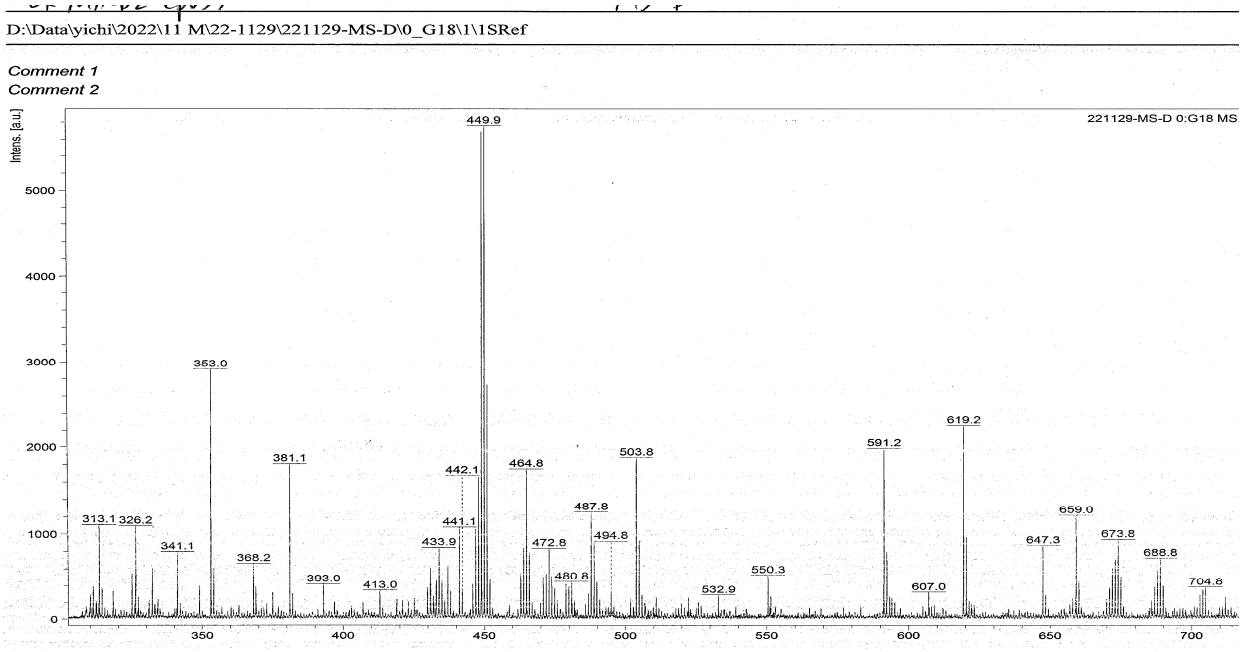

Appendix 77: ^{1}H-NMR (600 MHz, DMSO) Spectrum of Compound **84**

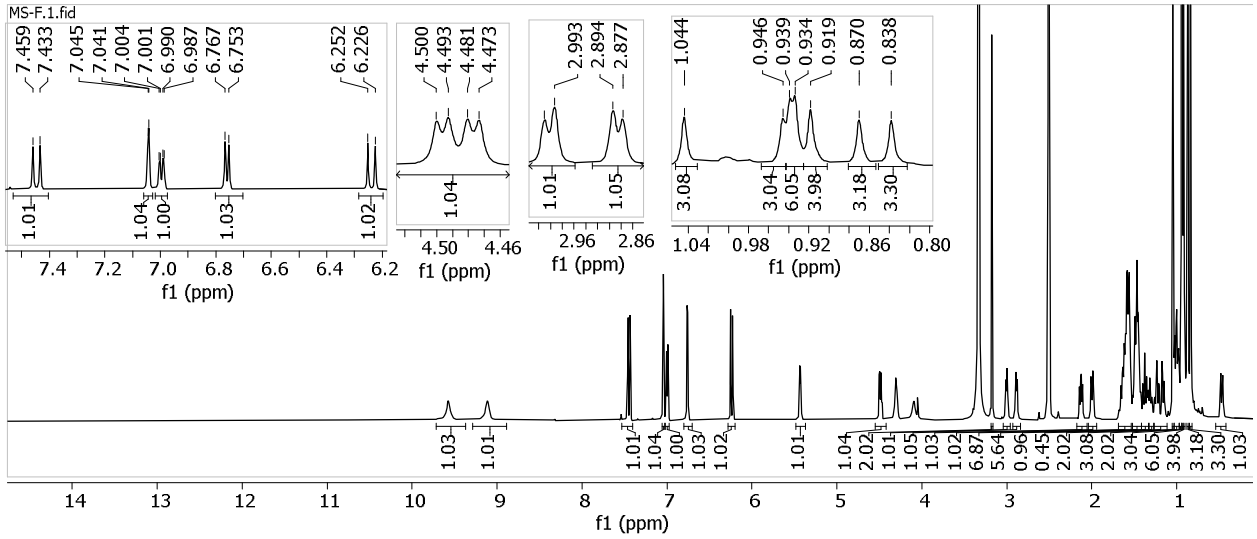

Appendix 78: ^{13}C-NMR (151 MHz, DMSO) Spectrum of Compound **84**

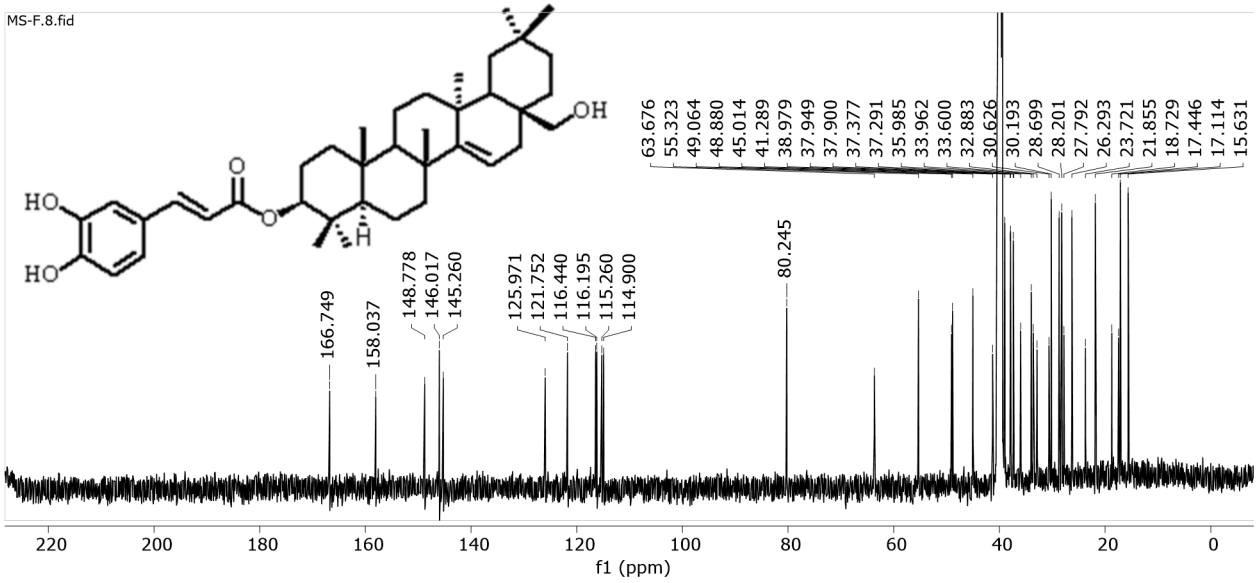

Appendix 79: DEPT-135 Spectrum of Compound **84**

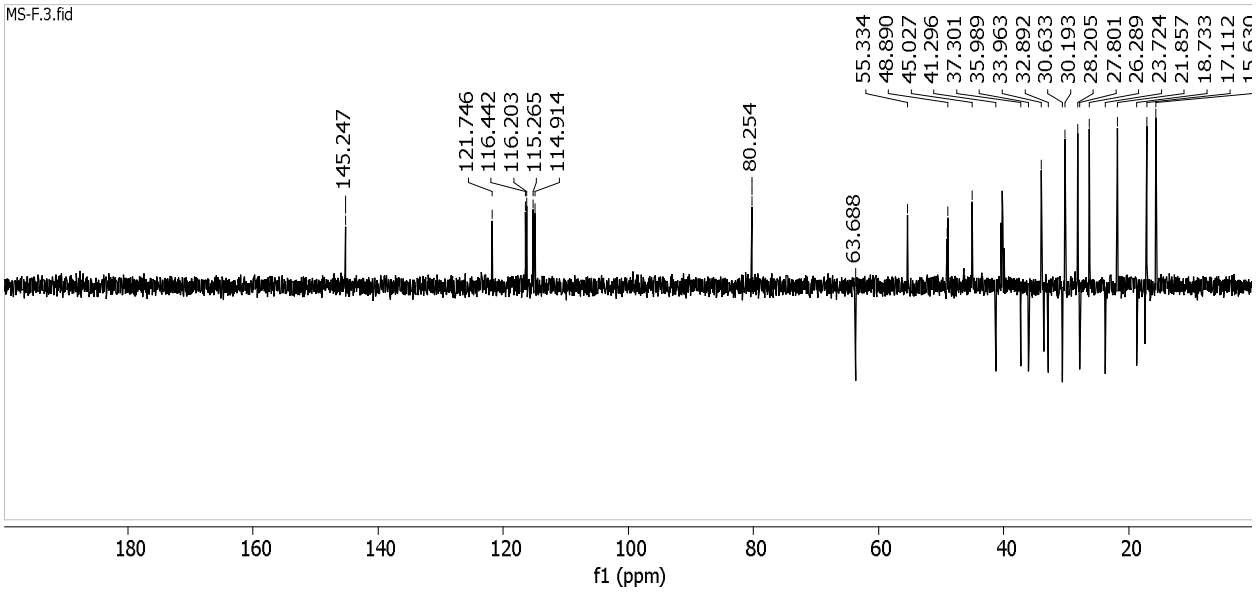

Appendix 80: ^{1}H-^{1}H COSY Spectrum of Compound **84**

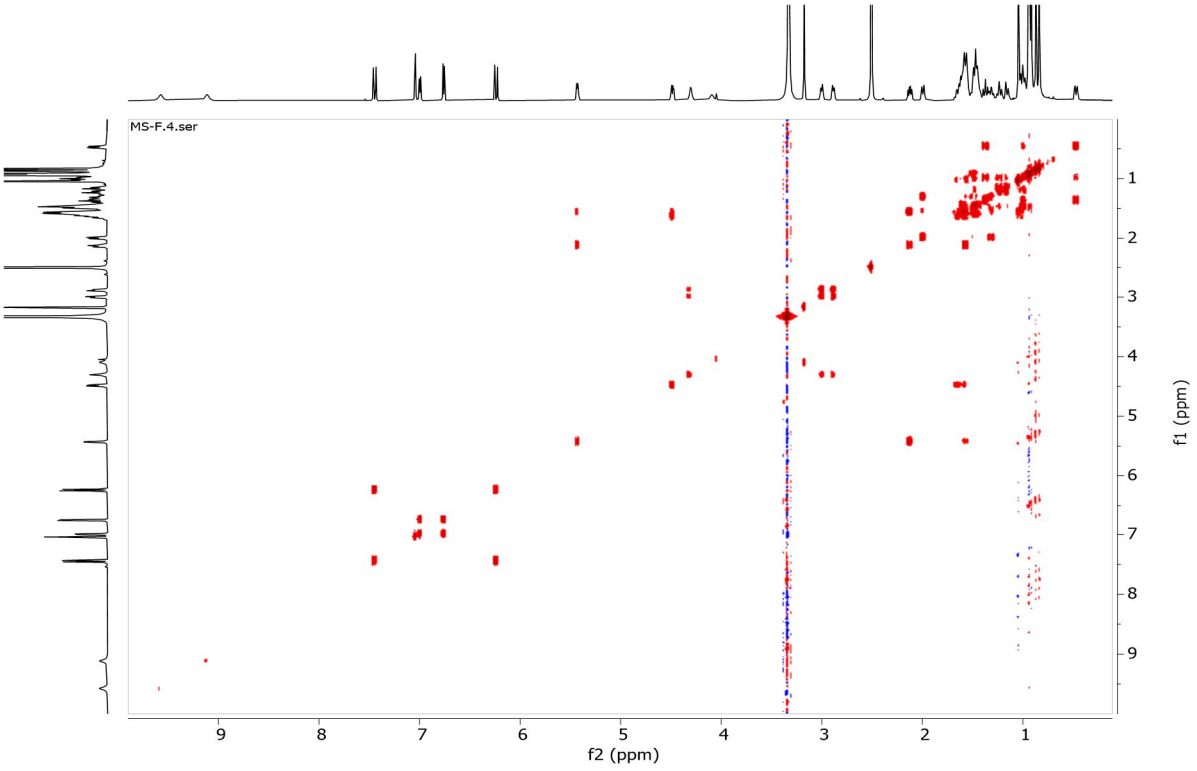

Appendix 81: HSQC Spectrum of Compound **84**

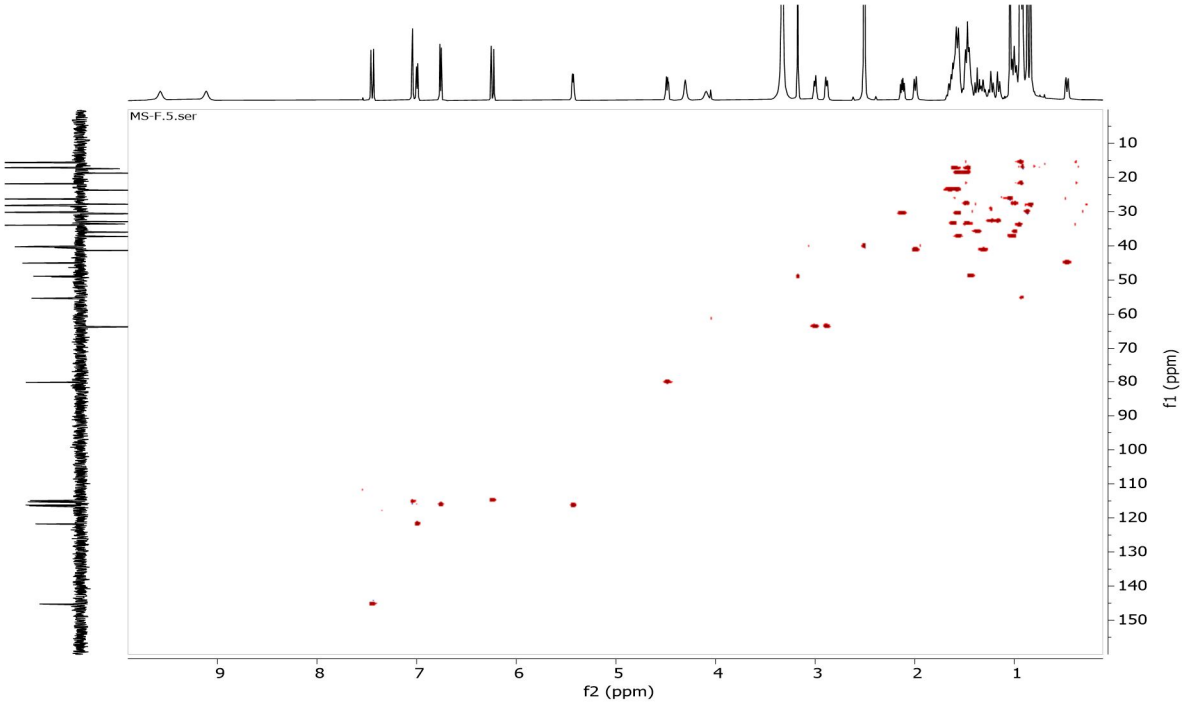

Appendix 82: HMBC Spectrum of Compound **84**

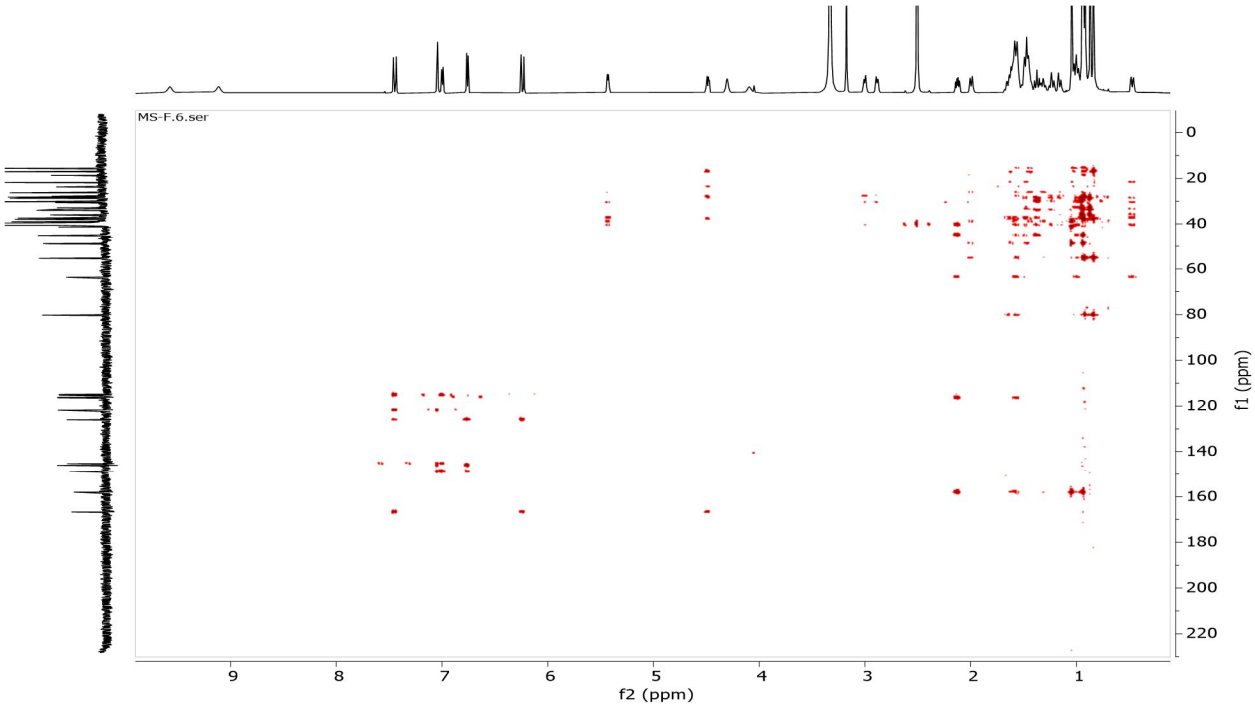

Appendix 83: NOES Spectrum of Compound **84**

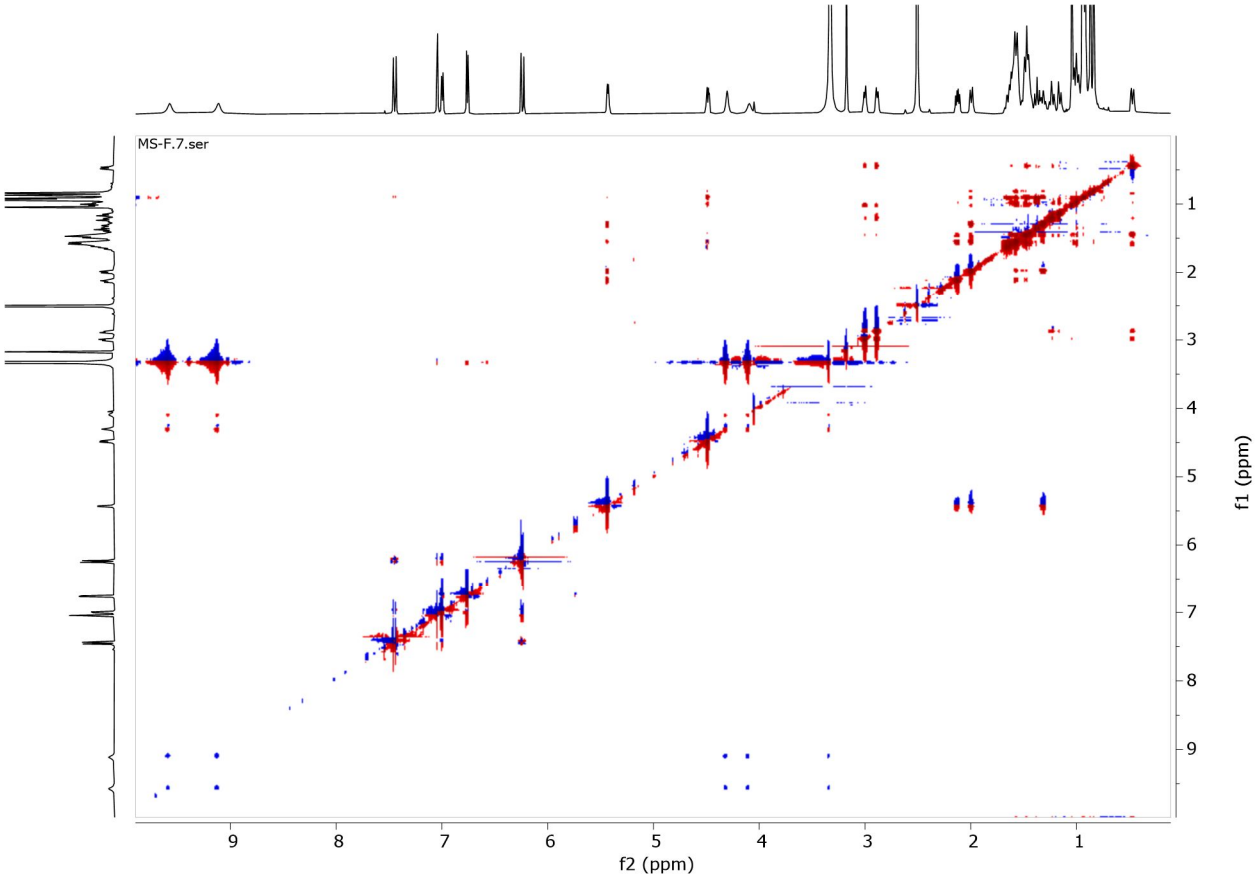

Appendix 84: MALDI-MS Spectrum of Compound **84**

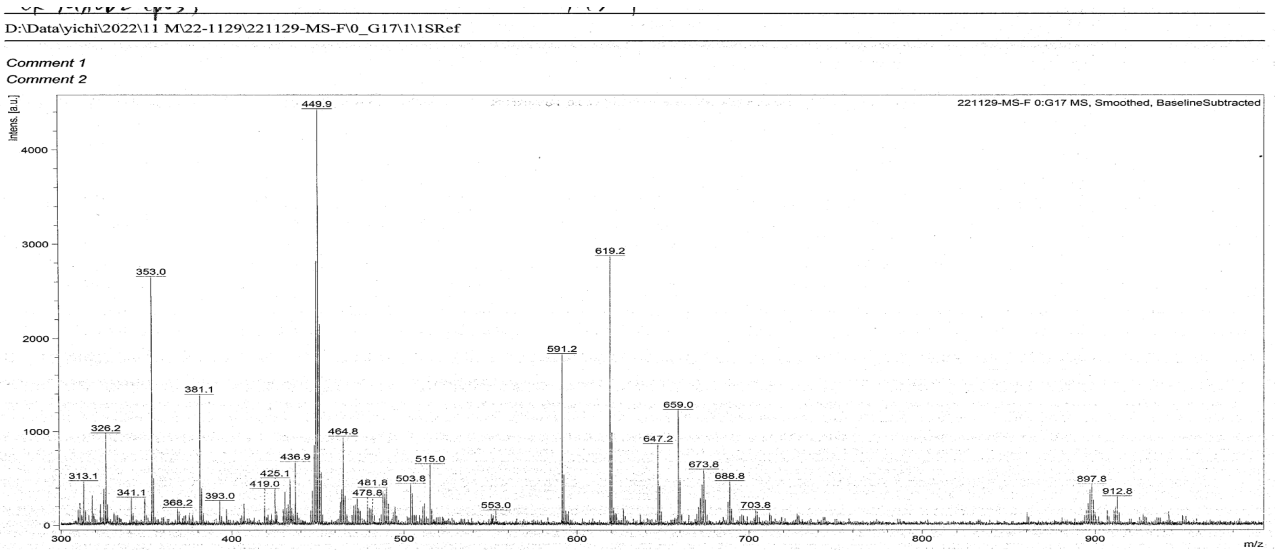

Appendix 85: FT-IR Spectrum of Compound **78**

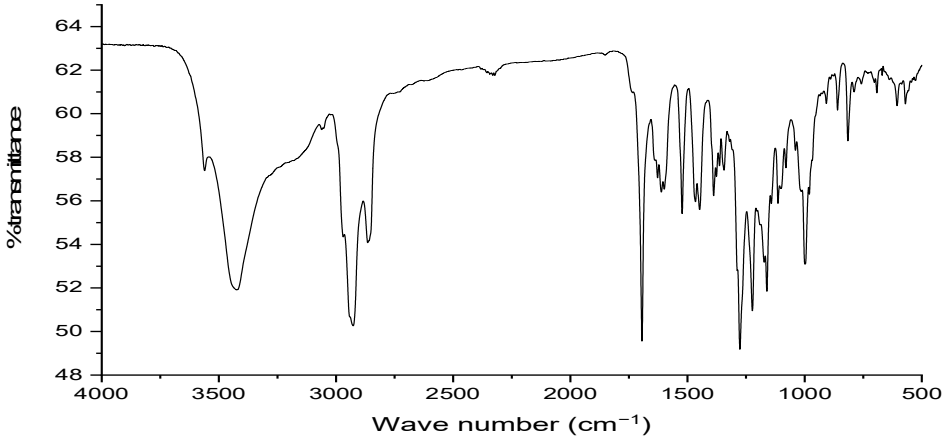

Appendix 86: ^{1}H-NMR (600 MHz, MeOD) Spectrum of Compound **85**

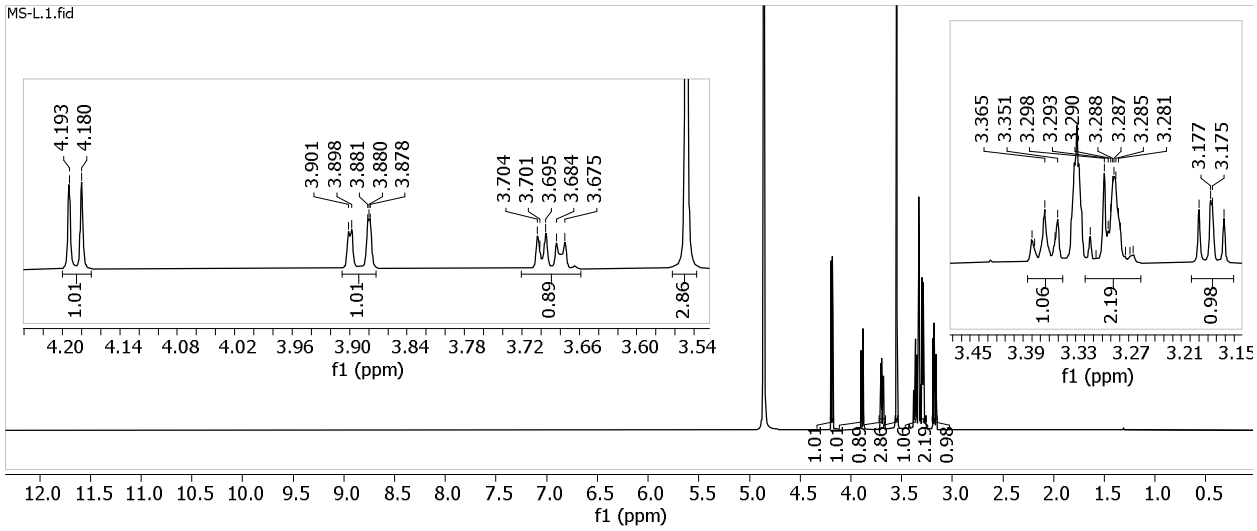

Appendix 87: ^{13}C-NMR (151 MHz, MeOD) Spectrum of Compound **85**

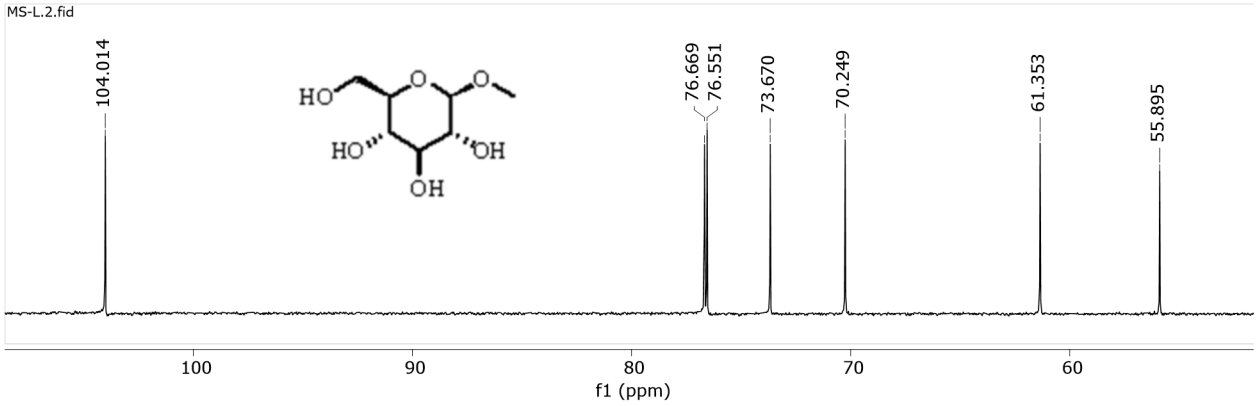

Appendix 88: DEPT-135 Spectrum of Compound **85**

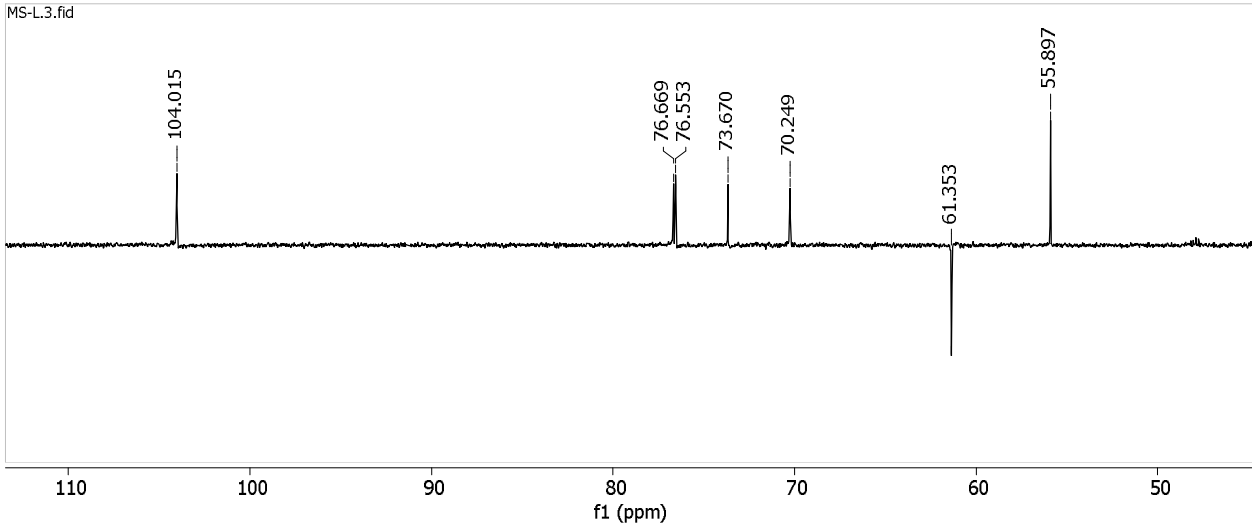

Appendix 89: ^{1}H-^{1}H COSY Spectrum of Compound **85**

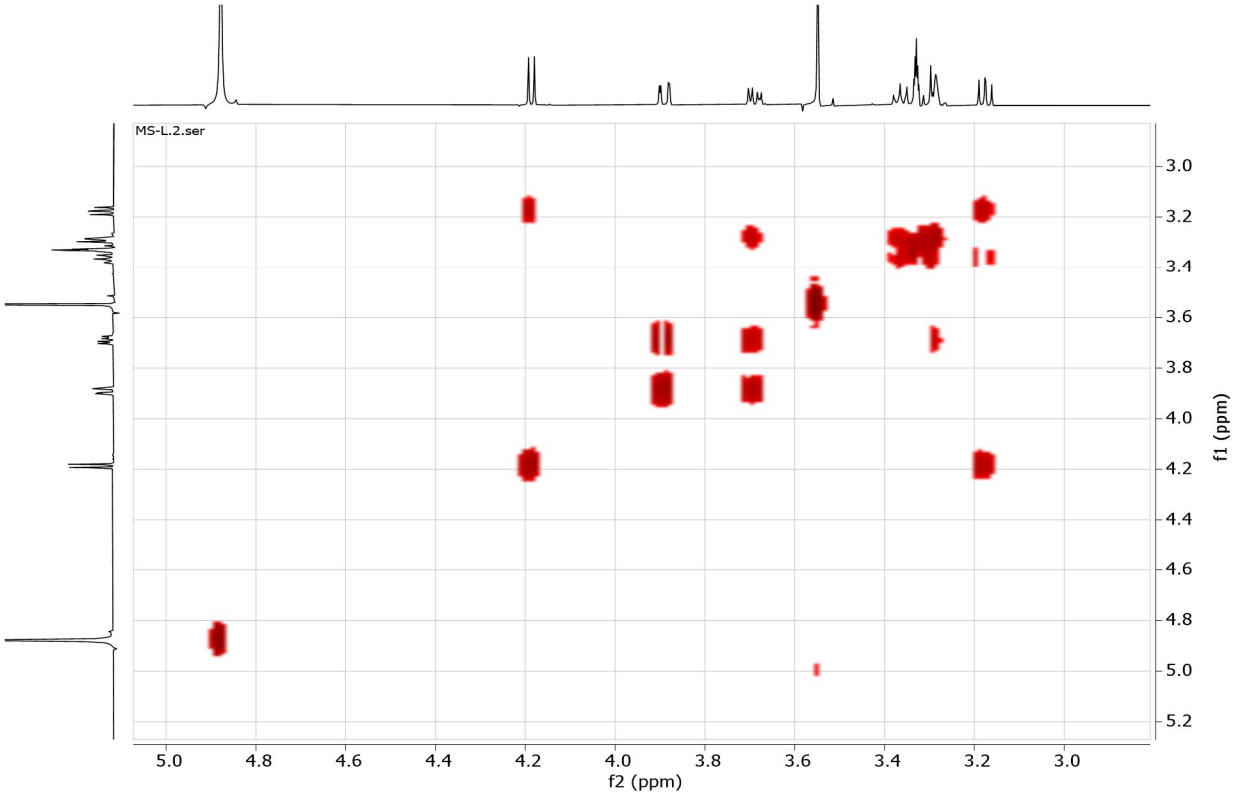

Appendix 90: HSQC Spectrum of Compound **85**

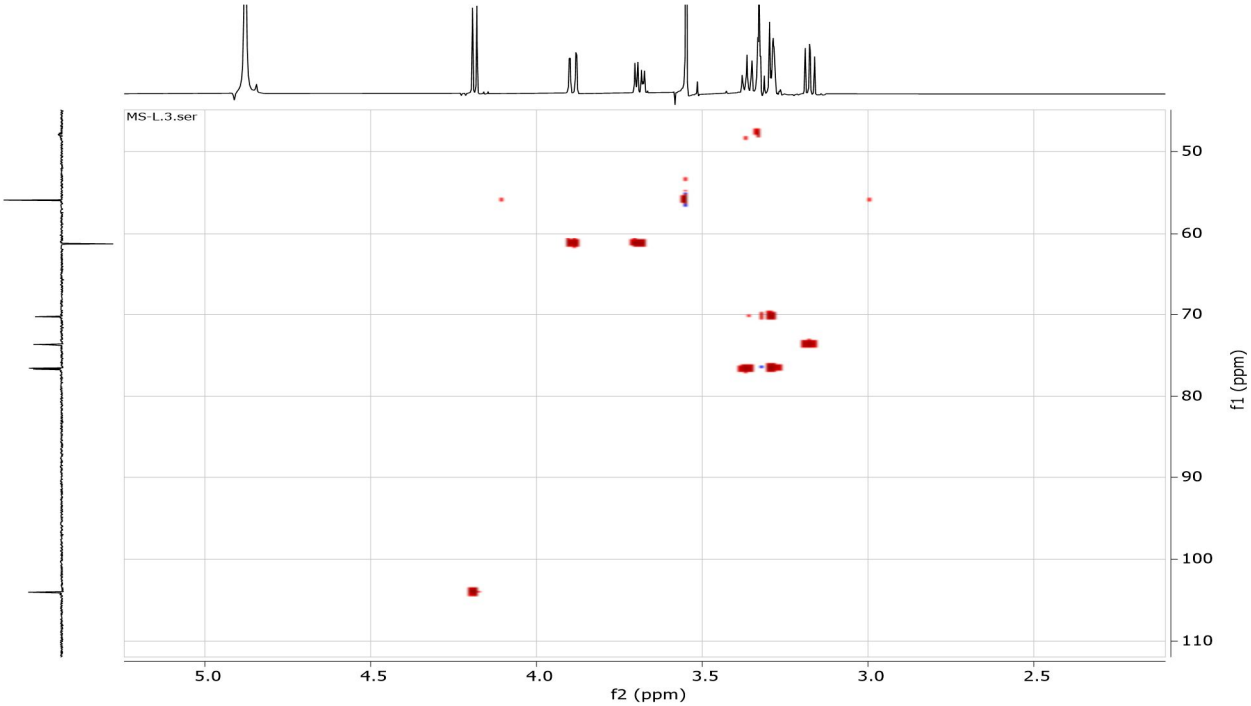

Appendix 91: HMBC Spectrum of Compound **85**

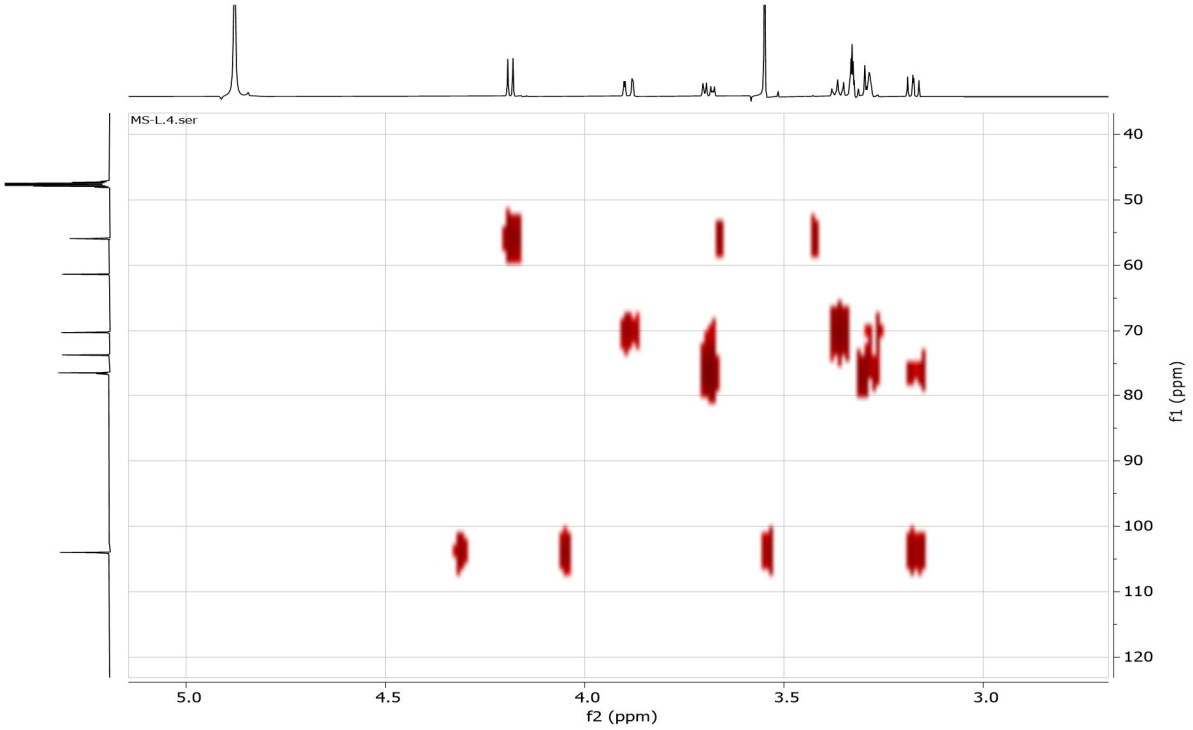

Appendix 92: HPLC-MS Spectrum of Compound **85**

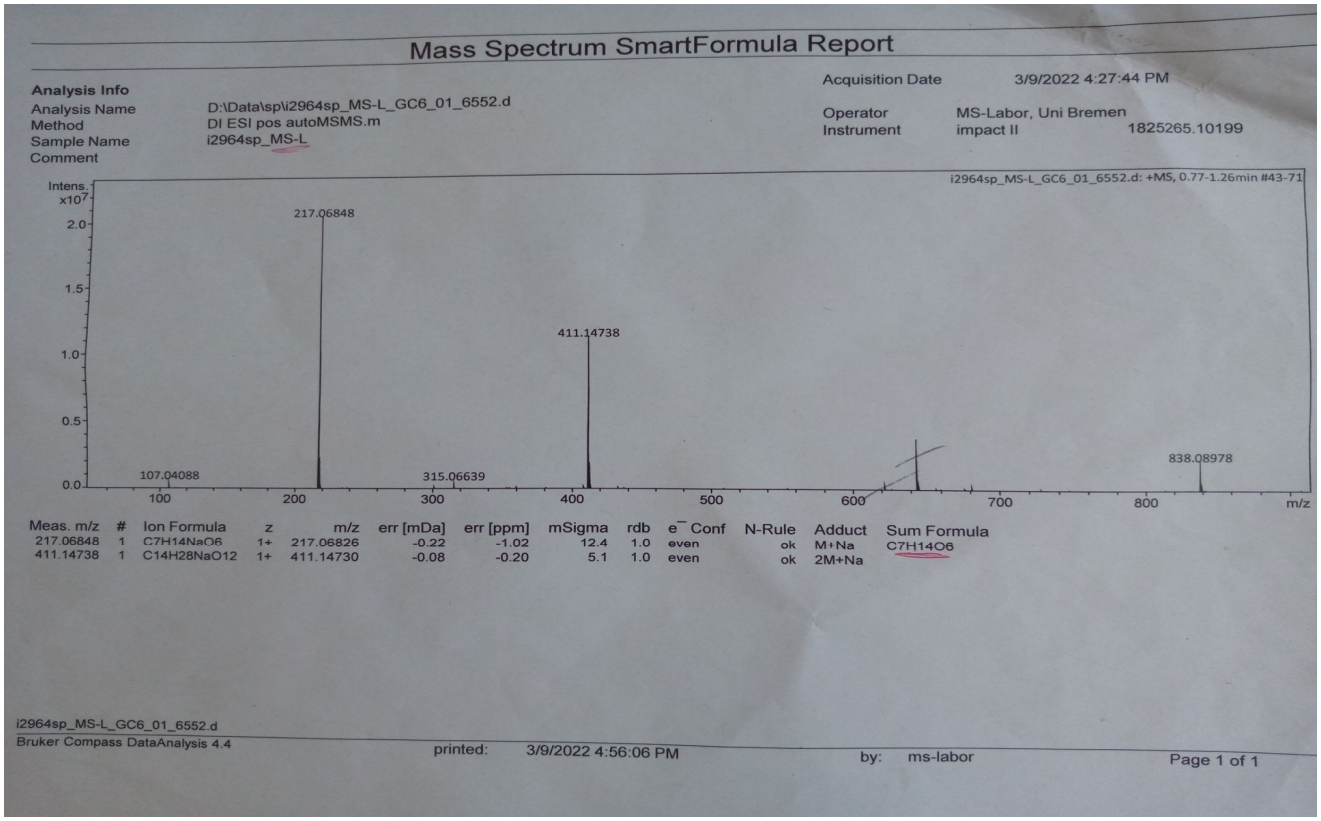

Appendix 93: ^{1}H-NMR (600 MHz, MeOD) Spectrum of Compound **86**

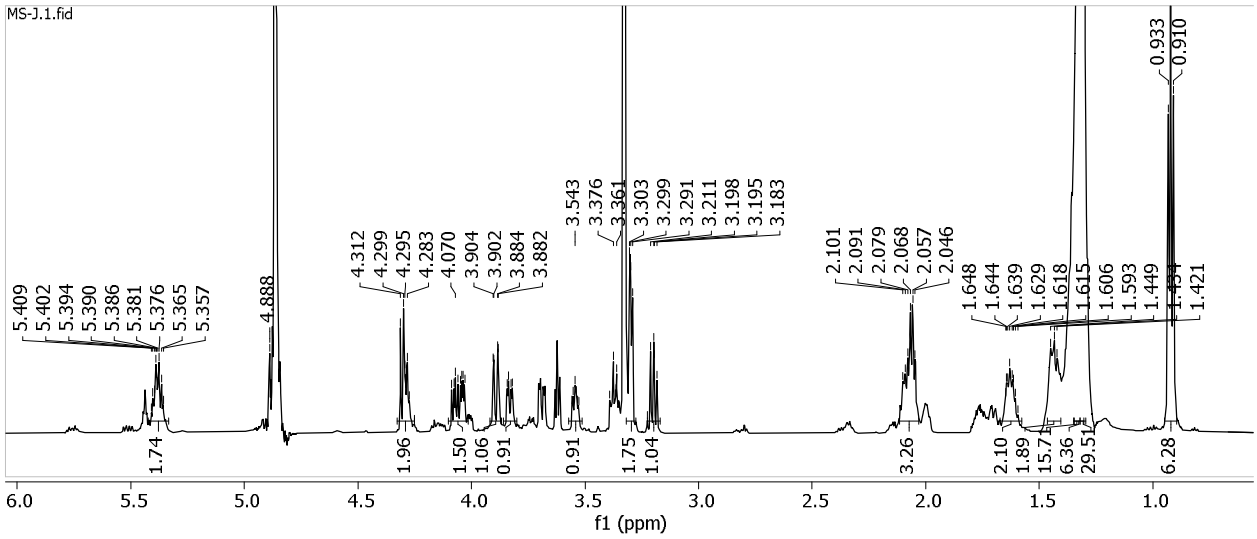

Appendix 94: ^{13}C-NMR (151 MHz, MeOD) Spectrum of Compound **86**

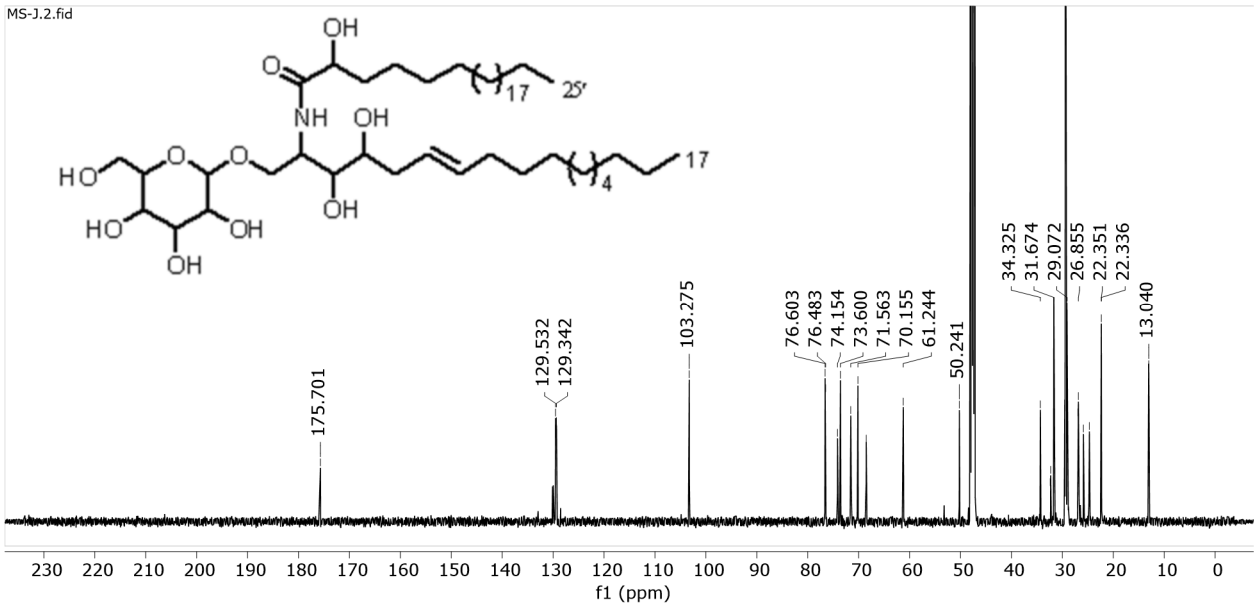

Appendix 95: DEPT-135 Spectrum of Compound **86**

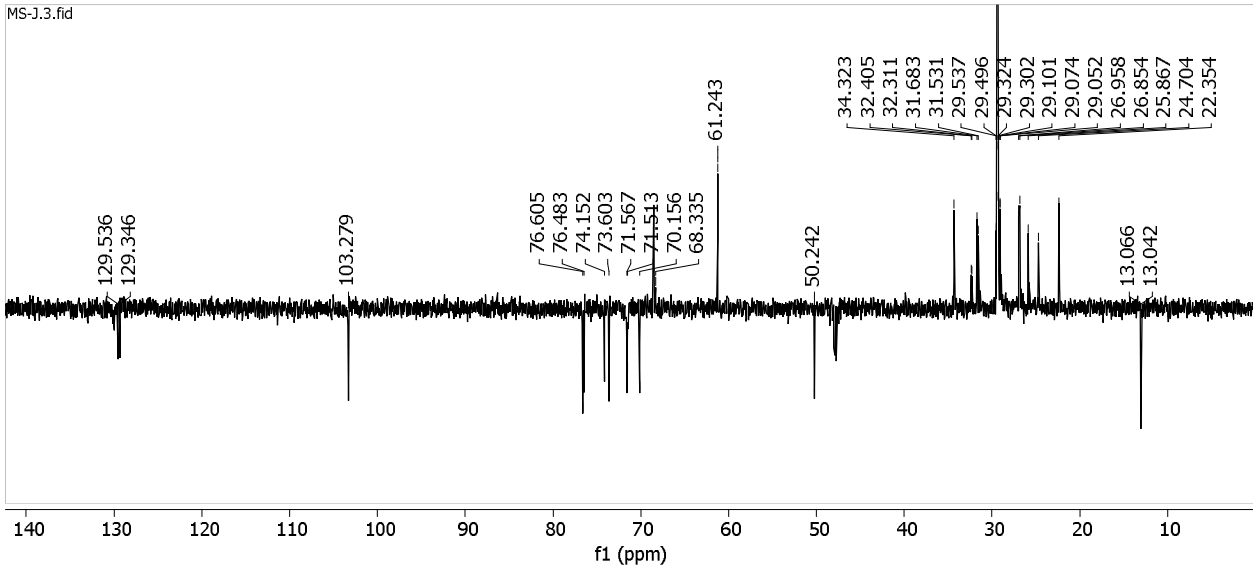

Appendix 96: ^{1}H-^{1}H COSY Spectrum of Compound **86**

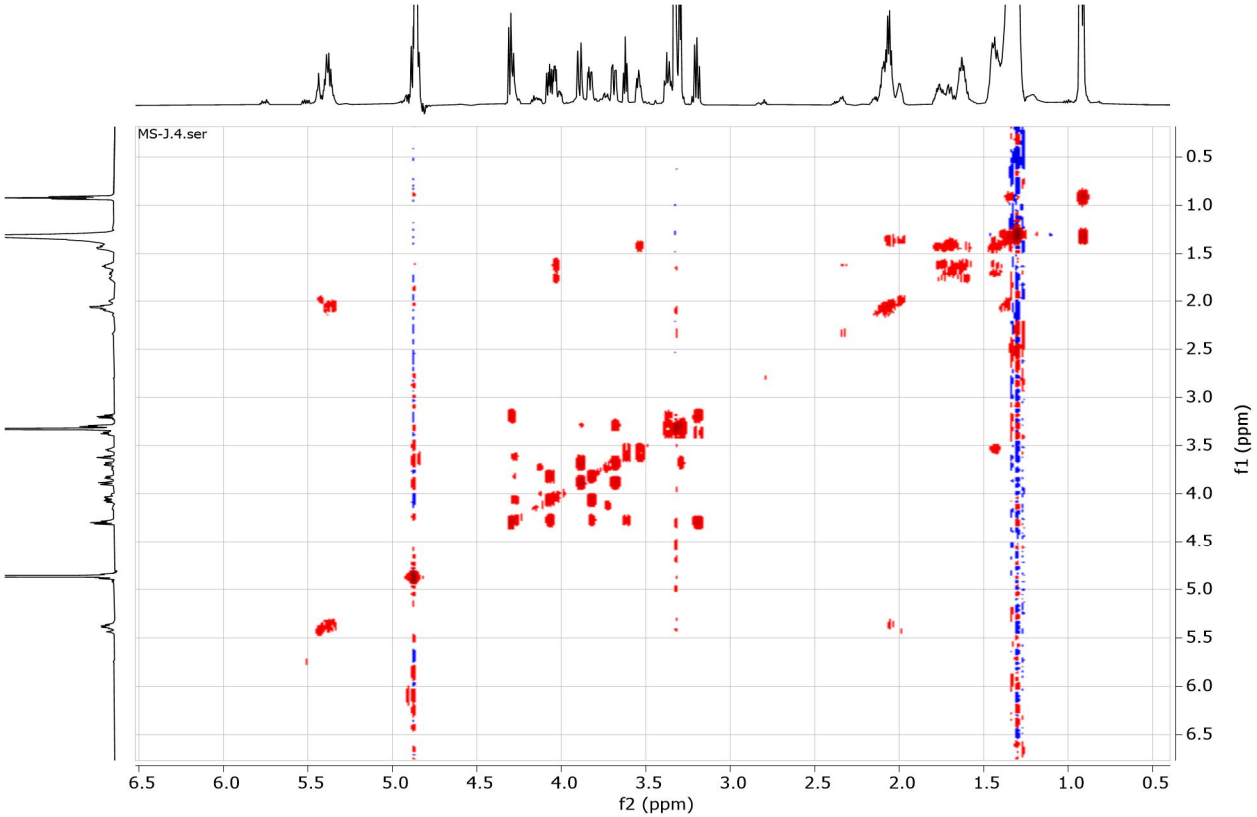

Appendix 97: HSQC Spectrum of Compound **86**

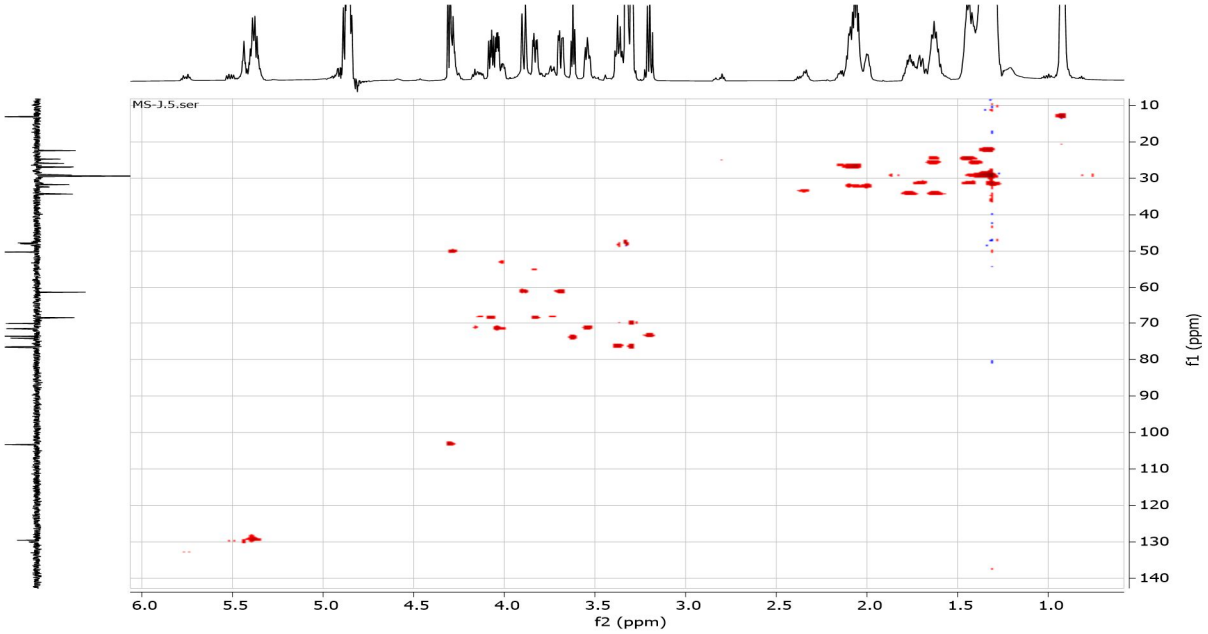

Appendix 98: HMBC Spectrum of Compound **86**

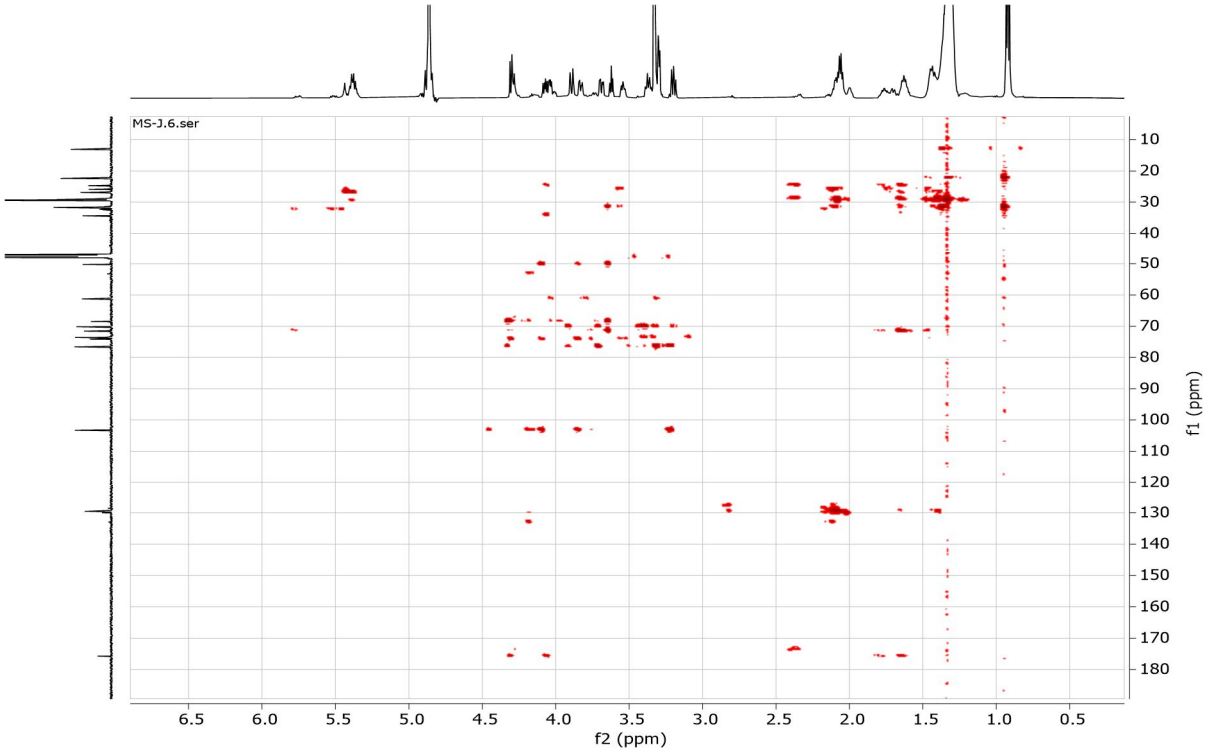

Appendix 99: ^{1}H-NMR (600 MHz, $CDCl_3$) Spectrum of Compound **82**

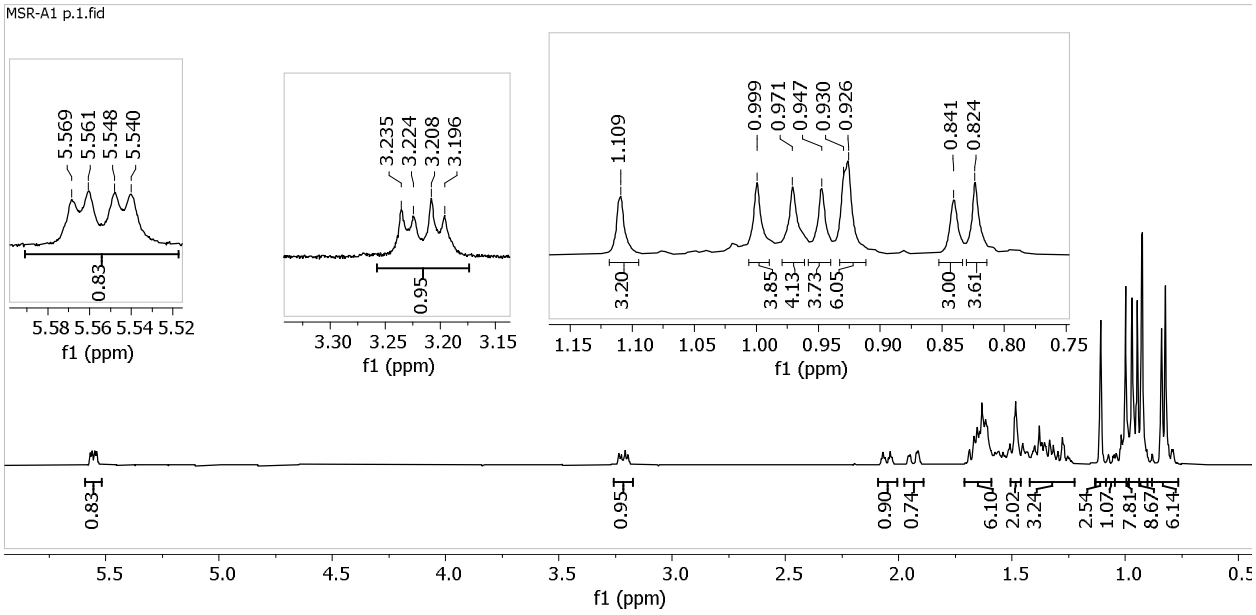

Appendix 100: ^{13}C-NMR (100 MHz, $CDCl_3$) Spectrum of Compound **82**

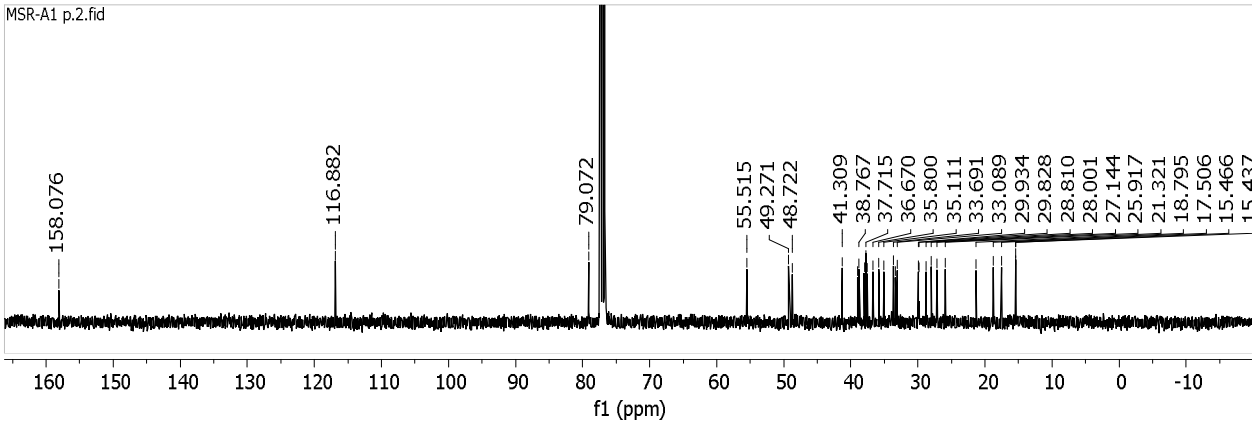

Appendix 101: DEPT-135 Spectrum of Compound **82**

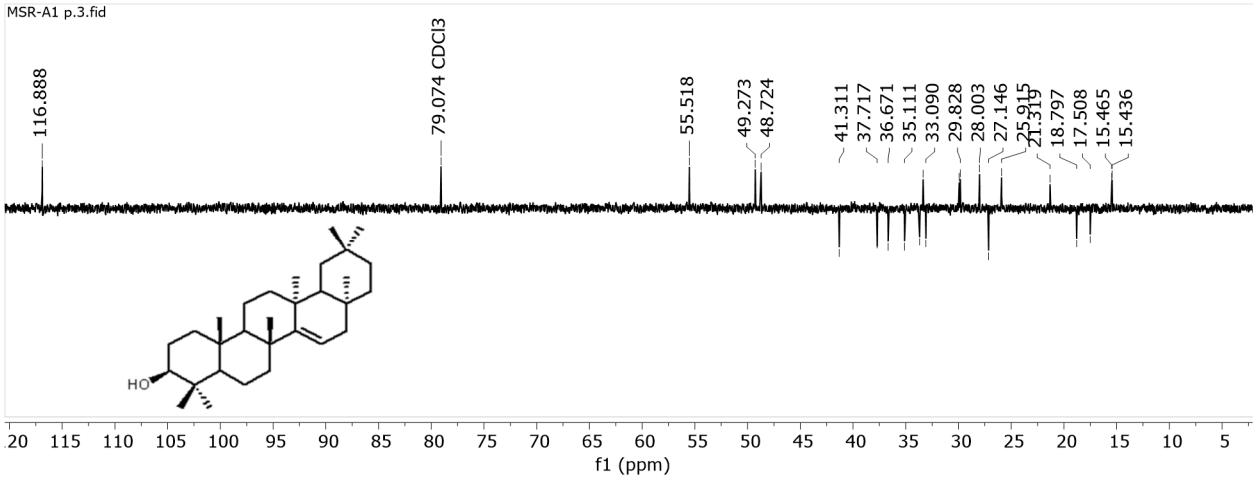

Appendix 102: ^{1}H-^{1}H COSY Spectrum of Compound **82**

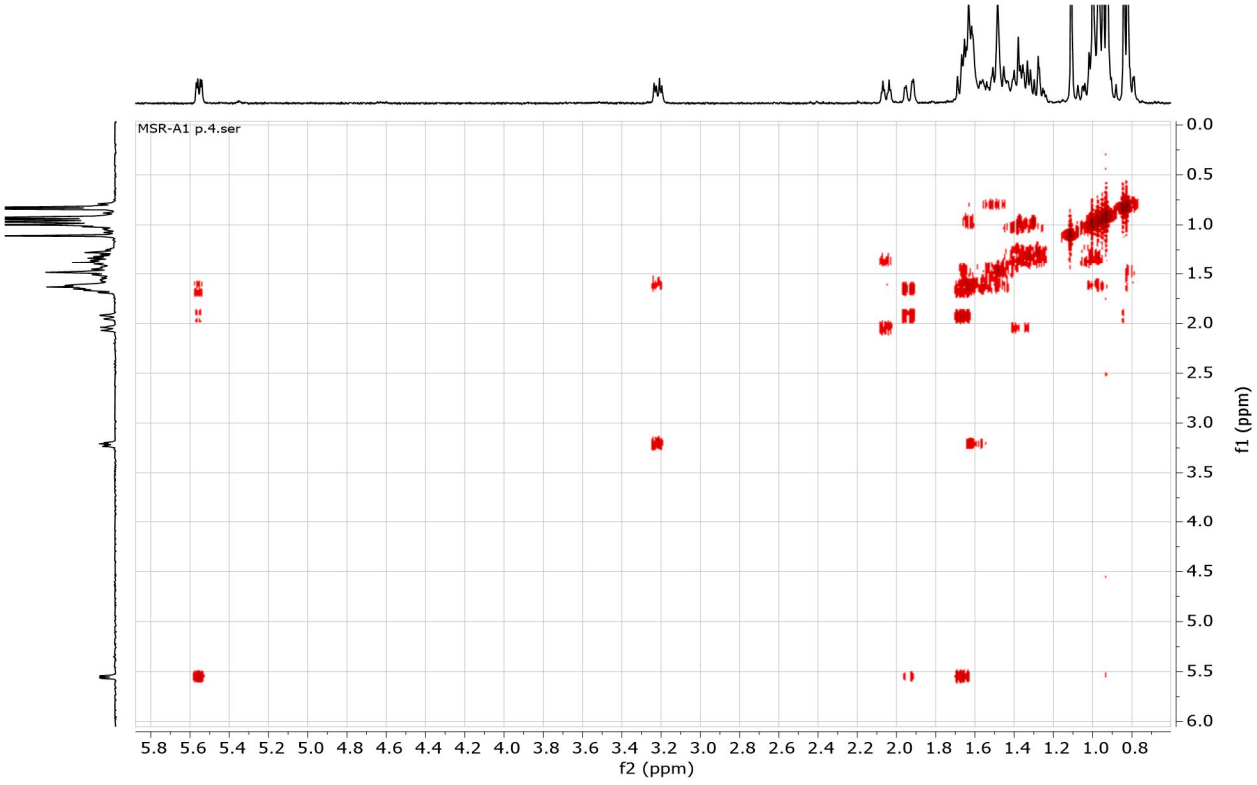

Appendix 103: HSQC Spectrum of Compound **82**

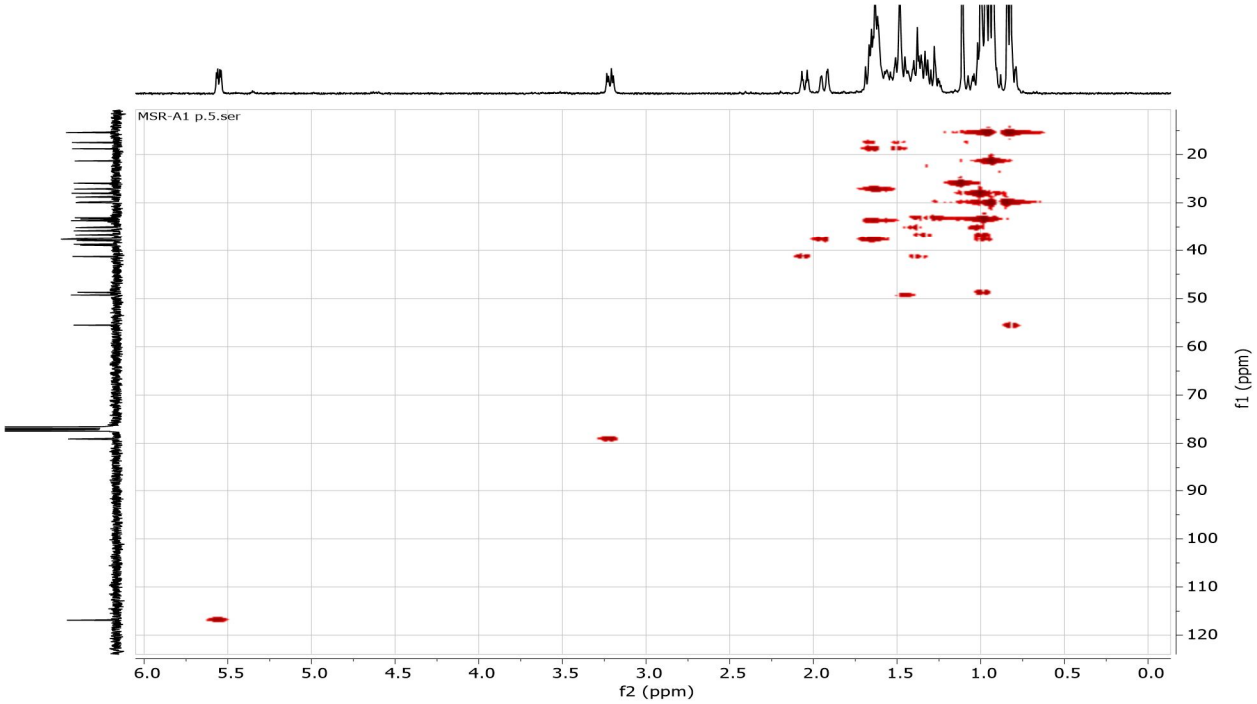

Appendix 104: HMBC Spectrum of Compound **82**

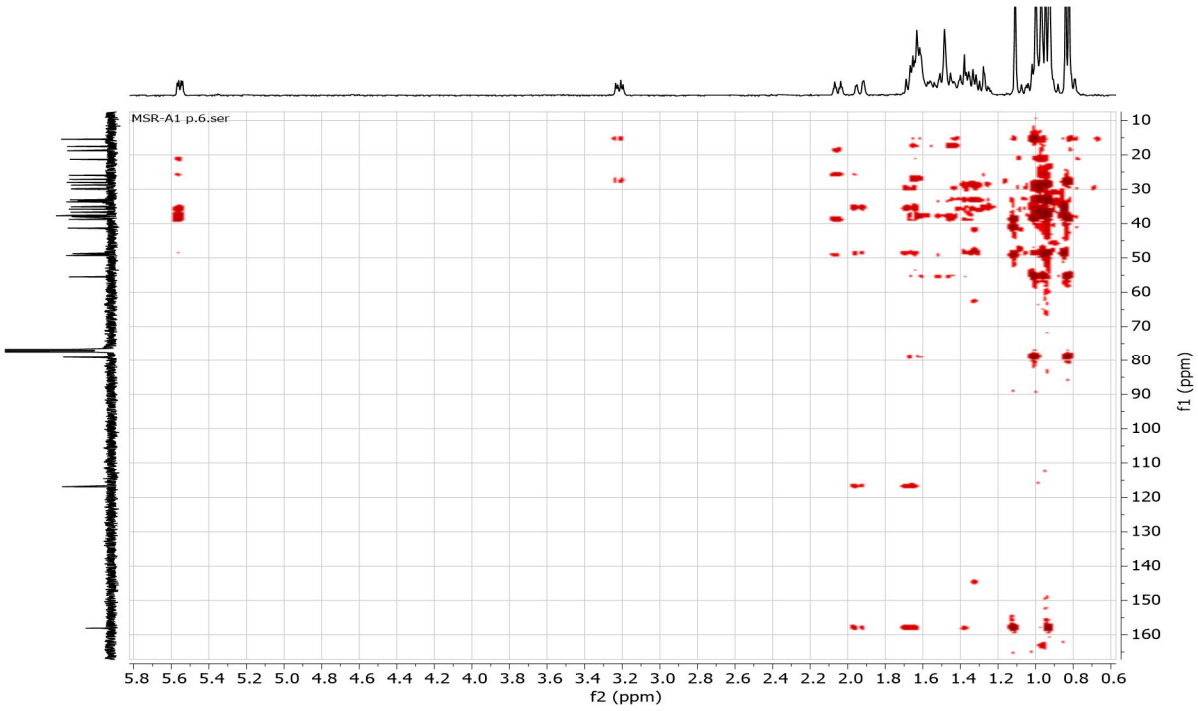

Appendix 105: TOF-MS Spectrum of Compound **82**

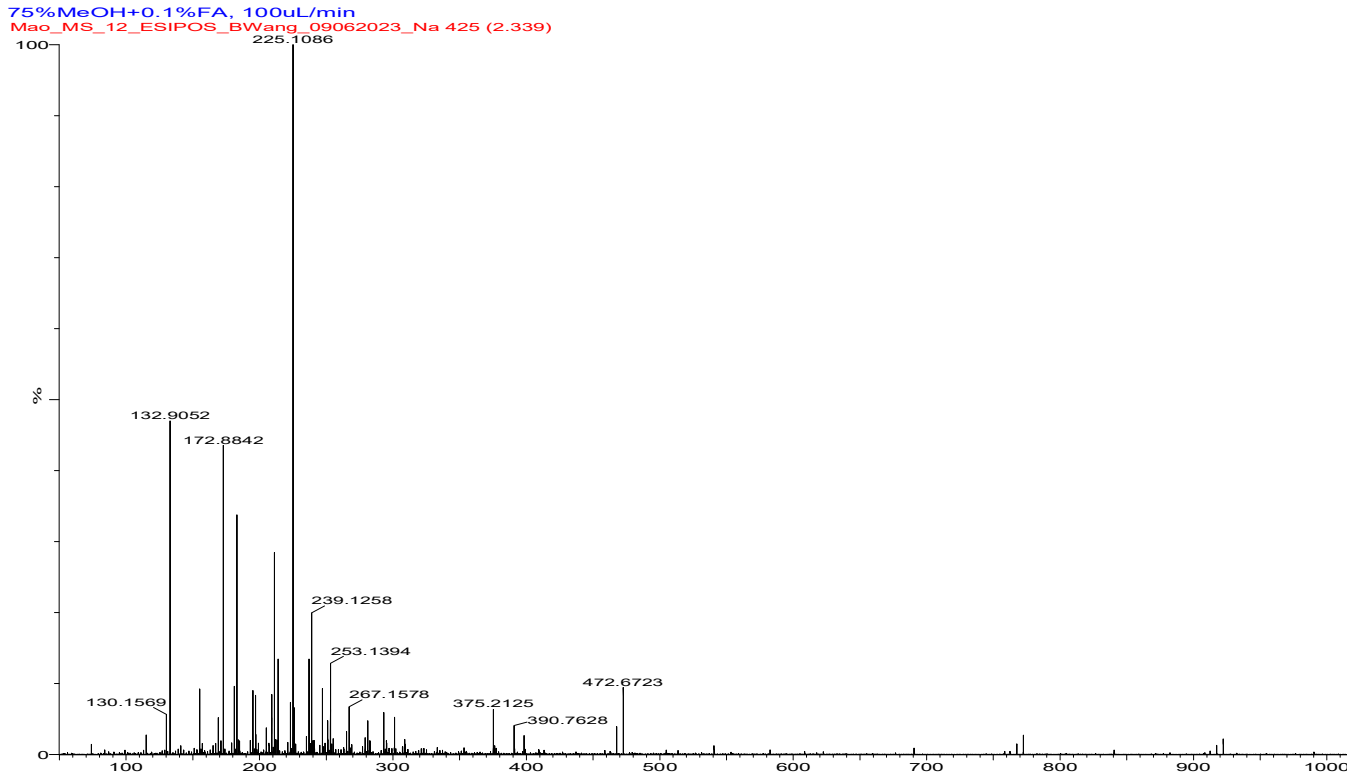

Appendix 106: ^{1}H-NMR (400 MHz, $CDCl_3$) Spectrum of Compound **80**

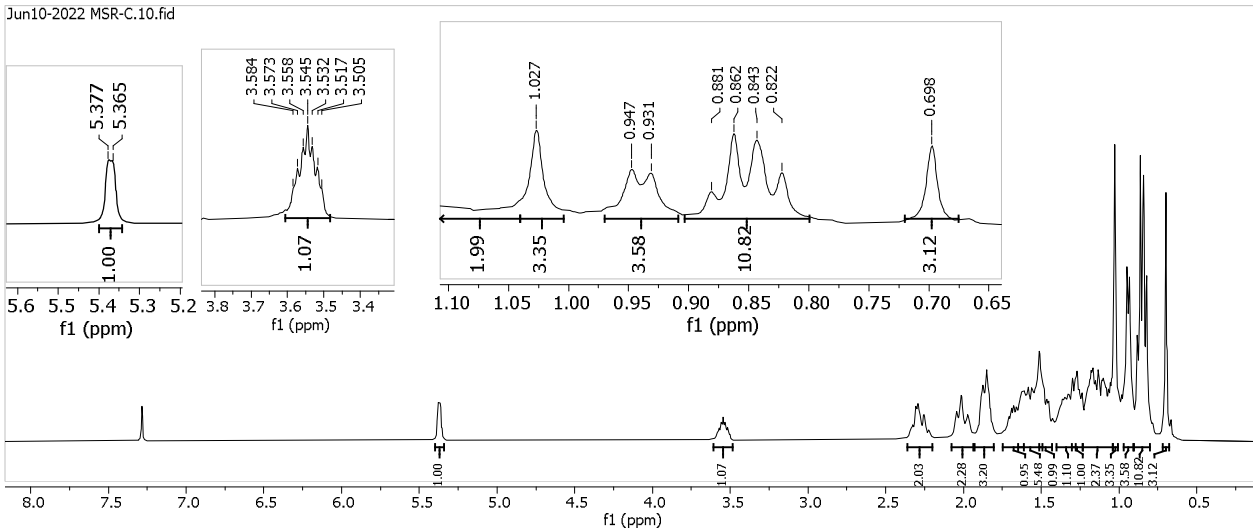

Appendix 107: ^{13}C-NMR (101 MHz, $CDCl_3$) Spectrum of Compound **80**

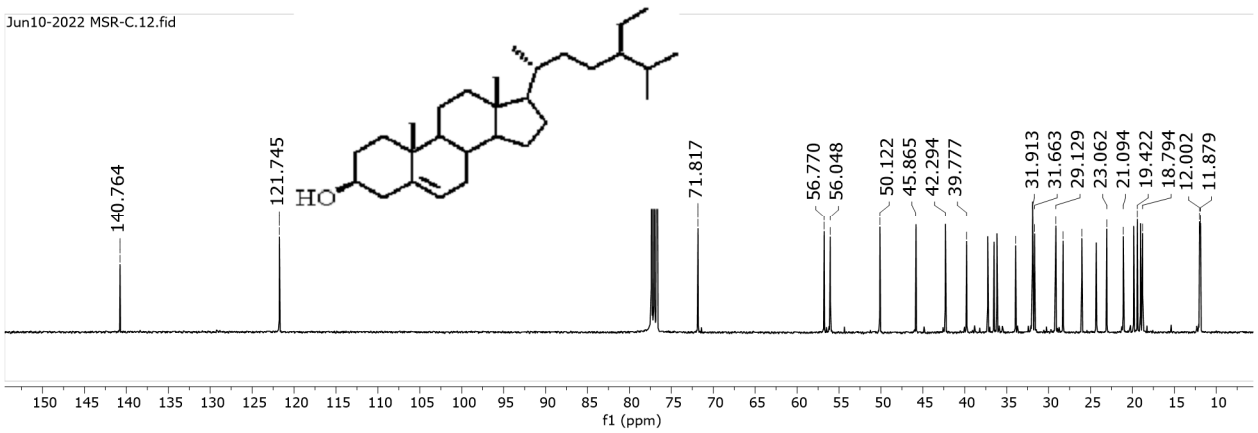

Appendix 108: DEPT-135 Spectrum of Compound **80**

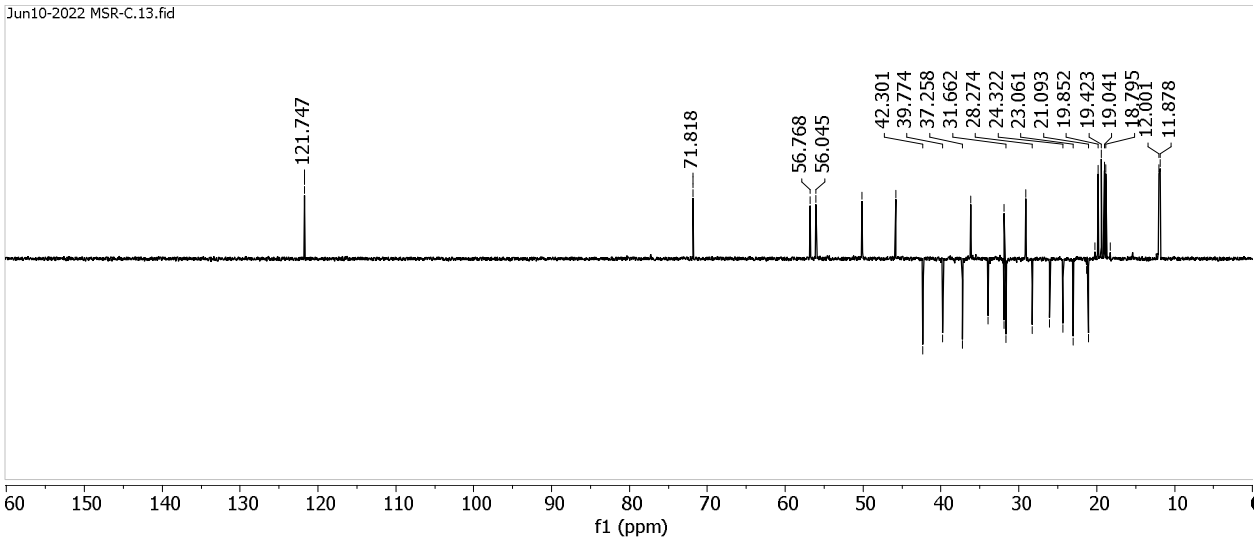

Appendix 109: ^{1}H-^{1}H COSY Spectrum of Compound **80**

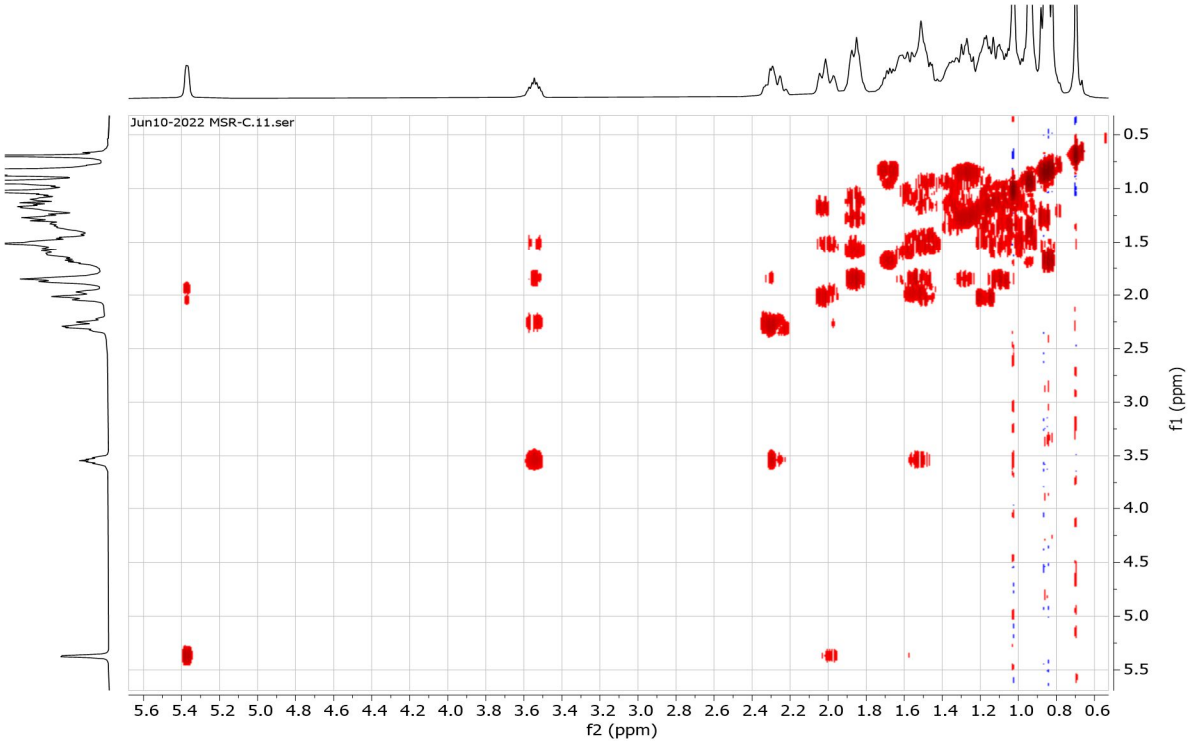

Appendix 110: HSQC Spectrum of Compound **80**

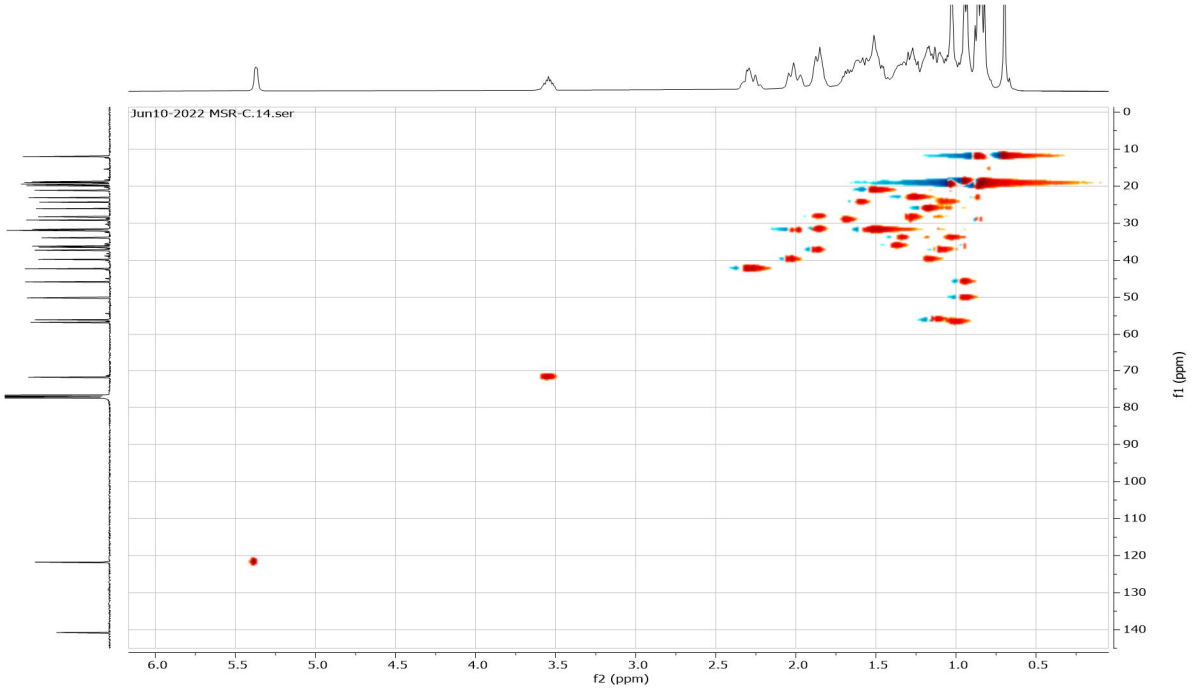

Appendix 111: HMBC Spectrum of Compound **80**

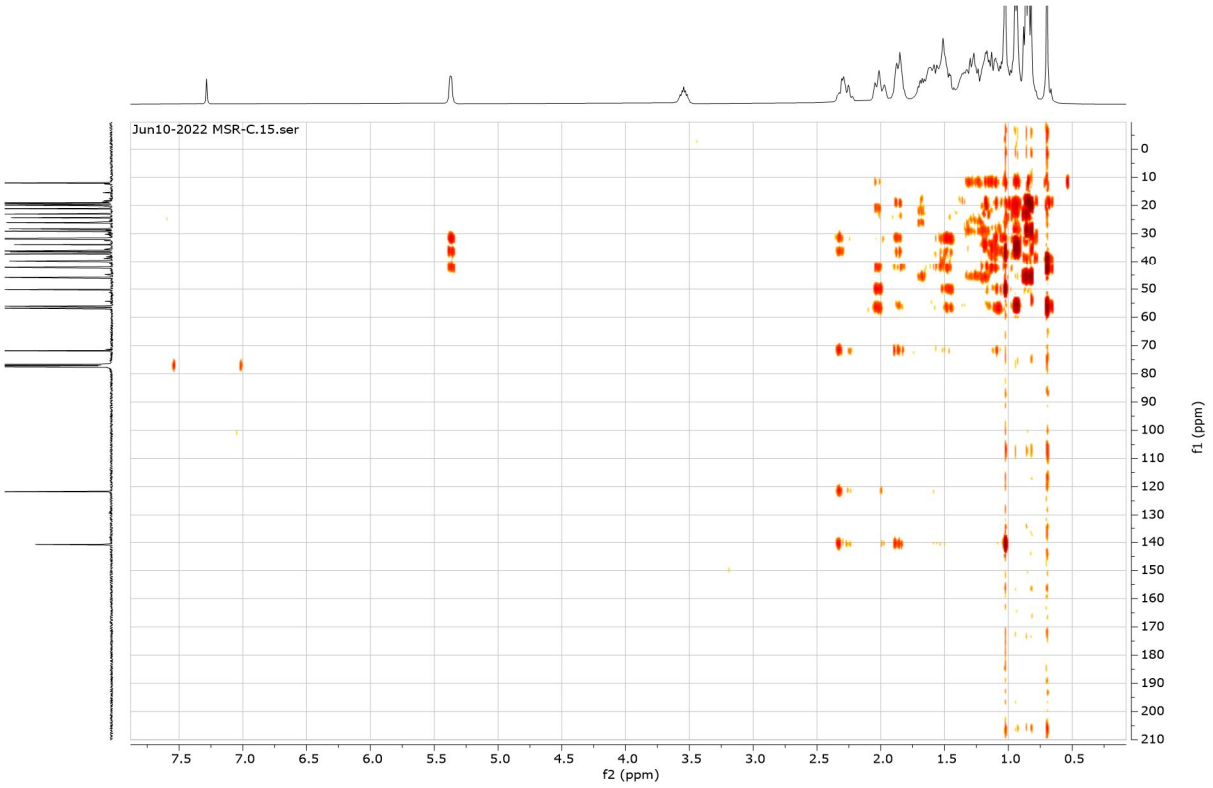

Appendix 112: TOF-MS Spectrum of Compound **80**

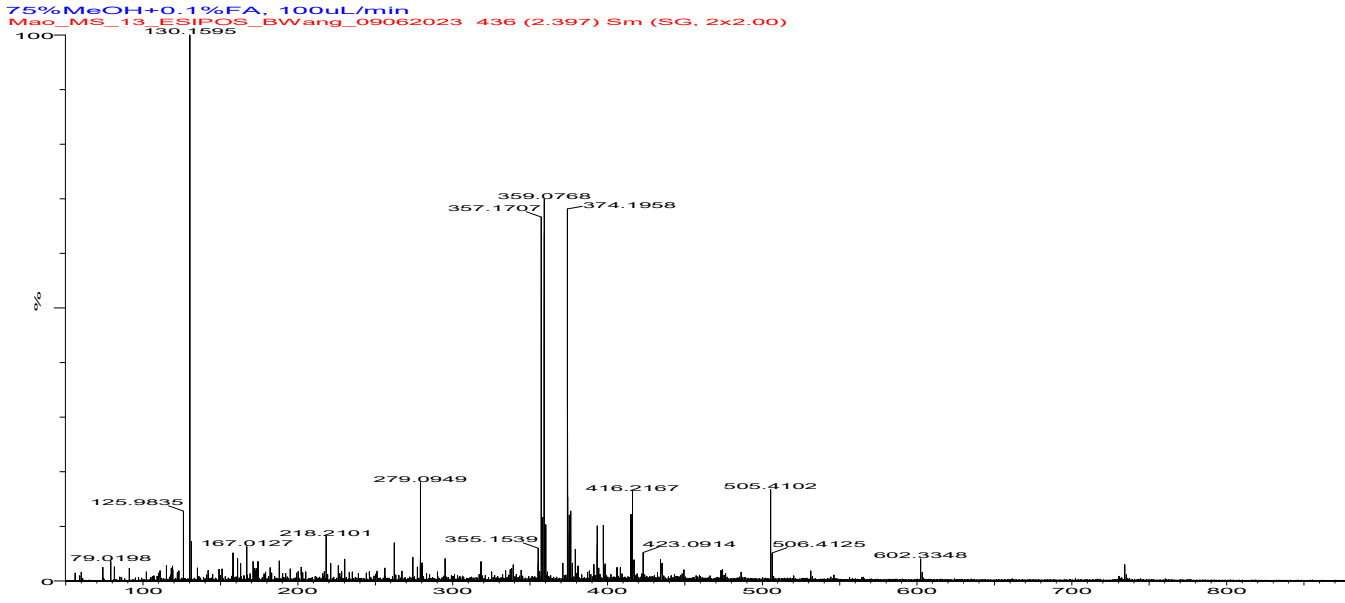

Appendix 113: ^{1}H-NMR (400 MHz, $CDCl_3$) Spectrum of Compound **87**

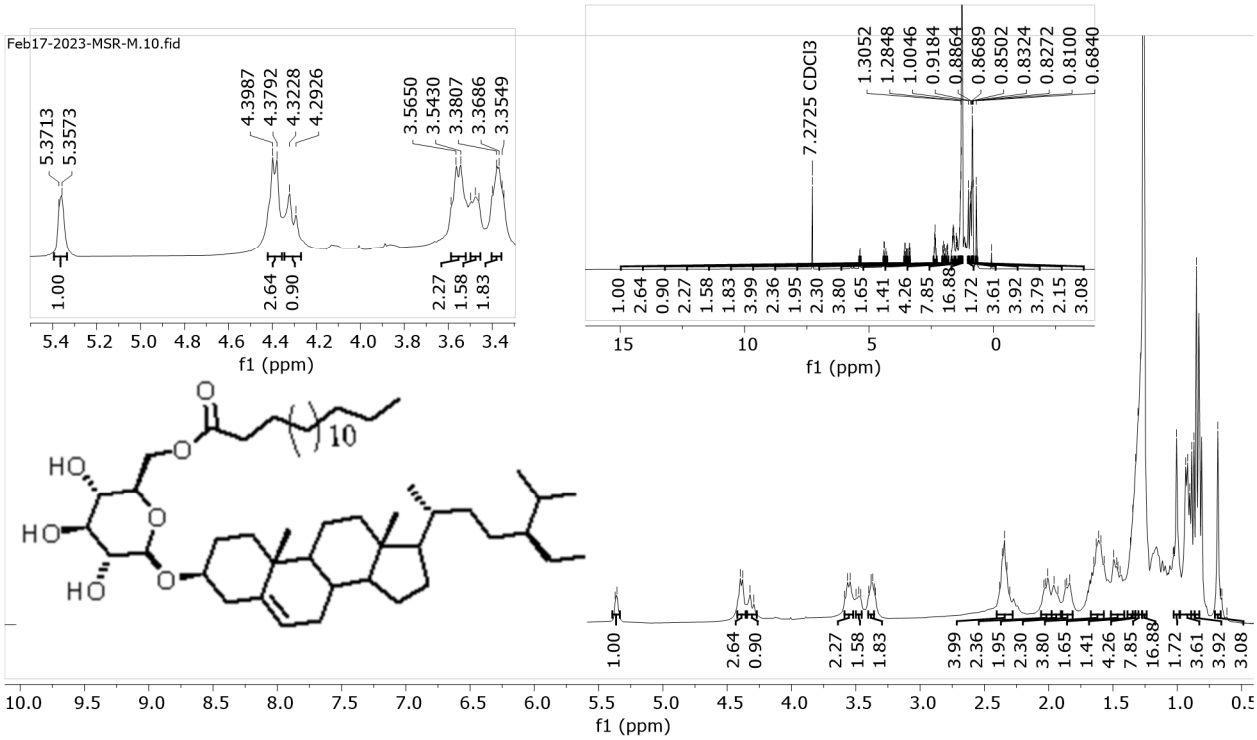

Appendix 114: ^{13}C-NMR (101 MHz, $CDCl_3$) Spectrum of Compound **87**

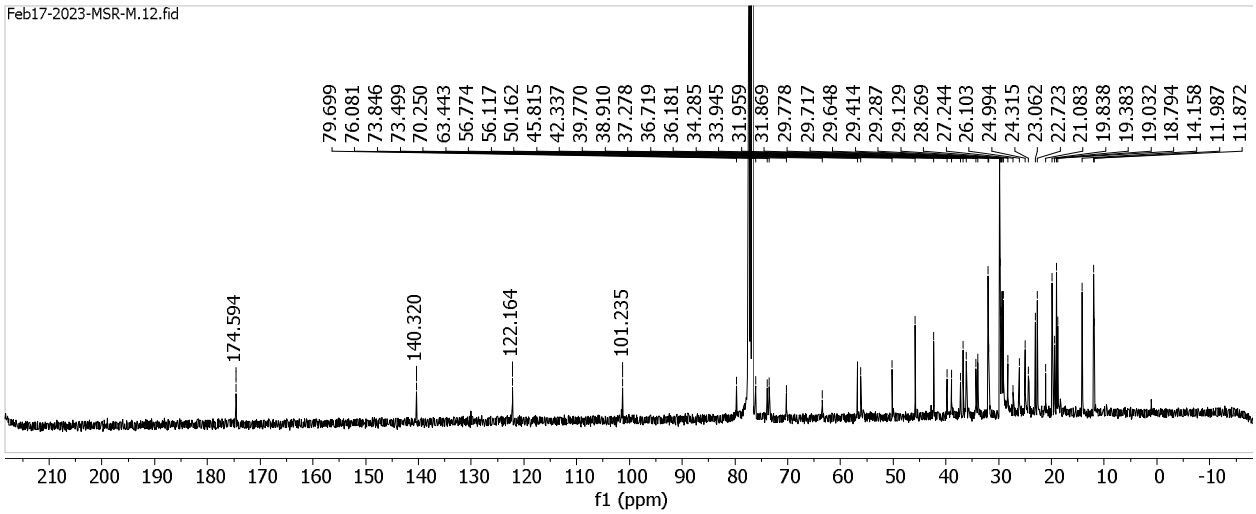

Appendix 115: DEPT-135 Spectrum of Compound **87**

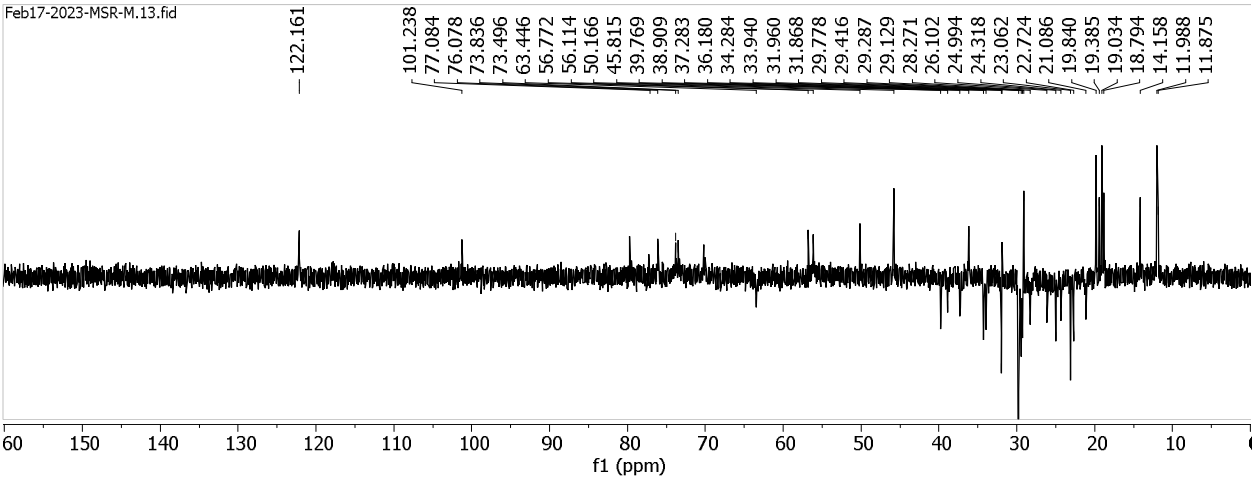

Appendix 116: ^{1}H-^{1}H COSY Spectrum of Compound **87**

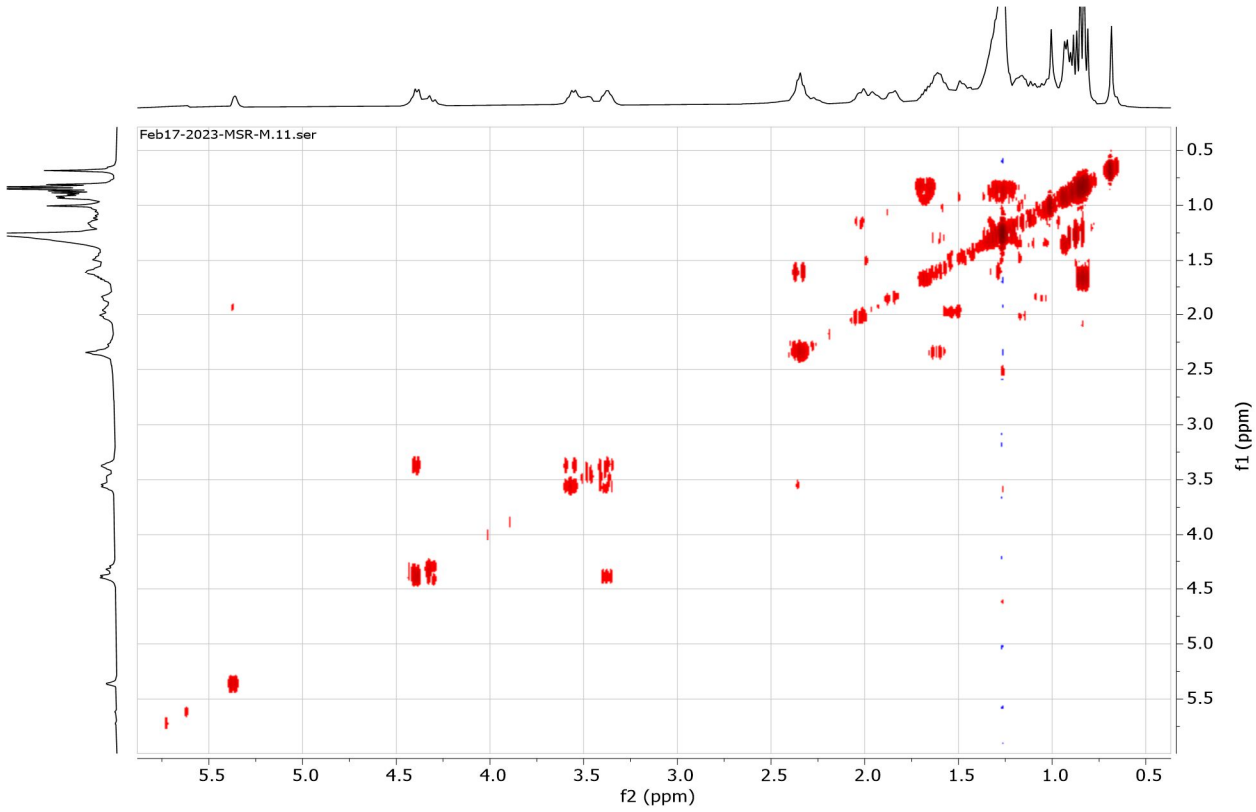

Appendix 117: HSQC Spectrum of Compound **87**

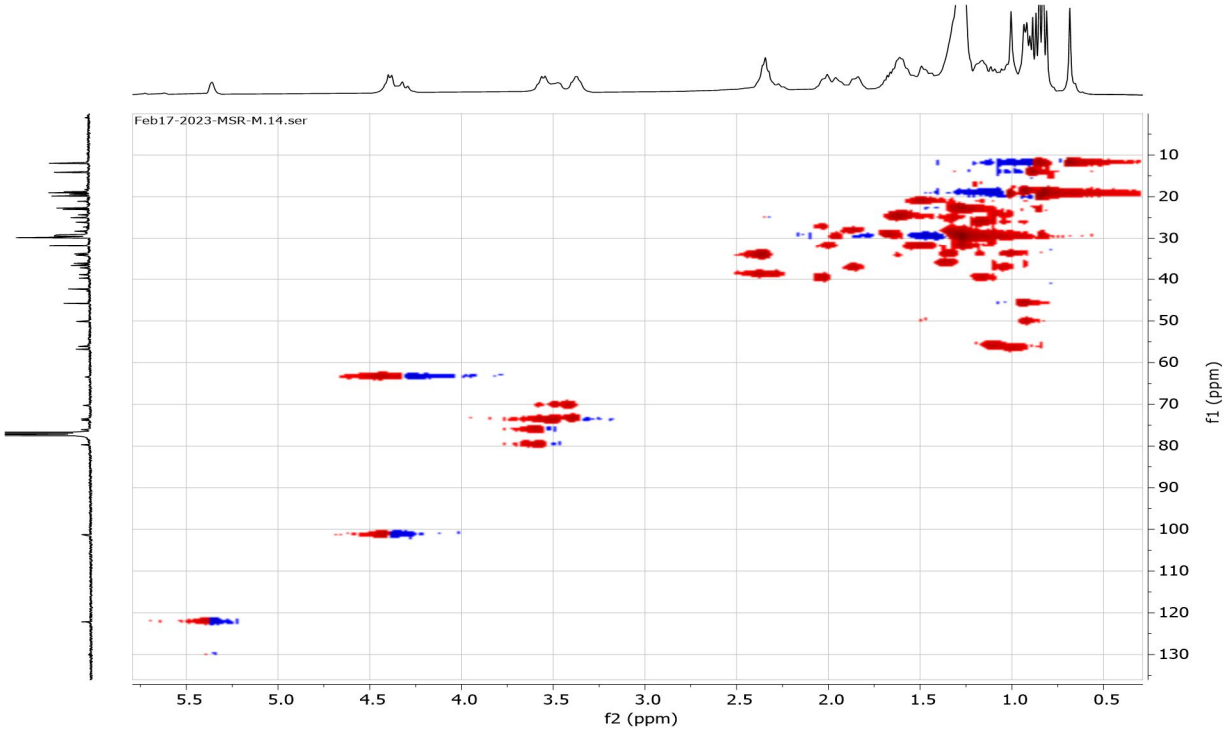

Appendix 118: HMBC Spectrum of Compound **87**

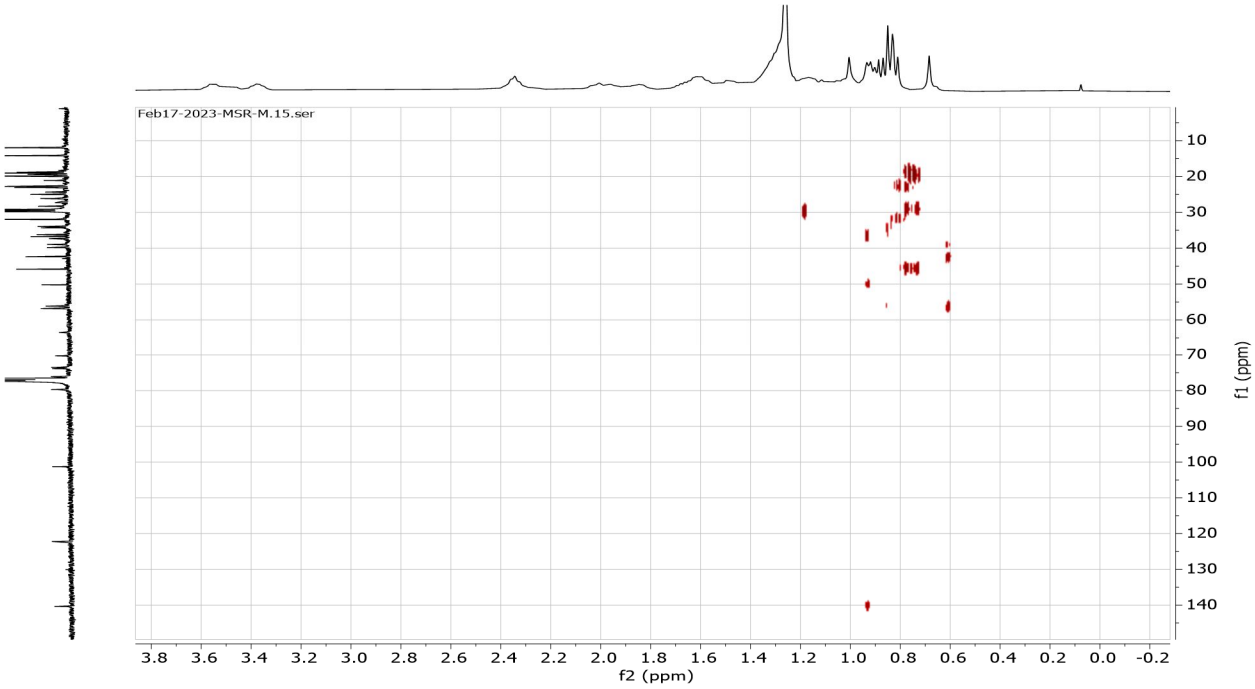

Appendix 119: TOF-MS Spectrum of Compound **87**

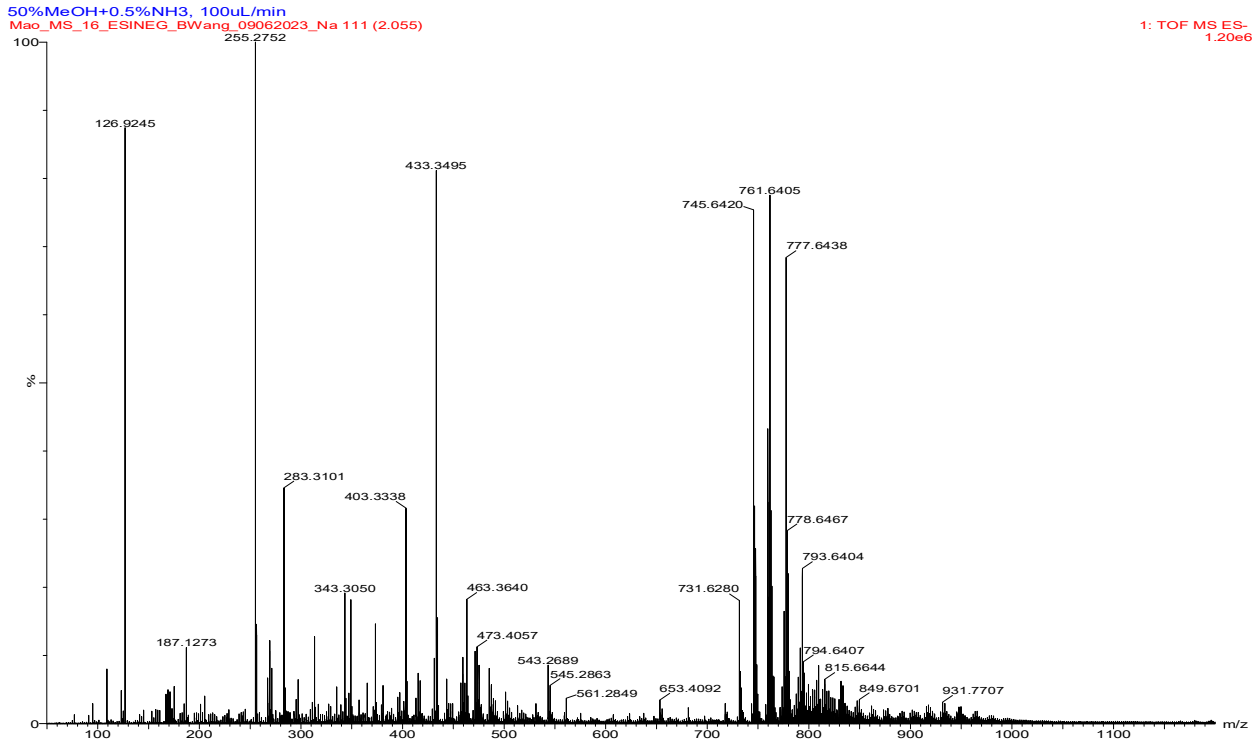

Appendix 120: ^{1}H-NMR (400 MHz, $CDCl_3$) Spectrum of Compound **28**

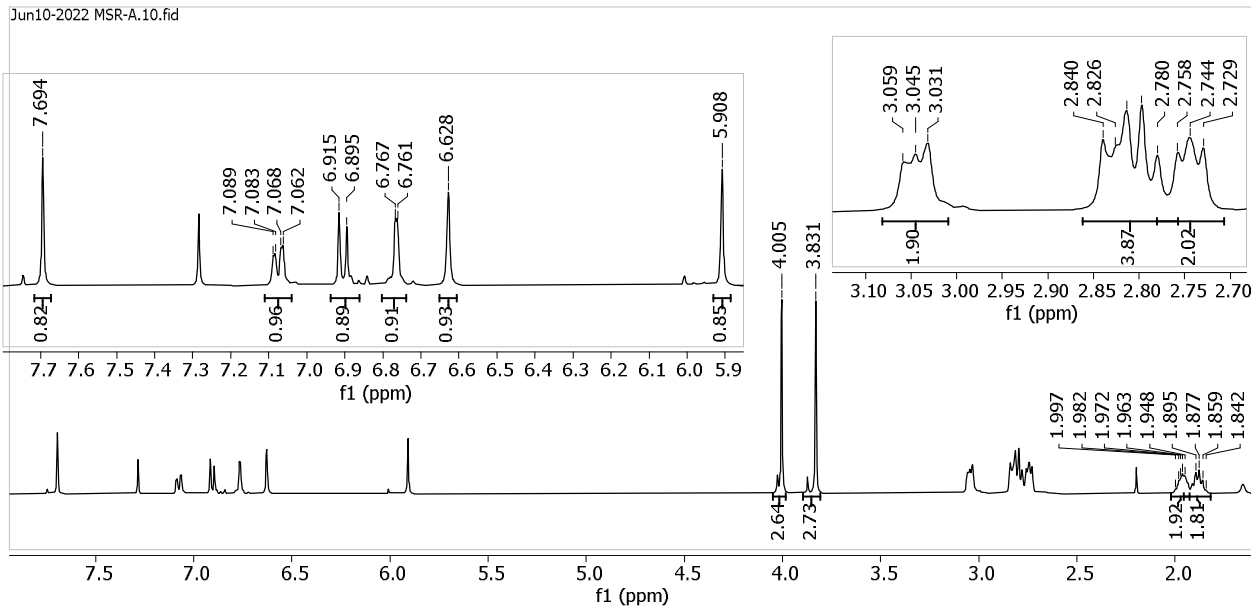

Appendix 121: ^{13}C-NMR (101 MHz, $CDCl_3$) Spectrum of Compound **28**

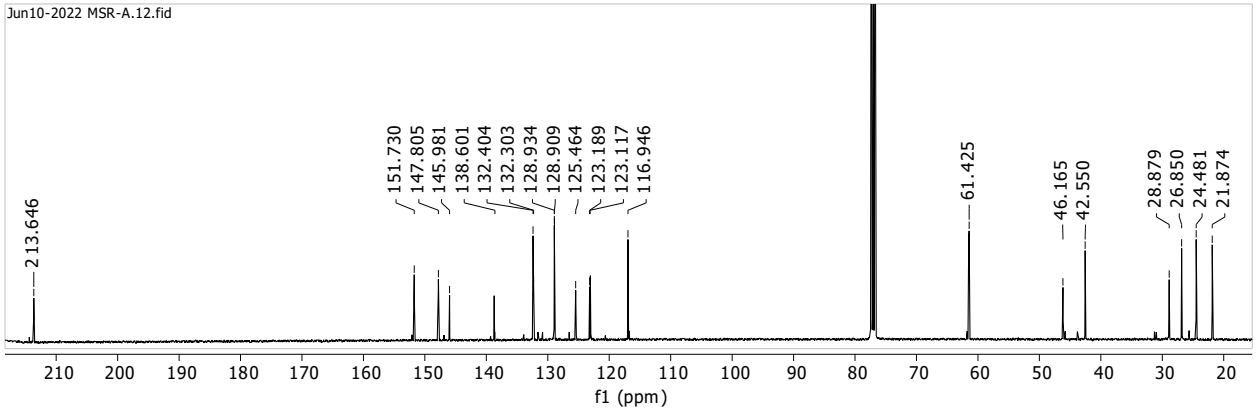

Appendix 122: DEPT-135 Spectrum of Compound **28**

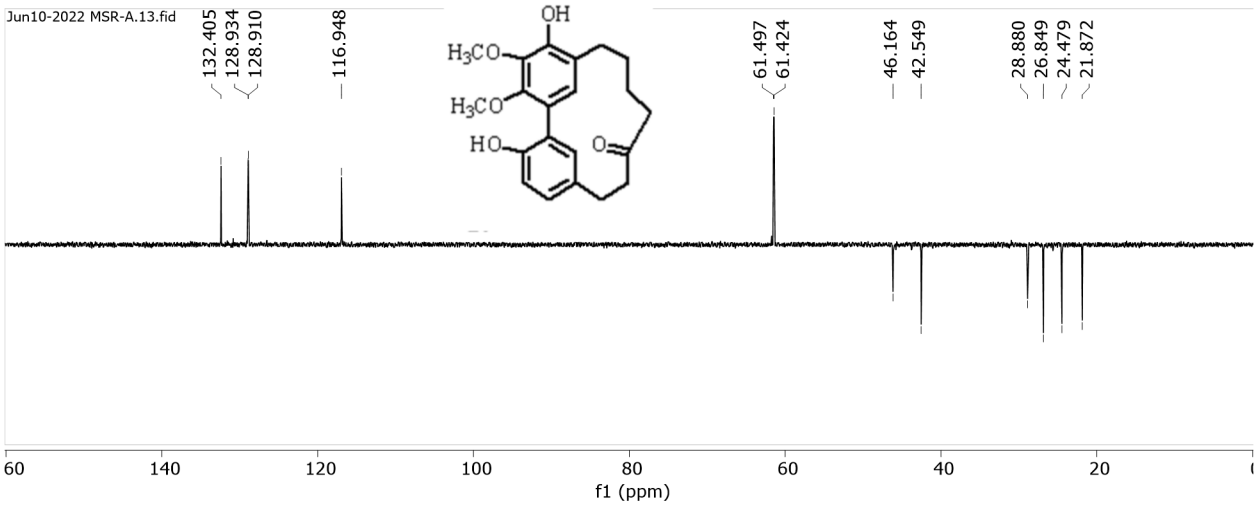

Appendix 123: ^{1}H-^{1}H COSY Spectrum of Compound **28**

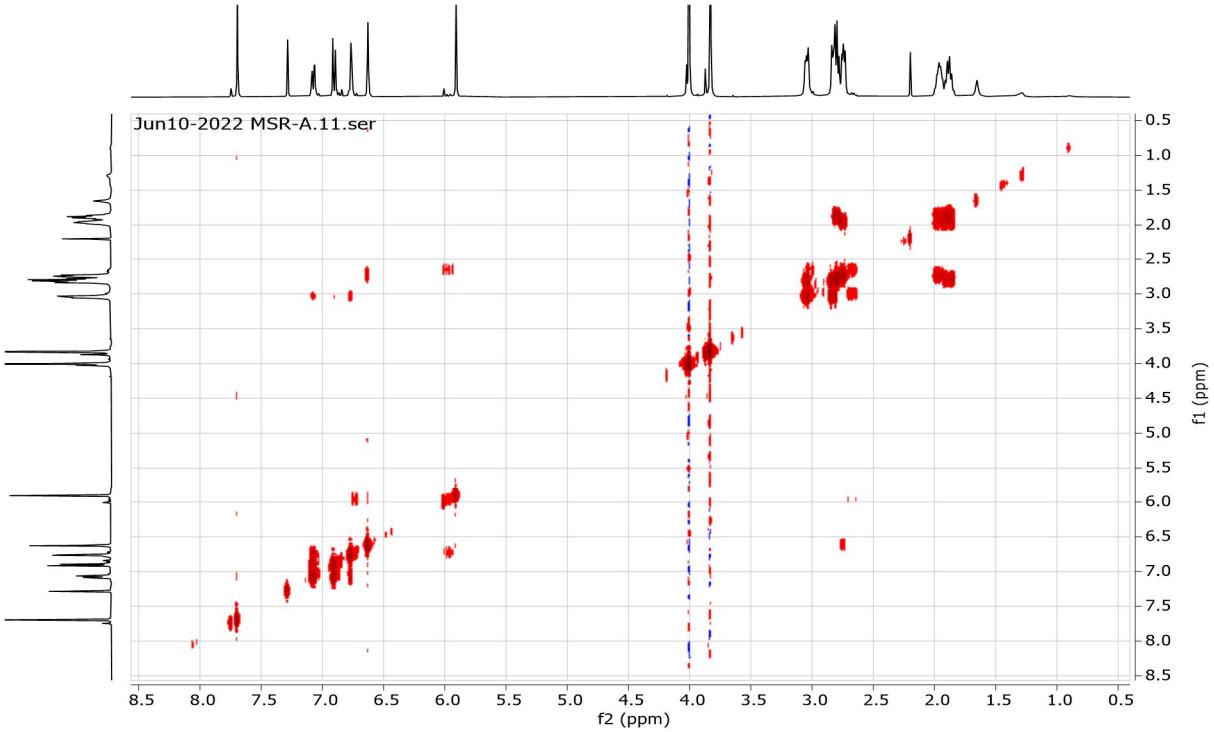

Appendix 124: HSQC Spectrum of Compound **28**

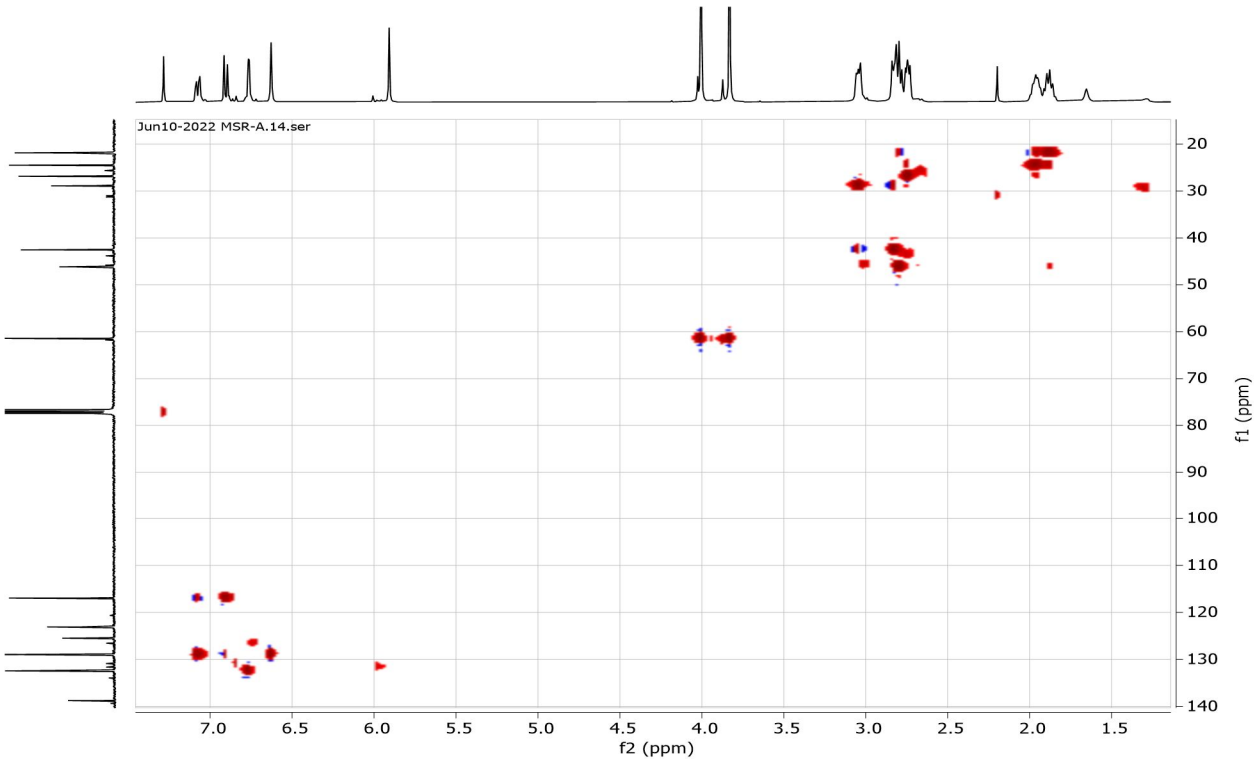

Appendix 125: TOF-MS Spectrum of Compound **28**

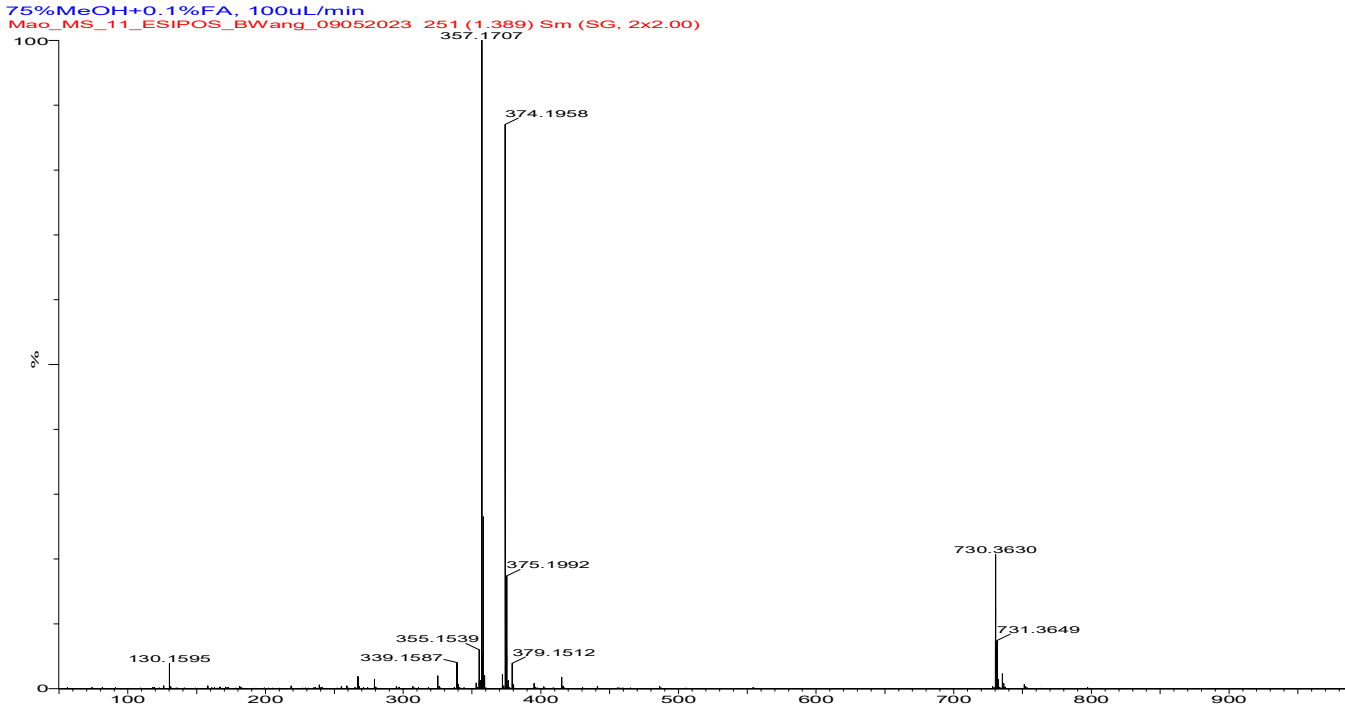

Appendix 126: ^{1}H-NMR (400 MHz, MeOD) Spectrum of Compound **30**

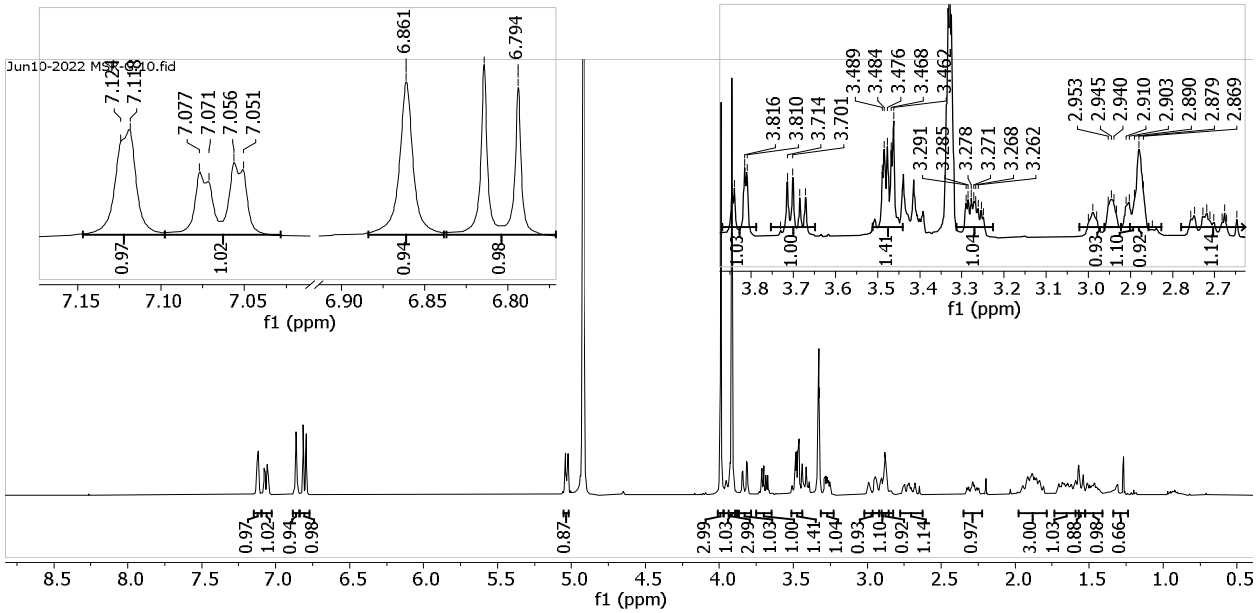

Appendix 127: ^{13}C-NMR (101 MHz, MeOD) Spectrum of Compound **30**

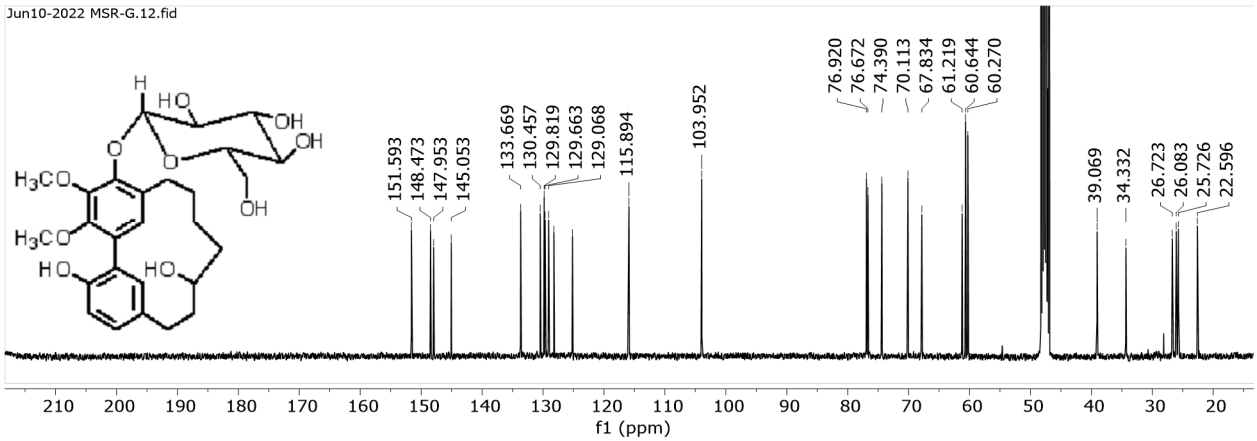

Appendix 128: DEPT-135 Spectrum of Compound **30**

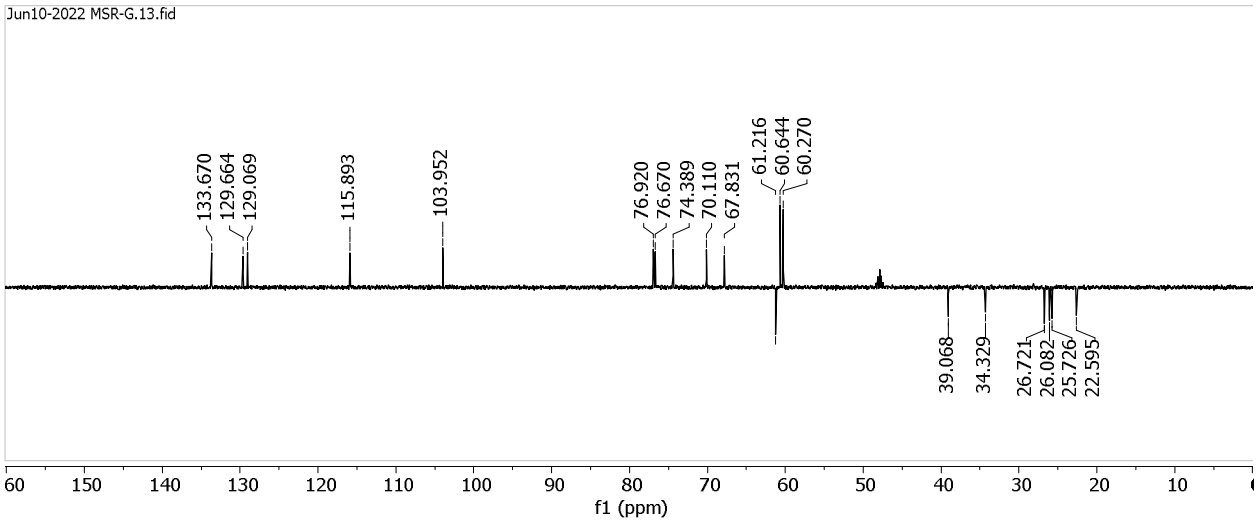

Appendix 129: ^{1}H-^{1}H COSY Spectrum of Compound **30**

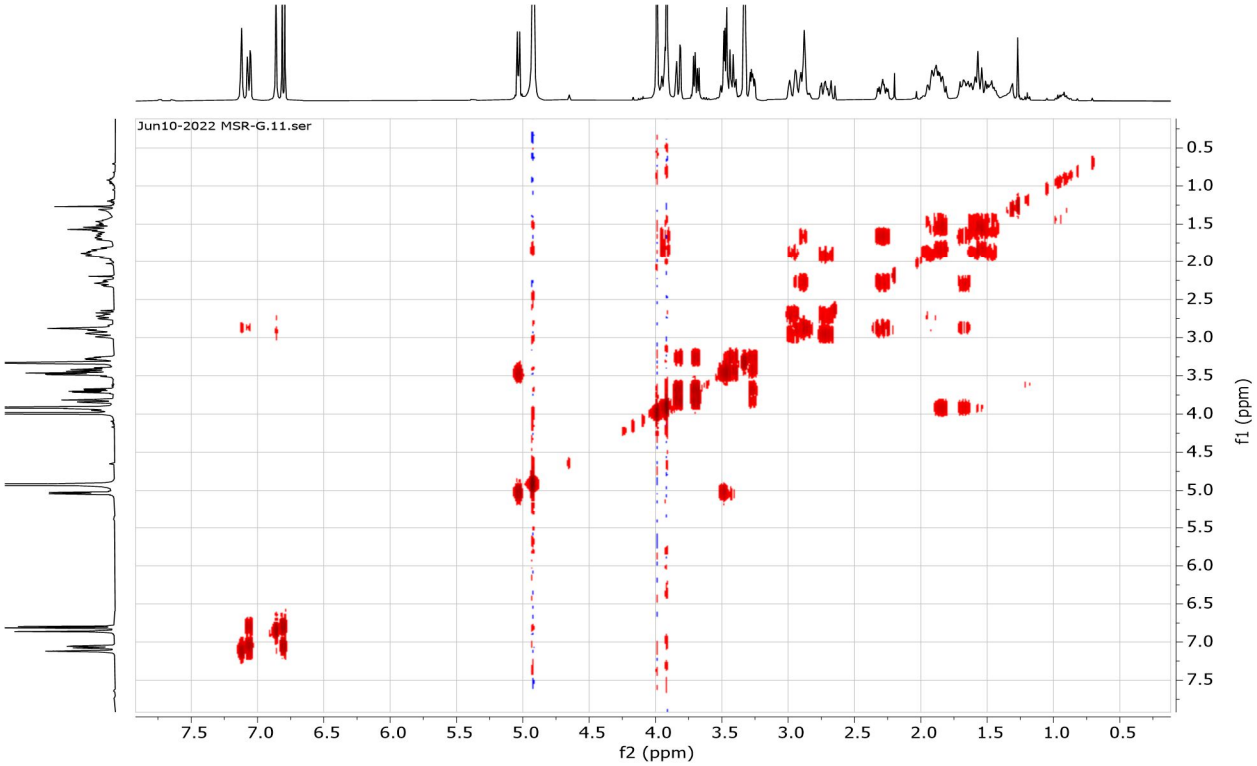

Appendix 130: HSQC Spectrum of Compound **30**

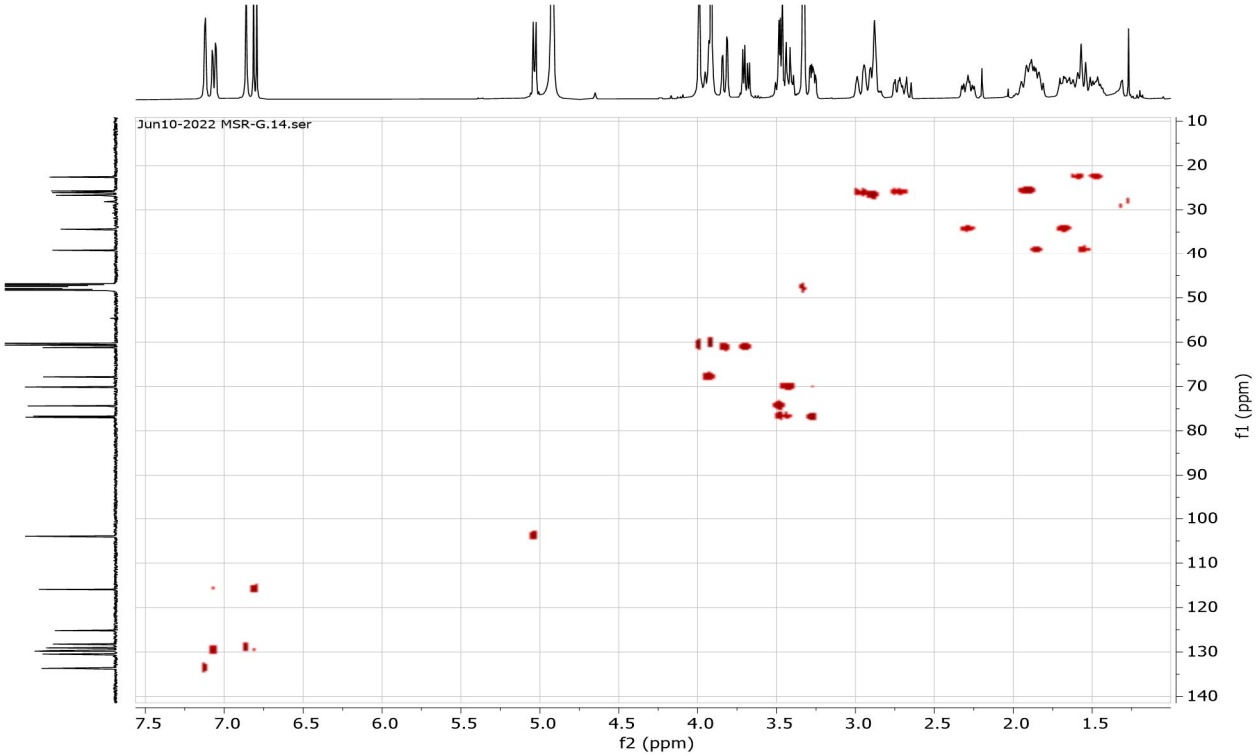

Appendix 131: HMBC Spectrum of Compound **30**

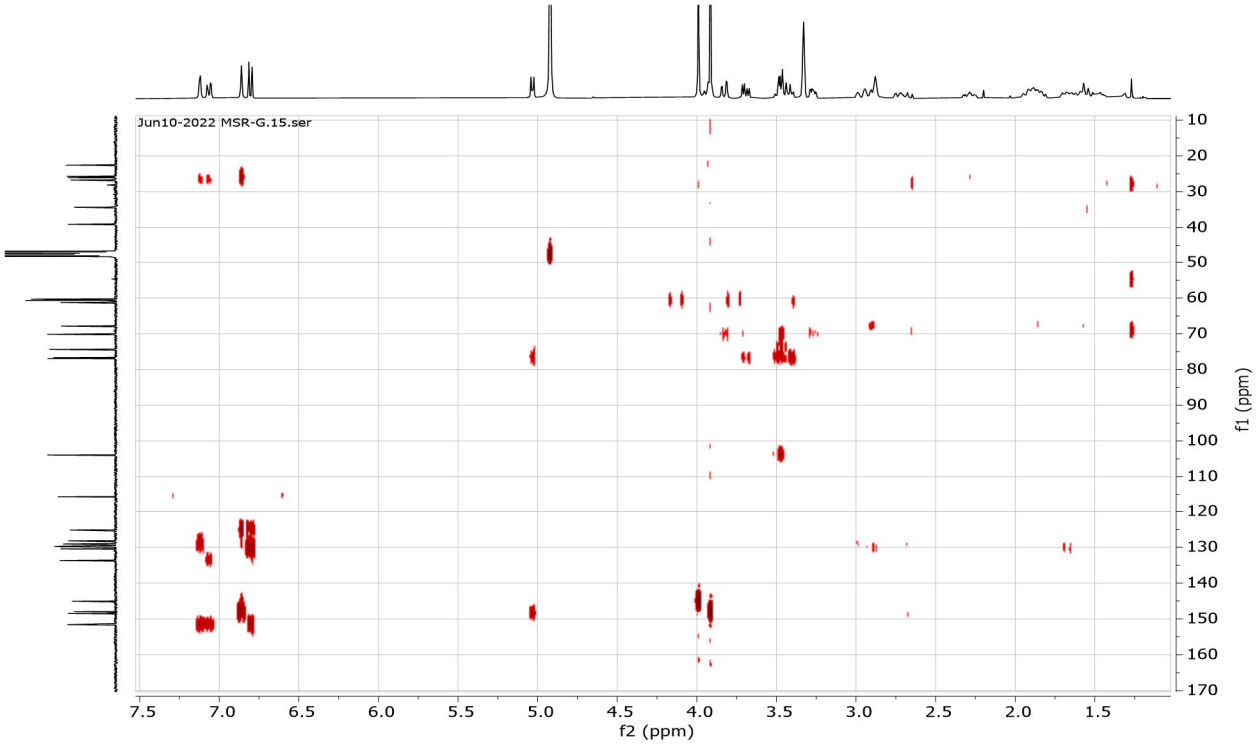

Appendix 132: TOF-MS Spectrum of Compound **30**

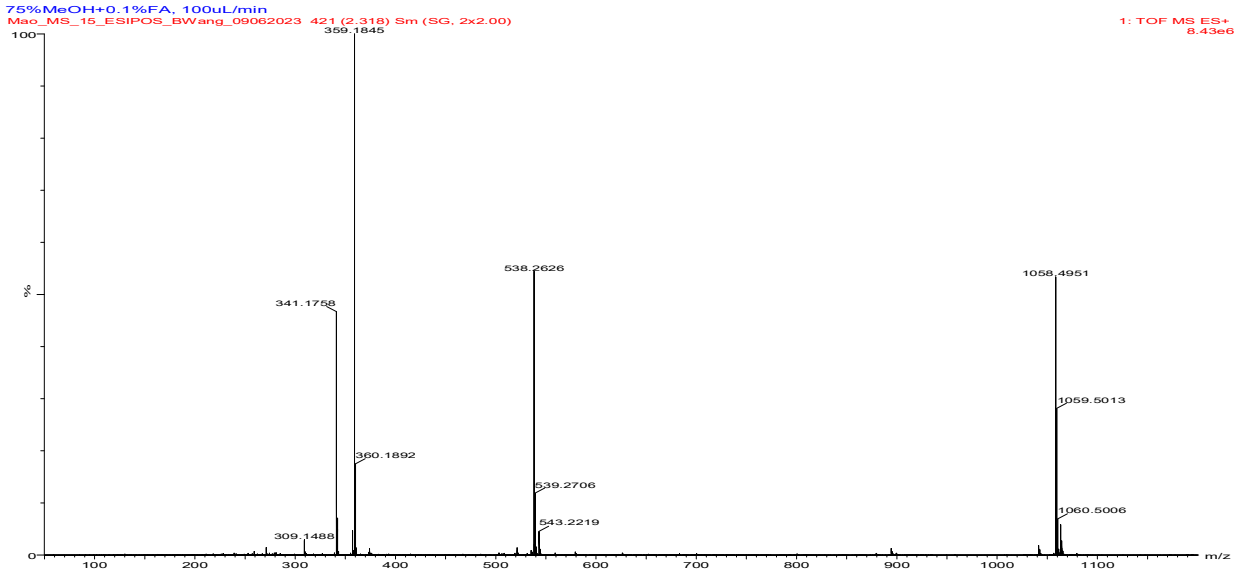

Appendix 133: ^{1}H-NMR (600 MHz, DMSO) Spectrum of Compound **88**

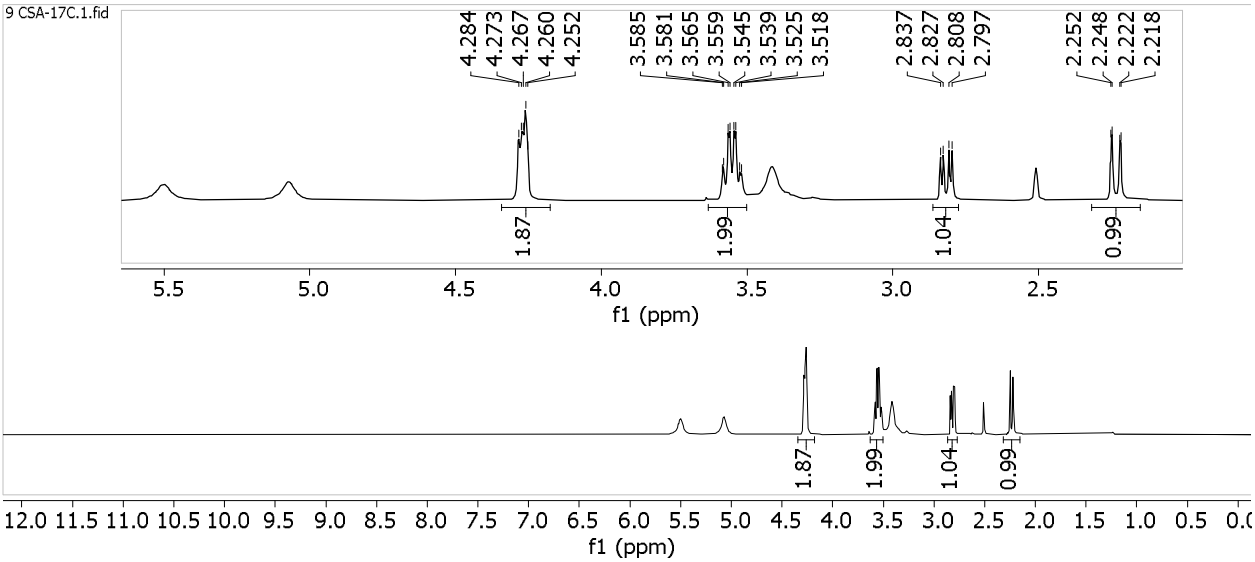

Appendix 134: ^{13}C-NMR (125 MHz, DMSO) Spectrum of Compound **88**

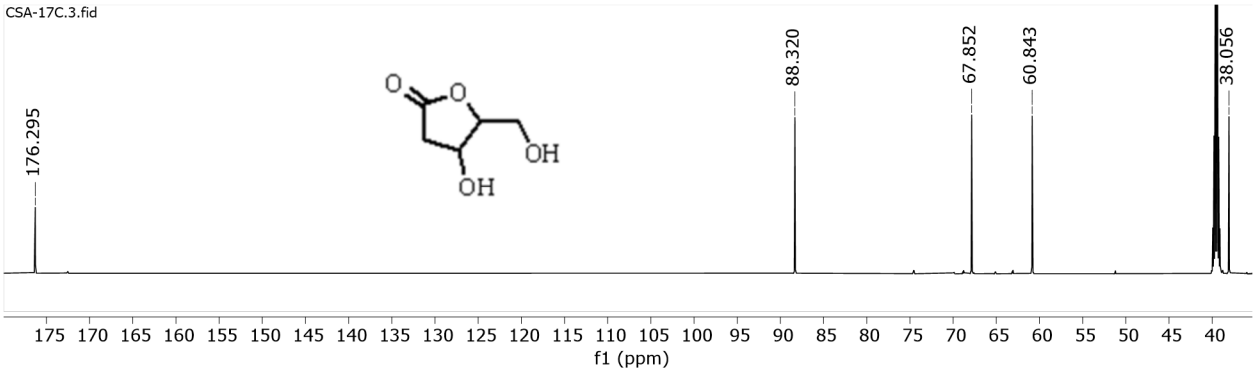

Appendix 135: DEPT-135 Spectrum of Compound **88**

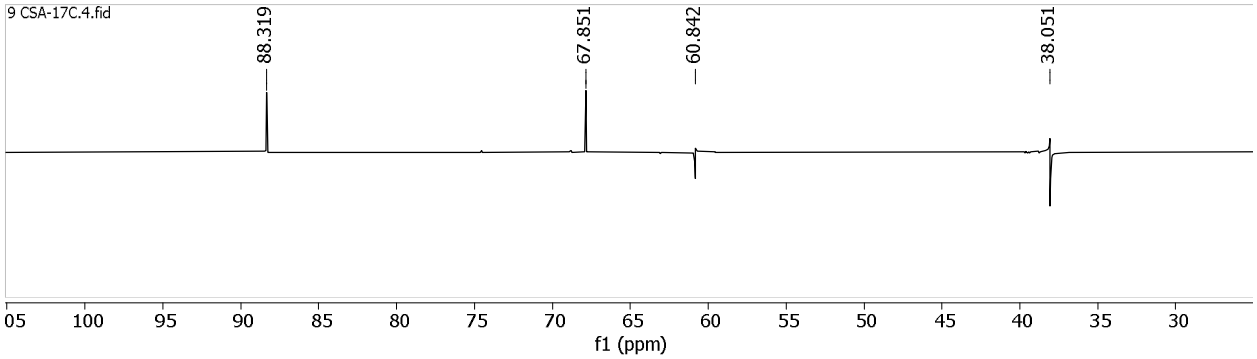

Appendix 136: ^{1}H-^{1}H COSY Spectrum of Compound **88**

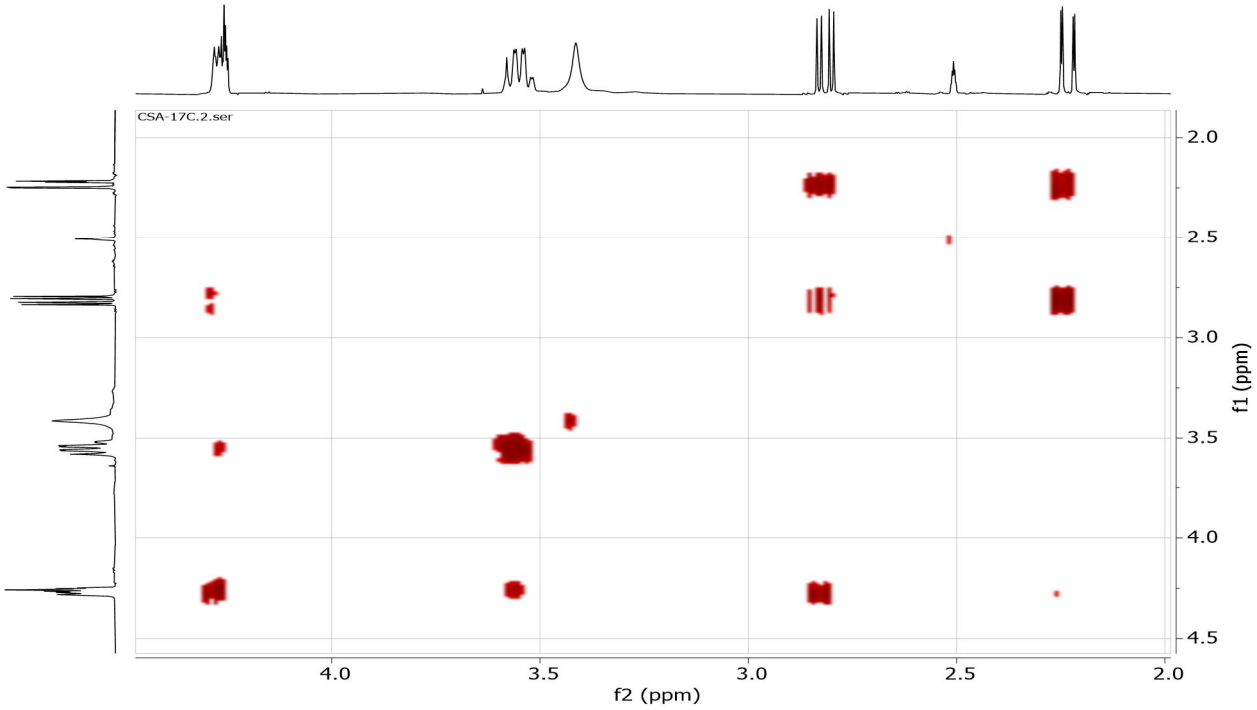

Appendix 137: HSQC Spectrum of Compound **88**

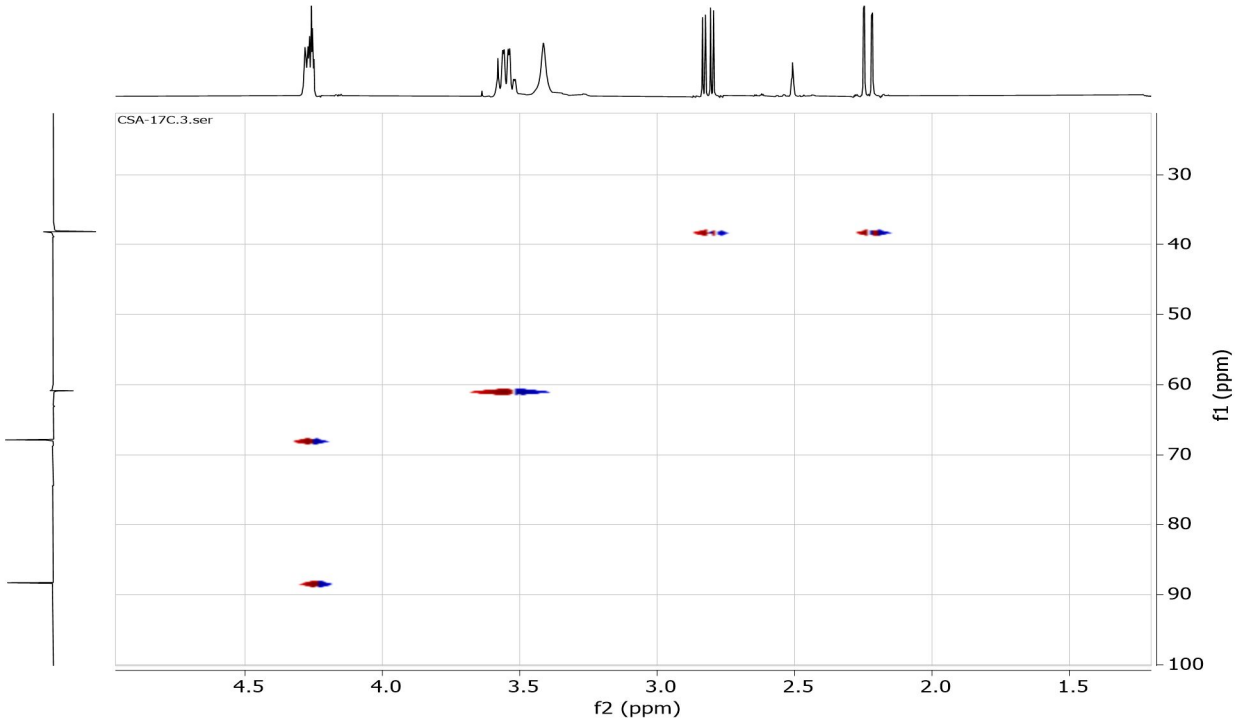

Appendix 138: HMBC Spectrum of Compound **88**

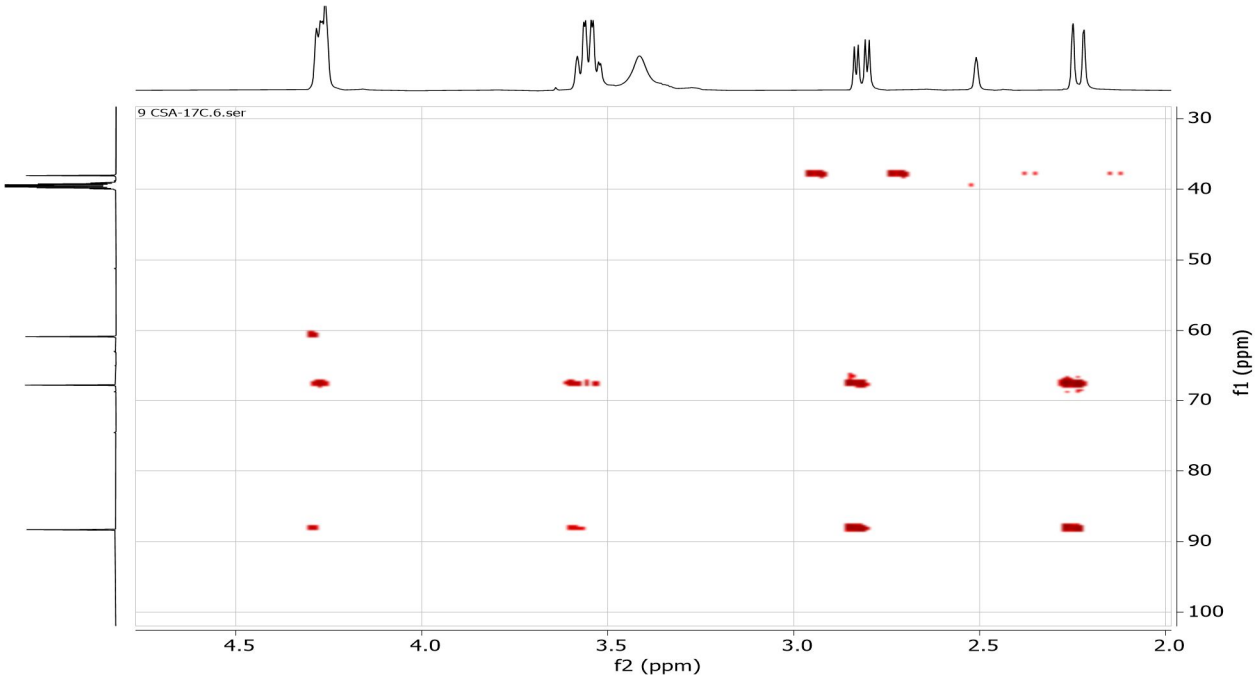

Appendix 139: HR-MS Spectrum of Compound **88**

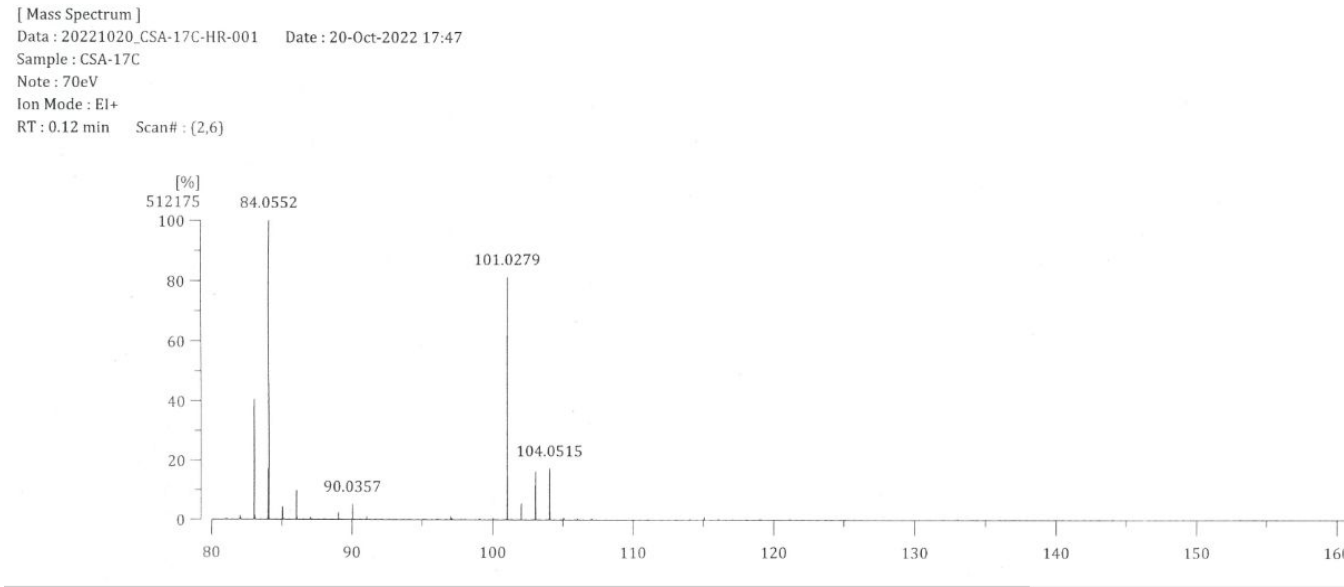

Appendix 140: ^{1}H-NMR (600 MHz, CH_3OH) Spectrum of Compound **89**

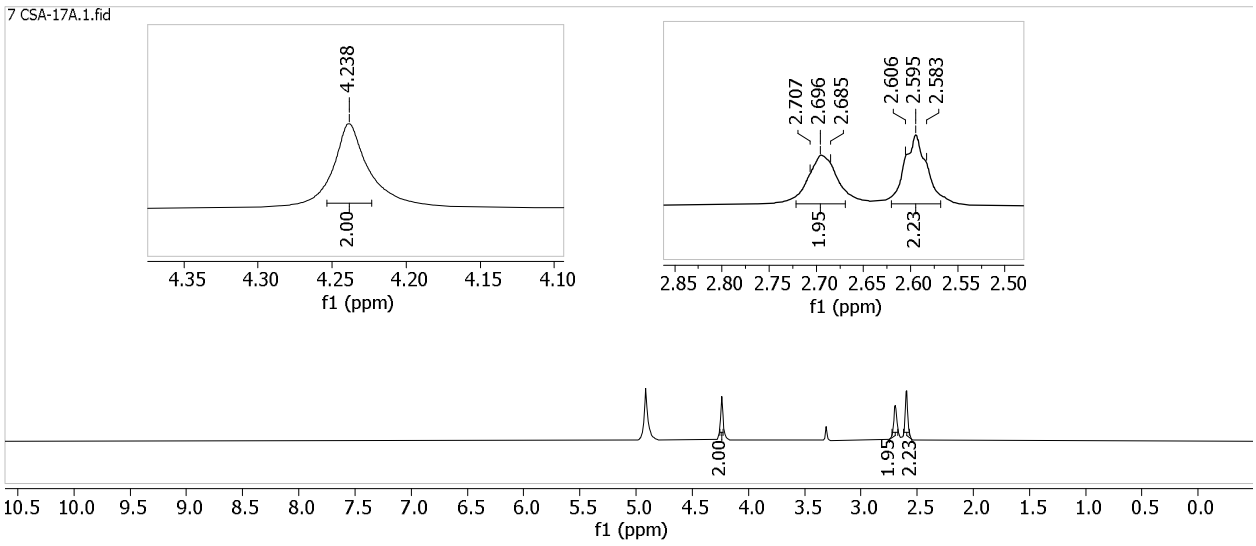

Appendix 141: ^{13}C-NMR (151 MHz, CH_3OH) Spectrum of Compound **89**

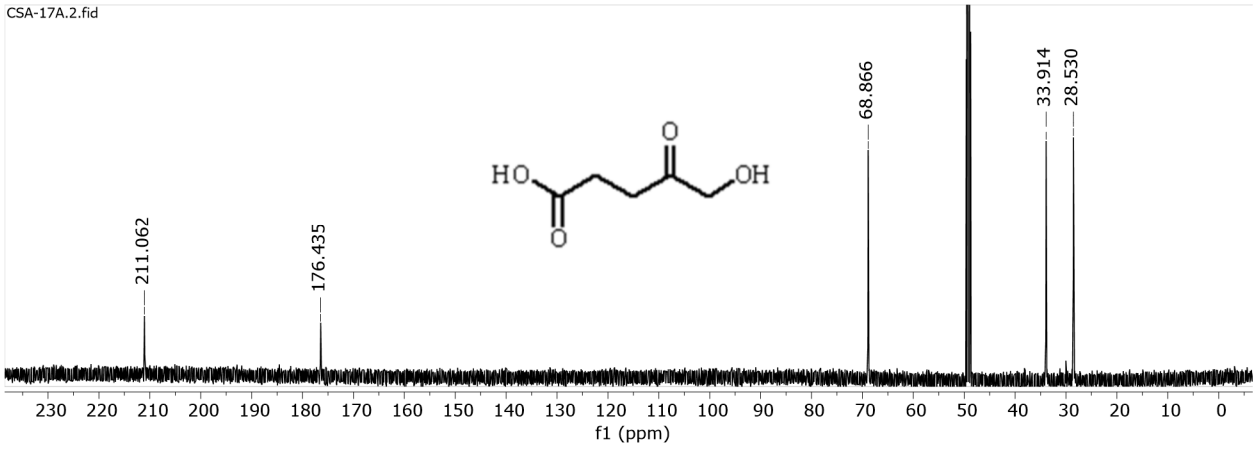

Appendix 142: ^{1}H-^{1}H COSY Spectrum of Compound **89**

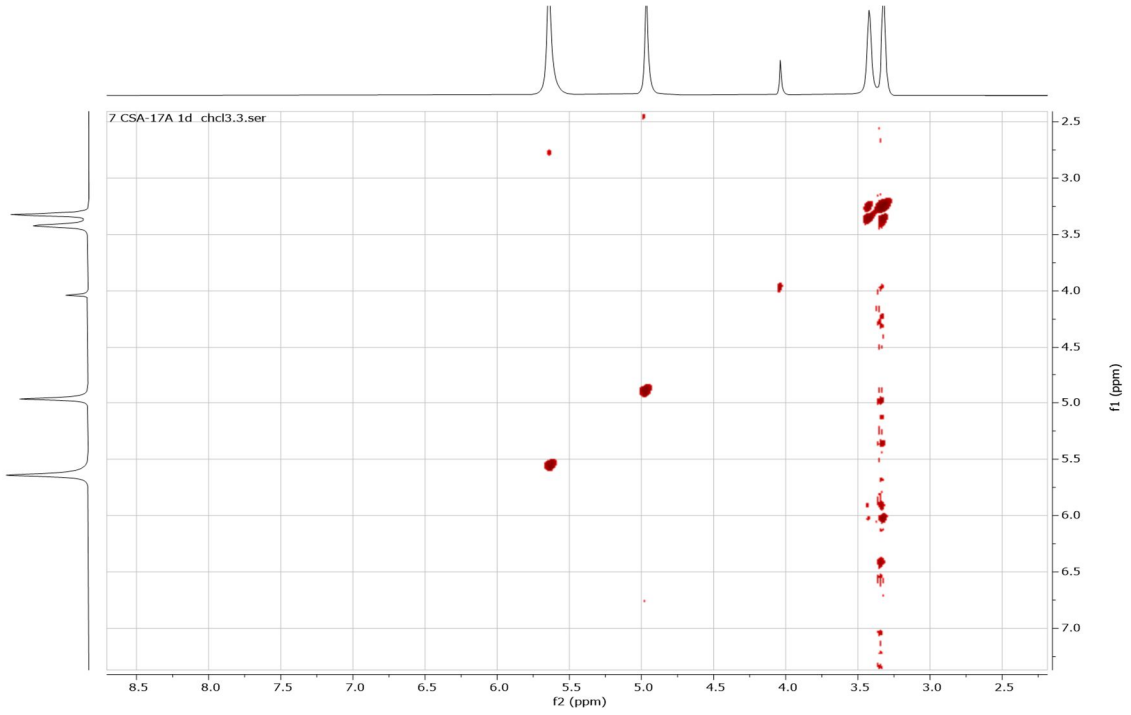

Appendix 143: HSQC Spectrum of Compound **89**

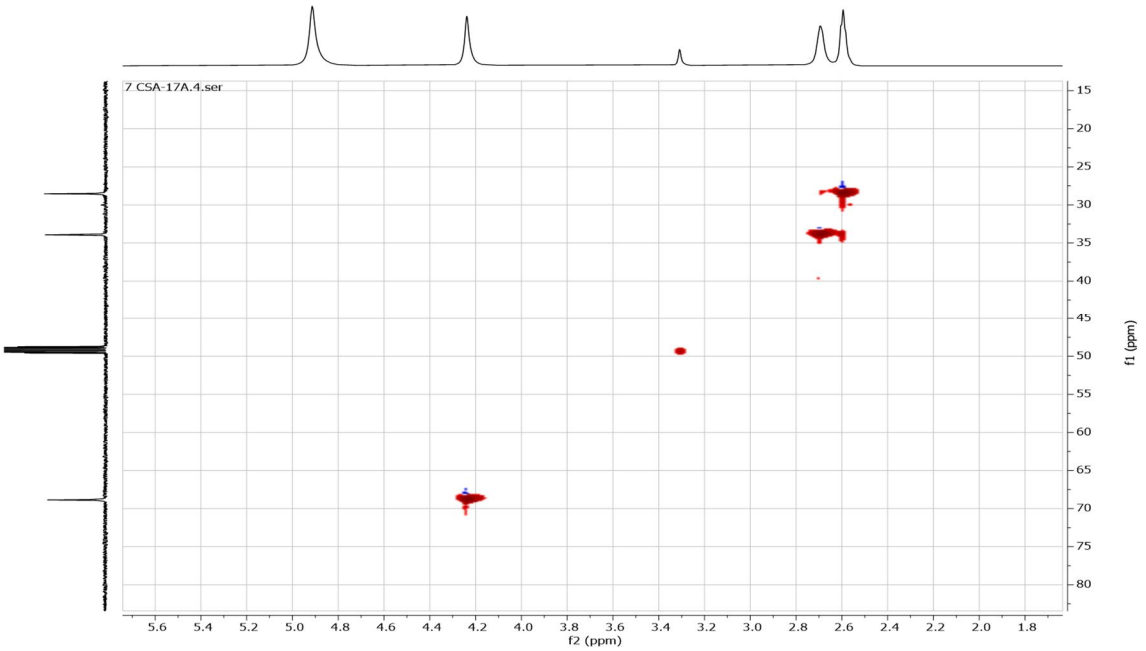

Appendix 144: HMBC Spectrum of Compound **89**

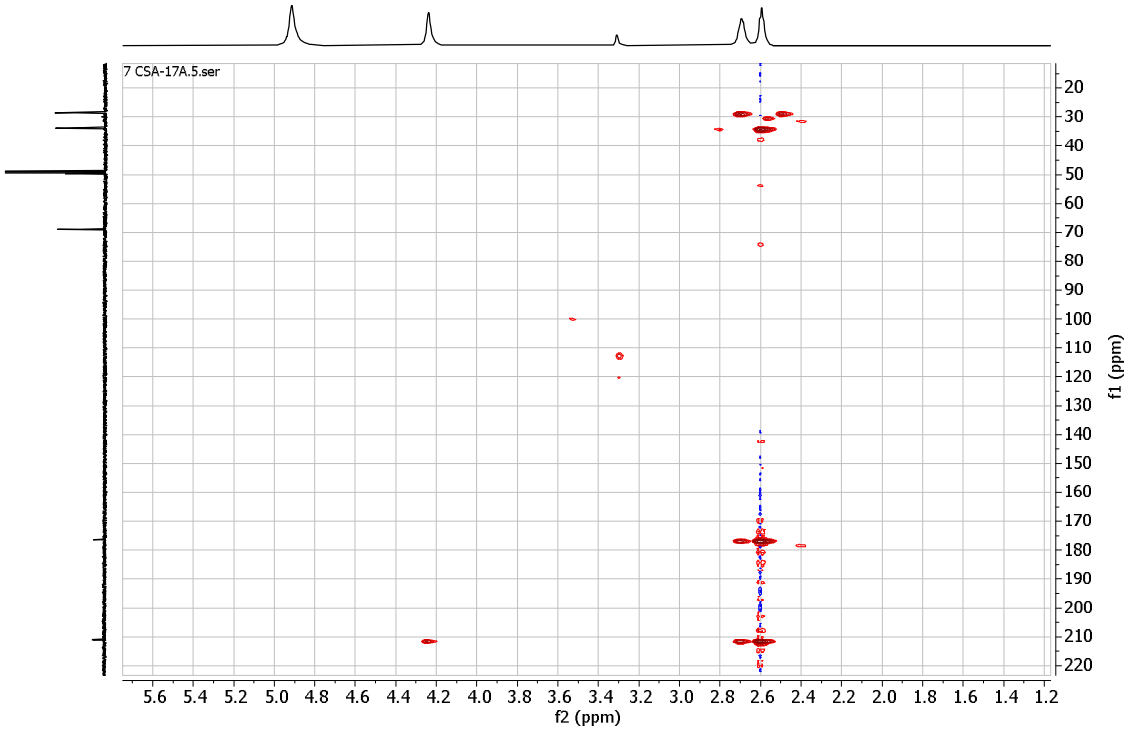

Appendix 145: HR-MS Spectrum of Compound **89**

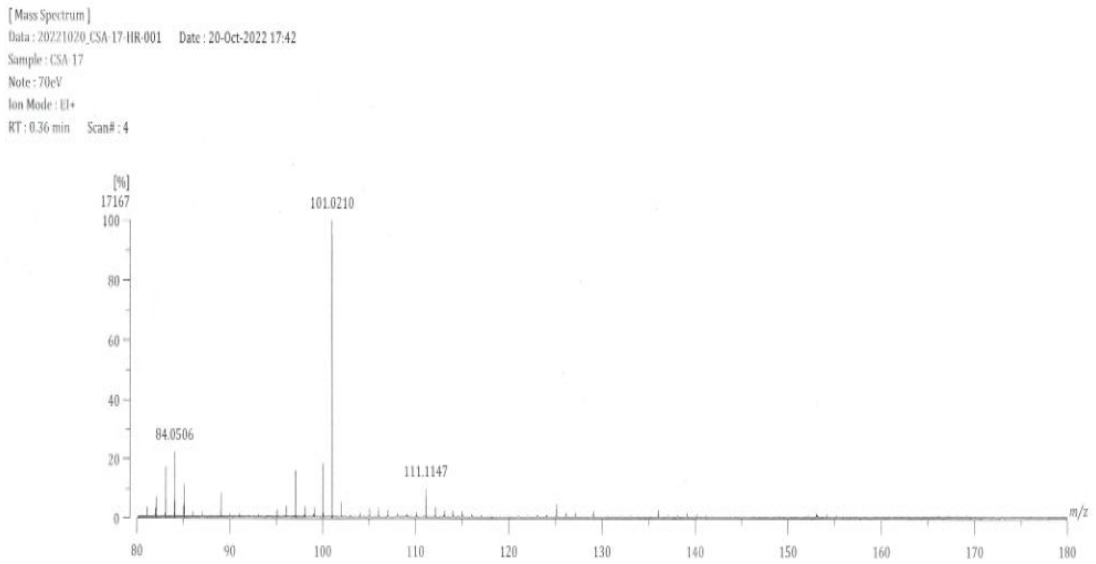

Appendix 146: [1]H-NMR (601 MHz, DMSO) Spectrum of Compound **90**

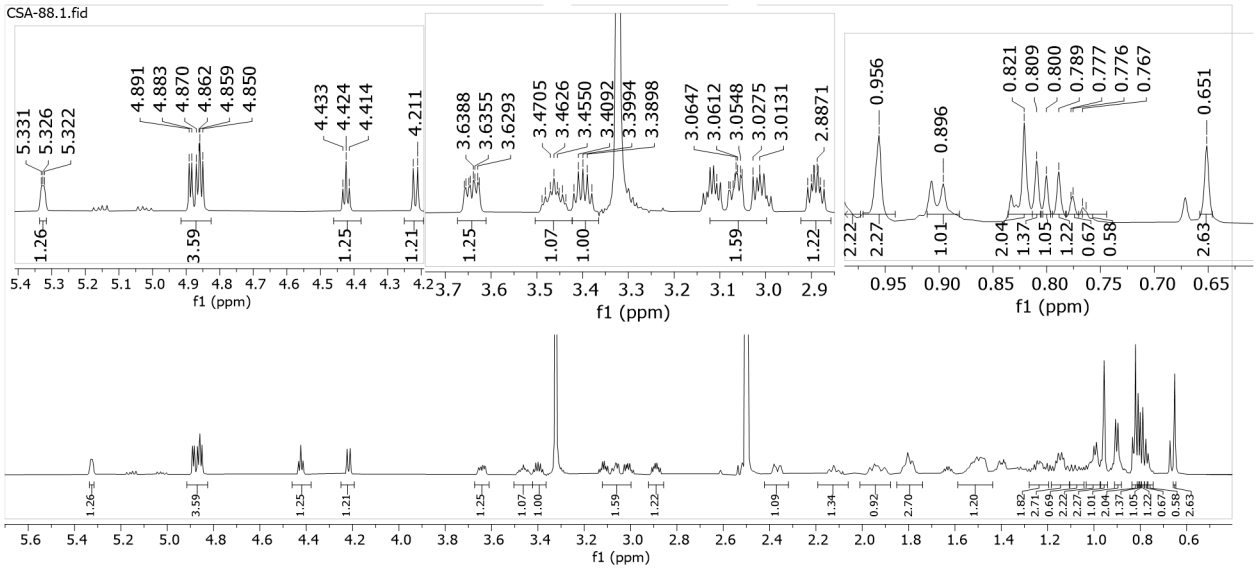

Appendix 147: ^{13}C-NMR (151 MHz, DMSO) Spectrum of Compound **90**

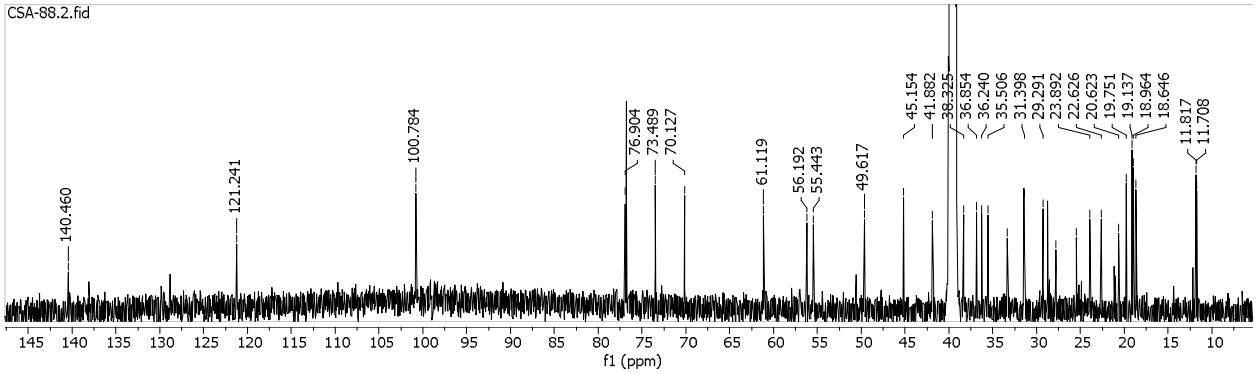

Appendix 148: DEPT-135 Spectrum of Compound **90**

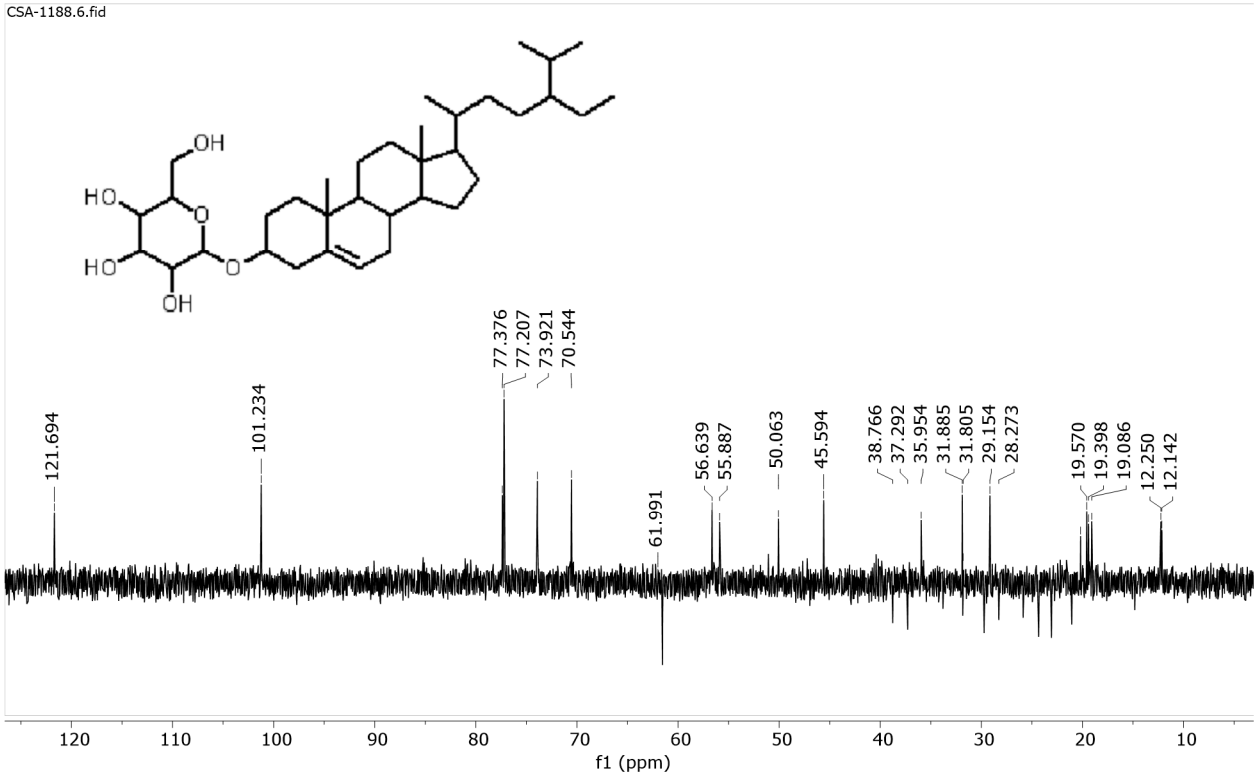

Appendix 149: ^{1}H-^{1}H COSY Spectrum of Compound **90**

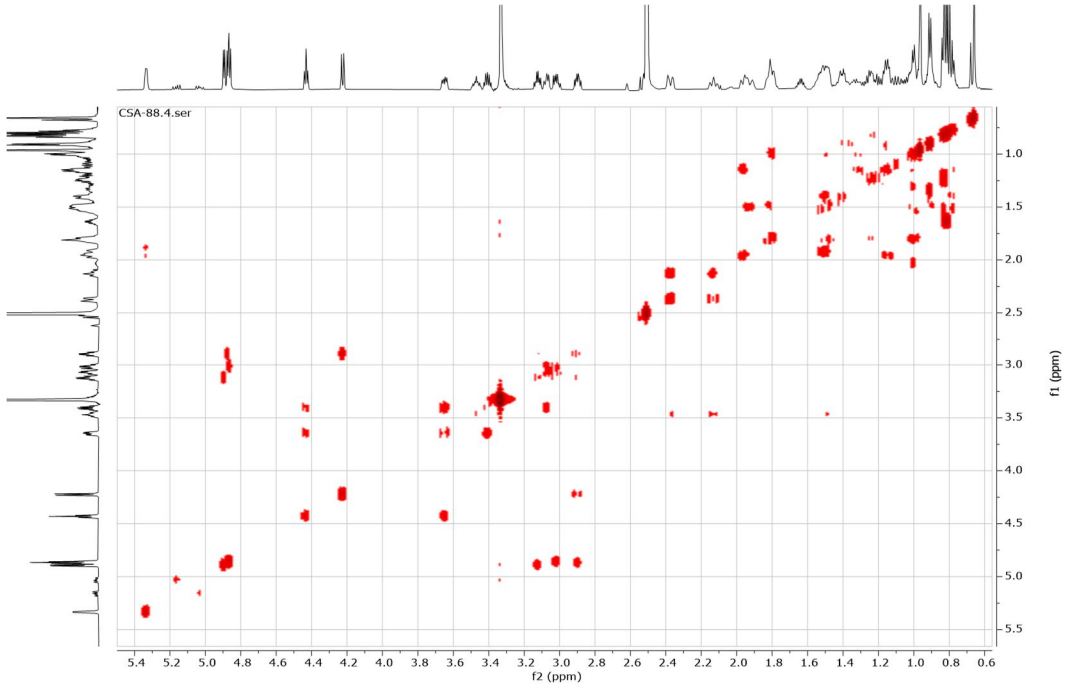

Appendix 150: HSQC Spectrum of Compound **90**

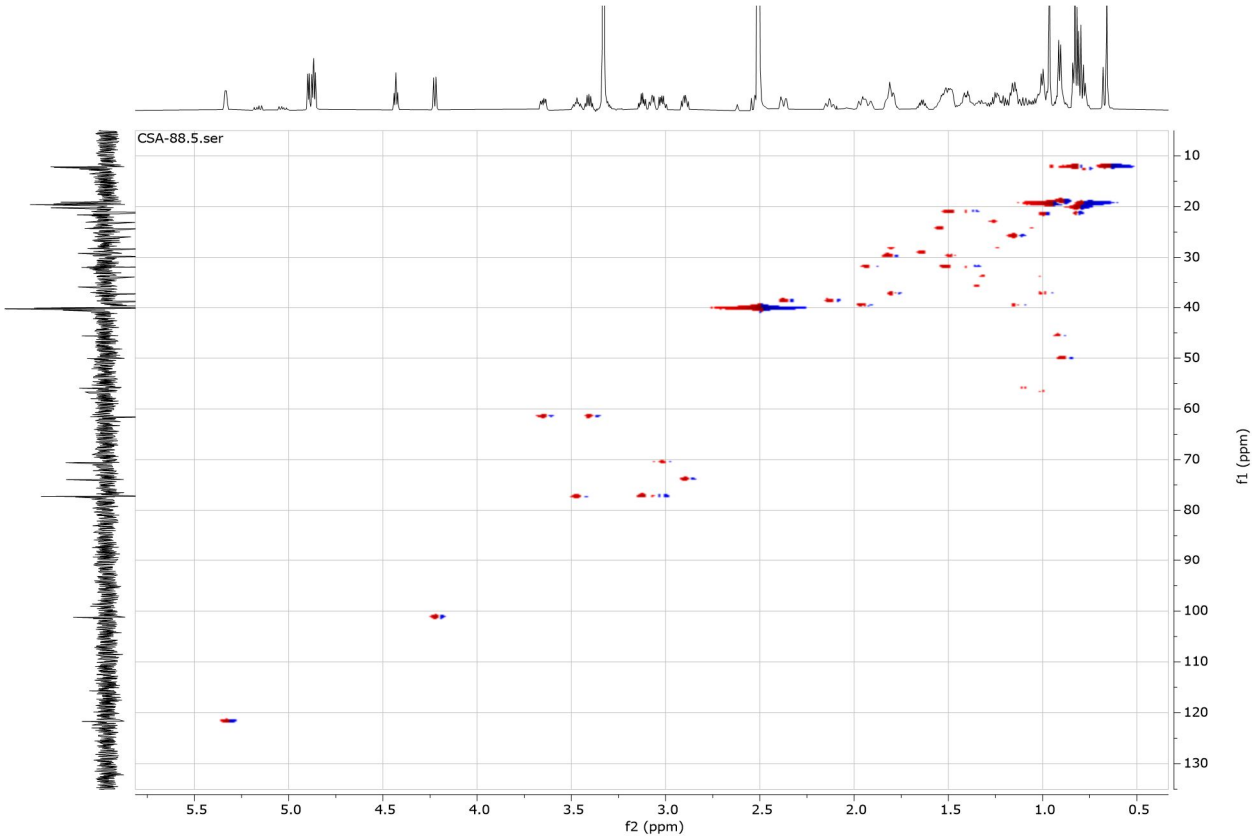

Appendix 151: HMBC Spectrum of Compound **90**

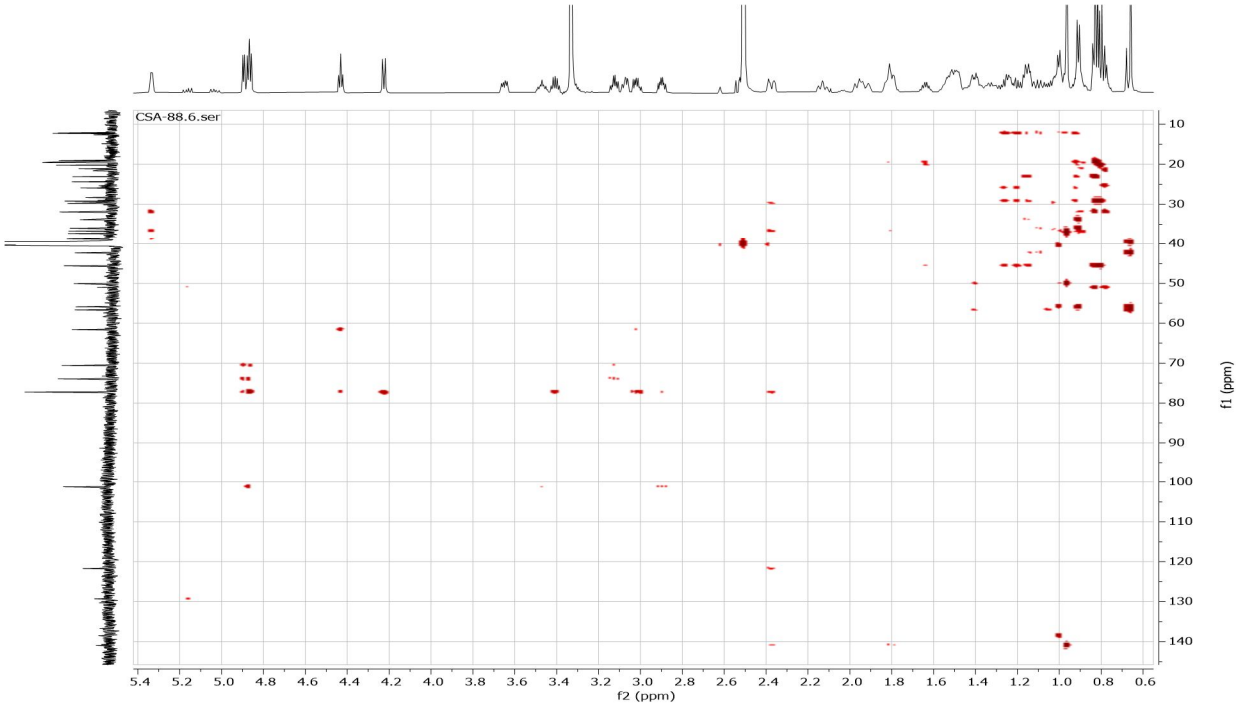

Appendix 152: FAB-MS Spectrum of Compound **90**

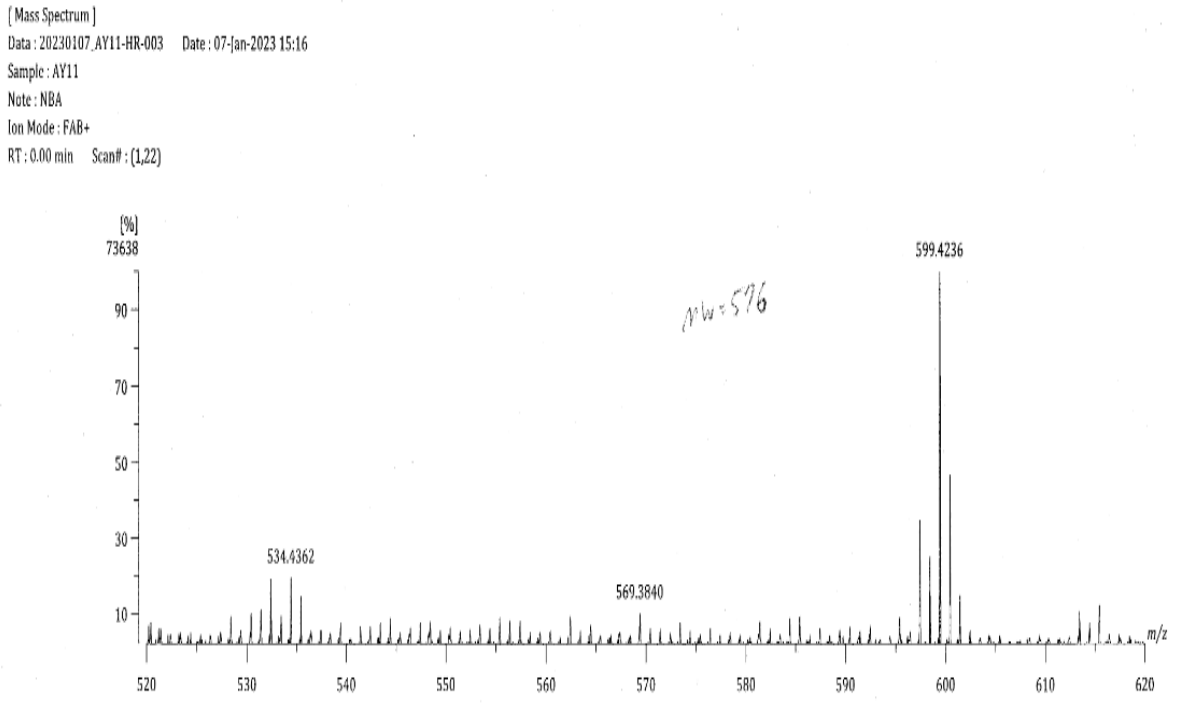

Appendix 153: ^{1}H-NMR (400 MHz, $CDCl_3$) Spectrum of Compound **91**

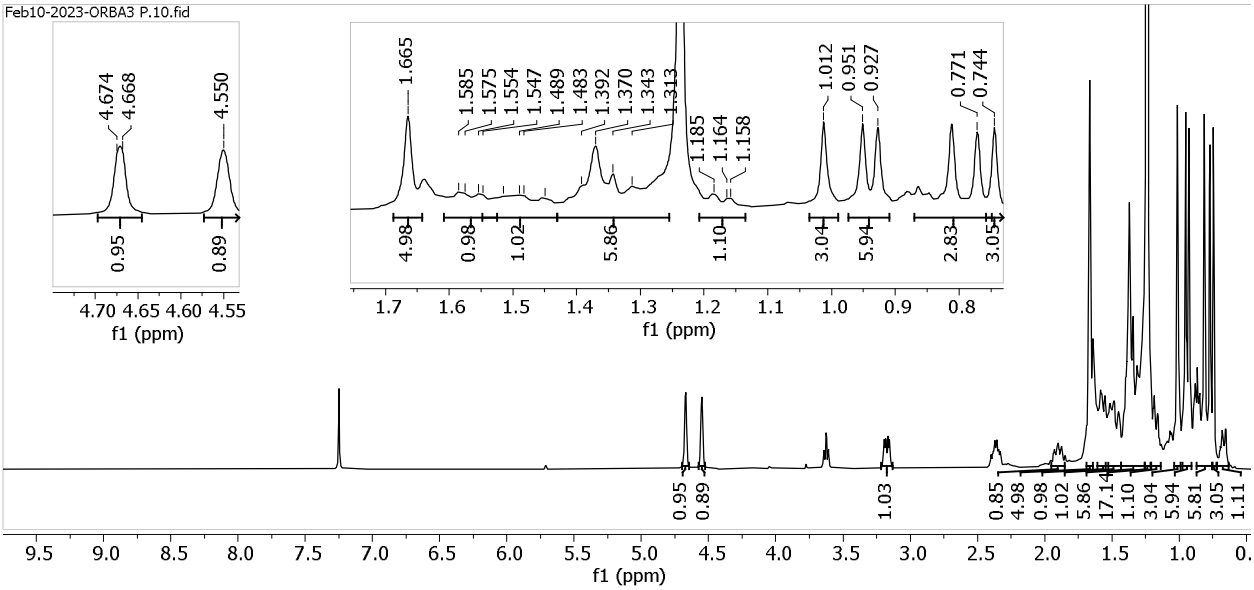

Appendix 154: ^{13}C-NMR (101 MHz, $CDCl_3$) Spectrum of Compound **91**

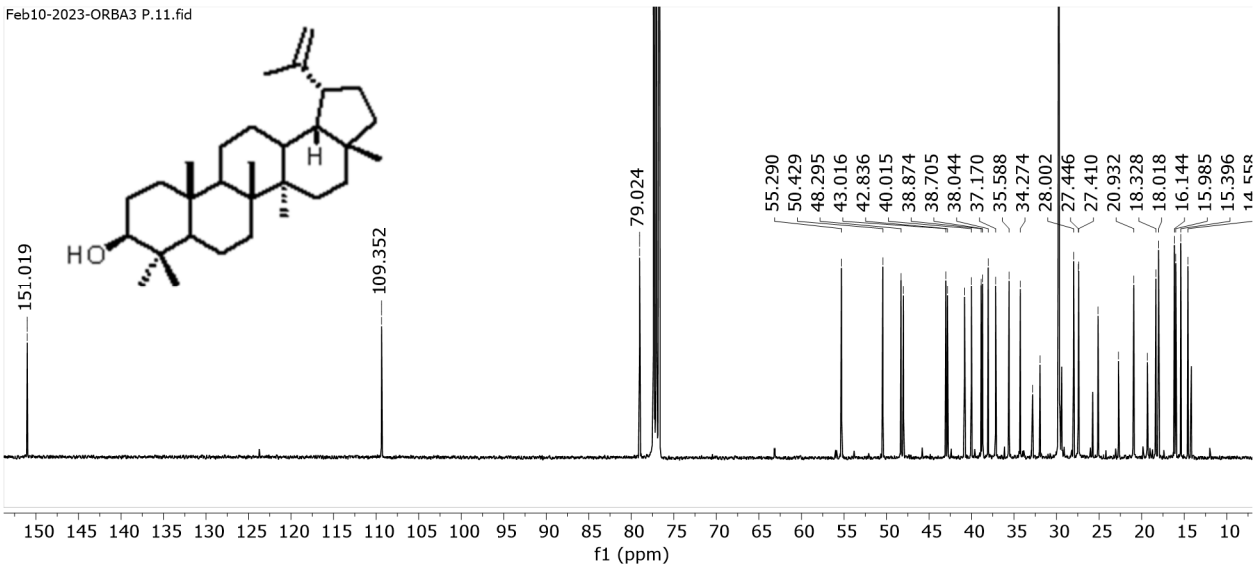

Appendix 155: DEPT-135 Spectrum of Compound **91**

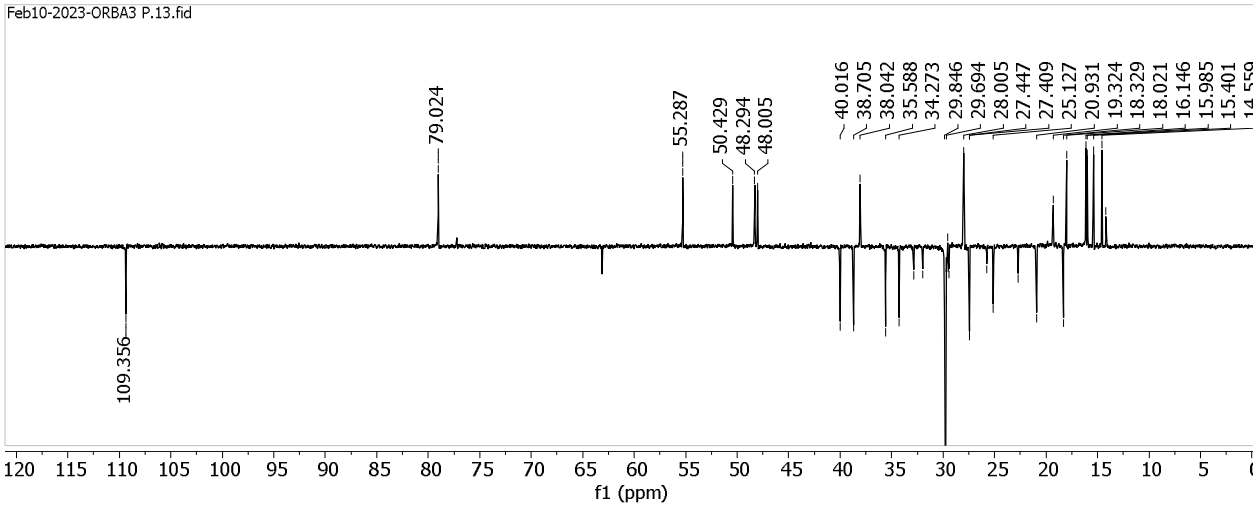

Appendix 156: ^{1}H-^{1}H COSY Spectrum of Compound **91**

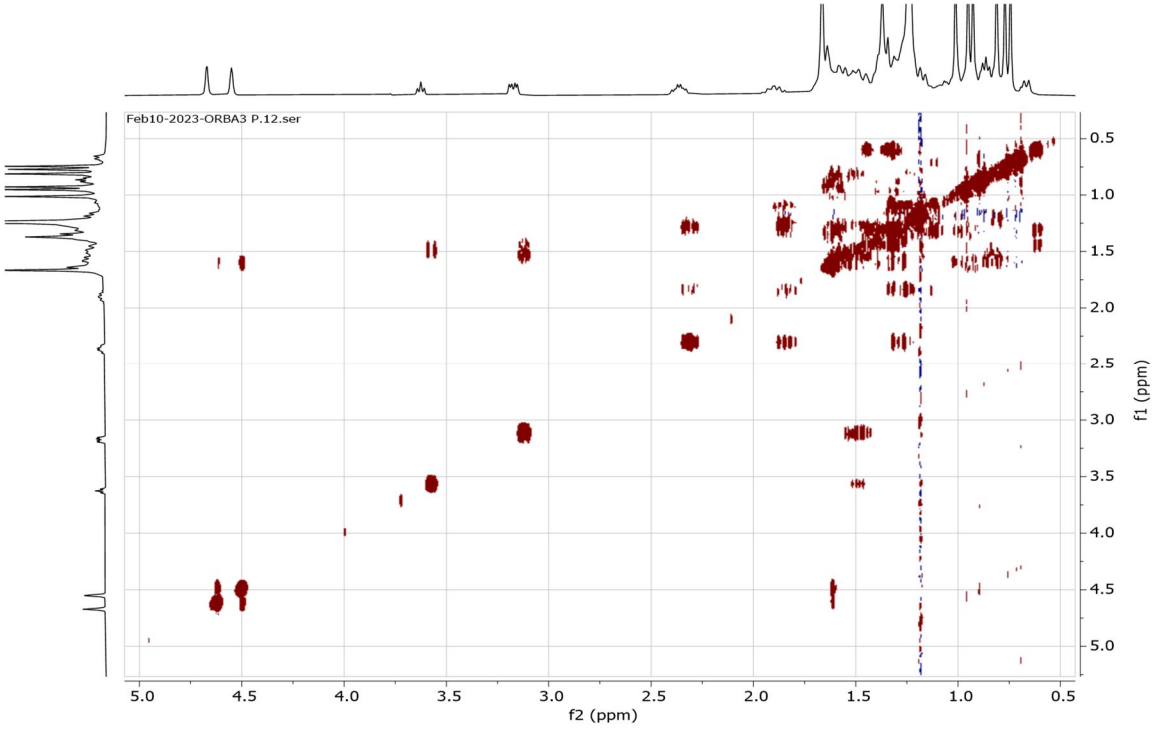

Appendix 157: HSQC Spectrum of Compound **91**

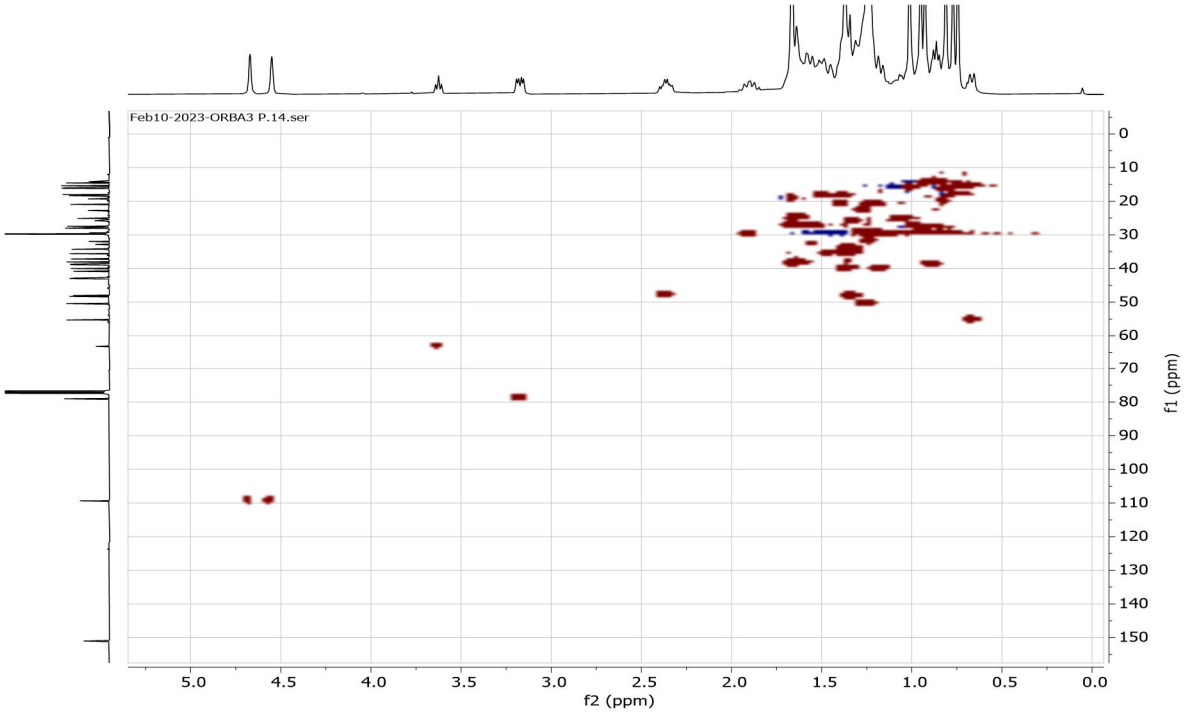

Appendix 158: HMBC Spectrum of Compound **91**

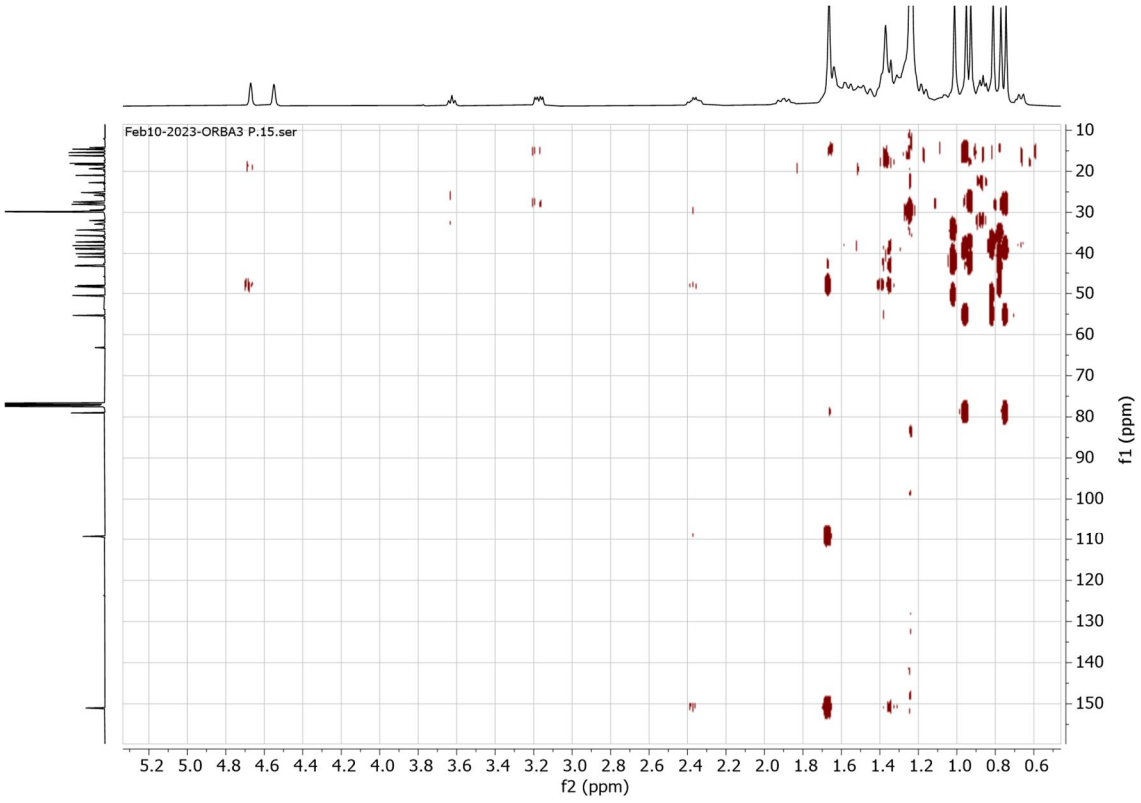

Appendix 159: TOF-MS Spectrum of Compound **91**

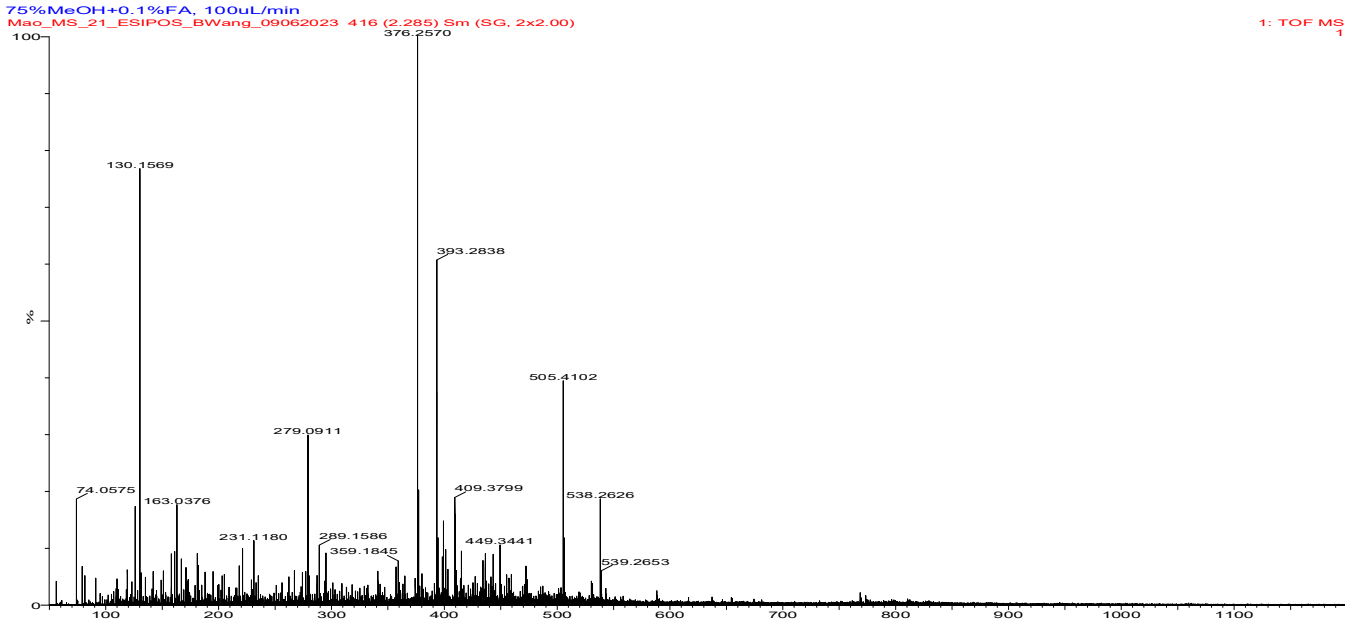

Appendix 160: ^{1}H-NMR (400 MHz, $CDCl_3$) Spectrum of Compound **92**

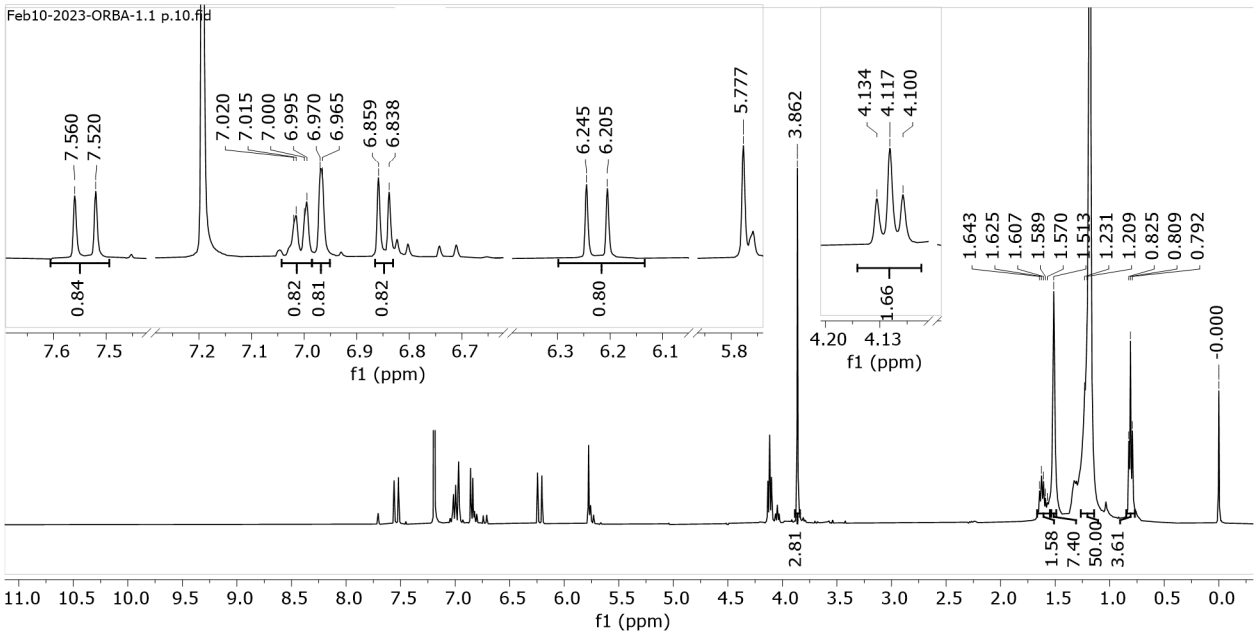

Appendix 161: ^{13}C-NMR (101 MHz, $CDCl_3$) Spectrum of Compound **92**

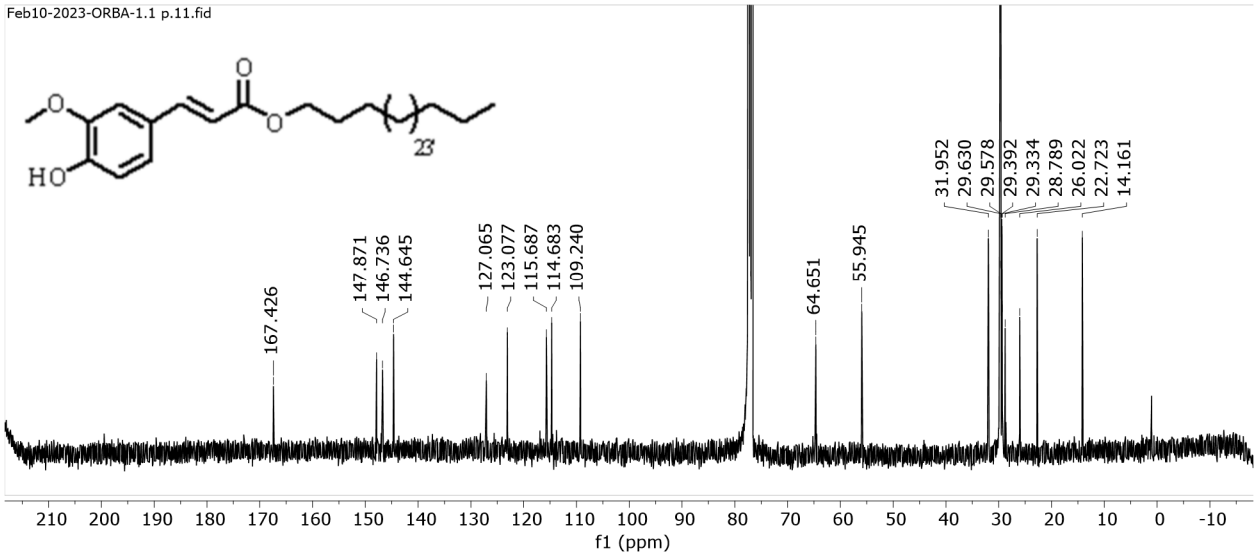

Appendix 162: DEPT-135 Spectrum of Compound **92**

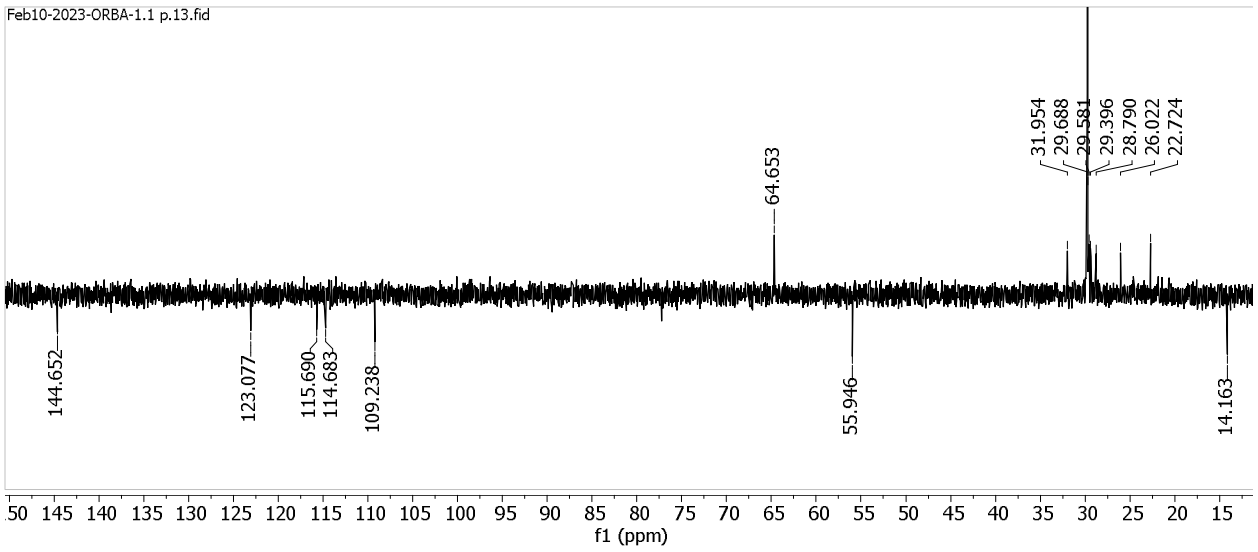

Appendix 163: ^{1}H-^{1}H COSY Spectrum of Compound **92**

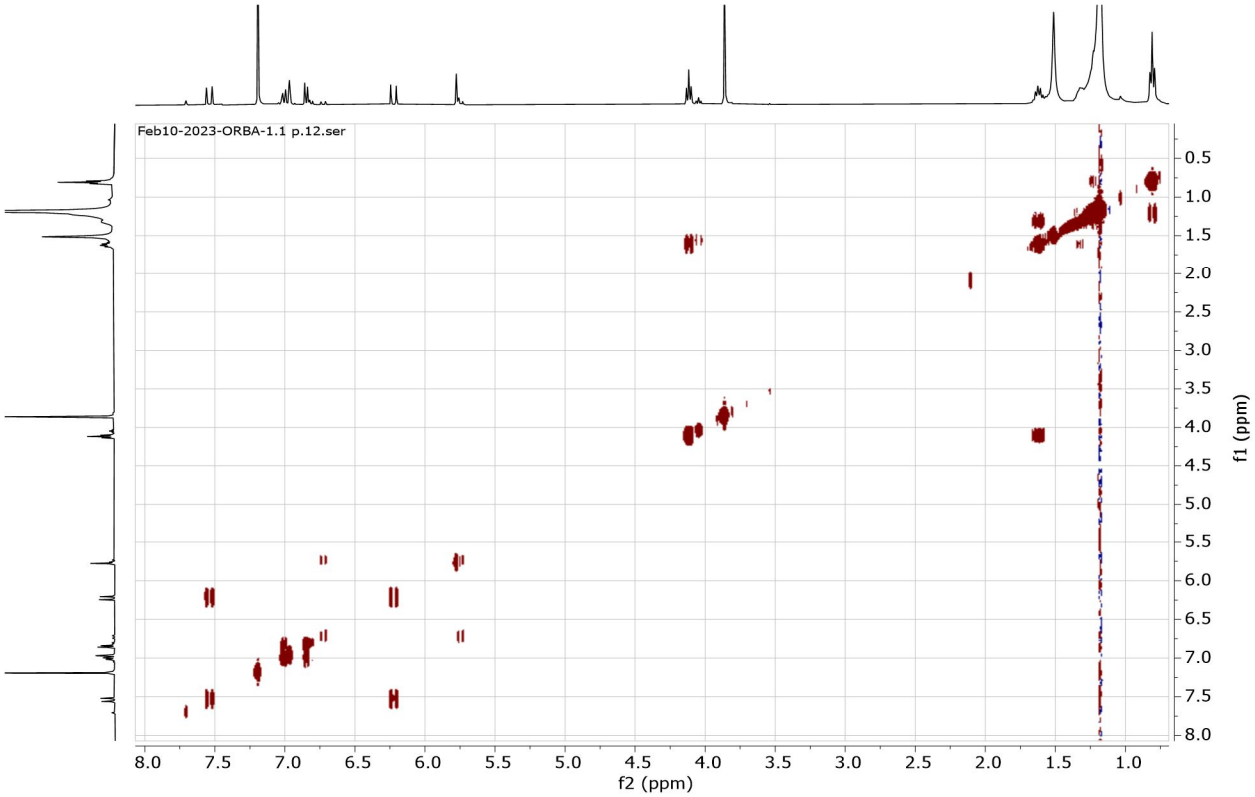

Appendix 164: HSQC Spectrum of Compound **92**

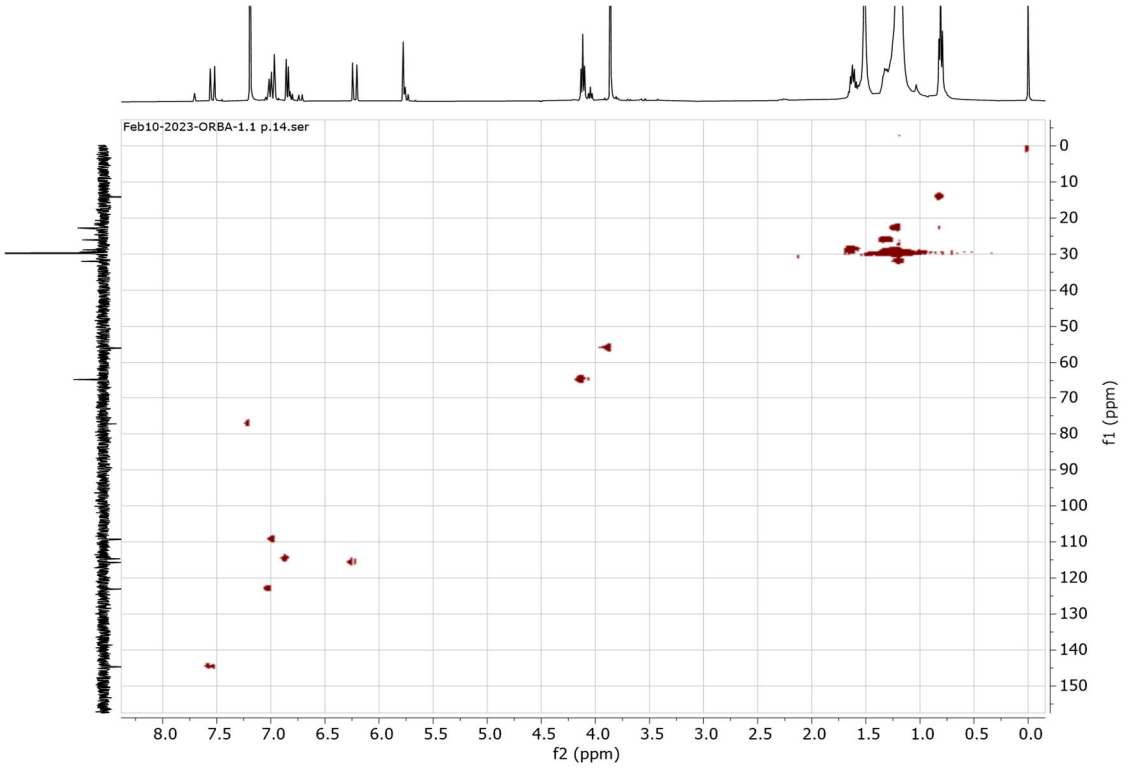

Appendix 165: HMBC Spectrum of Compound **92**

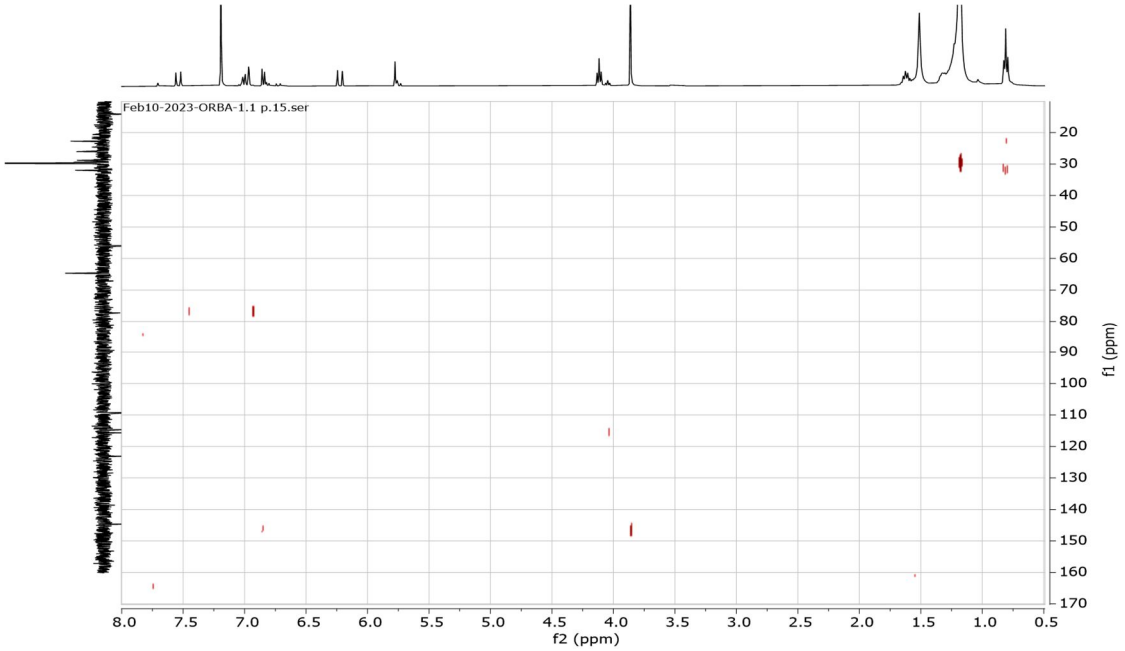

Appendix 166: TOF-MS Spectrum of Compound **92**

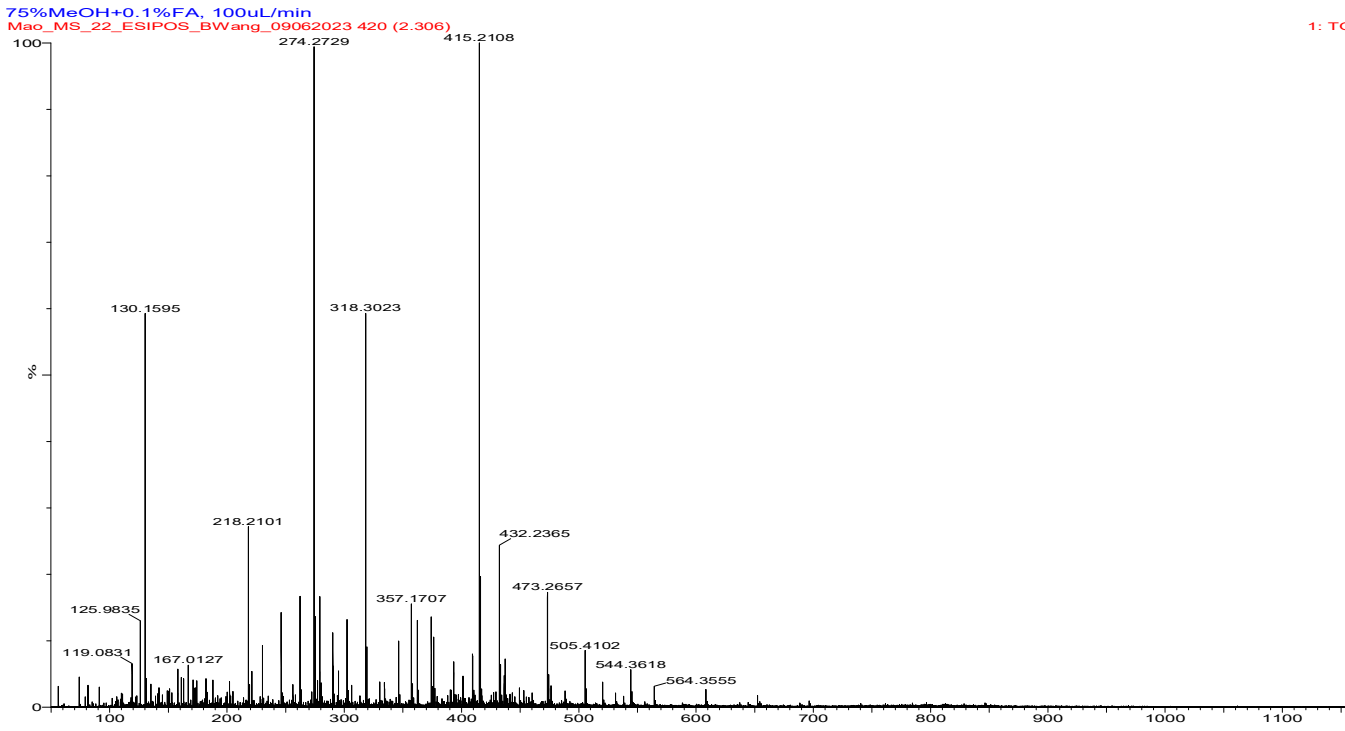

Appendix 167: ^{1}H-NMR (400 MHz, MeOD) Spectrum of Compound **72**

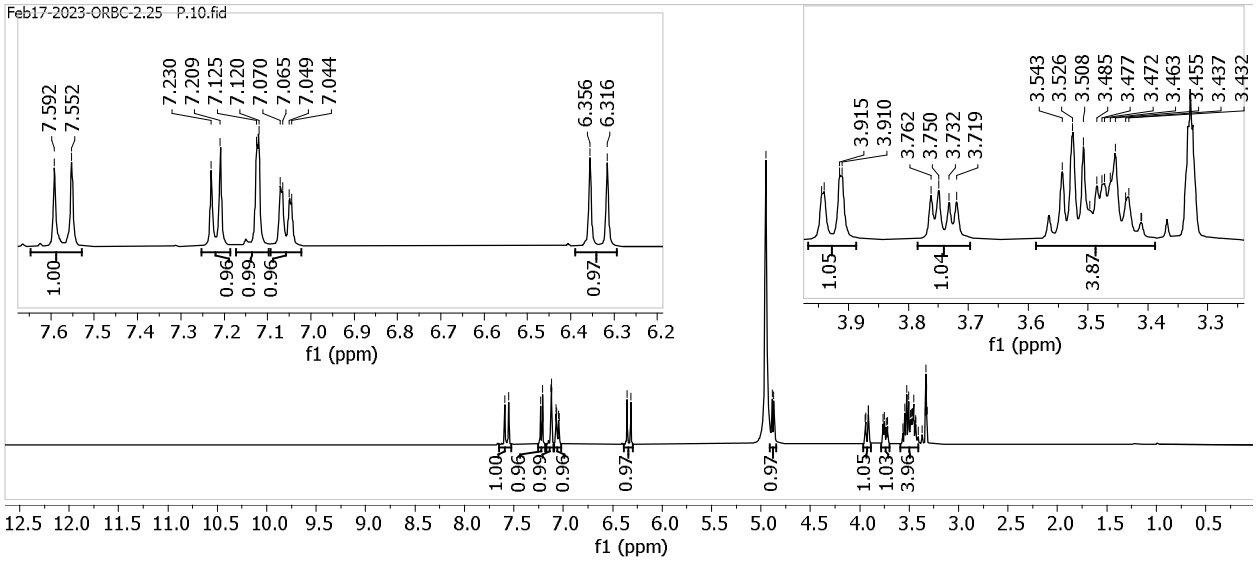

Appendix 168: ^{13}C-NMR (101 MHz, MeOD) Spectrum of Compound **72**

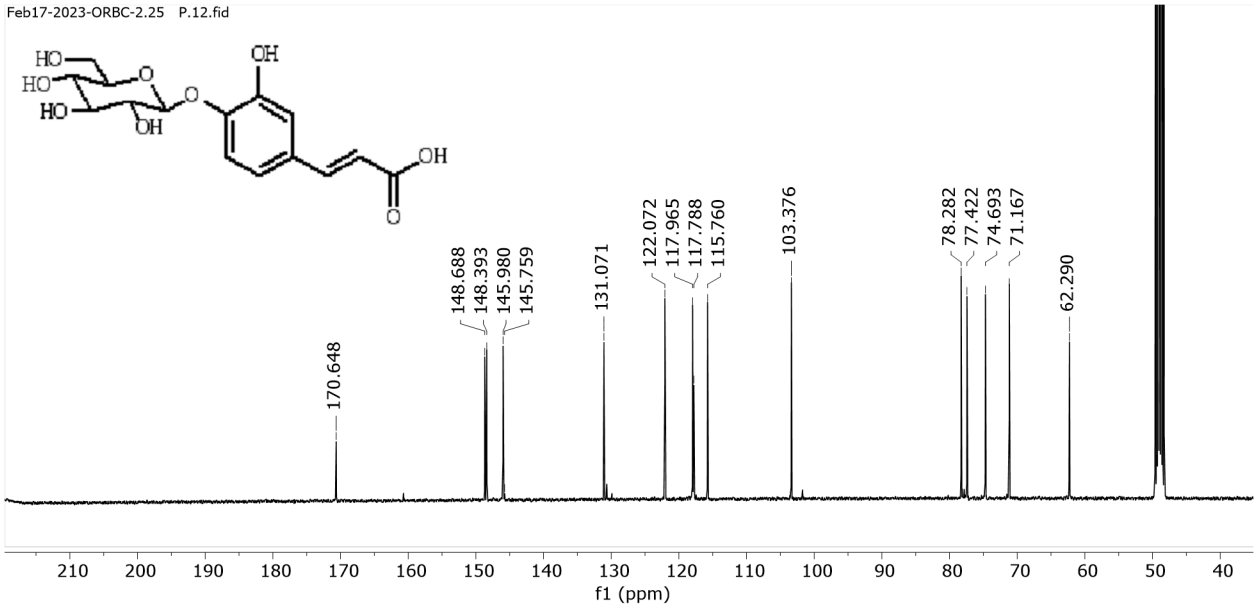

Appendix 169: DEPT-135 Spectrum of Compound **72**

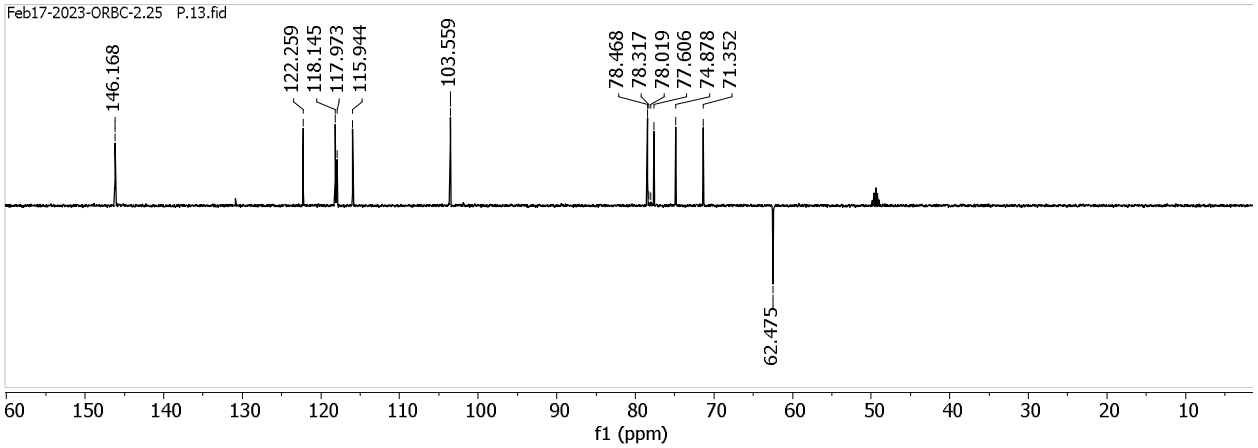

Appendix 170: ^{1}H-^{1}H COSY Spectrum of Compound **72**

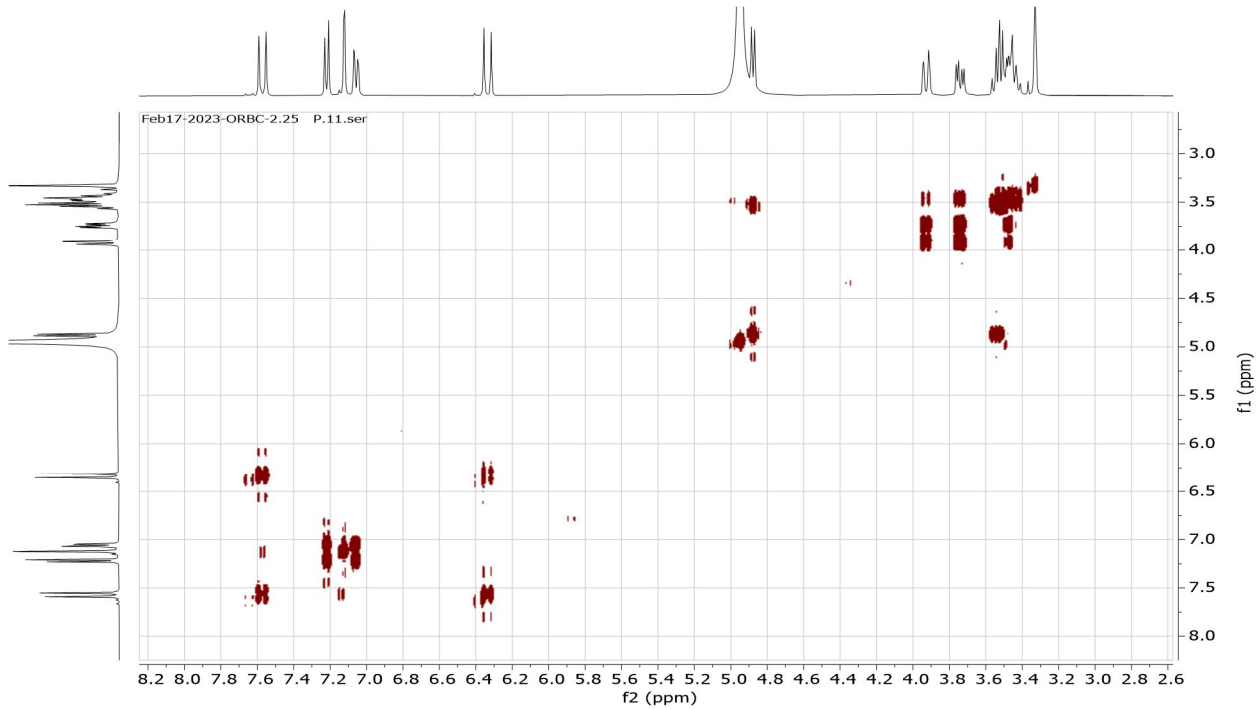

Appendix 171: HSQC Spectrum of Compound **72**

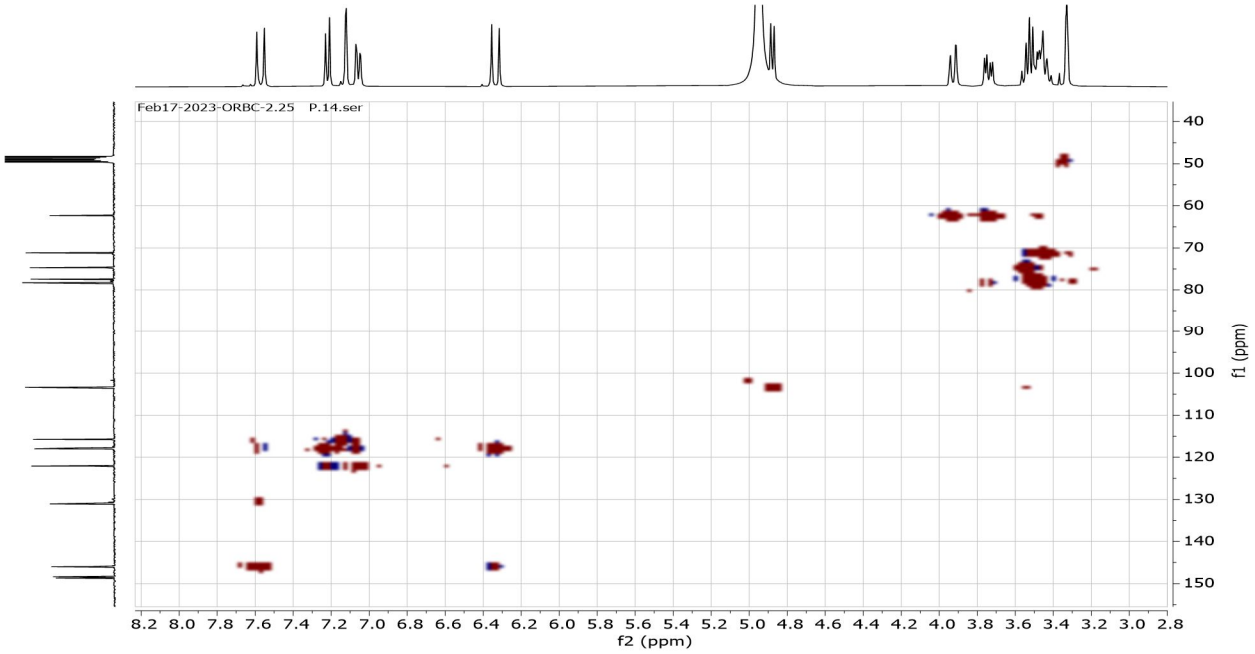

Appendix 172: HMBC Spectrum of Compound **72**

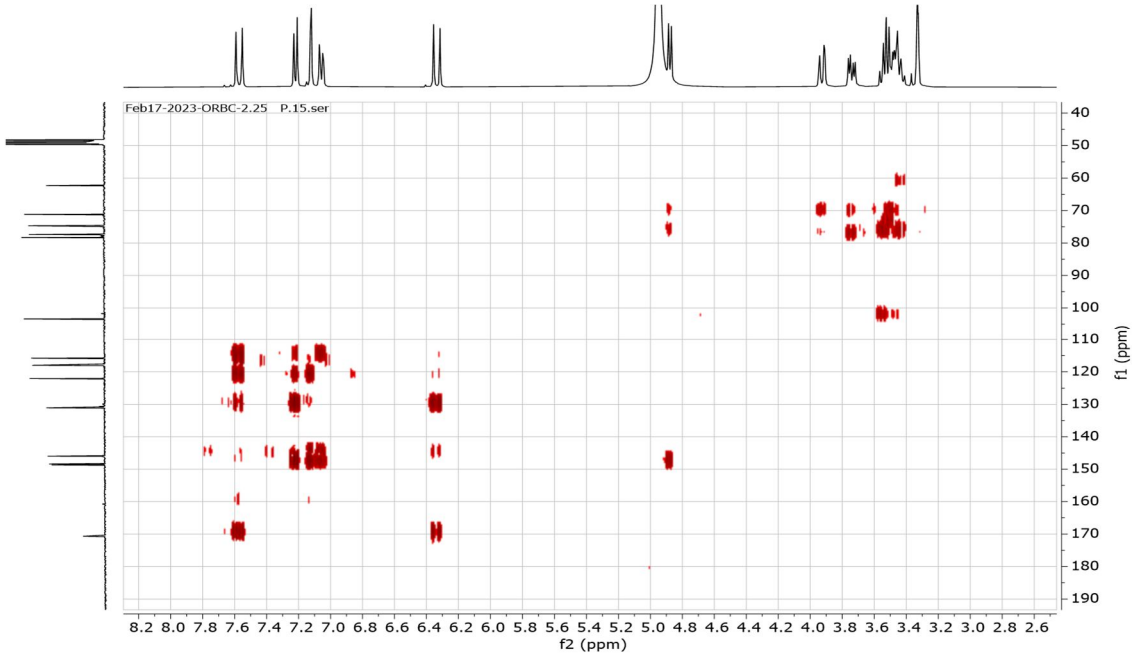

Appendix 173: TOF-MS Spectrum of Compound **72**